

Mid-Holocene marine faunas from the Bangkok Clay deposits in Nakhon Nayok, the Central Plain of Thailand

Parin Jirapatrasilp^{1,2}, Gilles Cuny³, László Kocsis⁴, Chirasak Sutcharit¹, Nom Ngamnissai⁵, Thasinee Charoentitirat⁶, Satapat Kumpitak⁶, Kantapon Suraprasit⁷

1 *Animal Systematics Research Unit, Department of Biology, Faculty of Science, Chulalongkorn University, Bangkok 10330, Thailand*

2 *Leibniz-Institut zur Analyse des Biodiversitätswandels - Standort Hamburg, Martin-Luther-King-Platz 3, Hamburg 20146, Germany*

3 *Université Claude Bernard Lyon 1, LEHNA UMR 5023, CNRS, ENTPE, F-69622, Villeurbanne, France*

4 *Institute of Earth Surface Dynamics, University of Lausanne, Rue de la Mouline, 1015 Lausanne, Switzerland*

5 *Department of Geography, Faculty of Social Sciences, Srinakharinwirot University, Bangkok 10110, Thailand*

6 *Department of Geology, Faculty of Science, Chulalongkorn University, Bangkok 10330, Thailand*

7 *Center of Excellence in Morphology of Earth Surface and Advanced Geohazards in Southeast Asia (MESA CE), Department of Geology, Faculty of Science, Chulalongkorn University, Bangkok 10330, Thailand*

Corresponding author: Kantapon Suraprasit (Kantapon.S@chula.ac.th)

Abstract

Based on several field investigations, many molluscan shells and chondrichthyan teeth, together with other invertebrate and actinopterygian remains were found from the marine Bangkok Clay deposits in Ongkharak, Nakhon Nayok, at a depth of ~ 5–7 m below the topsoil surface. Animal macrofossils recovered from these Holocene marine deposits were identified and their chronological context was investigated in order to reconstruct the paleoenvironments of the area at that time. The majority of marine fossils recovered from the site consist of molluscs, with a total of 63 species identified. Other invertebrate species include a stony coral, a mud lobster, barnacles, and a sea urchin. The vertebrates are represented by fish remains, including carcharhinid shark teeth from at least nine species, stingray and trichiurid teeth, and one sciaenid otolith. The molluscan fauna indicates that the paleoenvironments of the area corresponded to intertidal to sublittoral zones, where some areas were mangrove forests and intertidal mudflats. The fish fauna is dominated by the river shark *Glyphis*, indicating freshwater influences and possibly occasional brackish conditions. The carbon-14 analysis of mollusc and charcoal remains shows that deposition of the marine sediment sequence began during the mid-Holocene, spanning approximately from 8,800 to 5,300 cal yr BP. This study provides in-depth insights into the diversity of fishes, marine molluscs, and other invertebrates from the Bangkok Clay deposits, supporting the existence of a marine transgression onto the Lower Central Plain of Thailand during the mid-Holocene.

Key words: carbon-14 dating, Chao Phraya River Basin, Chondrichthyes, marine transgression, mollusc, paleoenvironment



Academic editor: Fedor Konstantinov

Received: 25 January 2024

Accepted: 24 March 2024

Published: 15 May 2024

ZooBank: <https://zoobank.org/D04EE090-0D05-4EB2-ADA6-3EE4E19F59D9>

Citation: Jirapatrasilp P, Cuny G, Kocsis L, Sutcharit C, Ngamnissai N, Charoentitirat T, Kumpitak S, Suraprasit K (2024) Mid-Holocene marine faunas from the Bangkok Clay deposits in Nakhon Nayok, the Central Plain of Thailand. ZooKeys 1202: 1–110. <https://doi.org/10.3897/zookeys.1202.119389>

Copyright: © Parin Jirapatrasilp et al.
This is an open access article distributed under terms of the Creative Commons Attribution License (Attribution 4.0 International – CC BY 4.0).

Table of contents

Introduction	3
Geological settings of the study area	4
Materials and methods	7
Results	8
Systematic palaeontology	8
Phylum Cnidaria	8
Class Anthozoa Ehrenberg, 1834	8
Family Rhizangiidae d’Orbigny, 1851	8
Phylum Mollusca	9
Class Gastropoda Cuvier, 1795	9
Family Colloniidae Cossmann, 1917	9
Family Neritidae Rafinesque, 1815	9
Family Potamididae H. Adams & A. Adams, 1854	12
Family Naticidae Guilding, 1834	16
Family Calyptraeidae Lamarck, 1809	20
Family Bursidae Thiele, 1925	21
Family Cancellariidae Forbes & Hanley, 1851	21
Family Buccinidae Rafinesque, 1815	23
Family Melongenidae Gill, 1871	23
Family Nassariidae Iredale, 1916	25
Family Muricidae Rafinesque, 1815	26
Family Borsoniidae Bellardi, 1875	29
Family Clathurellidae H. Adams & A. Adams, 1858	30
Family Clavatulidae Gray, 1853	30
Family Horaiclavidae Bouchet et al., 2011	32
Family Pseudomelatomidae Morrison, 1966	32
Family Terebridae Mörch, 1852	33
Family Architectonicidae Gray, 1850	36
Family Cylichnidae H. Adams & A. Adams, 1854	36
Family Ellobiidae Pfeiffer, 1854	37
Class Bivalvia Linnaeus, 1758	39
Family Nuculanidae H. Adams & A. Adams, 1858	39
Family Arcidae Lamarck, 1809	41
Family Noetiidae Stewart, 1930	45
Family Ostreidae Rafinesque, 1815	46
Family Placunidae Rafinesque, 1815	47
Family Pectinidae Rafinesque, 1815	49
Family Lucinidae J. Fleming, 1828	49
Family Cyrenidae Gray, 1840	50
Family Mactridae Lamarck, 1809	50
Family Tellinidae Blainville, 1814	53
Family Ungulinidae Gray, 1854	53
Family Veneridae Rafinesque, 1815	54
Family Corbulidae Lamarck, 1818	56
Family Pholadidae Lamarck, 1809	58
Family Pharidae H. Adams & A. Adams, 1856	60
Class Scaphopoda Bronn, 1862	62

Family Dentaliidae Children, 1834.....	62
Phylum Arthropoda	62
Class Malacostraca Latreille, 1802.....	62
Family Thalassinidae Latreille, 1831.....	62
Class Thecostraca Gruvel, 1905.....	63
Family Balanidae Leach, 1817.....	63
Phylum Echinodermata.....	64
Class Echinoidea Schumacher, 1817.....	64
Family Temnopleuridae Agassiz, 1872.....	64
Phylum Chordata.....	65
Family Carcharhinidae Jordan & Evermann, 1896.....	65
Family Dasyatidae Jordan & Gilbert, 1879.....	82
Class Actinopterygii Klein, 1885.....	82
Family Trichiuridae Rafinesque, 1810.....	82
Family Sciaenidae Cuvier, 1829.....	85
Discussion.....	85
Acknowledgments.....	89
Additional information.....	89
References.....	90

Introduction

The Holocene began approximately 11,700 years ago and belongs to one of the interglacial periods. Prior to the Holocene, during the period of the Last Glacial Maximum (LGM), the global climate was much colder and dryer and was a period of significant landscape changes in many areas due to a lowered sea level, approximately 120 m below the present-day stands (Clark et al. 2009). During the Holocene, however, the climate became warmer, and the sea level rose and inundated a previously emerged landmass. Southeast Asia is one of the regions impacted by sea level inundations (Sathiamurthy and Voris 2006), due in part to an increase in precipitation level after the cold and dry period (Chabangborn 2017). Differences in climatic and environmental conditions between the Pleistocene and Holocene have therefore had impacts on the ecological adaptations of both terrestrial and marine organisms, leading to dispersal, migration, and extinction of species.

The Central Plain of Thailand is an important area where the topography and climate changes were under the influence of a sea level rise starting at ~ 12 ka. The region covers the plains between the mountain ranges along the lower northern part of Thailand, including the Yom and Nan River basins, and the low-lying plains of the Chao Phraya, Tha Chin, Mae Klong and Bang Pakong River basins near the Gulf of Thailand (Sinsakul 2000). During the Holocene, the Sing Buri Plain (5–15 m above mean sea level (amsl)) and the Bangkok Lowland (0–5 m amsl), forming the Central plain of Thailand, were inundated (Takaya 1969). Approximately 8–7 ka, the sea level was 2–4 m higher than present-day stands and inundated the whole lowland areas of Bangkok. Later, the sea level subsided along with a new sedimentation regime and a new landmass started to develop, shaping the current coastal shorelines (Umitsu et al. 2002; Tanabe et al. 2003).

The extent of marine intrusion into the Central Plain of Thailand during the Holocene was largely interpreted based on various studies (e.g., geomorphological, sedimentological, paleontological, palynological, and stratigraphical data as well as carbon-14 dating of peat layers). These studies indicated that the ancient coastal shoreline of the Gulf of Thailand was located further north in Phra Nakhon Si Ayutthaya Province during 7.3–6.5 ka (Jarupongsakul and Thiramongkol 1992). The ancient coastal shoreline was also reconstructed based on a 4,500-year-old coastal archaeological site in Chonburi Province (Boyd et al. 1996), open-pit mining of clay deposits at a depth of 7 m under the ground surface in many provinces, dated to ~8–7 ka (Songtham et al. 2007, 2015), and geological studies of coastal berms in Chumphon and Prachuap Khiri Khan provinces, dated between 8.9–5.6 ka and 6.5–6 ka, respectively (Nimnate et al. 2015; Surakiatchai et al. 2018).

In addition to the inference of ancient coastal shorelines during the Holocene, studies on faunas and floras along the ancient coast of the Gulf of Thailand are crucial to understand paleoenvironmental and palaeoecological changes in response to climatic oscillations. The ancient coastal habitats occupied by these animals are investigated based on the identification and dating of fossils (e.g., molluscs, arthropods, and vertebrates). According to accurate species-level identification, microhabitats can be investigated based on comparisons between fossils and living species or related taxa. The paleoenvironments of the area are also reconstructed based on the identification of various groups of animals because each of them has a different mode of life in a specific habitat (Negri 2009, 2012; Oliver and Terry 2019).

Marine faunas from the Holocene Bangkok Clay deposits of the Central Plain of Thailand have infrequently been analysed in detail, and we identify the animal macrofossils recovered from the clay pit of Ongkharak, Nakhon Nayok Province in central Thailand (Fig. 1). We also date the Bangkok Clay sequence deposited in the area, using a carbon-14 dating technique. Although the Bangkok Clay deposits have previously been described from some areas of Nakhon Nayok Province (Songtham et al. 2007; Royal Irrigation Department 2009), the fauna and its paleoenvironments have not yet been thoroughly studied and compared to other sites from different regions (e.g., Negri 2009, 2012). This study not only fulfils the gap regarding the paleoenvironments of the Gulf of Thailand during the Holocene, but also illustrates the ancient coastlines in the eastern part of the Central Plain of Thailand to some extent. The reconstruction of ancient coastlines and paleoenvironments is crucial to advance the knowledge of archaeological contexts in terms of prehistoric human settlements and cultures, and probably helpful in forecasting changes in coastal ecosystems and environments in response to sea level oscillations due to the present-day global warming situation.

Geological settings of the study area

The study area is located at the clay pit in Ban Lad Chang, Chumpon Subdistrict, Ongkharak District, Nakhon Nayok Province (13°59'30.9"N, 100°55'11.5"E) in the Lower Central Plain of Thailand (Fig. 1), which is covered by the thick marine deposits of the Chao Phraya River delta, also known as the Bangkok Clay. These marine clay deposits have been dated between the Late Pleistocene and Holocene (Cox 1968; Moh et al. 1969; Sinsakul 2000). The Bangkok clay sequence comprises three main zones (Ohtsubo et al. 2000): 1) weathered

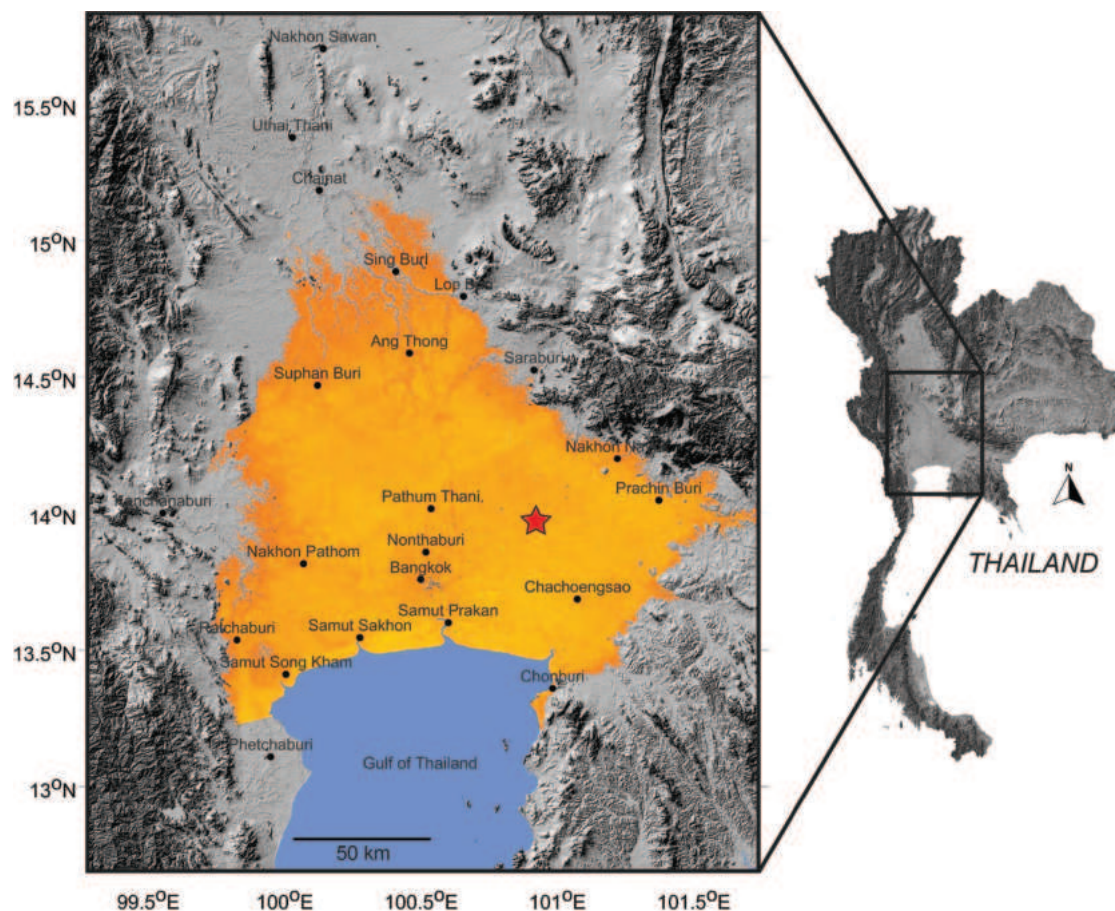


Figure 1. Map of the lower central plain of Thailand (orange). A red star indicates the location of the study area.

clay with a thickness of 0–2 m in the uppermost part, 2) soft marine clay in the middle part, and 3) medium stiff clay at the bottom. The Holocene Bangkok Soft Clay in the middle part, with a thickness ranging from 10 to 20 m, is olive grey and medium to dark grey in colour, indicating reducing environments (Sinsakul 2000; Choowong 2002; Tanabe et al. 2003). This Bangkok Soft Clay layer is further divided into lower transgressive peaty (mangrove swamp) and upper regressive deltaic sediments (Tanabe et al. 2003). Some marine shells and remains of mangrove trees were found from this middle layer, indicating intertidal and shallow sublittoral inner bay conditions, with local mangrove and freshwater influences (Robba et al. 2002, 2003, 2004, 2007; Songtham et al. 2007; Negri 2009, 2012). This evidence supports the occurrence of a marine transgression into the Central Plain of Thailand after the LGM (Songtham et al. 2015).

The rectangular mine is 1,000 m long × 400 m wide and 30 m deep. It was opened to produce clay material used in construction sites. The active mining operations of the clay pit allow us to have access to the stratigraphic sequence of the Quaternary deposits of the area (Fig. 2). The topsoil (0.5–1 m thick) consists of coarse-grained sand with FeO grains and black mud nodules, underlain by a 5 m thick layer of black clay and organic soil (dark layer) partially interbedded with thin layers of silt to very fine-grained sand. Marine invertebrate and vertebrate remains were only found from this organic-rich clay unit, also known as the Bangkok Clay, which overlies the layers of Pleistocene stiff clay (Rau and Nutalaya 1983). In this site, the Pleistocene stiff clay contains seven different

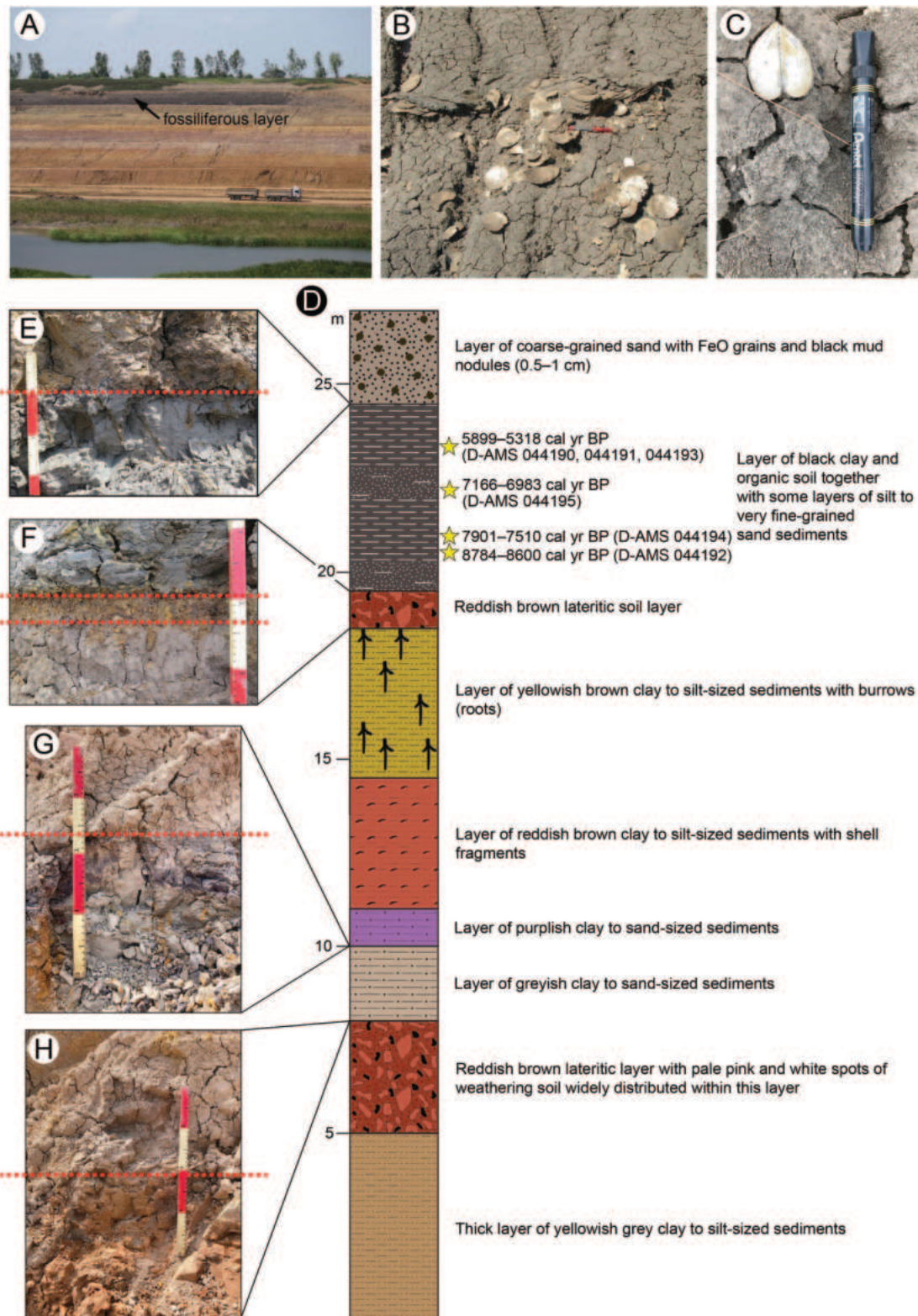


Figure 2. The study area and the sediment profile of the clay pit **A** the clay pit of Ongkharak, Nakhon Nayok Province in central Thailand **B** the Bangkok clay layer bearing numerous *in situ* complete shells of *Placuna placenta* **C** Shells of a bivalve *Anadara inaequalvis* buried *in situ* in the Bangkok clay deposits **D** lithological profile of the clay pit **E** the contact between two successive layers: coarse-grained sand (upper) and black clay (lower) **F** the contact between three successive layers: black clay (upper), lateritic soil (middle), and yellowish brown clay to silt (lower) **G** the contact between two successive layers: purplish (upper) and greyish (lower) clay to sand **H** the contact between two successive layers: greyish clay to sand (upper) and reddish brown lateritic layer (lower).

lithological units from the top to bottom of the pit: 1) reddish brown lateritic soil (1 m thick), 2) yellowish brown clay to silt-sized sediments with root-trace burrows (4 m thick), 3) reddish brown clay to silt-sized sediments with shell fragments (4 m thick), 4) purplish clay to sand-sized sediments (1 m thick), 5) greyish clay to sand-sized sediments (2 m thick), 6) reddish brown lateritic soil with pale pink and white spots of weathering soil (3 m thick), and 7) yellowish grey clay to silt-sized sediments (5 m thick), respectively (Fig. 2).

The Bangkok clay layer at the clay pit of Ongkharak has yielded nearly *in situ* fossil deposits as indicated by preservation of complete shells with both valves attached (Fig. 2C) as well as the orientation of shell valves of *Pholas orientalis*, which has been recovered in natural position within its burrows during field collection (see also Songtham et al. 2007: fig. 3). Although remains of marine molluscs were found throughout the sequence of dark clay deposits, they were most abundant in the middle part of the layer (Fig. 2D–F), at a depth of ~ 2 m below the upper contact that separates it from the topsoil. Numerous wood fragments, plant remains, and giant oyster shells were found from the lower part of the dark clay unit below the shell-rich layer.

Materials and methods

Species identification of specimens is mainly based on the existing literature specified under the treatment of each taxon. The specimens are kept at the Department of Geology, Faculty of Science, Chulalongkorn University, and coded as the name of the collection (**CUF**: Chulalongkorn fossil collection), followed by the locality (**NKNY**: Nakhon Nayok) and the catalogue number. Fish remains including teeth and otolith as well as some small shells were photographed with a scanning electron microscope (SEM; JEOL, JSM-5410 LV) or a Leica M205C stereo light microscope with fusion optics and the Leica Application Suite Image System. L and R designate left and right valves of bivalve shells, respectively.

We selected six samples (shells and charcoal) collected from the marine clay deposits at different depths in the clay pit for carbon-14 dating (Table 1). The samples were pretreated and analysed at the DirectAMS (USA), using an accelerated mass spectrometer (AMS). According to the convention outlined by Stuiver and Polach (1977), the ^{14}C age \pm one standard deviation (SD) was calculated using the Libby half-life of 5,568 years and an isotopic fractionation correction based on $\delta^{13}\text{C}$ measurements obtained from the AMS. The DirectAMS results were calibrated and corrected for the marine reservoir effect, using the Calib 8.2 program with IntCal20.14c for charcoal (Reimer et al. 2020) and with Marine20 (Heaton et al. 2020) for shells.

Table 1. AMS ^{14}C ages of shells and charcoal collected from the clay pit of Ongkharak in Nakhon Nayok, central Thailand.

Lab Code	Sample type	Depths (m) below the uppermost part of a marine clay layer	^{14}C age (yr BP)	Calibrated ^{14}C (2-sigma) age (cal yr BP)
D-AMS 044190	Shell (<i>Tellinides conspicuus</i>)	2.2	5303 \pm 26	5882–5464
D-AMS 044191	Shell (<i>Pholas orientalis</i>)	2.2	5202 \pm 28	5757–5318
D-AMS 044193	Charcoal	2.2	5047 \pm 26	5899–5726
D-AMS 044195	Charcoal	3.4	6186 \pm 29	7166–6983
D-AMS 044194	Shell (<i>Magallana cf. gigas</i>)	4	7241 \pm 32	7901–7510
D-AMS 044192	Charcoal	4.6	7913 \pm 26	8784–8600

Results

The ages of the Bangkok Clay deposits in the clay pit of Ongkharak range from 8,784 calibrated years before the present (cal yr BP) to 5,318 cal yr BP (mid-Holocene) based on the radiocarbon dating of several shell and charcoal fragments collected along the stratigraphic section of the layer (Table 1). The majority of marine faunas are molluscs, where a total of 63 species were identified, including 35 gastropod species from 20 families, 27 bivalve species from 15 families, and one scaphopod species. The most common gastropods are *Architectonica perdix*, *Natica stellata*, and *Indothais lacera*, whereas the most common bivalves are *Corbula fortisulcata*, *Magallana* cf. *gigas*, and *Joannisiella oblonga*. Other invertebrate remains include one species of stony corals (*Oulangia* cf. *stokesiana*), one unidentified species of mud lobsters (*Thalassina* sp.), two species of barnacles (*Fistulobalanus kondakovi* and *Megabalanus* cf. *tintinnabulum*), and one species of sea urchins (*Temnotrema siamense*).

The vertebrate remains include at least nine species (two families) of chondrichthyan fishes and at least two species (two families) of actinopterygian taxa. Altogether, 100 cartilaginous fish fossils were recovered, including 97 remains identified as belonging to the family Carcharhinidae and three to the family Dasyatidae. The teeth of the latter belong to the stingray genus *Pastinachus*. Among the carcharhinids, the genus *Glyphis* dominates the shark fauna (61%). There are also at least six species of *Carcharhinus*, representing 26% of the shark fauna. The accurate identification of *Carcharhinus* species is often hindered by the preservation of teeth or by the morphological similarities of tooth positions among these taxa. A few teeth among the carcharhinids belong to the genus *Scoliodon*. Few actinopterygian remains were also found, including three teeth that belong to the family Trichiuridae and one sciaenid otolith that represents the genus *Johnius*.

Systematic palaeontology

Phylum Cnidaria

Class Anthozoa Ehrenberg, 1834

Subclass Hexacorallia Haeckel, 1896

Order Scleractinia Bourne, 1900

Family Rhizangiidae d'Orbigny, 1851

Oulangia Milne Edwards & Haime, 1848

Oulangia cf. *stokesiana* Milne Edwards & Haime, 1848

Figs 3A, 5A

cf. *Oulangia stokesiana* Milne Edwards & Haime, 1848: pl. 7, fig. 4, 4a. Type locality: Philippines. Milne Edwards and Haime 1849: 183. Lam et al. 2008: 742, fig. 4e.

cf. *Oulangia stokesiana stokesiana*. Cairns et al. 1999: 39.

Referred material. CUF-NKNY-007 (1 specimen; Figs 3A, 5A).

Habitat. Shallow waters as well as in submarine caves (Lam et al. 2008).

Distribution. Indian Ocean; Indo-West Pacific, from Japan to the Philippines, and central Pacific (Cairns et al. 1999; Lam et al. 2008).

Taxonomic remarks and comparisons. This specimen is classified into the genus *Oulangia* based on the descriptions and figures of Cairns and Kitahara (2012) and Baron-Szabo and Cairns (2016). We tentatively identify this specimen as belonging to *O. stokesiana* according to Lam et al. (2008).

Phylum Mollusca

Class Gastropoda Cuvier, 1795

Subclass Vetigastropoda Salvini-Plawen, 1980

Order Trochida Cox & Knight, 1960

Superfamily Trochoidea Rafinesque, 1815

Family Colloniidae Cossmann, 1917

***Homalopoma* Carpenter, 1864**

***Homalopoma* cf. *sangarensis* (Schrenck, 1861)**

Figs 3F, 5B

cf. *Turbo sangarensis* Schrenck, 1861: 409–410. Type locality: the Sangaric strait near the shore of the island of Jesso [Sangar (Tsugaru) Strait, Hakodate Bay, Hokkaido, Japan].

cf. *Homalopoma sangarensis*. Habe 1958: 5, pl. 2, fig. 1. Golikov and Kussakin 1978: 65–66, fig. 40a, b. Egorov 2000: 66, with in-text fig. Kantor and Sysoev 2006: 42, pl. 18h. Lebedev 2014: 57.

Referred material. CUF-NKNY-G24 (1 shell; Figs 3F, 5B).

Habitat. On silty-sandy or rarely on rocky substrates at a depth from 2 to 22 m (Egorov 2000; Kantor and Sysoev 2006).

Distribution. Sea of Japan and southern Kuril Islands (Kantor and Sysoev 2006; Lebedev 2014).

Record in Thailand. This is the first record of this species in Thailand.

Taxonomic remarks and comparisons. Although there is only one incomplete specimen, it is tentatively identified as *H. sangarensis* based on shell size and shape and several strong spiral cords on the surface as in the descriptions and figures in Habe (1958), Golikov and Kussakin (1978), and Egorov (2000).

Subclass Neritimorpha Golikov & Starobogatov, 1975

Order Cycloneritida Frýda, 1998

Superfamily Neritoidea Rafinesque, 1815

Family Neritidae Rafinesque, 1815

***Neripteron* Lesson, 1831**

***Neripteron violaceum* (Gmelin, 1791)**

Figs 3B, 5C

Nerita violacea Gmelin, 1791: 3686. Type locality: unknown.

Neritina violacea. Tantanasiwong 1978: 6, fig. 52. Nateewathana et al. 1981: 56. Wilson 1993: 41, pl. 2, figs 18a, b, 19a–d. Hylleberg and Kilburn 2003: 31.

Robba et al. 2004: 24–25, pl. 2, fig. 5a, b. Robba et al. 2007: 89 (appendix). Printrakoon et al. 2008: table 1. Tan and Clements 2008: 490–491, fig. 3-33, 3-34. Nabhitabhata 2009: 39. Sanpanich and Duangdee 2013: 53. Ng et al. 2016: fig. 1-28. Yang et al. 2017: 20, fig. 75. Tudu et al. 2018: table 1.

Dostia violacea. Way and Purchon 1981: 314. Subba Rao and Dey 2000: 35. Sri-aroon et al. 2004: table 1, fig. 2-1. Dechruksa et al. 2014: fig. 2k.

Neripteron violacea. Swennen et al. 2001: 52, 108, text-fig. 275, fig. 275.

Neritina (Dostia) violacea. Gemert 2003: 103. Sri-aroon et al. 2005: tables 2, 3, 5, 6. Dey 2006: 22, figs 11, 12. Ramakrishna et al. 2007: 5, 37. Kesavan et al. 2009: 382, with in-text fig. Eichhorst 2016: 392–395, pl. 102, figs 1–15.

Neritina (Neripteron) violacea. Thach 2005: 38, pl. 6, figs 8, 9.

Neripteron violaceus. Eichhorst 2008: 268, pl. 79, fig. 7a, b.

Neripteron violaceum. Baharuddin et al. 2017: fig. 3o. BEDO 2017b: 97, with in-text fig. Kantharajan et al. 2017: table 1, fig. 4-34. Yadav et al. 2019: table 2, fig. 1h. Mustapha et al. 2021: 52–53, figs 3e, f, 4i. Wells et al. 2021: 154–155.

Referred material. CUF-NKYN-G26 (28 shells; Figs 3B, 5C).

Habitat. On Nipa palms, muddy surfaces, old wood and rocks in brackish habitats and mangrove forests (Swennen et al. 2001; Mustapha et al. 2021) as well as on gravels in high tidal zones (Yang et al. 2017).

Distribution. India (Kantharajan et al. 2017; Yadav et al. 2019); Indo-West Pacific, from Japan to Australia (Wilson 1993; Yang et al. 2017).

Record in Thailand. Gulf of Thailand and Andaman Sea (Wells et al. 2021).

Taxonomic remarks and comparisons. The shell of *N. violaceum* is highly similar to that of *N. cornucopia* (Benson, 1836) but differs in having a purple to orangish red ventral side, and denticulations along the columellar edge often only present in the central part (Huang 1997; Tan and Clements 2008). Although the columella edge of the specimens is corroded, there are still some traces of purple colour at the ventral side. Therefore, these specimens are identified as belonging to *N. violaceum*.

***Nerita* Linnaeus, 1758**

***Nerita articulata* Gould, 1847**

Figs 3C, 5D

Nerita lineata Gmelin, 1791: 3684 [junior homonym of *Nerita lineata* Müller, 1774]. Type locality: Strait of Malacca. Way and Purchon 1981: 314. Hylleberg and Kilburn 2003: 29–30. Yang et al. 2017: 20, fig. 67.

Nerita (Ritena) lineata. Cernohorsky 1972: 51, pl. 11, fig. 5.

Nerita articulata Gould, 1847: 220. Type locality: Tavoy. Wium-Andersen 1977: 5, fig. 8. Tantanasiwong 1978: 6, fig. 42. Nateewathana et al. 1981: 56. Tan and Clements 2008: 483–485, fig. 2-3, 2-4. Nabhitabhata 2009: 36. Hamli et al. 2013: tables 2, 3, fig. 2g. Tudu et al. 2018: table 1.

Nerita balteata Reeve, 1855: pl. 6, fig. 28. Type locality: unknown. Wilson 1993: 40, pl. 2, fig. 9a, b. Nateewathana 1995: 95, with in-text fig. Nabhitabhata 2009: 36. Sanpanich and Duangdee 2013: 53. Chen et al. 2015: 75, fig. 1a–c. BEDO 2017b: 99, with in-text fig. Kantharajan et al. 2017: table 1, fig. 4-36. Tudu et al. 2018: table 1. Raven 2019: figs 4–6. Yadav et al. 2019: table 2, fig. 1i. Mustapha et al. 2021: 48, figs 2m, n, 4g. Wells et al. 2021: 155.



Figure 3. Size comparison of coral and gastropods found in this study **A** *Oulangia* cf. *stokesiana* **B** *Neripteron violaceum* **C** *Nerita articulata* **D** *Natica stellata* **E** *Natica vitellus* **F** *Homalopoma* cf. *sangarensis* **G** *Eunaticina papilla* **H** *Ergaea walshi* **I** *Pirenella incisa* **J** *Scalptia scalariformis* **K** *Telescopium telescopium* **L** *Merica elegans* **M** *Cerithidea obtusa* **N** *Bufonaria rana* **O** *Nassarius micans* **P** *Nassarius siquijorensis* **Q** *Paratectonatica tigrina*.

- Nerita (Ritena) balteata*. Cernohorsky 1978: 42, pl. 11, fig. 1. Dharma 2005: 68, pl. 9, fig. 3a, b.
Nerita (Amphinerita) articulata. Subba Rao and Dey 2000: 31. Dey 2006: 20, figs 7, 8.
Nerita (Nerita) articulata. Sri-aroon et al. 2004: table 1.
Nerita (Theliostyla) balteata. Thach 2005: 37, pl. 6, figs 36, 37.
Nerita balteata forma *articulata*. Eichhorst 2008: 280, pl. 85, fig. 1a, b.
Nerita (Cymostyla) balteata. Eichhorst 2016: 455–457, pl. 113, figs 1–9.

Referred material. CUF-NKNY-G61 (3 shells; Figs 3C, 5D).

Habitat. On tree trunks, branches, roots and on muddy banks and rocky areas or near mangrove forests (Tan and Clements 2008; Mustapha et al. 2021) as well as on rocks in intertidal zones (Yang et al. 2017).

Distribution. India (Kantharajan et al. 2017; Yadav et al. 2019); Indo-West Pacific, from China to Australia (Wilson 1993; Yang et al. 2017). Also reported from the Hawaiian Islands (Cernohorsky 1978).

Record in Thailand. Gulf of Thailand and Andaman Sea (Wells et al. 2021).

Taxonomic remarks and comparisons. This species is recognised by numerous raised spiral cords and a crenulated outer lip (Tan and Clements 2008). Although this species is widely known as *N. balteata* Reeve, 1855, the name *N. articulata* was made available earlier by Gould (1847). Thus, it has a priority over *N. balteata*.

Subclass Caenogastropoda Cox, 1960

Cohort Sorbeoconcha Ponder & Lindberg, 1997

Subcohort Cerithiimorpha Golikov & Starobogatov, 1975

Superfamily Cerithioidea Fleming, 1822

Family Potamididae H. Adams & A. Adams, 1854

***Cerithidea* Swainson, 1840**

***Cerithidea obtusa* (Lamarck, 1822)**

Figs 3M, 5E

Cerithium obtusum Lamarck, 1822: 71. Type locality: Timor.

Cerithidea obtusa. Cernohorsky 1972: 60 (in part). Tantanasiriwong 1978: 7, fig. 70. Nateewathana et al. 1981: 57. Way and Purchon 1981: 315. Nateewathana 1995: 97, with in-text fig. Poutiers 1998b: 450, with in-text figs. Gemert 2003: 104. Hylleberg and Kilburn 2003: 37–38. Robba et al. 2004: 31–32, pl. 3, fig. 4a, b. Dharma 2005: 92, pl. 21, fig. 8; 308, pl. 119, fig. 8a, b. Thach 2005: 49, pl. 10, fig. 4. Dey 2006: 35–36, figs 38–40. Robba et al. 2007: 89 (appendix). Printrakoon et al. 2008: table 1. Kesavan et al. 2009: 382, with in-text fig. Hamli et al. 2013: tables 2, 3, fig. 2a. Dechruksa et al. 2014: fig. 2f. Reid 2014: 27–29, 31, figs 2b, 8, 9. BEDO 2017b: 26, with in-text fig. Tudu et al. 2018: table 1. Wells et al. 2021: 125–126.

Cerithidea (Cerithidea) obtusa. Brandt 1974: 192–193, pl. 14, fig. 52. Houbrick 1984: 15–16, fig. 5c. Sri-aroon et al. 2004: table 1, fig. 3-1. Sri-aroon et al. 2005: tables 2–6. Ramakrishna et al. 2007: 6, 47. Nabhitabhata 2009: 95.

Referred material. CUF-NKNY-G14 (23 shells; Figs 3M, 5E).



Figure 4. Size comparison of gastropods found in this study **A** *Brunneifusus ternatanus* **B** *Murex trapa* **C** *Indothais lacera* **D** *Pristiterebra miranda* **E** *Chicoreus capucinus* **F** *Indothais gradata* **G** *Ellobium aurisjudae* **H** *Inquisitor vulpionis* **I** *Turricula javana* **J** *Architectonica perdix* **K** *Pseudoneptunea varicosa* **L** *Cassidula nucleus* **M** *Pseudoetrema fortilirata* **N** *Paradrillia melvilli* **O** *Duplicaria tricincta* **P** *Granuliterebra bathyrhappe* **Q** *Comitas ilariae* **R** *Cylichna modesta* **S** *Maoritomella vallata*.

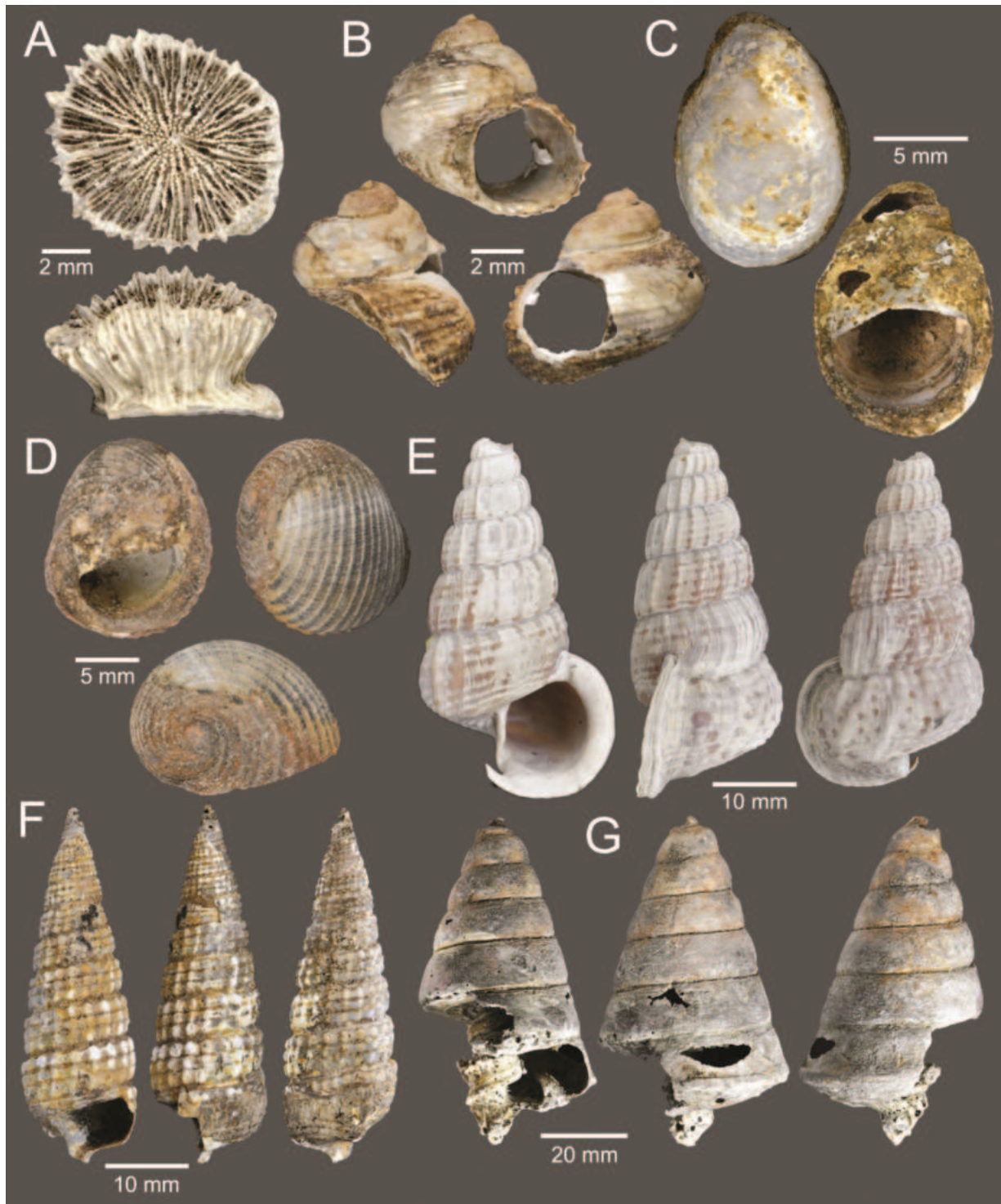


Figure 5. Coral and gastropods **A** *Oulangia* cf. *stokesiana* **B** *Homalopoma* cf. *sangarensis* **C** *Neripteron* *violaceum* **D** *Nerita* *articulata* **E** *Cerithidea* *obtusa* **F** *Pirenella* *incisa* **G** *Telescopium* *telescopium*.

Habitat. On firm mud and on trunks and stilt roots in mangrove forests as well as in fully marine and estuarine areas (Reid 2014).

Distribution. Bay of Bengal; Indo-West Pacific, from southern Vietnam to Java and East Borneo (Reid 2014). Records of fossils from the Late Pliocene in Central and West Java, Indonesia, and from the Holocene in Thailand (Robba et al. 2004; Dharma 2005).

Record in Thailand. Chanthaburi River, Gulf of Thailand and Andaman Sea (Nabhitabhata 2009; Wells et al. 2021).

Taxonomic remarks and comparisons. This species has a more thickened and flared aperture compared to two similar species, *Cerithidea anticipata* Iredale, 1929 and *C. reidi* Houbrick, 1986. These two species are also common in Sahul (New Guinea and Australia), whereas *C. obtusa* is present in Sunda (Reid 2014). See also comprehensive taxonomic remarks in Reid (2014).

***Pirenella* Gray, 1847**

***Pirenella incisa* (Hombron & Jacquinot, 1848)**

Figs 3I, 5F

Cerithium incisum Hombron & Jacquinot, 1848: 97, pl. 23, figs 8, 9. Type locality: Borneo.

Cerithidea (Cerithideopsilla) djadjariensis [non Martin]. Sri-aroon et al. 2004: table 1, fig. 2-7.

Cerithideopsilla djadjariensis [non Martin]. Lozouet 2008: 284, pl. 87, fig. 9; pl. 88, fig. 2.

Pirenella incisa. Reid and Ozawa 2016: 30–32, figs 1, 2g, h, 4i, 10, 11a. Zvonareva and Kantor 2016: 415, fig. 5a–d. BEDO 2017b: 28, with in-text fig. Wells et al. 2021: 126.

Referred material. CUF-NKNY-G10 (47 shells; Figs 3I, 5F).

Habitat. On damp mud in mangrove forests. Also found on open surface areas of intertidal mudflats and on muddy shores of shrimp ponds (Reid and Ozawa 2016; Zvonareva and Kantor 2016).

Distribution. East India; Indo-West Pacific, from southern China, the Philippines to West Sulawesi, and Flores Island (Reid and Ozawa 2016).

Record in Thailand. Gulf of Thailand and Andaman Sea (Wells et al. 2021).

Taxonomic remarks and comparisons. This species differs from the other two similar species, *Pirenella pupiformis* Ozawa & Reid, 2016 and *P. caiyingyai* (Qian, Fang & He, 2013), by the presence of an almost columnar appearance, a more oblique and more flared aperture with the projection of a lip next to a deep anterior canal, and three equal cords on each spire whorl with strong square nodules on axial ribs (Reid and Ozawa 2016). See comprehensive taxonomic remarks in Reid and Ozawa (2016).

***Telescopium* Montfort, 1810**

***Telescopium telescopium* (Linnaeus, 1758)**

Figs 3K, 5G

Trochus telescopium Linnaeus, 1758: 760. Type locality: unknown.

Telescopium telescopium. Tesch 1920: 58–59, pl. 132, fig. 191. Cernohorsky 1972: 61, pl. 13, fig. 6. Brandt 1974: 196, pl. 15, fig. 61. Tantanasiwong 1978: 7, fig. 69. Nateewathana et al. 1981: 57. Way and Purchon 1981: 315. Houbrick 1991: 291–304, figs 1–6. Wilson 1993: 133, pl. 15, fig. 21. Bosch et al. 1995: 56–57, fig. 186. Nateewathana 1995: 97–98, with in-text fig. Pout-

iers 1998b: 451, with in-text figs. Subba Rao and Dey 2000: 53. Swennen et al. 2001: 52, 111–112, with in-text fig., fig. 295. Hylleberg and Kilburn 2003: 38. Sri-aroon et al. 2004: table 1, fig. 3-3. Dharma 2005: 92, pl. 21, fig. 1; 308, pl. 119, fig. 4. Thach 2005: 45, pl. 9, figs 4, 7. Dey 2006: 31–32, figs 29–32. Ramakrishna et al. 2007: 48–49. Lozouet 2008: 284, pl. 87, figs 1, 3. Printrakoon et al. 2008: table 1. Kesavan et al. 2009: 382, with in-text fig. Nabhitabhata 2009: 97. Hamli et al. 2013: tables 2, 3, fig. 2e. Sanpanich and Duangdee 2013: 54. Dechruksa et al. 2014: fig. 2h. BEDO 2017b: 29, with in-text fig. Kantharajan et al. 2017: table 1, fig. 3-18. Okutani 2017: 797, pl. 63, fig. 11. Yang et al. 2017: 28, fig. 109. Tudu et al. 2018: table 1. Yadav et al. 2019: table 2, fig. 1o. Palanisamy et al. 2020: 2, fig. 1a–d. George et al. 2021: 1532, fig. 2a, b. Wells et al. 2021: 126.

Referred material. CUF-NKNY-G64 (2 shells; Figs 3K, 5G).

Habitat. On muddy floors of mangrove forests and intertidal mud flats (Poutiers 1998b; Okutani 2017).

Distribution. Indian Ocean; Indo-West Pacific, from Japan to India (Poutiers 1998b; Okutani 2017; Palanisamy et al. 2020). Records of fossils from the Miocene to Quaternary in Indonesia (Tesch 1920; Dharma 2005).

Record in Thailand. Gulf of Thailand and Andaman Sea (Wells et al. 2021).

Taxonomic remarks and comparisons. This species is recognised by its high conical spire with a broad, rather flat base, and a twisted columella with a strong and central spiral ridge (Houbrick 1991; Poutiers 1998b).

Subcohort Hypsogastropoda Ponder & Lindberg, 1997

Superfamily Naticoidea Guilding, 1834

Family Naticidae Guilding, 1834

***Eunaticina* Fischer, 1885**

***Eunaticina papilla* (Gmelin, 1791)**

Figs 3G, 6A

Nerita papilla Gmelin, 1791: 3675. Type locality: Tranquebar [Tharangambadi, Tamil Nadu, India].

Eunaticina papilla. Cernohorsky 1971: 201–202, fig. 69. Cernohorsky 1972: 102, pl. 27, fig. 5. Tantanasiwong 1978: 11, fig. 151. Nateewathana et al. 1981: 58. Way and Purchon 1981: 317. Majima 1989: 68–69, pl. 10, fig. 16, text-figs 15.36, 23.1a–d. Wilson 1993: 223, pl. 36, fig. 7. Bosch et al. 1995: 87, fig. 326. Swennen et al. 2001: 54, 122, fig. 378. Gemert 2003: 105. Hylleberg and Kilburn 2003: 56. Beu et al. 2004: 206, 208–211, fig. 22d–f, h. Robba et al. 2004: 75–76, pl. 9, fig. 7a, b. Dharma 2005: 176, pl. 63, fig. 25a–d; 342, pl. 136, fig. 12a, b. Ramakrishna et al. 2007: 9, 69–70. Robba et al. 2007: 91 (appendix). Hollmann 2008: 500, pl. 195, figs 1, 2. Nabhitabhata 2009: 123. Beu 2010: 152, fig. 21a. Torigoe and Inaba 2011: 55–56, pl. 2, fig. 17. Gopalakrishnan et al. 2012: 73. Öztürk and Bitlis 2013: 7, with in-text fig. Sanpanich and Duangdee 2013: 56. BEDO 2017b: 159, with in-text fig. Okutani 2017: 862, pl. 148, fig. 6. Yang et al. 2017: 52, fig. 215. Tudu et al. 2018: table 1. Albano et al. 2021: 12, fig. 5. Wells et al. 2021: 82.

Eunaticina papilla papilla. Thach 2005: 90, pl. 26, figs 3, 5.

Referred material. CUF-NKNY-G19 (5 shells; Figs 3G, 6A).

Habitat. Fine sandy bottoms in intertidal zones down to 30 m depth (Robba et al. 2004; Okutani 2017).

Distribution. Red Sea to Indian Ocean; Indo-West Pacific, from Japan to Australia and Fiji Islands (Robba et al. 2004; Okutani 2017), as well as the Israeli Mediterranean shelf (Albano et al. 2021). Several records of fossils during the Late Miocene to Holocene in Indonesia, Japan, Taiwan, and Thailand (Beu et al. 2004; Robba et al. 2004; Dharma 2005).

Record in Thailand. Gulf of Thailand and Andaman Sea (Wells et al. 2021).

Taxonomic remarks and comparisons. This species is recognised by a regularly oval shell with a small spire and a large body whorl with low and wide spiral cords, which are broader than their interspaces and crossed by prominent axial ridges (Öztürk and Bitlis 2013). See also comprehensive taxonomic remarks in Beu et al. (2004).

Natica Scopoli, 1777

Natica stellata Hedley, 1913

Figs 3D, 6B

Natica stellata Hedley, 1913: 299–300. Type locality: unknown. Cernohorsky 1972: 94–95, pl. 24, fig. 6. Wilson 1993: 217, pl. 36, fig. 24. Poutiers 1998b: 513, with in-text figs. Robba et al. 2004: 71, pl. 9, fig. 2a, b. Dharma 2005: 176, pl. 63, fig. 18. Robba et al. 2007: 91 (appendix). Hollmann 2008: 492, pl. 191, figs 9, 10a, b. Nabhitabhata 2009: 125. Torigoe and Inaba 2011: 76–77. Mukhopadhyay et al. 2013: 152–153, fig. 6. Sanpanich and Duangdee 2013: 57. Okutani 2017: 862, pl. 149, fig. 7. Wells et al. 2021: 83.

Natica (Natica) stellata. Cernohorsky 1971: 176–177, figs 6, 8–13.

Referred material. CUF-NKNY-G05 (126 shells; Figs 3D, 6B).

Habitat. Sandy gravel bottoms in sublittoral zones down to 20 m depth (Hollmann 2008; Okutani 2017).

Distribution. Indo-West Pacific, from Japan to Australia (Cernohorsky 1972; Wilson 1993; Okutani 2017). Probably present in the Indian Ocean (Poutiers 1998b). Records of fossils from the Holocene in central Thailand (Robba et al. 2003, 2004).

Record in Thailand. Gulf of Thailand and Andaman Sea (Wells et al. 2021).

Taxonomic remarks and comparisons. This species differs from its similar species, *Natica vitellus*, in having a parietal callus forming a tongue-shaped extension over the posterior part of the umbilicus (Cernohorsky 1971). See also comprehensive taxonomic remarks in Cernohorsky (1971).

Natica vitellus (Linnaeus, 1758)

Figs 3E, 6C

Nerita vitellus Linnaeus, 1758: 776. Type locality: Asiatic Ocean.

Natica vitellus. Tesch 1920: 70–71, pl. 132, fig. 207a, b. Cernohorsky 1972: 94, pl. 24, fig. 5. Tantanasiwong 1978: 11, fig. 141. Nateewathana et al. 1981: 58. Way and Purchon 1981: 317. Majima 1989: 74–76, pl. 10, figs 1–12, text-figs 4.1,

15.38. Wilson 1993: 217, pl. 36, fig. 28. Bosch et al. 1995: 87, fig. 322. Poutiers 1998b: 515, with in-text figs. Subba Rao and Dey 2000: 78. Swennen et al. 2001: 54, 121, fig. 371. Hylleberg and Kilburn 2003: 57. Robba et al. 2003: table 5. Robba et al. 2004: 71–73, pl. 9, fig. 3a, b. Dharma 2005: 176, pl. 63, fig. 17; 342, pl. 136, fig. 5a, b. Ramakrishna et al. 2007: 8, 67. Robba et al. 2007: 91 (appendix). Hollmann 2008: 492, pl. 191, fig. 7. Nabhitabhata 2009: 125. Torigoe and Inaba 2011: 69–70. Sanpanich and Duangdee 2013: 57. BEDO 2017b: 162, with in-text fig. Okutani 2017: 862, pl. 149, fig. 4. Yang et al. 2017: 56, fig. 230. Harzhauser et al. 2018: 7–8, pl. 1, figs 7–15. Tudu et al. 2018: table 1. Wells et al. 2021: 83. *Natica (Natica) vitellus*. Cernohorsky 1971: 173–174, 176, figs 2–5. Ladd 1982: 39, pl. 6, fig. 7. *Natica vitellus vitellus*. Thach 2005: 86, pl. 26, fig. 8.

Referred material. CUF-NKNY-G04 (5 shells; Figs 3E, 6C).

Habitat. Fine sandy or muddy bottoms in intertidal zones down to ~ 120 m depth (Robba et al. 2004); in clean coral-sand pockets and weedy-sand lagoons (Cernohorsky 1971).

Distribution. Persian Gulf to Indian Ocean; Indo-West Pacific, from Japan to Australia (Bosch et al. 1995; Poutiers 1998b; Okutani 2017). Several records of fossils from the Early Miocene to Holocene in India, Indonesia, Japan, Malaysia, Myanmar, the Philippines, Polynesia, Taiwan, Vanuatu, and Thailand (Ladd 1982; Robba et al. 2004; Dharma 2005).

Record in Thailand. Gulf of Thailand and Andaman Sea (Wells et al. 2021).

Taxonomic remarks and comparisons. This species differs from its similar species, *Natica stellata*, in lacking a tongue-shaped extension of a parietal callus over the posterior part of the umbilicus (Cernohorsky 1971). See also comprehensive taxonomic remarks in Cernohorsky (1971).

***Paratectonatica* Azuma, 1961**

***Paratectonatica tigrina* (Röding, 1798)**

Figs 3Q, 6D

Cochlis tigrina Röding, 1798: 147. Type locality: unknown.

Natica tigrina. Tantanasiwong 1978: 11, fig. 142. Nateewathana et al. 1981: 58. Dheeradilok et al. 1984: pl. 3, figs 9, 10. Wilson 1993: 217, pl. 36, fig. 10. Nateewathana 1995: 98, with in-text fig. Poutiers 1998b: 514, with in-text figs. Swennen et al. 2001: 54, 121, fig. 369. Hylleberg and Kilburn 2003: 57. Dharma 2005: 176, pl. 63, fig. 14. Ramakrishna et al. 2007: 8, 66–67, pl. 4, figs 45, 46. Nabhitabhata 2009: 125. Okutani 2017: 864, pl. 150, fig. 10. Yang et al. 2017: 56, fig. 229. Surakiatchai et al. 2018: table 5, pl. 1, fig. 6a, b.

Paratectonatica tigrina. Majima 1989: pl. 14, fig. 18. Robba et al. 2003: tables 2–5. Robba et al. 2004: 73, pl. 9, fig. 4a, b. Robba et al. 2007: 91 (appendix). Torigoe and Inaba 2011: 101–102, pl. 3, fig. 30. Kang et al. 2018: 357–358, 360, fig. 4.

Tectonatica tigrina. Thach 2005: 87, pl. 26, fig. 24.

Notocochlis tigrina. Gopalakrishnan et al. 2012: 73. Sanpanich and Duangdee 2013: 57. BEDO 2017b: 165, with in-text fig. Tudu et al. 2018: table 1. Yadav et al. 2019: table 2, fig. 1a. Wells et al. 2021: 84.

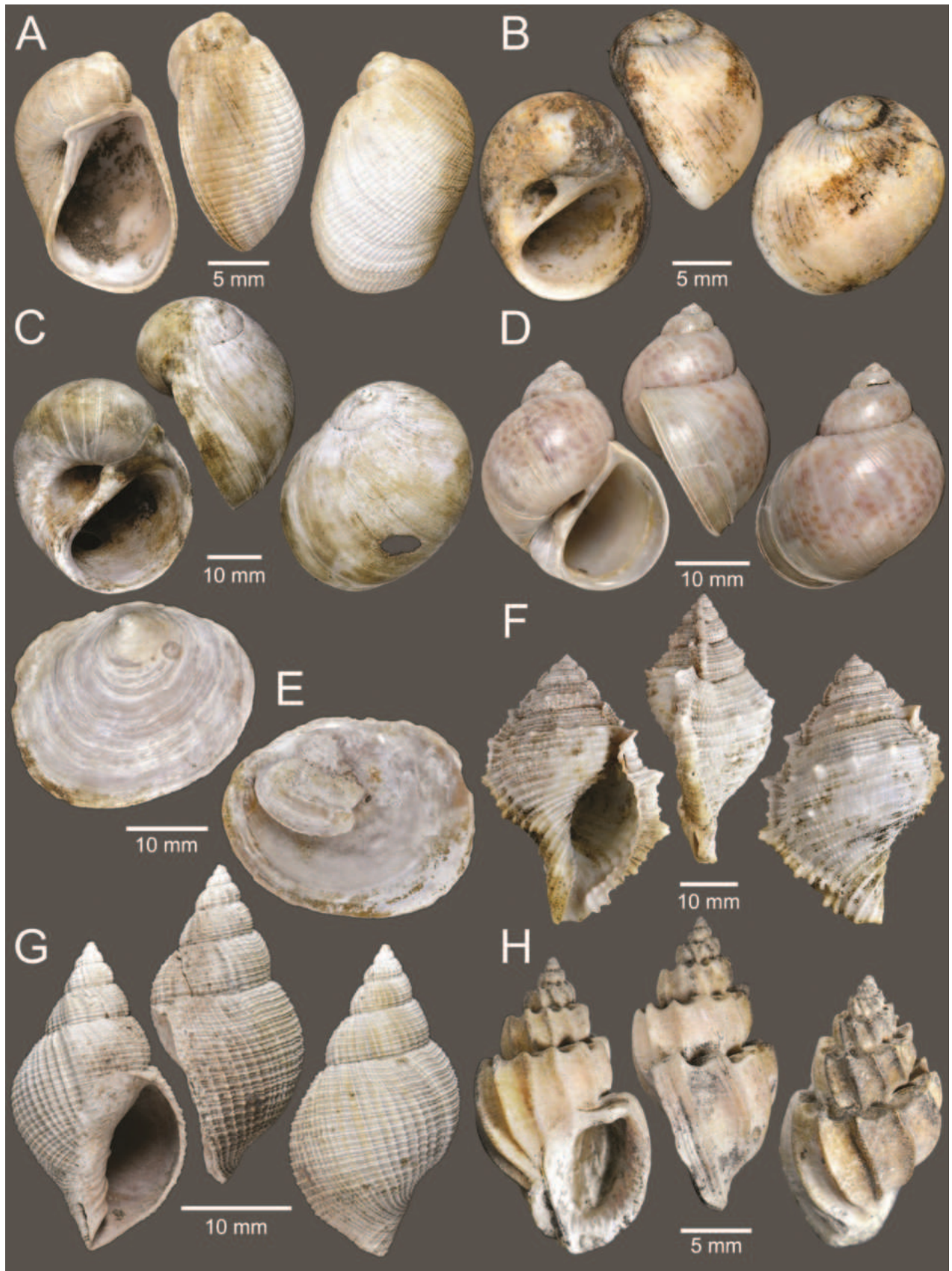


Figure 6. Gastropods **A** *Eunaticina papilla* **B** *Natica stellata* **C** *Natica vitellus* **D** *Paratectonatica tigrina* **E** *Ergaea walshi* **F** *Bufonaria rana* **G** *Merica elegans* **H** *Scalptia scalariformis*.

Referred material. CUF-NKNY-G03 (70 shells; Figs 3Q, 6D).

Habitat. Sandy mud in intertidal zones down to 30 m depth (Thach 2005; Okutani 2017).

Distribution. India (Yadav et al. 2019); Indo-West Pacific, from Japan to Australia (Wilson 1993; Poutiers 1998b; Okutani 2017). Records of fossils from the Late Miocene to Quaternary in Indonesia and from the Quaternary in Thailand (Robba et al. 2003, 2004; Surakiatchai et al. 2018).

Record in Thailand. Gulf of Thailand and Andaman Sea (Wells et al. 2021).

Taxonomic remarks and comparisons. This species is recognised by its tall-spired shell with deeply impressed sutures and spiral rows of reddish-brown spots on a white background (Poutiers 1998b; Robba et al. 2004).

Superorder Latrogastropoda Riedel, 2000

Superfamily Calyptraeoidea Lamarck, 1809

Family Calyptraeidae Lamarck, 1809

***Ergaea* H. Adams & A. Adams, 1854**

***Ergaea walshi* (Reeve, 1859)**

Figs 3H, 6E

Crepidula walshi Reeve, 1859: *Crepidula*, pl. 3, sp. 17. Type locality: Singapore; Ceylon [Sri Lanka]. Tantanasiriwong 1978: 9. Bosch et al. 1995: 69, fig. 230. Subba Rao and Dey 2000: 64. Swennen et al. 2001: 54, 117, text-fig. 344, fig. 344. Gemert 2003: 104. Robba et al. 2003: tables 3–5. Robba et al. 2004: 66–67, pl. 8, fig. 8a, b. Ramakrishna et al. 2007: 7, 55–56. Robba et al. 2007: 91 (appendix).

Ergaea walshi. Nateewathana et al. 1981: 57. Nabhitabhata 2009: 109. Low and Tan 2014: 11–13, fig. 1. BEDO 2017b: 117, with in-text fig. Tudu et al. 2018: table 1. Wells et al. 2021: 75.

Crepidula walshii [sic]. Way and Purchon 1981: 316.

Siphopatella walshi. Hylleberg and Kilburn 2003: 47. Sanpanich and Duangdee 2013: 55. Okutani 2017: 838, pl. 114, fig. 3. Yang et al. 2017: 32, fig. 117.

Crepidula (Siphopatella) walshi. Dharma 2005: 78, pl. 14, fig. 13a, b; 342, pl. 136, fig. 15a, b.

Crepidula (Ergaea) walshi. Thach 2005: 66, pl. 10, fig. 27.

Referred material. CUF-NKNY-G25 (10 shells; Figs 3H, 6E).

Habitat. Attached to the aperture of other shelled marine organisms, in intertidal zones down to 40 m depth (Robba et al. 2004; Thach 2005; Low and Tan 2014).

Distribution. Persian Gulf; Indo-West Pacific, from Japan to the Arafura Sea (Robba et al. 2004; Okutani 2017). Several records of fossils from the Late Miocene to Holocene in India, Indonesia, Japan, Taiwan, and Thailand (Robba et al. 2004; Dharma 2005).

Record in Thailand. Gulf of Thailand and Andaman Sea (Wells et al. 2021).

Taxonomic remarks and comparisons. This species is recognised by an irregularly subrectangular and flattened shell, with a small apex close to the posterior margin, and a shelf-like internal septum attached just inside the posterior margin (Robba et al. 2004). See also comprehensive taxonomic remarks in Low and Tan (2014).

Superfamily Tonnoidea Suter, 1913

Family Bursidae Thiele, 1925

***Bufonaria* Schumacher, 1817**

***Bufonaria rana* (Linnaeus, 1758)**

Figs 3N, 6F

Murex rana Linnaeus, 1758: 748. Type locality: Asiatic Ocean.

Bursa (Bufonaria) rana. Cernohorsky 1972: 119, pl. 32, fig. 8.

Bursa rana. Tantanasiwong 1978: 12, fig. 170. Nateewathana et al. 1981: 59.

Way and Purchon 1981: 317. Swennen et al. 2001: 55, 122, fig. 380.

Bufonaria rana. Wilson 1993: 226, pl. 43, fig. 1a, b. Aungtonya and Hylleberg 1998: 319. Poutiers 1998b: 551, with in-text figs. Subba Rao and Dey 2000: 92. Hylleberg and Kilburn 2003: 59. Robba et al. 2004: 76–77, pl. 9, fig. 9a, b. Dharma 2005: 194, pl. 72, fig. 1a–e; 352, pl. 141, fig. 7a–c. Ramakrishna et al. 2007: 10, 81, pl. 6, figs 69, 70. Robba et al. 2007: 91 (appendix). Beu 2008: 618, pl. 254, figs 6, 7a, b. Nabhitabhata 2009: 137. Sanpanich and Duangdee 2013: 58. BEDO 2017b: 112, with in-text fig. Okutani 2017: 867–868, pl. 154, fig. 5. Yang et al. 2017: 64, fig. 266. Harzhauser et al. 2018: 13–14, pl. 3, figs 6–9. Tudu et al. 2018: table 1. Yadav et al. 2019: table 2, fig. 1b. Wells et al. 2021: 89.

Bufonaria (Bufonaria) rana. Cossignani 1994: 33–35, with in-text figs. Bosch et al. 1995: 102, fig. 372. Gemert 2003: 105. Thach 2005: 96, pl. 28, fig. 8.

Referred material. CUF-NKNY-G06, G07 (18 shells; Figs 3N, 6F).

Habitat. Muddy or sandy bottoms at a depth from 20 to 100 m (Okutani 2017; Yang et al. 2017).

Distribution. Red Sea to Indian Ocean; Indo-West Pacific, from Japan to Australia (Robba et al. 2004; Okutani 2017; Yadav et al. 2019). Several records of fossils from the Miocene to Quaternary in Indonesia, Japan, the Philippines, and Taiwan (Robba et al. 2004; Dharma 2005; Harzhauser et al. 2018).

Record in Thailand. Gulf of Thailand and Andaman Sea (Wells et al. 2021).

Taxonomic remarks and comparisons. This species is recognised based on the descriptions and figures in Robba et al. (2004) and Harzhauser et al. (2018), specifically in having two prominent varices placed at either periphery, running vertically uninterrupted, or slightly staggered, from apex to base, and bearing three short spines.

Order Neogastropoda Wenz, 1938

Superfamily Volutoidea Rafinesque, 1815

Family Cancellariidae Forbes & Hanley, 1851

***Merica* H. Adams & A. Adams, 1854**

***Merica elegans* (Sowerby I, 1822)**

Figs 3L, 6G

Cancellaria elegans Sowerby I, 1822: *Cancellaria*, pl. 218, fig. 3. Type locality: unknown. Tantanasiwong 1978: 17. Nateewathana et al. 1981: 61. Robba et al. 2007: 51–52, fig. 19d, e; 93 (appendix).

Cancellaria asperella [sic]. Cernohorsky 1972: 179, pl. 50, fig. 3 right.
Merica elegans. Verhecken 1986: 40–41, fig. 9. Verhecken 1997: 307–308, fig. 36. Swennen et al. 2001: 57, 133, fig. 461. Hylleberg and Kilburn 2003: 100. Dharma 2005: 134, pl. 42, fig. 1. Thach 2005: 188, pl. 58, figs 6, 10. Hemmen 2007: 128–129, with in-text fig. Verhecken 2008: 818, pl. 704, fig. 5a, b. BEDO 2017b: 221, with in-text fig. Tudu et al. 2018: table 1. Wells et al. 2021: 121.

Referred material. CUF-NKNY-G18 (3 shells; Figs 3L, 6G).

Habitat. Sandy and muddy bottoms at a depth from 10 to 30 m (Robba et al. 2004; Thach 2005).

Distribution. Indo-West Pacific, from Japan to the Philippines. Records of fossils from the Miocene in Indonesia, and from the Quaternary in Japan (Robba et al. 2007).

Record in Thailand. Gulf of Thailand and Andaman Sea (Wells et al. 2021).

Taxonomic remarks and comparisons. This species differs from its similar species, *Merica asperella* (Lamarck, 1822), in having a slenderer and more fusiform shell with a narrower aperture and a sculptured shell with finer and more numerous ribs crossed by spiral ridges nearly of the same strength, showing a rectangular reticulated pattern (Robba et al. 2007).

***Scalptia* Jousseume, 1887**

***Scalptia scalariformis* (Lamarck, 1822)**

Figs 3J, 6H

Cancellaria scalariformis Lamarck, 1822: 115. Type locality: unknown.

Cancellaria (Trigonostoma) scalariformis. Tesch 1915: 39, pl. 79, fig. 81a, b.

Trigonostoma scalariformis. Cernohorsky 1972: 180, pl. 50, fig. 2, 2a. Garrard 1975: 27–29, figs 4 (3, 4). Way and Purchon 1981: 320. Wilson 1994: 178, pl. 37, fig. 7a, b.

Scalptia scalariformis. Verhecken 1986: 53–55, figs 28–35. Swennen et al. 2001: 57, 133, fig. 462. Hylleberg and Kilburn 2003: 101. Robba et al. 2004: 129–130, pl. 17, fig. 6. Dharma 2005: 134, pl. 42, fig. 12a, b. Hemmen 2007: 277–278, with in-text figs. Robba et al. 2007: 93 (appendix). Okutani 2017: 1054, pl. 344, fig. 4. Yang et al. 2017: 102, fig. 415. Tudu et al. 2018: table 1. Wells et al. 2021: 121. Chan and Lau 2022: 1–2, figs 1–3.

Scalptia (Scalptia) scalariformis. Thach 2005: 188, pl. 58, figs 25, 27, 29.

Referred material. CUF-NKNY-G64 (1 shell; Figs 3J, 6H).

Habitat. Sand and muddy bottoms at a depth from 20 to 40 m in sublittoral zones (Thach 2005; Okutani 2017; Yang et al. 2017).

Distribution. Indian Ocean; Indo-West Pacific, from Japan to Australia (Robba et al. 2004; Okutani 2017). Several records of fossils from the Pliocene to Holocene in the Indo-Pacific area, including Indonesia and Thailand (Robba et al. 2004).

Record in Thailand. Gulf of Thailand (Wells et al. 2021).

Taxonomic remarks and comparisons. This species differs from its similar species, *Scalptia bicolor* (Hinds, 1843), by having a higher and narrower body whorl and a less widely open umbilicus (Robba et al. 2007).

Superfamily Buccinoidea Rafinesque, 1815

Family Buccinidae Rafinesque, 1815

***Pseudoneptunea* Kobelt, 1882**

***Pseudoneptunea varicosa* (Röding, 1798)**

Figs 4K, 7A

Neptunea varicosa Röding, 1798: 116. Type locality: unknown.

Siphonalia (*Pseudoneptunea*) aff. *varicosa*. Tesch 1915: 53, pl. 80, fig. 114a, b.

Pseudoneptunea varicosa. Cernohorsky 1975: 217–218, figs 10–12. Way and Purchon 1981: 318. Swennen et al. 2001: 56, 128, fig. 428. Robba et al. 2004: 106–107, pl. 14, fig. 5a, b. Dharma 2005: 100, pl. 25, fig. 7a, b; 312, pl. 121, fig. 9a, b. Thach 2005: 135, pl. 39, figs 12, 15. Robba et al. 2007: 93 (appendix). Nabhitabhata 2009: 148. Sanpanich and Duangdee 2013: 63. Wells et al. 2021: 95.

Referred material. CUF-NKNY-G13, G16, G17 (25 shells; Figs 4K, 7A).

Habitat. Shallow water at a depth from 10 to 15 m (Thach 2005).

Distribution. Indo-West Pacific, from Vietnam to Indonesia (Robba et al. 2004; Dharma 2005; Thach 2005). Records of fossils from the Pliocene and Quaternary in Indonesia and from the Holocene in Thailand (Robba et al. 2004).

Record in Thailand. Gulf of Thailand and Andaman Sea (Wells et al. 2021).

Taxonomic remarks and comparisons. This species is recognised based on the descriptions and figures in Cernohorsky (1975) and Robba et al. (2004), specifically in having subangulate whorls and a sculpture of crisp main spirals with an occasional intermediate spiral thread.

Family Melongenidae Gill, 1871

***Brunneifusus* Dekkers, 2018**

***Brunneifusus ternatanus* (Gmelin, 1791)**

Figs 4A, 7B

Murex ternatanus Gmelin, 1791: 3554. Type locality: Ternate Island, North Maluku, Indonesia.

Pugilina ternatana. Tantanasiriwong 1978: 15. Nateewathana et al. 1981: 60. Poutiers 1998b: 586, with in-text figs.

Hemifusus ternatanus. Yokoyama 1927: 393. Way and Purchon 1981: 318. Swennen et al. 2001: 56, 130, fig. 445. Gemert 2003: 106, with in-text fig. Hylleberg and Kilburn 2003: 88. Robba et al. 2004: 122–123, pl. 16, fig. 7a, b. Dharma 2005: 108, pl. 29, fig. 2a, b; 316, pl. 123, fig. 7a, b. Robba et al. 2007: 93 (appendix). Nabhitabhata 2009: 162. Sanpanich and Duangdee 2013: 61. BEDO 2017b: 288, with in-text fig. Tudu et al. 2018: table 1.

Brunneifusus ternatanus. Dekkers 2018: 41–42, pl. 2, figs 5, 6. Alf and Thach 2021: pl. 1, figs 1–9, pl. 2, figs 1–3. Wells et al. 2021: 97.

Referred material. CUF-NKNY-G21, G22 (71 shells; Figs 4A, 7B).

Habitat. Mud and muddy sand bottoms from the low tide mark to ~ 10–50 m depth (Poutiers 1998b; Swennen et al. 2001; Dekkers 2018).

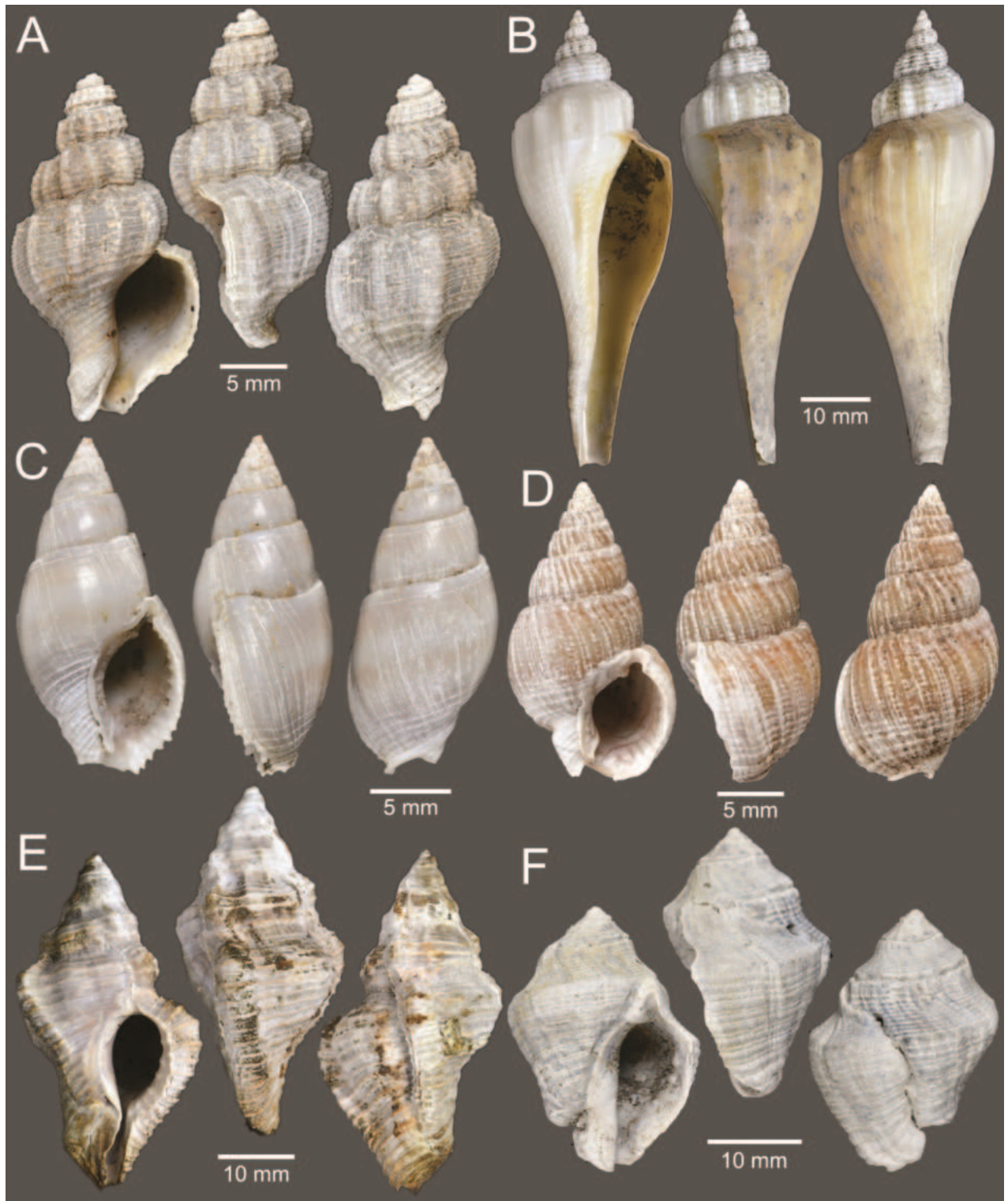


Figure 7. Gastropods **A** *Pseudoneptunea varicosa* **B** *Brunneifusus ternatanus* **C** *Nassarius micans* **D** *Nassarius siquijorensis* **E** *Chicoreus capucinus* **F** *Indothis gradata*.

Distribution. Eastern Indian Ocean; Indo-West Pacific, from Taiwan to Indonesia and the Philippines (Poutiers 1998b; Robba et al. 2004). Records of fossils from the Pliocene and Quaternary in Indonesia, Japan, and Taiwan (Robba et al. 2004; Dharma 2005).

Record in Thailand. Gulf of Thailand and Andaman Sea (Wells et al. 2021).

Taxonomic remarks and comparisons. This species is the sole member of the genus *Brunneifusus*, characterised by a determinate outer lip, compared to the indeterminate growth of the outer lip in *Hemifusus* Swainson, 1840 (Alf and Thach 2021). See also comprehensive taxonomic remarks in Alf and Thach (2021).

Family Nassariidae Iredale, 1916

***Nassarius* Duméril, 1805**

***Nassarius micans* (A. Adams, 1852)**

Figs 30, 7C

Nassa micans A. Adams, 1852: 106. Type locality: Cagayan, Misamis, Mindanao. *Nassarius (Zeuxis) micans*. Cernohorsky 1984: 147–148, pl. 29, figs 8–11. Robba et al. 2003: table 5. Robba et al. 2004: 120, pl. 16, fig. 4a, b. Dharma 2005: 106, pl. 28, fig. 16a, b. Robba et al. 2007: 93 (appendix). Okutani 2017: 914, pl. 202, fig. 11

Nassarius micans. Gopalakrishnan et al. 2012: 77. Wells et al. 2021: 99.

Referred material. CUF-NKNY-G27 (53 shells; Figs 30, 7C).

Habitat. Sandy bottoms in subtidal zones down to 50 m depth (Robba et al. 2004; Okutani 2017).

Distribution. Gulf of Oman to India; Indo-West Pacific, from Japan to Papua New Guinea (Cernohorsky 1984; Robba et al. 2004; Okutani 2017). Records of fossils from the Holocene in Thailand (Robba et al. 2004).

Record in Thailand. Gulf of Thailand (Wells et al. 2021).

Taxonomic remarks and comparisons. This species differs from its similar species, *Nassarius comptus* (A. Adams, 1852), by having a longer body whorl with narrowly subcanaliculate sutures, a more prominent varix, and a narrower and more elongate aperture (Cernohorsky 1984). See also comprehensive taxonomic remarks in Cernohorsky (1984).

***Nassarius siquijorensis* (A. Adams, 1852)**

Figs 3P, 7D

Nassa siquijorensis A. Adams, 1852: 97. Type locality: Island of Siquijor, Philippines.

Nassa (Zeuxis) siquijorensis. Tesch 1915: 59, pl. 81, figs 128a, b, 129a, b.

Nassarius (Zeuxis) siquijorensis. Cernohorsky 1978: 88, pl. 27, fig. 8. Cernohorsky 1984: 134–136, pl. 25, figs 12–14, pl. 26, figs 1–5. Robba et al. 2003: table 5. Robba et al. 2004: 120–121, pl. 16, fig. 5a, b. Dharma 2005: 106, pl. 28, fig. 14a–c. Robba et al. 2007: 93 (appendix).

Nassarius siquijorensis. Nobuhara 1993: fig. 8-1a, 8-1b. Swennen et al. 2001: 56, 130, fig. 442. Hylleberg and Kilburn 2003: 87. Kool 2007: figs 17–20. Martin 2008: 120, pl. 355, fig. 13; 128, pl. 359, fig. 13. Surakiatchai et al. 2018: table 5, pl. 1, fig. 9a, b. Wells et al. 2021: 99.

Zeuxis siquijorensis. Thach 2005: 148, pl. 44, fig. 25.

Nassarius siquijorensis [sic]. Yang et al. 2017: 90, fig. 371.

Referred material. CUF-NKNY-G01 (10 shells; Figs 3P, 7D).

Habitat. Sandy and muddy bottoms from subtidal zones to 450 m depth (Cernohorsky 1984; Thach 2005; Yang et al. 2017).

Distribution. Red Sea to India; Indo-West Pacific, from Japan to Indonesia and New Caledonia (Cernohorsky 1984; Dharma 2005; Yang et al. 2017). Records of fossils from the Pliocene in Indonesia and from the Holocene in Thailand (Cernohorsky 1984; Surakiatchai et al. 2018).

Record in Thailand. Gulf of Thailand and Andaman Sea (Wells et al. 2021).

Taxonomic remarks and comparisons. This species differs from its similar species, *Nassarius castus* (Gould, 1850), in having a more tapering spire, canaliculate sutures, and considerably more numerous axial ribs (Cernohorsky 1984). See also comprehensive taxonomic remarks in Cernohorsky (1984) and Kool (2007).

Superfamily Muricoidea Rafinesque, 1815

Family Muricidae Rafinesque, 1815

***Chicoreus* Montfort, 1810**

***Chicoreus capucinus* (Lamarck, 1822)**

Figs 4E, 7E

Murex capucinus Lamarck, 1822: 164. Type locality: unknown.

Naquetia capucina. Tantanasiriwong 1978: 13. Nateewathana et al. 1981: 59. Way and Purchon 1981: 318. Bussarawit 1991: 31.

Chicoreus (Rhizophorimurex) capucinus. Houart 1992: 106–109, fig. 217. Tan 2000: 504. Dharma 2005: 164, pl. 57, fig. 20; 336, pl. 133, fig. 9a–c. Thach 2005: 114, pl. 36, fig. 2. Merle et al. 2011: 99, text-fig. 39.

Chicoreus capucinus. Wilson 1994: 27, pl. 3, fig. 12a, b. Middelfart 1997: 358, pl. 2, fig. 7. Hylleberg and Kilburn 2003: 69. Sri-aroon et al. 2005: tables 2, 3, 5, 6. Houart 2008: 154, pl. 372, fig. 1. Printrakoon et al. 2008: table 1. Nabhitabhata 2009: 141. BEDO 2017b: 300, with in-text fig. Sanpanich and Duangdee 2013: 62. Dechruksa et al. 2014: fig. 4d. Wells et al. 2021: 113.

Chicoreus (Naquetia) capucinus. Subba Rao and Dey 2000: 100.

Chicoreus copucinus [sic]. Sri-aroon et al. 2004: table 1.

Referred material. CUF-NKNY-G11, G12 (30 shells; Figs 4E, 7E).

Habitat. Muddy sand and rocks in mangrove forests (Thach 2005).

Distribution. Indo-West Pacific, from the Philippines to Australia to Fiji Islands (Houart 1992). Records of fossils from the Middle Miocene to Late Pliocene in Indonesia (Dharma 2005).

Record in Thailand. Gulf of Thailand and Andaman Sea (Wells et al. 2021).

Taxonomic remarks and comparisons. This species is recognised based on the descriptions and figures in Houart (1992) and Merle et al. (2011), specifically in having a rounded last whorl usually associated with three spineless varices, each with a short and webbed expansion on adapical section, an aperture with a characteristically small callus with straight, adherent columellar lip, and a broad siphonal canal. See also comprehensive taxonomic remarks in Houart (1992).

***Indothais* Claremont et al., 2013**

***Indothais gradata* (Jonas, 1846)**

Figs 4F, 7F

Purpura gradata Jonas, 1846: 14–15. Type locality: Indian Ocean, near Singapore.
Thais gradata. Bussarawit 1991: 33. Middelfart 1997: 367–368, pl. 4, fig. 1. Tan 2000: 499. Hylleberg and Kilburn 2003: 76. Dharma 2005: 170, pl. 60, fig. 11a, b; 340, pl. 135, fig. 1a–e. Printrakoon et al. 2008: table 1. Yang et al. 2017: 76, fig. 316.
Stramonita gradata. Wilson 1994: 47, pl. 4, fig. 5a, b. Thach 2005: 128, pl. 37, figs 33, 37.
Indothais gradata. Okutani 2017: 963, pl. 255, fig. 9. Wells et al. 2021: 114.

Referred material. CUF-NKNY-G29 (1 shell; Figs 4F, 7F).

Habitat. Rocky bottom at a depth from 1 to 5 m (Thach 2005; Okutani 2017).

Distribution. Indo-West Pacific, from Japan to Australia (Okutani 2017; Yang et al. 2017). Records of fossils from the Middle to Late Pliocene in Indonesia (Dharma 2005).

Record in Thailand. Andaman Sea (Wells et al. 2021).

Taxonomic remarks and comparisons. This species is recognised based on the descriptions and figures in Middelfart (1997), specifically in having an erect and crenulate outer lip, which has a pronounced indentation in the subsutural ramp area, and an aperture with four denticles with proceeding lirae present inside.

***Indothais lacera* (Born, 1778)**

Figs 4C, 8A

Murex lacerus Born, 1778: 107–108. Type locality: unknown.

Cymia lacera. Bussarawit 1991: 32. Poutiers 1998b: 561, with in-text figs. Thach 2005: 123, pl. 36, fig. 1.

Thais lacera. Bosch et al. 1995: 123, fig. 491. Middelfart 1997: 369, pl. 4, fig. 4. Subba Rao and Dey 2000: 113. Tan 2000: 499. Swennen et al. 2001: 56, 127, fig. 422. Hylleberg and Kilburn 2003: 76–77. Robba et al. 2003: table 2. Robba et al. 2004: 102, pl. 13, fig. 6a, b. Dharma 2005: 170, pl. 60, fig. 12a–c; 338, pl. 134, fig. 15a–h. Dey 2006: 40–41, figs 45, 46. Ramakrishna et al. 2007: 11, 93, pl. 7, figs 79, 80. Robba et al. 2007: 92 (appendix). Nolf 2009: 9–10, figs 1–14. Kumar et al. 2017: 1101, fig. 1a, b.

Cuma lacera. Nabhitabhata 2009: 143. Yang et al. 2017: 78, fig. 324.

Indothais lacera. Sanpanich and Duangdee 2013: 63. BEDO 2017b: 305, with in-text fig. Kantharajan et al. 2017: table 1, fig. 3-11. Tudu et al. 2018: table 1. Wells et al. 2021: 114.

Referred material. CUF-NKNY-G08 (106 shells; Figs 4C, 8A).

Habitat. Mangrove forests (Kantharajan et al. 2017) and rocky bottom at a depth of 1–25 m (Thach 2005).

Distribution. South Africa to India; Indo-West Pacific, from Japan to New Caledonia (Poutiers 1998b; Robba et al. 2004; Kantharajan et al. 2017; Yang et al. 2017) as well as from western Mediterranean Sea (Nolf 2009). Records of

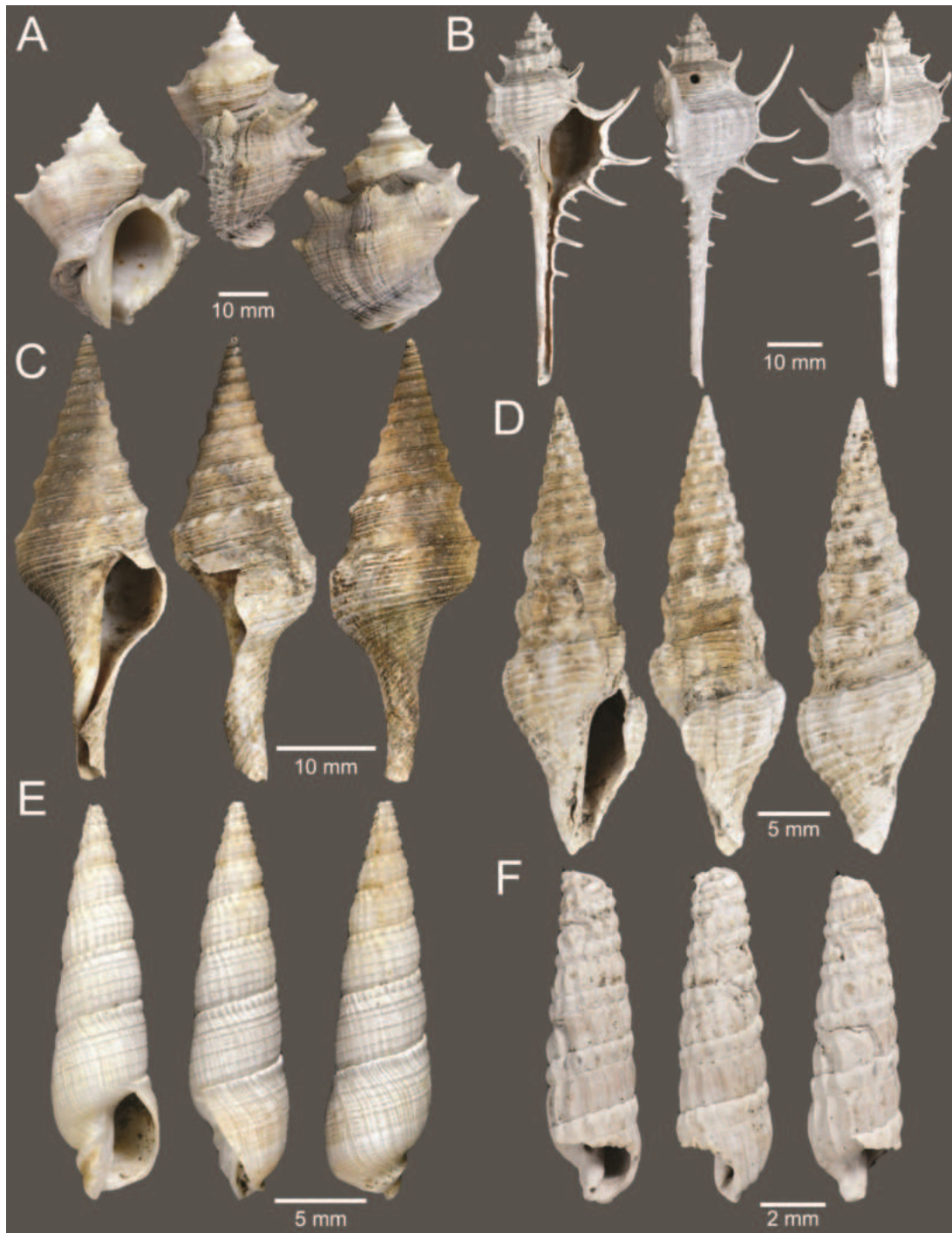


Figure 8. Gastropods **A** *Indothis lacera* **B** *Murex trapa* **C** *Turricula javana* **D** *Inquisitor vulpionis* **E** *Pristiterebra miranda* **F** *Granuliterebra bathyrhaphe*.

fossils from the Middle Miocene to Quaternary in Indonesia and from the Holocene in Thailand (Robba et al. 2004; Dharma 2005).

Record in Thailand. Gulf of Thailand and Andaman Sea (Wells et al. 2021).

Taxonomic remarks and comparisons. This species is recognised based on the descriptions and figures in Middlefart (1997) and Poutiers (1998b), specifically in having a body whorl bearing one to two spiral ridges, in which the prominent one bears eight spines, and an elaborate crenulate outer lip with a strong incision where the spiral ridge(s) and the anal sulcus are positioned.

Murex Linnaeus, 1758

Murex trapa Röding, 1798

Figs 4B, 8B

Murex trapa Röding, 1798: 145. Type locality: Tranquebar, India. Tantanasiwong 1978: 13, fig. 174. Nateewathana et al. 1981: 59. Way and Purchon 1981: 318. Ponder and Vokes 1988: 41–45, figs 17–19, 67g, h, 71b, c, 73d, 83g, h. Bussarawit 1991: 31. Middelfart 1997: 352, pl. 1, fig. 1. Poutiers 1998b: 565, with in-text figs. Subba Rao and Dey 2000: 102. Tan 2000: 503. Swennen et al. 2001: 55, 126, fig. 410. Hylleberg and Kilburn 2003: 72–73. Robba et al. 2003: table 5. Robba et al. 2004: 96–97, pl. 12, fig. 9a, b. Dharma 2005: 158, pl. 54, fig. 4a, b; 334, pl. 132, fig. 3a–c. Ramakrishna et al. 2007: 10, 85–86. Robba et al. 2007: 92 (appendix). Houart 2008: 136, pl. 636, fig. 2. Nabhitabhata 2009: 147. BEDO 2017b: 312, with in-text fig. Yang et al. 2017: 70, fig. 288. Surakiatchai et al. 2018: table 5, pl. 1, fig. 7a, b. Tudu et al. 2018: table 1. Wells et al. 2021: 116.

Murex cf. trapa. Aungtonya and Hylleberg 1998: 319.

Murex (Murex) trapa. Gemert 2003: 105. Thach 2005: 119, pl. 34, fig. 9. Merle et al. 2011: 59, text-fig. 27e; pl. 4, fig. 7; pl. 5, figs 8–10. Gopalakrishnan et al. 2012: 77. Sanpanich and Duangdee 2013: 63. Okutani 2017: 947, pl. 238, fig. 6.

Referred material. CUF-NKNY-G09 (33 shells; Figs 4B, 8B).

Habitat. Fine sand and muddy sand bottoms at a depth of 5–60 m (Swennen et al. 2001; Robba et al. 2004).

Distribution. Indian Ocean; Indo-West Pacific, from Japan to Fiji Islands (Dharma 2005; Okutani 2017). Records of fossils from the Middle Miocene to Holocene in Indonesia, Malaysia, the Philippines, Taiwan, and Thailand (Ponder and Vokes 1988; Robba et al. 2004; Dharma 2005; Surakiatchai et al. 2018).

Record in Thailand. Gulf of Thailand and Andaman Sea (Wells et al. 2021).

Taxonomic remarks and comparisons. This species differs from other related species in having a higher spire, angulated whorls, and shorter spines (Ponder and Vokes 1988). See also comprehensive taxonomic remarks in Ponder and Vokes (1988).

Superfamily Conoidea Fleming, 1822

Family Borsoniidae Bellardi, 1875

Maoritomella Powell, 1942

Maoritomella vallata (Gould, 1860)

Figs 4S, 9A

Drillia vallata Gould, 1860: 336. Type locality: Hong Kong. Johnson 1964: 164, pl. 7, fig. 6.

Asthenotoma vallata. Yen 1944: 575, pl. 51, figs 6, 7.

Maoritomella vallata. Robba et al. 2003: table 5. Robba et al. 2004: 134–135, pl. 18, fig. 5a, b. Robba et al. 2007: 94 (appendix). Wells et al. 2021: 100.

Referred material. CUF-NKNY-G30 (5 shells; Figs 4S, 9A).

Habitat. Probably present in shallow sublittoral areas (Robba et al. 2004).

Distribution. Indo-West Pacific. Records of fossils from the Holocene in Thailand (Robba et al. 2004).

Record in Thailand. Gulf of Thailand (Wells et al. 2021).

Taxonomic remarks and comparisons. This species is recognised based on the descriptions and figures in Yen (1944), Johnson (1964), and Robba et al. (2004), specifically in having a high-spired and claviform shell, with the sculpture of one rather strong and peripheral spiral cord, a weaker one abapical to the spiral cord, and one or two spiral threads on the shoulder slope, resulting in a total of 12–14 spirals occurring along the body whorl. This species is poorly known and has been assigned to *Maoritomella* due to a blunt, smooth, and paucispiral protoconch (1.5 whorls in this species), which is the diagnostic character of the genus (Powell 1942).

Family Clathurellidae H. Adams & A. Adams, 1858

***Pseudoetrema* Oyama, 1953**

***Pseudoetrema fortilirata* (Smith, 1879)**

Figs 4M, 9B

Drillia fortilirata Smith, 1879b: 194, pl. 19, fig. 22. Type locality: Station 14, east of Goto Islands, 32°48'N, 129°6'E; 47 fathoms, and station 21, between south-western extremity of Nippon and the island of Shikoku, 33°45'N, 132°30'E, 30 fathoms. Yokoyama 1927: 393, 410, pl. 46, fig. 20.

Pseudoetrema fortilirata. Oyama 1953: 154. Robba et al. 2004: 141, pl. 19, fig. 6. Robba et al. 2007: 94 (appendix). Okutani 2017: 1017, pl. 311, fig. 7. Wells et al. 2021: 101.

Referred material. CUF-NKNY-G38 (5 shells; Figs 4M, 9B).

Habitat. Sand and sandy mud in sublittoral areas to 50 m depth (Robba et al. 2004; Okutani 2017).

Distribution. Japan and Thailand. Records of fossils from the Pliocene to Holocene in Japan, Taiwan, and Thailand (Robba et al. 2004).

Record in Thailand. Gulf of Thailand (Wells et al. 2021).

Taxonomic remarks and comparisons. This species is recognised based on the descriptions and figures in Smith (1879b), Yokoyama (1927), and Robba et al. (2004), specifically in having a high-spired, claviform shell with the sculpture of nine broad and low collabral ribs fading away shortly before the subsutural cord and overriding spirals, three closely set spiral cords: adapical, peripheral, and abapical cords, and a weaker more adapical one on the penultimate whorl, resulting in a total of 14 spirals occurring along the body whorl. This species is the type species of *Pseudoetrema* (Oyama 1953).

Family Clavatulidae Gray, 1853

***Turricula* Schumacher, 1817**

***Turricula javana* (Linnaeus, 1767)**

Figs 4I, 8C

Murex javanus Linnaeus, 1767: 1221. Type locality: Java.

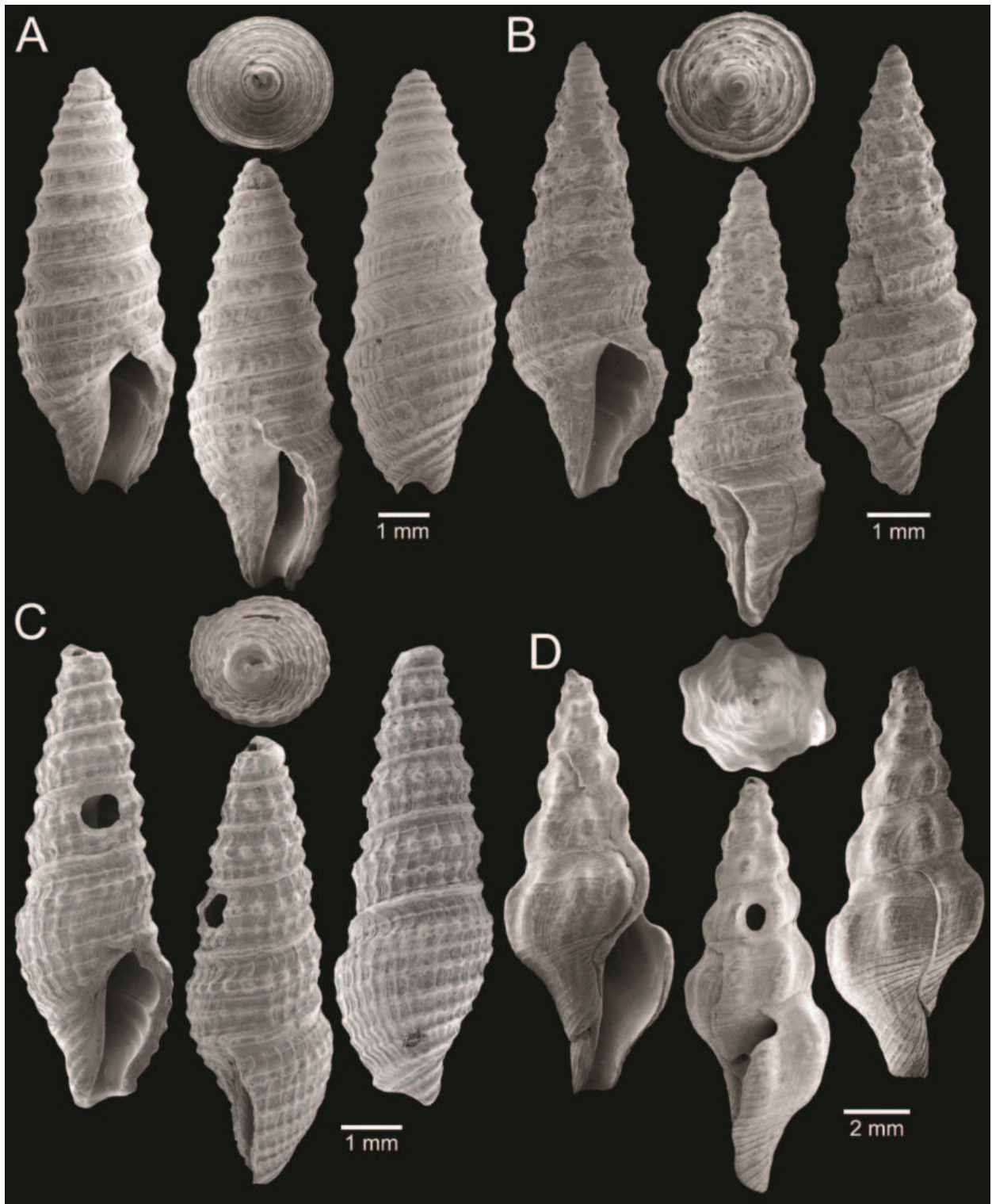


Figure 9. Gastropods **A** *Maoritomella vallata* **B** *Pseudoetrema fortilirata* **C** *Paradrillia melvilli* **D** *Comitas ilariae*.

Turricula (Vulpecula) javana. Tesch 1915: 48–49, pl. 80, fig. 104a, b.

Turricula javana. Powell 1969: 235–237, pl. 192, figs 10, 11; pl. 201, fig. 11. Tantana-siriwong 1978: 17. Nateewathana et al. 1981: 61. Way and Purchon 1981: 320. Poutiers 1998b: 630, with in-text figs. Swennen et al. 2001: 57, 133, fig. 463. Hylleberg and Kilburn 2003: 104. Robba et al. 2003: tables 3, 5. Robba et al. 2004: 136, pl. 18, fig. 8a, b. Dharma 2005: 130, pl. 40, fig. 8a, b. Thach 2005: 214, pl. 59,

fig. 16; pl. 60, fig. 24. Ramakrishna et al. 2007: 15, 133, 134. Robba et al. 2007: 93 (appendix). Nabhitabhata 2009: 196. Sanpanich and Duangdee 2013: 60. BEDO 2017b: 354, with in-text fig. Yang et al. 2017: 114, fig. 472. Surakiatchai et al. 2018: table 5, pl. 1, fig. 11a, b. Tudu et al. 2018: table 1. Wells et al. 2021: 101.

Referred material. CUF-NKNY-G15, G20 (53 shells; Figs 4I, 8C).

Habitat. Intertidal sand and rocks and muddy bottoms at a depth from 20 to 80 m (Robba et al. 2004; Thach 2005).

Distribution. Indian Ocean; Indo-West Pacific, from Japan to Australia (Robba et al. 2004; Yang et al. 2017). Records of fossils from the Late Miocene to Holocene in India, Indonesia, and Thailand (Robba et al. 2004; Surakiatchai et al. 2018).

Record in Thailand. Gulf of Thailand and Andaman Sea (Wells et al. 2021).

Taxonomic remarks and comparisons. This species is recognised based on the descriptions and figures in Powell (1969) and Robba et al. (2004), specifically in having an elongate-fusiform shell with the sculpture of oblique nodes on the peripheral angulation and finer spiral cords over the shoulder slope as well as a twin cord forming a weak subsutural margin. See also comprehensive taxonomic remarks in Powell (1969).

Family Horaiclavidae Bouchet et al., 2011

***Paradrillia* Makiyama, 1940**

***Paradrillia melvilli* Powell, 1969**

Figs 4N, 9C

Paradrillia melvilli Powell, 1969: 314–315, pl. 242, fig. 2; pl. 245, figs 1, 2. Type locality: Persian Gulf. Robba et al. 2004: 137, 139, pl. 19, fig. 2. Robba et al. 2007: 95 (appendix). Wells et al. 2021: 107.

Referred material. CUF-NKNY-G52 (7 shells; Figs 4N, 9C).

Habitat. Sublittoral and upper bathyal zones (Robba et al. 2004).

Distribution. Persian Gulf and Indian Ocean; Gulf of Thailand. Records of fossils from the Holocene in Thailand (Robba et al. 2004).

Record in Thailand. Gulf of Thailand (Wells et al. 2021).

Taxonomic remarks and comparisons. This species is recognised based on the descriptions and figures in Powell (1969) and Robba et al. (2004), specifically in having a light built claviform shell with a medially situated blunt peripheral keel bearing rather weak cog-like axial nodes, approximately 18 or 19 per whorl.

Family Pseudomelatomidae Morrison, 1966

***Inquisitor* Hedley, 1918**

***Inquisitor vulpionis* Kuroda & Oyama, 1971**

Figs 4H, 8D

Inquisitor vulpionis Kuroda & Oyama in Kuroda et al., 1971: 215, pl. 56, fig. 4; pl. 110, fig. 15. Type locality: Sagami Bay, Japan. Robba et al. 2004: 133, pl. 18, fig. 2a–c. Robba et al. 2007: 93 (appendix). Wells et al. 2021: 108.

Referred material. CUF-NKNY-G28 (1 shell; Figs 4H, 8D).

Habitat. Sandy bottoms at a depth from 10 to 100 m (Robba et al. 2004).

Distribution. Japan and the Philippines. Records of fossils from the Holocene in Thailand (Robba et al. 2004).

Record in Thailand. Gulf of Thailand (Wells et al. 2021).

Taxonomic remarks and comparisons. This species is recognised based on the descriptions and figures in Robba et al. (2004), specifically in having a claviform shell with the sculpture of nine collabral ribs resulting in a nodose appearance at the periphery and gradually fading away on the shoulder slope as well as the very faint spiral sculpture all over the shell except for the base where more prominent cords are developed.

***Comitas* Finlay, 1926**

***Comitas ilariae* Bozzetti, 1991**

Figs 4Q, 9D

Comitas ilariae Bozzetti, 1991: 26–28, figs 1–3. Type locality: island of Bohol, central Philippines. Olivera and Sysoev 2008: 786, pl. 688, figs 9, 10.

Referred material. CUF-NKNY-G55 (1 shell; Figs 4Q, 9D).

Habitat. Sandy bottoms at a depth from 100 to 150 m (Bozzetti 1991).

Distribution. Known only from the type locality (Bozzetti 1991).

Record in Thailand. New record in Thailand from this study.

Taxonomic remarks and comparisons. This species is recognised based on the descriptions and figures in Bozzetti (1991) and Olivera and Sysoev (2008), specifically in having a slight, fusiform, and high-spired shell with the axial sculpture made of 7–9 very pronounced, long, and thick tubercles positioned obliquely on each whorl as well as numerous dense spiral cords.

Family Terebridae Mörch, 1852

***Duplicaria* Dall, 1908**

***Duplicaria tricineta* (Smith, 1877)**

Figs 4O, 10A

Terebra tricineta Smith, 1877: 225. Type locality: Persian Gulf. Bratcher and Cernohorsky 1987: 76, pl. 17, fig. 58a, b. Wilson 1994: 229, with in-text fig. Hylleberg and Kilburn 2003: 106. Robba et al. 2004: 157, pl. 21, fig. 8. Robba et al. 2007: 95 (appendix).

Granuliterebra tricineta. BEDO 2017b: 360, with in-text fig. Okutani 2017: 1050, pl. 339, fig. 14. Tudu et al. 2018: table 1. Wells et al. 2021: 109.

Duplicaria tricineta. Fedosov et al. 2019: 365, fig. 3b. Aubry et al. 2021: pl. 36. Bibi et al. 2021: 51, pl. 1, figs 9–11.

Referred material. CUF-NKNY-G33 (5 shells; Figs 4O, 10A).

Habitat. Sandy mud bottoms at a depth from 10 to 50 m (Robba et al. 2004; Okutani 2017).

Distribution. Persian Gulf; Indo-West Pacific, from Japan to Australia (Robba et al. 2004; Okutani 2017). Records of fossils from the Holocene in Thailand (Robba et al. 2004).

Record in Thailand. Gulf of Thailand and Andaman Sea (Wells et al. 2021).

Taxonomic remarks and comparisons. This species is recognised based on the descriptions and figures in Bratcher and Cernohorsky (1987) and Aubry et al. (2021), and differs from its similar species, *Granuliterebra bathyrhaphe* (Smith, 1875), in having a smaller shell and two additional minutely beaded spiral cords abapical to the subsutural margin and on the lower base.

***Granuliterebra* Oyama, 1961**

***Granuliterebra bathyrhaphe* (Smith, 1875)**

Figs 4P, 8F

Terebra (Myurella) bathyrhaphe Smith, 1875: 415. Type locality: Gulf of Yedo [Edo Bay, Honshu, Japan].

Terebra sp. Dheeradilok et al. 1984: pl. 3, fig. 11.

Terebra bathyrhaphe. Bratcher and Cernohorsky 1987: 75, pl. 17, fig. 57a–e. Wilson 1994: 223, with in-text fig. Bosch et al. 1995: 171, fig. 765. Robba et al. 2004: 155, pl. 21, fig. 5. Robba et al. 2007: 95 (appendix).

Granuliterebra bathyrhaphe. Okutani 2017: 1049–1050, pl. 339, fig. 13. Fedosov et al. 2019: 379, fig. 10a. Aubry et al. 2021: pl. 73. Bibi et al. 2021: 50, pl. 1, figs 14–17. Wells et al. 2021: 109.

Referred material. CUF-NKNY-G66 (1 shell; Figs 4P, 8F).

Habitat. Muddy and sandy bottoms from intertidal zones to 200 m depth (Robba et al. 2004; Aubry et al. 2021).

Distribution. Persian Gulf and Indian Ocean; Indo-West Pacific, from Japan to Australia (Robba et al. 2004; Okutani 2017; Aubry et al. 2021). Records of fossils from the Quaternary in Japan and Thailand (Robba et al. 2004).

Record in Thailand. Gulf of Thailand (Wells et al. 2021).

Taxonomic remarks and comparisons. This species is recognised based on the descriptions and figures in Bratcher and Cernohorsky (1987) and Aubry et al. (2021), and differs from its similar species, *Duplicaria tricincta* (Smith, 1877), by lacking the band anterior to the subsutural band and by having the other two bands that are connected by well-developed ribs rather than by thin cords.

***Pristiterebra* Oyama, 1961**

***Pristiterebra miranda* (Smith, 1873)**

Figs 4D, 8E

Myurella miranda Smith, 1873: 267–268. Type locality: Malacca.

Terebra miranda. Bratcher and Cernohorsky 1987: 78, pl. 18, fig. 63a, b; colour pl. D, fig. 13. Swennen et al. 2001: 57, 134, fig. 471. Robba et al. 2004: 155–156, pl. 21, fig. 6a, b. Dharma 2005: 114, pl. 32, fig. 5a, b. Robba et al. 2007: 95 (appendix).

Pristiterebra miranda. Aubry et al. 2021: pl. 296. Wells et al. 2021: 109.

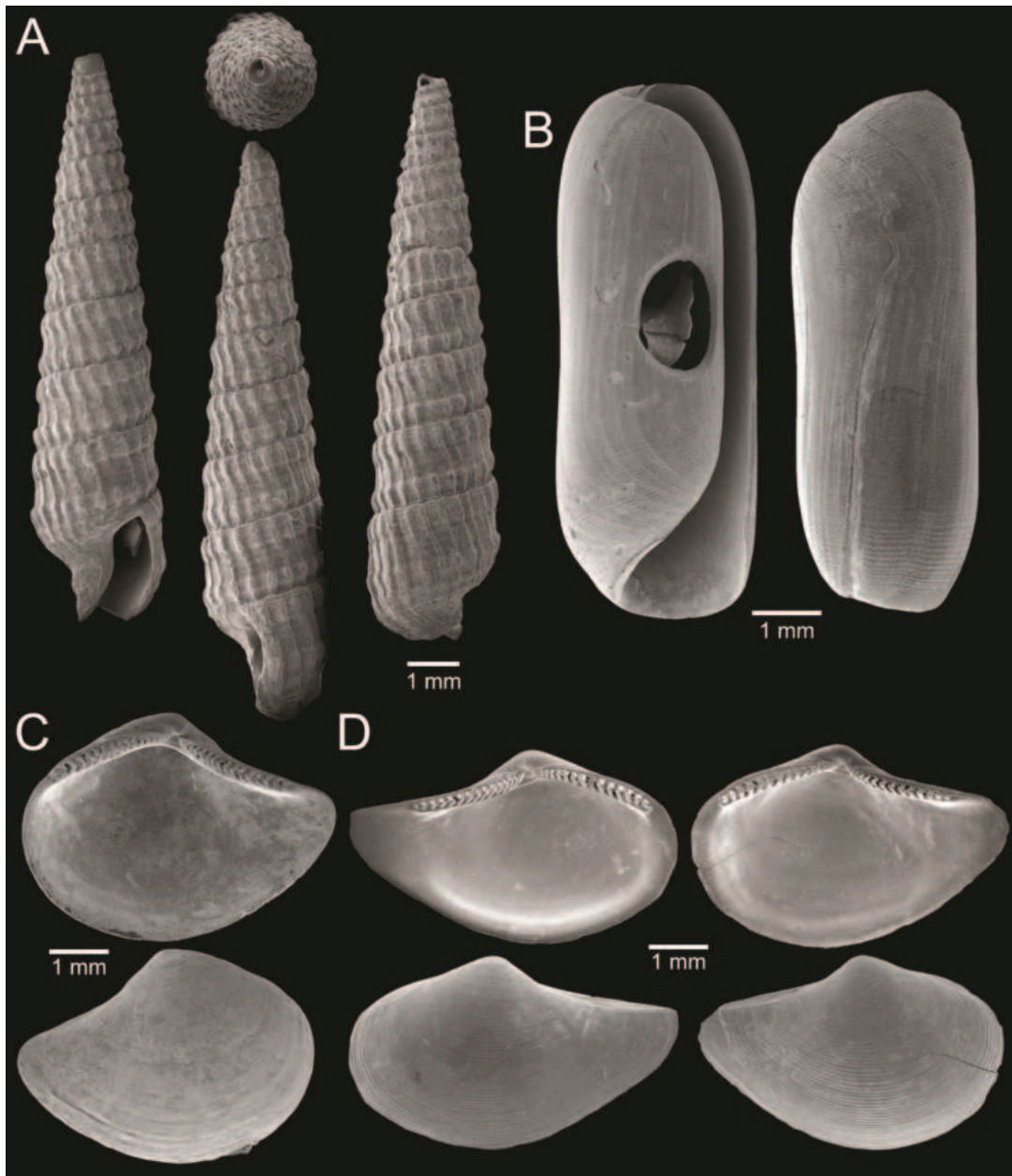


Figure 10. Gastropods and bivalves. **A** *Duplicaria tricineta* **B** *Cylichna modesta* **C** *Jupiteria puellata* **D** *Saccella mauritiana*.

Referred material. CUF-NKNY-G23 (17 shells; Figs 4D, 8E).

Habitat. At sea depth of 6–10 m (Bratcher and Cernohorsky 1987; Robba et al. 2004).

Distribution. Indo-West Pacific, from Thailand to Indonesia (Bratcher and Cernohorsky 1987; Robba et al. 2004). Records of fossils from the Holocene in Thailand (Robba et al. 2004).

Record in Thailand. Gulf of Thailand (Wells et al. 2021).

Taxonomic remarks and comparisons. This species is recognised based on the descriptions and figures in Bratcher and Cernohorsky (1987) and Aubry et al. (2021), specifically in having a turreted and slightly cyrtconoid shell with the sculpture completely cancellate throughout and with numerous and unevenly spaced axial cords crossed by ~ 6 spiral cords forming small bead-like nodes at intersections.

Subclass Heterobranchia Burmeister, 1837
Grade “Lower Heterobranchia”
Superfamily Architectonicoidea Gray, 1850
Family Architectonicidae Gray, 1850
***Architectonica* Röding, 1798**

***Architectonica perdix* (Hinds, 1844)**

Figs 4J, 11A

Solarium perdix Hinds, 1844: 22–23. Type locality: Ceylon; north-west coast of Australia.

Architectonica perdix. Bieler 1993: 48–52, figs 35–38. Swennen et al. 2001: 57, 135, fig. 477. Hylleberg and Kilburn 2003: 113. Robba et al. 2004: 158, pl. 21, fig. 10a, b. Dharma 2005: 204, pl. 77, fig. 2a, b; 358, pl. 144, fig. 7a, b. Thach 2005: 224. Robba et al. 2007: 95 (appendix). Nabhitabhata 2009: 200. BEDO 2017b: 73, with in-text fig. Yang et al. 2017: 118, 120, fig. 493. Surakiatchai et al. 2018: table 5, pl. 1, fig. 12a, b. Tudu and Balakrishnan 2018: 199–200, fig. 1a–f. Wells et al. 2021: 131.

Referred material. CUF-NKKNY-G02, G31 (155 shells; Figs 4J, 11A).

Habitat. Sandy and muddy bottoms at a depth from 10 to 60 m (Bieler 1993; Thach 2005; Yang et al. 2017).

Distribution. Indian Ocean; Indo-West to Central Pacific, from China to Australia and Polynesia (Robba et al. 2004; Tudu and Balakrishnan 2018). Records of fossils from the Middle Pliocene in Indonesia and from the Holocene in Thailand (Dharma 2005; Surakiatchai et al. 2018).

Record in Thailand. Gulf of Thailand and Andaman Sea (Wells et al. 2021).

Taxonomic remarks and comparisons. This species differs from its similar species, *Adelphotectonica reevei* (Hanley, 1862), by having a much smaller protoconch and a much higher upper point of attachment of the whorls (Bieler 1993). See also comprehensive taxonomic remarks in Bieler (1993).

Cohort Tectipleura Schrödl et al., 2011

Subcohort Euopisthobranchia Jörger et al., 2010

Order Cephalaspidea Fischer, 1883

Superfamily Cylichnoidea H. Adams & A. Adams, 1854

Family Cylichnidae H. Adams & A. Adams, 1854

***Cylichna* Lovén, 1846**

***Cylichna modesta* Thiele, 1925**

Figs 4R, 10B

Cylichna modesta Thiele, 1925: 241–242 [275–276], pl. 44 [32], fig. 7. Type locality: “Neu-Amsterdam”, Station 167 (37° 47' südl. Br., 77° 33.7' östl. L., 496 m). Swennen et al. 2001: 137, fig. 497. Wells et al. 2021: 144.

Adamnestia modesta. Robba et al. 2004: 230, pl. 34, fig. 5a, b. Robba et al. 2007: 97 (appendix). Negri et al. 2014: table 3.

Referred material. CUF-NKKNY-G39 (11 shells; Figs 4R, 10B).

Habitat. Sublittoral in muddy or fine sandy bottoms (Robba et al. 2004).

Distribution. Southwest Pacific. Records of fossils from the Holocene in Thailand (Robba et al. 2004).

Record in Thailand. Gulf of Thailand (Wells et al. 2021).

Taxonomic remarks and comparisons. This species differs from its similar species, *Cylichna sibogae* Schepman, 1913, by having a less slender shell and an adapical umbilicus unbounded by sharp angulation (Robba et al. 2004). The generic assignment to either *Adamnestia* Iredale, 1936 or *Cylichna* requires further investigation.

Subcohort Panpulmonata Jörger et al., 2010

Superorder Eupulmonata Haszprunar & Huber, 1990

Order Ellobiida Van Mol, 1967

Superfamily Ellobioidea Pfeiffer, 1854

Family Ellobiidae Pfeiffer, 1854

***Ellobium* Röding, 1798**

***Ellobium aurisjudae* (Linnaeus, 1758)**

Figs 4G, 11B

Bulla aurisjudae Linnaeus, 1758: 728. Type locality: unknown.

Ellobium aurisjudae. Cernohorsky 1972: 211, pl. 60, fig. 7. Brandt 1974: 227–228, pl. 16, fig. 94. Tantanasiriwong 1978: 20, fig. 256. Nateewathana et al. 1981: 62. Way and Purchon 1981: 321. Bosch et al. 1995: 183, fig. 852. Nateewathana 1995: 100, with in-text fig. Poutiers 1998b: 643, with in-text figs. Subba Rao and Dey 2000: 187. Swennen et al. 2001: 60, 143, fig. 524. Gemert 2003: 107, with in-text fig. Hylleberg and Kilburn 2003: 133. Robba et al. 2003: tables 1, 2. Robba et al. 2004: 241–242, pl. 35, fig. 5. Sri-aroon et al. 2004: table 1. Dharma 2005: 206, pl. 78, fig. 18; 360, pl. 145, fig. 11. Sri-aroon et al. 2005: tables 2, 3, 5, 6. Thach 2005: 232, pl. 71, figs 11, 14. Dey 2006: 56, figs 75, 76. Raven and Vermeulen 2007: 37, 39, pl. 2, figs 10–13. Robba et al. 2007: 98 (appendix). Printrakoon et al. 2008: table 1. Kesavan et al. 2009: 382, with in-text fig. Nabhitabhata 2009: 227. Groh 2010: 446, pl. 914, figs 8, 9. Hamli et al. 2013: tables 2, 3, fig. 2t. Hylleberg and Aungtonya 2013: 97. Sanpanich and Duangdee 2013: 64. Dechruksa et al. 2014: fig. 3e. BEDO 2017b: 81, with in-text fig. Tudu et al. 2018: table 1. Wells et al. 2021: 146.

Ellobium (Ellobium) cf. aurisjudae. Matsubara and Komori 2007: 326–328, fig. 2a–d.

Ellobium (Ellobium) aurisjudae. Matsubara and Komori 2007: fig. 2e–h.

Referred material. CUF-NKNY-G65 (25 shells; Figs 4G, 11B).

Habitat. In estuaries, mangrove and coastal forests, on salt marshes above the normal high tide line in or under rotting wood, and on sandy soil bordering a sandy beach (Raven and Vermeulen 2007).

Distribution. Arabian Gulf and Indian Ocean; Indo-West Pacific, from South China Sea to Australia (Poutiers 1998b; Robba et al. 2004). Records of fossils from the Early Miocene to Holocene in Indonesia, Japan, Malaysia, and Thailand (Robba et al. 2004; Dharma 2005; Matsubara and Komori 2007; Raven and Vermeulen 2007).

Record in Thailand. Gulf of Thailand and Andaman Sea (Wells et al. 2021).

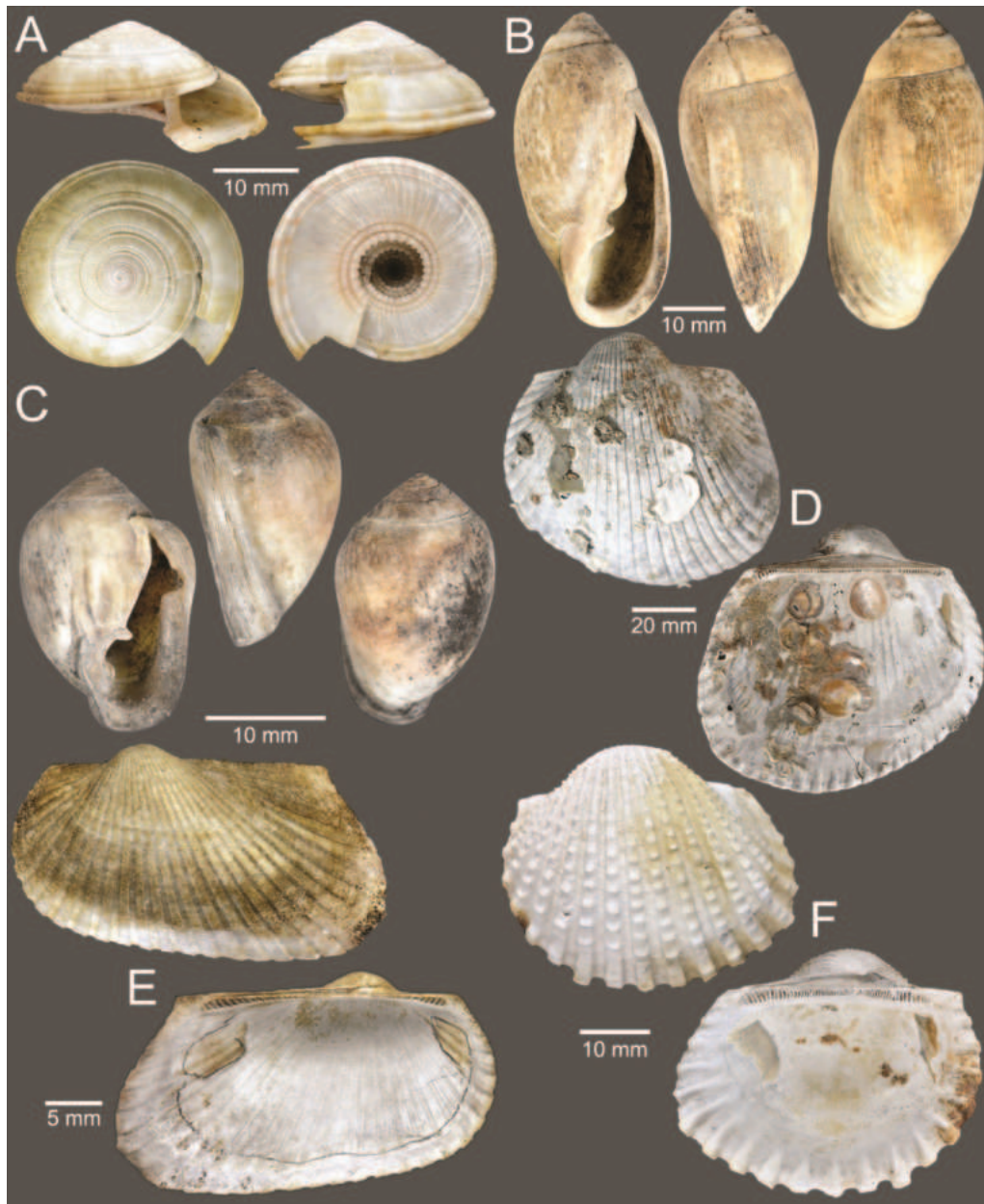


Figure 11. Gastropods and bivalves **A** *Architectonica perdix* **B** *Ellobium aurisjudae* **C** *Cassidula nucleus* **D** *Anadara inaequalis* **E** *Anadara indica* **F** *Tegillarca granosa*.

Taxonomic remarks and comparisons. This species is recognised based on the descriptions and figures in Brandt (1974), Poutiers (1998b), and Robba et al. (2004), specifically in having an elongate-oval and unshouldered shell with the sculpture of numerous axial grooves and fine spiral lines.

***Cassidula* Férussac, 1821**

***Cassidula nucleus* (Gmelin, 1791)**

Figs 4L, 11C

Helix nucleus Gmelin, 1791: 3193. Type locality: "Tahiti" [Cooktown, Queensland, Australia].

Auricula mustelina Deshayes, 1830: 92. Type locality: "New Zealand".

Cassidula nucleus. Cernohorsky 1972: 212, pl. 60, fig. 8. Bosch et al. 1995: 183, fig. 851. Subba Rao and Dey 2000: 188. Swennen et al. 2001: 60, 143, fig. 526. Hylleberg and Kilburn 2003: 133. Robba et al. 2004: 242–243, pl. 35, fig. 6. Dharma 2005: 208, pl. 79, fig. 1a, b. Thach 2005: 233, pl. 72, fig. 8. Dey 2006: 55–56, figs 73, 74. Raven and Vermeulen 2007: 50–51, pl. 4, figs 35, 36. Robba et al. 2007: 98 (appendix). Kesavan et al. 2009: 382, with in-text fig. Nabhitabhata 2009: 227. Groh 2010: 448, pl. 915, figs 9–11. Zvonareva and Kantor 2016: 429–430, fig. 8s, t. BEDO 2017b: 80, with in-text fig. Kantharajan et al. 2017: table 1, fig. 4–32. Yang et al. 2017: 134, fig. 545. Tudu et al. 2018: table 1. Wells et al. 2021: 145.

Cassidula mustelina. Brandt 1974: 221, pl. 16, fig. 88. Tantanasiwong 1978: 20, fig. 259. Nateewathana et al. 1981: 62. Way and Purchon 1981: 321. Hylleberg and Kilburn 2003: 133. Sri-aroon et al. 2004: table 1, fig. 2–9. Sri-aroon et al. 2005: tables 2–6. Dechruksa et al. 2014: fig. 3c. BEDO 2017b: 80, with in-text fig. Okutani 2017: 1128, pl. 427, fig. 4.

Referred material. CUF-NKNY-G63 (1 shell; Figs 4L, 11C).

Habitat. On mud in shaded areas and on tree trunks in mangrove and nipa palm forests, sometimes present in salt marsh or on muddy tidal flats (Brandt 1974; Raven and Vermeulen 2007; Zvonareva and Kantor 2016).

Distribution. Arabian Gulf and Indian Ocean; Indo-West Pacific, from Japan to Australia (Brandt 1974; Bosch et al. 1995; Subba Rao and Dey 2000; Okutani 2017). Records of fossils from the Holocene in Thailand (Robba et al. 2004).

Record in Thailand. Gulf of Thailand and Andaman Sea (Brandt 1974; Swennen et al. 2001; Wells et al. 2021).

Taxonomic remarks and comparisons. This species differs from its similar species, *Cassidula aurisfelis* (Bruguière, 1789), by having a normal and non-bifurcated columellar fold, a less rounded outline with a less convex shoulder, a straighter aperture, and a thinner palatal ridge (Raven and Vermeulen 2007). See also comprehensive taxonomic remarks in Raven and Vermeulen (2007).

Class Bivalvia Linnaeus, 1758

Subclass Protobranchia Pelseneer, 1889

Order Nuculanida Carter et al., 2000

Superfamily Nuculanoidea H. Adams & A. Adams, 1858

Family Nuculanidae H. Adams & A. Adams, 1858

***Jupiteria* Bellardi, 1875**

***Jupiteria puellata* (Hinds, 1843)**

Figs 10C, 12O

Nucula puellata Hinds, 1843: 100. Type locality: Malacca; from 10 to 17 fathoms, coarse sand.

Nuculana puellata. Lyngø 1909: 105. Hylleberg and Kilburn 2003: 139.

Nuculana (Jupiteria) puellata. Robba et al. 2002: 53, pl. 1, fig. 4a, b. Robba et al. 2003: tables 1, 2, 4–5. Robba et al. 2007: 83 (appendix). Nabhitabhata 2009: 279. Negri et al. 2014: table 3. Huber 2015: C666.

Jupiteria puellata. Wells et al. 2021: 50.



Figure 12. Size comparison of bivalves, scaphopod and other invertebrates found in this study **A** *Tegillarca nodifera* **B** *Volachlamys singaporina* **C** *Tegillarca granosa* **D** *Noetiella pectunculiformis* **E** *Magallana* cf. *gigas* **F** *Estellacar olivacea* **G** *Anadara indica* **H** *Dentalium variable* **I** *Siliqua minima* **J** *Corbula fortisulcata* **K** *Fistulobalanus kondakovi* **L** *Placamen lamellatum* **M** *Martesia striata* **N** *Potamocorbula* sp. **O** *Jupiteria puellata* **P** *Saccella mauritiana* **Q** *Paratapes undulatus* **R** *Dosinia dilecta* **S** *Joannisiella oblonga* **T** *Temnotrema siamense* **U** *Pholas orientalis*.

Referred material. CUF-NKNY-B25 (37 shells; Figs 10C, 12O).

Habitat. Subtidal on coarse sand, soft clay, and mud bottoms at a depth from 5 to 40 m (Huber 2015).

Distribution. Indo-West Pacific, from southern China to New Guinea (Huber 2015). Records of fossils from the Holocene in Thailand (Robba et al. 2002).

Record in Thailand. Gulf of Thailand (Wells et al. 2021).

Taxonomic remarks and comparisons. This species is recognised based on the descriptions and figures in Robba et al. (2002), specifically in having an unsculptured surface bearing only faint growth markings.

***Sacella* Woodring, 1925**

***Sacella mauritiana* (Sowerby I, 1833)**

Figs 10D, 12P

Nucula mauritiana Sowerby I, 1833: 15, fig. 7. Type locality: Mauritius.

Nuculana mauritiana. Lynge 1909: 105. Swennen et al. 2001: 43, 62, fig. 4. Gopalakrishnan et al. 2012: 61.

Nuculana (Scaeoleda) caspidata [non Gould]. Robba et al. 2002: 53, pl. 1, fig. 3a, b.

Nuculana (Scaeoleda) mauritiana. Robba et al. 2003: tables 1, 3, 5. Robba et al. 2004: 245. Robba et al. 2007: 83 (appendix). Negri et al. 2014: table 3.

Sacella mauritiana [sic]. Nabhitabhata 2009: 278.

Nuculana (Sacella) mauritiana. Huber 2010: 97, with in-text fig. Huber 2015: C612.

Sacella mauritiana. Wells et al. 2021: 50.

Referred material. CUF-NKNY-B24 (20 shells; Figs 10D, 12P).

Habitat. Sublittoral on mainly mud and clay with sand and shells at a depth from 11 to 92 m (Huber 2015).

Distribution. Indian Ocean; Indo-West Pacific, from China to Indonesia (Huber 2015). Records of fossils from the Holocene in Thailand (Robba et al. 2002).

Record in Thailand. Gulf of Thailand and Andaman Sea (Swennen et al. 2001; Nabhitabhata 2009; Wells et al. 2021).

Taxonomic remarks and comparisons. This species is recognised based on the descriptions and figures in Robba et al. (2002) and Huber (2010), specifically in having strong commarginal ridges in the umbonal area then changing into flat and somewhat imbricate low rugae which are more raised on crossing the postero-dorsal keel. This species often co-occurs with *Jupiteria puellata*, which has an unsculptured shell (Robba et al. 2002).

Superorder Pteriomorphia Beurlen, 1944

Order Arcida Stoliczka, 1871

Superfamily Arcoidea Lamarck, 1809

Family Arcidae Lamarck, 1809

***Anadara* Gray, 1847**

***Anadara inaequalvis* (Bruguière, 1789)**

Figs 11D, 13D

Arca inaequalvis Bruguière, 1789: 106–107. Type locality: East India. Reeve 1844: *Arca*, pl. 8, sp. 54.

Scapharca inaequalvis. Tantanasiriwong 1979: 4. Morris and Purchon 1981: 322. Natewathana et al. 1981: 63. Poutiers 1998a: 152, with in-text

figs. Subba Rao and Dey 2000: 205. Robba et al. 2002: 58–59, pl. 2, fig. 8. Robba et al. 2003: tables 4, 5. Robba et al. 2007: 83 (appendix). Nabhitabhata 2009: 294. Negri et al. 2014: table 3. Okutani 2017: 1168, pl. 468, fig. 3. Yang et al. 2017: 148, fig. 580.

Anadara (Scapharca) inaequalvis. Vongpanich 1996: 182, figs 21–23. Aungtonya et al. 1999: 372. Dharma 2005: 242, pl. 96, fig. 10. Dey and Ramakrishna 2007: 151, 174. Huber 2010: 137, with in-text fig. Huber 2015: C3218.

Anadara cf. inaequalvis. Swennen et al. 2001: 44, 65–66, fig. 29.

Anadara inaequalvis. Hylleberg and Kilburn 2003: 148. Poppe 2010a: 474, pl. 928, figs 5, 6. Sanpanich 2011: table 2. Gopalakrishnan et al. 2012: 59. Surakiatchai et al. 2018: table 6, pl. 3, fig. 1a, b. Tudu et al. 2018: table 1. Tudu et al. 2019: 38–40, fig. 3c–e. Wells et al. 2021: 52.

Referred material. CUF-NKNY-B03, B21 (21L+30R shells; Figs 11D, 13D).

Habitat. Sandy and muddy bottoms in intertidal and upper sublittoral zones (Robba et al. 2002; Huber 2015).

Distribution. Red Sea to India Ocean; Indo-West Pacific, from Japan to Australia as well as from Mediterranean and Black Sea (Robba et al. 2002; Tudu et al. 2019). Records of fossils from the Late Miocene and Pliocene in Indonesia and from the Holocene in Thailand (Robba et al. 2002; Surakiatchai et al. 2018).

Record in Thailand. Gulf of Thailand and Andaman Sea (Wells et al. 2021).

Taxonomic remarks and comparisons. This species is recognised based on the descriptions and figures in Poutiers (1998a) and Tudu et al. (2019), specifically in having an inflated, inequilateral, and roughly quadrate shell shape with 30–37 radial ribs.

***Anadara indica* (Gmelin, 1791)**

Figs 11E, 12G

Arca indica Gmelin, 1791: 3312. Type locality: the Indian Ocean. Reeve 1844: *Arca*, pl. 9, sp. 56.

Anadara (Scapharca) indica. Lynge 1909: 126–127, pl. 2, figs 5–12.

Scapharca indica. Morris and Purchon 1981: 322. Bosch et al. 1995: 211, fig. 928. Poutiers 1998a: 153, with in-text figs. Robba et al. 2002: 59, pl. 2, fig. 9. Gemert 2003: 107. Robba et al. 2003: tables 1–5. Thach 2005: 243, pl. 75, fig. 17. Robba et al. 2007: 83 (appendix). Nabhitabhata 2009: 294. Yang et al. 2017: 148, fig. 581. Surakiatchai et al. 2018: pl. 3, fig. 3a, b.

Anadara indica. Vongpanich 1996: 183, figs 26, 27. Aungtonya et al. 1999: 372. Tudu et al. 2018: table 1. Wells et al. 2021: 52.

Anadara (Anadara) indica. Huber 2010: 136, with in-text fig. Huber 2015: C3220.

Referred material. CUF-NKNY-B06 (16L+24R shells; Figs 11E, 12G).

Habitat. In soft sand or sandy mud bottoms at bays, river mouths, and intertidal zones down to 15 m depth (Huber 2015).

Distribution. Persian Gulf to India Ocean; Indo-West Pacific, from Japan to Australia (Poutiers 1998a; Robba et al. 2002). Records of fossils from the Holocene in Thailand (Robba et al. 2002; Surakiatchai et al. 2018).

Record in Thailand. Gulf of Thailand and Andaman Sea (Wells et al. 2021).

Taxonomic remarks and comparisons. This species is recognised based on the descriptions and figures in Poutiers (1998a), Robba et al. (2002), and Huber (2010), specifically in having an inequilateral, laterally compressed, and sub-rectangular shell shape with 30–36 flat radial ribs.

***Tegillarca lredale*, 1939**

***Tegillarca granosa* (Linnaeus, 1758)**

Figs 11F, 12C

Arca granosa Linnaeus, 1758: 694. Type locality: southern European ocean. Reeve 1844: *Arca*, pl. 3, sp. 15. Yokoyama 1927: 403. Lutaenko 2015: 135–136, pl. 1, fig. a–d.

Arca (Anadara) granosa. Lynge 1909: 118. Tesch 1920: 92–93, pl. 137, figs 248a, b, 249a–c.

Anadara granosa. Tantanasiwong 1979: 4. Morris and Purchon 1981: 322. Nateewathana et al. 1981: 63. Nateewathana 1995: 101, with in-text fig. Poutiers 1998a: 147, with in-text figs. Aungtonya et al. 1999: 372. Subba Rao and Dey 2000: 204. Hylleberg and Kilburn 2003: 148, pl. 1, fig. 3. Robba et al. 2002: 57–58, pl. 2, fig. 4. Robba et al. 2003: tables 1–5. Dey 2006: 61, figs 86, 87. Dey and Ramakrishna 2007: 151, 172. Robba et al. 2007: 83 (appendix). Printrakoon et al. 2008: table 1. Nabhitabhata 2009: 284. Sanpanich 2011: table 2. Hylleberg and Aungtonya 2013: 94. Negri et al. 2014: table 3. Surakitachai et al. 2018: table 6, pl. 2, fig. 7a, b.

Anadara (Tegillarca) granosa. Vongpanich 1996: 187, 189, figs 47–50. Dharma 2005: 242, pl. 96, fig. 9; 362, pl. 146, fig. 10. Lutaenko et al. 2019: 174, pl. 3, fig. c, d.

Tegillarca granosa. Swennen et al. 2001: 44, 66, fig. 35. Gemert 2003: 107. Thach 2005: 244, pl. 75, fig. 8. Huber 2010: 141, with in-text fig. Poppe 2010a: 486, pl. 934, figs 9, 10. Huber 2015: C3352. BEDO 2017a: 27, with in-text fig. Kantharajan et al. 2017: table 1, fig. 2–10. Okutani 2017: 1168, pl. 468, fig. 9. Yang et al. 2017: 150, fig. 586. Tudu et al. 2018: table 1. Tudu et al. 2019: 42–44, fig. 5c, d. Wells et al. 2021: 54.

Referred material. CUF-NKNY-B20 (15L+15R shells; Figs 11F, 12C).

Habitat. Mud down to 10 m depth in mangrove forests and muddy estuaries (Swennen et al. 2001; Thach 2005; Kantharajan et al. 2017).

Distribution. East Africa to India; Indo-West Pacific, from Japan to Australia and Polynesia (Poutiers 1998a; Kantharajan et al. 2017; Tudu et al. 2019). Records of fossils from the Late Miocene to Holocene in Indonesia, Japan, the Philippines, Taiwan, and Thailand (Robba et al. 2002; Dharma 2005; Surakitachai et al. 2018).

Record in Thailand. Gulf of Thailand and Andaman Sea (Wells et al. 2021).

Taxonomic remarks and comparisons. This species differs from its similar species, *Tegillarca nodifera*, by having a less elongated shell with a lower number of ribs (15–21) and a lower number of nodules on ribs (Tudu et al. 2019).

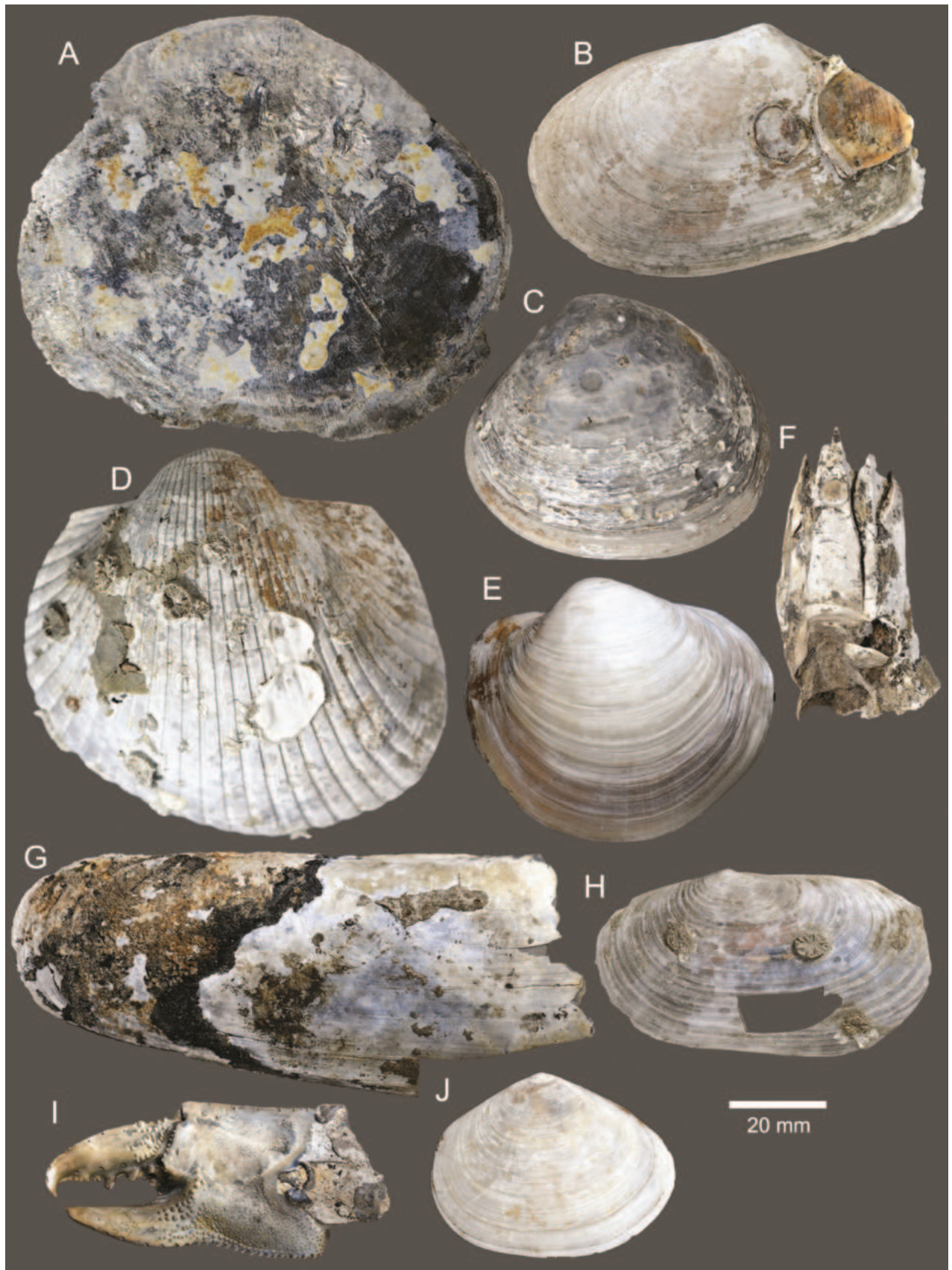


Figure 13. Size comparison of bivalves and other invertebrates found in this study **A** *Placuna placenta* **B** *Standella pellucida* **C** *Geloina bengalensis* **D** *Anadara inaequalis* **E** *Pegophysema bialata* **F** *Megabalanus* cf. *tintinnabulum* **G** *Cultellus maximus* **H** *Lutraria complanata* **I** *Thalassina* sp. **J** *Tellinides conspicuus*.

***Tegillarca nodifera* (Martens, 1860)**

Figs 12A, 14A

Arca nodifera Martens, 1860: 17. Type locality: Bangkok [Bangkok, Thailand].
Anadara nodifera. Nateewathana et al. 1981: 63. Nateewathana 1995: 101, with in-text fig. Poutiers 1998a: 148, with in-text figs. Aungtonya et al. 1999: 372. Hylleberg and Kilburn 2003: 148–149, pl. 1, fig. 5. Nabhitabhata 2009: 284. Hylleberg and Aungtonya 2013: 94.
Anadara (Tegillarca) nodifera. Vongpanich 1996: 189–190, figs 51–54.
Tegillarca nodifera. Swennen et al. 2001: 44, 67, text-fig. 26, fig. 36. Thach 2005: 244, pl. 75, fig. 18. Huber 2010: 141, with in-text fig. Huber 2015: C3366. BEDO 2017a: 28, with in-text fig. Yang et al. 2017: 150, fig. 587. Tudu et al. 2018: table 1. Tudu et al. 2019: 44, fig. 5e, f. Wells et al. 2021: 54.

Referred material. CUF-NKNY-B01, B02, B15 (26L+31R shells; Figs 12A, 14A).

Habitat. On mud and sand bottoms, in intertidal or near mangrove forests and shallow sublittoral waters down to a depth of 10 m (Poutiers 1998a; Huber 2015).

Distribution. Eastern Indian Ocean; Indo-West Pacific, from East China Sea to Indonesia (Poutiers 1998a; Huber 2015; Tudu et al. 2019).

Record in Thailand. Gulf of Thailand and Andaman Sea (Wells et al. 2021).

Taxonomic remarks and comparisons. This species differs from its similar species, *Tegillarca granosa*, by having a more elongated shell with a higher number of ribs (19–23) and a higher number of nodules on ribs (Tudu et al. 2019).

Family Noetiidae Stewart, 1930

***Estellacar* Iredale, 1939**

***Estellacar olivacea* (Reeve, 1844)**

Figs 12F, 14B

Arca olivacea Reeve, 1844: *Arca*, pl. 16, sp. 113. Type locality: San Nicolas, island of Zebu [the Philippines] (found in sandy mud at the depth of four fathoms).

Estellacar olivacea. Poutiers 1998a: 160, with in-text figs. Swennen et al. 2001: 44, 68, fig. 42. Robba et al. 2002: 61, pl. 2, fig. 13. Hylleberg and Kilburn 2003: 153. Robba et al. 2003: table 2. Vongpanich and Matsukuma 2004: 41, pl. 2, figs. r, s. Robba et al. 2007: 84 (appendix). Nabhitabhata 2009: 297. Huber 2010: 146, with in-text fig. Negri et al. 2014: table 3. Huber 2015: C3594. BEDO 2017a: 42, with in-text fig. Wells et al. 2021: 55.

Striarca olivacea. Printrakoon et al. 2008: table 1.

Referred material. CUF-NKNY-B18 (16L+14R shells; Figs 12F, 14B).

Habitat. In mud and sand from intertidal zones, often near mangrove forests, down to 20 m depth (Poutiers 1998a; Robba et al. 2002).

Distribution. India; Indo-West Pacific, from South China to the Philippines (Huber 2015). Records of fossils from the Holocene in Thailand (Robba et al. 2002).

Record in Thailand. Gulf of Thailand and Andaman Sea (Wells et al. 2021).

Taxonomic remarks and comparisons. This species differs from its similar species *Estellacar galactodes* (Benson, 1842) by having a higher number of coarser riblets (Robba et al. 2002).

Noetiella Thiele, 1931

***Noetiella pectunculiformis* (Dunker, 1866)**

Figs 12D, 14C

Barbatia pectunculiformis Dunker, 1866: 88–89, pl. 28, figs 4–6. Type locality: Borneo.

Arca (Fossularca) pectunculiformis. Lynge 1909: 115.

Striarca pectunculiformis. Tantanasiwong 1979: 4. Morris and Purchon 1981: 323. Nateewathana et al. 1981: 63. Aungtonya et al. 1999: 373.

Scelidionarca pectunculiformis. Robba et al. 2002: 61, pl. 2, fig. 14q, b. Robba et al. 2007: 84 (appendix). Nabhitabhata 2009: 297.

Noetiella pectunculiformis. Huber 2010: 146, with in-text fig. Huber 2015: C3575. BEDO 2017a: 43, with in-text fig. Kantharajan et al. 2017: table 1, fig. 2-11. Wells et al. 2021: 55.

Referred material. CUF-NKYN-B27 (4L+4R shells; Figs 12D, 14C).

Habitat. In soft clay, mud or sand, in subtidal zones from a depth of 2–43 m, and in mangrove forests (Huber 2015; Kantharajan et al. 2017).

Distribution. India Ocean; Indo-West Pacific, from South China to Indonesia (Huber 2015; Kantharajan et al. 2017). Records of fossils from the Holocene in Thailand (Robba et al. 2002).

Record in Thailand. Gulf of Thailand and Andaman Sea (Wells et al. 2021).

Taxonomic remarks and comparisons. This species is recognised based on the descriptions and figures in Robba et al. (2002) and Huber (2010), specifically in having a roundly trapezoidal and inequilateral shell shape with the sculpture of dense, faint radials, and coarse growth markings.

Order Ostreida Férussac, 1822

Superfamily Ostreoidea Rafinesque, 1815

Family Ostreidae Rafinesque, 1815

***Magallana* Salvi & Mariottini, 2016**

***Magallana cf. gigas* (Thunberg, 1793)**

Figs 12E, 14D

cf. *Ostrea gigas* Thunberg, 1793: 140–142, pl. 6, figs 1–3. Type locality: Japan. Yokoyama 1927: 402.

cf. *Crassostrea gigas*. Tantanasiwong 1979: 7. Nateewathana et al. 1981: 65. Poutiers 1998a: 233, with in-text figs. Aungtonya et al. 1999: 375. Robba et al. 2002: 69, 71, pl. 5, fig. 3a, b. Hylleberg and Kilburn 2003: 162. Beu et al. 2004: 154–156, fig. 9d. Thach 2005: 257. Robba et al. 2007: 84 (appendix). Printrakoon et al. 2008: table 1. Huber 2010: 180, with in-text fig. Sanpanich 2011: table 2. Huber 2015: C5155. Okutani 2017: 1183, pl. 483, fig. 7. Yang

et al. 2017: 176, 178, fig. 685. Surakiatchai et al. 2018: table 6, pl. 3, fig. 6a, b. Tudu et al. 2018: table 1.
cf. *Crassostrea* cf. *gigas*. Swennen et al. 2001: 45, 72, text-fig. 62, fig. 62.
cf. *Crassostrea (Magallana) gigas*. Lutaenko et al. 2019: 187–188, pl. 15, fig. a–f.
cf. *Magallana gigas*. Wells et al. 2021: 60.

Referred material. CUF-NKNY-B13 (130L+16R shells; Figs 12E, 14D).

Habitat. Attached to rocks from intertidal zones down to 30 m depth, in mud, bays, and sheltered areas that are often brackish with low salinity water (Thach 2005; Huber 2015).

Distribution. Cosmopolitan (Huber 2015). Records of fossils from the Miocene to Holocene in Japan, New Zealand, Taiwan, and Thailand (Robba et al. 2002; Beu et al. 2004; Surakiatchai et al. 2018).

Record in Thailand. Gulf of Thailand and Andaman Sea (Wells et al. 2021).

Taxonomic remarks and comparisons. The cupped oysters in the subfamily Crassostreinae could not be identified at species level based on shell characters or soft tissue alone (Salvi and Mariottini 2021). Therefore, we tentatively identify these specimens of giant cupped oysters as belonging to *Magallana gigas*, due to large and thick shells and the presence of this species in Thailand (Wells et al. 2021).

Order Pectinida Gray, 1854

Superfamily Anomioidea Rafinesque, 1815

Family Placunidae Rafinesque, 1815

***Placuna* Lightfoot, 1786**

***Placuna placenta* (Linnaeus, 1758)**

Figs 13A, 14E

Anomia placenta Linnaeus, 1758: 703. Type locality: unknown.

Placuna placenta. Lyngø 1909: 107–108. Tantanasiriwong 1979: 6. Morris and Purchon 1981: 324. Nateewathana et al. 1981: 64. Oliver 1992: 86, pl. 17, fig. 6a, b. Bosch et al. 1995: 234, fig. 1018. Poutiers 1998a: 218, with in-text figs. Aungtonya et al. 1999: 376. Subba Rao and Dey 2000: 230. Swennen et al. 2001: 46, 76, text-fig. 80, fig. 80. Robba et al. 2002: 77, pl. 6, fig. 10a, b. Hylleberg and Kilburn 2003: 169–170. Robba et al. 2003: table 5. Dharma 2005: 246, pl. 98, fig. 17. Dey and Ramakrishna 2007: 154, 197. Robba et al. 2007: 84 (appendix). Nabhitabhata 2009: 20, with in-text fig., 347. Huber 2010: 190, with in-text fig. Sanpanich 2011: table 2. Huber 2015: C5627. Yang et al. 2017: 176, fig. 681. Surakiatchai et al. 2018: table 6, pl. 3, fig. 8a, b. Tudu et al. 2018: table 1. Wells et al. 2021: 64.

Placuna (Placuna) placenta. Dheeradilok et al. 1984: pl. 2, fig. 14. Thach 2005: 266, pl. 81, fig. 4.

Referred material. CUF-NKNY-B22 (19L+18R shells; Figs 13A, 14E).

Habitat. Sandy mud in intertidal zones and shallow waters down to 35 m depth, in quiet waters of lagoons, protected bays, and mangrove areas, or near estuaries (Poutiers 1998a; Thach 2005; Yang et al. 2017).

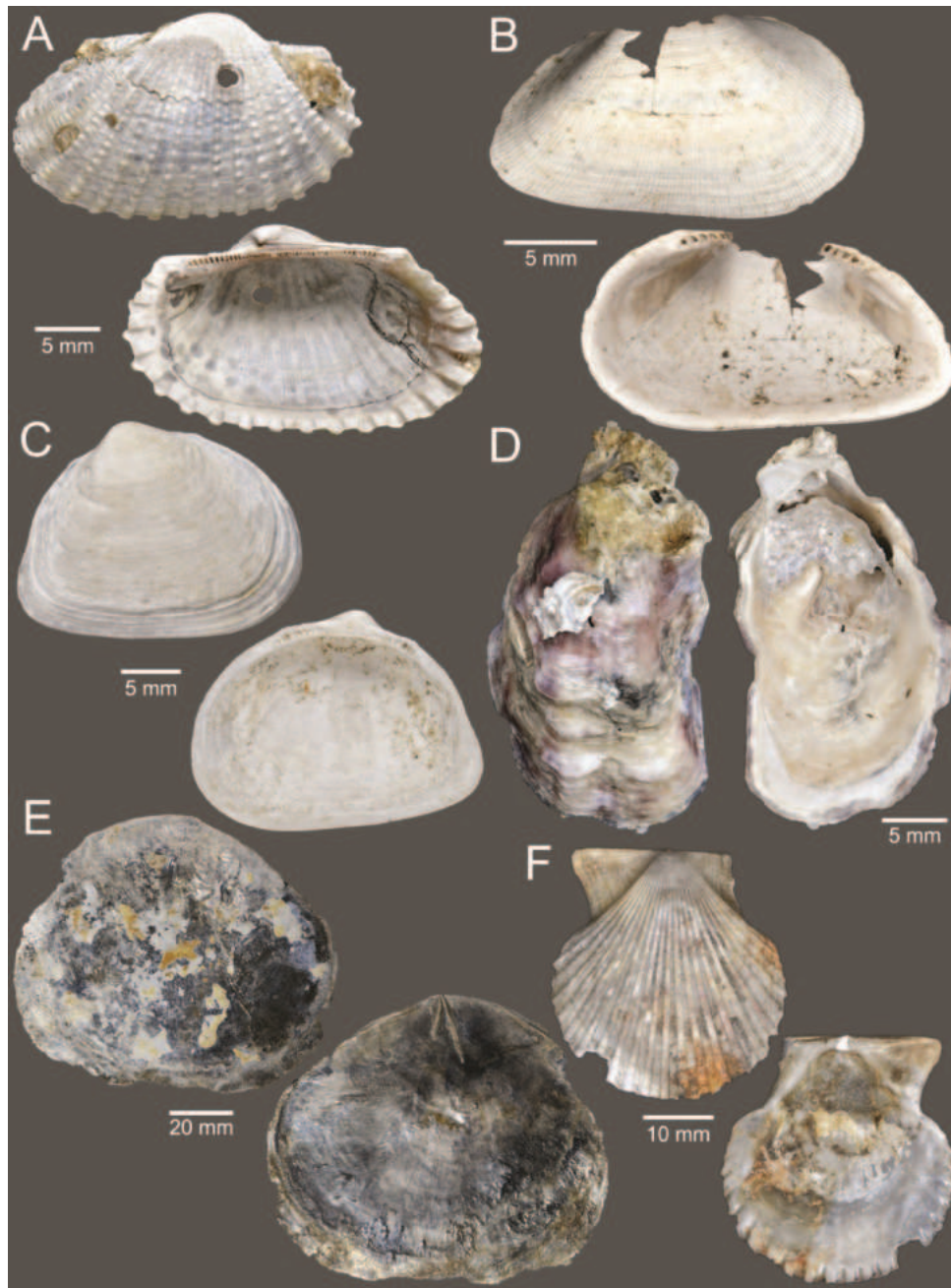


Figure 14. Bivalves **A** *Tegillarca nodifera* **B** *Estellacar olivacea* **C** *Noetiella pectunculiformis* **D** *Magallana* cf. *gigas* **E** *Placuna placenta* **F** *Volachlamys singaporina*.

Distribution. Indian Ocean; Indo-West Pacific, from Japan to Australia (Huber 2015). Records of fossils from the Late Miocene to Holocene in Indonesia, Japan, the Philippines, Taiwan, and Thailand (Robba et al. 2002; Surakiatchai et al. 2018).

Record in Thailand. Gulf of Thailand and Andaman Sea (Wells et al. 2021).

Taxonomic remarks and comparisons. This species differs from its similar species, *Placuna ehippium* (Philipsson, 1788), by having an almost circular shell and a right valve bearing a hinge plate with arrowhead-shaped lamellar teeth with the posterior ridge distinctly longer than the anterior one (Poutiers 1998a; Swennen et al. 2001).

Superfamily Pectinoidea Rafinesque, 1815

Family Pectinidae Rafinesque, 1815

***Volachlamys* Iredale, 1939**

***Volachlamys singaporina* (Sowerby II, 1842)**

Figs 12B, 14F

Pecten singaporinus Sowerby II, 1842: 74, pl. 13, fig. 55; pl. 14, fig. 71. Type locality: Singapore. Lynge 1909: 155.

Volachlamys singaporina. Roussy 1991: 21. Poutiers 1998a: 210, with in-text figs. Aungtonya et al. 1999: 376. Swennen et al. 2001: 45, 74, fig. 70. Gemert 2003: 108. Hylleberg and Kilburn 2003: 169. Dharma 2005: 248, pl. 99, fig. 13a–e; 364, pl. 147, fig. 3a, b. Thach 2005: 263, pl. 80, fig. 13. Nabhitabhata 2009: 342. Huber 2010: 203, with in-text fig. Huber 2015: C6118. BEDO 2017a: 236, with in-text fig. Yang et al. 2017: 172, fig. 667. Dijkstra and Beu 2018: 296–298, figs 98, 100j, l, 101d, e. Wells et al. 2021: 67.

Referred material. CUF-NKNY-B07 (32L+32R shells; Figs 12B, 14F).

Habitat. Byssally attached under coral boulders and rocks, on sand and sandy mud in intertidal zones down to 22 m depth (Huber 2015).

Distribution. Indo-West Pacific, from China to Australia (Huber 2015; Dijkstra and Beu 2018). Records of fossils from the Middle to Late Pliocene in Indonesia (Dharma 2005).

Record in Thailand. Gulf of Thailand and Andaman Sea (Wells et al. 2021).

Taxonomic remarks and comparisons. This species differs from its similar species, *Volachlamys tranquebaria* (Gmelin, 1791) and *V. hirasei* (Bavay, 1904), by having square and well-defined 18–24 ribs with wider interspaces between the ribs (Dharma 2005; Dijkstra and Beu 2018). See also comprehensive taxonomic remarks in Dijkstra and Beu (2018)

Superorder Heteroconchia Gray, 1854

Order Lucinida Gray, 1854

Superfamily Lucinoidea J. Fleming, 1828

Family Lucinidae J. Fleming, 1828

***Pegophysema* Stewart, 1930**

***Pegophysema bialata* (Pilsbry, 1895)**

Figs 13E, 15A

Loripes bialata Pilsbry, 1895: 133–134, pl. 3, figs 13, 14. Type locality: Inland Sea, Japan.

Anodontia (?*Pegophysema*) *bialata*. Taylor and Glover 2005: 305–306, figs 11a, 12a, 22, 23.

Pegophysema bialata. Huber 2015: 102, 455–456, with in-text figs; C10244. Wells et al. 2021: 35.

Referred material. CUF-NKNY-B11 (3L+3R shells; Figs 13E, 15A).

Habitat. Muddy bottoms and sandy mud among weed in intertidal zones down to 60 m depth (Huber 2015).

Distribution. Indian Ocean; Indo-West Pacific, from Japan to Malaysia (Taylor and Glover 2005; Huber 2015).

Record in Thailand. Gulf of Thailand (Wells et al. 2021).

Taxonomic remarks and comparisons. This species differs from its similar species, *Pegophysema philippiana* (Reeve, 1850), by having a ligament that is shallowly inset and an absence of secondary pallial attachment scars (Taylor and Glover 2005). See also comprehensive taxonomic remarks in Taylor and Glover (2005).

Order Venerida Gray, 1854

Superfamily Cyrenoidea Gray, 1840

Family Cyrenidae Gray, 1840

***Geloina* Gray, 1842**

***Geloina bengalensis* (Lamarck, 1818)**

Figs 13C, 15B

Cyrena bengalensis Lamarck, 1818: 554. Type locality: Bengal.

Polymesoda (Geloina) bengalensis. Brandt 1974: 310–311, pl. 28, fig. 83. Nateewathana 1995: 106, with in-text fig. Aungtonya et al. 1999: 380. Robba et al. 2002: 106, pl. 16, fig. 9. Robba et al. 2003: tables 1, 2. Robba et al. 2007: 87 (appendix). Nabhitabhata 2009: 21, with in-text fig, 471.

Polymesoda bengalensis. Poutiers 1998a: 319, with in-text figs. Dharma 2005: 266, pl. 108, fig. 25. Dey 2006: 74–75, figs 113, 114. Tudu et al. 2018: table 1.

Geloina bengalensis. Huber 2015: 319; C20908. BEDO 2017a: 252, with in-text fig. Wells et al. 2021: 39.

Referred material. CUF-NKNY-B31 (2L+3R shells; Figs 13C, 15B).

Habitat. In intertidal zones, river deltas, estuaries, mud flats, and in mangrove areas (Poutiers 1998a; Huber 2015).

Distribution. Bay of Bengal; Indo-West Pacific, from Taiwan to Indonesia (Huber 2015). Records of fossils from the Holocene in Thailand (Robba et al. 2002).

Record in Thailand. Gulf of Thailand and Andaman Sea (Wells et al. 2021).

Taxonomic remarks and comparisons. This species is recognised based on the descriptions and figures in Robba et al. (2002) and Huber (2015), specifically in having a solid, inflated, pronounced inequilateral, and subtriangular shell shape.

Superfamily Mactroidea Lamarck, 1809

Family Mactridae Lamarck, 1809

***Lutraria* Lamarck, 1799**

***Lutraria complanata* (Gmelin, 1791)**

Figs 13H, 15C

Mactra complanata Gmelin, 1791: 3261. Type locality: the Indian Ocean.

Lutraria (Lutrophora) cf. *complanata*. Dheeradilok et al. 1984: pl. 2, fig. 5.

Lutraria complanata. Swennen et al. 2001: 47, 82, fig. 112. Hylleberg and Kilburn 2003: 186. Yang et al. 2017: 194, fig. 742. Wells et al. 2021: 40.

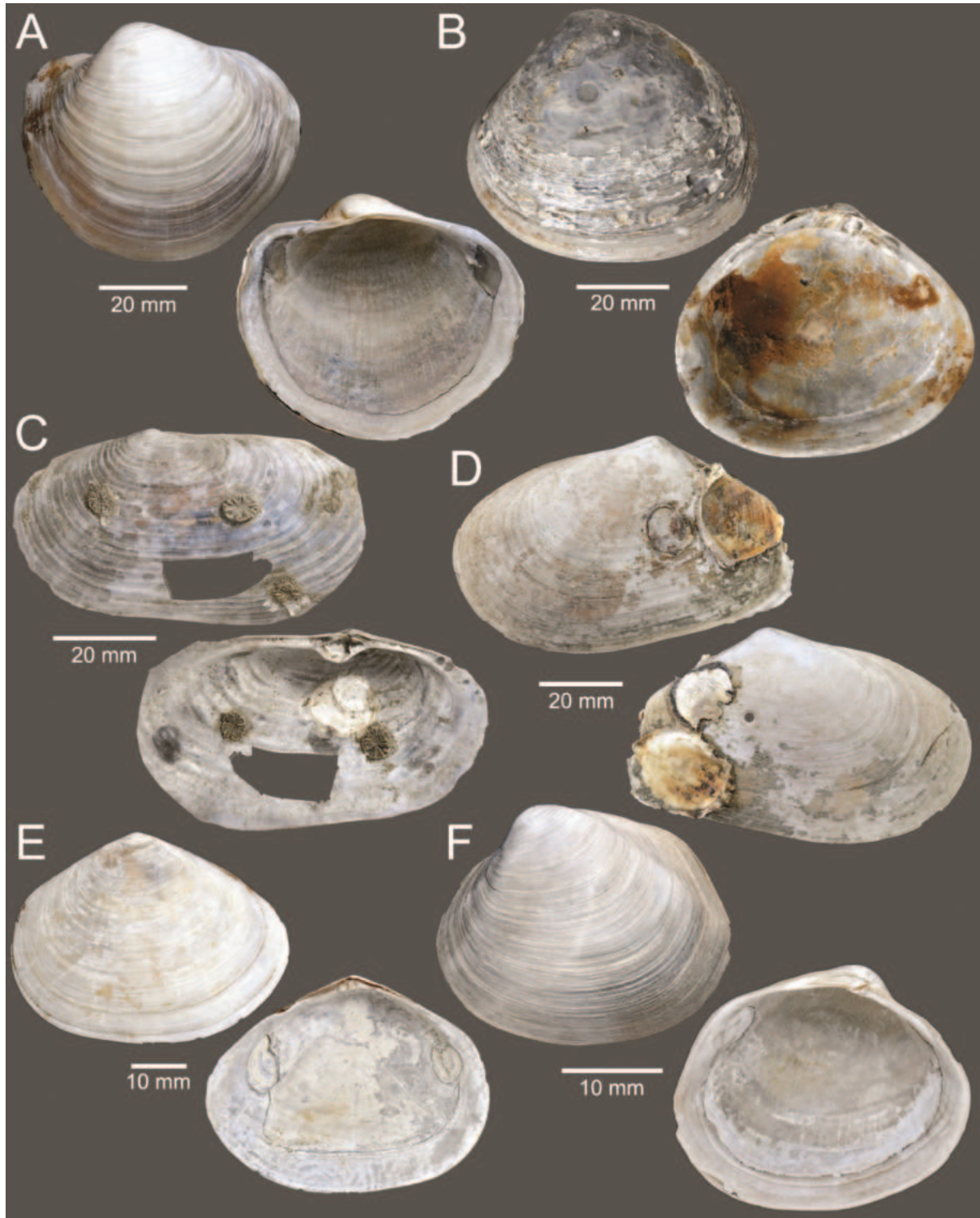


Figure 15. Bivalves **A** *Pegophysema bialata* **B** *Geloina bengalensis* **C** *Lutraria complanata* **D** *Standella pellucida* **E** *Tellinides conspicuus* **F** *Joanniella oblonga*.

Lutraria (Lutrophora) complanata. Robba et al. 2002: 91, pl. 12, fig. 4. Robba et al. 2007: 86 (appendix). Huber 2010: 451, with in-text figs. Huber 2015: C21984.
Lutraria (Goniomactra) complanata. Beu 2006: 242.
Lutraria (Lutrobora) complanata [sic]. Nabhitabhata 2009: 412.

Referred material. CUF-NKYN-B29 (1L+2R shells; Figs 13H, 15C).

Habitat. Sandy and muddy sand in subtidal zones from a depth of 8–20 m (Huber 2015).

Distribution. Indian Ocean; Indo-West Pacific, from South China to Indonesia (Huber 2015; Yang et al. 2017). Records of fossils from the Holocene in Thailand (Robba et al. 2002).

Record in Thailand. Gulf of Thailand (Wells et al. 2021).

Taxonomic remarks and comparisons. This species is recognised based on the descriptions and figures in Robba et al. (2002) and Huber (2010), specifically in having an elongate-elliptical and markedly inequilateral thin shell with arched anterior and posterior margins, and an outer surface sculptured with irregular crenulated growth lines.

***Standella* Gray, 1853**

***Standella pellucida* (Gmelin, 1791)**

Figs 13B, 15D

Macra pellucida Gmelin, 1791: 3260–3261. Type locality: “Guinea coast.” Sanpanich 2011: table 2.

Standella pellucida. Lynge 1909: 224. Nabhitabhata 2009: 418. Huber 2010: 451, with in-text figs. Huber 2015: C22028. Tudu et al. 2018: table 1. Wells et al. 2021: 42.

Meropesta pellucida. Bosch et al. 1995: 248, fig. 1100. Poutiers 1998a: 281, with in-text figs. Swennen et al. 2001: 47, 83, text-fig. 116, fig. 116. Robba et al. 2002: 91–92, pl. 12, fig. 6. Dey and Ramakrishna 2007: 211. Robba et al. 2007: 86 (appendix). Meyer et al. 2008: tables 2, 3. Nabhitabhata 2009: 417. Wong 2009: 289, figs 9a, b, 22. BEDO 2017a: 155. Yang et al. 2017: 196, fig. 752.

Referred material. CUF-NKYN-B30 (1L+1R shells; Figs 13B, 15D).

Habitat. Fine sand and mud in intertidal zones down to 4 m depth, in lagoons, and at the fringe of mangrove areas (Poutiers 1998a; Huber 2015).

Distribution. Arabian Gulf and Indian Ocean; Indo-West Pacific, from Japan to Australia (Bosch et al. 1995; Wong 2009; Huber 2015). Records of fossils from the Quaternary in Indonesia and from the Holocene in Thailand (Robba et al. 2002).

Record in Thailand. Gulf of Thailand and Andaman Sea (Wells et al. 2021).

Taxonomic remarks and comparisons. This species is recognised based on the descriptions and figures in Robba et al. (2002) and Huber (2010), specifically in having a longer than high, inequilateral, and elliptical shell with an oval-shaped anterior margin and a somewhat pointed posterior margin, an outer surface sculptured with uneven and fine growth markings, and faint posterior radial striation. An exceedingly shallow radial depression is sometimes observed in the mid-anterior part. Huber (2015) indicated that the type locality in Guinea is erroneous.

Superfamily Tellinoidea Blainville, 1814

Family Tellinidae Blainville, 1814

***Tellinides* Lamarck, 1818**

***Tellinides conspicuus* (Hanley, 1846)**

Figs 13J, 15E

Tellina conspicua Hanley, 1846b: 293, pl. 58, fig. 100. Type locality: unknown.
Coan and Kabat 2012: 309.

Tellina (*Tellinides*) sp. Robba et al. 2002: 98, pl. 14, fig. 7a, b.

Tellinides conspicuus. Huber 2015: 220, 639, with in-text figs; C14877. Wells et al. 2021: 30.

Referred material. CUF-NKNY-B04 (33L+40R shells; Figs 13J, 15E).

Habitat. Shallow water (Huber 2015).

Distribution. Indo-West Pacific, from southern China to New Guinea (Huber 2015).

Record in Thailand. Gulf of Thailand (Wells et al. 2021).

Taxonomic remarks and comparisons. *Tellina* (*Tellinides*) sp. in Robba et al. (2002) was identified as belonging to this species by Huber (2015). This species differs from its similar species, *Tellinides timorensis* Lamarck, 1818, by having a higher shell that lacks the posterior truncation with oblique anterior striae fading posteriorly (Robba et al. 2002; Huber 2015).

Superfamily Ungulinoidea Gray, 1854

Family Ungulinidae Gray, 1854

***Joannisiella* Dall, 1895**

***Joannisiella oblonga* (Hanley, 1846)**

Figs 12S, 15F

Cyrenoidea oblonga Hanley, 1846a: 10 (plate explanation). Type locality: Philippines. Hanley 1856: 353, pl. 15, fig. 6. Coan and Kabat 2012: 320.

Diplodonta (*Joannisiella*) *oblonga*. Lynge 1909: 176.

Cycladicama oblonga. Dheeradilok et al. 1984: pl. 2, figs 6, 7. Robba et al. 2002: 79, pl. 7, fig. 9a, b. Hylleberg and Kilburn 2003: 174. Robba et al. 2003: tables 3, 4. Robba et al. 2007: 85 (appendix). Nabhitabhata 2009: 389. Yang et al. 2017: 182, fig. 704. Surakiatchai et al. 2018: table 6, pl. 3, fig. 10a, b.

Joannisiella oblonga. Huber 2015: 341, 829, with in-text figs; C21436. Wells et al. 2021: 42.

Referred material. CUF-NKNY-B09, B17 (59L+66R shells; Figs 12S, 15F).

Habitat. Muddy bottom with soft clay, muddy sediments on mud flats, and in the shallow waters from intertidal zones down to 36 m depth (Huber 2015; Yang et al. 2017).

Distribution. Indo-West Pacific, from Japan to Indonesia and the Philippines (Huber 2015; Yang et al. 2017). Records of fossils from the Middle Miocene to Holocene in Indonesia, Japan, the Philippines, Taiwan, and Thailand (Robba et al. 2002; Surakiatchai et al. 2018).

Record in Thailand. Gulf of Thailand (Wells et al. 2021).

Taxonomic remarks and comparisons. This species is characterised by its elongate, ovate-triangular shaped, and posteriorly grooved shell (Robba et al. 2002; Huber 2015).

Superfamily Veneroidea Rafinesque, 1815

Family Veneridae Rafinesque, 1815

***Dosinia* Scopoli, 1777**

***Dosinia dilecta* A. Adams, 1856**

Figs 12R, 16A

Dosinia dilecta A. Adams, 1856: 224. Type locality: Malacca. Lynge 1909: 249–250, pl. 5, figs 11–13. Morris and Purchon 1981: 326. Swennen et al. 2001: 49, 95, text-fig. 201, fig. 201. Robba et al. 2002: 115, pl. 19, fig. 4. Dharma 2005: 266, pl. 108, fig. 30. Robba et al. 2007: 88 (appendix). Sartori et al. 2008: table 1. Nabhitabhata 2009: 482. Poppe 2010c: 304, pl. 1147, figs 5, 6. Surakiatchai et al. 2018: table 6, pl. 5, fig. 8a, b. Wells et al. 2021: 44.

Dosinia (Dosinella) dilecta. Fischer-Piette and Delmas 1967: 77, pl. 14, figs 1–3. Dheeradilok et al. 1984: pl. 2, figs 9–12. Huber 2010: 414, with in-text fig. Huber 2015: C19500.

Referred material. CUF-NKNY-B10 (2L+5R shells; Figs 12R, 16A).

Habitat. Soft clay and mud bottoms in subtidal zones at a depth from 5 to 20 m (Huber 2015).

Distribution. Indo-West Pacific, from southern China to Indonesia (Huber 2015). Records of fossils from the Holocene in Thailand (Robba et al. 2002; Surakiatchai et al. 2018).

Record in Thailand. Gulf of Thailand and Andaman Sea (Wells et al. 2021).

Taxonomic remarks and comparisons. This species is recognised based on the descriptions and figures in Fischer-Piette and Delmas (1967), Robba et al. (2002), and Huber (2010), specifically in having deeply demarcated and exceedingly small lunulae and a shell with low concentric ribs. See also comprehensive taxonomic remarks in Fischer-Piette and Delmas (1967).

***Paratapes* Stoliczka, 1870**

***Paratapes undulatus* (Born, 1778)**

Figs 12Q, 16B

Venus undulata Born, 1778: 54–55. Type locality: unknown.

Tapes (Paratapes) undulatus. Lynge 1909: 237.

Paphia undulata. Tantanasiriwong 1979: 13. Morris and Purchon 1981: 326. Nateewathana et al. 1981: 67. Dheeradilok et al. 1984: pl. 2, fig. 13. Oliver 1992: 191, pl. 43, fig. 6a, b. Bosch et al. 1995: 273, fig. 1227. Nateewathana 1995:

111, with in-text fig. Poutiers 1998a: 339, with in-text figs. Aungtonya et al. 1999: 382. Subba Rao and Dey 2000: 283. Swennen et al. 2001: 49, 95, text-fig. 198, fig. 198. Hylleberg and Kilburn 2003: 217. Dharma 2005: 270, pl. 110, fig. 16; 368, pl. 149, fig. 13. Thach 2005: 300, pl. 90, fig. 3. Dey and Ramakrishna 2007: 160, 244–245. Nabhitabhata 2009: 492. Poppe 2010c: 296, pl. 1143, figs 7–9. Sanpanich 2011: table 2. Okutani 2017: 1248, pl. 543, fig. 4. Yang et al. 2017: 232, fig. 871. Surakiatchai et al. 2018: table 6, pl. 5, fig. 4a, b.

Paphia cf. *undulata*. Aungtonya and Hylleberg 1998: 320.

Paphia (*Paphia*) *undulata*. Gemert 2003: 109. Robba et al. 2002: 113, pl. 18, fig. 8a, b. Robba et al. 2003: tables 1, 3–5. Robba et al. 2007: 88 (appendix). Negri et al. 2014: table 3.

Neotapes undulata. Sartori et al. 2008: 115, table 1, figs 4l, 5l.

Paphia (*Neotapes*) *undulata*. Huber 2010: 423, with in-text fig.

Paratapes undulatus. Huber 2015: C19932. Tudu et al. 2018: table 1. Wells et al. 2021: 47.

Paratapes undulata. BEDO 2017a: 281, with in-text fig.

Referred material. CUF-NKNY-B12 (2L shells; Figs 12Q, 16B).

Habitat. Fine sandy sediments and mud as well as silty clay bottoms in intertidal to subtidal zones at a depth of 1–50 m (Huber 2015).

Distribution. Red Sea and Indian Ocean; Indo-West Pacific, from Japan to Australia (Robba et al. 2002; Huber 2015). Records of fossils from the Late Miocene to Holocene in Indonesia, Japan, the Philippines, Taiwan, and Thailand (Robba et al. 2002; Dharma 2005; Surakiatchai et al. 2018).

Record in Thailand. Gulf of Thailand and Andaman Sea (Wells et al. 2021).

Taxonomic remarks and comparisons. Despite having no colour and patterns, the elongate-oval and inequilateral shell shape with growth lines as well as slightly oblique and somewhat undulating commarginal grooves on outer surface of the specimens conform to the characters of this species (Robba et al. 2002; Huber 2010).

Placamen Iredale, 1925

***Placamen lamellatum* (Röding, 1798)**

Figs 12L, 16C

Venus lamellata Röding, 1798: 183. Type locality: the East Indian Seas.

Venus tiara Dillwyn, 1817: 162. Type locality: the East Indian Seas.

Venus calophylla Philippi, 1836: 229–230, pl. 8, fig. 2 Type locality: the Chinese Sea.

Chione (*Circomphalus*) *calophylla*. Lynge 1909: 150–151.

Callanaitis calophylla. Tantanasiwong 1979: 13. Nateewathana et al. 1981: 67.

Placamen tiara. Tantanasiwong 1979: 13. Nateewathana et al. 1981: 67. Poutiers 1998a: 351, with in-text figs. Aungtonya et al. 1999: 382. Hylleberg and Kilburn 2003: 219. Dharma 2005: 268, pl. 109, fig. 24. Thach 2005: 292. Dey and Ramakrishna 2007: 159, 238. Nabhitabhata 2009: 495. Poppe 2010c: 274, pl. 1132, figs 1–3.

Bassina calophylla. Bosch et al. 1995: 266, fig. 1191. Subba Rao and Dey 2000: 284.

Placamen calophyllum. Kilburn and Hylleberg 1998: 315. Aungtonya et al. 1999: 382. Swennen et al. 2001: 48, 92, fig. 180. Robba et al. 2002: 107, pl. 17, fig. 4. Gemert 2003: 15. Hylleberg and Kilburn 2003: 218–219. Dharma 2005: 268, pl. 109, fig. 25. Thach 2005: 292, pl. 89, fig. 11. Robba et al. 2007: 87 (appendix). Meyer et al. 2008: tables 2, 4. Sartori et al. 2008: table 1. Nabhitabhata 2009: 494. Poppe 2010c: 272, pl. 1131, figs 4–7. Sanpanich 2011: table 2.
Placamen lamellatum. Huber 2010: 369, with in-text figs. Huber 2015: C18043. BEDO 2017a: 287. Tudu et al. 2018: table 1. Wells et al. 2021: 48.
Clausinella calophylla. Yang et al. 2017: 222, 224, fig. 834.
Clausinella tiara. Yang et al. 2017: 224, fig. 836.

Referred material. CUF-NKKNY-B28 (1R shell; Figs 12L, 16C).

Habitat. Muddy sand, sand, and shell gravels from intertidal zones down to 100 m depth (Bosch et al. 1995; Robba et al. 2002; Yang et al. 2017).

Distribution. Arabian Gulf and Indian Ocean; Indo-West Pacific, from Japan to Indonesia (Bosch et al. 1995; Huber 2015; Yang et al. 2017). Records of fossils from the Late Neogene to Holocene in Fiji, India, Indonesia, Japan, the Philippines and Taiwan (Robba et al. 2002).

Record in Thailand. Gulf of Thailand and Andaman Sea (Wells et al. 2021).

Taxonomic remarks and comparisons. This species differs from its similar species, *Placamen chloroticum* (Philippi, 1849), by having a somewhat shallower and trigonal pallial sinus as well as more widely spaced and more raised commarginal lamellae (Robba et al. 2002).

Order Myida Stoliczka, 1870

Superfamily Myoidea Lamarck, 1809

Family Corbulidae Lamarck, 1818

***Corbula* Bruguière, 1797**

***Corbula fortisulcata* Smith, 1879**

Figs 12J, 16D

Corbula fortisulcata Smith, 1879a: 819–820, pl. 50, fig. 23, 23b. Type locality: the Andaman Islands. Subba Rao and Dey 2000: 286. Swennen et al. 2001: 49, 97, text-fig. 212, fig. 212. Hylleberg and Kilburn 2003: 222. Poppe 2010b: 388, pl. 1189, figs 6, 7a, b. Yang et al. 2017: 240, 242, fig. 899. Surakiatchai et al. 2018: table 6, pl. 5, fig. 10a, b. Wells et al. 2021: 36.

Corbula (*Corbula*) *fortisulcata*. Robba et al. 2002: 117–118, pl. 20, fig. 5. Robba et al. 2003: table 3. Robba et al. 2007: 88 (appendix). Nabhitabhata 2009: 506.

Corbula (*Notocorbula*) cf. *fortisulcata*. Thach 2005: 303, pl. 91, fig. 4.

Corbula (*Notocorbula*) *fortisulcata*. Huber 2010: 467, with in-text fig. Huber 2015: C22606.

Referred material. CUF-NKKNY-B19 (154 shells; Figs 12J, 16D).

Habitat. Fine sand, sandy mud and muddy bottoms at intertidal to sublittoral zones at a depth from 1 to 70 m (Huber 2015).

Distribution. Indian Ocean; Indo-West Pacific, from Taiwan to Australia (Huber 2015). Records of fossils from the Late Miocene in the Philippines and from the Holocene in Thailand (Robba et al. 2002; Surakiatchai et al. 2018).

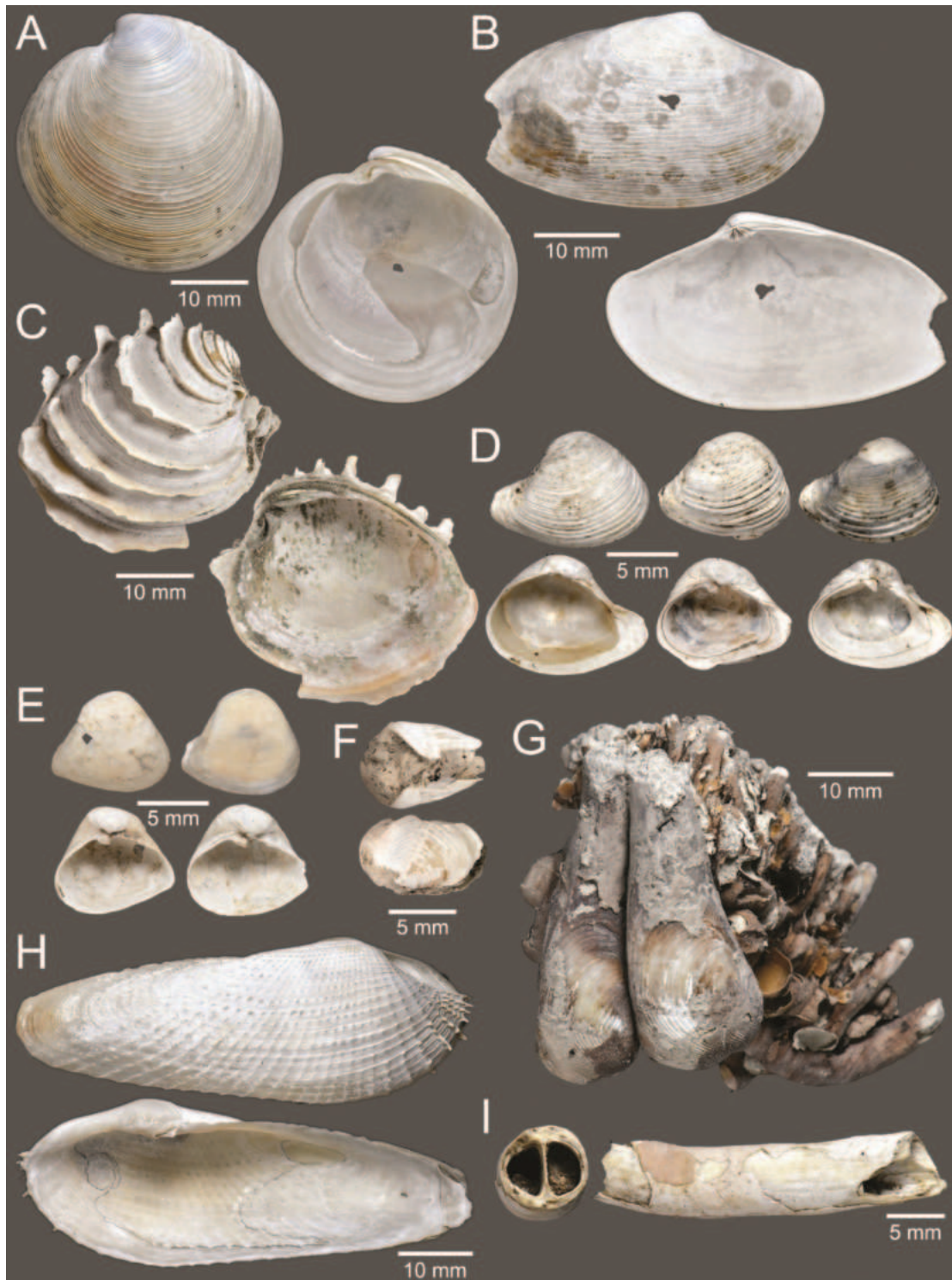


Figure 16. Bivalves **A** *Dosinia dilecta* **B** *Paratapes undulatus* **C** *Placamen lamellatum* **D** *Corbula fortisulcata* **E** *Potamocorbula* sp. **F, G** *Martesia striata* **G** showing the shells with burrow casts along with mangrove roots **H** *Pholas orientalis* **I** calcareous burrows of Teredinidae indet.

Record in Thailand. Gulf of Thailand and Andaman Sea (Wells et al. 2021).

Taxonomic remarks and comparisons. This species differs from its similar species, *Corbula tunicata* Reeve, 1843, by having a weaker keel on the juvenile shell part (Swennen et al. 2001).

Potamocorbula Habe, 1955

Potamocorbula sp.

Figs 12N, 16E

Referred material. CUF-NKNY-B26 (112 shells; Figs 12N, 16E).

Habitat. Mostly present in intertidal zones, estuarine and brackish habitats (Huber 2015).

Distribution. This genus is mostly distributed in the Indian Ocean and Indo-West Pacific, except for the species *Potamocorbula adusta* (Reeve, 1844), which is recorded only from West Africa (Huber 2015).

Taxonomic remarks and comparisons. These specimens are assigned to *Potamocorbula* based on the descriptions in Coan (2002), specifically in having smooth shells. Currently, there are a total of nine species in this genus (Huber 2015; MolluscaBase 2023), in which two species, *P. fasciata* (Reeve, 1843) and *P. laevis* (Hinds, 1843), are recorded from Thailand (Wells et al. 2021). However, our specimens have a more quadrate shell shape, probably suggesting the presence of other different species.

Superfamily Pholadoidea Lamarck, 1809

Family Pholadidae Lamarck, 1809

Martesia Sowerby I, 1824

Martesia striata (Linnaeus, 1758)

Figs 12M, 16F, G

Pholas striatus Linnaeus, 1758: 669. Type locality: southern Europe.

Pholas (Martesia) striata. Lynge 1909: 283–284.

Martesia striata. Cernohorsky 1978: 188, pl. 68, fig. 4. Morris and Purchon 1981: 327. Oliver 1992: 203, pl. 45, fig. 4a, b. Bosch et al. 1995: 279, fig. 1263. Yoosukh and Jitkaew 1997: 402, fig. 1a, b. Poutiers 1998a: 358, with in-text figs. Subba Rao and Dey 2000: 287. Swennen et al. 2001: 49, 99, fig. 223. Hylleberg and Kilburn 2003: 224. Dey and Ramakrishna 2007: 161, 252. Nabhitabhata 2009: 21, with in-text fig, 509. Haga 2010: 394, pl. 1192, figs 3, 4. Gopalakrishnan et al. 2012: 61. Okutani 2017: 1270, pl. 563, fig. 5. Yang et al. 2017: 246, fig. 914. Tudu et al. 2018: table 1. Wells et al. 2021: 37.

Martesia (Martesia) striata. Robba et al. 2002: 121–122, pl. 21, fig. 7a. Thach 2005: 304, pl. 91, fig. 10. Robba et al. 2007: 23, fig. 9p; 88 (appendix). Huber 2010: 476, with in-text figs. Huber 2015: C22956.

Referred material. CUF-NKNY-B14 (8L+8R shells; Figs 12M, 16F, G).

Habitat. Bored in old wood pilings, waterlogged tree trunks, and in driftwood but rarely in astroid corals, in soft rocks, or mangroves *Rhizophora stylosa*; from intertidal zones down to 20 m depth (Huber 2015).

Distribution. Cosmopolitan (Huber 2015). Records of fossils from the Middle Miocene to Holocene in Japan, Indonesia, New Hebrides, and Thailand (Robba et al. 2002).

Record in Thailand. Gulf of Thailand and Andaman Sea (Wells et al. 2021).

Taxonomic remarks and comparisons. This species is recognised based on the descriptions and figures in Poutiers (1998a), Robba et al. (2002), and Huber (2010), specifically in having an outer surface bearing a radial groove at the anterior one-third of the shell, sculptured with commarginal ridges that are minutely nodose and anterior to the radial groove with nodes arranged into radial rows.

***Pholas* Linnaeus, 1758**

***Pholas orientalis* Gmelin, 1791**

Figs 12U, 16H

Pholas orientalis Gmelin, 1791: 3216. Type locality: Siam [Thailand] and Tranquebar. Morris and Purchon 1981: 327. Nateewathana 1995: 111, with in-text fig. Poutiers 1998a: 356, with in-text figs. Subba Rao and Dey 2000: 286. Swennen et al. 2001: 50, 98, fig. 219. Haga 2010: 396, pl. 1193, figs 2, 3. BEDO 2017a: 168, with in-text fig. Hylleberg and Kilburn 2003: 224. Dey and Ramakrishna 2007: 160, 251–252. Nabhitabhata 2009: 510. Gopalakrishnan et al. 2012: 61. Yang et al. 2017: 246, fig. 916. Tudu et al. 2018: table 1. Wells et al. 2021: 37.

Pholas siamensis Spengler, 1792: 88–89. Type locality: the Gulf of Thailand, the mouth of the river Qweda, where it goes up to Alastav. Knudsen and Jensen 2001: 547–556, figs 1–4.

Pholas (Monothyra) orientalis. Lynge 1909: 282. Aungtonya et al. 1999: 383. Robba et al. 2002: 121, pl. 21, fig. 5. Robba et al. 2003: tables 3–5. Dharma 2005: 270, pl. 110, fig. 25; 368, pl. 149, fig. 18a, b. Thach 2005: 304, pl. 91, fig. 6. Robba et al. 2007: 88 (appendix). Huber 2010: 473, with in-text fig. Huber 2015: C22846.

Referred material. CUF-NKNY-B05 (26L+73R shells; Figs 12U, 16H).

Habitat. Boring down to 50 cm depth in peat, soft rocks, stiff clay, or sticky and soft sandy-mud bottoms rich in silt and detritus, often near river mouths, from intertidal and sublittoral zones at a depth from 1 to 30 m (Poutiers 1998a; Huber 2015).

Distribution. Indian Ocean; Indo-West Pacific, from Taiwan to Australia (Huber 2015). Records of fossils from the Middle Miocene to Holocene in Indonesia, Myanmar, and Thailand (Robba et al. 2002; Dharma 2005).

Record in Thailand. Gulf of Thailand and Andaman Sea (Wells et al. 2021).

Taxonomic remarks and comparisons. This species is recognised based on the descriptions and figures in Poutiers (1998a), Swennen et al. (2001), and Robba et al. (2002), specifically in having antero-dorsal reflection that has axial supports.

Famliy Teredinidae Rafinesque, 1815

Teredinidae indet.

Fig. 16I

Referred material. CUF-NKNY-B14-4 (83 tube pieces; Fig. 16I).

Habitat. Boring into submerged wood and other plant material (Poutiers 1998a).

Taxonomic remarks and comparisons. The calcareous burrows have a septum dividing the cavity in half, indicating that these burrows belong to the shipworm family Teredinidae (e.g., Chan and Lau 2021). Due to the absence of shells, it is impossible to assign the inhabitants to species or even genus level based on these trace fossils.

Order Adapedonta Cossmann & Peyrot, 1909

Superfamily Solenoidea Lamarck, 1809

Family Pharidae H. Adams & A. Adams, 1856

***Cultellus* Schumacher, 1817**

***Cultellus maximus* (Gmelin, 1791)**

Figs 13G, 17A

Solen maximus Gmelin, 1791: 3227. Type locality: Nicobar.

Solen lacteus Spengler, 1794: 94–95. Type locality: Nicobar.

Cultellus lacteus. Tantanasiwong 1979: 11. Morris and Purchon 1981: 325.

Nateewathana et al. 1981: 66. Aungtonya et al. 1999: 379. Robba et al. 2002: 92, pl. 12, fig. 10. Robba et al. 2007: 86 (appendix). Nabhitabhata 2009: 423.

Cultellus maximus. Subba Rao and Dey 2000: 251. Swennen et al. 2001: 47, 83, text-fig. 121, fig. 121. Huber 2010: 271, with in-text fig. Negri et al. 2014: table 3. Huber 2015: C12478. BEDO 2017a: 48, with in-text fig. Tudu et al. 2018: table 1. Wells et al. 2021: 18.

Referred material. CUF-NKNY-B23 (6L+3R shells; Figs 13G, 17A).

Habitat. Deeply (down to 40 cm) buried in soft mud at seaward fringes of mangrove forests or intertidal zones down to 3 m depth (Huber 2015).

Distribution. Indian Ocean; Indo-West Pacific, from Taiwan to Borneo Island (Huber 2015). Records of fossils from the Holocene in Thailand (Robba et al. 2002).

Record in Thailand. Gulf of Thailand and Andaman Sea (Wells et al. 2021).

Taxonomic remarks and comparisons. Due to the large size and oblong-elliptical shape of shells (Robba et al. 2002; Huber 2010), we identified these specimens as belonging to *Cultellus maximus*.

***Siliqua* Megerle von Mühlfeld, 1811**

***Siliqua minima* (Gmelin, 1791)**

Figs 12I, 17B

Solen minimus Gmelin, 1791: 3227. Type locality: Tranquebar.

Siliqua minima. Lyngé 1909: 278. Swennen et al. 2001: 47, 84, text-fig. 126, fig.

126. Robba et al. 2002: 93, pl. 12, fig. 11a, b. Robba et al. 2003: tables 3–5. Robba et al. 2007: 86 (appendix). Nabhitabhata 2009: 424. Negri et al. 2014: table 3. Yang et al. 2017: 218, fig. 822. Wells et al. 2021: 19.

Siliqua cf. *minima*. Hylleberg and Kilburn 2003: 195–196, pl. 8, fig. 10. Thach 2005: 281.

Siliqua (*Neosiliqua*) *minima*. Huber 2010: 273, with in-text fig. Huber 2015: C12603.

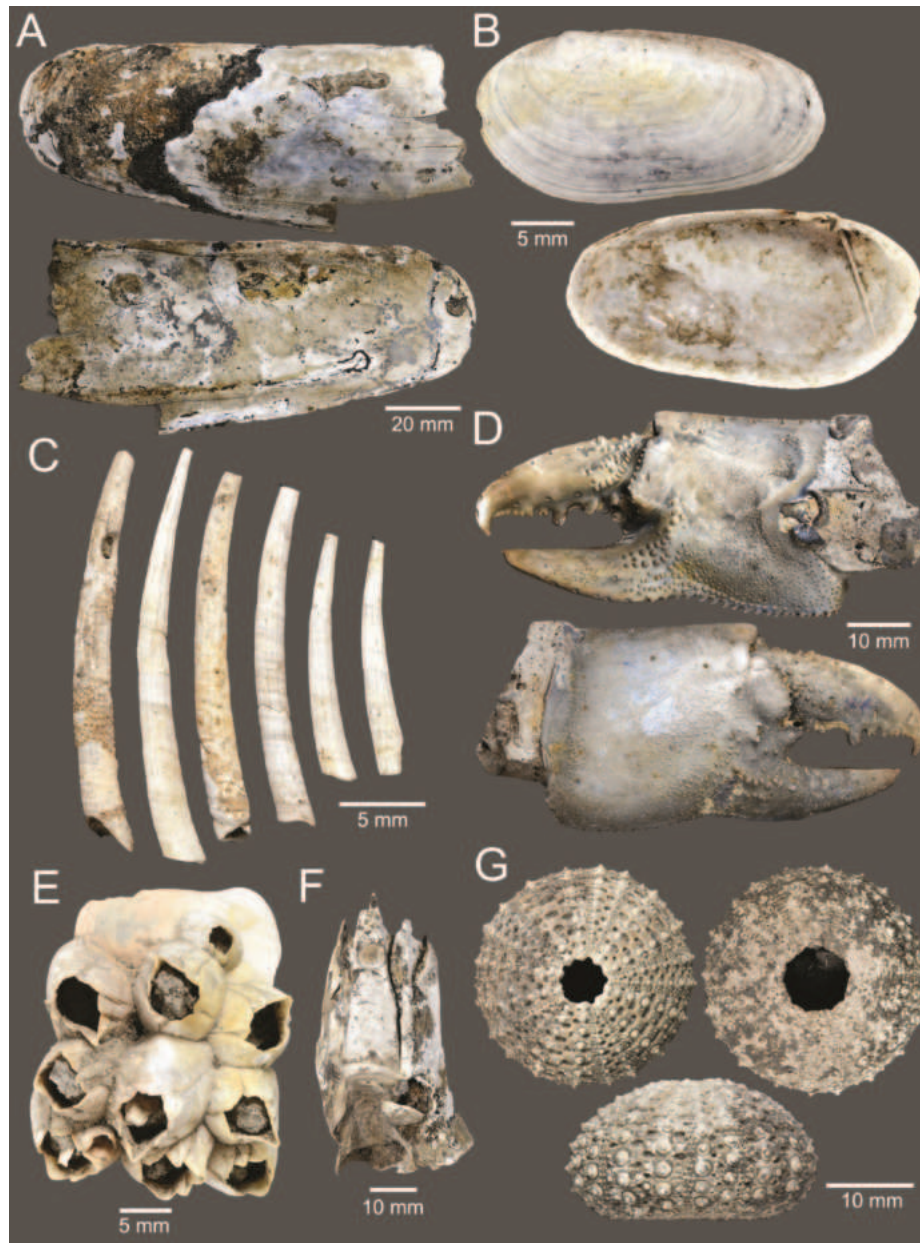


Figure 17. Bivalves and other invertebrates **A** *Cultellus maximus* **B** *Siliqua minima* **C** *Dentalium variabile* **D** *Thalassina* sp. **E** *Fistulobalanus kondakovi* **F** *Megabalanus* cf. *tintinnabulum* **G** *Temnotrema siamense*.

Referred material. CUF-NKNY-B16 (6L+6R shells; Figs 12I, 17B).

Habitat. Sand and mud bottoms from intertidal zones down to 30 m depth (Huber 2015).

Distribution. Indian Ocean; Indo-West Pacific, from Japan to the Philippines (Robba et al. 2002; Huber 2015). Records of fossils from the Holocene in Thailand (Robba et al. 2002).

Record in Thailand. Gulf of Thailand (Wells et al. 2021).

Taxonomic remarks and comparisons. This species is recognised based on the descriptions and figures in Robba et al. (2002) and Huber (2010), specifically in having an ovate-rectangular and inequilateral shell with a widely rounded and deep pallial sinus, the lower border of which coincides with the pallial line, and a thin and slightly oblique inner rib.

Class Scaphopoda Bronn, 1862
Order Dentaliida Starobogatov, 1974
Family Dentaliidae Children, 1834
***Dentalium* Linnaeus, 1758**

***Dentalium variabile* Deshayes, 1826**
Figs 12H, 17C

Dentalium variabile Deshayes, 1826: 352–353, pl. 16, fig. 30. Type locality: possibly India. Scarabino 1995: 200–201, fig. 16d, e. Robba et al. 2003: tables 1, 3–5. Robba et al. 2004: 13, pl. 1, fig. 1. Steiner and Kabat 2004: 660. Chaiwath-ee et al. 2007: table 1. Robba et al. 2007: 89 (appendix). Sahlmann and Poppe 2010: 406, pl. 1198, fig. 8. Negri et al. 2014: tables 3, 4. Wells et al. 2021: 164. *Dentalium (Lentigodentalium) variabile*. Dey and Ramakrishna 2007: 162, 257.

Referred material. CUF-NKNY-001 (48 shells; Figs 12H, 17C).

Habitat. Mud bottoms from a depth of 10–75 m (Robba et al. 2004).

Distribution. Indo-West Pacific, from Japan to Reunion Island and New Caledonia. Records of fossils from the Quaternary in Thailand (Robba et al. 2004).

Record in Thailand. Gulf of Thailand (Wells et al. 2021).

Taxonomic remarks and comparisons. This species is recognised based on the descriptions and figures in Scarabino (1995) and Robba et al. (2004), specifically in having a polygonal cross-section of apex and a circular aperture. See also comprehensive taxonomic remarks in Scarabino (1995).

Phylum Arthropoda
Subphylum Crustacea Brünnich, 1772
Class Malacostraca Latreille, 1802
Order Decapoda Latreille, 1802
Family Thalassinidae Latreille, 1831
***Thalassina* Latreille, 1806**

***Thalassina* sp.**
Figs 13I, 17D

Referred material. CUF-NKNY-009 (130 pieces; Figs 13I, 17D).

Habitat. Littoral and sublittoral zones, mangrove swamps and forests, and edges of estuaries (Ngoc-Ho and de Saint Laurent 2009).

Distribution. Indo-West Pacific, from Japan to Australia (Hyžný and de Angeli 2022). Records of fossils from the Miocene to Holocene in Indo-West Pacific, and from the Oligocene in Italy (Hyžný and de Angeli 2022).

Taxonomic remarks and comparisons. These specimens are assigned to *Thalassina* based on descriptions in Ngoc-Ho and de Saint Laurent (2009), Sakai and Türkay (2012), and Hyžný and de Angeli (2022), specifically in having a subchelate pereopod 1 with its propodus having dorsomesially tuberculated or spinuous carinae. There is a total of 13 species within this genus (Hyžný and de Angeli 2022), in which three species, *T. anomala* (Herbst, 1804), *T. gracilis* Dana, 1852, and *T. squamifera* De Man, 1915, are recorded from Thailand

(Ngoc-Ho and de Saint Laurent 2009; Sakai and Türkay 2012) (but see the comment on the record of *T. squamifera* in Thailand in Moh et al. (2013)). However, the pereopod 1 observed in our specimens is shorter and has a more quadrate shape. The dactylus that has a hooked tip is nearly as long as the fixed finger, suggesting an as yet unidentified species.

Class Thecostraca Gruvel, 1905

Subclass Cirripedia Burmeister, 1834

Order Balanomorpha Pilsbry, 1916

Family Balanidae Leach, 1817

Subfamily Amphibalaninae Pitombo, 2004

***Fistulobalanus* Zullo, 1984**

***Fistulobalanus kondakovi* (Tarasov & Zevina, 1957)**

Figs 12K, 17E

Balanus amphitrite var. *kondakovi* Tarasov & Zevina, 1957: 179, 191, fig. 76a–d.

Type locality: Japan.

Balanus kondakovi. Henry and Mclaughlin 1975: 114–123, text-figs 21, 22b, c, f; pl. 2, figs a–m. Yamaguchi 1977a: pl. 19, figs 6, 7; pl. 20, figs 4, 8, 12; pl. 21, fig. 4; pl. 22, figs 13–18. Yamaguchi 1977b: 176, 178, text-fig. 18. Kim and Kim 1980: 176, pl. 6, figs 1–8. Yamaguchi 1980: tables 1, 2. Jones et al. 2000: 279. Puspasari et al. 2000: tables 1, 2. Kim 2011: 119–121, fig. 64.

Balanus amphitrite kondakovi. Rosell 1973: 88, fig. 8a–j. Newman and Ross 1976: 63.

Fistulobalanus kondakovi. Zullo 1984: 1330. Pitombo 2004: 275. Prabowo and Yamaguchi 2005: table 3, fig. 3f. Chan et al. 2009: 248–251, figs 214–217. Jones and Hosie 2016: 287–288. Kepel' 2018: 50–51, fig. 1. Kim 2020: 75–78, figs 48, 49, table 2. Karasawa and Kobayashi 2022: 71, pl. 5, fig. 10a, b.

Referred material. CUF-NKNY-006-1 (217 individuals; Figs 12K, 17E).

Habitat. Attached to hard substrates, mainly shells of oysters and gastropod molluscs and stalks of seaweed, as well as wooden piles and supports, bamboo, various objects installed under water on muddy beds for oyster culture, and buoys, in freshened closed inner parts of bays and estuarine coastal areas, from intertidal to subtidal zones (Henry and Mclaughlin 1975; Chan et al. 2009; Kepel' 2018).

Distribution. Indian Ocean; Indo-West Pacific, from Japan to New Zealand (Henry and Mclaughlin 1975; Puspasari et al. 2000; Jones and Hosie 2016). Records of fossils from the Pleistocene and Holocene in Japan (Yamaguchi 1977b; Karasawa and Kobayashi 2022).

Record in Thailand. Gulf of Thailand (Henry and Mclaughlin 1975; Puspasari et al. 2000).

Taxonomic remarks and comparisons. The subfamily Amphibalaninae was erected to incorporate most of the species under the *Balanus amphitrite* complex/group (Pitombo 2004). Currently, there are a total of six species from this subfamily recorded from Thailand: *Amphibalanus amphitrite* (Darwin, 1854), *A. reticulatus* (Utinomi, 1967), *A. thailandicus* (Puspasari, Yamaguchi & Angsupanich, 2001), *A. variegatus* (Darwin, 1854), *Fistulobalanus kondakovi* (Tarasov

& Zevina, 1957), and *F. patelliformis* (Bruguère, 1789) (Henry and McLaughlin 1975; Puspasari et al. 2000, 2001; Pochai et al. 2017). The presence of two or more rows of parietal tubes on shell walls assigns these specimens to the genus *Fistulobalanus* (Zullo 1984; Chan et al. 2009). We attribute these specimens to *F. kondakovi* because of the smooth outer surface of shells without any longitudinal ribs (Henry and McLaughlin 1975; Chan et al. 2009; Kim 2011; Kepel' 2018).

Subfamily Megabalaninae Leach, 1817

***Megabalanus* Hoek, 1913**

***Megabalanus* cf. *tintinnabulum* (Linnaeus, 1758)**

Figs 13F, 17F

cf. *Lepas tintinnabulum* Linnaeus, 1758: 668. Type locality: Amboina, Indonesia [lectotype designation by Henry and McLaughlin (1986)].

cf. *Balanus (Megabalanus) tintinnabulum tintinnabulum*. Pilsbry 1916: 55–57, pl. 10, fig. 1, 1e. Hiro 1939: 258, fig. 7a–b.

cf. *Balanus tintinnabulum* var. *tintinnabulum*. Oliveira 1941: 11–14, text-fig. 1, pl. 2, figs. 1, 2; pl. 4, fig. 1; pl. 5, fig. 3; pl. 8, fig. 6.

cf. *Balanus tintinnabulum*. Holthuis and Heerebout 1972: 24–31, pl. 1, fig. a–e.

cf. *Megabalanus tintinnabulum*. Newman and Ross 1976: 68. Henry and McLaughlin 1986: 17–21, figs 1e, 2a, g, h, 3a–c, 5a–l. Jones et al. 2000: 282. Pitombo 2004: 275. Lozano-Cortés and Londoño-Cruz 2013: 466–467. Jones and Hosie 2016: 289–290. Pochai et al. 2017: 28–29, fig. 11

Referred material. CUF-NKNY-006-2 (2 individuals; Figs 13F, 17F).

Habitat. Attached on low exposed rocky shores in littoral areas, ship bottoms, and floating pontoons (Chan et al. 2009; Jones and Hosie 2016)

Distribution. Cosmopolitan (Jones and Hosie 2016).

Record in Thailand. Andaman Sea (Pochai et al. 2017). This is the first record of this species from Gulf of Thailand.

Taxonomic remarks and comparisons. These specimens are tentatively identified as belonging to *Megabalanus tintinnabulum* based on the descriptions and figures in Henry and McLaughlin (1986), Chan et al. (2009), and Pochai et al. (2017), specifically in having large cylindrical shells with smooth parietal surfaces and without spines.

Phylum Echinodermata

Class Echinoidea Schumacher, 1817

Order Camarodonta Jackson, 1912

Family Temnopleuridae Agassiz, 1872

***Temnotrema* Agassiz, 1864**

***Temnotrema siamense* (Mortensen, 1904)**

Figs 12T, 17G

Pleurechinus siamensis Mortensen, 1904: 79–82, pl. 1, figs 2, 7, 11, 20; pl. 2, figs 2, 9, 14, 15, 22; pl. 6, figs 16, 36; pl. 7, figs 14, 44, 53. Type locality: Koh

Mesan, 3–15 fathoms; Koh Chuen, 15–38 faths.; Koh Kram, 20–30 faths.; Koh Kahdat, 10 faths.

Temnotrema siamense. Clark 1925: 92. Mortensen 1940: 45. Mortensen and Gislén 1940: 103. Mortensen 1943: 259–262, fig. 139. Clark and Rowe 1971: 155. Price 1981: 8. Liao 1998: table 1. Lane et al. 2000: 485. Samyn 2003: table 2. Marsh and Morrison 2004: tables 1, 2, 5. Gopalakrishnan et al. 2012: 32. Filander and Griffiths 2014: 53. Schultz 2015: 258, 263–264, fig. 4.169b, c. Arachchige et al. 2017: table 3. Putchakarn 2018: 57, table 1. Arachchige et al. 2019: table 1. Köhler 2020: 9, 72–73, pl. 14, figs 11, 14. Mucharin and Sumitrakij 2022: 6, pl. 4, fig. 1.

Temnotrema siamensis. Putchakarn and Sonchaeng 2004: table 1.

Referred material. CUF-NKYN-002 (23 shells; Figs 12T, 17G).

Habitat. Coarse and high energy subtidal sand from a depth of 5–350 m (Price 1981; Schultz 2015).

Distribution. Persian Gulf and Indian Ocean; Indo-West Pacific, from South China Sea to Australia (Mortensen 1904; Price 1981; Schultz 2015; Arachchige et al. 2019).

Record in Thailand. Gulf of Thailand and Andaman Sea (Putchakarn and Sonchaeng 2004).

Taxonomic remarks and comparisons. This species is recognised based on the descriptions and figures in Mortensen (1904), Clark and Rowe (1971) and Schultz (2015), specifically in having deep horizontal grooves in ambulacral and interambulacral plates and in lacking a horizontal series of tubercles.

Phylum Chordata

Subphylum Vertebrata Lamarck, 1801

Class Chondrichthyes Huxley, 1880

Subcohort Selachimorpha Nelson, 1984

Superorder Galeomorphii Compagno, 1973

Order Carcharhiniformes Compagno, 1977

Family Carcharhinidae Jordan & Evermann, 1896

Carcharhinus Blainville, 1816

Carcharhinus cf. *amblyrhynchoides* (Whitley, 1934)

Fig. 18A–E

cf. *Gillisqualus amblyrhynchoides* Whitley, 1934: 189–191, text-fig. 4. Type locality: Cape Bowling Green, Queensland.

cf. *Carcharhinus amblyrhynchoides*. Compagno 1984: 458–459, with in-text figs. Krajangdara et al. 2022: 49, with in-text figs.

Referred material. CUF-NKYN-S3-2 (Fig. 18A–E) (1 upper tooth).

Description. The crown of CUF-NKYN-S3-2 is triangular and erect with fine serrations and displays well-developed heels mesially and distally. Its lingual face is distinctly more convex than the labial one. Its base presents a damaged lingual face.

Habitat. Tropical, inshore and offshore, coastal-pelagic species, found over the continental and insular shelves (Compagno 1984).

Distribution. Gulf of Aden and Indian Ocean; Indo-West Pacific, from southern China to Australia (Compagno 1984).

Record in Thailand. Gulf of Thailand and Andaman Sea (Compagno 1984; Krajangdara et al. 2022).

Taxonomic remarks and comparisons. The specimen CUF-NKNY-S3-2 represents an anterior upper tooth. Several species of *Carcharhinus* have similar upper teeth in terms of morphology. Additional teeth and larger assemblages are needed for a more precise identification. Nevertheless, the tooth most resembles the upper teeth of *C. amblyrhynchoides* (Garrick 1982: fig. 20). Male individuals of *C. brachyurus* have somewhat similar upper teeth (Garrick 1982: fig. 51), but the mesial cutting edge of their crown is often more convex. *Carcharhinus limbatus* also shows the same characters, but the serration on the cusps at the base of the crown is much finer (Bass et al. 1973: pl. 5; Garrick 1982: fig. 18). The pattern of serration also resembles that of the lower teeth of *C. sorrah*, although in the latter, the base of the root is more concave and the heels of the crown are better developed, the teeth being longer mesio-distally than high baso-apically (Voigt and Weber 2011). Regarding the fossil record in Southeast Asia, similar teeth have been reported from the Late Miocene deposits of Brunei in Borneo (Kocsis et al. 2019).

***Carcharhinus cf. amblyrhynchos* (Bleeker, 1856)**

Fig. 18F–J

cf. *Carcharias (Prionodon) amblyrhynchos* Bleeker, 1856: 467–468. Type locality: Java Sea near Solombo Island.

cf. *Carcharhinus amblyrhynchos*. Compagno 1984: 459–461, with in-text figs. Krajangdara et al. 2022: 49, with in-text figs.

Referred material. CUF-NKNY-S3-10 (Fig. 18F–J) (1 upper tooth).

Description. The crown of CUF-NKNY-S3-10 displays a rather narrow main cusp with well-developed heels. The main cusp is regularly serrated, with an almost straight mesial edge and a distal one that is slightly concave. It is thus inclined distally. The labial side of the main cusp is nearly flat, whereas the lingual one is convex. Both the mesial and distal heels of the crown are poorly preserved and their serration pattern cannot thus be observed. The base of the root is concave and the nutritive groove on the bulged lingual face is poorly developed or heavily worn. The labial face of the root is nearly flat.

Habitat. Continental and insular shelves and adjacent oceanic waters (Compagno 1984).

Distribution. Indo-western to Central Pacific (Compagno 1984).

Record in Thailand. Gulf of Thailand and Andaman Sea (Compagno 1984; Krajangdara et al. 2022).

Taxonomic remarks and comparisons. The general shape of the crown, the regular serration of the main cusp, and the arched root are reminiscent of *C. amblyrhynchos* (Bass et al. 1973; Garrick 1982; Kocsis et al. 2019; Malyskina et al. 2023), but the poorly preserved heels of the teeth make a definite identification difficult to ascertain.

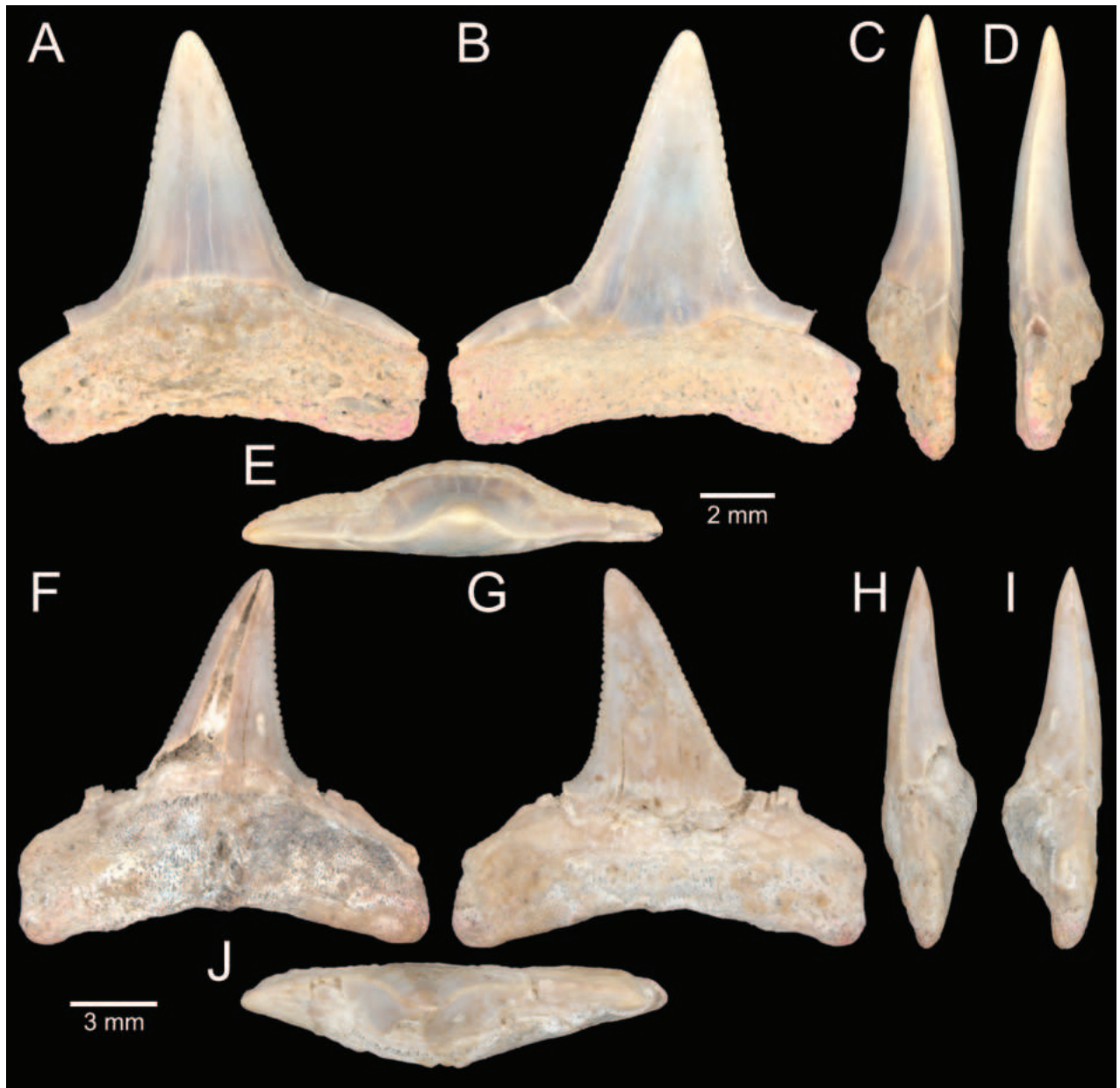


Figure 18. Carcharhinid shark teeth **A–E** *Carcharhinus* cf. *amblyrhynchoides*, specimen CUF-NKNY-S3-2 in **A** lingual **B** labial **C** mesial **D** distal and **E** apical views **F–J** *Carcharhinus* cf. *amblyrhynchos*, specimen CUF-NKNY-S3-10 in **F** lingual **G** labial **H** mesial **I** distal and **J** apical views.

***Carcharhinus* cf. *leucas* (Valenciennes, 1839)**

Fig. 19

cf. *Carcharias* (*Prionodon*) *leucas* Valenciennes in Müller & Henle, 1839: 42–43.
Type locality: Antilles.

cf. *Carcharhinus leucas*. Compagno 1984: 478–481, with in-text figs. Krajang-dara et al. 2022: 52, with in-text figs.

Referred material. CUF-NKNY-Q04 (Fig. 19A–I), CUF-NKNY-SA-1 (Fig. 19J–N), CUF-NKNY-SB-3, CUF-NKNY-SC-5 (4 upper teeth).

Description. Crowns show well-developed serrations, becoming larger and more complex in the basal part of the distal side of the crown. In labial or lingual view, the mesial side is almost straight, whereas the distal one is concave in its lower third. The outline of the base of the crown is more concave on the lingual face than on the labial one. The root is deep, slightly concave at its base, and does not display a nutritive groove in lingual view.

Habitat. Close inshore in reef-associated marine habitats, mostly in water less than 30 m depth (Compagno 1984; Krajangdara et al. 2022).

Distribution. Cosmopolitan in tropical and subtropical seas, but also reported from estuaries and rivers, tolerant of freshwater conditions (Compagno 1984).

Record in Thailand. Gulf of Thailand and Andaman Sea (Compagno 1984; Krajangdara et al. 2022).

Taxonomic remarks and comparisons. Teeth of *C. amboiensis* are very similar to those of *C. leucas* so that it is very difficult to differentiate them (Kocsis et al. 2019). As a result, ten incomplete teeth may belong either to *C. leucas* or *C. amboiensis*: CUF-NKNY-S2-1, CUF-NKNY-S3-9, CUF-NKNY-S5-1, CUF-NKNY-S5-5, CUF-NKNY-SA-6, CUF-NKNY-SB-2, CUF-NKNY-SC-10, CUF-NKNY-SD-7, CUF-NKNY-SE-3 and CUF-NKNY-SE-9.

***Carcharhinus cf. sorrah* (Valenciennes, 1839)**

Fig. 20

cf. *Carcharias (Prionodon) sorrah* Valenciennes in Müller & Henle, 1839: 45–46, pl. 16. Type locality: Java.

cf. *Carcharhinus sorrah*. Compagno 1984: 500–501, with in-text figs. Krajangdara et al. 2022: 57, with in-text figs.

Referred material. CUF-NKNY-3.1 (Fig. 20A–G), CUF-NKNY-3.2 (Fig. 20H–N) (2 upper teeth).

Description. The crown is compressed labio-lingually. The labial face is slightly flatter than the lingual one. The cusp is inclined distally and presents a notch on its distal part. The serrations do not reach the apex of the main cusp and are enlarged, becoming more complex basally, especially on the distal heel. The mesial edge of the crown is almost straight in labial or lingual view. The base of the root is slightly concave in lingual or labial view. There is a well-developed groove with a nutritive foramen at the base of the root in lingual view.

Habitat. Coastal, shallow-water zones of the continental and insular shelves, primarily around coral reefs at intertidal zones down to 73 m depth (Compagno 1984; Krajangdara et al. 2022).

Distribution. Red Sea and Indian Ocean; Indo-West Pacific, from China to Australia (Compagno 1984).

Record in Thailand. Gulf of Thailand and Andaman Sea (Compagno 1984; Krajangdara et al. 2022).

Taxonomic remarks and comparisons. Some upper teeth of *C. sorrah* appear to display a mesial cutting edge slightly more convex than on our specimens, but this character is known to depend on ontogenetic stages and the position

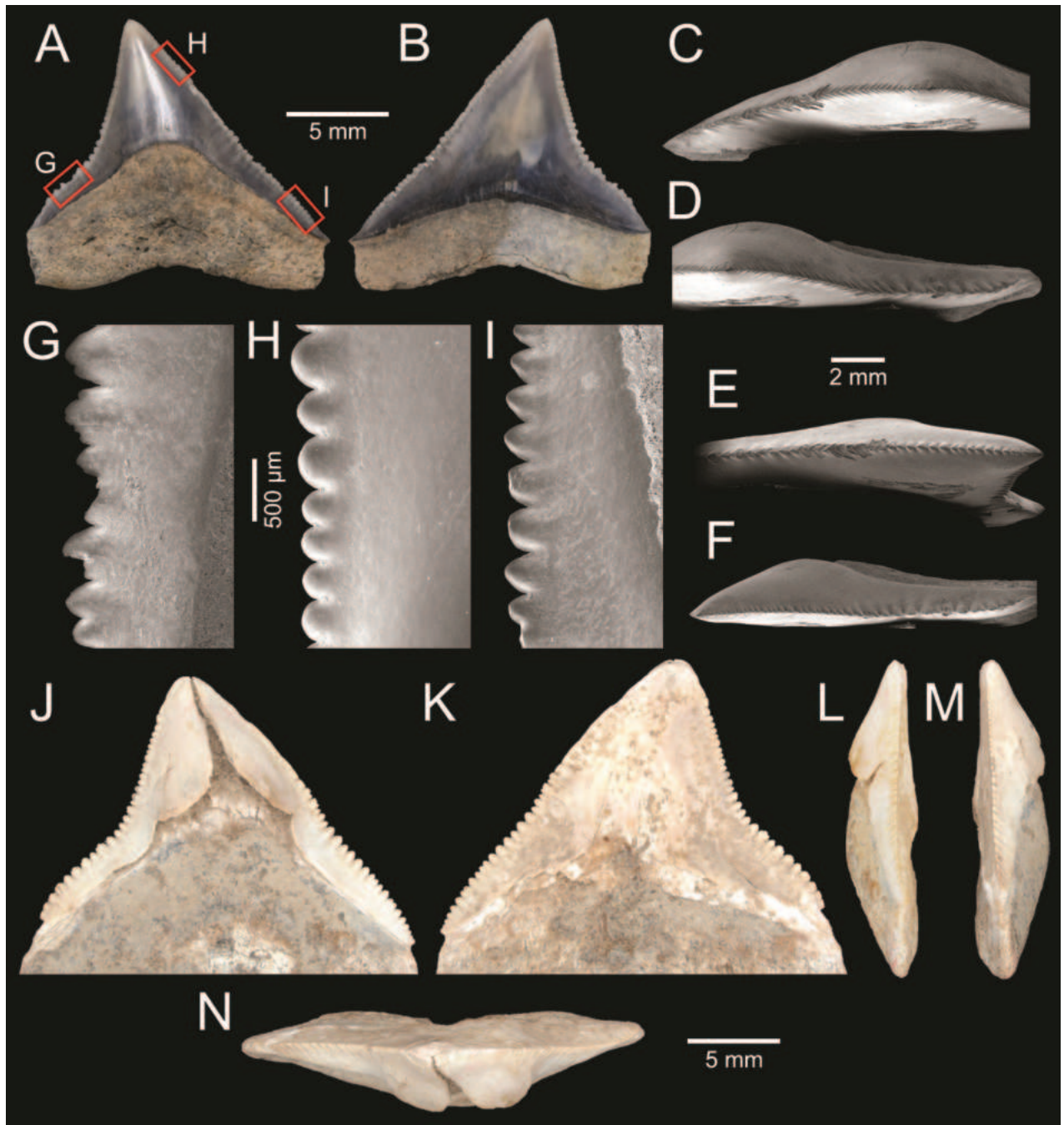


Figure 19. Carcharhinid shark teeth - *Carcharhinus* cf. *leucas* **A–I** specimen CUF-NKNY-Q04 in **A** lingual **B** labial and **C–F** different apical views **G–I** close-ups on the serrations of the distal cutting edge at the level of **G** distal heel and mesial cutting edge at the level of **H** upper part of the cusp and **I** heel. **J–N** specimen CUF-NKNY-SA-1 in **J** lingual **K** labial **L** mesial **M** distal and **N** apical views.

of the teeth in the jaw (e.g., Bass et al. 1973: pl. 13; Garrick 1982: fig. 76). Juveniles of *C. dussumieri* may have upper teeth with similar characteristics, but the distal cutting edge of the main cusp is not serrated. This latter character appears in larger specimens, but the mesial cutting edge of the main cusp becomes slightly concave. In addition, the distal heels and the distal root lobe of the fossil teeth are more elongated than the upper teeth of *C. dussumieri* (White 2012).

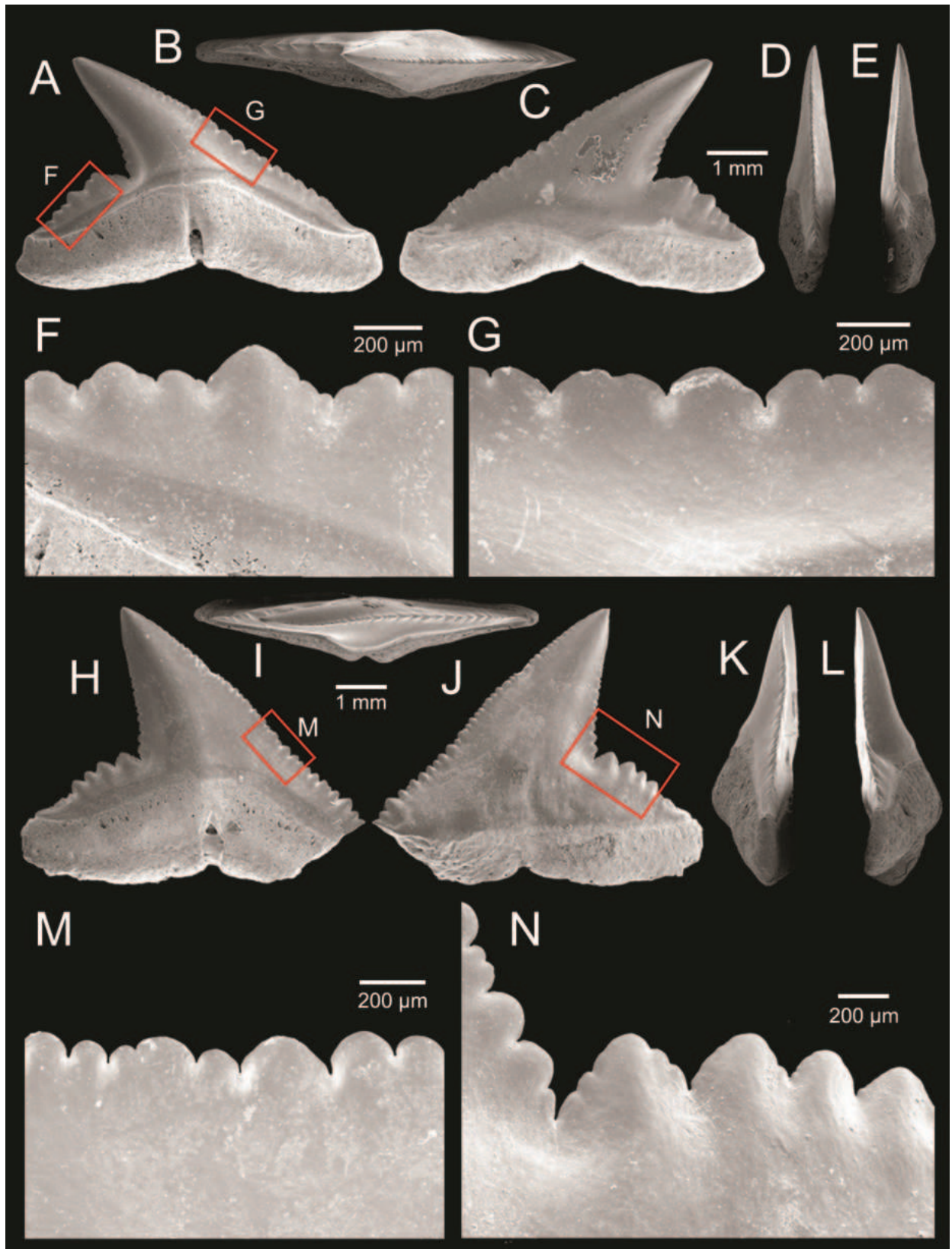


Figure 20. Carcharhinid shark teeth - *Carcharhinus* cf. *sorrah* **A–G** specimen CUF-NKNY-3.1 **A** lingual **B** apical **C** labial **D** mesial and **E** distal views **F**, **G** close-ups of the serration **F** on the distal heel and **G** on the middle part of the cusp mesial cutting-edge **H–N** specimen CUF-NKNY-3.2 **H** lingual **I** apical **J** labial **K** mesial and **L** distal views **M** close-up of the serration on the lower part of the mesial cutting-edge and **N** close-up of the serration between the heel and the base of the distal cutting edge.

***Carcharhinus* spp.**

Figs 21, 22

Referred material. CUF-NKNY-16.1 (Fig. 21A–G), CUF-NKNY-S2 (Fig. 21H–L), CUF-NKNY-S3-4, CUF-NKNY-S3-8, CUF-NKNY-S4-7 (5 lower teeth), CUF-NKNY-S1 (Fig. 22A–H), CUF-NKNY-S3-7 (two upper teeth).

Description. The specimens CUF-NKNY-16.1, CUF-NKNY-S3-4, CUF-NKNY-S3-8, and CUF-NKNY-S4-7 display a narrow main cusp that is inclined lingually. Their labial face is flatter than the lingual one. The serrations are well-developed in the upper two-third of the cusp. The serrations appear to be very fine on the mesial and distal heels in CUF-NKNY-16.1, CUF-NKNY-S3-4, and CUF-NKNY-S3-8, but the serrations are damaged in CUF-NKNY-S4-7. The root is well preserved only in CUF-NKNY-S3-4 and CUF-NKNY-S3-8, both of which display a slightly arched base, a moderately bulged lingual face with a nutritive foramen in its centre in CUF-NKNY-S3-4 and a faint nutritive groove in CUF-NKNY-S3-4. The specimen CUF-NKNY-S2 is asymmetric, with a mesial heel almost twice as elongated as the distal one and displays a sigmoid main cusp in labial or lingual view as well as in mesial or distal view, separated from the distal heel by a notch. The heels are serrated, but the main cusp is smooth. This tooth appears quite bulbous in mesial or distal view, being less compressed labio-lingually than the specimens described above. There is a well-developed nutritive groove on the root in lingual view, forming a basal notch in labial view.

A heavily worn tooth (CUF-NKNY-S3-7) is better attributed to an upper tooth. The lingual and distal faces of the crown are strongly damaged and a part of the distal end of the root is missing. The serration is only preserved in the middle part of the mesial cutting edge and appears to be quite regular. The root has a basal face slightly arched with a well-developed nutritive groove on its lingual face, forming a notch at the base of the root in labial view.

Another upper tooth, CUF-NKNY-S1, displays a crown with a quite coarse, irregular serration pattern nearly reaching the apex of the main cusp. The latter is bent lingually and slightly inclined distally. Its root shows a well-developed nutritive groove in lingual view, forming a notch at the base of the root in labial view. Apart from this notch, the base is almost straight.

Taxonomic remarks and comparisons. Lower teeth of *C. amblyrhynchos* (*C. wheeleri* in Garrick (1982): fig 51) display features similar to the specimen CUF-NKNY-16.1. They are characterised by a narrow main cusp that displays serrations ending at mid-height. Some of the lower teeth of *C. longimanus* also have these morphological patterns, though their crown is often more robust and wider at their base (Bass et al. 1973: pl. 17; Garrick 1982: fig. 70). Nevertheless, teeth very similar to the specimens CUF-NKNY-16.1, CUF-NKNY-S3-4, CUF-NKNY-S3-8, and CUF-NKNY-S4-7 from the Pliocene of Italy were attributed to *C. longimanus* (Marsili 2007).

The sigmoid crown of the specimen CUF-NKNY-S2 is reminiscent of the posterior lower teeth of *C. borneensis* and *C. tjtjtjot* (Voigt and Weber 2011). The dentition attributed to *C. dussumieri* by Voigt and Weber (2011) belongs in fact to *C. tjtjtjot* (White 2012). A sigmoid cusp, when present, is less developed in *C. sealei* and *C. sorrah* (Voigt and Weber 2011), and the distal heel is coarsely serrated in *C. coatesi* (White 2012). The morphology of the crown recalls that

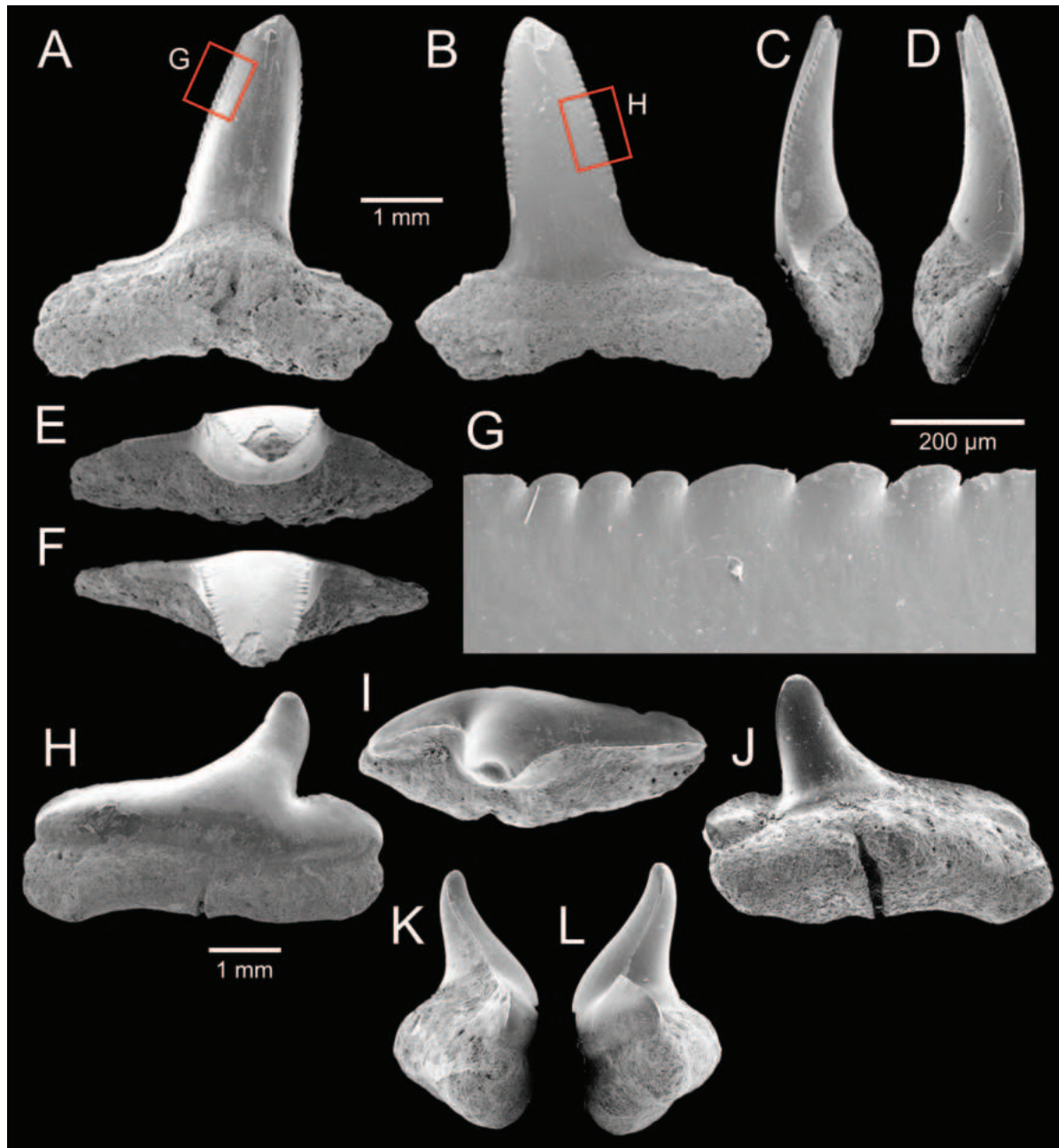


Figure 21. Carcharhinid shark teeth - *Carcharhinus* spp. **A–G** specimen CUF-NKNY-16.1 in **A** lingual **B** labial **C** mesial **D** distal and **E, F** apical views **G** close-ups of the serration on the upper part of the cusp mesial cutting edge in lingual view **H–L** specimen CUF-NKNY-S2 in **H** labial **I** apical **J** lingual **K** mesial and **L** distal views.

of *Rhizoprionodon*, but in the latter genus, the distal heel is often more convex than in the specimen CUF-NKNY-S2 (Cappetta 2012: fig. 283; Carrillo-Briceño et al. 2015). This set of lower teeth is therefore attributed to the genus *Carcharhinus* but represents more than a single species, whereas the specimen CUF-NKNY-S3-7 is poorly preserved. Moreover, the posterior part is only preserved in the specimen CUF-NKNY-S1 and this does not allow us to reach the species-level identification.

There are 27 species of the genus *Carcharhinus* reported from the Southeast Asian region (Froese and Pauly 2024), and at least 20 taxa were recorded in Thai waters (Krajangdara et al. 2022) including all the ones mentioned above.

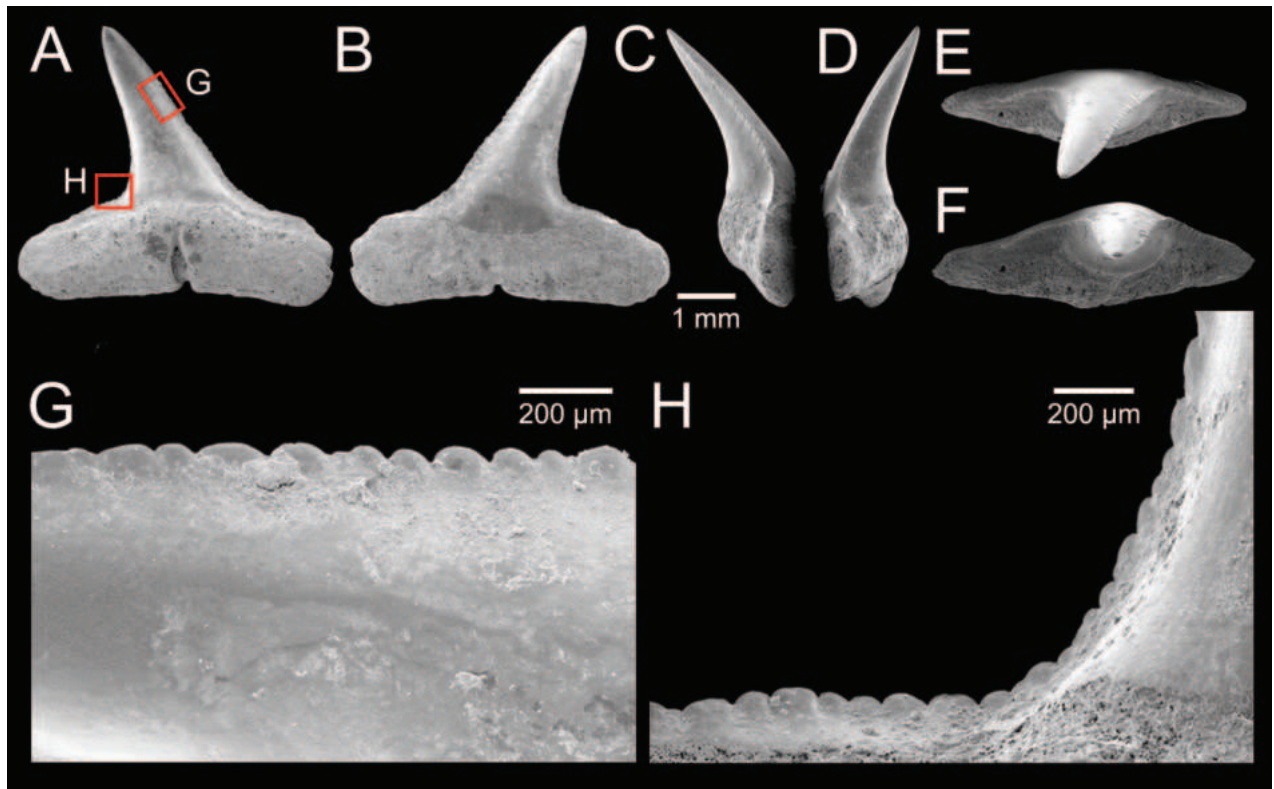


Figure 22. Carcharhinid shark teeth - *Carcharhinus* sp. **A–H** specimen CUF-NKNY-S1 in **A** lingual **B** labial **C** mesial **D** distal and **E, F** apical views **G, H** close-ups on the serration **G** at mid-height of the cusp mesial cutting-edge and **H** at the level of the distal heel and base of the cusp.

Glyphis Agassiz, 1843

Glyphis sp.

Figs 23–28

Referred material. CUF-NKNY-8.2 (Fig. 23A–H), CUF-NKNY-Q03 (Fig. 24A–H), CUF-NKNY-S5-2, CUF-NKNY-S5-4, CUF-NKNY-S5-6, CUF-NKNY-S5-7, CUF-NKNY-SA-2 to 5, CUF-NKNY-SA-7, CUF-NKNY-SA-8, CUF-NKNY-SB-1, CUF-NKNY-SB-4 to 9, CUF-NKNY-SC-1, CUF-NKNY-SC-3 (Fig. 25A–E), CUF-NKNY-SC-4, CUF-NKNY-SC-6, CUF-NKNY-SC-8, CUF-NKNY-SC-9, CUF-NKNY-SD1 to 3 (Fig. 25F–J), CUF-NKNY-SD6, CUF-NKNY-SD-8 to 10, CUF-NKNY-SE1 to 2, CUF-NKNY-SE-4 to 7, CUF-NKNY-SE-10 to 15, CUF-NKNY-SE-17 to 18 (46 upper teeth), CUF-NKNY-14 (Fig. 26A–H), CUF-NKNY-S1-1 to 4 (Fig. 26I–M), CUF-NKNY-S3-1 (Fig. 27A–E), CUF-NKNY-S3-5 to 6 (Fig. 27F–J), CUF-NKNY-S4-1 to 2 (Fig. 28A–E), CUF-NKNY-S4-4 to 6 (Fig. 28F–J) (13 lower teeth).

Description. Many teeth are poorly preserved. The crown of the upper teeth is triangular in outline, with a concavity at the base on both the mesial and distal sides in labial and lingual view, although the distal one is better marked, especially in anterior teeth (CUF-NKNY-S5-7). The serrations are quite fine and homogeneous in size along the cutting edges. The crown is strongly compressed labio-lingually and may be slightly curved lingually. When being broken, the crown displays a pulp cavity compressed labio-lingually, indicating an orthodont tooth histology (CUF-NKNY-SE-11). The base of the root is

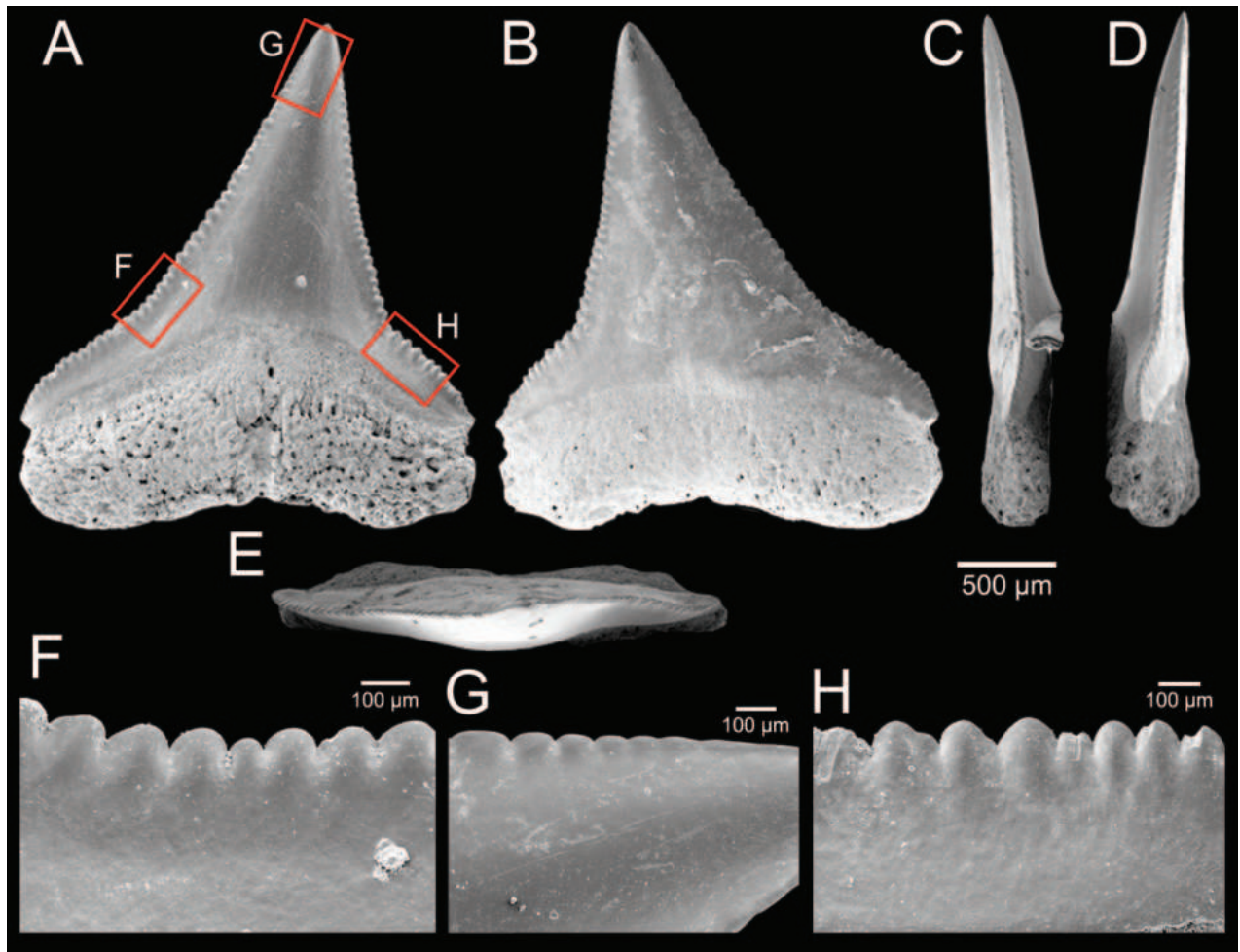


Figure 23. Carcharhinid shark teeth - *Glyphis* sp. specimen CUF-NKNY-8.2, upper lateral tooth in **A** lingual **B** labial **C** mesial **D** distal and **E** apical views **F–H** close-ups of the serration **F** at the base of the cusp mesial cutting-edge, **G** at the tip of the cusp and **H** on the distal heel.

slightly concave in labial or lingual view. A well-developed nutritive groove and/or a nutritive foramen may be present on the lower half of the lingual side of the root.

The lower teeth may reach 40 mm in height. They are narrower and less compressed labio-lingually than the upper ones. The enameloid is smooth and the labial face of the crown is flatter than the lingual one. The main cusp is inclined lingually, sometimes with a sigmoid outline (CUF-NKNY-S4-2, CUF-NKNY-S4-5). Three different crown morphologies are noted. (1) On the specimens CUF-NKNY-S1-1, CUF-NKNY-S1-2, and CUF-NKNY-S1-4, the crown is devoid of heels and the tip of the main cusp is spearhead-shaped, the latter being regularly serrated, whereas the rest of the crown is smooth. (2) The specimens CUF-NKNY-S4-1 and CUF-NKNY-S4-4 have a narrow and upright triangular main cusp devoid of serration, showing a tiny accessory cusplet on each side of the main cusp in CUF-NKNY-S4-4 or only lingually in CUF-NKNY-S4-1. (3) On the specimen CUF-NKNY-S3-6, the main cusp is also upright, narrow, triangular in shape, and serrated on their mesial and distal edges. Well-developed heels are present on each side of the main cusp, separated from the latter by a notch. The heel is

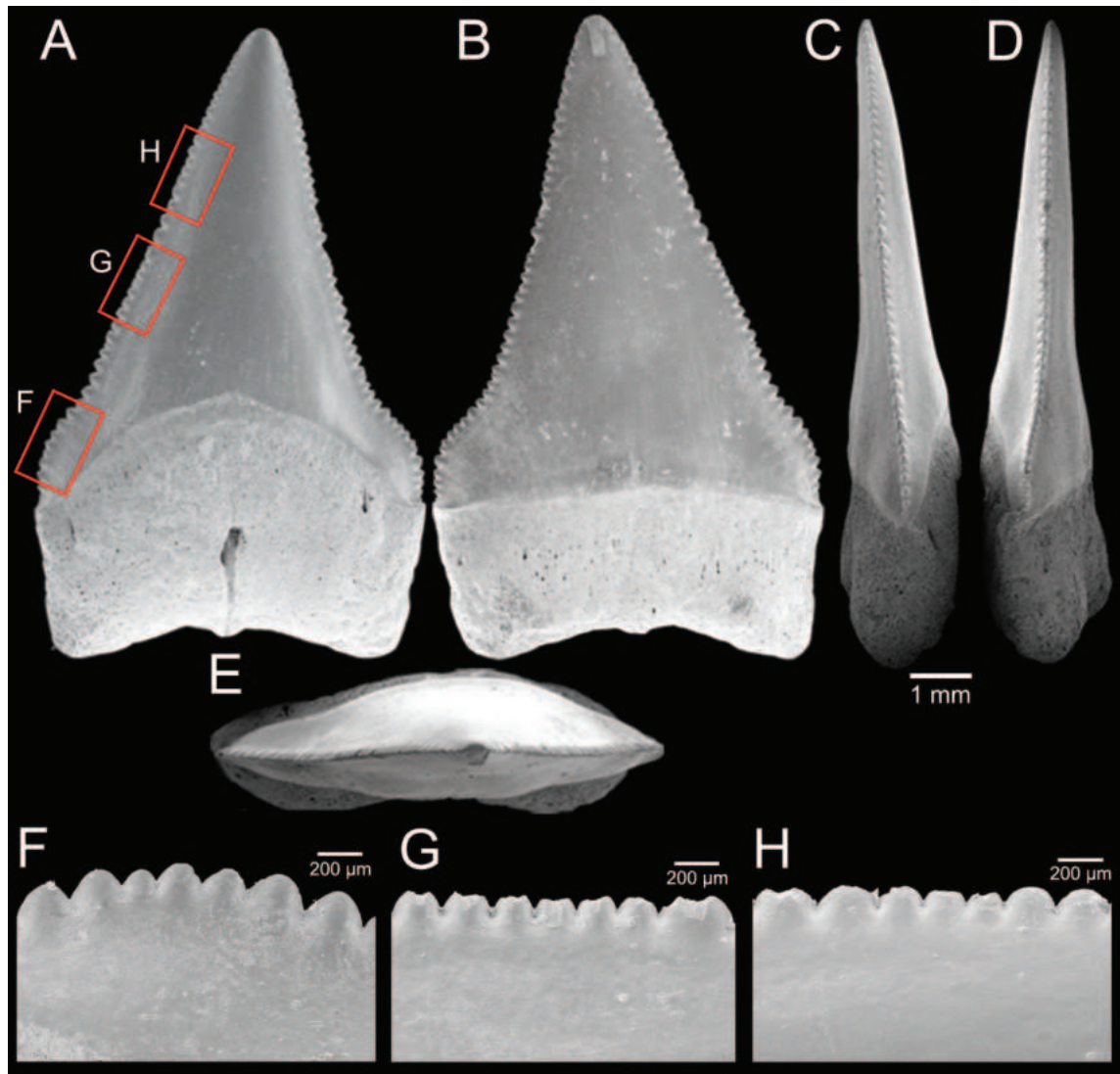


Figure 24. Carcharhinid shark teeth - *Glyphis* sp. specimen CUF-NKNY-Q03, upper anterior tooth in **A** lingual **B** labial **C** mesial **D** distal and **E** apical views **F–H** close-ups of the serration **F** at the base, **G** in the middle and **H** in the upper part of the cusp mesial cutting-edge.

sometimes less marked on the mesial side (CUF-NKNY-S3-1). The heels display less developed serration than on the main cusp. Many teeth belonging to this morphotype display a broken apex of the main cusp (CUF-NKNY-14).

The root displays a bulged lingual face. It is more massive and more arched in spearhead-shaped teeth than in heeled ones. There is a nutritive groove in the lingual side of the root with a nutritive foramen in its middle part that can be observed in most of the teeth. The specimen CUF-NKNY-S1-1 displays a double groove.

Taxonomic remarks and comparisons. Upper anterior teeth (CUF-NKNY-Q03) are more erect and narrower than the lateral ones (CUF-NKNY-8.2). Lower teeth with a spearhead-shaped apex correspond to the larger teeth in our sample, in agreement with the fact that this morphology is known only in anterior teeth of adult specimens of *Glyphis glyphis* and *G. garricki*. However, lateral teeth of these species display serrated heels and teeth of juveniles can display a pair of tiny lateral cusplets (Compagno et al. 2008; White et al. 2015). As a result, the three lower tooth morphotypes described above could be encountered into

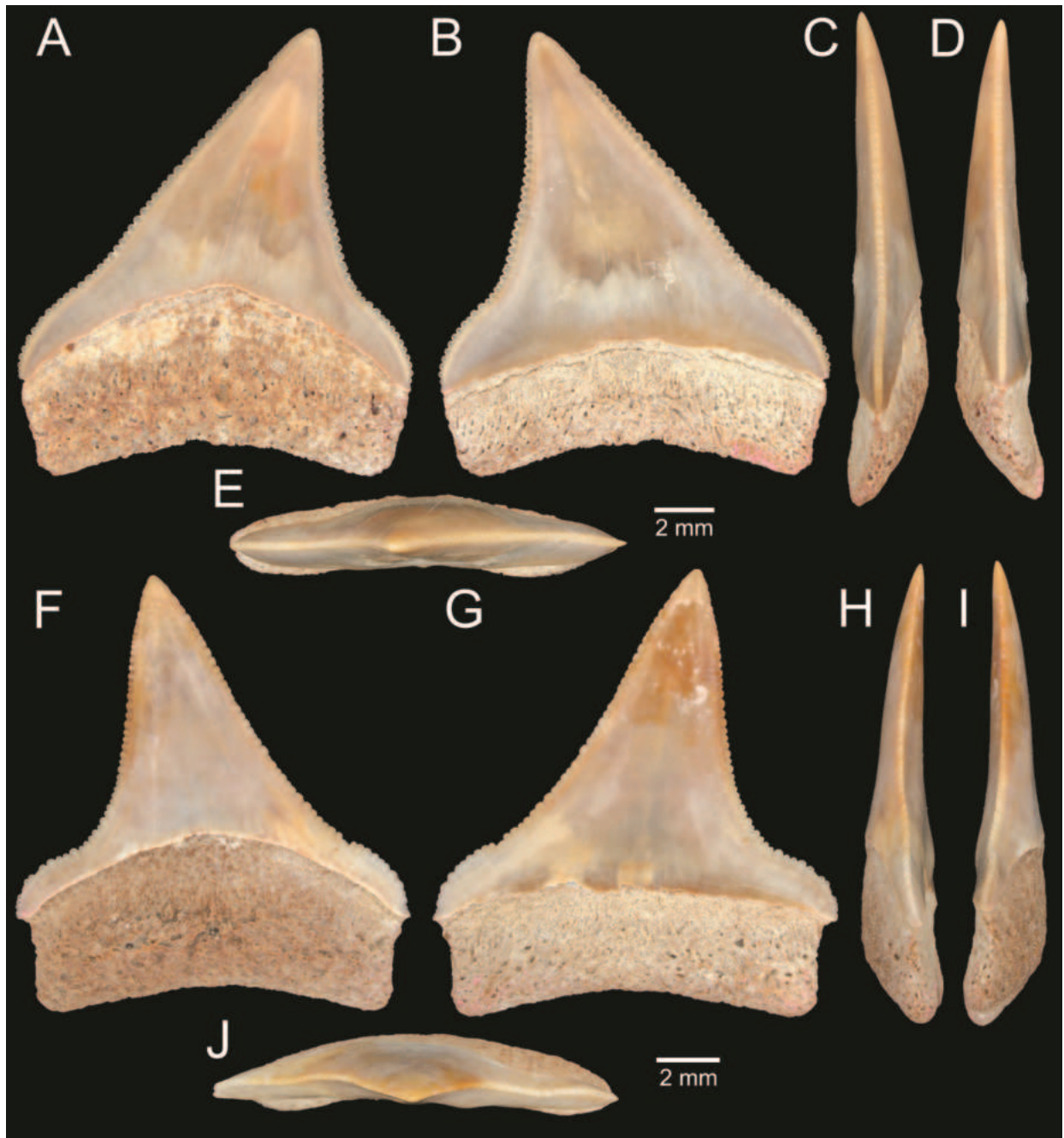


Figure 25. Carcharhinid shark teeth - *Glyphis* sp. **A–E** specimen CUF-NKNY-SC-3, upper anterolateral tooth in **A** lingual **B** labial **C** mesial **D** distal and **E** apical views **F–J** specimen CUF-NKNY-SD-3, upper lateral tooth in **F** lingual **G** labial **H** mesial **I** distal and **J** apical views.

a single species during its ontogeny. Otherwise, it could indicate the presence of more than one species, possibly three: *G. glyphis*, *G. garricki*, and *G. gangeticus*, as the latter species often possesses anterior lower teeth with tiny lateral cusplets but lacks the spearhead-shaped apex (Roberts 2006; Cappetta 2012). Consequently, the teeth described above are left in open nomenclature as *Glyphis* sp. This taxon appears to be most common in the studied fauna, although the discrepancies between the number of upper and lower teeth recovered suggest some degree of collecting bias.

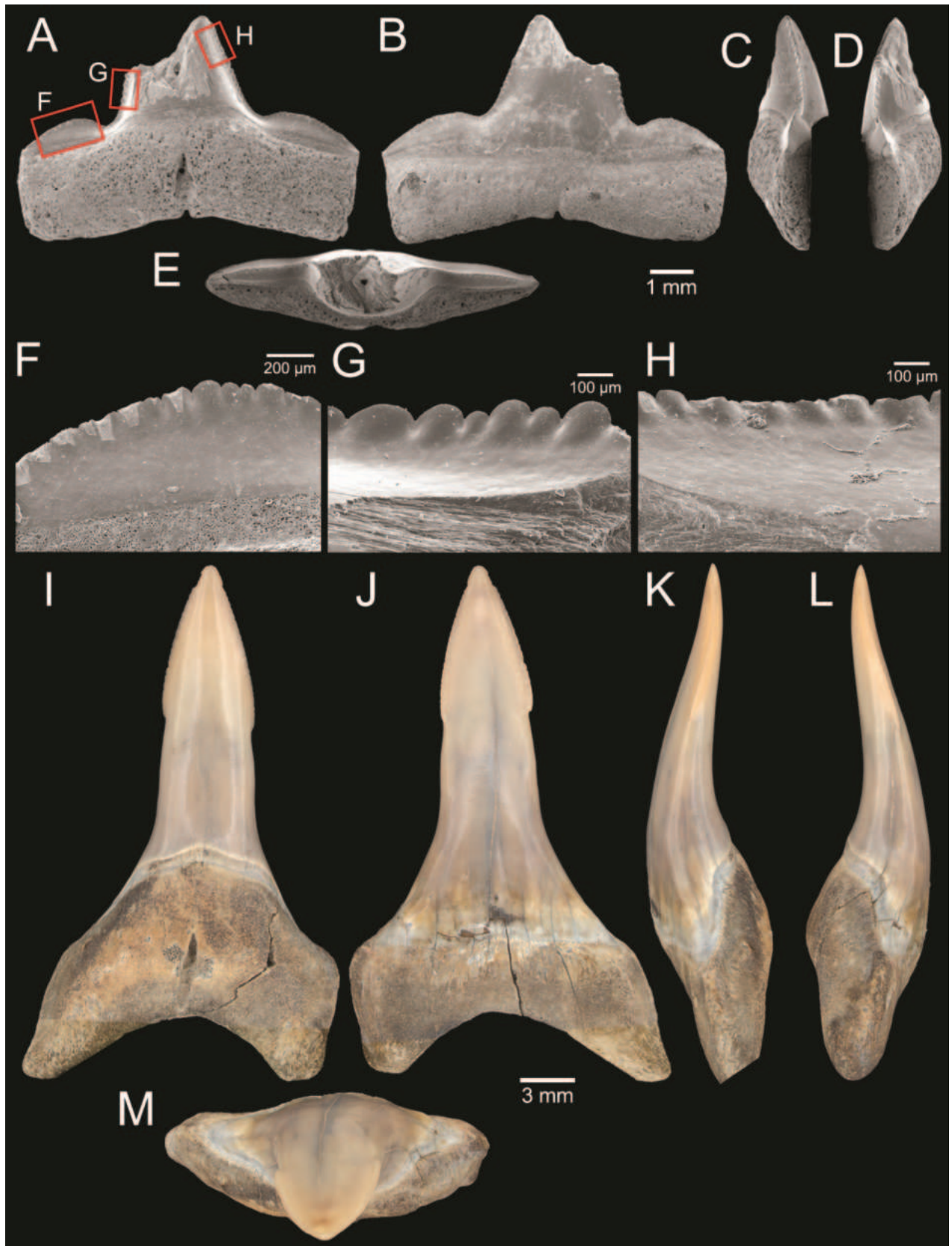


Figure 26. Carcharhinid shark teeth - *Glyphis* sp. **A–H** specimen CUF-NKNY-14, lower tooth in **A** lingual **B** labial **C** mesial **D** distal and **E** apical views **F–H** close-ups on the serration **F** on the distal heel, **G** at the base of the cusp distal cutting-edge and **H** in the middle part of the cusp mesial cutting-edge **I–M** specimen CUF-NKNY-S1-2, lower anterior tooth in **I** lingual **J** labial **K** mesial **L** distal and **M** apical views.

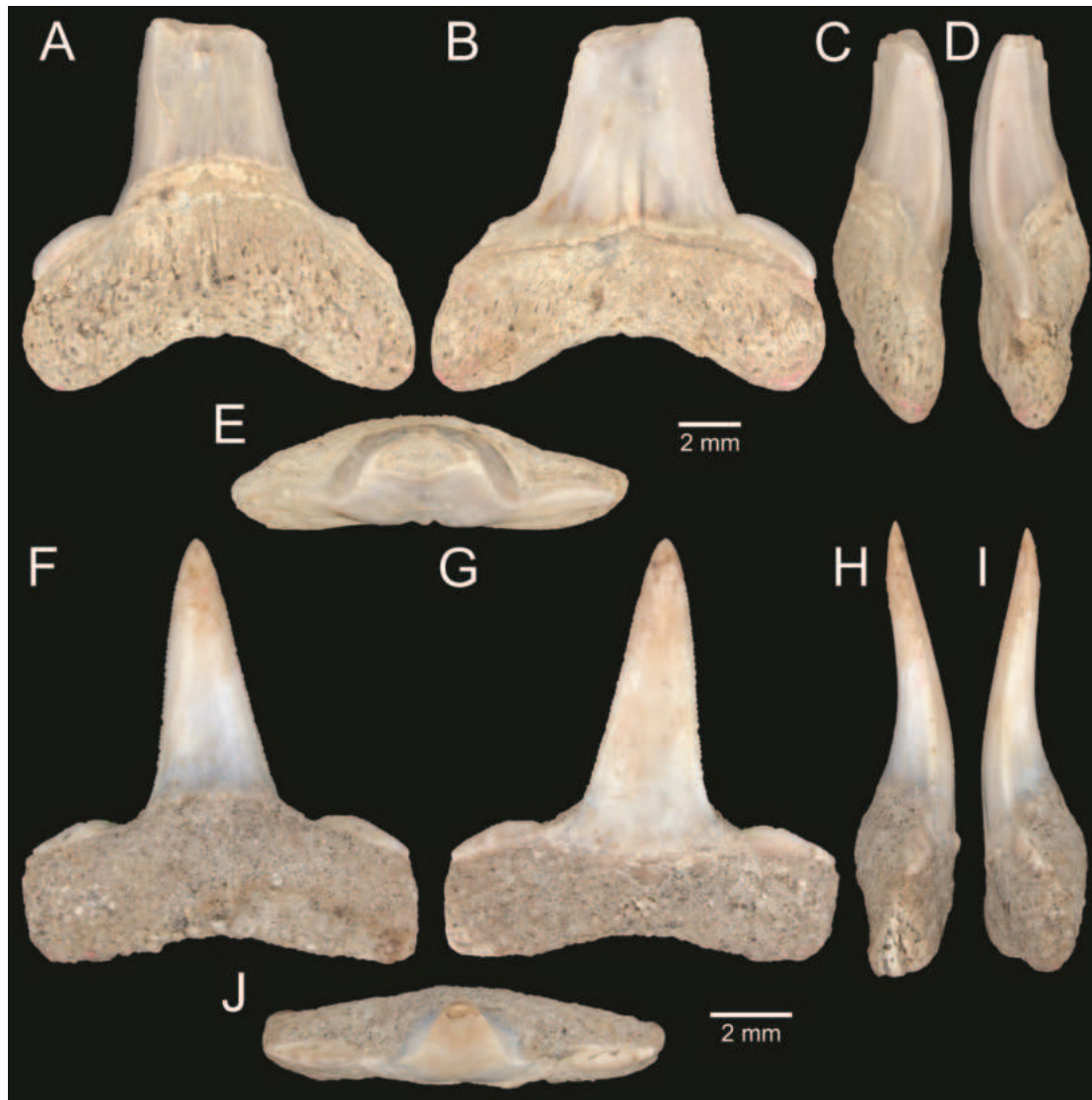


Figure 27. Carcharhinid shark teeth - *Glyphis* sp. **A–E** specimen CUF-NKNY-S3-1, lower tooth in **A** lingual **B** labial **C** mesial **D** distal and **E** apical views **F–J** specimen CUF-NKNY-S3-6, lower tooth in **F** lingual **G** labial **H** mesial **I** distal and **J** apical views.

The genus is specific to the Indo-West Pacific tropical region and often referred as “river shark” due to its habitat in or nearby rivers and estuaries. They are quite rare, hence difficult to study. Five living species are known (Froese and Pauly 2024), but DNA analyses suggest that some of these are conspecific (Li et al. 2015). On the other hand, teeth of *Glyphis* are often recorded from South-east Asia (Shimada et al. 2016; Kocsis et al. 2019 and references therein).

***Scoliodon* Müller & Henle, 1837**

***Scoliodon* cf. *laticaudus* Müller & Henle, 1838**

Fig. 29

cf. *Carcharias* (*Scoliodon*) *laticaudus* Müller & Henle, 1838: 28–29, pl. 8. Type locality: India.

cf. *Scoliodon laticaudus*. Compagno 1984: 534–535, with in-text figs. Krajang-dara et al. 2022: 62, with in-text figs.



Figure 28. Carcharhinid shark teeth - *Glyphis* sp. **A–E** specimen CUF-NKNY-S4-1, lower tooth in **A** lingual **B** labial **C** mesial **D** distal and **E** apical views **F–J** specimen CUF-NKNY-S4-4, lower anterior tooth in **F** lingual **G** labial **H** mesial **I** distal and **J** apical views.

Referred material. CUF-NKNY-S3–S5 (Fig. 29A–O) (3 teeth).

Description. The specimen CUF-NKNY-S3 is a small and elongated tooth with a low crown and a worn off root. The mesial cutting edge is concave and smooth and continues along the mesial heel. The distal edge of the crown is convex and separated by a notch from a distinct distal heel.

The specimen CUF-NKNY-S4 is a well-preserved tooth, with a crown strongly curved distally. The mesial cutting edge is sinusoid, starting convex, then becoming concave towards the apex. The apex of the crown overhangs distally the basal part of the tooth. The distal cutting edge is also sinusoid, though less so than the mesial one, and it is separated by a distinct notch from a well-developed distal heel. The enameloid of the crown extends more basally on the labial side of the tooth. The root is thick and the lobes run rather horizontally. It bears a well-developed and deep nutritive groove in the centre.

The cusp of the specimen CUF-NKNY-S5 is strongly sigmoid in labial and lingual view, and similar to that of CUF-NKNY-S4, but its cusp is narrower and less wide at the base, with more apparent mesial heels. The cutting edge is smooth and does not reach the apex of the cusp on its mesial side. The heels of the crown display faint serrations. The root is asymmetric and projected lingually and distally. There is a well-defined groove distally on the lingual side of the basal face, forming a deep notch in apical view.

Habitat. Tropical zones of continental and insular shelves close to inshore, frequently in rocky areas (Compagno 1984).

Distribution. Indian Ocean; Indo-West Pacific, from Japan to Indonesia (Compagno 1984).

Record in Thailand. Andaman Sea (Krajangdara et al. 2022).

Taxonomic remarks and comparisons. The three teeth best fit the dentition of the modern species *S. laticaudus* (spadenose shark). The specimen CUF-NKNY-S5 has a slender sigmoidal cusp and its mesial cutting edge does not reach the apex. It displays an asymmetric root, corresponding perfectly to a parasymphyseal tooth of a male specimen (Herman et al. 1991). The specimen CUF-NKNY-S4 likely represents an upper anterior-anterolateral tooth, whereas the specimen CUF-NKNY-S3 is probably a lower anterolateral tooth (see Springer 1964: fig. 3a). White et al. (2010) recognised another species, *S. macrorhynchus*, in the Western Pacific, meanwhile a molecular study also indicates the possible third *Scoliodon* species from the region (Lim et al. 2022), hence these fossil teeth are described in open nomenclature.

It may be mentioned that the specimen CUF-NKNY-S3 also resembles that of the lower anterolateral teeth of other common sharks in Southeast Asia (Krajangdara et al. 2022) such as *Loxodon macrorhinus* (slit-eye shark) and two *Rhizoprionodon* species, *R. acutus* (milk shark) and *R. oligolinx* (grey sharpnose shark). For the teeth of *Loxodon*, the apex of the crown is higher and somewhat aligned in a more distal position than that of the specimen CUF-NKNY-S3 (Springer 1964: fig. 4; Bass et al. 1975: pl. 8). The teeth of *R. oligolinx* seem to have a less concave mesial cutting edge (Springer 1964: fig. 13), whereas for *R. acutus*, the distal heel appears less elongated and vertically higher, but a clear distinction is difficult here (Springer 1964: fig. 6; Bass et al. 1975: pl. 9).

Carcharhinidae indet.

Referred material. CUF-NKNY-S3-3, CUF-NKNY-S4-3, CUF-NKNY-S5-3, CUF-NKNY-SC-2, CUF-NKNY-SC-7, CUF-NKNY-SD-4, CUF-NKNY-SD-5, CUF-NKNY-SD-11, CUF-NKNY-SE-8, CUF-NKNY-SE-16 (10 teeth).

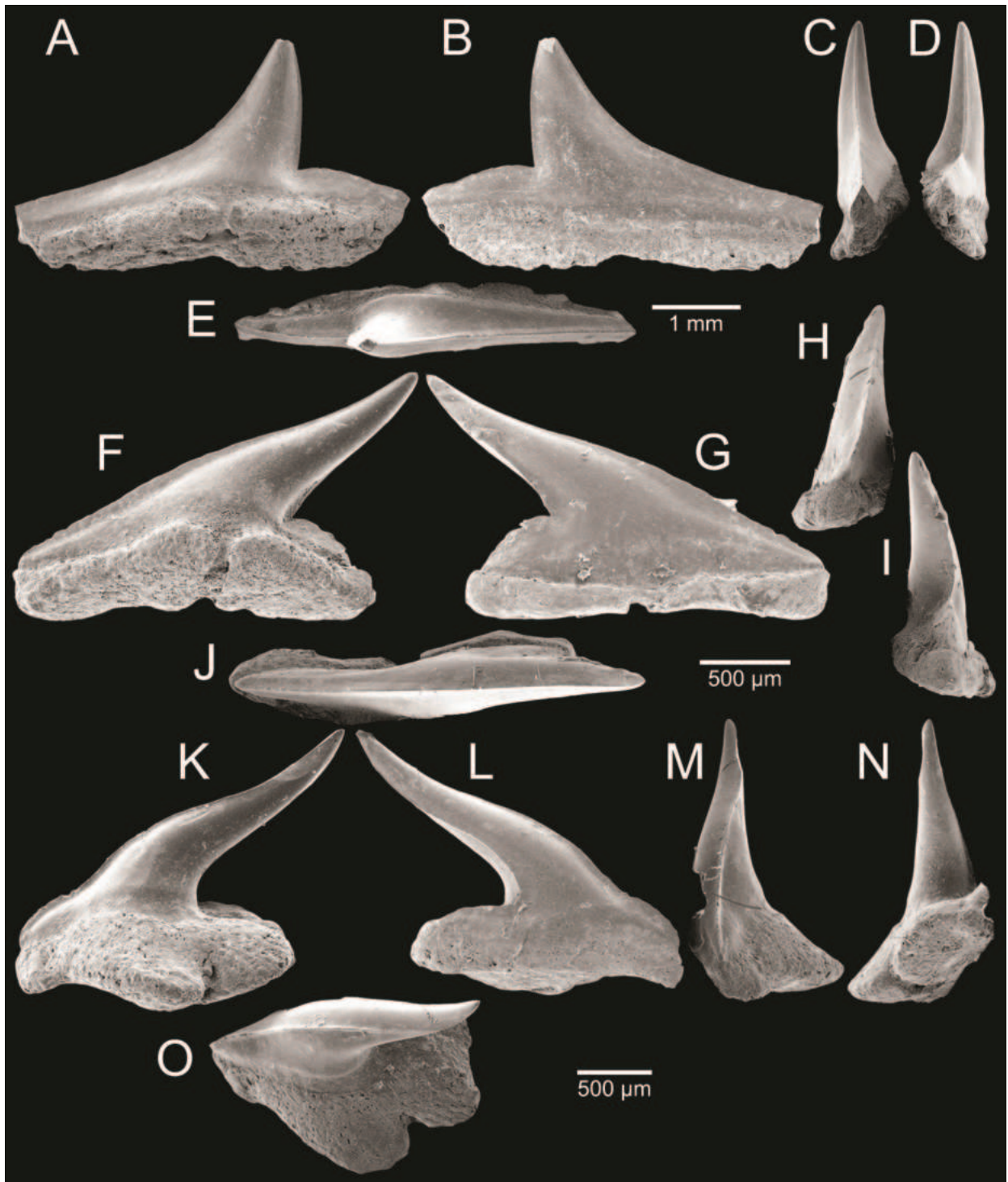


Figure 29. Carcharhinid shark teeth - *Scoliodon* cf. *laticaudus* **A–E** specimen CUF-NKNY-S3, lower anterolateral tooth in **A** lingual **B** labial **C** mesial **D** distal and **E** apical views **F–J** specimen CUF-NKNY-S4, upper anterior-anterolateral tooth in **F** lingual **G** labial **H** mesial **I** distal and **J** apical views **K–O** specimen CUF-NKNY-S5, parasymphyseal tooth in **K** lingual **L** labial **M** mesial **N** distal and **O** apical views.

Description. These teeth are poorly preserved. The crown is generally triangular, more or less narrow, and symmetric with serration incompletely preserved. The root is broken away or does not display the details of its vascularisation pattern.

Taxonomic remarks and comparisons. The presence of triangular serrated crowns suggests that most of the teeth belong to upper ones of *Carcharhinus* and/or *Glyphis*, but their poor preservation does not allow a more precise identification. The specimen CUF-NKNY-SC-7 may represent a lower tooth of *C. leucas*/*C. amboinensis*, but without the root and the base of the crown preserved, this is impossible to ascertain.

Superorder Batomorphii Capetta, 1980
Order Myliobatiformes Compagno, 1973
Family Dasyatidae Jordan & Gilbert, 1879
***Pastinachus* Rüppell, 1829**

***Pastinachus* sp.**

Fig. 30

Referred material. CUF-NKNY-7.1 (Fig. 30A–F), CUF-NKNY-7.2 (Fig. 30G–L), CUF-NKNY-8.1 (Fig. 30M–R) (3 teeth).

Description. The crown is hexagonal to diamond-shaped in apical view, longer mesio-distally than labio-lingually. The crown surface is rather smooth to heavily pitted. The labial face of the crown displays a salient horizontal bulge. There is a well-developed horizontal groove in the basal part of the crown on the lingual face. The vascularisation of the teeth is holaulacorhize. There is a row of small foramina positioned under the crown on the labial face and between one and four foramina present in the groove separating the two branches of the root in basal view.

Taxonomic remarks and comparisons. Heavily pitted crowns probably belong to non-functional teeth (Adnet et al. 2019). Four species of cowtail rays (*Pastinachus ater*, *P. gracilicaudus*, *P. solocirostris*, and *P. stellurostris*) are known in Southeast Asia (Last et al. 2016), all of them having been recorded in Thai waters (Krajangdara et al. 2022). Regarding the nearby fossil record, teeth of *Pastinachus* were reported from India, Taiwan, and Borneo (see discussion in Kocsis et al. 2019).

Class Actinopterygii Klein, 1885
Infraclass Teleostei Müller, 1845
Order Scombriformes Rafinesque, 1810
Family Trichiuridae Rafinesque, 1810

Trichiuridae indet.

Fig. 31

Referred material. CUF-NKNY-2.1 (Fig. 31A–F), CUF-NKNY-2.2 (Fig. 31G–K), CUF-NKNY-18.2 (Fig. 31L–P) (3 teeth).

Description. Labiolingually flattened teeth seem to thin out at their mesial edge. They are covered with elongated and fine striation. This striation becomes coarser basally and distally on the more elongated specimens (specimens CUF-NKNY-2.1 and CUF-NKNY-2.2). The latter two teeth are strongly curved distally with a concave distal edge and the more completely preserved specimen CUF-NKNY-2.1 bears an apical barb. The specimen

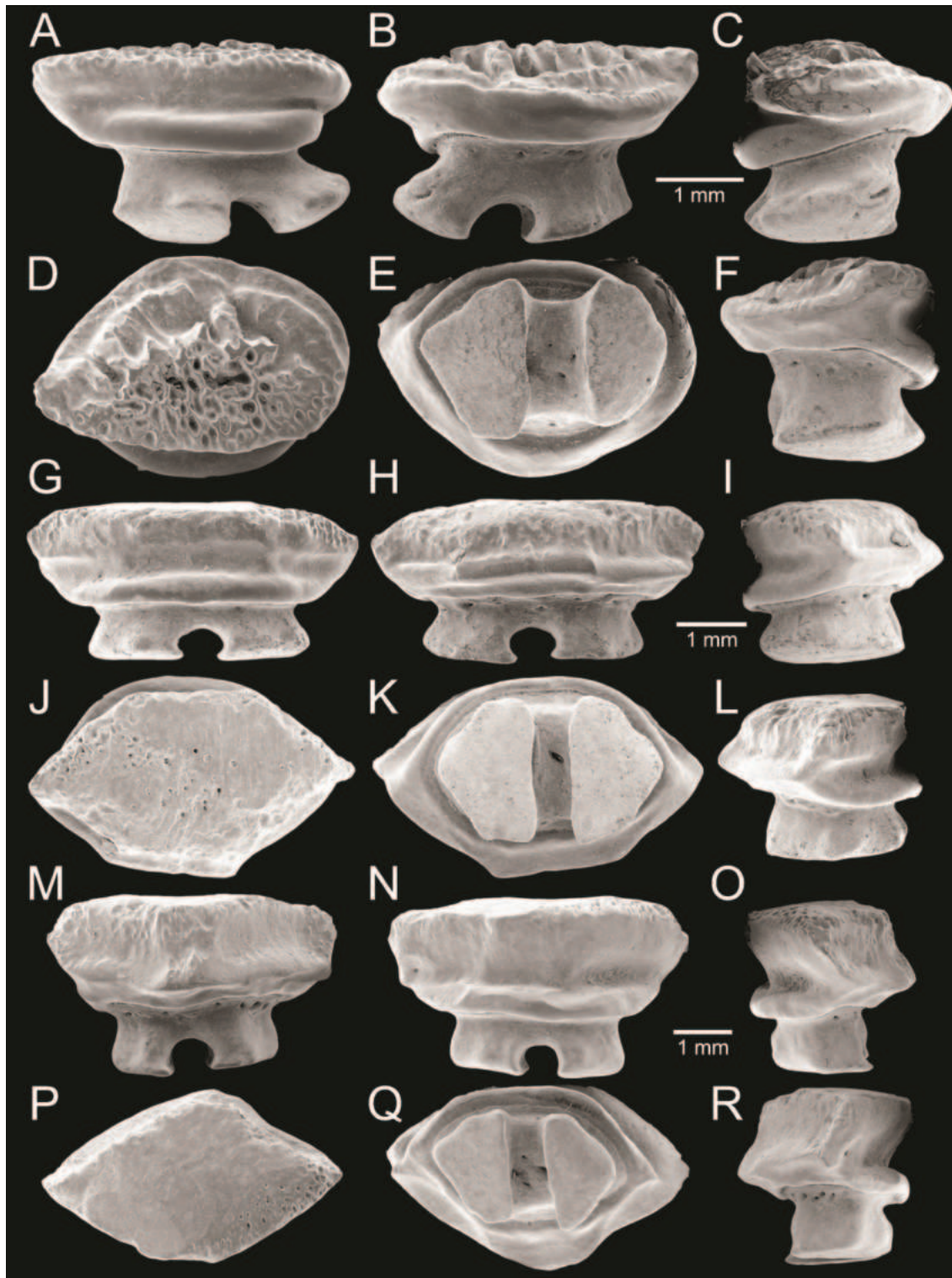


Figure 30. Dasyatid ray teeth - *Pastinachus* sp. **A–F** specimen CUF-NKNY-7.1 in **A** lingual **B** labial **C**, **F** profile **D** occlusal and **E** basal views **G–L** specimen CUF-NKNY-7.2 in **G** lingual **H** labial **I**, **L** profile **J** occlusal and **K** basal views **M–R** specimen CUF-NKNY-8.1 in **M** lingual **N** labial **O**, **R** profile **P** occlusal and **Q** basal views.

CUF-NKNY-18.2 has a curved mesial margin, whereas the distal one is vertical and straight.

Taxonomic remarks and comparisons. The two strongly curved teeth (specimens CUF-NKNY-2.1 and CUF-NKNY-2.2) represent fang-like features

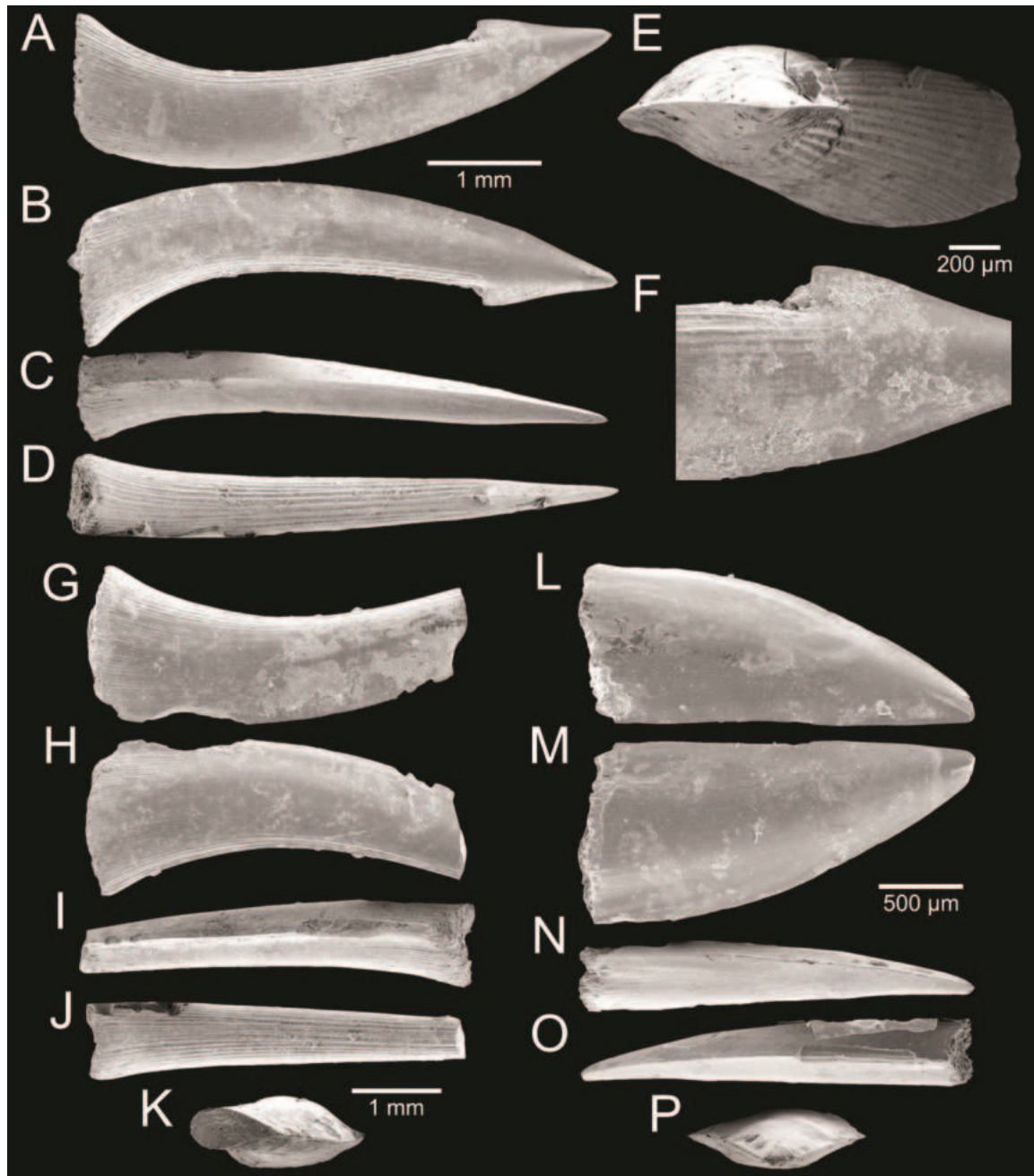


Figure 31. Trichiuridae indet. **A–F** specimen CUF-NKNY-2.1, anterior tooth in **A, B** lateral **C** anterior **D** posterior and **E** apical views **F** close-up of the tip of the tooth **G–K** specimen CUF-NKNY-2.2, anterior tooth in **G, H** lateral **I** anterior **J** posterior and **K** apical views **L–P** specimen CUF-NKNY-18.2, lateral tooth in **L, M** lateral **N** anterior **O** posterior and **P** apical views.

from the front of the jaw, while the specimen CUF-NKNY-18.2 comes from a rather distal position. This latter tooth resembles somewhat the lateral teeth of *Sphyranea* (barracuda, e.g., Gottfried et al. 2017), but those are more symmetrical. The global species database (Fishbase: www.fishbase.org) reports twenty-seven cutlassfishes from the wider region of South and Southeast Asia (Froese and Pauly 2024). Two common genera, *Trichurus* and *Lepuracanthus*, contain some species that bear such barbed fang-like teeth (Nakamura and Parin 1993; 1998).

Order *incertae sedis* in Eupercaria Betancur-R. et al., 2014
Family Sciaenidae Cuvier, 1829
***Johnius* Bloch, 1793**

***Johnius* sp.**

Fig. 32

Referred material. CUF-NKNY-16.2 (Fig. 32A–D) (1 right sagitta otolith).

Description. Thick otolith with a smooth external surface, whereas the internal surface bears a sulcus characteristic of the genus. The ostium is shallow, vertically positioned, higher than long, and it widens ventrally. The anterior and horizontal portion of the cauda is short and shallow, then opening posteriorly into a deep caudal funnel with an external circular shape.

Taxonomic remarks and comparisons. Otoliths of *Johnius* are unique and have distinct characteristics that make them easily distinguishable from those of other sciaenids or teleosts (Schwarzhan 1993). There are 21 species of *Johnius* in Southeast Asia (Froese and Pauly 2024), and most of them inhabit shallow coastal waters and estuaries but some species are capable of entering rivers. They are also known from the fossil records in Japan (Ohe 1976) and Taiwan (Lin et al. 2022).

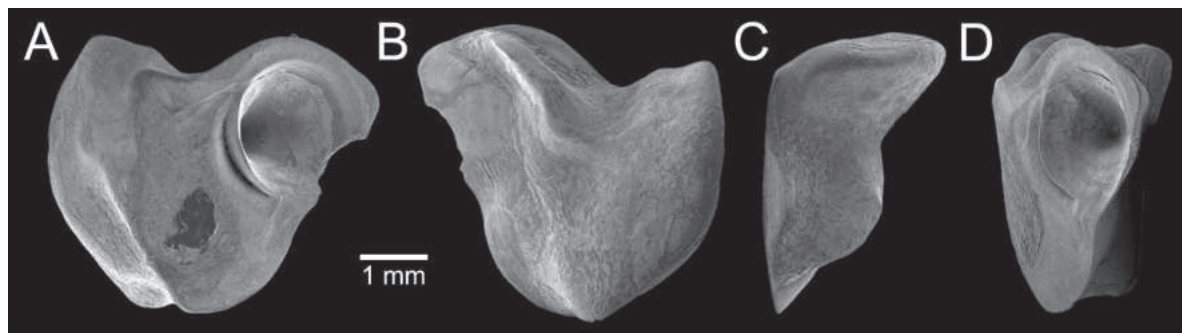


Figure 32. Sciaenid otolith of *Johnius* sp., specimen CUF-NKNY-16.2, right sagitta otolith in **A** inner **B** external **C** anterior and **D** posterior views.

Discussion

Based on the survey of mid-Holocene marine faunas from the clay pit of Nakhon Nayok Province in Thailand, many fossils of molluscs together with other invertebrates and vertebrates have been found in the Bangkok clay layer at a depth of ~ 5–7 m below the surface. The faunal assemblages, especially molluscs (Table 2), depict the palaeo-ecosystem of the area at that time as corresponding to the intertidal to sublittoral zones. Some molluscan taxa, i.e., *Cerithidea obtusa*, *Pirenella incisa*, *Telescopium telescopium*, *Ellobium aurisjudae*, *Cassidula nucleus*, and *Geloina bengalensis*, also indicate that some parts of the area corresponded to mangrove forests and intertidal mudflats. The occurrence of mangrove forests has previously been corroborated by evidence of peat and pollens from the same, as well as nearby, sites (Songtham et al. 2007, 2015). In this study, several described mollusc taxa correspond to those reported from the Lower Central Plain of Bangkok and Samut Prakan and from the inland of Phetchaburi coasts (Somboon 1988; Somboon and Thiramongkol

1992; Robba et al. 2007; Negri 2009, 2012; Surakiatchai et al. 2018), suggesting similar paleoenvironments of these sites.

Most of the marine and mangrove shells were found at a depth of 2.2 m below the uppermost part of a marine clay layer. The carbon-14 dating analysis indicates a mid-Holocene age for this level as being approximately 5,900–5,300 cal yr BP, whereas charcoal material was found at a greater depth of 2.2–4.6 m, spanning approximately an age from 8,800 to 5,700 cal yr BP (Table 1). However, the abundance of tree trunks and carbonised woods as well as the accumulation of peat at greater depth than most shells indicate the predominance of mangrove forests, suggesting an early stage of marine incursion further inland (Songtham et al. 2007). The ages of the Bangkok Clay deposits determined by this study are also in good agreement with those retrieved by Songtham et al. (2007). This duration corresponds to the depositional stage 2 (7,000–3,000 cal yr BP), a marine transgression time proposed by Tanabe et al. (2003). During this stage, a large mud shoal was formed around Samut Prakan Province and the Chao Phraya delta prograded toward the head of the palaeo-Gulf of Ayutthaya southward (Fig. 33; Tanabe et al. 2003). However, our chronological results suggest that the area of Ongkharak, Nakhon Nayok in central Thailand was possibly an ancient coastal shoreline between 7,900 and 5,300 cal yr BP, which was located further southward compared to the palaeogeographic scheme proposed by Tanabe et al. (2003).

The vertebrate fauna is dominated by cartilaginous fishes, among which the family Carcharhinidae is most common (Table 3). The genus *Glyphis*, also known as “river shark”, is dentally most abundant in the area due to its habitat

Table 2. Molluscan species assemblages from the Bangkok Clay deposits of Ongkharak in Nakhon Nayok recovered in the present study and from other sites retrieved from previous literature (indicated by an asterisk). NA = data not available.

Class	Species in this study	Lower Central Plain and Chao Phraya delta (Somboon 1988; Somboon and Thiramongkol 1992)	Lower Central Plain of Bangkok and inland of Phetchaburi coast (Robba et al. 2007; Negri 2009)	Ban Praksa, Samut Prakan (Negri 2012)	Sam Roi Yot National Park, Phetchaburi (Surakiatchai et al. 2018)	Habitat	Substrate preference
Gastropoda	1. <i>Homalopoma</i> cf. <i>sangarensis</i>	–	–	–	–	Sublittoral	Sand, hard
	2. <i>Neripteron violaceum</i>	–	–	–	–	Intertidal, mangrove	Mud, hard
	3. <i>Nerita articulata</i>	*	–	–	–	Intertidal, mangrove	Mud, hard
	4. <i>Cerithidea obtusa</i>	–	*	–	–	Intertidal, mangrove	Mud, hard
	5. <i>Pirenella incisa</i>	–	–	–	–	Intertidal, mangrove	Mud
	6. <i>Telescopium telescopium</i>	–	–	–	–	Intertidal, mangrove	Mud
	7. <i>Eunaticina papilla</i>	–	*	–	–	Intertidal–sublittoral	Sand
	8. <i>Natica stellata</i>	–	*	–	–	Sublittoral	Sand
	9. <i>Natica vitellus</i>	–	*	–	–	Intertidal–sublittoral	Sand, mud
	10. <i>Paratectonatica tigrina</i>	*	*	*	*	Intertidal–sublittoral	Sand, mud
	11. <i>Ergaea walshi</i>	–	*	–	–	Intertidal–sublittoral	Hard
	12. <i>Bufo nana</i>	–	–	–	–	Sublittoral	Sand, mud
	13. <i>Merica elegans</i>	–	–	–	–	Sublittoral	Sand, mud
	14. <i>Scalptia scalariformis</i>	–	*	–	–	Sublittoral	Sand, mud
	15. <i>Pseudoneptunea varicosa</i>	–	*	–	–	Sublittoral	NA
	16. <i>Brunneifusus ternatanus</i>	*	–	–	–	Sublittoral	Sand, mud
	17. <i>Nassarius micans</i>	–	*	–	–	Intertidal–sublittoral	Sand

Class	Species in this study	Lower Central Plain and Chao Phraya delta (Somboon 1988; Somboon and Thiramongkol 1992)	Lower Central Plain of Bangkok and inland of Phetchaburi coast (Robba et al. 2007; Negri 2009)	Ban Praksa, Samut Prakan (Negri 2012)	Sam Roi Yot National Park, Phetchaburi (Surakiatchai et al. 2018)	Habitat	Substrate preference	
Gastropoda	18. <i>Nassarius siquijorensis</i>	-	*	-	*	Intertidal- sublittoral	Sand, mud	
	19. <i>Chicoreus capucinus</i>	*	-	-	-	Intertidal, mangrove	Sand, mud, hard	
	20. <i>Indothais gradata</i>	*	-	-	-	Sublittoral	Hard	
	21. <i>Indothais lacera</i>	-	*	-	-	Intertidal- sublittoral	Mud, hard	
	22. <i>Murex trapa</i>	*	*	-	*	Sublittoral	Sand, mud	
	23. <i>Maoritomella vallata</i>	-	*	-	-	Sublittoral	NA	
	24. <i>Pseudoetrema fortilirata</i>	-	*	-	-	Sublittoral	Sand, mud	
	25. <i>Turricula javana</i>	*	*	-	*	Intertidal- sublittoral	Sand, mud, hard	
	26. <i>Paradrillia melvilli</i>	-	*	-	-	Sublittoral-upper bathyal	NA	
	27. <i>Inquisitor vulpionis</i>	-	*	-	-	Sublittoral	Sand	
	28. <i>Comitas ilariae</i>	-	-	-	-	Sublittoral	Sand	
	29. <i>Duplicaria tricincta</i>	-	*	-	-	Sublittoral	Sand, mud	
	30. <i>Granuliterebra bathyrhaphe</i>	-	*	*	-	Intertidal- sublittoral	Sand, mud	
	31. <i>Pristiterebra miranda</i>	-	*	-	-	Sublittoral	NA	
	32. <i>Architectonica perdix</i>	-	*	-	*	Sublittoral	Sand, mud	
	33. <i>Cylichna modesta</i>	-	*	-	-	Sublittoral	Sand, mud	
	34. <i>Ellobium aurisjudae</i>	-	*	-	-	Intertidal, mangrove	Sand, mud, hard	
	35. <i>Cassidula nucleus</i>	-	*	-	-	Intertidal, mangrove	Mud, hard	
	Bivalvia	1. <i>Jupiteria puellata</i>	-	*	*	-	Sublittoral	Sand, mud
		2. <i>Saccella mauritiana</i>	-	*	-	-	Sublittoral	Sand, mud, hard
		3. <i>Anadara inaequivalvis</i>	-	*	-	*	Intertidal- sublittoral	Sand, mud
		4. <i>Anadara indica</i>	-	*	-	*	Intertidal- sublittoral	Sand, mud
		5. <i>Tegillarca granosa</i>	*	*	-	*	Intertidal, mangrove	Mud
		6. <i>Tegillarca nodifera</i>	-	-	-	-	Intertidal- sublittoral, mangrove	Sand, mud
		7. <i>Estellacar olivacea</i>	*	*	-	-	Intertidal- sublittoral, mangrove	Sand, mud
		8. <i>Noetiella pectunculiformis</i>	-	*	-	-	Intertidal- sublittoral, mangrove	Sand, mud
		9. <i>Magallana cf. gigas</i>	-	*	-	*	Intertidal- sublittoral	Mud, hard
		10. <i>Placuna placenta</i>	-	*	*	*	Intertidal- sublittoral	Sand, mud
		11. <i>Volachlamys singaporina</i>	-	-	-	-	Intertidal- sublittoral	Sand, mud, hard
		12. <i>Pegophysema bialata</i>	-	-	-	-	Intertidal- sublittoral	Sand, mud
		13. <i>Geloina bengalensis</i>	-	*	-	-	Intertidal, mangrove	Mud
		14. <i>Lutraria complanata</i>	-	*	-	-	Sublittoral	Sand, mud
		15. <i>Standella pellucida</i>	-	*	-	-	Intertidal- sublittoral, mangrove	Sand, mud
		16. <i>Tellinides conspicuus</i>	-	-	-	-	Sublittoral	NA
		17. <i>Joannisiella oblonga</i>	*	*	-	*	Intertidal- sublittoral	Mud
18. <i>Dosinia dilecta</i>		-	*	-	*	Sublittoral	Mud	
19. <i>Paratapes undulatus</i>		*	*	*	*	Intertidal- sublittoral	Sand, mud	
20. <i>Placamen lamellatum</i>		-	*	-	-	Intertidal- sublittoral	Sand, mud	
21. <i>Corbula fortisulcata</i>		-	*	-	*	Intertidal- sublittoral	Sand, mud, hard	
22. <i>Potamocorbula</i> sp.		NA	NA	NA	NA	Intertidal	NA	
23. <i>Martesia striata</i>		-	*	-	-	Intertidal- sublittoral	Hard	
24. <i>Pholas orientalis</i>		-	*	-	-	Intertidal- sublittoral	Sand, mud, hard	
25. <i>Teredinidae</i> indet.		NA	NA	NA	NA	Intertidal- sublittoral	Hard	
26. <i>Cultellus maximus</i>		-	*	-	-	Intertidal- sublittoral, mangrove	Mud	
27. <i>Siliqua minima</i>		-	*	-	-	Intertidal- sublittoral	Sand, mud	
Scaphopoda	1. <i>Dentalium variabile</i>	-	*	*	-	Sublittoral	Mud	

in or nearby rivers and estuaries. It is a cryptic shark that is difficult to study, but it has been reported that these sharks also live in coastal and shallow marine regions, while the young grow up in a river habitat where the predation pressure is reduced (Li et al. 2015). The dominant presence of this taxon is indicative of the vicinity of freshwater input and/or habitats close to rivers, corresponding to the paleogeographic context of the region (Fig. 33) and the results of other studies from the Bangkok Clay (Robba et al. 2002, 2003, 2004, 2007; Songtham et al. 2007; Negri 2009, 2012). Several *Carcharhinus* species including *C. amblyrhynchoides*, *C. amblyrhynchos*, *C. leucas*, *C. amboinensis*, and *C. sorrah* were

Table 3. Fish remains recovered from the Bangkok Clay deposits of Ongkharak in Nakhon Nayok.

Class Chondrichthyes				
Order	Family	Species	No.	Material
Carcharhiniformes	Carcharhinidae	<i>Carcharhinus</i> cf. <i>amblyrhynchoides</i>	1	tooth
		<i>Carcharhinus</i> cf. <i>amblyrhynchos</i>	1	tooth
		<i>Carcharhinus</i> cf. <i>leucas</i>	4	teeth
		<i>Carcharhinus leucas</i> / <i>Carcharhinus amboinensis</i>	10	teeth
		<i>Carcharhinus</i> cf. <i>sorrah</i>	2	teeth
		<i>Carcharhinus</i> spp.	7	teeth
		<i>Glyphis</i> sp.	59	teeth
		<i>Scoliodon</i> cf. <i>laticaudus</i>	3	teeth
		Carcharhinidae indet.	10	teeth
Myliobatiformes	Dasyatidae	<i>Pastinachus</i> sp.	3	teeth
Class Actinopterygii				
Scombriformes	Trichiuridae	Trichiuridae indet.	3	teeth
<i>incertae sedis</i> in Eupercaria	Sciaenidae	<i>Johnius</i> sp.	1	otolith

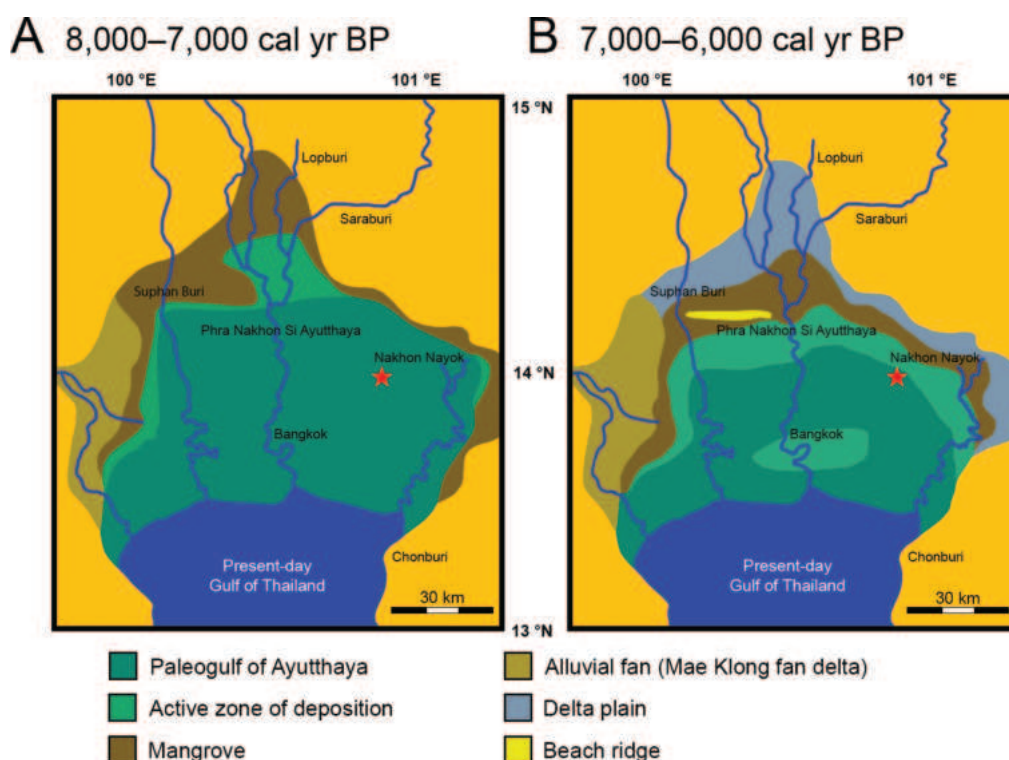


Figure 33. Paleogeographic maps illustrating the evolution of the Chao Phraya delta modified from Tanabe et al. (2003), during **A** 8,000–7,000 cal yr BP and **B** 7,000–6,000 cal yr BP. Red stars indicate the location of the study area.

also found. As the position of the teeth in the jaws cannot be ascertained, other taxa could not be ruled out based on some similarities in tooth morphology. Nevertheless, the bull shark (*C. leucas*) appears to be abundant and is also known to live in freshwater environments. Moreover, the genus *Scoliodon* present in the area is reported from brackish environments (Riede 2004). The other recovered taxa, the stingray (*Pastinachus*), cutlassfish (Trichiuridae), and the sciaenid *Johnius* are all compatible with shallow marine coastal environments, as supported by the presence of molluscan faunas, although some species are reported from brackish environments. Due to the fact that the fish remains are almost entirely represented by isolated teeth and only one single otolith has been found so far (*Johnius*), the rarity of this type of remains could be the consequence of sampling biases and/or taphonomic processes. Therefore, targeting otoliths in future studies could shed more light on the bony fish fauna of the Bangkok Clay.

Acknowledgments

We thank the following colleagues from the Department of Biology, Faculty of Science, Chulalongkorn University: Wichase Khonsue who led us to the locality and provided information on the sites, Somsak Panha who facilitated access to collection storage and working area, Arthit Polyotha for providing SEM images, and Kittipum Chansri and Buntika A. Butcher for providing access and taking photographs with a Leica M205C stereo light microscope. We also thank Falls Jindewha, Sutan Saehan, Jirapan Sumpaonthong, and Suwijak Pata for their assistance in the field, Santi Pailoplee (Department of Geology, Faculty of Science, Chulalongkorn University) for his help in generating the map, Mana Rugbumrung (Department of Mineral Resources) for his technical assistance and supports, and Thierry Backeljau (Royal Belgian Institute of Natural Sciences, Brussels) and Bernhard Hausdorf (Leibniz Institute for the Analysis of Biodiversity Change, Hamburg) for the access to the relevant literature. We are grateful to Montri Inthasaeng who allowed us to work at the site. Finally, we thank Jürgen Kriwet and Matthias Harzhauser for their comments on the first version of this manuscript.

Additional information

Conflict of interest

The authors have declared that no competing interests exist.

Ethical statement

No ethical statement was reported.

Funding

This research was supported by the Sci-Super VII grant, Faculty of Science, Chulalongkorn University (Grant No. Sci-Super VII_64_001, to KS and CS).

Author contributions

Conceptualization: PJ, LK, KS, CS, GC. Data curation: NN, SK, KS. Formal analysis: PJ, KS, NN, LK, SK, GC, TC. Funding acquisition: CS, KS. Investigation: CS, TC, NN, KS. Method-

ology: CS, TC, PJ, LK, GC, KS. Project administration: KS. Resources: NN, CS, KS. Validation: LK, PJ, GC, KS. Visualization: KS, LK, GC, PJ. Writing - original draft: KS, GC, PJ, LK. Writing - review and editing: PJ, LK, GC, KS.

Author ORCIDs

Parin Jirapatrasilp  <https://orcid.org/0000-0002-5591-6724>

Gilles Cuny  <https://orcid.org/0000-0001-7680-1697>

László Kocsis  <https://orcid.org/0000-0003-4613-1850>

Chirasak Sutcharit  <https://orcid.org/0000-0001-7670-9540>

Kantapon Suraprasit  <https://orcid.org/0000-0002-3428-9549>

Data availability

All of the data that support the findings of this study are available in the main text.

References

- Adams A (1852) Catalogue of the species of *Nassa*, a genus of gasteropodous Mollusca belonging to the family Buccinidae, in the collection of Hugh Cuming, Esq., with the description of some new species. *Proceedings of the Zoological Society of London* 19: 94–114. <https://doi.org/10.1111/j.1096-3642.1851.tb01137.x>
- Adams A (1856) Descriptions of twenty-five new species of shells from the collection of Hugh Cuming, Esq. *Proceedings of the Zoological Society of London* 23: 221–226. <https://www.biodiversitylibrary.org/page/30748138>
- Adnet S, Mouana M, Charruault A-L, Essid EM, Ammar HK, Marzougui W, Merzeraud G, Tabuce R, Vianey-Liaud M, Marivaux L (2019) Teeth, fossil record and evolutionary history of the cowtail stingray *Pastinachus* Rüppell, 1829. *Historical Biology* 31: 1213–1222. <https://doi.org/10.1080/08912963.2018.1431779>
- Albano PG, Steger J, Bakker PAJ, Bogi C, Bošnjak M, Guy-Haim T, Huseyinoglu MF, La-Follette PI, Lubinevsky H, Mulas M, Stockinger M, Azzarone M, Sabelli B (2021) Numerous new records of tropical non-indigenous species in the Eastern Mediterranean highlight the challenges of their recognition and identification. *ZooKeys* 1010: 1–95. <https://doi.org/10.3897/zookeys.1010.58759>
- Alf A, Thach NN (2021) Some remarks on *Lenifusus*, *Brunneifusus* and *Hemifusus* and description of two new species of *Hemifusus* (Buccinoidea, Melongenidae). *Conchylia* 52: 95–108.
- Arachchige GM, Jayakody S, Mooi R, Kroh A (2017) A review of previous studies on the Sri Lankan echinoid fauna, with an updated species list. *Zootaxa* 4231(2): 151–168. <https://doi.org/10.11646/zootaxa.4231.2.1>
- Arachchige GM, Jayakody S, Mooi R, Kroh A (2019) An annotated species list of regular echinoids from Sri Lanka with notes on some rarely seen temnopleurids. *Zootaxa* 4571(1): 35–57. <https://doi.org/10.11646/zootaxa.4571.1.3>
- Aubry U, Gargiulo R, Russo S (2021) Terebridae: Descriptive and Iconographic Review from 1713 to 2021. *L'Informatore Piceno*, Ancona, Italy, 515 pp.
- Aungtonya C, Hylleberg J (1998) Check list of sublittoral molluscs, with nine new records for the Andaman Sea. *Phuket Marine Biological Center Special Publication* 18: 317–322.
- Aungtonya C, Thaiklang N, Srisawan D (1999) Recent records of Bivalvia in the reference collection of Phuket Marine Biological Center, Thailand. *Phuket Marine Biological Center Special Publication* 19: 371–383.

- Baharuddin N, Martin MB, Nagappan T, Borkhanuddin MH (2017) Checklist of mangrove snails (Mollusca: Gastropoda) in Setiu Wetlands. In: Abdullah DM, Nasir MZ, Mazlan NM, Jusoh WFAW (Eds) Prosiding Seminar Ekspedisi Saintifik Tanah Bencah Setiu 2016. WWF-Malaysia, 9 pp.
- Baron-Szabo RC, Cairns SD (2016) Treatise on Invertebrate Paleontology: Part F, Revised, Volume 2, Chapter 10: Systematic descriptions of the Scleractinia family Rhizangiidae. Treatise Online 80: 1–10. <https://doi.org/10.17161/to.v0i0.6462>
- Bass AJ, D'Aubrey JD, Kistnasamy N (1973) Sharks of the East Coast of southern Africa. I. The genus *Carcharhinus* (Carcharhinidae). Investigational Report – Issue 33. Oceanographic Research Institute, Durban, South Africa, 168 pp.
- Bass AJ, D'Aubrey JD, Kistnasamy N (1975) Sharks of the East Coast of Southern Africa. III. The Families Carcharhinidae (excluding *Mustelus* and *Carcharhinus*) and Sphyrnidae. Investigational Report Oceanographic Research Institute, Durban, South Africa, 100 pp.
- BEDO (2017a) Marine Bivalves: Checklist of Molluscan Biodiversity in Thailand. BEDO, Bangkok, 296 pp. [in Thai]
- BEDO (2017b) Marine Gastropods: Checklist of Molluscan Biodiversity in Thailand. BEDO, Bangkok, 376 pp. [in Thai]
- Beu AG (2006) Marine Mollusca of oxygen isotope stages of the last 2 million years in New Zealand. Part 2. Biostratigraphically useful and new Pliocene to recent bivalves. Journal of the Royal Society of New Zealand 36(4): 151–338. <https://doi.org/10.1080/03014223.2006.9517808>
- Beu AG (2008) Bursidae. In: Poppe GT (Ed.) Philippine Marine Mollusks Volume I. ConchBooks, Hackenheim, Germany, 612–627.
- Beu AG (2010) Marine Mollusca of isotope stages of the last 2 million years in New Zealand. Part 3. Gastropoda (Vetigastropoda - Littorinimorpha). Journal of the Royal Society of New Zealand 40(3-4): 59–180. <https://doi.org/10.1080/03036758.2010.500717>
- Beu AG, Alloway BV, Pillans BJ, Naish TR, Westgate JA (2004) Marine Mollusca of oxygen isotope stages of the last 2 million years in New Zealand. Part 1: Revised generic positions and recognition of warm-water and cool-water migrants. Journal of the Royal Society of New Zealand 34(2): 111–265. <https://doi.org/10.1080/03014223.2004.9517766>
- Bibi S, Terryn Y, Siddiqui PJA, Iqbal P (2021) In the wake of Captain Townsend – Poorly known and cryptic Terebridae (Gastropoda: Conoidea) of Pakistan. Gloria Maris 60: 43–59.
- Bieler R (1993) Architectonicidae of the Indo-Pacific (Mollusca, Gastropoda). Abhandlungen des Naturwissenschaftlichen Vereins in Hamburg 30: 1–376.
- Bleeker P (1856) *Carcharias (Prionodon) amblyrhynchus*, eene nieuwe haaisoort, gevangen nabij het eiland Solombo. Natuurkundig Tijdschrift voor Nederlandsch Indië 10: 467–468. <https://www.biodiversitylibrary.org/part/4267>
- Born I von (1778) Index rerum naturalium Musei Cæsarei Vindobonensis. Pars I.ma. Testacea. Verzeichniß der natürlichen Seltenheiten des k. k. Naturalien Cabinets zu Wien. Erster Theil. Schalthiere. [1–40], 1–458, [1–82]. Vindobonae [Vienna]. <https://doi.org/10.5962/bhl.title.11581>
- Bosch DT, Dance SP, Moolenbeek RG, Oliver PG (1995) Seashells of Eastern Arabia. Montivate Publsihing, Dubai, 296 pp.
- Boyd WE, Higham CFW, Thosarat R (1996) The Holocene palaeogeography of the south-east margin of the Bangkok plain, Thailand, and its archaeological implications. Asian Perspective 35: 193–207. <https://www.jstor.org/stable/42928387>

- Bozzetti L (1991) *Comitas ilariae* new species from the Philippines. *La Conchiglia* 22: 26–28.
- Brandt RAM (1974) The non-marine aquatic Mollusca of Thailand. *Archiv für Molluskenkunde* 105: 1–423.
- Bratcher T, Cernohorsky WO (1987) Living terebras of the world. A monograph of the recent Terebridae of the world. American Malacologists, Melbourne, Florida & Burlington, Massachusetts, 240 pp.
- Bruguière JG (1789) *Encyclopédie méthodique ou par ordre de matières. Histoire naturelle des vers*, volume 1. Pancoucke, Paris, xviii, 344 pp. [Dates after Evenhuis 2003] <https://doi.org/10.5962/bhl.title.82248>
- Bussarawit S (1991) The family Muricidae in the PMBC reference collection: Application of a database system. *Phuket Marine Biological Center Special Publication* 9: 29–34.
- Cairns S, Kitahara MV (2012) An illustrated key to the genera and subgenera of the Recent azooxanthellate Scleractinia (Cnidaria, Anthozoa), with an attached glossary. *ZooKeys* 227: 1–47. <https://doi.org/10.3897/zookeys.227.3612>
- Cairns SD, Hoeksema BW, Van der Land J (1999) Appendix: List of extant stony corals. *Atoll Research Bulletin* 459: 13–46. <https://doi.org/10.5479/si.00775630.459.1>
- Cappetta H (2012) Chondrichthyes. Mesozoic and Cenozoic Elasmobranchii: teeth. *Handbook of paleoichthyology*. Vol. 3E. Verlag Dr. Friedrich Pfeil, Munich, 512 pp.
- Carrillo-Briceño JD, Maxwell E, Aguilera OA, Sánchez R, Sánchez-Villagra MR (2015) Sawfishes and other elasmobranch assemblages from the Mio-Pliocene of the South Caribbean (Urumaco Sequence, Northwestern Venezuela). *PLoS ONE* 10(10): 1–30. <https://doi.org/10.1371/journal.pone.0139230>
- Cernohorsky WO (1971) The family Naticidae (Mollusca: Gastropoda) in the Fiji Islands. *Records of the Auckland Institute and Museum* 8: 169–208. <https://www.jstor.org/stable/42906168>
- Cernohorsky WO (1972) *Marine Shells of the Pacific: v. 2*. Pacific Publications, Sydney, 411 pp.
- Cernohorsky WO (1975) The taxonomy of some Indo-Pacific Mollusca part 3. With descriptions of new taxa and remarks on an Ecuadorian fossil species of Turridae. *Records of the Auckland Institute and Museum* 12: 212–234. <https://www.jstor.org/stable/42906228>
- Cernohorsky WO (1978) *Tropical Pacific Marine Shells*. Pacific Publications, Sydney, 352 pp.
- Cernohorsky WO (1984) Systematics of the family Nassariidae (Mollusca: Gastropoda). *Bulletin of the Auckland Institute and Museum* 14: i–iv, 1–356. <https://www.biodiversitylibrary.org/item/281235>
- Chabangborn A (2017) Review of paleoclimatic reconstruction in Thailand between the last glacial maximum and the mid Holocene. *Burapha Science Journal* 22: 61–77. [in Thai] <https://scijournal.buu.ac.th/index.php/sci/article/view/1263>
- Chaiwathee S, Dumrongrojwattana P, Matchacheep S, Chalermwat C (2007) Pre-list of some marine microsnails from Bangsaen beach, Chonburi province (Mollusca: Scaphopoda and Gastropoda). In: *Proceedings of 45th Kasetsart University Annual Conference: Science*. Kasetsart University, Bangkok, 573–576.
- Chan S-Y, Lau WL (2021) Biodiversity Record: The edible shipworm, *Bactronophorus thoracites*. *Nature in Singapore* 14: e2021112. <https://lknhm.nus.edu.sg/wp-content/uploads/sites/10/2021/10/NIS-2021-0112.pdf>

- Chan S-Y, Lau WL (2022) Biodiversity Record: The scalariform nutmeg snail, *Scalptia scalariformis*, in Singapore. Nature in Singapore 15: e2022103. <https://lkcnhm.nus.edu.sg/wp-content/uploads/sites/10/2022/09/NIS-2022-0103.pdf>
- Chan BK-K, Prabowo RE, Lee K-S (2009) Crustacean Fauna of Taiwan: Barnacles, Volume 1. Cirripedia: Thoracica Excluding the Pyrgomatidae and Acastinae. National Taiwan Ocean University, Taiwan, 297 pp.
- Chen Z-y, Tan Y-h, Lian X-p (2015) Taxonomic note on the Lineate Nerite: *Nerita balteata* Reeve, 1855 (Gastropoda, Neritidae, *Nerita*). Journal of Tropical Oceanography 34: 74–76.
- Choowong M (2002) The geomorphology and assessment of indicators of sea-level change to study coastal evolution from the gulf of Thailand. International Symposium on “Geology of Thailand”. Department of Mineral Resource, Bangkok, Thailand, 207–220.
- Clark HL (1925) A catalogue of the recent sea-urchins (Echinoidea) in the collection of the British Museum (Natural History). Trustees of the Museum, London, 250 pp.
- Clark AM, Rowe FWE (1971) Monograph of shallow-water indo-west Pacific Echinoderms. Trustees of the British Museum (Natural History), London, x + 238 pp.
- Clark PU, Dyke AS, Shakun JD, Carlson AE, Clark J, Wohlfarth B, Mitrovica JX, Hostetler SW, McCabe AM (2009) The Last Glacial Maximum. Science 325(5941): 710–714. <https://doi.org/10.1126/science.1172873>
- Coan EV (2002) The eastern Pacific recent species of the Corbulidae (Bivalvia). Malacologia 44: 47–105. <https://www.biodiversitylibrary.org/part/2779>
- Coan EV, Kabat AR (2012) The malacological works and taxa of Sylvania Hanley (1819–1899). Malacologia 55(2): 285–359. <https://doi.org/10.4002/040.055.0208>
- Compagno LJV (1984) FAO Species Catalogue. Vol. 4. Sharks of the world. An annotated and illustrated catalogue of shark species known to date. Part 2 - Carcharhiniformes. FAO Fisheries Synopsis 4(125): 251–655.
- Compagno LJV, White WT, Last PR (2008) *Glyphis garricki* sp. nov., a new species of river shark (Carcharhiniformes: Carcharhinidae) from northern Australia and Papua New Guinea, with a redescription of *Glyphis glyphis* (Müller & Henle, 1839). CSIRO Marine and Atmospheric Research Paper 22: 203–225.
- Cossignani T (1994) Bursidae of the world. L'Informatore Piceno, Ancona, 119 pp.
- Cox JB (1968) A review of the engineering characteristics of the recent marine clays in southeast Asia. Asian Institute of Technology Research Report 6, Bangkok.
- Dechruksa W, Sritongtae S, Namchote S, Krailas D (2014) Species diversity of molluscs obtained from mangrove forest and estuary of river in the Eastern coast of Thailand. Tokyo International Conference on Life Science and Biological Engineering, Tokyo, Japan, 931–937.
- Dekkers A (2018) Two new genera in the family Melongenidae from the Indo-Pacific and comments on the identity of *Hemifusus zhangyii* Kosuge, 2008 and *Pyruলা elongata* Lamarck, 1822 (Gastropoda, Neogastropoda: Buccinoidea). Gloria Maris 57: 40–50.
- Deshayes GP (1826) Anatomie et monographie du genre Dentale. Mémoires de la Société d'Histoire Naturelle de Paris (2) 2: 321–378. <https://www.biodiversitylibrary.org/item/227705>
- Deshayes GP (1830) Encyclopédie méthodique ou par ordre de matières. Histoire naturelle des Vers et Mollusques. Vol. 2: viii+1-594 [part 1: i-vi, 1-256, Livraison 101, 1 Feb 1830; part 2: 1-144, Livraison 101, 1 Feb. 1830]. <https://www.biodiversitylibrary.org/bibliography/49857>

- Dey A (2006) Handbook on mangrove associate molluscs of Sundarbans. Zoological Survey of India, Kolkata, xi + 96 pp.
- Dey A, Ramakrishna (2007) Marine molluscs: Bivalvia, Scaphopoda and Cephalopoda. Fauna of Andhra Pradesh, State Fauna Series Vol 5 Part 7. Zoological Survey of India, Kolkata, 149–260.
- Dharma B (2005) Recent and fossil Indonesian shells. ConchBooks, Hackenheim, 424 pp.
- Dheeradolok P, Chaimanee N, Piccoli G, Robba E (1984) On the Quaternary stratigraphy and fossils of Senanivate Housing Project area, Bangkok Metropolis. *Memorie di Scienze Geologiche* 36: 413–426.
- Dijkstra HH, Beu AG (2018) Living scallops of Australia and adjacent waters (Mollusca: Bivalvia: Pectinoidea: Propeamussiidae, Cyclochlamydidae and Pectinidae). *Records of the Australian Museum* 70(2): 113–330. <https://doi.org/10.3853/j.2201-4349.70.2018.1670>
- Dillwyn LW (1817) A descriptive catalogue of Recent shells, arranged according to the Linnean method; with particular attention to the synonymy, Vol. 1. John and Arthur Arch, London, 580 pp. <https://doi.org/10.5962/bhl.title.10437>
- Dunker W (1866) *Novitates Conchologicae. Mollusca Marina. Beschreibung und Abbildung neuer oder wenig gekannter Meeres-Conchylien. Abt. II: Meeres Conchylien.* Theodor Fischer, Cassel, iv + 144 pp. [145 pls]
- Egorov R (2000) *Treasure of Russian Shells Vol. 4: Trochiformes: Trochidae, Calliostomatidae, Liotiidae, Turbinidae, Tricoliidae.* Colus-Doverie, Moscow, 84 pp.
- Eichhorst TE (2008) Neritidae. In: Poppe GT (Ed) *Philippine Marine Mollusks Volume I.* ConchBooks, Hackenheim, Germany, 266–281.
- Eichhorst TE (2016) *Neritidae of the world. Volume 1.* ConchBooks, Hackenheim, 695 pp.
- Evenhuis NL (2003) Dating and publication of the *Encyclopédie Méthodique* (1782–1832), with special reference to the parts of the *Histoire Naturelle* and details on the *Histoire Naturelle des Insectes*. *Zootaxa* 166: 1–48. <https://doi.org/10.11646/zootaxa.166.1.1>
- Fedosov AE, Malcolm G, Terryn Y, Gorson J, Modica MV, Holford M, Puillandre N (2019) Phylogenetic classification of the family Terebridae (Neogastropoda: Conoidea). *Journal of Molluscan Studies* 85(4): 359–388. <https://doi.org/10.1093/mollus/eyz004>
- Filander Z, Griffiths CL (2014) Additions to and revision of the South African echinoid fauna (Echinodermata: Echinoidea). *African Natural History* 10: 47–56. http://www.scielo.org.za/scielo.php?script=sci_arttext&pid=S2305-79632014000100002
- Fischer-Piette E, Delmas D (1967) Révision des Mollusques Lamellibranches du genre *Dosinia* Scopoli. *Mémoires du Muséum national d'Histoire naturelle, Sér A – Zoologie* 47: 1–91. <https://www.biodiversitylibrary.org/part/280654>
- Froese R, Pauly D (2024) FishBase. World Wide Web electronic publication. <https://www.fishbase.org> [version (02/2024)] [Verified 18 February 2024]
- Garrard TA (1975) A revision of Australian Cancellariidae (Gastropoda: Mollusca). *Records of the Australian Museum* 30(1): 1–62. <https://doi.org/10.3853/j.0067-1975.30.1975.212>
- Garrick JAF (1982) *Sharks of the genus Carcharhinus.* NOAA Technical Report NMFS Circular vol. 445. NMFS Scientific Publications Office, Seattle, USA, 194 pp.
- Gemert L van (2003) Marine schelpen verzamelen op Ko Samui (Golf van Thailand). *De Kreukel* 39: 95–109.
- George N, Siddiqui G, Muhammad F, George Z (2021) DNA barcoding of gastropod *Telescopium telescopium* (Linnaeus, 1758) found at the Karachi coast, Pakistan.

- Journal of Animal and Plant Sciences 31: 1530–1536. <https://thejaps.org.pk/docs/2021/05/35.pdf>
- Gmelin JF (1791) Vermes. In: Gmelin JF (Ed.) *Caroli a Linnaei Systema Naturae per Regna Tria Naturae*, Ed 13 Tome 1(6). G.E. Beer, Lipsiae [Leipzig], 3021–3910.
- Golikov AN, Kussakin OG (1978) Shell-bearing gastropods of the intertidal zone of the seas of the USSR. *Opredeliteli po faune SSSR, izdavayemye Zoologicheskim Institutom AN SSSR* 116: 1–292.
- Gopalakrishnan A, Divya PR, Basheer VS, Swaminathan TR, Kathirvelpandian A, Bineesh KK, Kumar RG, Jena JK (2012) Macro Flora & Fauna of the Gulf of Mannar: a checklist. National Bureau of Fish Genetic Resources, Lucknow, 127 pp.
- Gottfried MD, Samonds KE, Ostrowski SA, Andrianavalona TH, Ramihangihajason TN (2017) New evidence indicates the presence of barracuda (Sphyraenidae) and supports a tropical marine environment in the Miocene of Madagascar. *PLoS ONE* 12(5): e0176553. <https://doi.org/10.1371/journal.pone.0176553>
- Gould AA (1847) Descriptions of new shells, received from Rev. Mr. Mason, of Burmah. *Proceedings of the Boston Society of Natural History* 2: 218–221. <https://www.biodiversitylibrary.org/page/9490902>
- Gould AA (1860) Descriptions of new shells collected by the United States North Pacific Exploring Expedition. *Proceedings of the Boston Society of Natural History* 7: 323–340, 382–384. <https://www.biodiversitylibrary.org/page/9249883>
- Groh K (2010) Ellobiidae. In: Poppe GT (Ed.) *Philippine Marine Mollusks Volume III*. ConchBooks, Hackenheim, Germany, 446–457.
- Habe T (1958) The Fauna of Akkeshi Bay: XXV. Gastropoda. *Publication of the Akkeshi Marine Biological Station* 8: 1–39. <https://eprints.lib.hokudai.ac.jp/dspace/handle/2115/68354>
- Haga T (2010) Pholadidae. In: Poppe GT (Ed.) *Philippine Marine Mollusks Volume IV*. ConchBooks, Hackenheim, Germany, 392–397.
- Hamli H, Idris MH, Abu Hena MK, Wong SK, Arshad A (2013) Checklist and habitat descriptions of edible gastropods from Sarawak, Malaysia. *Journal of Fisheries and Aquatic Science* 8(2): 412–418. <https://doi.org/10.3923/jfas.2013.412.418>
- Hanley SCT (1846a) An illustrated and descriptive catalogue of Recent shells, by Sylvanus Hanley, B.A., F.L.S. The plates forming a third edition of the *Index Testaceologicus*, by William Wood. W. Wood, London, 272 + 218 pp.
- Hanley SCT (1846b) Monograph of the genus *Tellina*. In: Sowerby II GB (Ed.) *Thesaurus conchyliorum; or, monographs of the genera of shells*. Sowerby II, G. B., London, 221–336. <https://doi.org/10.5962/bhl.title.10916>
- Hanley SCT (1856) *An Illustrated and Descriptive Catalogue of Recent Bivalve Shells*. Williams & Norgate, London, xviii + 392 + 324 pp.
- Harzhauser M, Raven H, Landau BM, Kocsis L, Adnan A, Zuschin M, Mandic O, Briguglio A (2018) Late Miocene gastropods from northern Borneo (Brunei Darussalam, Seria Formation). *Palaeontographica, Abt A: Palaeozoology – Stratigraphy* 313: 1–79. <https://doi.org/10.1127/pala/2018/0077>
- Heaton TJ, Köhler P, Butzin M, Bard E, Reimer RW, Austin WEN, Bronk Ramsey C, Grootes PM, Hughen KA, Kromer B, Reimer PJ, Adkins J, Burke A, Cook MS, Olsen J, Skinner LC (2020) Marine20—The marine radiocarbon age calibration curve (0–55,000 cal BP). *Radiocarbon* 62(4): 779–820. <https://doi.org/10.1017/RDC.2020.68>
- Hedley C (1913) Studies on Australian Mollusca, part XI. *Proceedings of the Linnean Society of New South Wales* 38: 258–339. <https://doi.org/10.5962/bhl.part.13561>

- Hemmen J (2007) Recent Cancellariidae. Annotated and illustrated catalogue of Recent Cancellariidae. Privately published, Wiesbaden, 428 pp.
- Henry DP, McLaughlin PA (1975) The barnacles of the *Balanus amphitrite* complex (Cirripedia, Thoracica). Zoologische Verhandlungen 141: 1–254. <https://repository.naturalis.nl/pub/317846>
- Henry DP, McLaughlin PA (1986) The recent species of *Megabalanus* (Cirripedia: Balanomorpha) with special emphasis on *Balanus tintinnabulum* (Linnaeus) sensu lato. Zoologische Verhandlungen 235: 3–69. <https://repository.naturalis.nl/pub/317744>
- Herman J, Hovestadt-Euler M, Hovestadt DC (1991) Contributions to the study of the comparative morphology of teeth and other relevant ichthyodorulites in living supra-specific taxa of chondrichthyan fishes. Part A: Selachii. No 2c: Order: Carcharhiniformes. Families: Proscylliidae, Hemigaleidae, Pseudotriakidae, Leptochariidae and Carcharhinidae. Bulletin de l'Institut royal des Sciences naturelles de Belgique, Biologie 61: 73–120.
- Hinds RB (1843) Descriptions of new species of *Nucula*, from the collections of Sir Edward Belcher, C.B., and Hugh Cuming, Esq. Proceedings of the Zoological Society of London 11: 97–101. <https://www.biodiversitylibrary.org/page/30680075>
- Hinds RB (1844) Description of new species of shells. Proceedings of the Zoological Society of London 12: 21–26. <https://www.biodiversitylibrary.org/item/46217>
- Hiro F (1939) Studies on the cirripedian fauna of Japan IV. Cirripeds of Formosa (Taiwan), with some geographical and ecological remarks on the littoral forms. Memoirs of the College of Science, Kyoto Imperial University, Series B 15: 245–284. https://repository.kulib.kyoto-u.ac.jp/dspace/bitstream/2433/257900/1/mcskiu-b_15_2_245.pdf
- Hollmann M (2008) Naticidae. In: Poppe GT (Ed.) Philippine Marine Mollusks Volume I. ConchBooks, Hackenheim, Germany, 482–501.
- Holthuis LB, Heerebout GR (1972) Vondsten van de zeepok *Balanus tintinnabulum* (Linnaeus, 1758) in Nederland. Zoologische Bijdragen 13: 24–31. <https://repository.naturalis.nl/pub/317248>
- Hombron JB, Jacquinot H (1848) Atlas d'Histoire Naturelle Zoologie par MM. Hombron et Jacquinot, Chirurgiens de l'Expédition. In: Jacquinot H (Ed.) Voyage au Pole Sud et dans l'Océanie sur les corvettes l'Astrolabe et la Zélée...Livre 26. Gide et Cie, Paris.
- Houart R (1992) The genus *Chicoreus* and related genera (Gastropoda: Muricidae) in the Indo-West Pacific. Mémoires du Muséum national d'Histoire naturelle Série A. Zoologie 154: 1–188. <https://www.biodiversitylibrary.org/part/283031>
- Houart R (2008) Muricidae. In: Poppe GT (Ed.) Philippine Marine Mollusks Volume II. ConchBooks, Hackenheim, Germany, 132–221.
- Houbrick RS (1984) Revision of higher taxa in genus *Cerithidea* (Mesogastropoda: Potamididae) based on comparative morphology and biological data. American Malacological Bulletin 2: 1–20. https://repository.si.edu/bitstream/handle/10088/6218/sms_houbrick_1984.pdf
- Houbrick RS (1991) Systematic review and functional morphology of the mangrove snails *Terebralia* and *Telescopium* (Potamididae; Prosobranchia). Malacologia 33: 289–338. <https://www.biodiversitylibrary.org/part/271736>
- Huang Q (1997) Morphological, allozymic, and karyotypic distinctions between *Neritina* (*Dostia*) *violacea* and *N. (D.) cornucopia* (Gastropoda: Neritoidea). Journal of Zoology 241(2): 343–369. <https://doi.org/10.1111/j.1469-7998.1997.tb01964.x>
- Huber M (2010) Compendium of bivalves. A full-color guide to 3,300 of the world's marine bivalves. A status on Bivalvia after 250 years of research. ConchBooks, Hackenheim, 901 pp.

- Huber M (2015) Compendium of Bivalves 2. A Full-Color Guide to the Remaining Seven Families. A Systematic Listing of 8'500 Bivalve Species and 10'500 Synonyms. ConchBooks, Hackenheim.
- Hylleberg J, Aungtonya C (2013) Biodiversity survey in Chalong Bay and surrounding areas, east coast of Phuket Island. Phuket Marine Biological Center Special Publication 32: 81–112.
- Hylleberg J, Kilburn RN (2003) Marine molluscs of Vietnam: annotations, voucher material, and species in need of verification. Phuket Marine Biological Center Special Publication 28: 1–300.
- Hyžný M, de Angeli A (2022) Mud lobster *Thalassinia* Latreille, 1806 (Decapoda: Gebiidea: Thalassinidae), its Cenozoic occurrences in Italy and palaeobiogeography. *Geodiversitas* 44(13): 417–425. <https://doi.org/10.5252/geodiversitas2022v44a13>
- Jarupongsakul S, Thiramongkol N (1992) Holocene highstand shoreline of the Chao Phraya delta, Thailand. *Journal of Southeast Asian Earth Sciences* 7(1): 53–60. [https://doi.org/10.1016/0743-9547\(92\)90014-3](https://doi.org/10.1016/0743-9547(92)90014-3)
- Johnson RI (1964) The recent Mollusca of Augustus Addison Gould. *Bulletin - United States National Museum* 239(239): 1–182. <https://doi.org/10.5479/si.03629236.239>
- Jonas JH (1846) Ueber die Gattung Proserpina, und Beschreibungen neuer Conchylien. *Zeitschrift für Malakozoologie* 1846: 10–16. <https://www.biodiversitylibrary.org/page/16291804>
- Jones DS, Hosie AM (2016) A checklist of the barnacles (Cirripedia: Thoracica) of Singapore and neighbouring waters. *Raffles Bulletin of Zoology (Supplement No. 34)*: 241–311. <https://lkcnhm.nus.edu.sg/wp-content/uploads/sites/10/app/uploads/2017/06/S34rbz241-311.pdf>
- Jones DS, Hewitt MA, Sampey A (2000) A checklist of the Cirripedia of the South China Sea. *The Raffles Bulletin of Zoology (Supplement No. 8)*: 233–307. <https://lkcnhm.nus.edu.sg/wp-content/uploads/sites/10/app/uploads/2017/04/s08rbz233-307.pdf>
- Kang D-R, Tan KS, Liu L-L (2018) Egg-collar morphology and identity of nine species of Naticidae (Gastropoda) in Taiwan, with an assessment of their phylogenetic relationships. *Journal of Molluscan Studies* 84: 354–378. <https://doi.org/10.1093/mollus/eyy041>
- Kanthalajan G, Pandey PK, Krishnan P, Deepak Samuel V, Bharti VS, Purvaja R (2017) Molluscan diversity in the mangrove ecosystem of Mumbai, west coast of India. *Regional Studies in Marine Science* 14: 102–111. <https://doi.org/10.1016/j.rsma.2017.06.002>
- Kantor YI, Syssoev AV (2006) Marine and brackish water Gastropoda of Russia and adjacent countries: an illustrated catalogue. KMK Scientific Press, Moscow, 372 pp.
- Karasawa H, Kobayashi N (2022) Cirripedes from the middle Pleistocene Atsumi Group, Japan, with a reevaluation of the genus *Adna* Sowerby, 1823 (Balanoidea: Pyrgomatidae). *Bulletin of the Mizunami Fossil Museum* 49: 67–93. https://doi.org/10.50897/bmf.49.0_67
- Kepel' AA (2018) The first finding of *Fistulobalanus kondakovi* (Tarasov & Zevina, 1957) (Cirripedia: Thoracica) in the Russian waters of the Sea of Japan. *Russian Journal of Biological Invasions* 9(1): 50–52. <https://doi.org/10.1134/S2075111718010101>
- Kesavan K, Palpandi C, Shanmugam A (2009) A checklist of malacofauna of the Vellar Estuarine Mangroves, India. *Journal of Threatened Taxa* 1(7): 382–384. <https://doi.org/10.11609/JoTT.o1912.382-4>
- Kilburn R, Hylleberg J (1998) Gastropods and bivalves from Thailand; with taxonomic notes and new records. *Phuket Marine Biological Center Special Publication* 18: 311–316.

- Kim IH (2011) Flora and Fauna of Korea, Invertebrate Fauna of Korea, vol. 21, no. 6. Arthropoda: Crustacea: Cirripedia. Barnacles. National Institute of Biological Resources, Incheon, 144 pp.
- Kim HK (2020) Taxonomic Study of the Thoracican Barnacles (Crustacea: Thecostraca: Thoracica) in Korean Waters. Diversity, Host specificity, Distribution. PhD Thesis, Seoul National University, Seoul, South Korea. <http://dcollection.snu.ac.kr/common/orgView/000000160138>
- Kim IH, Kim HS (1980) Systematic studies on the cirripeds (Crustacea) from Korea. I. Balanomorph barnacles (Cirripedia, Thoracica, Balanomorpha). *Tongmul Hakhoe Chi* 23: 161–185. <https://koreascience.kr/article/JAKO198011919887096.page>
- Knudsen J, Jensen KR (2001) Translations into English of Lorenz Spengler's papers on *Bivalvia* (1783–1798). Part 3. 1788: *Pholas siamensis* with notes on the type specimen. The oldest marine bivalve with a type locality in the Gulf of Thailand. *Phuket Marine Biological Center Special Publication* 25: 547–556.
- Kocsis L, Razak H, Briguglio A, Szabo M (2019) First report on a diverse Neogene cartilaginous fish fauna from Borneo (Ambug Hill, Brunei Darussalam). *Journal of Systematic Palaeontology* 17(10): 791–819. <https://doi.org/10.1080/14772019.2018.1468830>
- Köhler R (2020) Echinoids of the Indian Museum at Calcutta. III. Regular Echinoids: A Translation of *Échinides du Musée indien à Calcutta*. III. Echinides réguliers (J. M. Lawrence, Trans.). Herizos Press, Tampa, 147 pp.
- Kool HH (2007) *Nassarius garuda* n. sp., a new deepwater species from the Indonesian Tanimbar and Kai Islands and a review of the species *N. crematus* (Hinds, 1844), *N. euglyptus* (Sowerby III, 1914) and *N. siquijorensis* (A. Adams, 1852) (Gastropoda: Buccinoidea: Nassariidae). *Miscellanea Malacologica* 2: 87–92.
- Krajangdara T, Vidthayanon C, Ali A, Lim A, Sumontha M, Rodpradit S, Chansue N, Haetrakul T (2022) The Cartilaginous Fishes of Thailand and Adjacent Waters. Department of Fisheries, Thailand, 233 pp.
- Kumar R, Jaiswar AK, Jahageerdar S, Chakraborty SK, Pavan Kumar A, Prasad L (2017) Comparative taxonomic evaluation of *Thais* species (Order: Gastropoda; Family: Muricidae) of Mollusca from Maharashtra coast of India. *Indian Journal of Geo-Marine Sciences* 46: 1098–1104. <http://nopr.niscpr.res.in/handle/123456789/42018>
- Kuroda T, Habe T, Oyama K (1971) The Sea Shells of Sagami Bay. Maruzen Co., Tokyo, xix, 741 (Japanese), 489 (English), 751 (index) pp.
- Ladd HS (1982) Cenozoic fossil mollusks from western Pacific islands; gastropods (Eulimidae and Volutidae through Terebridae). *Professional Paper* 1171: 1–100. <https://doi.org/10.3133/pp1171>
- Lam K, Morton B, Hodgson P (2008) Ahermatypic corals (Scleractinia: Dendrophylliidae, Oculinidae and Rhizangiidae) recorded from submarine caves in Hong Kong. *Journal of Natural History* 42(9–12): 729–747. <https://doi.org/10.1080/00222930701862724>
- Lamarck J-BM de (1818) *Histoire naturelle des animaux sans vertèbres*. Tome 5. Deterville/Verdière, Paris, 612 pp.
- Lamarck J-BM de (1822) *Histoire naturelle des animaux sans vertèbres*. Tome septième. de Lamarck, J.-B. M., Paris, 711 pp.
- Lane DJW, Marsh LM, Vandenspiegel D, Rowe FWE (2000) Echinoderm fauna of the South China Sea: An inventory and analysis of distribution patterns. *The Raffles Bulletin of Zoology (Supplement No. 8)*: 459–493. <https://lknhm.nus.edu.sg/wp-content/uploads/sites/10/app/uploads/2017/04/s08rbz459-493.pdf>

- Last PR, White WT, de Carvalho MR, Séret B, Stehmann MFW, Naylor GJP (2016) Rays of the World. CSIRO Publishing, Clayton South, 790 pp. <https://doi.org/10.1071/9780643109148>
- Lebedev EB (2014) Intertidal gastropod mollusks of the Far Eastern Marine Biosphere Natural Reserve. In: Sayenko EM, Lutaenko KA (Eds) Abstracts of the Conference Mollusks of the Eastern Asia and Adjacent Seas. Dalnauka, Vladivostok, Russia, 56–59.
- Li C, Corrigan S, Yang L, Straube N, Harris M, Hofreiter M, White WT, Naylor GJP (2015) DNA capture reveals transoceanic gene flow in endangered river sharks. *Proceedings of the National Academy of Sciences of the United States of America* 112(43): 13302–13307. <https://doi.org/10.1073/pnas.1508735112>
- Liao Y (1998) The Echinoderm fauna of Hainan Island. In: Morton B (Ed.) *The Marine Biology of the South China Sea III: Proceedings of the Third International Conference on the Marine Biology of the South China Sea*. Hong Kong University Press, Hong Kong, 75–82.
- Lim KC, White WT, Then AYH, Naylor GJP, Arunrugstichai S, Loh K-H (2022) Integrated taxonomy revealed genetic differences in morphologically similar and non-sympatric *Scoliodon macrorhynchos* and *S. laticaudus*. *Animals* 12(6): 681. <https://doi.org/10.3390/ani12060681>
- Lin C-H, Wang Y-C, Ribas-Deulofeu L, Chang C-W, Li K-T (2022) Changes in marine resource consumption over the past 5000 years in southwestern Taiwan revealed by fish otoliths. *Journal of Archaeological Science, Reports* 42: 103400. <https://doi.org/10.1016/j.jasrep.2022.103400>
- Linnaeus C (1758) *Systema naturae per regna tria naturae: secundum classes, ordines, genera, species, cum characteribus, differentiis, synonymis, locis. Editio decima, reformata* [10th revised edn.], vol. 1. Laurentius Salvius, Holmiae, 824 pp. <https://doi.org/10.5962/bhl.title.542>
- Linnaeus C (1767) *Systema naturae per regna tria naturae: secundum classes, ordines, genera, species, cum characteribus, differentiis, synonymis, locis. Ed. 12. 1., Regnum Animale. 1 & 2. Laurentii Salvii, Holmiae* [Stockholm]. <https://doi.org/10.5962/bhl.title.157601>
- Low MEY, Tan SK (2014) *Ergaea* H. Adams & A. Adams, 1854, the correct genus for *Crepidula walshi* Reeve, 1859, with nomenclatural notes on *Syphopatella* Lesson, 1831, *Siphonipatella* L. Agassiz, 1846, and the incorrect subsequent spelling “*Siphopatella*” of authors (Gastropoda: Calyptraeioidea: Calyptraeidae). *Occasional Molluscan Papers* 3: 11–14. <https://archive.org/details/ErgaeaH.AdamsA.Adams1854TheCorrectGenusForCrepidulaWalshiReeve/omp-v003-p011/>
- Lozano-Cortés DF, Londoño-Cruz E (2013) Checklist of barnacles (Crustacea; Cirripedia: Thoracica) from the Colombian Pacific. *Marine Biodiversity* 43(4): 463–471. <https://doi.org/10.1007/s12526-013-0175-2>
- Lozouet P (2008) Batillariidae & Potamididae. In: Poppe GT (Ed.) *Philippine Marine Mollusks Volume I*. ConchBooks, Hackenheim, Germany, 284–285.
- Lutaenko K (2015) The arcid collection of Carl Emil Lischke in the Zoological Institute, St. Petersburg. *Archiv für Molluskenkunde International Journal of Malacology* 144: 125–138. <https://doi.org/10.1127/arch.moll/1869-0963/144/125-138>
- Lutaenko K, Noseworthy RG, Choi K-S (2019) Marine bivalve mollusks of Jeju Island (Korea). Part 1. *The Korean Journal of Malacology* 35: 149–238.
- Lynge H (1909) *Marine Lamellibranchia. The Danish Expedition to Siam 1899–1900. Det Kongelige Danske Videnskabernes Selskab Skrifter, Naturvidenskab og Matematik Afdeling, Ser 7 5: 97–299*. <https://www.biodiversitylibrary.org/part/25913>

- Majima R (1989) Cenozoic fossil Naticidae (Mollusca: Gastropoda) in Japan. *Bulletins of American Paleontology* 96: 1–159. <https://www.biodiversitylibrary.org/item/40603>
- Malyshkina TP, Ward DJ, Nazarkin MV, Nam G-S, Kwon S-H, Lee J-H, Kim T-W, Kim D-K, Baek D-S (2023) Miocene Elasmobranchii from the Duho Formation, South Korea. *Historical Biology* 35(9): 1726–1741. <https://doi.org/10.1080/08912963.2022.2110870>
- Marsh LM, Morrison SM (2004) Echinoderms of the Dampier Archipelago, Western Australia. *Records of the Western Australian Museum Supplement No. 66*: 293–342. <https://doi.org/10.18195/issn.0313-122x.66.2004.293-342>
- Marsili S (2007) Revision of the teeth of the genus *Carcharhinus* (Elasmobranchii; Carcharhinidae) from the Pliocene of Tuscany, Italy. *Rivista Italiana di Paleontologia e Stratigrafia* 113: 79–95. <https://doi.org/10.13130/2039-4942/6360>
- Martens E von (1860) On the Mollusca of Siam. *Proceedings of the Zoological Society of London* 28: 6–18. <https://www.biodiversitylibrary.org/item/46225>
- Martin JC (2008) Nassariidae. In: Poppe GT (Ed) *Philippine Marine Mollusks Volume II*. ConchBooks, Hackenheim, Germany, 114–129.
- Matsubara T, Komori K (2007) The first record of fossil *Ellobium* (Gastropoda: Ellobiidae) from northeastern Japan. *Venus* 65: 325–331. https://doi.org/10.18941/venus.65.4_325
- Merle D, Garrigues B, Pointier J-P (2011) *Fossil and Recent Muricidae of the world. Part Muricinae*. Conchbooks, Hackenheim, 648 pp.
- Meyer E, Nilkerd B, Glover EA, Taylor JD (2008) Ecological importance of chemoautotrophic lucinid bivalves in a peri-mangrove community in eastern Thailand. *The Raffles Bulletin of Zoology (Supplement 18)*: 41–55. <https://lknhm.nus.edu.sg/app/uploads/2017/06/s18rbz041-055.pdf>
- Middlefart P (1997) An illustrated checklist of Muricidae (Gastropoda: Prosobranchia) from the Andaman Sea, Thailand. *Phuket Marine Biological Center Special Publication* 17: 348–388.
- Milne Edwards H, Haime J (1848) *Recherches sur les polypiers. Mémoire 3. Monographie des eupsammides*. *Annales des Sciences Naturelles, Zoologie, Series 3* 10: 65–114. <https://www.biodiversitylibrary.org/item/49250>
- Milne Edwards H, Haime J (1849) *Recherches sur les polypiers. Quatrième mémoire. Monographie des astréides (1). Suite. Quatrième section. Astréens agglomérés. As-treinae aggregatae*. *Annales des sciences naturelles, Zoologie, Series 3* 12: 95–197. <https://www.biodiversitylibrary.org/item/48069>
- Moh ZC, Nelson JD, Brand EW (1969) Strength and deformation behavior of Bangkok Clay. In: *Proceedings of the Seventh International Conference on Soil Mechanics, Vol 1*. Mexico City, 287 pp.
- Moh HH, Chong VC, Lim PE, Tan J (2013) Verification of four species of the mud lobster genus *Thalassina* (Crustacea: Decapoda: Gebiidea: Thalassinidae) using molecular and morphological characters. *The Raffles Bulletin of Zoology* 61: 579–588. <https://lknhm.nus.edu.sg/app/uploads/2017/06/61rbz579-588.pdf>
- MolluscaBase (2023) MolluscaBase taxon details: *Potamocorbula* Habe, 1955. <https://www.marinespecies.org/aphia.php?p=taxdetails&id=397174> [Verified 3 January 2023]
- Morris S, Purchon RD (1981) The marine shelled Mollusca of West Malaysia and Singapore part 3, Bivalvia. *Journal of Molluscan Studies* 47: 322–327. <https://doi.org/10.1093/oxfordjournals.mollus.a065575>

- Mortensen T (1904) The Danish Expedition to Siam 1899–1900. III. Echinoidea (1). Kongelige Danske Videnskabelige Selskabs, Skrifter, Serie 7 1: 1–124. <https://www.biodiversitylibrary.org/item/31830>
- Mortensen T (1940) Contributions to the biology of the Philippine Archipelago and adjacent regions: Report on the Echinoidea collected by the United States Fisheries steamer "Albatross" during the Philippine Expedition, 1907–1910. Part 2: The Echinothuridae, Saleniidae, Arbaciidae, Aspidodiadematidae, Micropygidae, Diadematidae, Pedinidae, Temnopleuridae, Toxopneustidae, and Echinometridae. Bulletin - United States National Museum 14: i–vi, 1–52. <https://repository.si.edu/handle/10088/21253>
- Mortensen T (1943) Monograph of the Echinoidea. III. 2 Camarodonta. I. Orthopsidae, Glyphocyphidae, Temnopleuridae and Toxopneustidae. C. A. Reitzel, Copenhagen, 533 pp.
- Mucharin A, Sumitrakij R (2022) Echinoderms (Phylum Echinodermata) of Ko Yao Noi-Ko Yao Yai and nearby islands, Pang-Nga Province, Thailand. Science, Technology, and Social Sciences Procedia 2022: rspg002. <https://wjst.wu.ac.th/index.php/stssp/article/download/25685/2291/73007>
- Mukhopadhyay AK, Sharma K, Ramakrishna (2013) Two new records of the genus *Polinices* and one of the *Natica* from India. Records of the Zoological Survey of India 113: 151–154.
- Müller J, Henle FGJ (1838) Systematische Beschreibung der Plagiostomen. Veit und Comp., Berlin, xxii, 200 pp. [Pp. 201–228: 1838]
- Müller J, Henle FGJ (1839) Systematische Beschreibung der Plagiostomen. Veit und Comp., Berlin, xxii, 200 pp. [reset pp. 227–228, 229–102: 1839]
- Mustapha N, Baharuddin N, Tan SK, Marshall DJ (2021) The neritid snails of Brunei Darussalam: their geographical, ecological and conservation significance. Ecologica Montenegrina 42: 45–61. <https://doi.org/10.37828/em.2021.42.2>
- Nabhitabhata J (2009) Checklist of Mollusca Fauna in Thailand. Office of Natural Resources and Environmental Policy and Planning, Bangkok, 576 pp.
- Nakamura I, Parin NV (1993) FAO species catalogue. Vol. 15. Snake mackerels and cutlassfishes of the world (Families Gempylidae and Trichiuridae). An annotated and illustrated catalogue of the snake mackerels, snoeks, escolars, gemfishes, sackfishes, domine, oilfish, cutlassfishes, scabbardfishes, hairtails, and frostfishes known to date. FAO Fisheries Synopsis No 125 15: 1–136. <http://www.fao.org/3/a-t0539e.pdf>
- Nakamura I, Parin NV (1998) Trichiuridae Cutlassfishes. In: Carpenter KE, Niem VH (Eds) FAO species identification guide for fishery purposes The living marine resources of the Western Central Pacific Volume 6 Bony fishes part 4 (Labridae to Latimeriidae), estuarine crocodiles, sea turtles, sea snakes and marine mammals. FAO, Rome, 3709–3720.
- Nateewathana A (1995) Taxonomic account of commercial and edible molluscs, excluding cephalopods, of Thailand. Phuket Marine Biological Center Special Publication 15: 93–116.
- Nateewathana A, Tantichodok P, Bussarawich S, Sirivejabandhu R (1981) Marine organisms in the Reference Collection. Research Bulletin - Phuket Marine Biological Center 28: 43–86.
- Negri MP (2009) Fossil mollusc-faunas: Their bearing on the Holocene evolution of the Lower Central Plain of Bangkok (Thailand). Journal of Asian Earth Sciences 35(6): 524–544. <https://doi.org/10.1016/j.jseaes.2009.04.003>

- Negri MP (2012) A Late Pleistocene transgression in Thailand: A marine molluscan fauna from Ban Praksa (Samut Prakan Province). *Journal of Asian Earth Sciences* 43(1): 145–149. <https://doi.org/10.1016/j.jseaes.2011.09.006>
- Negri MP, Sanfilippo R, Basso D, Rosso A, Di Geronimo SI (2014) Molluscan associations from the Pak Phanang Bay (SW Gulf of Thailand) as a record of natural and anthropogenic changes. *Continental Shelf Research* 84: 204–218. <https://doi.org/10.1016/j.csr.2014.04.019>
- Newman WA, Ross A (1976) Revision of the balanomorph barnacles: including a catalog of the species. *Memoirs of the San Diego Society of Natural History* 9: 1–108. <https://www.biodiversitylibrary.org/page/4328558>
- Ng TH, Tan SK, Wong WH, Meier R, Chan S-Y, Tan HH, Yeo DCJ (2016) Molluscs for sale: Assessment of freshwater gastropods and bivalves in the ornamental pet trade. *PLoS ONE* 11(8): e0161130. <https://doi.org/10.1371/journal.pone.0161130>
- Ngoc-Ho N, de Saint Laurent M (2009) The genus *Thalassina* Latreille, 1806 (Crustacea: Thalassinidea: Thalassinidae). *The Raffles Bulletin of Zoology (Supplement No. 20)*: 121–158. <https://lknhm.nus.edu.sg/app/uploads/2017/04/s20rbz121-158.pdf>
- Nimnate P, Chutakositkanon V, Choowong M, Pailoplee S, Phantu Wongraj S (2015) Evidence of Holocene sea level regression from Chumphon coast of the Gulf of Thailand. *ScienceAsia* 41(1): 55–63. <https://doi.org/10.2306/scienceasia1513-1874.2015.41.055>
- Nobuhara T (1993) The relationship between bathymetric depth and climate change and its effect on molluscan faunas of the Kakegawa Group, central Japan. *Transactions and Proceedings of the Paleontological Society of Japan New series* 170: 159–185. https://doi.org/10.14825/prpsj1951.1993.170_159
- Nolf F (2009) *Thais lacera* (Born, 1778) (Mollusca: Gastropoda: Muricoidae: Muricidae): an early record of an exotic species from the western Mediterranean Sea. *Neptunea* 8: 9–15.
- Ohe F (1976) Fossil otoliths of Sciaenid fishes from the Tertiary and Quaternary formations, Tobai district, central Japan and their paleontological vicissitudes. *Bulletin of the Mizunami Fossil Museum* 3: 73–97. <http://www2.city.mizunami.gifu.jp/bulletin/list/20/detail7.html>
- Ohtsubo M, Egashira K, Koumoto T, Bergado DT (2000) Mineralogy and chemistry, and their correlation with the geotechnical index properties of Bangkok clay: Comparison with Ariake clay. *Soil and Foundation* 40(1): 11–21. <https://doi.org/10.3208/sandf.40.11>
- Okutani T (2017) *Marine mollusks in Japan*, ed. 2. 2 vols. Tokai University Press, Tokyo, Japan, 1375 pp.
- Oliveira LPH de (1941) Contribuição ao conhecimento dos crustáceos do Rio de Janeiro, Sub-ordem 'Balanomorpha' (Cirripédia, Thoracica). *Memórias do Instituto Oswaldo Cruz* 36: 1–31. <https://doi.org/10.1590/S0074-02761941000100004>
- Oliver PG (1992) *Bivalved seashells of the Red Sea*. National Museum of Wales, Cardiff, 330 pp.
- Oliver GJH, Terry JP (2019) Relative sea-level highstands in Thailand since the Mid-Holocene based on ¹⁴C rock oyster chronology. *Palaeogeography, Palaeoclimatology, Palaeoecology* 517: 30–38. <https://doi.org/10.1016/j.palaeo.2018.12.005>
- Olivera B, Sysoev A (2008) Turridae. In: Poppe GT (Ed) *Philippine Marine Mollusks Volume II*. ConchBooks, Hackenheim, Germany, 764–787.
- Oyama K (1953) Review of the known species of the Japanese Turridae (1). *Venus* 17: 151–160. https://doi.org/10.18941/venusijmc.17.3_151

- Öztürk B, Bitlis BB (2013) *Eunaticina papilla* (Gmelin, 1791) (Naticidae, Gastropoda): A new alien mollusc in the eastern Mediterranean. *Triton* 28: 7–8.
- Palanisamy SK, Prasanna Kumar C, Paramasivam P, Sundaresan U (2020) DNA barcoding of horn snail *Telescopium telescopium* (Linnaeus C, 1758) using mt-COI gene sequences. *Regional Studies in Marine Science* 35: 101109. <https://doi.org/10.1016/j.rsma.2020.101109>
- Philippi RA (1836) Beschreibung einiger neuen Conchylien-Arten und Bemerkungen über die Gattung *Lacuna* von Turton. *Archiv für Naturgeschichte* 2: 224–235. <https://www.biodiversitylibrary.org/page/45630143>
- Pilsbry HA (1895) Catalogue of the marine molluscs of Japan, with descriptions of new species, and notes on others collected by F. Stearns. F. Stearns, Detroit, viii + 196 pp. <https://doi.org/10.5962/bhl.title.32672>
- Pilsbry HA (1916) The sessile barnacles (Cirripedia) collected in the collections of the U. S. National Museum: Including a monograph of the American species. *Bulletin - United States National Museum* 93(93): 1–366. <https://doi.org/10.5479/si.03629236.93.1>
- Pitombo FB (2004) Phylogenetic analysis of the Balanidae (Cirripedia, Balanomorpha). *Zoologica Scripta* 33(3): 261–276. <https://doi.org/10.1111/j.0300-3256.2004.00145.x>
- Pochai A, Kingtong S, Sukparangsi W, Khachonpisitsak S (2017) The diversity of acorn barnacles (Cirripedia, Balanomorpha) across Thailand's coasts: The Andaman Sea and the Gulf of Thailand. *Zoosystematics and Evolution* 93(1): 13–34. <https://doi.org/10.3897/zse.93.10769>
- Ponder WF, Vokes EH (1988) A revision of the Indo-West Pacific fossil and recent species of *Murex* s.s. and *Haustellum* (Mollusca: Gastropoda: Muricidae). *Records of the Australian Museum (Supplement 8)*: 1–160. <https://doi.org/10.3853/j.0812-7387.8.1988.96>
- Poppe GT (2010a) Arcidae. In: Poppe GT (Ed.) *Philippine Marine Mollusks Volume III*. ConchBooks, Hackenheim, Germany, 468–491.
- Poppe GT (2010b) Corbulidae. In: Poppe GT (Ed.) *Philippine Marine Mollusks Volume IV*. ConchBooks, Hackenheim, Germany, 386–391.
- Poppe GT (2010c) Veneridae. In: Poppe GT (Ed.) *Philippine Marine Mollusks Volume IV*. ConchBooks, Hackenheim, Germany, 258–309.
- Poutiers JM (1998a) Bivalve (Acephala, Lamellibranchia, Pelecypoda). In: Carpenter KE, Niem VH (Eds) *FAO Species Identification Guide for Fishery Purposes The Living Marine Resources of the Western Central Pacific Volume 1 Seaweeds, corals, bivalves and gastropods*. Food and Agriculture Organization of the United Nations, Rome, Italy, 123–362.
- Poutiers JM (1998b) Gastropods. In: Carpenter KE, Niem VH (Eds) *FAO Species Identification Guide for Fishery Purposes The Living Marine Resources of the Western Central Pacific Volume 1 Seaweeds, corals, bivalves and gastropods*. Food and Agriculture Organization of the United Nations, Rome, Italy, 363–648.
- Powell AWB (1942) The New Zealand Recent and fossil Mollusca of the family Turridae with general notes on turrid nomenclature and systematics. *Bulletin of the Auckland Institute and Museum* 2: 1–188. <https://www.biodiversitylibrary.org/item/278251>
- Powell AWB (1969) The family Turridae in the Indo-Pacific. Part 2. The subfamily Turriculinae. *Indo-Pacific Mollusca* 2: 215–416. <https://www.biodiversitylibrary.org/page/49824050>
- Prabowo RE, Yamaguchi T (2005) A new mangrove barnacle of the genus *Fistulobalanus* (Cirripedia: Amphibalaninae) from Sumbawa Island, Indonesia. *Journal of the Marine Biological Association of the United Kingdom* 85(4): 929–936. <https://doi.org/10.1017/S0025315405011902>

- Price ARG (1981) Studies on the echinoderm fauna of the western Arabian Gulf. *Journal of Natural History* 15(1): 1–15. <https://doi.org/10.1080/00222938100770011>
- Printrakoon C, Wells FE, Chitramvong Y (2008) Distribution of molluscs in mangroves at six sites in the upper Gulf of Thailand. *The Raffles Bulletin of Zoology* 18: 247–257. <https://lkcnm.nus.edu.sg/wp-content/uploads/sites/10/app/uploads/2017/04/s18rbz247-257.pdf>
- Puspasari IA, Yamaguchi T, Angsupanich S (2000) Reexamination of a little-known mangrove barnacle, *Balanus patelliformis* Bruguière (Cirripedia, Thoracica) from the Indo-West Pacific. *Sessile Organisms* 16(2): 1–13. https://doi.org/10.4282/sosj.16.2_1
- Puspasari IA, Yamaguchi T, Angsupanich S (2001) *Balanus thailandicus* sp. nov., a new mangrove barnacle of the *Balanus amphitrite* complex (Cirripedia, Balanomorpha) from Satun, Southwest Thailand. *Sessile Organisms* 18(1): 27–33. <https://doi.org/10.4282/sosj.18.27>
- Putchakarn S (2018) Biodiversity of sea urchins (Echinoidea, Echinodermata) in Thai Waters. Institute of Marine Science, Burapha University, 108 pp.
- Putchakarn S, Sonchaeng P (2004) Echinoderm fauna of Thailand: History and inventory reviews. *ScienceAsia* 30(4): 417–428. <https://doi.org/10.2306/scienceasia1513-1874.2004.30.417>
- Ramakrishna DA Barua S, Mukhopadhyaya A (2007) Marine molluscs: Polyplacophora and Gastropoda. Fauna of Andhra Pradesh, State Fauna Series Vol 5 Part 7. Zoological Survey of India, Kolkata, 1–148.
- Rau JL, Nutalaya P (1983) Geology of the Bangkok clay. *Buletin Persatuan Geologi Malaysia* 16: 99–116. <https://doi.org/10.7186/bgsm16198309>
- Raven JGM (2019) Notes on molluscs from NW Borneo - Dispersal of molluscs through nipa rafts. *The Festivus* 51(1): 3–10. <https://doi.org/10.54173/F511003>
- Raven H, Vermeulen JJ (2007) Notes on molluscs from NW Borneo and Singapore. 2. A synopsis of the Ellobiidae (Gastropoda, Pulmonata). *Vita Malacologica* 4: 29–62.
- Reeve L (1844) Monograph of the genus *Arca*. *Conchologia Iconica, or, illustrations of the shells of molluscous animals, vol 2, pls 1–17, and unpaginated text*. Lovell Reeve & Co., London. [without pagination] [stated dates: pl. 1–2: 1843; 1843–1817: 1844].
- Reeve LA (1855) Monograph of the genus *Nerita*. *Conchologia Iconica, or, illustrations of the shells of molluscous animals, vol 9, pls 1–19, and unpaginated text*. L. Reeve & Co., London.
- Reeve LA (1859) Monograph of the genus *Crepidula*. *Conchologia Iconica, or, illustrations of the shells of molluscous animals, vol 11, pl 1–5 and unpaginated text*. L. Reeve & Co., London.
- Reid DG (2014) The genus *Cerithidea* Swainson, 1840 (Gastropoda: Potamididae) in the Indo-West Pacific region. *Zootaxa* 3775(1): 1–65. <https://doi.org/10.11646/zootaxa.3775.1.1>
- Reid DG, Ozawa T (2016) The genus *Pirenella* Gray, 1847 (= *Cerithideopsis* Thiele, 1929) (Gastropoda: Potamididae) in the Indo-West Pacific region and Mediterranean Sea. *Zootaxa* 4076(1): 1–91. <https://doi.org/10.11646/zootaxa.4076.1.1>
- Reimer PJ, Austin WEN, Bard E, Bayliss A, Blackwell PG, Bronk Ramsey C, Butzin M, Cheng H, Edwards RL, Friedrich M, Grootes PM, Guilderson TP, Hajdas I, Heaton TJ, Hogg AG, Hughen KA, Kromer B, Manning SW, Muscheler R, Palmer JG, Pearson C, van der Plicht J, Reimer RW, Richards DA, Scott EM, Southon JR, Turney CSM, Wacker L, Adolphi F, Büntgen U, Capano M, Fahrni SM, Fogtmann-Schulz A, Friedrich R, Köhler P, Kudsk S, Miyake F, Olsen J, Reinig F, Sakamoto M, Sookdeo A, Talamo S (2020) The IntCal20 Northern Hemisphere radiocarbon age calibration curve (0–55 cal kBP). *Radiocarbon* 62(4): 725–757. <https://doi.org/10.1017/RDC.2020.41>

- Riede K (2004) Global register of migratory species from global to regional scales. Final Report of the R & D Project 808 05 081 (p. 329). Federal Agency for Nature Conservation, Bonn, Germany.
- Robba E, Di Geronimo I, Chaimanee N, Negri MP, Sanfilippo R (2002) Holocene and Recent shallow soft-bottom mollusks from the northern Gulf of Thailand area: Bivalvia. *Bollettino Malacologico* 38: 49–132.
- Robba E, Di Geronimo I, Chaimanee N, Negri M, Sanfilippo R (2003) Mollusc associations of the Northern Gulf of Thailand and Holocene analogs from the Bangkok Clay. *Maharakham University Journal* 22: 191–213.
- Robba E, Di Geronimo I, Chaimanee N, Negri MP, Sanfilippo R (2004) Holocene and recent shallow soft-bottom mollusks from the Northern Gulf of Thailand area: Scaphopoda, Gastropoda, additions to Bivalvia. *La Conchiglia. International Shell Magazine* 35: 1–290.
- Robba E, Di Geronimo I, Chaimanee N, Negri MP, Sanfilippo R (2007) Holocene and recent shallow soft-bottom mollusks from the Western Gulf of Thailand: Pak Phanang Bay and additions to Phetchaburi fauna. *Bollettino Malacologico* 43: 1–98.
- Roberts TR (2006) Rediscovery of *Glyphis gangeticus*: Debunking the mythology of the supposed “Gangetic freshwater shark”. *The Natural History Bulletin of the Siam Society* 54: 261–278. https://thesiamsociety.org/wp-content/uploads/2020/04/NHBSS_054_2I_Roberts_RediscoveryOfGlyp.pdf
- Röding PF (1798) *Museum Boltenianum sive Catalogus cimeliorum e tribus regnis naturæ quæ olim collegerat Joa. Fried Bolten, M. D. p. d. per XL. annos proto physicus Hamburgensis. Pars secunda continens Conchylia sive Testacea univalvia, bivalvia & multivalvia.* Trapp, Hamburg, viii, 199 pp.
- Rosell NC (1973) Some thoracic barnacles (Crustacea: Cirripedia) of Manila Bay. *Kalikaan, the Philippine Journal of Biology* 2: 69–95.
- Roussy H (1991) Family Pectinidae recorded – a checklist. *Phuket Marine Biological Center Special Publication* 9: 21.
- Royal Irrigation Department (2009) Soil and Geological Survey Report, Preparation of Cross Sections and Soil Classification in Irrigation Bureau Area No. 11. Royal Irrigation Department, Bangkok, 1–28 pp.
- Sahlmann B, Poppe GT (2010) Dentaliidae. In: Poppe GT (Ed.) *Philippine Marine Mollusks Volume IV.* ConchBooks, Hackenheim, Germany, 402–411.
- Sakai K, Türkay M (2012) A review of the species of the genus *Thalassina* (Thalassinidea, Thalassinidae). *Crustaceana* 85(11): 1339–1376. <https://doi.org/10.1163/15685403-00003114>
- Salvi D, Mariottini P (2021) Revision shock in Pacific oysters taxonomy: The genus *Magallana* (formerly *Crassostrea* in part) is well-founded and necessary. *Zoological Journal of the Linnean Society* 192(1): 43–58. <https://doi.org/10.1093/zoolinnean/zlaa112>
- Samyn Y (2003) Shallow-water regular echinoids (Echinodermata: Echinoidea) from Kenya. *African Zoology* 38: 193–212. <https://journals.co.za/doi/abs/10.10520/EJC17893>
- Sanpanich K (2011) Marine bivalves occurring on the east coast of the Gulf of Thailand. *ScienceAsia* 37(3): 195–204. <https://doi.org/10.2306/scienceasia1513-1874.2011.37.195>
- Sanpanich K, Duangdee T (2013) The biodiversity of marine gastropods of Thailand in the late decade. *Malaysian Journal of Science. Series B, Physical & Earth Sciences* 32(3): 47–64. <https://doi.org/10.22452/mjs.vol32no3.5>
- Sartori AF, Printrakoon C, Mikkelsen PA, Bieler R (2008) Siphonal structure in the Veneridae (Bivalvia: Heterodonta) with an assessment of its phylogenetic application and a

- review of venerids in the Gulf of Thailand. *The Raffles Bulletin of Zoology* (Supplement 18): 103–125. <https://lknhm.nus.edu.sg/app/uploads/2017/06/s18rbz103-125.pdf>
- Sathiamurthy E, Voris H (2006) Maps of Holocene sea level transgression and submerged lakes on the Sunda shelf. *The Natural History Journal of Chulalongkorn University* 2: 1–43. <https://li01.tci-thaijo.org/index.php/tnh/article/view/102930>
- Scarabino V (1995) Scaphopoda of the tropical Pacific and Indian Oceans, with description of 3 new genera and 42 new species. *Mémoires du Muséum national d'histoire naturelle* 167: 189–379. <https://www.biodiversitylibrary.org/part/288160>
- Schrenck LI (1861) Vorläufige Diagnosen einiger neuer Molluskenarten aus der Meerenge der Tartarei und dem Nordjapanischen Meere. *Bulletin de l'Académie Impériale des Sciences de St Pétersbourg* 4: 408–413. <http://hdl.handle.net/10062/3640>
- Schultz H (2015) *Handbook of Zoology: Echinodermata, Volume 1: Echinoidea*. Walter de Gruyter GmbH, Berlin/Boston, 386 pp.
- Schwarzhan W (1993) A comparative morphological treatise of recent and fossil otoliths of the family Sciaenidae (Perciformes). *Piscium catalogus: Part Otolithi Piscium*. Vol. 1. Verlag Dr. Friedrich Pfeil, München, 245 pp.
- Shimada K, Egi N, Tsubamoto T, Maung-Maung MM, Thaug-Htike TH, Zin-Maung-Maung-Thein ZM, Nishioka Y, Sonoda T, Takai M (2016) The extinct river shark *Glyphis pagoda* from the Miocene of Myanmar and a review of the fossil record of the genus *Glyphis* (Carcharhiniformes: Carcharhinidae). *Zootaxa* 4161(2): 237–251. <https://doi.org/10.11646/zootaxa.4161.2.6>
- Sinsakul S (2000) Late Quaternary geology of the lower central plain, Thailand. *Journal of Asian Earth Sciences* 18(4): 415–426. [https://doi.org/10.1016/S1367-9120\(99\)00075-9](https://doi.org/10.1016/S1367-9120(99)00075-9)
- Smith EA (1873) Remarks on a few species belonging to the family Terebridae, and descriptions of several new forms in the collection of the British Museum. *Annals & Magazine of Natural History* 11(64): 262–271. <https://doi.org/10.1080/00222937308696811>
- Smith EA (1875) A list of the Gasteropoda collected in Japanese seas by Commander H. C. St. John, R. N. *Annals & Magazine of Natural History* 15(90): 414–427. <https://doi.org/10.1080/00222937508681111>
- Smith EA (1877) Descriptions of new species of Conidae and Terebridae. *Annals & Magazine of Natural History* 19(111): 222–231. <https://doi.org/10.1080/00222937708682126>
- Smith EA (1879a) On a collection of marine shells from the Andaman Islands. *Proceedings of the Zoological Society of London* 1878(1): 804–821. <https://doi.org/10.1111/j.1469-7998.1878.tb08026.x>
- Smith EA (1879b) On a collection of Mollusca from Japan. *Proceedings of the Zoological Society of London* 1879(1): 181–218. <https://doi.org/10.1111/j.1096-3642.1879.tb02650.x>
- Somboon JRP (1988) Paleontological study of the recent marine sediments in the lower central plain, Thailand. *Journal of Southeast Asian Earth Sciences* 2(3–4): 201–210. [https://doi.org/10.1016/0743-9547\(88\)90031-1](https://doi.org/10.1016/0743-9547(88)90031-1)
- Somboon JRP, Thiramongkol N (1992) Holocene highstand shoreline of the Chao Phraya delta, Thailand. *Journal of Southeast Asian Earth Sciences* 7(1): 53–60. [https://doi.org/10.1016/0743-9547\(92\)90014-3](https://doi.org/10.1016/0743-9547(92)90014-3)
- Songtham W, Phanwong P, Seelanan T (2007) Middle Holocene peat and mollusk shells from Ongkharak area, Nakhon Nayok, central Thailand: evidence of in situ deposits during a marine transgression period. *International Conference on Geology of Thailand: Towards Sustainable Development and Sufficiency Economy*, 177–179.
- Songtham W, Musika S, Mildenhall DC, Cochran UA, Kojevnikova D (2015) Development of the lower central plain of Thailand with history of human settlements: Evidence

- from pollen, spores and diatoms. *Journal of Geological Resource and Engineering* 2(2): 98–107. <https://doi.org/10.17265/2328-2193/2015.02.004>
- Sowerby GB I (1822) The genera of recent and fossil shells, for the use of students, in conchology and geology. Published in 42 numbers. Vol. 1, pls 1–126 [1821–1825]; vol. 2, pls 127–262 + text (unpaginated) [1825–1834]. Sowerby I, G. B., London.
- Sowerby GB I (1833) [1832–1841] The conchological illustrations or, Coloured figures of all the hitherto unfigured recent shells. Sowerby I, G. B., London. <https://doi.org/10.5962/bhl.title.51602>
- Sowerby GB II (1842) Monograph of the genus *Pecten*. In: Sowerby GB II (Ed) *Thesaurus Conchyliorum, or monographs of Genera of Shells*. Sowerby II, G. B., London, 45–78.
- Spengler L (1792) Betragtninger og Anmærkninger ved den Linneiske Slægt *Pholas* blant de mangeskallede Muskeler, med dens hidindtil bekiendte gamle og nye Arter, samt den dermed i Forbindelse staaende Slægt *Teredo* Linn. *Skrivter af Naturhistorie-Selskabet, Kiøbenhavn* 2: 72–106. http://gdz.sub.uni-goettingen.de/dms/load/img/?PPN=PPN608227374_0002&DMDID=DMDLOG_0006
- Spengler L (1794) Nøiere Bestemmelse og Udvidelse af det Linneiske Genus *Solen*. *Skrivter af Naturhistorie-Selskabet, Kiøbenhavn* 3: 81–114. http://gdz.sub.uni-goettingen.de/dms/load/img/?PID=PPN608227374_0003%7CLOG_0033
- Springer VG (1964) A revision of the carcharhinid shark genera *Scoliodon*, *Loxodon*, and *Rhizoprionodon*. *Proceedings of the United States National Museum* 115(3493): 559–632. <https://doi.org/10.5479/si.00963801.115-3493.559>
- Sri-aroon P, Lohachit C, Harada M (2004) Survey of brackish-water snails in eastern Thailand. *The Southeast Asian Journal of Tropical Medicine and Public Health* 35: 150–155. <https://www.tm.mahidol.ac.th/seameo/2004-35-suppl-1/27-150.pdf>
- Sri-aroon P, Lohachit C, Harada M (2005) Brackish-water mollusks of Surat Thani Province, southern Thailand. *The Southeast Asian Journal of Tropical Medicine and Public Health* 36: 180–188. https://www.tm.mahidol.ac.th/seameo/2005_36_spp4/36sup4_180.pdf
- Steiner G, Kabat AR (2014) Catalog of species-group names of Recent and fossil Scaphopoda (Mollusca). *Zoosystema* 26: 549–726. <https://sciencepress.mnhn.fr/en/periodiques/zoosystema/26/4/catalogue-des-noms-du-groupe-espece-de-scaphopodes-mollusca-recents-et-fossiles>
- Stuiver M, Polach HA (1977) Discussion: Reporting of ¹⁴C data. *Radiocarbon* 19(3): 355–363. <https://doi.org/10.1017/S0033822200003672>
- Subba Rao NV, Dey A (2000) Catalogue of the marine molluscs of Andaman and Nicobar Islands. *Records of the Zoological Survey of India, Occasional Paper* 187: 1–323. <https://faunaofindia.nic.in/PDFVolumes/occpapers/187/index.pdf>
- Surakiatchai P, Choowong M, Charusiri P, Charoentitirat T, Chawchai S, Pailoplee S, Chabangborn A, Phantuwongraj S, Chutakositkanon V, Kongsen S, Nimnate P, Bissen R (2018) Paleogeographic reconstruction and history of the sea level change at Sam Roi Yot National Park, Gulf of Thailand. *Tropical Natural History* 18: 112–134. <https://li01.tci-thaijo.org/index.php/tnh/article/view/148171>
- Swennen C, Moolenbeek RG, Ruttanadakul N, Hobbelink H, Dekker H, Hajisamae S (2001) *The Molluscs of the Southern Gulf of Thailand*. The Biodiversity Research and Training Program, Bangkok, 210 pp.
- Takaya Y (1969) Topographical analysis of the southern basin of the central plain, Thailand. *Tonan Ajia Kenkyu (The Southeast Asian Studies)* 7: 293–300. https://doi.org/10.20495/tak.7.3_293

- Tan KS (2000) Species checklist of Muricidae (Mollusca: Gastropoda) in the South China Sea. The Raffles Bulletin of Zoology (Supplement No. 8): 495–512. <https://lkcnhm.nus.edu.sg/wp-content/uploads/sites/10/app/uploads/2017/04/s08r-bz495-512.pdf>
- Tan SK, Clements R (2008) Taxonomy and distribution of the Neritidae (Mollusca: Gastropoda) in Singapore. Zoological Studies 47: 481–494. <https://zoolstud.sinica.edu.tw/Journals/47.4/481.pdf>
- Tanabe S, Saito Y, Sato Y, Suzuki Y, Sinsakul S, Tiyaipairach S, Chaimanee N (2003) Stratigraphy and Holocene evolution of the mud-dominated Chao Phraya delta, Thailand. Quaternary Science Reviews 22(8–9): 789–807. [https://doi.org/10.1016/S0277-3791\(02\)00242-1](https://doi.org/10.1016/S0277-3791(02)00242-1)
- Tantanasiriwong R (1978) An illustrated checklist of marine shelled gastropods from Phuket Island, adjacent mainland and offshore island, western peninsular Thailand. Research Bulletin - Phuket Marine Biological Center 21: 1–63.
- Tantanasiriwong R (1979) A checklist of marine bivalves from Phuket Island, adjacent mainland and offshore island, western peninsular Thailand. Research Bulletin - Phuket Marine Biological Center 27: 1–15.
- Tarasov NI, Zevina GB (1957) Barnacles (Cirripedia, Thoracica) of the Soviet Seas. Fauna SSSR. Crustacea 6: 1–267.
- Taylor JD, Glover EA (2005) Cryptic diversity of chemosymbiotic bivalves: A systematic revision of worldwide *Anodontia* (Mollusca: Bivalvia: Lucinidae). Systematics and Biodiversity 3(3): 281–338. <https://doi.org/10.1017/S1477200005001672>
- Tesch P (1915) Jungtertiäre und quartäre Mollusken von Timor. I. Teil. Palaontologie von Timor, Stuttgart 5: 1–70.
- Tesch P (1920) Jungtertiäre und quartäre Mollusken von Timor. II. Teil. Palaontologie von Timor, Stuttgart 8: 41–121.
- Thach NN (2005) Shells of Vietnam. ConchBooks, Hackenheim, 338 pp.
- Thiele J (1925) Gastropoden der Deutschen Tiefsee-Expedition. II Teil. Wissenschaftliche Ergebnisse der Deutschen Tiefsee-Expedition auf dem Dampfer "Valdivia" 1898–1899 17: 35–382. [pls 313–346 [reprints paginated 381–348, pls 381–334]]
- Thunberg CP (1793) Tekning och Beskrifning på en stor Ostronsort ifrån Japan. Kongliga Vetenskaps Akademiens Nya Handlingar 14: 140–142. <https://www.biodiversitylibrary.org/page/46957303>
- Torigoe K, Inaba A (2011) Revision on the classification of recent Naticidae. Bulletin of the Nishinomiya Shell Museum 7: 1–133.
- Tudu PC, Balakrishnan S (2018) First report of Patridge Sundial Snail *Architectonica perdix* (Hinds, 1844) from Northern part of East Coast of India. Records of the Zoological Survey of India 118(2): 198–201. <https://doi.org/10.26515/rzsi/v118/i2/2018/123516>
- Tudu PC, Yennawar P, Ghorai N, Tripathy B, Mohapatra A (2018) An updated checklist of marine and estuarine mollusc of Odisha coast. Indian Journal of Geo-Marine Sciences 47: 1537–1560. <http://nopr.niscpr.res.in/handle/123456789/44778>
- Tudu PC, Yennawar P, Mohapatra A (2019) First report of two ark shells, *Anadara consociata* (E.A. Smith, 1885) and *A. troscheli* (Dunker, 1882) (Arcidae: Anadarinae) from Indian waters with notes on morpho-taxonomy of some related species from east coast of India. Records of the Zoological Survey of India 119: 34–48.
- Umitsu M, Tiyaipairach S, Chaimanee N, Kawase K (2002) Late Holocene sea-level change and evolution of the central plain, Thailand. The Symposium on Geology of Thailand, Bangkok, Thailand, 201–206.

- Verhecken A (1986) The recent Cancellariidae of Indonesia (Neogastropoda: Cancellariacea). *Gloria Maris* 25: 29–66.
- Verhecken A (1997) Mollusca, Gastropoda: Arafura Sea Cancellariidae collected during the KARUBAR Cruise. In: Crosnier A, Bouchet P (Eds) Résultats des Campagnes MUSORSTOM 16 Campagne Franco-Indonésienne KARUBAR Mémoires du Muséum national d'Histoire naturelle Série A, Zoologie, 172, 295–324.
- Verhecken A (2008) Cancellariidae. In: Poppe GT (Ed.) Philippine Marine Mollusks Volume II. ConchBooks, Hackenheim, Germany, 816–825.
- Voigt M, Weber D (2011) Field guide for sharks of the genus *Carcharhinus*. Verlag Dr. Friedrich Pfeil, München, 155 pp.
- Vongpanich V (1996) The Arcidae of Thailand. Phuket Marine Biological Center Special Publication 16: 177–192.
- Vongpanich V, Matsukuma A (2004) Family Noetiidae in Thailand. Research Bulletin - Phuket Marine Biological Center 65: 31–44.
- Way K, Purchon RD (1981) The marine shelled Mollusca of West Malaysia and Singapore part 2. Polyplacophora and Gastropoda. *Journal of Molluscan Studies* 47: 313–321. <https://doi.org/10.1093/oxfordjournals.mollus.a065574>
- Wells FE, Sanpanich K, Tan SK, Duangdee T (2021) The Marine and Estuarine Molluscs of Thailand. Lee Kong Chian Natural History Museum National University of Singapore, Singapore, 195 pp. <https://lkcnhm.nus.edu.sg/wp-content/uploads/sites/10/2021/01/LKCNHM-EBOOK-2021-0001.pdf>
- White WT (2012) A redescription of *Carcharhinus dussumieri* and *C. seali*, with resurrection of *C. coatesi* and *C. tjtjot* as valid species (Chondrichthyes: Carcharhinidae). *Zootaxa* 3241(1): 1–34. <https://doi.org/10.11646/zootaxa.3241.1.1>
- White WT, Last PR, Naylor GJP (2010) *Scoliodon macrorhynchus* (Bleeker, 1852), a second species of spadenose shark from the Western Pacific (Carcharhiniformes: Carcharhinidae). In: Last PR, White WT, Pogonoski JJ (Eds) Descriptions of New Australian Chondrichthyans, CSIRO Marine and Atmospheric Research Paper 32. CSIRO, Hobart, Australia, 61–76.
- White WT, Appleyard SA, Sabub B, Kyne PM, Harris M, Lis R, Baje L, Usu T, Smart JJ, Corrigan S, Yang L, Naylor GJP (2015) Rediscovery of the threatened river sharks, *Glyphis garricki* and *G. glyphis*, in Papua New Guinea. *PLoS ONE* 10(10): e0140075. <https://doi.org/10.1371/journal.pone.0140075>
- Whitley GP (1934) Notes on some Australian sharks. *Memoirs of the Queensland Museum* 10: 180–200. <https://www.biodiversitylibrary.org/partpdf/244018>
- Wilson B (1993) Australian marine shells, Prosobranch Gastropods, Vol. 1. Odyssey Publishing, Kallroo, Australia, 408 pp.
- Wilson B (1994) Australian marine shells, Prosobranch Gastropods, Vol. 2. Odyssey Publishing, Kallroo, Australia, 370 pp.
- Wium-Andersen G (1977) Marine *Nerita* species from Phuket island and their chromosome numbers (Gastropoda: Neritidae). Research Bulletin - Phuket Marine Biological Center 15: 1–9.
- Wong HW (2009) The Mactridae (Mollusca: Bivalvia) of East Coast Park, Singapore. *Nature in Singapore* 2: 283–296. <https://lkcnhm.nus.edu.sg/wp-content/uploads/sites/10/app/uploads/2017/06/2009nis283-296.pdf>
- Yadav R, Malla PK, Dash D, Bhoi G, Patro S, Mohapatra A (2019) Diversity of gastropods and bivalves in the mangrove ecosystem of Paradeep, east coast of India: A comparative study with other Indian mangrove ecosystems. *Molluscan Research* 39(4): 325–332. <https://doi.org/10.1080/13235818.2019.1644701>

- Yamaguchi T (1977a) Taxonomic studies on some fossil and recent Japanese Balanoidea (Part 1). Transactions and Proceedings of the Paleontological Society of Japan New series 1977: 135–160. https://doi.org/10.14825/prpsj1951.1977.107_135
- Yamaguchi T (1977b) Taxonomic studies on some fossil and recent Japanese Balanoidea (Part 2). Transactions and Proceedings of the Paleontological Society of Japan New series 1977: 161–201. https://doi.org/10.14825/prpsj1951.1977.108_161
- Yamaguchi T (1980) A new species belonging to the *Balanus amphitrite* Darwin group (Cirripedia, Balanomorpha) from the late Pleistocene of Japan; an example of peripheral speciation. Journal of Paleontology 54: 1084–1101. <https://www.jstor.org/stable/1304372>
- Yang W, Cai Y, Kuang X (2017) Color Atlas of Molluscs of the South China Sea. China Agriculture Press, Beijing, 275 pp.
- Yen T-C (1944) Notes on some unfigured type-specimens of Chinese mollusks from the North Pacific Expedition. Proceedings of the California Academy of Sciences 23: 561–586. <https://www.biodiversitylibrary.org/partpdf/21394>
- Yokoyama M (1927) Mollusca from the Upper Musashino of Western Shimosa and Southern Musaski. Journal of the Faculty of Science, University of Tokyo, Section 2: Geology, Mineralogy, Geography, Geophysics 1: 439–457.
- Yoosukh W, Jitkaew M (1997) Marine wood-boring bivalves (Pholadacea) in the Gulf of Thailand. Phuket Marine Biological Center Special Publication 17: 401–405.
- Zullo V (1984) New genera and species of balanoid barnacles from the Oligocene and Miocene of North Carolina. Journal of Paleontology 58: 1312–1338. <https://www.jstor.org/stable/1304855>
- Zvonareva S, Kantor Y (2016) Checklist of gastropod molluscs in mangroves of Khanh Hoa province, Vietnam. Zootaxa 4162(3): 401–437. <https://doi.org/10.11646/zootaxa.4162.3.1>

Four new inquiline social parasite species in the dolichoderine ant genus *Tapinoma* (Hymenoptera, Formicidae)

Stefan P. Cover¹ , Christian Rabeling^{1,2,3,4} 

¹ Museum of Comparative Zoology, Harvard University, 26 Oxford Street, Cambridge, MA 02138, USA

² Department of Integrative Taxonomy of Insects, Institute of Biology, University of Hohenheim, Garbenstraße 30, 70599 Stuttgart, Germany

³ KomBioTa – Center for Biodiversity and Integrative Taxonomy Research, University of Hohenheim & State Museum of Natural History Stuttgart, Stuttgart, Germany

⁴ Social Insect Research Group, School of Life Sciences, Arizona State University, 550 E Orange Street, Tempe, AZ 85281, USA

Corresponding authors: Stefan P. Cover (coverstefan@gmail.com); Christian Rabeling (crabeling@gmail.com)

Abstract

Four new inquiline social parasites are described in the dolichoderine ant genus *Tapinoma* from the Nearctic region, and keys are provided for queens and males of the Nearctic *Tapinoma* species. The new social parasite species represent the first inquiline species in the genus *Tapinoma* and the first confirmed inquilines known from the ant subfamily Dolichoderinae. The four new species appear to be workerless inquilines that exploit a single host, *Tapinoma sessile* (Say), and they represent at least two distinct life history syndromes. *Tapinoma incognitum* Cover & Rabeling, **sp. nov.** is highly derived morphologically and is a host-queen-tolerant inquiline. In contrast, *T. inflatiscapus* Cover & Rabeling, **sp. nov.** shows a lesser degree of morphological modification and appears to be a host-queen-intolerant social parasite. The life history of *T. pulchellum* Cover & Rabeling, **sp. nov.** is presently unknown, but its close similarity to *T. incognitum* suggests that it is also a host-queen-tolerant inquiline. The life history of *T. shattucki* Cover & Rabeling, **sp. nov.** is still uncertain. Our findings provide novel insights into the complex biology of ant inquiline life history syndromes.

Key words: Brood parasitism, Dolichoderinae, Formicidae, integrative taxonomy, inquilinism, social parasitism



Academic editor: Brian Lee Fisher

Received: 7 February 2024

Accepted: 15 April 2024

Published: 15 May 2024

ZooBank: <https://zoobank.org/D9698204-3A76-4B93-A4E5-E2352A12871A>

Citation: Cover SP, Rabeling C (2024) Four new inquiline social parasite species in the dolichoderine ant genus *Tapinoma* (Hymenoptera, Formicidae). ZooKeys 1202: 111–134. <https://doi.org/10.3897/zookeys.1202.120478>

Copyright: © Stefan P. Cover & Christian Rabeling. This is an open access article distributed under terms of the Creative Commons Attribution License (Attribution 4.0 International – CC BY 4.0).

Introduction

Social parasitism, the dependence of one social insect species on another during colony founding and/or during its complete life cycle, is one of the most intriguing life history phenomena found in the eusocial Hymenoptera (see Hölldobler and Wilson 1990; Bourke and Franks 1991; Buschinger 2009; Rabeling 2021 for general reviews). Most ant social parasites belong to one of three basic life history syndromes. Temporary social parasites require the assistance of a host species during colony founding only, and established colonies of the parasite produce numerous workers and are fully independent (Wheeler 1904; Borowiec et al. 2021). Dulotic social parasites establish new colonies as

temporary social parasites, but in mature colonies the parasite workers raid host nests and steal their brood, some of which is eaten. The remaining brood complete development to become host workers that feed and maintain the parasite colony (Hölldobler and Wilson 1990). The vast majority of dulotic parasites are completely dependent on their host workers.

The third major life history syndrome of ant social parasites is permanent inquilinism (Wilson 1971). Inquiline ants live within the nests of their hosts for their entire life cycle, excepting a brief period during which dispersal (and mating in some species) occurs. In most cases the inquiline queen coexists with one or more host queens but “castrates” the colony by suppressing or greatly reducing the production of host sexual forms and substituting the production of parasite sexual offspring (Kutter 1968; Rabeling and Bacci 2010). In others, the inquiline somehow eliminates the host queen(s) or is adopted successfully only in host colonies that have lost their queen (Wilson 1971; Rabeling et al. 2019). The inquiline worker caste is usually absent or produced in very small numbers. Inquilines seem to be extremely rare, and their populations appear to be few in number, small in size, and sporadically distributed (Wilson 1963). In addition, inquiline ants are usually small and inconspicuous relative to their hosts and are thus seldom noticed or collected, reinforcing the impression of rarity. As a result, our knowledge of the ecology, life history, and distribution of most inquiline ant species is fragmentary.

Inquilinism has evolved at least 57 times convergently across the formicoid clade of the ant tree of life, and 88 inquiline species have been confirmed to date (Gray and Rabeling 2023). The majority of inquiline species are concentrated in the ant subfamilies Myrmicinae and Formicinae. Curiously, true inquilines are unknown from the subfamily Dolichoderinae, though temporary social parasites occur with some frequency. Temporary social parasites have been reported from the dolichoderine genera *Arnoldius*, *Azteca*, *Bothriomyrmex*, *Chronoxenus*, and *Dorymyrmex* (Trager 1988; Dubovikoff 2005; Longino 2007; Guerrero et al. 2010). Based on the morphology of the queens, inquilinism has been suggested for *Azteca nanogyna* and *Azteca diabolica* (Longino 2007; Guerrero et al. 2010). Both are known from only a handful of specimens collected by canopy fogging or in flight-interception traps (Longino 2007; Guerrero et al. 2010), and their hosts and life-histories remain unknown.

Until the present, social parasites of any kind were unknown in the dolichoderine genus *Tapinoma*. Currently, 72 extant species are recognized in the genus *Tapinoma* and the genus is distributed globally (Bolton 2024). The North American ant fauna contains only four described species (Fisher and Cover 2007). *Tapinoma litorale* Wheeler, *Tapinoma schreiberi* Hamm, and *Tapinoma sessile* (Say) are native, whereas *Tapinoma melanocephalum* (Fabricius) is a global tramp species established in Florida (Hamm 2010; Deyrup 2017). Here, we report the first inquilines discovered in the genus *Tapinoma*. Curiously, the new *Tapinoma* inquilines all parasitize a single host species, *Tapinoma sessile*. The evolution of several inquilines against the complex population genetic backdrop of a single, widespread host species makes this host-parasite complex unique in the context of ant social parasitism and deserving of further examination.

Materials and methods

Specimens examined

In addition to new collections, specimens from the insect collections listed below were examined for this study:

CASC California Academy of Sciences, San Francisco, CA, U.S.A.

CRC C. Rabeling Collection, University of Hohenheim, Stuttgart, Germany

LACM Los Angeles County Museum of Natural History, Los Angeles, CA, U.S.A.

MCZC Museum of Comparative Zoology, Harvard University, Cambridge, MA, U.S.A.

UCDC Bohart Museum of Entomology Collection, University of California at Davis, CA, U.S.A.

Morphometric measurements

Specimens were examined and measured using a Leica MS5 stereomicroscope fitted with a stage micrometer. Measurements were taken at 25× magnification. Morphometric conventions and indices follow Bolton (1987) and modifications described in Rabeling et al. (2007). Morphometric measurements and indices are defined as follows in Table 1.

Table 1. Morphometric measurements and indices.

HL	Head Length	Length of the head in full face view, excluding mandibles, measured in a straight line from the midpoint of the anterior clypeal margin to the midpoint of the posterior margin of the head. In species where the posterior margin or the clypeal margin (or both) is concave, the measurement is taken from the midpoint of a transverse line spanning the anteriormost or posteriormost projecting points, respectively.
HW	Head Width	Maximum width of head, not including the eye.
CI	Cephalic Index	$HW*100/HL$
SL	Scape Length	Maximum straight-line length of the antennal scape excluding the basal constriction or neck close to the condylar bulb.
SI	Scape Index	$SL*100/HW$
ML	Mesosoma Length	Diagonal length of the mesosoma in profile from the point at which the pronotum meets the cervical shield to the posterior base of the metapleuron.

Results

Key to the queens of *Tapinoma* species occurring in the Nearctic region north of Mexico

- 1 Maxillary palp segments 2–4 strikingly flattened and notably broader than palp segments 1, 5, and 6. Labial palp segments 2 and 3 also flattened. Workers distinctly bi-colored with dark, almost black head and mesosoma contrasting sharply with pale yellow-white metasoma and appendages. [pantropical tramp, heated greenhouses, and buildings, outdoors in southern Florida, exotic] ***T. melanocephalum* (Fabricius)**
- Maxillary and labial palp segments subcylindrical, not strikingly flattened and broad. Workers (if present) often uniformly colored; if bicolored, different from pattern described above **2**

- 2 At least some erect hairs present on gastric tergites 1–3, sometimes short erect hairs present on mesosomal dorsum as well. Pubescence on antennal scapes short but suberect **3**
- Erect hairs absent on mesosomal dorsum and gastric tergites 1–3. Pubescence on antennal scapes variable but generally appressed **4**
- 3 Short erect hairs present on mesosomal dorsum and gastric tergites 1–3. Antennal scapes long, projecting well beyond the posterior corners of the head, and reaching maximum diameter between the antennal insertion and the midpoint. Short but dense suberect pubescence present on scapes and most dorsal body surfaces. Palp formula (5,4). (Fig. 2) ***T. inflatiscapus* sp. nov.**
- Erect hairs absent on mesosomal dorsum. Antennal scapes short, barely, or just reaching the posterior corners of the head, subcylindrical, tapering in diameter only near the antennal insertion and near the apex. Palp formula (6,4). [subtropical Florida, the Caribbean region, arboreal] ***T. litorale* Wheeler**
- 4 In full-face view, head trapezoidal, broadest near the posterior border well behind the large compound eyes, sides straight or slightly convex (except for the broadly rounded posterior corners), and strongly converging anteriorly. In lateral view, dorsal petiolar scale absent. In dorsal view, anterodorsal margin of petiole convex; petiole broadest at midpoint **5**
- In full-face view, head shape variable, either subrectangular or sides of head convex with head widest at level of eyes. In lateral view, petiolar scale either absent or forming a small, rounded node. When small node present, shape of petiole when viewed from the rear trapezoidal or subrectangular, dorsal margin slightly convex to flat or concave. If petiolar scale absent, head widest at level of eyes in full-face view **6**
- 5 Queen bicolored with head and mesosoma orange to dull red, often with patches of darker infuscation, forming a strong contrast with the uniformly black or brown gaster. Note: workers combining the following: head and mesosoma orange to red, metasoma brown to black; in full-face view, posterior margin of head concave. [mountains of southern Nevada, and central to southern California] ***T. schreiberi* Hamm**
- Queen usually uniform gray or brownish gray, variable in size. Note: workers uniform gray to yellowish brown, sometimes weakly bicolored, but never as described above; in full-face view, posterior margin of head usually straight or weakly convex, rarely slightly concave. [omnipresent from sub-boreal Canada south through the Mexican highlands]. (Fig. 5) ***T. sessile* (Say)**
- 6 In lateral view, petiolar scale absent. In lateral view, propodeum forming a single, flat declivitous surface. Palp formula (5,4). (Fig. 4) ***T. shattucki* sp. nov.**
- In lateral view, petiole with a small dorsal rounded node. In lateral view, propodeum with dorsal and posterior surfaces that meet to form a convexity. Palp formula either (4,3) or (5,4) **7**
- 7 Palp formula (5,4). Shape of petiole when viewed from the rear subrectangular, dorsal margin slightly convex to flat. In side view, propodeum subangulate with dorsal face notably shorter than posterior face; posterior face slightly concave. Anterior clypeal margin flat. (Fig. 3) ***T. pulchellum* sp. nov.**
- Palp formula (4,3). Shape of petiole when viewed from the rear trapezoidal, broadest at apex, dorsal margin concave, rarely flat. In side view, propodeum broadly rounded, forming an even convexity. Anterior clypeal margin with small median impression. (Fig. 1) ***T. incognitum* sp. nov.**

Key to the males of *Tapinoma* species occurring in the Nearctic

- 1 Males minute, wings short, deformed, clearly non-functional. Number of antennal segments reduced to 12.....**2**
 - Males variable in size, fully alate. With 13 antennal segments**3**
- 2 Anterior border of clypeus weakly emarginate in full-face view. Cutting edge of mandible with 2–4 small denticles (clearly visible at high magnification) in addition to apical tooth. (Fig. 1) ***T. incognitum* sp. nov.**
 - Anterior border of clypeus flat in full-face view. Cutting edge of mandible smooth, lacking distinct subapical teeth or denticles; apical tooth present. (Fig. 3) ***T. pulchellum* sp. nov.**
- 3 Males minute (< 2 mm), fragile, gnat-like, pale yellow or pale gray.....**4**
 - Males larger (generally > 2.5 mm), more robust, solid gray or black**5**
- 4 Antennal scapes just reaching or barely surpassing the posterior border of the head. Maxillary palps delicate, filiform, segments uniformly thin and cylindrical ***T. litorale* Wheeler**
 - Antennal scapes long, surpassing the posterior border of the head by 2–3× the maximum diameter of the scape. Maxillary palps robust, segments 3 and 4 thicker than the preceding and terminal two segments (seldom collected) ***T. melanocephalum* (Fabricius)**
- 5 Very short, fine erect hairs present on mesosomal dorsum and gastric tergites. Pubescence on head and mesosoma short, dense, and suberect. (Fig. 2) ***T. inflatiscapus* sp. nov.**
 - Erect hairs absent on mesosoma and first three gastric tergites. Pubescence on head, and mesosoma variable, but appressed on most body surfaces.....**6**
- 6 In full-face view, sides of head strongly convex, head nearly circular exclusive of the compound eyes. As small or smaller than host workers. (Fig. 4) ***T. shattucki* sp. nov.**
 - In full-face view, head variable in shape with sides of head converging anteriorly; head shape but not as described above. Body size variable as well; often as large or larger than nestmate workers**7**
- 7 In full-face view, head distinctly longer than broad. Body color dark brown to black; tips of legs and antennal flagellum reddish-yellow..... ***T. schreiberi* Hamm**
 - In full-face view, head often as broad or broader than long. Body color brownish, yellowish, or battleship gray. (Fig. 5)..... ***T. sessile* (Say)**

Species accounts

***Tapinoma incognitum* Cover & Rabeling, sp. nov.**

<https://zoobank.org/6E385B56-D69F-4EB7-A75C-88C2D7D23A67>

Diagnosis. A workerless, host-queen-tolerant inquiline social parasite of *Tapinoma sessile* showing morphological and life history traits of the inquiline syndrome. Both females and males are miniaturized (i.e., smaller than the host workers), alate, and morphologically complete (Fig. 1, Table 2). Females eclose with intact wings, but the wings are fragile and quickly deciduous. Males are brachypterous. Females have a reduced 4,3 palp formula, anterior clypeal

border with weak median concavity, denticulate mandibles with only 2–4 denticles. In side view petiole with low, rounded node; viewed from the rear dorsal margin concave (rarely flat). Males similar in size and overall habitus to females but often darker in color and easily recognized by their extruding genitalia. Males have a reduced 5,3 palp formula and only 12 antennal segments. Females of *T. incognitum* are closely similar in habitus to those of *T. pulchellum* sp. nov., but can be easily distinguished by palp count, concave anterior clypeal border, mandibular dentition, and propodeal profile.

Description. Holotype queen: HL 0.53, HW 0.53, SL 0.44, ML 0.82, CI 100, SI 83. Head in full-face view nearly square, dorsal margin straight with corners evenly rounded. Anterior margin of clypeus with shallow median impression; posterior border rounded, not projecting forward between antennal insertions. Mandibles reduced, barely touching each other when mandibles are fully closed; apical tooth well developed, cutting edge of mandible with 2–4 small denticles. Antennae with 12 segments, scapes relatively short, surpassing the dorsal margin of head by less than their own maximum width. Palp count 4,3. Mesosoma with typical modifications related to wing bearing. In lateral view, propodeum forming an evenly rounded convexity and lacking distinct dorsal and posterior surfaces. Orifices of propodeal spiracles slightly elevated and conspicuous. Metapleural gland orifice significantly reduced. Petiole in side view with low, blunt node; viewed from the rear trapezoidal with concave dorsal margin. Petiolar spiracles located on top of laterally extended tubercles. In dorsal view, four gastric tergites visible. Integument thin, specimens can shrivel when dried. Body surface covered with short, appressed pubescence; posterior margin of all gastric sternites and fourth gastric tergite with sparse, long setae. Color pale brown to yellowish brown, appendages pale yellow. Paratype queens ($n = 8$): HL 0.50–0.53, HW 0.50–0.53, SL 0.41–0.47, ML 0.76–0.88, CI 94–100, SI 78–94.

Paratype male: HL 0.50, HW 0.47, SL 0.47, ML 0.76, CI 94, SI 100. Males small, approximately the same size as the queen, brachypterous, closely similar to the conspecific queen in habitus. Head in full-face view almost square. Eyes small, maximum diameter $\sim \frac{1}{4}$ of head length; individual ommatidia partly fused, lacking the distinct convex surface of each ommatidium; compound eyes appear to be coated with a translucent resin. Ocelli slightly elevated above the surface of the head. Anterior clypeal margin with a broad, median, shallow impression. Mandibles reduced, with a single large apical tooth; denticles on cutting edge of mandible indistinct. Antennae with 12 segments, scapes shorter than the head (CI), surpassing the dorsal margin of head by twice their maximum width. Palp count 5,3. Mesosoma enlarged with typical modifications related to wing bearing. In lateral view, propodeum rounded, convex, with dorsal and posterior of approximately equal length. Metapleural gland orifice absent/reduced. Petiole small, overhung by first gastric tergite, not entirely visible in dorsal view. In dorsal view, five gastric tergites visible. Hind wings reduced to wing remnants lacking venation. Body surface covered with short, appressed pubescence, except for the antennal scapes and flagellum, which are covered by a dense, short, suberect pubescence. Color medium brown to black. Paratype males ($n = 3$): HL 0.50–0.56, HW 0.47–0.53, SL 0.44–0.47, ML 0.76, CI 94–100, SI 83–100.

Etymology. When first seen in the field, the collector's initial impression was of a *Tapinoma sessile* colony infested by tiny diapiiid wasps of some kind.



Figure 1. Morphological comparison of the *Tapinoma incognitum* holotype queen **A, C, E** and a paratype male **B, D, F** in lateral **A, B** dorsal **C, D** and full-face **E, F** view. The type series was collected in Alumbed Hollow in Utah and belongs to a single nest series with the collection code SPC 7749. Scale bars: 0.5 mm (**A–D**); 0.2 mm (**E, F**).

A second look made it clear they were, in fact, tiny inquiline ants. Hence, the species name is the nominative neuter of the Latin adjective *incognitus*, meaning unknown, unrecognized, in disguise.

Type locality. U.S.A., Utah, Sevier County, Alumbed Hollow, 8.4 miles west of I-70 (Exit 71) on Salina County Frontage Rd., a dirt road paralleling I-70. GPS: 38.910°N, 111.697°W; elevation 5980' (1823 m). Small canyon running

southwest to northeast with dense, heavily grazed Gambel Oak (*Quercus gambelii*) thickets to 25' (8 m) tall on east-facing slope. Collected by SPC (SPC 7749), 16 July 2008. Collection Notes: SPC 7749. Site heavily grazed. Dense Gambel Oak thicket; forest floor protected from grazing by oak stem density. Superficial nest under rock in pale shade of dense Gambel Oak thicket. 2-cm thick oak litter present. Humusy sand soil. Very dry conditions. ~ 500 ants, multiple host queens present. Brood was mostly eggs and young larvae; just a few parasite and host worker pupae present.

Type material. *Holotype* queen (SPC 7749, MCZENT 00806456). *Paratype* male (SPC 7749, MCZENT 00806457), and the following additional paratypes: 13 queens, 17 males [16-VII-2008, SPC 7749]; 35 queens, 3 males [19-VII-2009, SPC 8077]; 19 queens, 4 males [19-VII-2013, SPC 8656]. Holotype and paratypes deposited in the MCZC. Additional paratypes deposited at CASC, CRC, LACM, and UCDC.

Additional material. (i) SPC 8077. Same site description as above. Site not as heavily grazed as in 2008. Nest under dead oak branch half buried in oak litter in shade. Very dry conditions. ~ 1500 ants. Multiple host queens present. Eggs and young larvae present plus some host worker pupae. No inquiline pupae seen.

(ii) SPC 8656. Same site description as above. Not as heavily grazed as in 2008. In 9 cm diameter hard, dead oak stump in shade. Very dry conditions. ~ 1000 ants. Multiple host queens present. Eggs, larvae, and a few inquiline and host worker pupae present.

Discussion and biology. *Tapinoma incognitum* is known from three collections that were made at the type locality on separate occasions. All were mixed colonies containing *T. incognitum* and its host *T. sessile*. Each colony contained multiple fertile host queens, numerous host workers, and some host worker pupae. In addition, each nest contained males and females of *T. incognitum*, and, in two collections, parasite pupae. No *T. incognitum* workers were found. In each colony, several *T. incognitum* queens were observed with enlarged metasomas, implying that multiple parasite queens were reproductively active (i.e., functional polygyny of social parasite; Table 2). A striking feature of this species is the strong convergence in size and habitus between females and males (i.e., gynaecomorphism; Table 2). Males, however, are easily recognizable by their externally visible genitalia and because they are brachypterous; the wing remnants are small, crumpled, distorted, and persistent. In addition, *T. incognitum* also displays other morphological characters typical of the inquiline syndrome (Fig. 1, Table 2). Hallmark characters include reduced body size, the reduction of antennal segments in the males, and the reduction of palp segments in both queens (palp formula 4,3) and males (palp formula 5,3). The wings of queens are extremely fragile, easily deciduous, and almost certainly non-functional, and the males cannot fly. Thus, mating must take place in or around the nest.

We kept a colony alive for a few days and made some behavioral observations. It was eye-catching that the host workers carried social parasite queens as if they were pupae and the parasites retracted their appendages against their bodies and became pupae-like when carried. The host workers also regurgitated to and groomed the social parasite queens. Host and social parasite queens encountered one another often but seemed to ignore each other. This suggests that *T. incognitum* is well integrated in the host society. Collectively these morphological and life history traits indicate that *T. incognitum* is a workerless, host-queen-tolerant inquiline social parasite of *T. sessile*.

Table 2. Morphological and life history traits characteristic of the inquiline syndrome in *Tapinoma* ants. Morphological reductions are determined by comparisons to the host, *Tapinoma sessile*, which is included in this table (traits modified from Kutter 1968; Wilson 1971, 1984; Rabeling et al. 2019; Prebus et al. 2023).

	Host		Social parasites		
	<i>T. sessile</i>	<i>T. shattucki</i>	<i>T. inflatiscapus</i>	<i>T. incognitum</i>	<i>T. pulchellum</i>
Worker caste absent	–	+	+	+	? (+)
Multiple egg laying host queens present (host polygyny)	+	? (–)	–	+	?
Multiple egg laying parasite queens present in host colony (parasite polygyny)	n/a	+	?	+	?
Parasite queen coexists with host queen (host queen tolerance)	n/a	? (–)	–	+	? (+)
Adelphogamy (inside nest mating)	–	? (–)	?	+	?
Gynaecomorphism (gyne-like male morphology)	–	–	–	+	+
Fragmented populations, limited geographic distribution	– (North America)	+	+	+	+
		(2 localities in MA)	(UT, CO)	(type locality, UT)	(type locality, NC)
Reduced body size	–	+	+	+	+
		(size of host worker)	(size of host worker)	(smaller than host worker)	(smaller than host worker)
Exoskeleton becomes thinner and less pigmented	–	+	+	+	+
Number of antennal segments reduced in females	– (♀: 12)	– (♀: 12)	– (♀: 12)	– (♀: 12)	– (♀: 12)
Number of antennal segments reduced in males	– (♂: 13)	– (♂: 13)	– (♂: 13)	+	+
				(♂: 12)	(♂: 12)
Number of maxillary and labial pals (palp formula) reduced in females	– (♀: 6,4)	+	+	+	+
		(♀: 5,4)	(♀: 5,4)	(♀: 4,3)	(♀: 5,4)
Number of maxillary and labial pals (palp formula) reduced in males	– (♂: 6,4)	+	–	+	+
		(♂: 5,4)	(♂: 6,4)	(♂: 5,3)	(♂: 5,4)
Reduced mandibular dentition	– 14 teeth	– (10–11 denticles)	– (11 denticles)	+	+
				(2–4 denticles, plus apical tooth)	(only apical tooth)
Reduced wings in females	– (♀ capable of flying)	– (♀ capable of flying)	– (♀ capable of flying)	+	–
				(♀: wings deciduous)	(♀: winged)
Reduced wings in males	– (♂ capable of flying)	– (♂ capable of flying)	– (♂ capable of flying)	+	+
				(♂: brachypterous)	(♂: brachypterous)
Petiole thickened	–	–	–	+	+

***Tapinoma inflatiscapus* Cover & Rabeling, sp. nov.**

<https://zoobank.org/6DB40425-2AF1-48D3-9D3A-E1B47FBB0F76>

Diagnosis. A unique, workerless, host-queen-intolerant inquiline social parasite of *Tapinoma sessile* with relatively few morphological adaptations to its parasitic lifestyle. Inquiline females and males are equal in size, smaller than the host females and males, and approximately the size of host workers (Fig. 2, Table 2). Both females and males are winged and seem capable of flying. Females have a reduced 5,4 palp formula whereas males have the same palp formula (6,4) as host males. Both sexes of *T. inflatiscapus* are easily distinguished from those of all other North American congeners by the presence of short, erect hairs on the

dorsal surface of the head, the mesosomal dorsum, and the first gastric tergite. In addition, the antennal scapes are covered by short, dense, suberect pubescence and may have one or two erect hairs near the distal end. Lastly, in females, the scape reaches its maximum diameter between the mid-point and the antennal insertion, not posterior to the mid-point as in many other *Tapinoma* species.

Description. *Holotype* queen: HL 0.76, HW 0.76, SL 0.74, ML 1.15, CI 100, SI 96. Head distinctly heart shaped, approximately as wide as long. Clypeus broad, anterior margin flat or slightly convex, median impression absent; posterior margin rounded, projecting between antennal insertions. Mandibles well developed, overlapping when closed; first three apical teeth well developed, continually decreasing in size from apex to base. Eleven teeth and denticles present, most denticles on cutting edge of mandible ill defined. Antennae with 12 segments, scapes relatively long, easily surpassing the dorsal margin of head; scape somewhat dorsoventrally flattened, basal third slightly curved. Scape widest between the insertion and the mid-point. Palp count 5,4. Mesosoma robust with typical modifications related to wing bearing. In side view, propodeum with dorsal surface approximately one third as long as posterior surface. Metapleural gland orifice large and rounded in oblique view; orifice guarded by long setae pointing inwards. Petiole reduced, overhung by first gastric tergite. In dorsal view, four gastric tergites visible. Integument thin. Body surfaces with micro-sculpture resembling a honeycomb. Entire body with dense, short, suberect to erect pubescence, including head and antennal scapes. Short erect hairs present on dorsal surface of head and mesosoma. Color pale to medium brown, legs and antennae paler, yellowish brown. Paratype queens ($n = 8$): HL 0.65–0.76, HW 0.65–0.76, SL 0.68–0.76, ML 1.03–1.15, CI 92–100, SI 96–113.

Paratype male: HL 0.62, HW 0.62, SL 0.62, ML 1.12, CI 100, SI 100. Males similar in size to the females, head as wide as long (CI). Eyes large, maximum diameter $\sim \frac{1}{3}$ of head width. Ommatidia clearly separated from each other; each ommatidium with a distinct convex surface. Ocelli slightly elevated above the surface of the head, but forming a raised, triangular turret in side view. Anterior margin of clypeus flat, median impression absent; posterior margin rounded, projecting between antennal insertions. Mandibles well developed with a single large apical tooth and ~ 18 denticles on cutting edge of mandible. Antennae with 13 segments, scapes surpassing the posterior border of the head by a bit less than $\frac{1}{2}$ their length. Palp formula 6,4. Mesosoma robust with typical modifications related to wing bearing. In side view, propodeum with dorsal surface $\sim \frac{1}{3}$ as long as the posterior surface. Metapleural gland orifice pointing backwards, circular in posterior view. Petiole visible in dorsal view. In dorsal view, six gastric tergites visible. Front and hind wings well developed. Dorsal body surfaces with short, suberect to erect pubescence, including head and antennal scapes. Short, erect hairs present on dorsal surfaces of head and mesosoma, long erect hairs irregularly dispersed over the body. Color uniformly pale to yellowish brown. Paratype males ($n = 6$): HL 0.53–0.71, HW 0.53–0.71, SL 0.59–0.65, ML 0.91–1.12, CI 90–100, SI 92–117.

Etymology. In *T. inflatiscapus* females, the antennal scape reaches its maximum diameter between the mid-point and the antennal insertion instead of posterior to the mid-point as in other *Tapinoma*. This unique, diagnostic morphological character is emphasized in the species epithet, which is a compound Latin noun in the nominative case used in apposition (*inflat* is the participle in the genitive case of *inflatus* + *scapus*, the noun in the nominative singular case).



Figure 2. Morphological comparison of the *Tapinoma inflatiscapus* holotype queen **A, E** and a paratype male **B, F** in lateral **A, B** and full-face **E, F** view. For the dorsal views of *T. inflatiscapus* **C, D** dealate queen **C** and male **D** paratypes were photographed. The type series was collected at Cove Mountain in Utah and belongs to a single nest series with the collection code SPC 7816. Scale bar: 0.5 mm (**A–F**).

Type locality. U.S.A., Utah, Sevier County, Cove Mountain, 13.4 miles south of Glenwood Fish Hatchery on FSR 068. GPS: 38.649°N, 111.950°W; elevation 9350' (2850 m). Enormous, grazed sagebrush (*Artemisia tridentata*) meadow around Big Lake. Superficial nest under rock and in adjacent grass clump in open on gentle south facing slope; fine silty sand. Small colony (~ 400 ants).

No host queens. Brood, mostly eggs and larvae, plus a few parasite queen pupae. Collected by SPC (SPC 7816), 20 July 2008.

Type material. **Holotype** queen (SPC 7816, MCZENT 00806458). **Paratype** male (SPC 7816, MCZENT 00806458), and the following paratypes: 63 queens, 4 males [20-VII-2008, SPC 7816]. Holotype and paratypes deposited in the MCZC. Additional paratypes deposited at CASC, CRC, LACM, and UCDC.

Additional material. (i) U.S.A., Colorado, El Paso County, Black Forest, 4.5 miles south of Hodgen Rd. on Meridian Rd. GPS (from Google Maps): 39.01°N, 104.61°W; elevation 7350' (2240 m). Open Ponderosa Pine (*Pinus ponderosa*) forest, 20–40' (6–12 m) tall with grassy understory and bearberry (*Arctostaphylos* sp.) in spots; medium sandy soil. Both colonies were under pine branches half buried in soil and litter. Collected by SPC (SPC 4117, 4120), 16 July 1994.

(ii) U.S.A., Colorado, Montrose County, 2.1 miles southeast of junction with Rt. 50 on P77 Road. GPS: 38.420°N, 107.628°W; elevation 8200' (2500 m). Rich, mixed shrubby northeast facing slope with some sagebrush (*Artemisia tridentata*), 3–4' (0.9–1.2 m) tall; fine sandy soil; sparse ground cover. Small colony consisting of two parasite females, ~ 30 host workers and no brood. Collected by SPC (SPC 7388), 16 July 2006.

(iii) One other collection from the type locality: SPC (SPC 8076), collected 18 July 2009, same collection data as type series, under rock in open, ~ 1000 ants, no host brood, a few inquiline pupae only.

Discussion and biology. *Tapinoma inflatiscapus* is a host-queen-intolerant inquiline that parasitizes *T. sessile* colonies in mid to high elevation habitats in the mountains of Utah and Colorado. So far it has been found in sagebrush meadows (*Artemisia tridentata*), mixed shrub and sagebrush, and Ponderosa Pine (*Pinus ponderosa*) woodlands. Morphologically, *T. inflatiscapus* is most similar to *T. shattucki* from Massachusetts from which it can be easily distinguished by the unique shape of the antennal scape, the presence of short, erect hairs on the dorsal body surfaces, and its comparatively robust habitus. In addition, the male palp formula is 6,4. All other *Tapinoma* inquiline males have reduced palp formulae (Table 2).

Tapinoma inflatiscapus has been collected from two localities in Colorado and a single locality in Utah. On all occasions, *T. inflatiscapus* was found in mixed colonies with its host, *T. sessile*. In every case these colonies lacked a host queen and any host brood, suggesting that *T. inflatiscapus* either kills the host queen(s) or can only colonize queenless host colonies. Parasite workers have not been observed, so *T. inflatiscapus* appears to be a workerless inquiline. We could not observe whether *T. inflatiscapus* is mono- or polygynous, although collection SPC 7388 contained two dealate queens.

The morphology of *T. inflatiscapus* queens and males reflects some characteristics of the inquiline syndrome (Fig. 2, Table 2), but the degree of specialization is not nearly as pronounced as in *T. incognitum* and *T. pulchellum*. *Tapinoma inflatiscapus* alates are smaller than those of the host and approximately the size of host workers. The number of antennal segments is not reduced, and the palp count is reduced in the queens (palp formula 5,3), but not in males. The mandibles are normal in size and dentation. Both queens and males are winged and mesosomal development is robust, thus the wings appear to be functional and dispersal by flight probable. Mating may take place outside of the nest. If so, there may be less inbreeding and much better dispersal than in inquilines where mating takes place inside the host nest and where flight is problematic or impossible.

***Tapinoma pulchellum* Cover & Rabeling, sp. nov.**

<https://zoobank.org/E469ABF5-240D-4F47-B950-1FB131C8407E>

Diagnosis. An apparently workerless, inquiline social parasite of *Tapinoma sessile* exhibiting morphological traits of the inquiline syndrome. Queens and males are tiny, much smaller than the host workers, and are very similar to each other in size and habitus (Fig. 3, Table 2). Females are apparently alate, but males are brachypterous. Both sexes have a reduced (5,4) palp formula and twelve antennal segments. Females have a flat anterior clypeal border, edentate mandibles, and a petiole with a small, dorsally rounded node in side view. Females most similar to but are readily distinguished from *T. incognitum* by differing palp count, edentate mandibles, anterior clypeal border, petiole shape, and propodeal profile (subangulate with short dorsal face and long, weakly concave posterior face versus rounded convexity in *T. incognitum*).

Description. Holotype queen: HL 0.44, HW 0.50, SL 0.44, ML 0.76, CI 113, SI 88. Parasite queen notably smaller than host workers. Head in full-face view nearly square, dorsal margin straight with corners evenly rounded. Anterior margin of clypeus flat, median impression absent, posterior margin rounded, not projecting forward between antennal insertions. Mandibles reduced, apical tooth well developed, barely touching each other when mandibles are closed; other mandibular teeth absent. Antennae with 12 segments, scapes relatively short, surpassing the dorsal margin of head by less than their own width. Palp count 5,4. Mesosoma fully developed with typical modifications related to wing bearing. Propodeum in side view rounded, with short dorsal face and longer, slightly concave posterior face. Propodeal spiracles slightly elevated and conspicuous. Metapleural gland orifice reduced. In side view petiole with low, blunt node; viewed from the rear subrectangular in shape with dorsal margin flat to slightly convex. In dorsal view, four gastric tergites visible. Integument thin. Body surface covered with short, appressed pubescence; posterior margin of all gastric sternites and fourth gastric tergite with long erect setae. Color dark brown to yellowish brown, appendages pale yellow.

Paratype male: HL 0.44, HW 0.50, SL 0.44, ML 0.76, CI 100, SI 113. Specimen damaged, but largely intact. Head glued on to point next to body. Male small, approximately the same size as the queen, brachypterous, closely similar to the conspecific queen in habitus. Head square. Eyes small, maximum diameter $\sim \frac{1}{4}$ of head length. Individual ommatidia partly fused, lacking the distinct convex surface of each ommatidium; compound eyes appear as if coated with a translucent resin. Ocelli slightly elevated above the surface the head. Anterior margin of clypeus with a broad, median, shallow impression. Mandibles reduced in size, with a single large apical tooth but lacking other teeth or denticles. Antennae with 12 segments, scapes short. Palp count 5,4. Mesosoma well-developed with typical modifications related to wing bearing. In sideview, propodeum rounded, divided into dorsal and posterior surfaces of approximately equal length. Metapleural gland orifice absent/reduced. Petiole small, overhung by first gastric tergite, not entirely visible in dorsal view. In dorsal view, five gastric tergites visible. Wings vestigial, distorted, lacking venation. Body surface densely covered with short, appressed pubescence, except for the antennal scapes and flagellum, which are covered by a dense, very short, suberect pubescence. Color medium brown, appendages yellowish brown.



Figure 3. Morphological comparison of the *Tapinoma pulchellum* holotype queen **A, C, E** and a paratype male **B, D, F** in lateral **A, B** dorsal **C, D** and full-face **E, F** view. The type series was collected in two adjacent pitfall traps at Eno River State Park in North Carolina. Scale bars 0.5 mm (**A, C–E**); 0.25 mm (**B, F**).

Etymology. *Tapinoma pulchellum* is a beautiful ant (Fig. 3) and also beautifully embodies the hallmark morphological traits of the inquiline syndrome. The specific epithet *pulchellum* is the singular nominative neuter of the Latin adjective *pulchellus*, which is the diminutive of *pulcher*, meaning pretty or beautiful.

Type locality. U.S.A., North Carolina, Orange County, Eno River State Park, 8 miles northwest of downtown Durham; open field adjacent to the Eno Trace trailhead. GPS: 36.073°N, 79.008°W; elevation 460' (140 m). Large, maintained open field surrounded by mature secondary oak-hickory forest. The field was dominated by scattered *Juniperus virginiana* to 30' tall plus a few young *Pinus virginiana*. Dense, grassy-herbaceous vegetation plus young Sweetgum (*Liquidambar styraciflua*) up

to 8' tall. Sandy clay soil. The holotype queen was found in pitfall sample 13F 4,2. The paratype male was found in pitfall sample 13F 5,1. There is also a worker of the potential host from pitfall sample 13F 5,3. Collected by Amy Arnett in June 1997.

Type material. **Holotype** queen (MCZENT 00806459). **Paratype** male (MCZENT 00806460; same collecting locality as holotype). Holotype and paratype deposited in the MCZC.

Discussion and biology. *Tapinoma pulchellum* is known from only two specimens: a dealate female and a damaged male, which both exhibit typical characters of the morphological inquiline syndrome (Fig. 3, Table 2). *Tapinoma pulchellum* is closely similar to *T. incognitum*, from which it can be readily distinguished by the palp formula of both queens and males, the edentate mandibles, the flat anterior clypeal border, the petiole shape, and the unique propodeal profile. This striking similarity makes it highly probable that *T. pulchellum* is a workerless inquiline, similar in its life-history to *T. incognitum*.

Both specimens were recovered from adjacent pitfall traps at the type locality in Eno River State Park in North Carolina. Accordingly, *T. pulchellum* has not been observed in mixed colonies with its host. However, *T. sessile* is the only *Tapinoma* species at the type locality, so *T. sessile* is almost certainly the host of *T. pulchellum*. Visits to the type locality in 2011 and 2012 failed to turn up additional specimens of *T. pulchellum* but allowed observations of the putative host at that site. The field contained a dense population of *Tapinoma sessile*, and nests were located at the base of grass clumps or in the dense grassy thatch that covered the ground under the living vegetation. The *T. sessile* population was unusual. Colonies were large, with more than 4,000–5,000 ants, and uniformly monogynous. Both workers and queens were larger than the average size for *T. sessile*. Sexuials were not present, indicating that the mating flights had taken place already in early July.

***Tapinoma shattucki* Cover & Rabeling, sp. nov.**

<https://zoobank.org/573C25EE-4870-459E-82B0-C54DD83F4990>

Diagnosis. An apparently workerless inquiline social parasite of *Tapinoma sessile* showing relatively few morphological indications of its parasitic lifestyle. *Tapinoma shattucki* queens and males superficially resemble those of the host, except for their smaller size, more delicate habitus, and notably reduced size of the metasoma relative to the mesosoma (Fig. 4, Table 2). Both sexes are fully alate and seem capable of flying. Female and male palp formulae reduced to 5,4. In lateral view, propodeum of female and male forming a single, flat posterior surface, and the petiolar scale is vestigial or absent. In the male, sides of head strongly convex, head nearly circular exclusive of the compound eyes in full-face view. In *T. shattucki*, males exhibit morphology similar to their free-living congeners. Females may be easily distinguished from other *Tapinoma* species by their palp count, propodeal profile, small body size, and reduced metasoma size relative to the mesosoma.

Description. **Holotype** queen: HL 0.65, HW 0.59, SL 0.59, ML 0.88, CI 91, SI 100. *Tapinoma shattucki* superficially resembles a miniature form of *T. sessile*. Head parallel sided, slightly longer than wide (CI), dorsal margin of head straight with corners evenly rounded. Anterior margin of clypeus with broad, shallow



Figure 4. Morphological comparison of the *Tapinoma shattucki* holotype queen **A, E** and a paratype male **B, D, F** in lateral **A, B** dorsal **D** and full-face **E, F** view. For the dorsal view of the *T. shattucki* queen **C**, a dealate paratype was photographed. The type series was collected in Stow, Massachusetts and belongs to a single nest series with the collection code SPC 7633. Scale bar: 0.5 mm (**A–F**).

median impression; posterior margin rounded, projecting between antennal insertions. Mandibles well developed, overlapping when closed, with 10 or 11 teeth or denticles; apical and preapical teeth well developed, distinctly larger than remaining teeth; apical tooth slightly larger than the subapical. Antennae with 12 segments, scapes long, clearly surpassing the dorsal margin of head by more than their own width. Palp formula 5,4. Mesosoma with typical modifications related to wing bearing; wings fully developed. In side view, propodeum lacking clear division into dorsal and posterior surfaces; appears as a single long, sloping posterior face. Metapleural gland orifice large and round in oblique view; orifice guarded by erect, long setae pointing inwards. Petiole

small, scale absent, overhung by first gastric tergite, not visible in dorsal view. In dorsal view, three gastric tergites visible; fourth tergite mostly hidden underneath the third. Body surface covered with micro-sculpture resembling a honeycomb, and short, appressed pubescence. Color medium to dark brown, appendages yellowish to reddish brown. Paratype queens ($n = 8$): HL 0.62–0.65, HW 0.53–0.59, SL 0.59–0.62, ML 0.85–0.94, CI 86–95, SI 100–111.

Paratype male: HL 0.53, HW 0.53, SL 0.50, ML 0.94, CI 100, SI 94. Medium sized males, head as wide as long (CI). Eyes large, maximum diameter little less than $\frac{1}{2}$ of head width. Ommatidia clearly separated from each other; each ommatidium with a distinctly convex surface. Ocelli slightly elevated above the surface of the head, but not forming a raised, triangular turret in side view. Anterior margin of clypeus straight, median impression lacking. Mandibles well developed with a single large apical tooth and ~ 14 denticles on cutting edge of mandible. Antennae with 13 segments, scapes surpassing the posterior corners of head by little less than $\frac{1}{2}$ their length. Palp formula 5,4. Mesosoma with typical modifications related to wing bearing; wings well developed. In lateral view, propodeum forming a single even slope, lacking division into dorsal and posterior surfaces. Metapleural gland orifice pointing backwards, circular in posterior view. Petiole small, scale absent, overhung by first gastric tergite; not visible in dorsal view. In dorsal view, six gastric tergites visible. Integument thin, specimens shrivel when dried. Body surface densely covered with short, appressed pubescence, except for antennal flagellum, which is covered with dense, short, suberect pubescence. Color pale to medium brown, appendages yellowish brown. Paratype males ($n = 4$): HL 0.53–0.56, HW 0.53, SL 0.50–0.53, ML 0.88–0.94, CI 95–100, SI 94–100.

Etymology. This species is named to honor our friend Steven O. Shattuck for his pioneering work on the ant genera of the Dolichoderinae, his invaluable contributions to the systematics of Australian ants, his important efforts in establishing the universal online ant research tool AntWiki.org, and for his and his wife Kathy's invaluable and deeply appreciated help in reorganizing the MCZ ant collection. The species epithet *shattucki* is used as a Latin noun in the genitive case.

Type locality. U.S.A., Massachusetts, Middlesex County, Stow, 47 Marlboro Road. GPS: 42.399°N, 71.524°W; elevation 230' (70 m). Large garden adjacent to Red Maple (*Acer rubrum*) forest and reforesting wetland. Small colony in flower pot in partial shade at garden edge. Specimens preserved from 26 August to 04 September as pupae eclosed and adults matured. Collected by SPC (SPC 7633), 26 August 2007.

Type material. **Holotype** queen (SPC 7633, MCZENT 00806461). **Paratype** male (SPC 7633, MCZENT 00806462), and the following additional paratypes: 39 queens, 10 males [26-VIII-2007, SPC 7633]. Holotype and paratypes deposited in the MCZC. Additional paratypes deposited at CASC, CRC, LACM, and UCDC. In addition, there are 26 *T. sessile* host workers, five host males, and two host worker-queen intermorphs from the same colony, which were also deposited in the MCZC.

Additional material. Wheeler's syntype series of "*Bothriomyrmex dimmocki*" (one winged and four dealate females) comprises the only other known specimens of *T. shattucki*. The collecting locality of Wheeler's type series is U.S.A., Massachusetts, Hampden County, Mount Tom, north of Springfield. Collected by George Dimmock, 27 August 1897. The specimens, including the lectotype worker of "*Bothriomyrmex dimmocki*" are deposited in the MCZC (MCZENT 00021289, MCZENT 00035244).

Discussion and biology. This taxon has a convoluted taxonomic history. Wheeler (1915: 418) described *Bothriomyrmex dimmocki* based on “two workers, one winged, and four dealate females taken by Dr. George Dimmock August 27, 1897, from a single colony on Mt. Tom, near Springfield, Mass.” Based primarily on the unusually small size of the queens, Wheeler placed the ants in *Bothriomyrmex*, a genus of temporary social parasites that exploits *Tapinoma* hosts during colony founding, which was then thought to be exclusively Old World in distribution (Santschi 1906; but see Dubovikoff and Longino 2004; Prebus and Lubertazzi 2016). Curiously, Wheeler’s description centered on the two workers, which he was at pains to distinguish from those of the Mediterranean *Bothriomyrmex meridionalis* (Roger). The four small, reproductive females were described afterwards and in much less detail. Emery (1925) correctly transferred *B. dimmocki* to *Tapinoma*, almost certainly without seeing the types. Creighton (1950) noted the close similarity of the *T. dimmocki* worker to that of *T. sessile*, but maintained provisional species status for *T. dimmocki*, given the problematic small size of the females. Shattuck, as part of his important re-assessment of the dolichoderine genera (Shattuck 1992), examined the types of *T. dimmocki* in the MCZC. He was able to affirm what Creighton suspected, namely the worker types of *T. dimmocki* did not belong in the genus *Bothriomyrmex*; instead, they were ordinary workers of *Tapinoma sessile*. Accordingly, Shattuck (1992) synonymized *T. dimmocki* with *T. sessile* and designated one of the two worker syntypes as the lectotype of *B. dimmocki*. This was an appropriate designation, as Wheeler’s description and discussion centered primarily on the worker caste. As Shattuck remarked at the time, his taxonomic action neatly disposed of a problematic name, leaving the significance of the minute females an open question.

In late August 2007, a new collection clarified the identity of the minute females. One of us (SPC) collected a colony of *Tapinoma sessile* in his garden in Stow, Massachusetts, in the bottom of a flowerpot. Surprisingly, alates of both sexes were present, though this was in late-August, a month or more later than the normal mating flights of *T. sessile* in eastern Massachusetts. In addition, the alates were notably smaller than normal *T. sessile* queens and males. A detailed examination revealed that the alates represented an inquiline parasite and that the females matched the miniature females in Wheeler’s syntype series of “*Bothriomyrmex dimmocki*.” Shattuck’s (1992) designation of a host worker as the *B. dimmocki* lectotype makes this name a junior synonym of *T. sessile*. Therefore, we describe *Tapinoma shattucki* as a new species. *Tapinoma shattucki* females may be readily distinguished from host queens by palp count, propodeal profile, small body size, and reduced metasoma size relative to the mesosoma.

Both times *T. shattucki* was collected, it was found in mixed colonies with its host. The type colony from Stow, Massachusetts, consisted of adult and pupal parasite females and males plus host workers and several adult host males. This suggests the possibility that, similar to *T. inflatiscapus*, *T. shattucki* might be a host-queen-intolerant inquiline that either kills the host queen(s) or preferentially exploits queenless host colonies. Two of the parasite females had swollen metasomas and were almost certainly reproductively active indicating parasite polygyny (Table 2). We did not observe any *T. shattucki* workers but instead numerous winged queens and males. Hence, our observations suggest that *T. shattucki* is a workerless inquiline social parasite of *T. sessile* and not a temporary social parasite as Wheeler (1915) suggested.



Figure 5. Morphological comparison of a *Tapinoma sessile* queen **A, C, E** and a male **B, D, F** in lateral **A, B**, dorsal **C, D**, and full-face **E, F** view. Individuals were collected in the Black Forest in Colorado and belong to a single nest series with the collection code SPC 4118. Scale bar: 0.5 mm (**A–F**).

Similar to *T. inflatiscapus*, *T. shattucki* queens and males show morphological differences between sexes comparable to the sexual dimorphism observed in the host (Table 2). The morphology of *T. shattucki* queens and males shows some characteristics of the inquiline syndrome (Fig. 4, Table 2) but the degree of morphological specialization is similar to that in *T. inflatiscapus* and not nearly as pronounced as seen in *T. incognitum* and *T. pulchellum*. *Tapinoma shattucki* alates are smaller than host sexuals and approximately the size of host workers. In addition, the number of maxillary palps is reduced in both queens and males (palp formula 5,4). As in *T. inflatiscapus*, the mandibles are normal in size and dentition, and both queens and males are fully winged and seem capable of flight. Hence, *T. shattucki* queens and males may mate outside the host nest and/or could disperse on the wing.

Discussion

In this study, we describe four new species of inquiline social parasites in the dolichoderine ant genus *Tapinoma* from the Nearctic region. These social parasites represent the first inquiline species in the genus *Tapinoma* as well as the first confirmed inquilines in the ant subfamily Dolichoderinae. All four *Tapinoma* inquiline species appear to be workerless and represent at least two very different life histories (Table 2). *Tapinoma incognitum* is polygynous and the parasite queens co-exist with host queens, revealing *T. incognitum* to be host-queen-tolerant. In contrast, *T. inflatiscapus* colonies contain neither host queens nor host brood, strongly suggesting that *T. inflatiscapus* is host-queen-intolerant. *Tapinoma shattucki* may also be host-queen-intolerant but we need additional collections to be certain. The life history of *T. pulchellum* is undocumented at present. However, close similarity of *T. pulchellum* to *T. incognitum* (Table 2) suggests that *T. pulchellum* might be a host-queen-tolerant inquiline as well.

For a host-queen-tolerant inquiline ant, the primary advantage of retaining the host queen(s) in the colony is the ongoing production of host workers. This secures the potential longevity of the host colony and allows the continuing reproduction of the parasite. Host queen intolerance is a more complex phenomenon. In some species, the parasite attacks and eliminates host queens some time after her acceptance by the host colony (Hölldobler and Wilson 1990; Brandt et al. 2005). Such aggressive replacement of the host queen has been observed in inquilines, such as *Leptothorax goesswaldi*, *Leptothorax wilsoni*, *Monomorium santschii*, and *Pseudomyrmex leptosus* (Forel 1906; Kutter 1968; Klein 1987; Buschinger and Klump 1988; Heinze 1989), and also in some inquilines that likely evolved from a dulotic ancestor, such as *Temnothorax adlerzi*, *T. birgatae*, *T. brunneus*, and *T. corsicus* (Buschinger 1989; Heinze et al. 2015).

Other so-called host-queen-intolerant inquilines do not aggressively replace the host queen but instead can only gain acceptance in host colonies that already lack a host queen (Hölldobler and Wilson 1990; Buschinger 2009). Examples include *Tetramorium atratum*, *Pseudoatta argentina*, and *Formica talbotae* (Bruch 1928; Kutter 1968; Talbot 1977; Rabeling et al. 2015). Host queen intolerance is a remarkably specialized life history strategy, and in the absence of host queens, no new host workers are produced. Thus, the lifespan of the parasitized colony must be short, limited to the time that existing host workers survive, and thus limiting the parasite to one or perhaps two annual reproductive cycles. Such life histories must be sustainable only where there are large, relatively stable host populations and where there is a rapid turnover among colonies, meaning that queenless host nests occur somewhat frequently. Note that at this point, we do not know whether *T. inflatiscapus* eliminates host queens aggressively or colonizes only queenless host nests, but either way, colonies are likely comparatively short lived.

The *Tapinoma* inquiline social parasites are especially interesting because they all exploit only a single host species, *T. sessile*. Systems like this, in which a single host is exploited by multiple species of inquilines, are rare, and their evolutionary ecology is not well understood. *Tapinoma sessile* is an extremely widespread and ecologically successful ant found throughout North America from central Canada to Florida and south into the Mexican highlands (Fisher

and Cover 2007). *Tapinoma sessile* occurs in a wide variety of habitats, nests almost anywhere, frequently moves its nest in response to changing conditions, and is often a nuisance in buildings. As one might expect, *T. sessile* exhibits variation in size, coloration, and colony structure over its enormous range. A phylogenetic analysis of *T. sessile* samples from across North America, identified four well-supported “*T. sessile*” clades (Menke et al. 2010). The analysis of DNA sequence variation in the mitochondrial marker *COI* revealed within clade genetic distances of less than 2.3% but between clade genetic distances of 7.5–10%. Accordingly, Menke and colleagues (2010) suggested that *T. sessile* might consist of a complex of cryptic species. Using genomic markers, we are revisiting these findings with a special emphasis on the evolutionary origin of the inquiline social parasites. Recent studies of inquiline social parasite evolution have revealed several convergent pathways by which inquilinism evolves. These include inquiline parasites speciating directly from their future hosts in sympatry, inquilines originating in allopatry and via host-shift speciation, as well as inquilines transitioning secondarily from a different parasitic life history, such as temporary social parasitism and dulosis, to inquilinism (e.g., Rabeling et al. 2014; Heinze et al. 2015; Messer et al. 2020; Borowiec et al. 2021; Degueldre et al. 2021; Ward and Branstetter 2022; Mera-Rodríguez et al. 2023). We are confident that further studies of host-parasite co-evolution in *Tapinoma* will reveal novel insights into the complex mosaic evolution of ant inquiline social parasites.

Acknowledgements

We gladly dedicate this paper to Bert Hölldobler in appreciation of his long tradition of exemplary scientific natural history, experimental behavioral physiology, and sociobiology research, his invaluable mentorship and encouragement of both of us, and most important of all for his friendship, company, and advice over the years. We thank Nick Gotelli for providing the pitfall trap samples that yielded the types of *Tapinoma pulchellum* and Brian Brown (LACM) for the loan of important specimens of *Tapinoma schreiberi*. We also would like to thank Jack Longino, Lorenzo Fraysse, and one anonymous reviewer for their constructive feedback and thoughtful suggestions which helped us improve the manuscript.

Additional information

Conflict of interest

The authors have declared that no competing interests exist.

Ethical statement

No ethical statement was reported.

Funding

This study was financially supported by the U.S. National Science Foundation (CAREER DEB-1943626), the Ernst Mayr Travel Grant in Animal Systematics from the Museum of Comparative Zoology, the Harvard Society of Fellows, the University of Hohenheim, and the Carl Zeiss Foundation.

Author contributions

SPC & CR: conceptualization, data generation, data curation, formal analysis, funding acquisition, investigation, methodology, visualization, writing.

Author ORCIDs

Stefan P. Cover  <https://orcid.org/0009-0000-1911-0283>

Christian Rabeling  <https://orcid.org/0000-0003-1292-0309>

Data availability

All of the data that support the findings of this study are available in the main text.

References

- Bolton B (1987) A review of the *Solenopsis* genus-group and a revision of the Afrotropical *Monomorium* Mayr (Hymenoptera: Formicidae). *Bulletin of the British Museum (Natural History). Entomology* 54: 263–452.
- Bolton B (2024) An online catalog of the ants of the world. <https://antcat.org> [accessed 05 January 2024]
- Borowiec ML, Cover SP, Rabeling C (2021) The evolution of social parasitism in *Formica* ants revealed by a global phylogeny. *Proceedings of the National Academy of Sciences of the United States of America* 118(38): e2026029118. <https://doi.org/10.1073/pnas.2026029118>
- Bourke AFG, Franks NR (1991) Alternative adaptations, sympatric speciation and the evolution of parasitic, inquiline ants. *Biological Journal of the Linnean Society. Linnean Society of London* 43(3): 157–178. <https://doi.org/10.1111/j.1095-8312.1991.tb00591.x>
- Brandt M, Foitzik S, Fischer-Blass B, Heinze J (2005) The coevolutionary dynamics of obligate ant social parasite systems – between prudence and antagonism. *Biological Reviews of the Cambridge Philosophical Society* 80(2): 251–267. <https://doi.org/10.1017/S1464793104006669>
- Bruch C (1928) Estudios mirmecológicos. *Anales del Museo Nacional de Historia Natural Buenos Aires* 34: 341–360.
- Buschinger A (1989) Evolution, speciation, and inbreeding in the parasitic ant genus *Epimyrma* (Hymenoptera, Formicidae). *Journal of Evolutionary Biology* 2(4): 265–283. <https://doi.org/10.1046/j.1420-9101.1989.2040265.x>
- Buschinger A (2009) Social parasitism among ants: A review (Hymenoptera: Formicidae). *Myrmecological News* 12: 219–235.
- Buschinger A, Klump B (1988) Novel strategy of host-colony exploitation in a permanently parasitic ant, *Doronomyrmex goesswaldi*. *Naturwissenschaften* 75(11): 577–578. <https://doi.org/10.1007/BF00377726>
- Creighton WS (1950) *Ants of North America*. *Bulletin of the Museum of Comparative Zoology* 104: 1–585.
- Degueldre F, Mardulyn P, Kuhn A, Pinel A, Karaman C, Lebas C, Schifani E, Bračko G, Wagner HC, Kiran K, Borowiec L, Passera L, Abril S, Espadaler X, Aron S (2021) Evolutionary history of inquiline social parasitism in *Plagiolepis* ants. *Molecular Phylogenetics and Evolution* 155: 107016. <https://doi.org/10.1016/j.ympev.2020.107016>
- Deyrup M (2017) *Ants of Florida: Identification and Natural History*. CRC Press, Boca Raton, Florida, 423 pp. <https://doi.org/10.1201/9781315368023>
- Dubovikoff DA (2005) The system of taxon *Bothriomyrmex* Emery, 1869 *sensu lato* (Hymenoptera: Formicidae) and relatives genera. *Kavkazskij Entomologiceskij Bjulleten*

- = Caucasian Entomological Bulletin 1(1): 89–94. <https://doi.org/10.23885/1814-3326-2005-1-1-89-94> [In Russian]
- Dubovikoff DA, Longino JT (2004) A new species of the genus *Bothriomyrmex* Emery, 1869 (Hymenoptera: Formicidae: Dolichoderinae) from Costa Rica. *Zootaxa* 776(1): 1–10. <https://doi.org/10.11646/zootaxa.776.1.1>
- Emery C (1925) Les espèces européennes et orientales du genre *Bothriomyrmex*. Bulletin de la Société Vaudoise des Sciences Naturelles 56: 5–22.
- Fisher BL, Cover SP (2007) *The Ants of North America: A Guide to the Genera*. University of California Press, Berkeley and Los Angeles, California, 308 pp. <https://doi.org/10.1525/9780520934559>
- Forel A (1906) Mœurs des fourmis parasites des genres *Wheeleria* et *Bothriomyrmex*. *Revue Suisse de Zoologie* 14: 51–69. <https://doi.org/10.5962/bhl.part.75182>
- Gray KW, Rabeling C (2023) Global biogeography of ant social parasites: Exploring patterns and mechanisms of an inverse latitudinal diversity gradient. *Journal of Biogeography* 50(2): 316–329. <https://doi.org/10.1111/jbi.14528>
- Guerrero RJ, Delabie JHC, Dejean A (2010) Taxonomic contribution to the *aurita* group of the ant genus *Azteca* (Formicidae: Dolichoderinae). *Journal of Hymenoptera Research* 19: 51–65.
- Hamm CA (2010) Multivariate discrimination and description of a new species of *Tapinoma* from the Western United States. *Annals of the Entomological Society of America* 103(1): 20–29. <https://doi.org/10.1603/008.103.0104>
- Heinze J (1989) *Leptothorax wilsoni* n. sp., a new parasitic ant from eastern North America (Hymenoptera: Formicidae). *Psyche* (Cambridge, Massachusetts) 96(1–2): 49–62. <https://doi.org/10.1155/1989/15931>
- Heinze J, Buschinger A, Poettinger T, Suefuji M (2015) Multiple convergent origins of workerlessness and inbreeding in the socially parasitic ant genus *Myrmoxenus*. *PLoS ONE* 10(7): e0131023. <https://doi.org/10.1371/journal.pone.0131023>
- Hölldobler B, Wilson EO (1990) *The Ants*. Harvard University Press, Cambridge, Massachusetts, 732 pp. <https://doi.org/10.1007/978-3-662-10306-7>
- Klein RW (1987) A workerless inquiline in *Pseudomyrmex* (Hymenoptera: Formicidae: Pseudomyrmecinae). Pp 623–624. In: Eder J, Rembold H (Eds) *Chemistry and Biology of Social Insects*. Verlag J. Peperny, München, 757 pp.
- Kutter H (1968) Die sozialparasitischen Ameisen der Schweiz. *Neujahrsblatt der Naturforschenden Gesellschaft in Zürich* 171: 1–62.
- Longino JT (2007) A taxonomic review of the genus *Azteca* (Hymenoptera: Formicidae) in Costa Rica and a global revision of the *aurita* group. *Zootaxa* 1491(1): 1–63. <https://doi.org/10.11646/zootaxa.1491.1.1>
- Menke SB, Booth W, Dunn RR, Schal C, Vargo EL, Silverman J (2010) Is it easy to be urban? Convergent success in urban habitats among lineages of a widespread native ant. *PLoS ONE* 5(2): e9194. <https://doi.org/10.1371/journal.pone.0009194>
- Mera-Rodríguez LD, Jourdan H, Ward PS, Shattuck S, Cover SP, Wilson EO, Rabeling C (2023) Biogeography and evolution of social parasitism in Australian *Myrmecia* bulldog ants revealed by phylogenomics. *Molecular Phylogenetics and Evolution* 186: 107825. <https://doi.org/10.1016/j.ympev.2023.107825>
- Messer SJ, Cover SP, Rabeling C (2020) Two new species of socially parasitic *Nyländeria* ants from the southeastern United States. *ZooKeys* 921: 23–48. <https://doi.org/10.3897/zookeys.921.46921>
- Prebus M, Lubertazzi D (2016) A new species of the ant genus *Bothriomyrmex* Emery, 1869 (Hymenoptera: Formicidae) from the Caribbean region. *European Journal of Taxonomy* 211(211): 1–12. <https://doi.org/10.5852/ejt.2016.211>

- Prebus M, Georgiev BB, van de Kamp T, Hamann E, Baker I, Rabeling C (2023) The rediscovery of the putative ant social parasite *Manica parasitica* syn. nov. (Hymenoptera: Formicidae) reveals an unexpected endoparasite syndrome. *Biology Letters* 19(12): 20230399. <https://doi.org/10.1098/rsbl.2023.0399>
- Rabeling C (2021) Social Parasitism. Pp. 836–858. In: Starr CK (Ed.) *Encyclopedia of Social Insects*. Springer Nature, Cham, Switzerland, 1049 pp. https://doi.org/10.1007/978-3-030-28102-1_175
- Rabeling C, Bacci M (2010) A new workerless inquiline in the Lower Attini (Hymenoptera: Formicidae), with a discussion of social parasitism in fungus-growing ants. *Systematic Entomology* 35(3): 379–392. <https://doi.org/10.1111/j.1365-3113.2010.00533.x>
- Rabeling C, Cover SP, Johnson RA, Mueller UG (2007) A review of the North American species of the fungus-gardening ant genus *Trachymyrmex* (Hymenoptera: Formicidae). *Zootaxa* 1664(1): 1–53. <https://doi.org/10.11646/zootaxa.1664.1.1>
- Rabeling C, Schultz TR, Pierce NE, Bacci Jr M (2014) A social parasite evolved reproductive isolation from its fungus-growing ant host in sympatry. *Current Biology* 24(17): 2047–2052. <https://doi.org/10.1016/j.cub.2014.07.048>
- Rabeling C, Schultz TR, Bacci Jr M, Bollazzi M (2015) *Acromyrmex charruanus*: A new inquiline social parasite species of leaf-cutting ants. *Insectes Sociaux* 62(3): 335–349. <https://doi.org/10.1007/s00040-015-0406-6>
- Rabeling C, Messer S, Lacau S, Nascimento IC, Bacci M, Delabie JHC (2019) *Acromyrmex fowleri*: A new inquiline social parasite species of leaf-cutting ants from South America, with a discussion of social parasite biogeography in the Neotropical region. *Insectes Sociaux* 66(3): 435–451. <https://doi.org/10.1007/s00040-019-00705-z>
- Santschi F (1906) A propos de mœurs parasitiques temporaires des fourmis du genre *Bothriomyrmex*. *Annales de la Société Entomologique de France* 75: 363–392.
- Shattuck SO (1992) Generic revision of the ant subfamily Dolichoderinae (Hymenoptera: Formicidae). *Sociobiology* 21: 1–181.
- Talbot M (1977) The natural history of the workerless ant parasite *Formica talbotae*. *Psyche* (Cambridge, Massachusetts) 83(3–4): 282–288. <https://doi.org/10.1155/1976/149241>
- Trager JC (1988) A revision of *Conomyrma* (Hymenoptera: Formicidae) from the southeastern United States, especially Florida, with keys to the species. *The Florida Entomologist* 71(1): 11–29. <https://doi.org/10.2307/3494888>
- Ward PS, Branstetter MG (2022) Species paraphyly and social parasitism: Phylogenomics, morphology, and geography clarify the evolution of the *Pseudomyrmex elongatus* group (Hymenoptera: Formicidae), a Mesoamerican ant clade. *Insect Systematics and Diversity* 6(1): 1–31. <https://doi.org/10.1093/isd/ixab025>
- Wheeler WM (1904) A new type of social parasitism among ants. *Bulletin of the American Museum of Natural History* 20: 347–375.
- Wheeler WM (1915) Some additions to the North American ant fauna. *Bulletin of the American Museum of Natural History* 34: 389–421.
- Wilson EO (1963) Social modification related to rareness in ant species. *Evolution; International Journal of Organic Evolution* 17(2): 249–253. <https://doi.org/10.2307/2406469>
- Wilson EO (1971) *The Insect Societies*. Belknap Press, Harvard University, Cambridge, Massachusetts, 548 pp.
- Wilson EO (1984) Tropical social parasites in the ant genus *Pheidole*, with an analysis of the anatomical parasitic syndrome (Hymenoptera: Formicidae). *Insectes Sociaux* 31(3): 316–334. <https://doi.org/10.1007/BF02223615>

New camaenid genus and species from Zhejiang, East China (Eupulmonata, Helicoidea)

Min Wu¹, Tian Chen², Wang Shen¹

¹ School of Life Sciences, Nanjing University, Xianlindadao 163, Qixia, Nanjing 210023, China

² Southern University of Science and Technology, Xueyandadao 1088, Nanshan, Shenzhen 518055, China

Corresponding author: Min Wu (minwu1969@aliyun.com)

Abstract

We report a new land snail species representing a new genus from the mountainous area of Zhejiang, China. The snail has a depressed shell with granules all over the surface. The soft part of the new taxon is characterized by the presence of a mantle lobe whose form is reviewed herein across a wide range of helicoid snails, the presence of a developed epiphallid papilla, and the absence of a penial sheath, a dart sac apparatus and a flagellum. As indicated by a molecular-based phylogeny (16S + ITS2), the new taxon is deeply nested in the eastern Asian camaenid genera and shows a close relationship with the camaenids distributed in Central China.

Key words: Anatomy, Camaenidae, mantle lobe, molecular phylogenetics, new genus, new species, taxonomy



Academic editor: Frank Köhler

Received: 17 January 2024

Accepted: 17 April 2024

Published: 15 May 2024

ZooBank: <https://zoobank.org/B73212F2-69AA-4703-826B-ADE235E8B7E0>

Citation: Wu M, Chen T, Shen W (2024) New camaenid genus and species from Zhejiang, East China (Eupulmonata, Helicoidea). ZooKeys 1202: 135–154. <https://doi.org/10.3897/zookeys.1202.118964>

Copyright: © Min Wu et al.

This is an open access article distributed under terms of the Creative Commons Attribution License (Attribution 4.0 International – CC BY 4.0).

Introduction

The first camaenid described in Zhejiang (= Dshè-dshiang, Chekiang [浙江]), China, was *Acusta ravid* (Benson, 1842). So far, there are about 20 species of camaenid land snails known from Zhejiang, grouped into seven genera, namely *Acusta* Martens, 1860, *Aegista* Albers, 1850, *Bradybaena* Beck, 1837, *Nesiohelix* Kuroda & Emura, 1943, *Plectotropis* Martens, 1860, *Satsuma* A. Adams, 1868 and *Traumatophora* Ancey, 1887. *Acusta ravid*, a widespread species in Central and East China (Möllendorff 1875, 1884; Gredler 1878; Heude 1882; Pilsbry 1888, 1934; Gude 1902b; Yen 1935, 1936, 1938, 1939, 1942, 1948; Hwang et al. 2021; etc.), is known from Zhoushan (= Chusan, Chowshan, the type locality [舟山]), Tonglu [桐庐], Moganshan [莫干山], Fuyang [富阳], Jiande [建德] (= Yenchow [严州]), Lutzepu [?芦茨村], Xiaoshan (= Hsiaoshan [萧山]) of Zhejiang (Benson 1842; Möllendorff 1884, 1899; Gude 1902a, 1902c; Yen 1948) and the neighboring provinces (Möllendorff 1875, 1899; Yen 1936). The congener *A. redfieldi* (Pfeiffer, 1852), widespread in Central and South China (Heude 1882; Möllendorff 1884, 1899; Pilsbry 1888; Gude 1902a, 1902c; Yen 1938, 1939, 1942), was recorded with imprecise localities from Zhejiang (Möllendorff 1884, 1899).

Bradybaena cremata (Heude, 1882), may not be a Zhejiang member because its only locality Wuyuan (= Wu-yüan [婺源]) (Heude 1882; Möllendorff 1884;

Pilsbry 1887; Yen 1939; Zilch 1968) belongs to Jiangxi [江西] but not mistakenly “Zhejiang” (Möllendorff 1884), which some authors subsequently followed (e.g., Gude 1902c). However, the distribution of this species in Zhejiang is possible because Wuyuan is close to West Zhejiang. A similar situation is also evident for *B. dichroa* (Pfeiffer, 1846), originally described from Shanghai [上海] (Möllendorff 1884; Pilsbry 1888; Yen 1942) neighboring northern Zhejiang, but treated as a species from Zhejiang (Gude 1902c). *Bradybaena similaris* (Rang, 1831), from Central China [including synonym *B. similaris nucleus* (Deshayes, 1873)] and Southeast China (Heude 1882; Möllendorff 1884; Gude 1902a, c; Jones and Preston 1904; Pilsbry and Hirase 1905; Yen 1936, 1939, 1942; Kuroda and Habe 1949; Zilch 1968, 1974) and “Nördlich von Shanghai scheint sie zu fehlen” (Möllendorff 1884), is also distributed in Zhejiang (Gude 1902c; Yen 1948). Interestingly, the distribution of *B. similaris* in northern China (e.g., Yen 1935) is possibly anthropogenic (personal observation by Wu M).

Considering that *Mastigeulota kiangsiensis* (Martens, 1875) is distributed in Central China including Hubei [湖北], Jiangxi, and Sichuan [四川], which are west of Hongzehu Lake [洪泽湖] of Anhui [安徽] (Heude 1882; Gredler 1884; Möllendorff 1884; Pilsbry 1934; Yen 1942; etc.), the distribution record of one of its subspecies *M. kiangsiensis hilberi* (Kobelt, 1894) in Zhejiang (Gude 1902c) rather than Hubei (Hankow = Hankou [汉口]) is the possible locality, Zilch 1968) is quite doubtful. Another species whose distribution was falsely recorded as Zhejiang is *Pseudiberus tectumsinense* (Martens, 1873) (Gude 1902a), as all evidence shows that it is a species geographically limited to Jinan [济南] of Shandong [山东] (Martens 1873; Möllendorff 1884; Pilsbry 1888; Gude 1902c; Yen 1939, 1942; Zilch 1968; Wu and Qi 2006; Zhang et al. 2021).

Aegista chinensis (Philippi, 1845) was recorded from Moganshan, Fengshiu (= Fenshui [分水] of Tonglu) and Tonglu (Yen 1948). Four *Plectotropis* were found in Zhejiang. *Plectotropis brevibarbis* (Pfeiffer, 1859) has the widest distribution as it is widespread in Wongkiang (= Oujiang [甌江]), Fengshiu of the SE region (Yen 1948) and the NW region (Zhou et al. 2011) of the province or so-called “north of China”, possibly referring more to Zhejiang (Pfeiffer 1859; Pilsbry 1887) than northern China in the present sense. *Plectotropis brevibarbis* is also known from Ningguo [宁国] of Anhui and the region between Shanghai and Wuyuan, both bordering northern Zhejiang (Heude 1882; Möllendorff 1884; Yen 1939). The species *P. sedentaria* (Heude, 1885), originally described from Fengjie [奉节] of Chongqing [重庆] (previously a part of Sichuan) (Heude 1885; Yen 1938) is present in Chiangshan [江山], Zhejiang (Yen, 1948). *Plectotropis barbosella* (Heude, 1882), the third species of the genus, was reported from Shanghai, Taihu Lake [太湖], and a variety of localities in Zhejiang (Heude 1882; Möllendorff 1884; Pilsbry 1888; Gude 1902c; Yen 1939, 1942 1948; Zilch 1968). *P. scitula* (Pilsbry & Hirase, 1908) was originally reported from Hangzhou [杭州] (Pilsbry and Hirase 1908). *Plectotropis trichotropis trichotropis* (Pfeiffer, 1850) was reported from Shanghai alongside northern Zhejiang, Wuyuan and Dongliu [东流] adjacent to western Zhejiang (Gredler 1881; Möllendorff 1884; Heude 1885; Pilsbry 1888; Yen 1942) and was listed as a species in Zhejiang by Gude (1902c) who similarly treated *P. trichotropis laciniata* (Heude, 1882) (Heude 1882; Pilsbry 1888; Gude 1902c; Yen 1939, 1942; Zilch 1968) as a species from Zhejiang. Another subspecies *P. trichotropis ningpoensis* (Boettger, 1892) was found in eastern Zhejiang (Pilsbry 1892; Gude 1902c; Yen 1939; Zilch 1968).

Three or four *Satsuma* species, with only one verified for generic position, have been reported from Zhejiang. *Satsuma* (?) *fortunei* (Pfeiffer, 1850) has been reported from several localities in Zhejiang (Yen 1948), from which the species from Anhui and Shanghai, each bordering West and North Zhejiang, has been reported (Heude 1882; Pilsbry 1887). *Satsuma laeva* (Pilsbry & Hirase, 1908) was first described from Hangzhou (Pilsbry and Hirase 1908; = *Satsuma uncopila* sensu Wang et al. 2014, see Zhang et al. 2019) and then Yen (1948) found it in nearby Tonglu and Lutzepu. *Satsuma* (?) *uncopila* (Heude, 1882), a species common in the Yangtze River valley (Heude 1882; Möllendorff 1884; Pilsbry 1887; Yen 1939, 1942; Zilch 1968; Zhang et al. 2019), was found in Moganshan at Southeast Anhui and South Jiangsu (Yen 1948). *Satsuma* (?) *latilabris* (Möllendorff, 1874) is distributed in Jiujiang [九江], Jiangxi (Möllendorff 1874, 1884; Zilch 1968; Zhang et al. 2019), which is located spatially near to West Zhejiang and was listed by Gude (1902c) as a member of Zhejiang.

Cathaica fasciola (Draparnaud, 1801), usually seen in horticulture environments, is a synanthropic species in Zhejiang (personal observation by Wu M).

With regard to the large-sized camaenids in the province, *Nesiohelix cecillei* (Philippi, 1849) is known from Tiantong (= Tien-tung or Tien-tong [天童]) of the east region (Möllendorff 1884; Pilsbry 1890; Gude 1902c; Yen 1939, 1942; Zilch 1968). *Nesiohelix moreletiana* (Heude, 1882) is distributed in Hangzhou and Moganshan (Pilsbry 1890; Gude 1902c; Yen 1939, 1948; Habe 1945; Wu and Asami 2017), and in Ningde [宁德] of NE Fujian and Guangde [广德] of Anhui neighboring North Zhejiang (Heude 1882; Möllendorff 1884). *Nesiohelix yeni* Wu & Asami, 2017 was found sympatrically with *N. moreletiana* in Hangzhou (Wu and Asami 2017). Another large camaenid distributed in Zhejiang is *Traumatophora triscalpta* (Martens, 1875), which is also known from Jiangxi (Boyanghu = Poyanghu [鄱阳湖], Fuzhou [抚州]), Hubei, and Zhejiang (Heude 1882; Gredler 1884; Möllendorff 1884; Pilsbry 1890; Gude 1902c; Yen 1939, 1942; Wu 2019). The fossils of *T. triscalpta*, along with those of *A. ravida*, *A. redfieldi*, and *B. similaris*, were found in the sedimentary outcrops of the Upper Pleistocene near Zhenjiang and Nanjing [南京] of Jiangsu [江苏], whose sites lie approximately 100 km north to North Zhejiang (Yen 1943).

In contrast to the northern parts of East China, more than 74% of the mountainous area in Zhejiang provides a considerable variety of microhabitats where speciation of land snails is expected. We have recently found a camaenid slightly smaller than *Nesiohelix moreletiana* and *N. yeni* in shell size that represents an unknown camaenid in terms of genital anatomy and molecular systematics. The presence of a lobe on the mantle collar in this new snail impels us to compare this body part in a wider range of helicoid snails.

Materials and methods

Morphology

Living specimens were relaxed by drowning in water and then fixed in 70% ethanol. The shell and genital system were measured with digital vernier calipers and from photograph to the nearest 0.1 mm, respectively. Whorl number was counted as described by Kerney and Cameron (1979), with 0.125 (= $\frac{1}{8}$) whorls

accuracy. Parts of the genital system were measured after the specimens were sufficiently fixed in 70% ethanol. Radula preparation: The buccal mass was removed and treated in 10% sodium hydroxide solution below 60 °C for up to 10 min before the radula was extracted. The released radula was cleaned with water using a sonic cleaner and then transferred into 75% ethanol before being mounted. The radula was examined under a scanning electron microscope (SEM; Sigma 500). To observe the possible lobe near the mantle edge, the hardened mucus and small pieces of dirt were carefully removed with a soft brush under water. Directions used in descriptions: proximal = towards the genital atrium; distal = away from the genital atrium.

The Chinese name for the person, new taxon or locality is provided only once in square brackets when necessary.

Molecular phylogenetic analyses

Whole genomic DNA was extracted from a piece of pedal muscle of the ethanol-preserved specimens using TIANamp Marine Animals DNA Kit. Each 25 µL PCR mixture consisted of 12.5 µL cwbio 2× Es Taq MasterMix Dye, 9.5 µL ddH₂O, 1 µL template DNA, 1 µL forward primer (10 µL/L) and 1 µL reverse primer (10 µL/L). Primers used for ITS2 were LSU1: 5'-CTAGCTGCGAGAAT-TAATGTGA-3', LSU3: 5'-ACTTTCCTCACGGTACTTG-3' (Wade and Mordan 2000), for 16S were 16SAR: 5'-CGCCTGTTTATCAAAAACAT-3', 16SBR: 5'-CCG-GTCTGAACCTCAGATCACGT-3' (Palumbi et al. 1991). The conditions for thermal cycling, performed on an Eastwin ETC811 Cycler, for 16S were 60 s at 96 °C for pre-denaturing, 35 cycles of 30 s at 94 °C, 30 s at 55 °C and 60 s at 72 °C, and a final extension at 72 °C for 10 min; for ITS2 4 min at 94 °C for pre-denaturing, 30 cycles of 20 s at 94 °C, 20 s at 55 °C and 40 s at 72 °C, and a final extension at 72 °C for 10 min. The amplicons were examined on a 1% agarose gel for quality and fragment size, then were purified and sequenced on an automated sequencer.

Chromatographs and sequences were studied and compiled in Sequencher v.4.5. For phylogenetic analysis, sequences of the new taxon (GenBank accession numbers: 16S, OR209732; ITS2, OR209722) and all those from a recently published work (see Wu et al. 2023, table 3) were included. The alignment of ITS2 and 16S was performed in batches with MAFFT v.7.505 (Kato and Standley 2013) in PhyloSuite v.1.2.3 (Zhang et al. 2020; Xiang et al. 2023) using '–auto' strategy and normal alignment mode. Gap sites of rRNA genes were removed with trimAl v.1.2rev57 (Capella-Gutiérrez et al. 2009) using "–automated1" command. DAMBE v.7.3.32 (Xia 2018) was employed to make the saturation tests. Unsaturated sequences were concatenated in the same order for subsequent analyses. The best-fit partition model (Edge-linked) was selected under the BIC criterion using ModelFinder (Kalyaanamoorthy et al. 2017). Bayesian inference phylogenies were inferred using MrBayes v.3.2.7a (Ronquist et al. 2012) under a partition model (2 parallel runs, 800,000 generations), in which the initial 25% of sampled data were discarded as burn-in. Maximum-likelihood phylogenies were inferred using IQ-TREE (Nguyen et al. 2015) under the Edge-linked partition model for 5000 ultra-fast (Minh et al. 2013) bootstraps, as well as the Shimodaira-Hasegawa-like approximate likelihood-ratio test (Guindon et al. 2010).

Abbreviations

At – atrium; **BC** – bursa copulatrix; **BCD** – bursa copulatrix duct; **Ep** – epiphallus; **EpP** – epiphallic papilla; **FO** – free oviduct; **P** – penis; **PR** – penial retractor muscle; **Va** – vagina; **VD** – vas deferens.

Depositories

HBUMM mollusc collection of the Museum of Hebei University, Baoding, China
IZCAS Zoological Museum, Institute of Zoology, Chinese Academy of Sciences, Beijing, China

Results

Phylogeny of the studied taxa

A concatenated matrix of 80 terminals (including outgroup) × 1045 bp (296 bp from partial 16S sequence and 749 bp from partial ITS2 sequence) was used in the subsequent analyses. Both 16S and ITS2 were unsaturated. For the Bayesian method, GTR+F+I+G4 was selected as the best evolution model for 16S, as well as K2P+G4 for ITS2. For the ML method, GTR+F+I+G4 was the best model for 16S I and K2P+I+I+R2 was the best model for ITS2.

The obtained phylograms using Bayesian inference and the maximum-likelihood analysis are topologically similar to each other except for two positions, as indicated in Fig. 7. Most clades received high support. The genera *Nesiohelix* Kuroda & Emura, 1943, *Traumatophora* Ancey, 1887, *Camaenella* Pilsbry, 1893, *Aegista*, *Plectotropis* Martens, 1860 are basal on the tree. *Sinocamaena* gen. nov. is inside the clade consisting of a variety of taxa that are almost exclusively endemic to the Southern Gansu Plateau. The phylogram topologically agrees well with that of Wu et al. (2023).

Comparative study of the mantle lobe in helicoids, especially for eastern Asian taxa

In some preserved specimens, the mantle lobe is covered with curdled mucus and is difficult to observe. At the mantle collar, the lobe-like flesh (literally indistinguishable from “lobe”, e.g., in Chen et al. 2021) near the anus+ pneumostome, forms a more or less developed elongating part of the structure of the anus orifice, i.e., the suprapneumostomal and subpneumostomal lobes (e.g., in *Napaeus nanodes*, fig. 6A in Henríquez et al. 1993). In this work, the mantle lobe refers to a single separate piece of fleshy lamina (e.g., Fig. 3B) on the opposite side of the lobe-like structure near the anus + pneumostome (e.g., Fig. 3A), which appears as a thin fleshy flap that is usually attached to the inner wall of the mantle collar. If present, the mantle lobe of a dextral-shelled snail is on the left side, and in the case of a sinistral-shelled snail on the right side of the mantle collar.

We observed mantle lobes in the voucher specimens phylogenetically investigated here and in other specimens including *Acusta*, *Aegista*, *Bradybaena*, *Camaena* Albers, 1850, *Camaenella*, *Euhadra* Pilsbry, 1890, *Nesiohelix*, *Plectotropis* Martens, 1860, *Satsuma*, *Sinocamaena* gen. nov. (see below), and *Traumatophora* (Table 1).

Table 1 Material examined for the comparative morphology of the mantle lobe in some helicoids.

Species	Collection information of the examined specimens
<i>Acusta ravida</i> (Benson, 1842)	HBUMM06242, Xiuning, Anhui, China, coll. Zheng W, Liu JY, 2007-V-19
<i>Aegista chinensis</i> (Philippi, 1845)	HBUMM06481, Nanshan, Zhenjiang, China, coll. Wu M & Xu Q, 2011-VI-12
<i>Angiomphalia</i> (<i>Angiomphalia</i>) <i>guljaensis</i> Wu, 2004	HBUMM05177, Gulja, Xinjiang, China, coll. Wu M, Ayken A, 2002-VI
<i>Bradybaena brevispira</i> (H. Adams, 1870)	HBUMM04167, Baidicheng, Fengjie, China, coll. Wu M, 2004-VII-20
<i>Bradybaena circula</i> (Pfeiffer, 1846)	HBUMM06859, Yoron-to Island, Japan. Individual, No. 3, coll. Hou L & Asami T, 2012-VI
" <i>Bradybaena</i> " <i>eris pachychila</i> (Möllendorff, 1899)	HBUMM05493, Wenxian, Gansu, coll. Wu M et al., 2006-IX-28
<i>Bradybaena linjun</i> Wu & Chen, 2019	HBUMM08241, types
<i>Bradybaena qixiaensis</i> Wu & Asami, 2017	HBUMM06841, paratypes, Qixiashan, Nanjing, China, coll. Wu M, Fang YX & Wang DB, 2012-6-26
<i>Bradybaena similis</i> (Rang, 1831)	HBUMM006861, Matsumoto, Nagano, Japan. No. 3; coll. Hou L & Asami T, 2012-VI-13
" <i>Bradybaena</i> " <i>strictotaenia</i> (Möllendorff, 1899)	HBUMM05467, Wenxian, Gansu, China, coll. Wu M, Liu JM, Zheng W and Gao LH, 2006-IX-27
" <i>Buliminidius</i> " <i>achatininus</i> (Möllendorff, 1899)	HBUMM00523, Gansu, China
" <i>Buliminidius</i> " <i>hirsutus</i> (Möllendorff, 1899)	HBUMM06565, Jiuzhaigou, Sichuan, coll. Wu, Xu & Buhda, 2011-VIII-14
<i>Camaena menglunensis</i> Chen & Zhang, 1999	HBUMM01701, Bubang, Yunnan, China, coll. Wu M & Wiktor A, 2002-VII-25
<i>Camaenella platyodon</i> (L. Pfeiffer, 1846)	HBUMM08457, Hainan, China, 2020-IX
<i>Cathaica buvigneri</i> (Deshayes, 1873)	HBUMM08140, Huanxian, Gansu, China, coll. Sheng XF et al., 2017-VII-29
<i>Cathaica fasciola</i> (Draparnaud, 1801)	HBUMM08144, Qingyang, Gansu, coll. Sheng XF et al., 2017-VII-28
" <i>Cathaica</i> " <i>gansuica</i> Möllendorff, 1899	HBUMM05666, Dangchang, Gansu, China, coll. Liu JM, Zheng W, 2006-X-02
" <i>Cathaica</i> " <i>pulveratricula</i> (Martens, 1882)	HBUMM08208, Dingxi, Gansu, coll. Sheng XF et al., 2017-VIII-4
<i>Cepaea hortensis</i> (Müller, 1774)	HBUMM05979, Slagelse, Denmark, coll. Guo JY, 2003-V-7–8
<i>Eueuhadra</i> sp.	HBUMM03341, Heishui, Sichuan, coll. Zhou HZ, 2001-VII-24–26
<i>Euhadra amaliae</i> (Kobelt, 1875)	HBUMM06851, Kyoto, Japan, No. 3, coll. Asami T, 2010; HBUMM06868–Kyoto, Japan, No. 2, coll. Asami T, 2010
<i>Euhadra sandai communis</i> Pilsbry, 1928	HBUMM06856, Kyoto, Japan, coll. Asami T
<i>Fruticicola fruticum</i> (Müller, 1774)	HBUMM01006, Lower Silesia Reserve Muszkowicki Las Bukowy near Henry Kow, Poland, coll. Wu M & Wiktor A, 1999-VI-26
<i>Helix pomatia</i> Linnaeus, 1758	HBUMM05972a, Nyborg, Denmark. coll. Guo JY, 2003-V-15
<i>Karftohelix middendorffi</i> (Gerstfeldt, 1859)	HBUMM05924, Cypancebua, Russia, coll. Sayenko EM, 2002-IX-27
<i>Laeocathaica</i> spp.	All known species, see Wu et al. 2023
<i>Mastigeulota kiangsiensis</i> (Martens, 1875)	HBUMM04190, Badong, Hubei, China, coll. Wu M, Wu Q, Qi G, 2004-VIII-1
<i>Metodontia wenxianensis</i> Chen & Zhang, 2004	HBUMM03335, Wenxian, Gansu, China, coll. Chen DN & Zhang GQ, 1998-V-17 (synonym: <i>Metodontia bidentatus</i> Wu & Prozorova, 2006)
<i>Nesiohelix moreletiana</i> (Heude, 1882)	HBUMM00054, Hangzhou, Zhejiang, China, coll. Chen DN, 1979-VIII-12
<i>Nesiohelix</i> sp.	HBUMM06873, Jiahe, Hunan, China, coll. Liu ZP, 2016-V-29
<i>Plectotropis sterilis</i> (Heude, 1890)	HBUMM04568, Badong, Hubei, China, coll. Wu M, 2003-VIII-20
<i>Ponsadenia</i> (<i>Mesasiata</i>) <i>duplocincta</i> (Martens, 1879)	HBUMM05886, Xinyuan, Xinjiang, China, coll. Wu M, Ayken A, 2002-VI-05
<i>Pseudiberus liuae</i> Wu, 2017	HBUMM06759, Shijiba, Wenxian, Gansu, China, types, coll. Wu M, Xu Q & Buhda P, 2011-VI-10
" <i>Pseudobuliminus</i> " <i>piligerus</i> (Möllendorff, 1899)	HBUMM05428, Wenxian, Gansu, China, coll. Wu M et al., 2006-IX-27
<i>Pseudobuliminus strigatus</i> (Möllendorff, 1899)	HBUMM05773, Wenxian, Gansu, China, coll. Wu M, 2006-IX-28
<i>Pseudobuliminus subcylindricus</i> (Möllendorff, 1899)	HBUMM04457, Wenxian, Gansu, coll. Chen DN & Zhang GQ, 1998-IV-27
<i>Pseudostegodera qilui</i> Chen, 2021	IZCAS TM206978, holotype
<i>Satsuma guandi</i> Zhang, Zhu & Lyu, 2019	HBUMM08239, Wenyuan, Shaoguan, Guangdong, China, coll. Yu D
<i>Satsuma uncopila</i> (Heude, 1882)	HBUMM03296, Zhongshanling, Nanjing, China, coll. Wu M, 2000-V-1. HBUMM06839, Tangshan, Nanjing, China, coll. Xu Q, Wang SY & Hou L, 2012-VI-29
<i>Sinochloritis lii</i> Wu & Chen, 2019	HBUMM08294, types
<i>Sinochloritis</i> sp.	HBUMM04525, Lushui, Yunnan, coll. Chen DN, 1981-VI-5
" <i>Stilpnodiscus</i> " <i>entochilus</i> Möllendorff, 1899	HBUMM00076, Jiuzhaigou, Sichuan, China, coll. Chen DN & Zhang GQ, 1998-V-18
<i>Traumatophora triscalpta</i> (Martens, 1875)	HBUMM06875, Tianmushan, Zhejiang, China, coll. Zhou DK, 2016-V
<i>Trichobradysbaena submissa</i> (Deshayes, 1873)	HBUMM01504, Meitan, Guizhou, China, coll. Wu M, 2003-VIII-2

The groups that do not have a mantle lobe are the following: “*Bradybaena*” in Central China, *Buliminidius* Heude, 1890, *Cathaica* Möllendorff, 1884, *Fruticicola* Held, 1837, *Metodontia* Möllendorff, 1886, *Pseudiberus* Ancey, 1887, *Pseudobuliminus* Gredler, 1886, *Stilpnodiscus* Möllendorff, 1899, and *Trichobrybaena* Wu & Guo, 2003 (Table 1).

Other groups of helicoids from Camaenidae, Hygromiidae and Helicidae, which are not included in the present phylogenetic study but have been anatomically examined, have mantle lobes as in Hygromiidae: *Angiomphalia* Schileyko, 1978; in Camaenidae: *Eueuhadra* Wu, 2004, *Mastigeulota* Pilsbry, 1894, *Ponsadenia* Schileyko, 1978, *Pseudostegodera* Wu & Chen, 2021, *Sinochloritis* Wu & Chen, 2019 (Wu et al. 2019b) and *Sinorachis* Wu & Chen, 2019 (Wu et al. 2019a); and in Helicidae: *Cepaea* Held, 1837 and *Helix* Linnaeus, 1758 (Table 1).

Systematics

Helicoidea Rafinesque, 1815

Camaenidae Pilsbry, 1895

Sinocamaena Wu, gen. nov.

<https://zoobank.org/40C4A6B6-BC44-4F77-87E3-1DDF85815DB3>

Chinese name. 中华坚螺属.

Type species. *Sinocamaena cheni* Wu, gen. et sp. nov.

Diagnosis. Shell depressed. Protoconch and teleoconch granulate. Protoconch strongly sculptured. Peristome expanded. Head wart low and tiny. Between the ommatophore insertions, a gland pore present. A mantle lobe present. Penial sheath absent. Epiphallus very short. Epiphallic papilla well developed. Flagellum absent.

Description. Shell depressed. Whorls slightly convex. Suture slightly impressed. Umbilicus broad. Protoconch with granules on strong radial sculpture. Peristome expanded. Adult shell surface without ribs, hairs or scales. Growth lines fine and evenly broken into granules on teleoconch. Shell with several thin bands above and beneath carina.

General anatomy. A small pore externally present between ommatophore insertions. Eversible head wart very weakly developed. A mantle lobe present.

Genitalia. Penial sheath absent. Penis externally without penial caecum. Pilasters inside penis low and weak. Epiphallus very short. Epiphallic papilla rather developed. Flagellum absent.

Etymology. This new genus is named after “sino” (= China) and “camaena” which is a camaenid genus that includes many large-sized helicoid species.

Distribution. China: Zhejiang.

Remarks. The new genus is conchologically close to many camaenids, such as *Camaena* Albers, 1850 and *Burmochloritis* Godwin-Austen, 1920, in having a large helicoid shell with multiple slender bands. In comparison to *Camaena* (sensu Schileyko 2003), the new genus has a strongly sculptured protoconch and an extremely short epiphallus (the part between penial retractor muscle insertion and vas deferens insertion), but has neither the axial corrugated pilasters within penis nor the flagellum. The new genus differs from *Burmochloritis* (Páll-Gergely et al. 2023) in the absence of the flagellum, the long cylin-

dricul epiphallus, the penial caecum and the dart sac. *Sinocamaena* gen. nov. shares with *Sinochloritis* the possession of granules on the protoconch and the characters from both general and genital anatomy, including the presence of a visible gland pore between the ommatophore insertions, a mantle lobe, a well-developed epiphallic papilla and the absence of a penial sheath and a dart sac apparatus. Compared to *Sinochloritis*, the new taxon has neither a flagellum nor a long epiphallus with the cylindrical trunk, nor prominent penial pilasters. In terms of shell morphology, generally, the new genus looks different from any other Chinese indigenous camaenid genus. Regardless of the shell morphology, all the other Chinese camaenid genera having no dart sac apparatus, i.e., *Amphidromus* Albers, 1850, *Landouria* Godwin-Austen, 1918, *Pancala* Kuroda & Habe, 1949, *Satsuma*, *Yakuchloritis* Habe, 1955, *Pseudostegodera* and the above mentioned *Sinochloritis*, possess a well-developed flagellum in the male part of genitalia (table 1 in Wu 2023). The present phylogeny (Fig. 7) suggests that the new taxon is possibly the nearest relative of almost all the members of dart sac-bearing bradybaenines endemic to the South Gansu Plateau or Central China.

It is noteworthy that the taxa that are basal on the phylogram, i.e., *Nesiohelix*, *Traumatophora*, *Acusta*, *Bradybaena*, *Plectotropis*, *Aegista*, *Euhadra*, *Satsuma*, *Camaena*, have mantle lobes. In general, the camaenids from Central China constitute a monophyly that receives high support values (clade X in Fig. 7), in which all terminals have a dart sac apparatus but lack a mantle lobe. The extended study of mantle lobes in helicoids taken here suggests that the presence of the mantle lobe could be a widely distributed and possibly a plesiomorphic character in the superfamily Helicoidea.

***Sinocamaena cheni* Wu, gen. et sp. nov.**

<https://zoobank.org/BAD768FA-1757-4938-83A2-E84FCE83B407>

Chinese name. 陈氏中华坚螺.

Type material. Holotype: a fully mature living snail, HBUMM08381-spec. 1, Zhangjiadi [张家地], Yunhe County [云和县], Lishui [丽水], Zhejiang Province; around oaks in remote forest, 27.974°N, 119.379°E, c. 820 m a.s.l., 2019-VIII, coll. Chen, Tian [陈天]; molecular voucher specimen HBUMM08381a. **Paratypes:** five fully mature empty shells, HBUMM08381-spec. 2–6, same collection data as holotype; HBUMM08367, a fully mature living snail; Zhangjiadi, Yunhe County, Lishui, Zhejiang Province; oak woods, coll. Chen, Tian; molecular voucher specimen HBUMM08367a-1; HBUMM08382-spec. 1, a living snail that reared to maturity at laboratory, same collection data as holotype; a fully mature empty shell, HBUMM08370-spec. 1, Mihougu [猕猴谷], Fengyangshan [凤阳山], Longquan County [龙泉县], Lishui, Zhejiang Province; 27.897°N, 119.159°E, 1100 m a.s.l., 2019-VIII-26, coll. Ye, Shi-Han [叶诗涵].

Measurement of holotype. Shell height 19.2 mm, shell breadth 44.3 mm, aperture height 15.9 mm, aperture breadth 22.2 mm, embryonic shell whorls $1\frac{1}{4}$, whorls $4\frac{5}{8}$.

Description. Shell (Fig. 1) large, depressed. Whorls slightly convex. Suture shallowly impressed. Umbilicus broad with embryonic whorls visible, approximately one-fifth of shell major diameter. Bottom-umbilicus transition

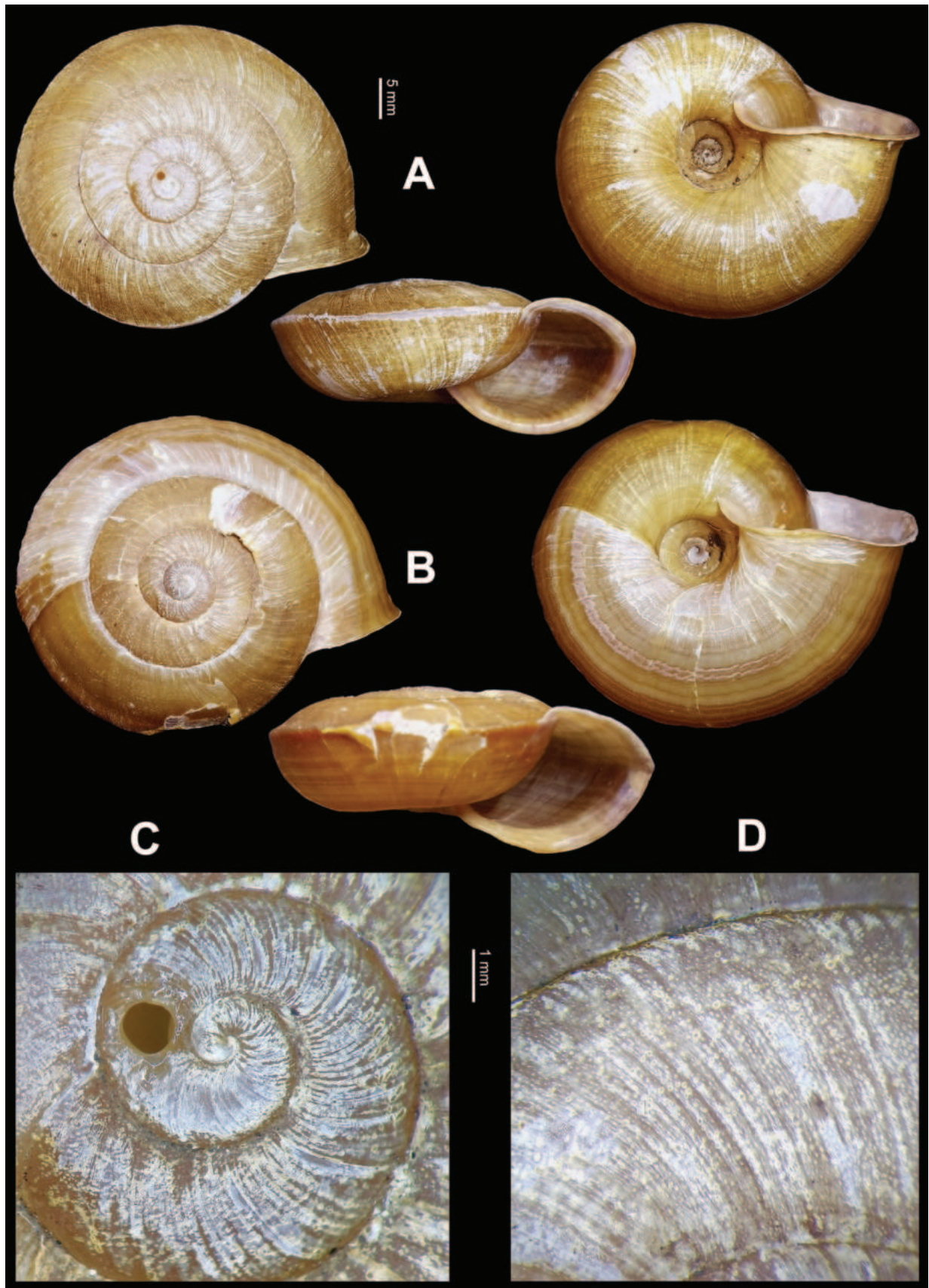


Figure 1. *Sinocamaena cheni* Wu, gen. et sp. nov. **A** holotype, HBUMM08381-spec. 1 **B** paratype, HBUMM08382-spec. 1, reared to maturity in laboratory **C**, **D** HBUMM08381, holotype **C** shell apex **D** shell surface. Upper scale for **A**, **B**; lower scale for **C**, **D**.



Figure 2. *Sinocamaena cheni* Wu, gen. et sp. nov., paratype, HBUMM08382-spec. 1, a specimen reared to maturity in laboratory.

changed gently. Columella oblique or obliquely curved. Columellar lip slightly covering umbilicus. Protoconch evenly granulate with strong radial sculpture (Fig. 1C). Teleoconch granulate, without hairs, scales or spiral furrows (Fig. 1D). Peristome evenly expanded, minutely sinuate. Aperture oblique, slightly expanded. Body whorl large, straight in front, sharply carinate above periphery. Aperture without inner ring-like thickening. Peristome thin, in faint purple. Shell dull and brownish yellow, with many clear thin brown bands above and beneath carina. Measurements (types, $N = 8$): shell height 17.5–21.0 mm (18.7 ± 1.15 mm), shell breadth 41.2–46.8 mm (43.9 ± 1.89 mm), aperture height 14.2–16.8 mm (15.4 ± 0.86 mm), aperture breadth 20.6–23.8 mm (22.3 ± 1.34 mm), embryonic shell whorls $1-1\frac{1}{4}$ (1.125 ± 0.1157 whorls), whorls $4\frac{3}{8}-4\frac{5}{8}$ (4.531 ± 0.1108 whorls), shell height/breadth ratio 0.41–0.45 (0.43 ± 0.013).

General anatomy (Figs 2–4). Externally, a small pore present between ommatophore insertions. Eversible head wart surrounding the pore very weakly present. A

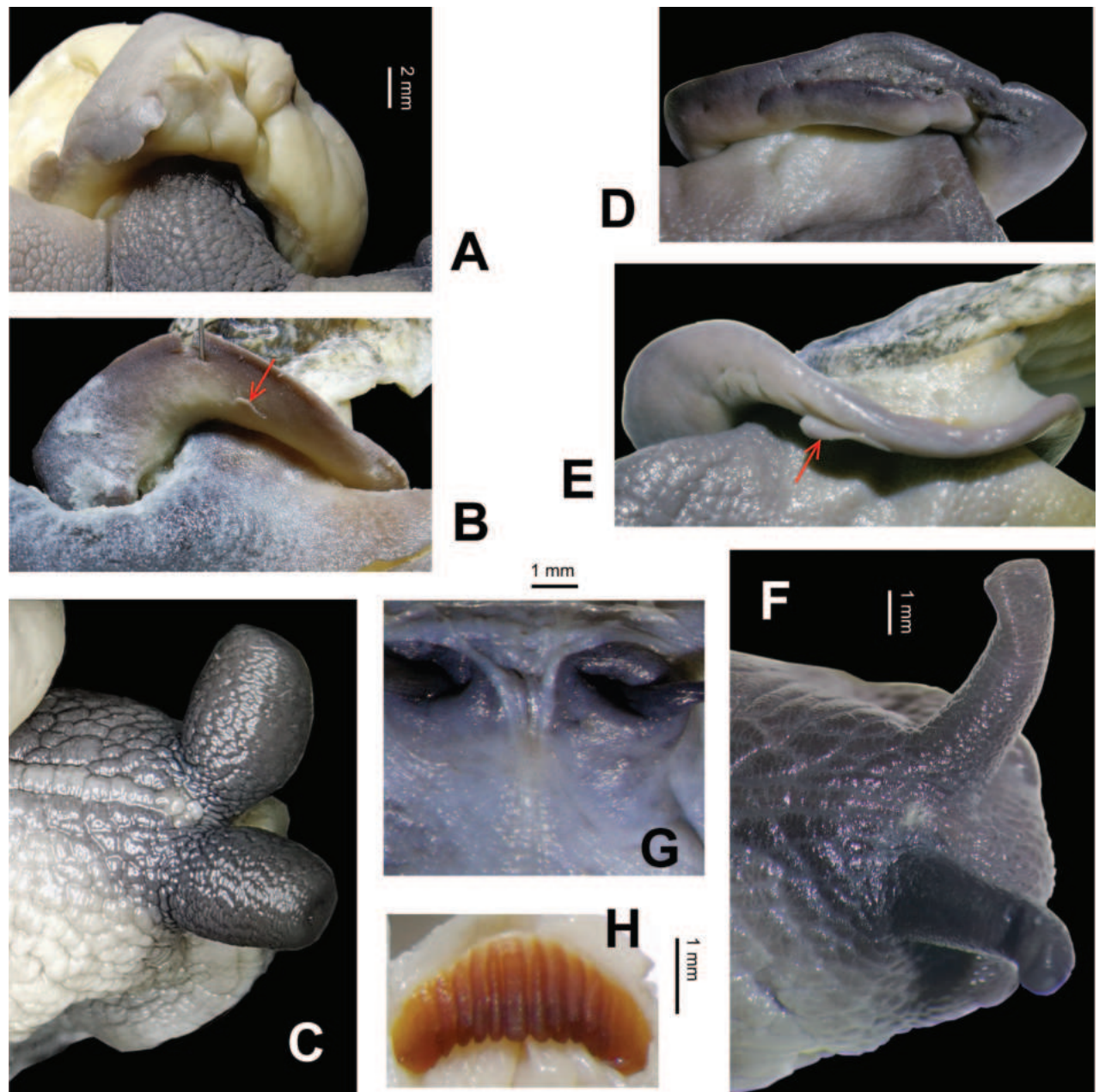


Figure 3. *Sinocamaena cheni* Wu, gen. et sp. nov., general anatomy **A–C** holotype, HBUMM08381-spec.1 **A** lobe-like structure near the anus+ pneumostome **B** mantle lobe on the left margin of mantle collar **C** anterior part of the animal, dorsal view, between ommatophore tentacles, showing the head gland where the pore/opening is not obvious **D–H** paratype, HBUMM08367-spec.1 **D** lobe-like structure near the anus+ pneumostome **E** mantle lobe on the left margin of mantle collar **F** dorsal view of anterior part of the animal, showing the pore among the contractive head gland **G** internal body wall of head, showing the head gland pore between the ommatophore tentacles **H** jaw, with basal muscle tissue remaining.

mantle lobe present. Tentacles and body in dark leaden-black; sole in color lighter than dorsal side. Jaw arcuate; with 12 more or less projecting ribs (Fig. 3H). Radula (HBUMM08367-spec. 1) comprises numerous transverse rows of teeth, each row containing approximately 131 teeth, 38+27+1+27+38. Central tooth symmetrically conic, without cuspid. Lateral tooth about more than two times larger than central tooth, strong conic medially, weakly uni-cuspid at both sides. Marginal teeth gradually changing from broadly tri-cuspid to tetra-cuspid (Fig. 4).

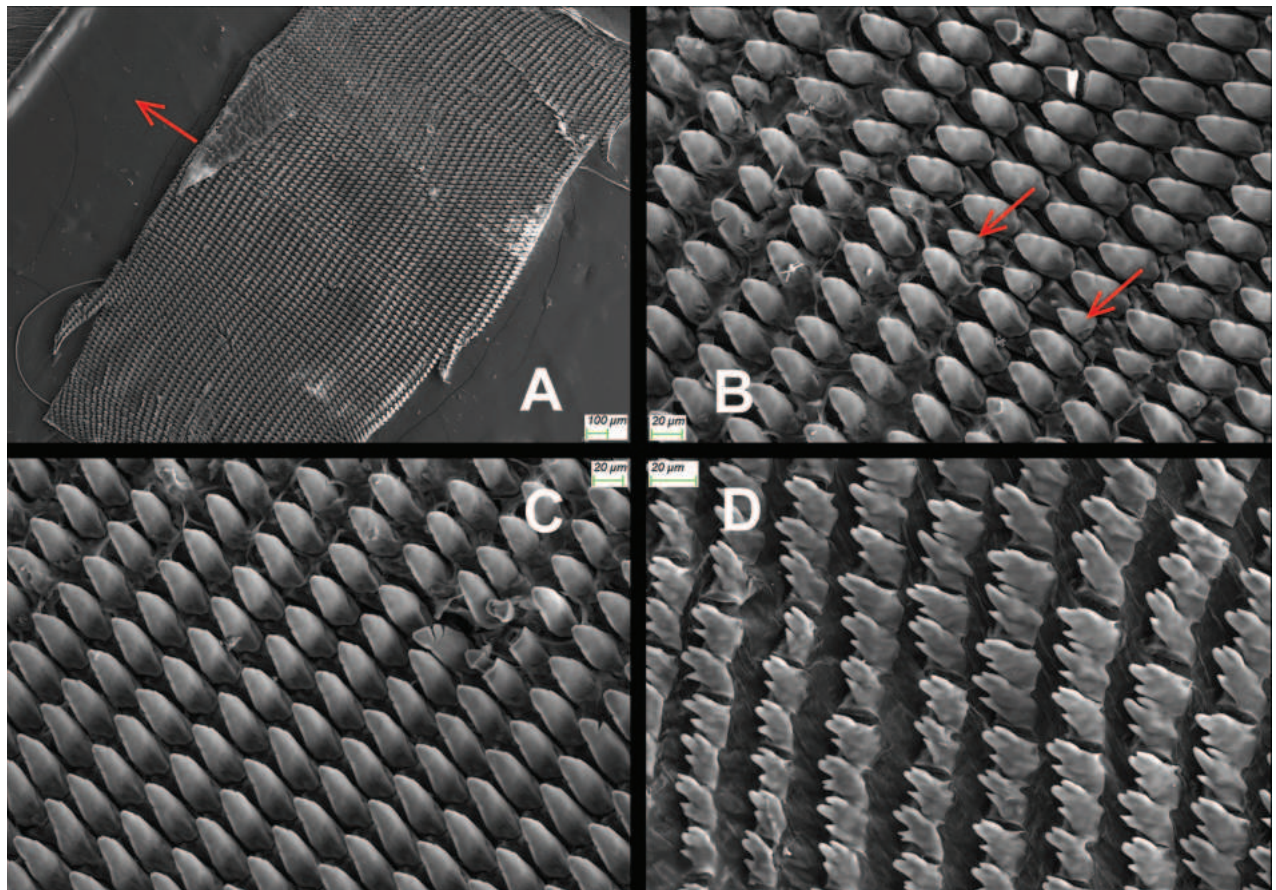


Figure 4. *Sinocamaena cheni* Wu, gen. et sp. nov. SEM photos. Paratype, HBUMM08367-spec.1 **A** section of radula, symmetry axis of radula arrowed **B** central teeth and lateral teeth; central teeth arrowed **C** lateral teeth **D** marginal teeth.

Genitalia (Figs 5, 6). Penial sheath absent. Penis club-shaped, swollen near insertion of penial retractor muscle. Penis externally simple, internally with numerous longitudinally arranged low projections like scales, which do not connect to each other into pilasters along the penial inner wall. Epiphallic papilla rather developed, on side of penial retractor muscle insertion with about several longitudinal pilasters which join apically. Epiphallus very short and stout, internally with a septum longitudinally dividing epiphallus into two separate chambers which one is empty and another one with about 10 pieces of high and low pilasters among which middle one is the strongest (Fig. 6). Flagellum absent. Membranous sac surrounding terminal genitalia absent. Dart sac apparatus absent. Vas deferens thin, slightly thickened near epiphallus. Vagina thick, subequal to penis in length. Bursa copulatrix duct thin, proximally not expanded. Measurement in holotype: P – 9.9 mm; Ep – 2.4 mm; VD – 19.4 mm; PR – 4.8 mm; Va – 7.2 mm; FO – 5.4 mm; BC plus BCD – 55.3 mm.

Ecology. This species was found in the litter layer in broad-leaved forest where oaks dominate (Fig. 8). However, the rediscovery of this species failed at one of the known localities (Zhangjiadi, Lishui) in April 2023.

Etymology. This new species is named in memory of Professor Chen De-Niu [陈德牛 Nov 1939 – March 2024], a known malacologist working on Chinese land molluscs. Prof. Chen was one of the doctoral supervisors for Wu M.

Distribution. Zhejiang (only from type localities: Yunhe, Longquan).

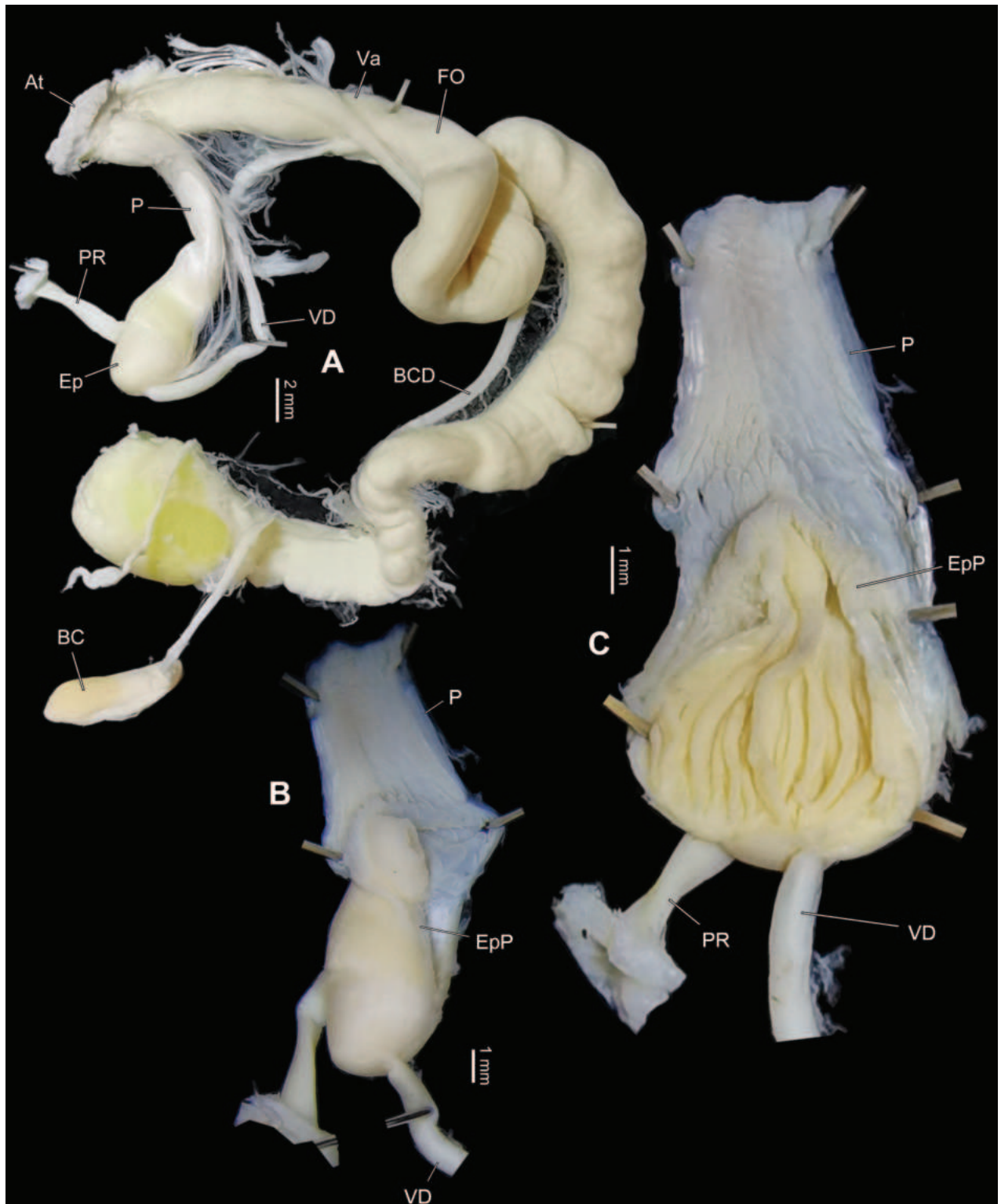


Figure 5. *Sinocamaena cheni* Wu, gen. et sp. nov., genitalia, holotype, HBUMM08381-spec.1 **A** general view of genitalia **B** exposed penis **C** exposed penial papilla.

Remarks. The new species and *Camaena vulpis* (Gredler, 1887) are superficially similar in having the densely and minutely granulate surface, numerous spiral thin bands and the general shape of shell. However, besides possessing a distinctly larger shell and a higher spire, the latter species has a totally differ-

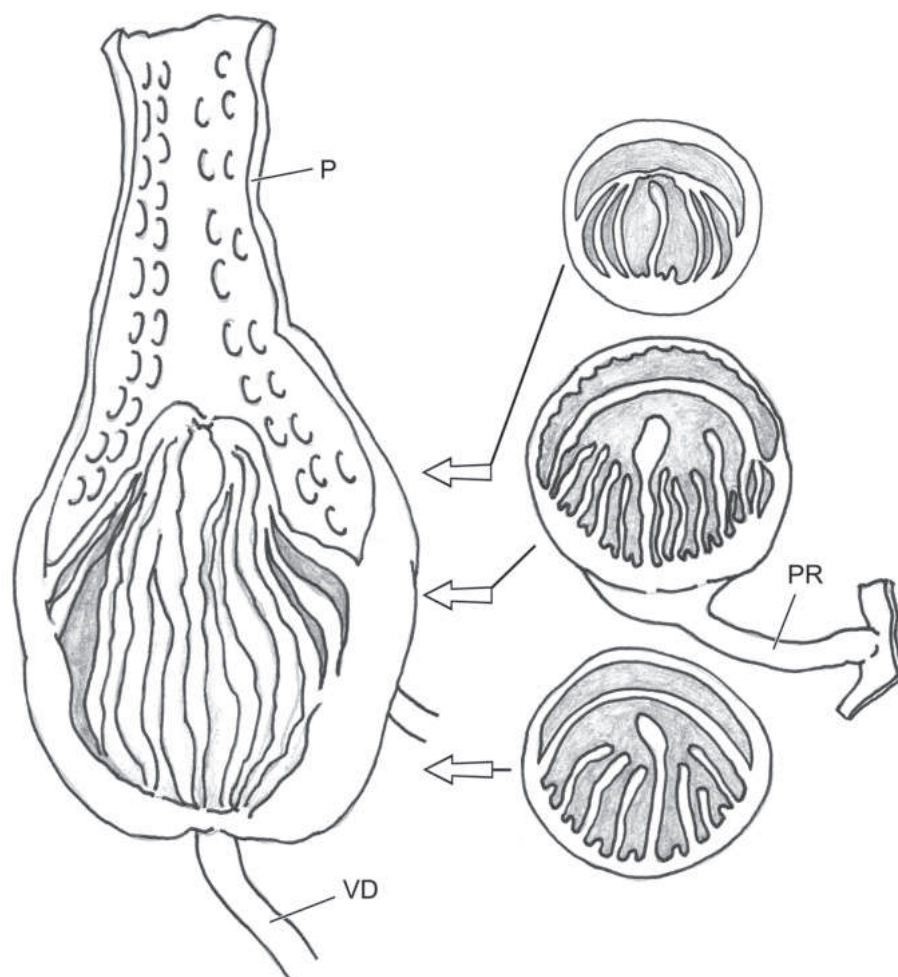


Figure 6. *Sinocamaena cheni* Wu, gen. et sp. nov., holotype, HBUMM08381-spec.1. exposed penis and exposed penial papillae, showing cross-sections.

ent genital system, which has a long flagellum (HBUMM08664, Liannan [连南], Nature Reserve of Giant Salamander, Guangdong, China, 2023-VII, coll. Wang Chong-Rui [王崇瑞], Chen Hui [陈辉]). The new species can be promptly distinguished from all the other Chinese camaenid taxa in genitalia because of the absence of the dart sac apparatus and the flagellum.

The phylogenetic analysis suggested that the new species/genus and the taxa distributed in Central China are possibly close relatives (Fig. 7). For other comments see the genus.

Acknowledgements

We are grateful to many people who collected the relevant specimens for this work. Thanks go to Dr Barna Páll-Gergely, Dr Frank Köhler and an anonymous reviewer for their helpful comments for an earlier manuscript and to Dr Christopher Glasby for linguistic editing. We must thank The Biodiversity Heritage Library (www.biodiversitylibrary.org) for access to old literature.

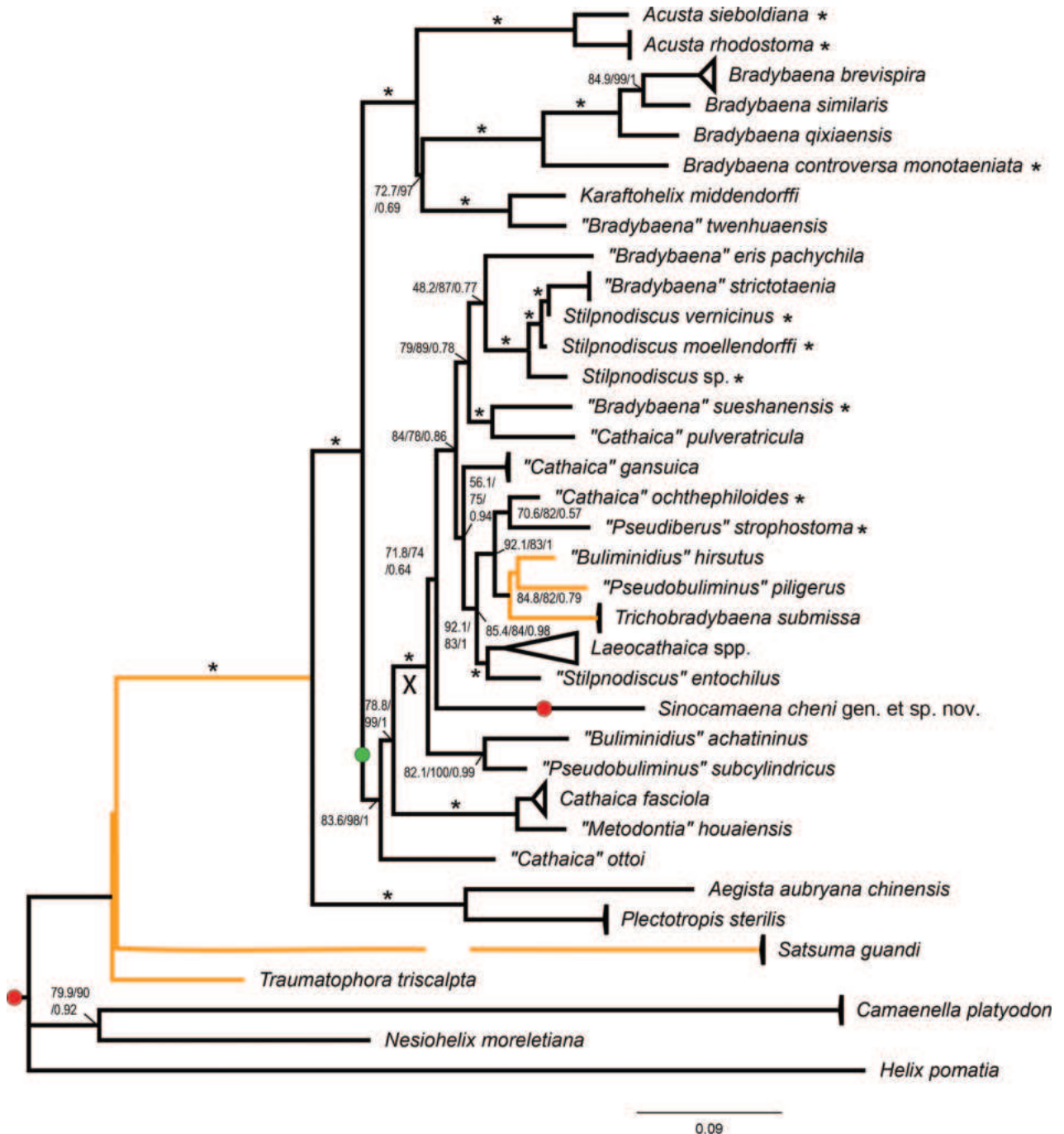


Figure 7. Maximum-likelihood phylogram based on the concatenated partial mitochondrial 16S and partial ITS2 sequences of East Asian camaenid species. The tree is rooted on *Helix pomatia*. Numbers near nodes indicate the Shimodaira and Hasegawa-approximate likelihood-ratios (SH-aLRT)/approximate Bayes test (aBayes)/ultra-fast bootstrap (IQ-TREE, maximum likelihood)/posterior probability (MrBayes, Bayesian inference). An asterisk on the branch indicates a clade with all well-supported values (SH-aLRT \geq 80%, aBayes \geq 0.95, BS \geq 95%, PP \geq 0.95). The broken branch indicates that the branch is shortened to exactly 1/2 the original length. Scale bar is for substitutions per site. Orange branches indicate where the BI tree topologically differs from the ML tree. Red dot/green dot indicates every terminal on that branch that has/has not a mantle lobe. An asterisk after the species name indicates that observation of the mantle lobe failed due to the bad condition of the specimen. The species under the genera in quotes are thought to be questionable generic assignments (Wu et al. 2023).



Figure 8. Habitat of *Sinocamaena cheni* Wu, gen. et sp. nov., Zhangjiadi, Yunhe County, Lishui.

Additional information

Conflict of interest

The authors have declared that no competing interests exist.

Ethical statement

No ethical statement was reported.

Funding

This study was supported by the National Natural Science Foundation of China (NSFC 31872196).

Author contributions

All authors have contributed equally.

Author ORCIDs

Min Wu  <https://orcid.org/0000-0000-0000-0000>

Data availability

All of the data that support the findings of this study are available in the main text.

References

- Benson WH (1842) Mollusca. In: Cantor T (Ed.) General features of Chusan, with remarks on the flora and fauna of that island. The Annals and Magazine of Natural History, London 9: 486–490. <https://doi.org/10.1080/03745484209445368>
- Capella-Gutiérrez S, Silla-Martínez JM, Gabaldón T (2009) trimAl: A tool for automated alignment trimming in large-scale phylogenetic analyses. *Bioinformatics* 25(15): 1972–1973. <https://doi.org/10.1093/bioinformatics/btp348>
- Chen Z-Y, Lyu Z-T, Wu M (2021) Systematic revision of *Stegodera* Martens, 1876 (Gastropoda, Stylommatophora, Camaenidae), with description of a new genus. *ZooKeys* 1059: 1–21. <https://doi.org/10.3897/zookeys.1059.68385>
- Gredler PV (1878) Zur Conchylien-Fauna von China. I. Stück *Nachrichtsblatt der deutschen Malakozoologischen Gesellschaft* 7: 101–105.
- Gredler PV (1881) Zur Conchylien-Fauna von China. III. Stück *Jahrbücher der Deutschen Malakozoologischen Gesellschaft* 8: 110–132.
- Gredler PV (1884) Zur Conchylien-Fauna von China. V. Stück *Jahrbücher der Deutschen Malakozoologischen Gesellschaft* 11: 129–161.
- Gude GK (1902a) A classified list of the helicoid land shells of Asia. (Part II) i. The Chinese Empire. *The Journal of Malacology* 9: 51–59.
- Gude GK (1902b) A classified list of the helicoid land shells of Asia (Part III) ii. Asiatic Russia. *The Journal of Malacology* 9: 97–129.
- Gude GK (1902c) A Classified list of the helicoid land shells of Asia. *The Journal of Malacology* 9: 1–11.
- Guindon S, Dufayard JF, Lefort V, Anisimova M, Hordijk W, Gascuel O (2010) New algorithms and methods to estimate maximum-likelihood phylogenies: Assessing the performance of PhyML 3.0. *Systematic Biology* 59(3): 307–321. <https://doi.org/10.1093/sysbio/syq010>
- Habe T (1945) Anatomical study of four snail species from Eastern Asia. *Japanese Journal of Malacology* 14(1–4): 14–21.
- Henríquez FC, Ibáñez M, Alonso R (1993) Revision of the genus *Napaeus* Albers, 1850 (Gastropoda Pulmonata: Enidae). The problem of *Napaeus* (*Napaeinus*) *nanodes* (Shuttleworth, 1852) and description of five new species from its conchological group. *The Journal of Molluscan Studies* 59(2): 147–163. <https://doi.org/10.1093/mollus/59.2.147>
- Heude PM (1882) Notes sur les mollusques terrestres de la vallée du Fleuve Bleu. *Mémoires concernant l'histoire naturelle de l'Empire chinois* 1: 1–84. <https://doi.org/10.5962/bhl.title.50365>
- Heude PM (1885) Notes sur les mollusques terrestres de la vallée du Fleuve Bleu. *Mémoires concernant l'histoire naturelle de l'Empire chinois* 2: 89–132.
- Hwang C-C, Zhou W-C, Ger M-J, Guo Y, Qian Z-X, Wang Y-C, Tsai C-L, Wu S-P (2021) Biogeography of land snail genus *Acusta* (Gastropoda: Camaenidae): Diversification on East Asian islands. *Molecular Phylogenetics and Evolution* 155: 106999. [Epub2020Oct30] <https://doi.org/10.1016/j.ympev.2020.106999>

- Jones KH, Preston HB (1904) List of Mollusca collected during the commission of H. M. S. "Waterwitch" in the China Seas, 1900–1903, with descriptions of new species. Proceedings of the Malacological Society, London 6: 138–151. <https://doi.org/10.1093/oxfordjournals.mollus.a066053>
- Kalyaanamoorthy S, Minh BQ, Wong TKF, von Haeseler A, Jermiin LS (2017) ModelFinder: Fast model selection for accurate phylogenetic estimates. Nature Methods 14(6): 587–589. <https://doi.org/10.1038/nmeth.4285>
- Katoh K, Standley DM (2013) MAFFT Multiple Sequence Alignment Software Version 7: Improvements in performance and usability. Molecular Biology and Evolution 30(4): 772–780. <https://doi.org/10.1093/molbev/mst010>
- Kerney MP, Cameron RAD (1979) A Field Guide to the Land Snails of Britain and North-West Europe. Collins, London, 288 pp. [24 pls]
- Kuroda T, Habe T (1949) Helicacea. 6 + 129 pp., 1 pl. Sanmeisha, Tokyo. [in Japanese]
- Martens EV (1873) Neue *Helix*-Arten aus China. Malakozoologische Blätter 21: 67–69.
- Minh BQ, Nguyen MAT, von Haeseler A (2013) Ultrafast approximation for phylogenetic bootstrap. Molecular Biology and Evolution 30(5): 1188–1195. <https://doi.org/10.1093/molbev/mst024>
- Möllendorff OF (1874) Diagnosen neuer Arten aus dem Binnenlande von China. Jahrbücher der Deutschen Malakozoologischen Gesellschaft 2: 78–80.
- Möllendorff OF (1875) Chinesische Landschnecken. Jahrbücher der Deutschen Malakozoologischen Gesellschaft 2: 118–135.
- Möllendorff OF (1884) Materialien zur Fauna von China. Jahrbücher der Deutschen Malakozoologischen Gesellschaft 11: 307–391.
- Möllendorff OF (1899) Binnen-Mollusken aus Westchina und Centralasien. I. Annuaire du Musée Zoologique de l'Académie Impériale des St.-Petersburg 4: 46–144 [pls 2–8]. <https://doi.org/10.5962/bhl.title.13125>
- Nguyen L-T, Schmidt HA, von Haeseler A, Minh BQ (2015) IQ-TREE: A fast and effective stochastic algorithm for estimating Maximum-Likelihood phylogenies. Molecular Biology and Evolution 32(1): 268–274. <https://doi.org/10.1093/molbev/msu300>
- Páll-Gergely B, Gojšina V, Neubert E (2023) Revision of *Burmochloritis* Godwin-Austen, 1920 in Southeast Asia (Gastropoda: Stylommatophora: Camaenidae). Archiv für Molluskenkunde 152(2): 183–216. <https://doi.org/10.1127/arch.moll/152/183-216>
- Palumbi S, Martin A, Romano S, McMillan WO, Stice L, Grabowwski G (1991) The Simple Fool's Guide to PCR. Department of Zoology, University of Hawaii, Honolulu.
- Pfeiffer L (1859) Descriptions of twenty-seven new species of land-shells, from the collection of H. Cuming, Esq. Proceedings of the Zoological Society of London 27: 23–29. [pls. XLIII.–XLIV.]
- Pilsbry HA (1887) In: GW Tryon and HA Pilsbry, Manual of Conchology (2) 3, 1–313 [63 pls].
- Pilsbry HA (1888) In: GW Tryon and HA Pilsbry, Manual of Conchology (2) 4, 1–296 [69 pls].
- Pilsbry HA (1890) In: GW Tryon and HA Pilsbry, Manual of Conchology (2) 6, 1–324 [69 pls].
- Pilsbry HA (1892) In: GW Tryon and HA Pilsbry, Manual of Conchology (2) 8, 1–314 [58 pls].
- Pilsbry HA (1934) Zoological results of the Dolan West China expedition of 1931, Part II, Mollusks. Proceeding of the Academy of Natural Sciences of Philadelphia 86: 5–28 [6 pls]
- Pilsbry HA, Hirase Y (1905) Catalogue of the land and fresh-water Mollusca of Taiwan (Formosa), with descriptions of new species. Proceedings. Academy of Natural Sciences of Philadelphia 57: 720–752.

- Pilsbry HA, Hirase Y (1908) New land shells of the Chinese Empire: I. Proceedings. Academy of Natural Sciences of Philadelphia 60(1): 37–43.
- Ronquist F, Teslenko M, Van Der Mark P, Ayres DL, Darling A, Höhna S, Larget B, Liu L, Suchard MA, Huelsenbeck JP (2012) MrBayes 3.2: Efficient Bayesian phylogenetic inference and model choice across a large model space. *Systematic Biology* 61(3): 539–542. <https://doi.org/10.1093/sysbio/sys029>
- Schileyko AA (2003) Treatise on recent terrestrial pulmonate molluscs. Part 11. Trigonochlamydidae, Papillodermidae, Vitrinidae, Limacidae, Bielziidae, Agriolimacidae, Boettgerillidae, Camaenidae. *Ruthenica* (Supplement 2): 1467–1626.
- Wade CM, Mordan PB (2000) Evolution within the gastropod molluscs; using the ribosomal RNA gene-cluster as an indicator of phylogenetic relationships. *The Journal of Molluscan Studies* 66(4): 565–570. <https://doi.org/10.1093/mollus/66.4.565>
- Wang P, Xiao Q, Zhou W-C, Hwang C-C (2014) Revision of three camaenid and one bradybaenid species (Gastropoda, Stylommatophora) from China based on morphological and molecular data, with description of a new bradybaenid subspecies from Inner Mongolia, China. *ZooKeys* 372: 1–16. <https://doi.org/10.3897/zookeys.372.6581>
- Wu M (2019) A taxonomic note on the helicoid land snail genus *Traumatophora* (Eupulmonata, Camaenidae). *ZooKeys* 835: 139–152. <https://doi.org/10.3897/zookeys.835.32697>
- Wu M (2023) A new *Aegistohadra* (Gastropoda: Camaenidae) from southwest China. *Ruthenica* 33(2): 59–71. [https://doi.org/10.35885/ruthenica.2023.33\(2\).2](https://doi.org/10.35885/ruthenica.2023.33(2).2)
- Wu M, Asami T (2017) Taxonomical notes on Chinese camaenids with description of three new species (Gastropoda: Pulmonata). *Molluscan Research* 38(2): 137–148. <https://doi.org/10.1080/13235818.2017.1380145>
- Wu M, Qi G (2006) A taxonomic note on *Pseudiberus* Ancey, 1887 (Gastropoda: Pulmonata: Bradybaenidae). *Folia Malacologica* 14(1): 25–30. <https://doi.org/10.12657/foimal.014.003>
- Wu M, Chen Z-Y, Zhang L (2019a) Jawless land snail *Sinorachis*, a new bradybaenine genus from China (Eupulmonata, Camaenidae). *ZooKeys* 853: 51–67. <https://doi.org/10.3897/zookeys.893.38445>
- Wu M, Chen Z-Y, Zhu X-R (2019b) Two new camaenid land snails (Eupulmonata) from Central China. *ZooKeys* 861: 129–144. <https://doi.org/10.3897/zookeys.861.35430>
- Wu M, Shen W, Chen Z-G (2023) Land snail diversity in central China: Revision of *Laeocathaica* Möllendorff, 1899 (Gastropoda, Camaenidae), with descriptions of seven new species. *ZooKeys* 1154: 49–147. <https://doi.org/10.3897/zookeys.1154.86237>
- Xia X (2018) DAMBE7: New and improved tools for data analysis in molecular biology and evolution. *Molecular Biology and Evolution* 35(6): 1550–1552. <https://doi.org/10.1093/molbev/msy073>
- Xiang C-Y, Gao F, Jakovlić I, Lei H-P, Hu Y, Zhang H, Zou H, Wang G-T, Zhang D (2023) Using PhyloSuite for molecular phylogeny and tree-based analyses. *iMeta* 2(1): e87. <https://doi.org/10.1002/imt2.87>
- Yen T-C (1935) The Non-marine gastropods of North China. Part I. Publications du Musée Hoangho Paiho de Tien Tsin No. 34: 1–57 [5 pls].
- Yen T-C (1936) Notes on the distribution of non-marine mollusks in the Soochow area. *China Journal* (Canberra, A.C.T.) 24(1): 44–47.
- Yen T-C (1938) Notes on the gastropod fauna of Szechwan Province. Sonderabdruck aus: *Mitteilungen aus dem Zoolog. Museum in Berlin* 23(2): 438–457 [1 pl.].

- Yen T-C (1939) Die chinesischen Land- und Süßwasser-Gastropoden des Natur-Museums Senckenberg. *Abhandlungen der Senckenbergischen Naturforschenden Gesellschaft* 444: 1–234 [16 pls].
- Yen T-C (1942) A Review of Chinese Gastropods in the British Museum. *Proceedings of the Malacological Society of London* 24: 170–288 [pl. 11–28].
- Yen T-C (1943) Review and summary of Tertiary and Quaternary non-marine mollusks of China. *Proceedings. Academy of Natural Sciences of Philadelphia* 95: 267–309, 346.
- Yen T-C (1948) Notes on land and fresh-water mollusks of Chekiang Province, China. *Proceedings of the California Academy of Sciences Fourth Series* 24(4): 69–99 [1 pl.].
- Zhang L-J, Zhu Y-J, Lyu Z-T (2019) A new sinistral species of the land-snail genus *Satsuma* (Pulmonata: Camaenidae) from China. *Molluscan Research*. <https://doi.org/10.1080/13235818.2019.1644721>
- Zhang D, Gao F, Jakovlić I, Zou H, Zhang J, Li WX, Wang GT (2020) PhyloSuite: An integrated and scalable desktop platform for streamlined molecular sequence data management and evolutionary phylogenetics studies. *Molecular Ecology Resources* 20(1): 348–355. <https://doi.org/10.1111/1755-0998.13096>
- Zhang G-Y, Wu M, Köhler F, Liu T-T (2021) Review of the genus *Pseudiberus* Ancey, 1887 (Eupulmonata: Camaenidae) in Shandong Province, China. *Malacologia* 63(2): 257–284. <https://doi.org/10.4002/040.063.0207>
- Zhou W-C, Xiao Q, Chen D-N, Hwang C-C (2011) *Plectotropis yonganensis* sp. nov. (Gastropoda: Bradybaenidae) from China, with revision of two Chinese camaenid species (Gastropoda: Camaenidae). *Zootaxa* 2929(1): 51–56. <https://doi.org/10.11646/zootaxa.2929.1.4>
- Zilch A (1968) Die Typen und Typoide des Natur-Museums Senckenberg. 41. *Archiv für Molluskenkunde* 98(3/4): 155–212.
- Zilch A (1974) Vinzenz Gredler und die Erforschung der Weichtiere Chinas durch Franziskaner aus Tirol. *Archiv für Molluskenkunde* 104(4/6): 171–228 [pls. 7–9].

On the enigmatic jumping spider genus *Ogdenia* Peckham, 1908 (Araneae, Salticidae, Chrysillini)

Zhiyong Yang^{1,2}, Quang Duy Hoang³, Weihang Wang^{1,2}, Wayne P. Maddison⁴, Junxia Zhang^{1,2}

1 Key Laboratory of Zoological Systematics and Application, College of Life Sciences, Hebei University, Baoding, Hebei 071002, China

2 Hebei Basic Science Center for Biotic Interaction, Hebei University, Baoding, Hebei 071002, China

3 Faculty of Natural Sciences and Technology, Tay Nguyen University, 567 Le Duan, Buon Ma Thuot, Dak Lak 630000, Vietnam

4 Departments of Zoology and Botany and Beaty Biodiversity Museum, University of British Columbia, 6270 University Boulevard, Vancouver, British Columbia, V6T 1Z4, Canada

Corresponding author: Junxia Zhang (jxzhang1976@163.com)

Abstract

The monotypic genus *Ogdenia* Peckham, 1908, is redefined based on the redescription of the holotype of *O. mutilla* (Peckham & Peckham, 1907), along with the newly discovered male specimens and intraspecific variation from China, Malaysia, Singapore, and Vietnam. Description, illustrations, and photographs are provided.

Key words: Chrysillini, *Ogdenia mutilla*, redescription, Southeast Asia

Introduction

In 1907, G.W. Peckham and E.G. Peckham established the monotypic genus *Rooseveltia* with the type species *Rooseveltia mutilla* Peckham & Peckham, 1907, based on a single female holotype from Borneo, Kuching, Malaysia (Peckham and Peckham 1907). *Rooseveltia* was later renamed *Ogdenia* due to its homonymy with *Rooseveltia* Jordan & Evermann, 1906 in Pisces (Peckham 1908). With the absence of diagnostic illustration in the original description, this genus long remained enigmatic until Prószyński (1984) provided drawings for the epigyne and retromarginal tooth based on the holotype of the type species. In addition, photographs of living females of *O. mutilla* from Singapore and Malaysia (Johor and Sarawak) were recently provided in "A Photographic Guide to Singapore Spiders" (Joseph et al. 2022). Although the information about *Ogdenia* has been accumulated in past decades, the male of this genus remained unknown.

Herein, we redescribe *O. mutilla* and provide photographs of the habitus and epigyne of the holotype specimen. In addition, we document the male for the first time. Furthermore, intraspecific variation based on specimens from China, Malaysia, Singapore, and Vietnam is presented.



Academic editor: Shuqiang Li

Received: 29 March 2024

Accepted: 24 April 2024

Published: 16 May 2024

ZooBank: <https://zoobank.org/8588FB35-9CA0-4889-8203-AC3403746C34>

Citation: Yang Z, Hoang QD, Wang W, Maddison WP, Zhang J (2024) On the enigmatic jumping spider genus *Ogdenia* Peckham, 1908 (Araneae, Salticidae, Chrysillini). ZooKeys 1202: 155–168. <https://doi.org/10.3897/zookeys.1202.124199>

Copyright: © Zhiyong Yang et al.

This is an open access article distributed under terms of the Creative Commons Attribution License (Attribution 4.0 International – CC BY 4.0).

Materials and methods

Specimens preserved in 75% or 95% ethanol were examined and measured under a Leica M205A stereomicroscope. All measurements are in millimetres using the associated Leica LAS v. 4.3 software. Photographs of living specimens were captured using a Canon 80D camera equipped with a Laowa 100 mm f/2.8 macro 2× lens and a KR-888 flash, a Sony ILCE-7RM2 camera with a Laowa 90 mm f/2.8 macro 2× lens and a KR-808 flash, and a Nikon D7200 camera with an AF-S DX Macro Nikkor 40 mm f/2.8G lens and a KR-888 flash. Ethanol-immersed body and genitalia photos were taken by a Kuy Nice CCD camera mounted on an Olympus BX53 microscope and then stacked by the Helicon Focus v. 7 software. Final photographs were retouched in Adobe Photoshop CC 2021. The male palp was macerated in clove oil to observe the trajectory of the spermophor, while the female vulva was cleaned with pancreatin. The holotype specimen is preserved in the Museum of Comparative Zoology, Harvard University, USA (**MCZ**); the examined specimens from China are preserved in the Museum of Hebei University, Baoding, China (**MHBU**), those from Vietnam are preserved at the Tay Nguyen University, Buon Ma Thuot, Vietnam (**TNU**), and those from Singapore and Malaysia are preserved in the Beaty Biodiversity Museum, University of British Columbia, Vancouver, Canada (**UBCZ**).

Abbreviations used: **AG**, accessory gland; **ALE**, anterior lateral eye; **AME**, anterior median eye; **BH**, basal haematodocha; **C**, cymbium; **CD**, copulatory duct; **CO**, copulatory opening; **E**, embolus; **FD**, fertilization duct; **IZ**, Invertebrate Zoology; **PL**, posterior tegular lobe; **PLE**, posterior lateral eye; **PME**, posterior median eye; **RTA**, retrolateral tibial apophysis; **S**, spermatheca; **SM**, spermophor; **TB**, tegular bump; **XTBG**, Xishuangbanna Tropical Botanical Garden.

Taxonomy

Genus *Ogdenia* Peckham, 1908

Rooseveltia Peckham & Peckham, 1907: 614; type species: *Rooseveltia mutilla* Peckham & Peckham, 1907, by original designation and monotypy.
Ogdenia Peckham, 1908: 171 (generic replacement name).

Diagnosis. The genus closely resembles *Siler* Simon, 1889, but can be distinguished by: (1) the larger body size (6–10 mm); (2) the male femur I with only sparse setae (Figs 4B, E, F, 5O; femur I and tibia I covered with dense setae in *Siler*); (3) the male palp with a blunt posterior tegular lobe (PL) (Figs 8B, C, 10A, 11E, 12D; PL longer and narrower in *Siler*); (4) the chelicerae with dense brown setae on the front surface (Figs 1B, D, 5M, N, P, Q, T, U, 6E, F, 7A, C, E; setae sparse in *Siler*); (5) the presence of accessory glands (AGs) (Figs 9B–F, 10D, 11B, D; AG not observed in *Siler*).

Description. Medium-sized spiders (total length 6.51–8.00 in males, 7.98–10.00 in females). Body dark with pale yellow patches, covered with dense scales (Figs 3A, B, 4A–L, 5A–D, 6A–D, 7B, D, F). Chelicerae with brown setae on front surface (male also with sparse blue scales), with two promarginal teeth and one retromarginal tooth (Figs 1C, D, 3C, 4B, E, F, H, 5P–U). Femur I of male covered with short and sparse setae (Figs 4B, E, F, 5O). Male

palp (Figs 8A–F, 10A, B, 11E, 12C–E) with short embolus, palpal bulb with tegular bump at lower right corner. Female epigyne large, copulatory ducts short (Figs 9A–G, 10C, D, 11A–D, 12A, B).

Distribution. China (Yunnan), Malaysia (Borneo, Johor, and Sarawak), Singapore (Bukit Timah Nature Reserve), Vietnam (Dak Lak).

***Ogdenia mutilla* (Peckham & Peckham, 1907)**

Figs 1–12

繆恐翠蛛

Rooseveltia mutilla Peckham & Peckham, 1907: 614; Prószyński 1984: 125.

Ogdenia mutilla: Peckham, 1908: 171; Prószyński 2017: 129, fig. 56I.

Type material. Holotype: MALAYSIA • ♀; Borneo, Kuching; 1 Jan. 1897; R. Sheldford & Peckham leg.; MCZ: IZ: 22236, examined.

Other material examined. CHINA – Yunnan Province • 7♂♂ 2♀♀; Xishuangbanna Dai Autonomous Prefecture, Mengla County, Menglun Town, XTBG; 21.9080°N, 101.2845°E, 669 m a.s.l.; 21 Apr. 2023; W. Wang & Z. Yang leg.; MHBU-ARA-00025193, 00025196, 00026514–00026517 • 1♀; same collection data as for preceding; 21.9077°N, 101.2824°E, 677 m a.s.l.; 17 Dec. 2022; W. Wang, B. Liu & Z. Yang leg.; MHBU-ARA-00025194 • 2♀♀; same collection data as for preceding; 21.9108°N, 101.2833°E, 669 m a.s.l.; 2 Aug. 2021; J. Zhang, Y. Mu, K. Yu, L. Zhang & W. Wang leg.; MHBU-ARA-00022704, 00022804 • 1♀; same collection data as for preceding; 21.9092°N, 101.2805°E, 605 m a.s.l.; 12 Jul. 2018; C. Jin & C. Zhang leg.; MHBU-ARA-00020807 • 1♂; Xishuangbanna Dai Autonomous Prefecture, Mengla County, Wangtianshu scenic area; 21.6223°N, 101.5892°E, 700 m a.s.l.; 23 Apr. 2023; L. Wang & Q. Lu leg.; MHBU-ARA-00025195.

MALAYSIA – 1♂; Johor, Gunung Belemut Forest, Lata Tengkorak; 2.0550°N, 103.5430°E, 250 m a.s.l.; 16 Jun. 2019; W.P. Maddison, N.I. Morehouse et al. leg.; UBCZ.

SINGAPORE – 1♀; Bukit Timah Nature Reserve, South Jungle Falls Path; 1.3551°N, 103.7739°E, 150 m a.s.l.; 5 Jun. 2019; W.P. Maddison leg.; UBCZ • 1♀; same collection data as for preceding; 1.3550°N, 103.7740°E–1.3570°N, 103.7750°E, 150–160 m a.s.l.; 12–14 Jun. 2019; W.P. Maddison, N.I. Morehouse et al. leg.; UBCZ.

VIETNAM – Dak Lak Province • 1♂; Buon Don District, Yok Don National Park; 12.8641°N, 107.7961°E, 180 m a.s.l.; 24 Apr. 2022; Q.D. Hoang leg.; TNU • 1♀ Krong Bong District, Chu Yang Sin National Park; 12.4796°N, 108.3391°E, 430 m a.s.l.; 14 May 2022; Q.D. Hoang leg.; TNU.

Diagnosis. See the diagnosis of the genus.

Description. Male. Habitus as shown in Figs 3A–C, 4A–G, L, 5A, B, 6C, D, 7F). Measurements (MHBU-ARA-00025193): carapace 3.27 long, 2.65 wide, abdomen 4.19 long, 2.39 wide; measurements of eyes: AME 0.55, ALE 0.31, PME 0.09, PLE 0.34; measurements of legs: I 10.52 (3.42, 1.30, 2.91, 1.80, 1.09), II 6.92 (2.20, 0.97, 1.67, 1.19, 0.89), III 7.54 (2.18, 0.90, 1.60, 1.72, 1.14), IV 10.07 (3.07, 1.03, 2.36, 2.47, 1.14); leg formula 1432. Body black and pale yellow except for blue carapace edge, covered with dense scales (Figs 3A–C, 4A–G, L, 5A, B, 6C, D, 7F). Chelicerae claybank color, with sparse blue scales (alive) and relatively dense setae on front surface, with two promarginal and one retromar-



Figure 1. *Ogdenia mutilla* (Peckham & Peckham, 1907), female holotype (©2024 W.P. Maddison) **A** habitus, dorsal view **B** prosoma **C**, **D** chelicerae, front (**D**) and back (**C**) views **E**, **F** epigyne, ventral views.



Figure 2. Habitats of *Ogdenia mutilla* (Peckham & Peckham, 1907) in XTBG, Yunnan, China.

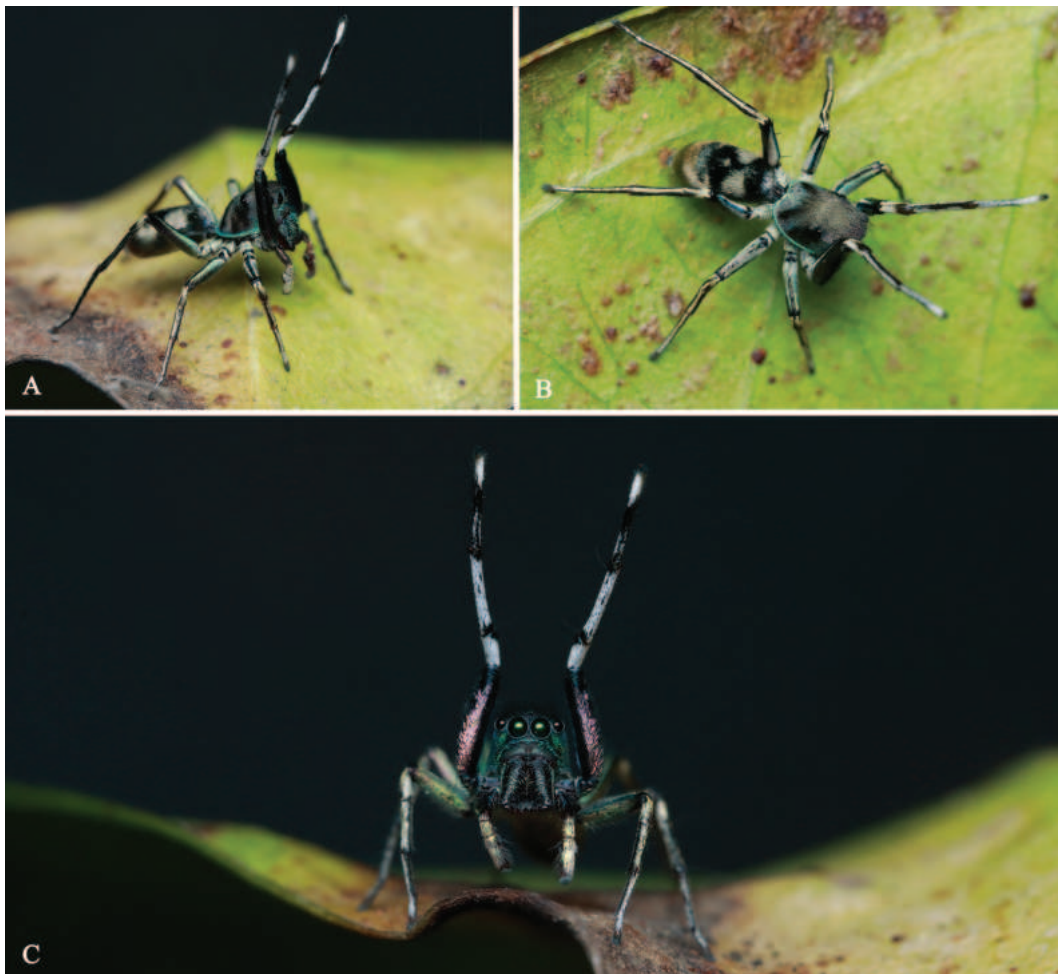


Figure 3. Living males of *Ogdenia mutilla* (Peckham & Peckham, 1907) from China (©2023 Q. Lu).

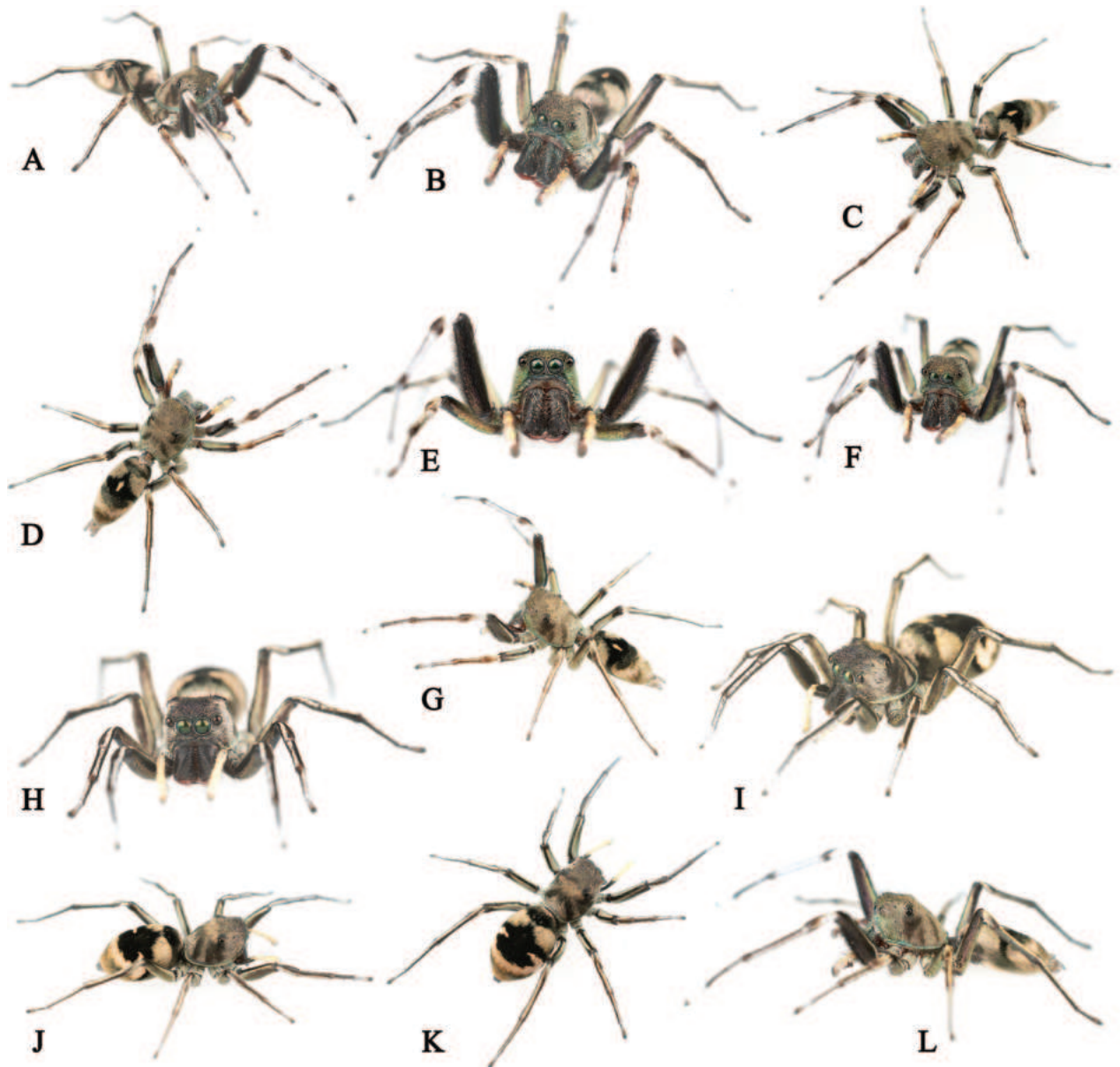


Figure 4. *Ogdenia mutilla* (Peckham & Peckham, 1907) from China **A–G, L** living males **H–K** living females.

ginal tooth (Figs 5M, P–R, 6F, 7E). Femur I covered with short setae (Figs 4B, E, F, 5O). Number of teeth in each tarsal claw varied (Fig. 5E–L).

Palp (Figs 8A–F, 10A, B, 11E, 12C–E): embolus short; cymbium yellow, longer than wide; retrolateral tibia apophysis around one-third of bulb length; palpal bulb like wax apple, with tegular bump at lower right corner.

Female. Habitus as shown in Figs 1A, 4H–K, 5C, D, 6A, B, 7B, D. Measurements (MHBV-ARA-00025194): carapace 3.45 long, 2.81 wide; abdomen 4.70 long, 3.04 wide; measurements of eyes: AME 0.58, ALE 0.35, PME 0.10, PLE 0.30; measurements of legs: I 8.11 (2.54, 0.96, 2.15, 1.47, 0.99), II 6.72 (2.18, 0.84, 1.62, 1.20, 0.88), III 7.71 (2.27, 0.94, 1.67, 1.87, 0.96), IV 10.5 (3.15, 0.91, 2.52, 2.87, 1.05); leg formula 4132. Body form and color pattern same as male, but without short setae on femur I. Chelicerae lacking blue scales, with slightly different shapes of teeth from males (Figs 1C, D, 4H, 5S–U, 6E, 7A, C).



Figure 5. *Ogdenia mutilla* (Peckham & Peckham, 1907), male (A, B, E–M, O–R) and female (C, D, N, S–U) from China A–D habitus, dorsal (A, C) and lateral (B, D) views E–L claws I (G, J), II (H, K), III (I, L), IV (E, F), prolateral (F–I) and retrolateral (E, J–L) views M, N prosomas O left leg I, front view P, Q, T, U chelicerae, front (P, T) and prolateral (Q, U) views R, S teeth of chelicerae, back views.



Figure 6. *Ogdenia mutilla* (Peckham & Peckham, 1907), male (C, D, F) and female (A, B, E) from Vietnam (©2023 Q.D. Hoang) A–D habitus, dorsal (A, C) and lateral (B, D) views E, F prosomas.

Epigyne (Figs 1E, F, 9A–G, 10C, D, 11A–D, 12A, B): copulatory openings elongate like curved butterfly antennae; copulatory ducts short; fertilization ducts at anterior of spermathecae; accessory glands small, located close to the junction between spermathecae and copulatory ducts.

Variation. The transition from the base of the embolus to the tegulum is smoother in some specimens (Figs 8B, 11E), but has an obvious junction in others (Figs 8C, 10A). For the females, differences in the size of accessory glands, the shape of spermathecae, copulatory openings and middle rim of epigyne are observed among different individuals (Figs 1E, F, 9A–E, 10C, D, 11A–D, 12A, B).

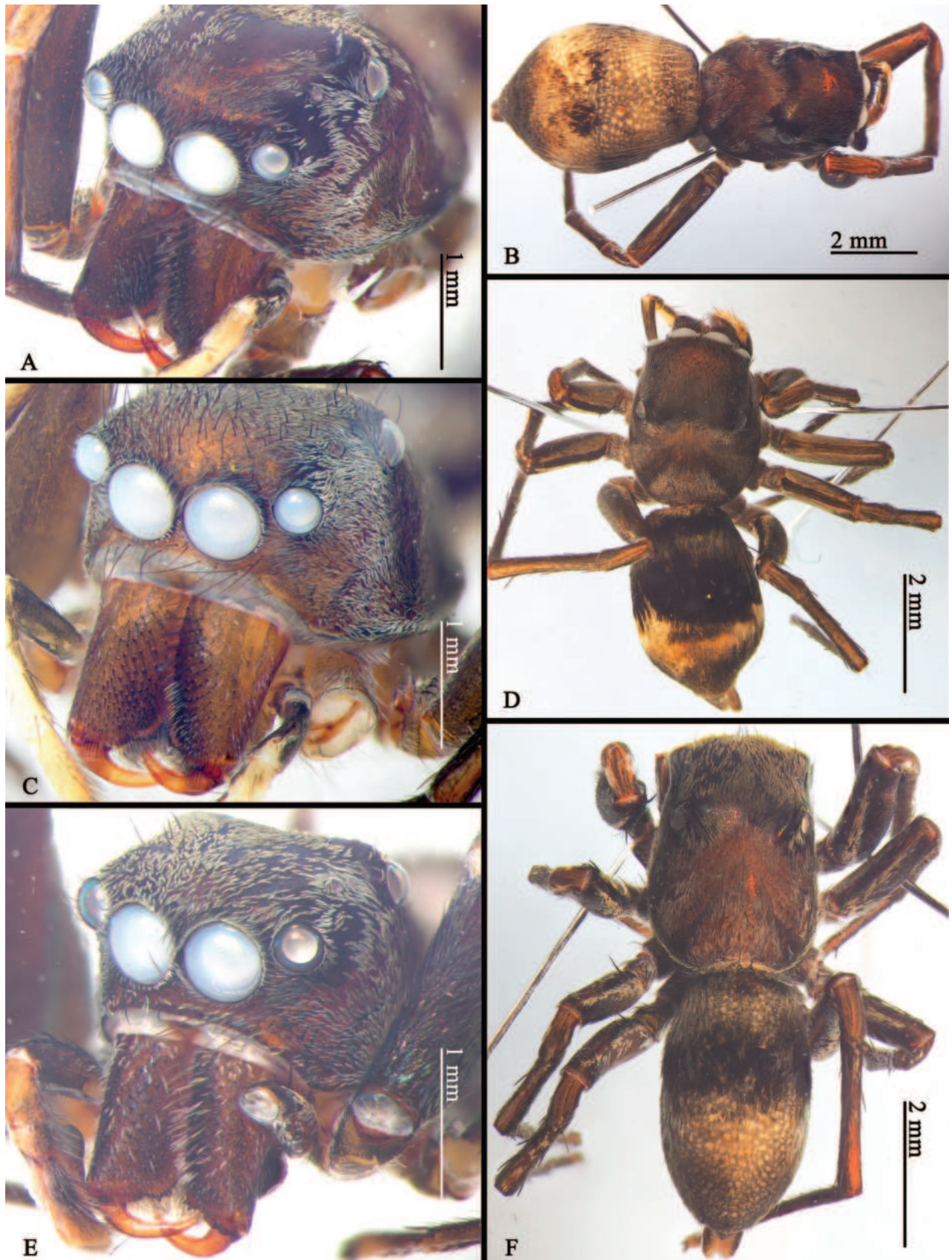


Figure 7. *Ogdenia mutilla* (Peckham & Peckham, 1907), male (E, F) and female (A–D) from Singapore (A–D) and Malaysia (E, F) (©2024 W.P. Maddison) A, C, E prosomas B, D, F habitus, dorsal views.

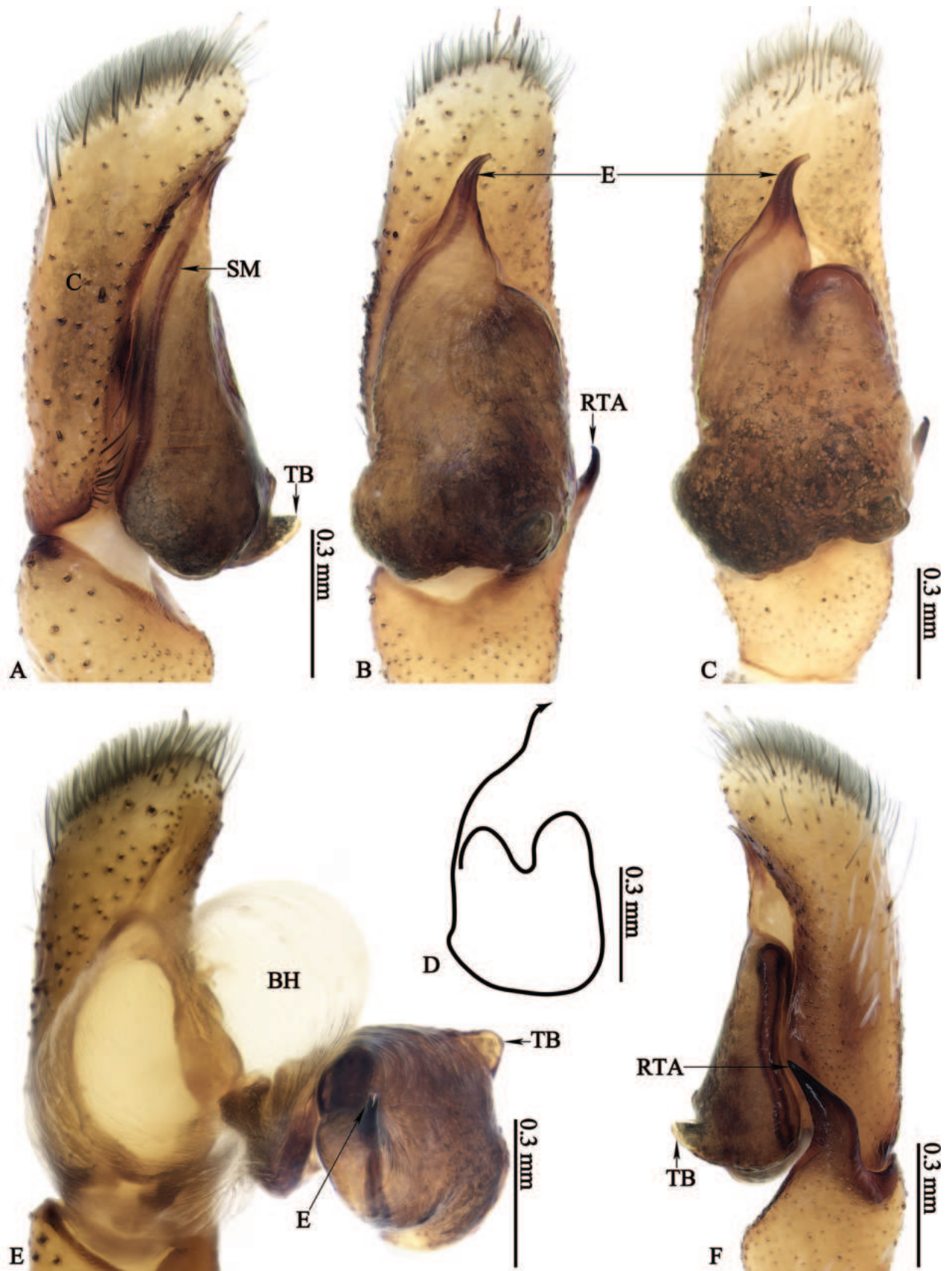


Figure 8. *Ogdenia mutilla* (Peckham & Peckham, 1907) from China A–C, E, F male left palp, prolateral (A), ventral (B, C), pro-ventral (E) and retrolateral (F) views D spermphor, ventral view B, C showing the intraspecific variation of the male palp.

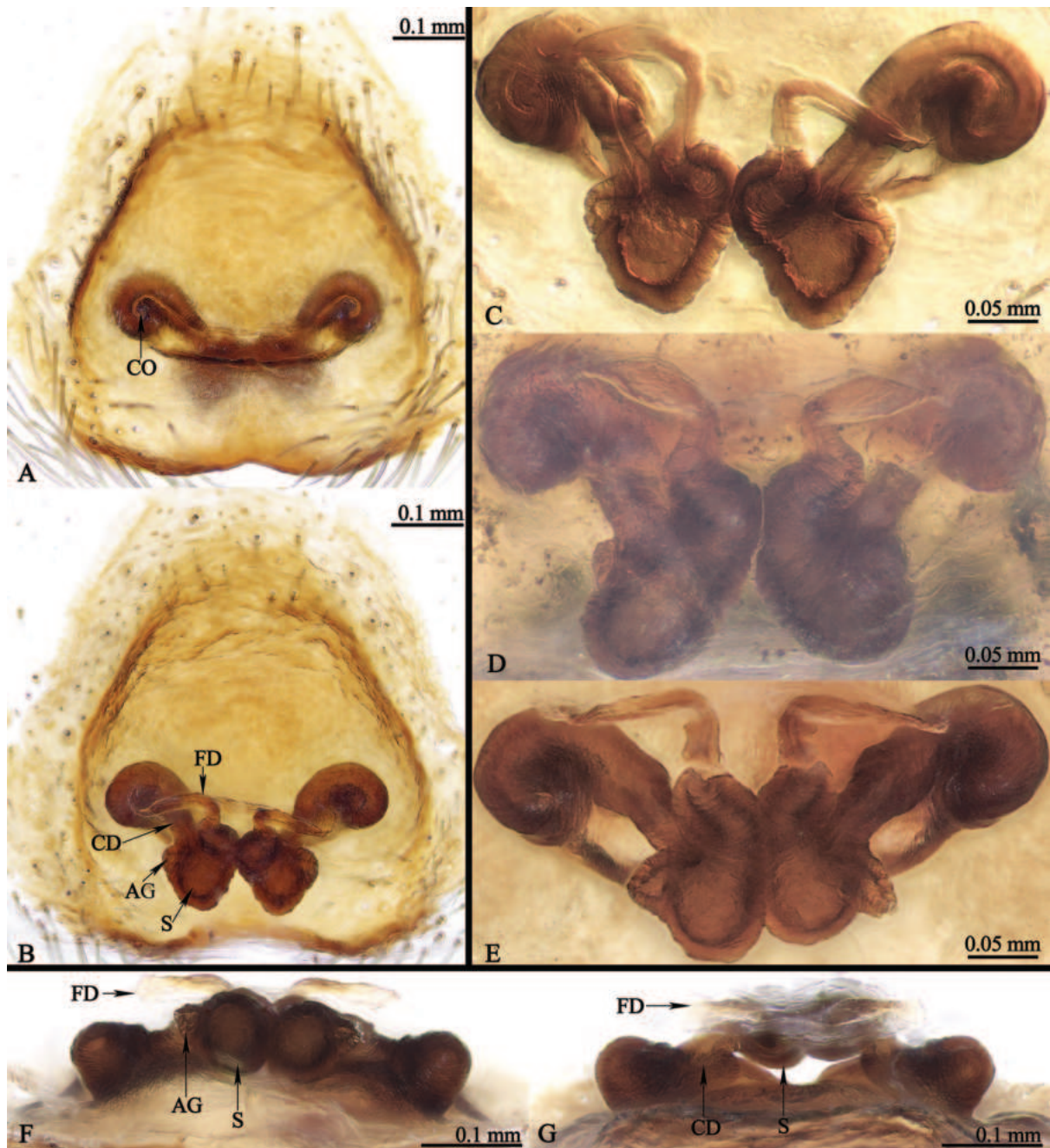


Figure 9. *Ogdenia mutilla* (Peckham & Peckham, 1907) from China. **A** epigyne, ventral view **B–G** vulvae, dorsal (**B–E**), front (**G**) and back (**F**) views **C–E** showing the intraspecific variation of the detailed structures of the vulvae.

Natural history. Specimens were discovered on the surface of leaf litter or in shrubs within tropical forests (Fig. 2A–D), moving actively and quickly. These specimens were collected during relatively dry seasons, and the subsequent lab observations showed that they may not prefer highly humid environments. While the original description of *O. mutilla* suggested that the species mimics *Mutilla* Linnaeus, 1758, a genus of parasitoid wasps (Peckham and Peckham 1907), our field observations indicated that *O. mutilla* possibly mimics large sympatric ants, similar to the imperfect ant-mimicry phenomenon reported in some species of *Siler* (Zeng et al. 2023).

Distribution. China, Malaysia, Singapore, and Vietnam.

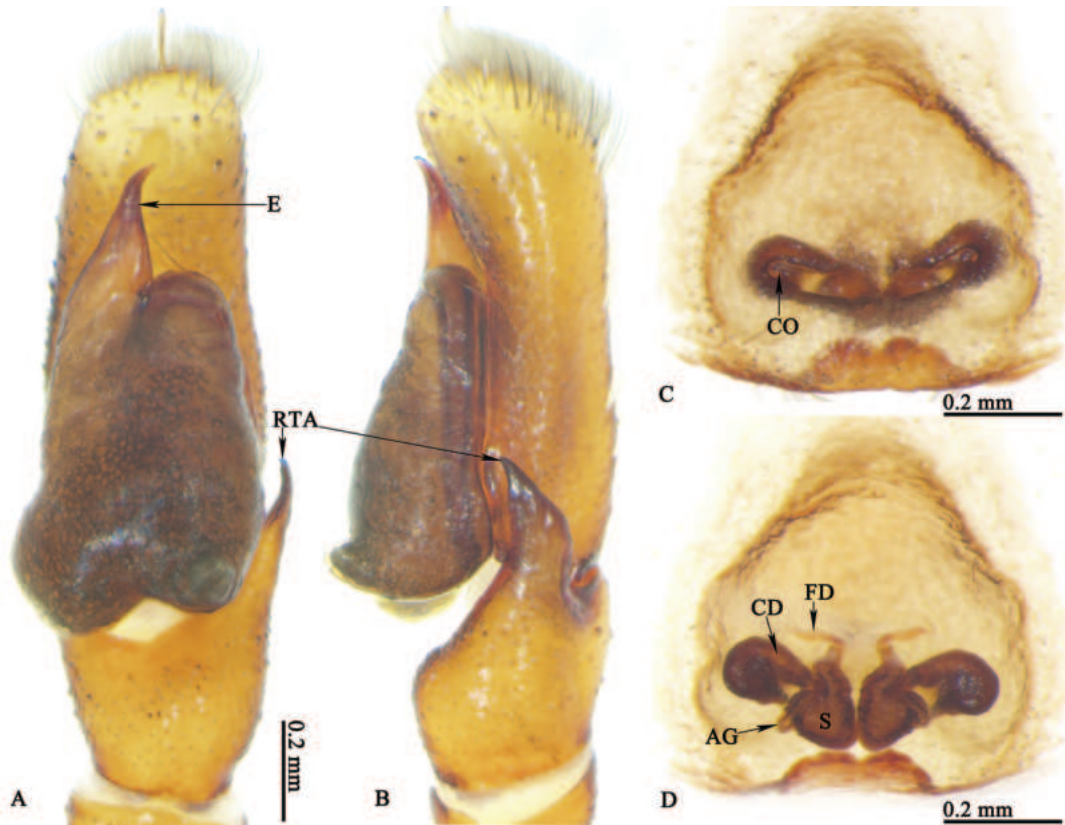


Figure 10. *Ogdenia mutilla* (Peckham & Peckham, 1907) from Vietnam (©2023 Q.D. Hoang) **A, B** male left palp, ventral (**A**) and retrolateral (**B**) views **C** epigyne, ventral view **D** vulva, dorsal view.

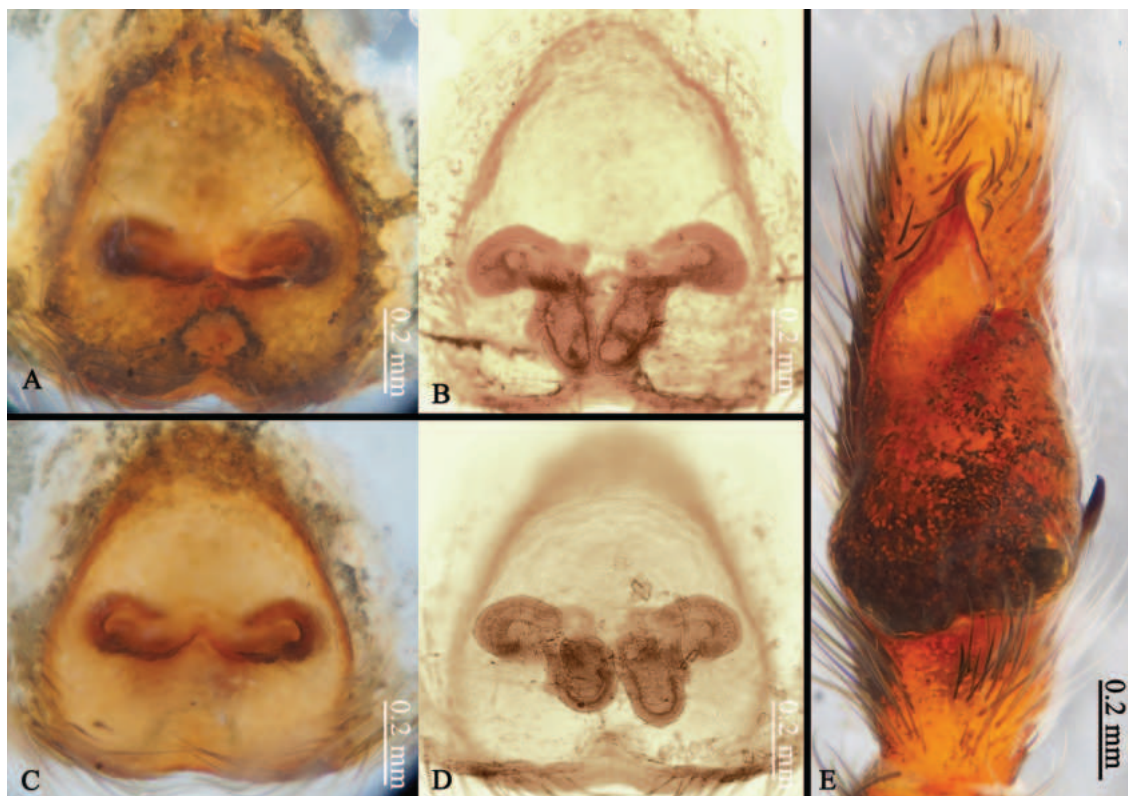


Figure 11. *Ogdenia mutilla* (Peckham & Peckham, 1907) from Singapore (**A–D**) and Malaysia (**E**) (©2024 W.P. Maddison) **A, C** epigynes, ventral views **B, D** vulvae, dorsal views **E** male left palp, ventral view.

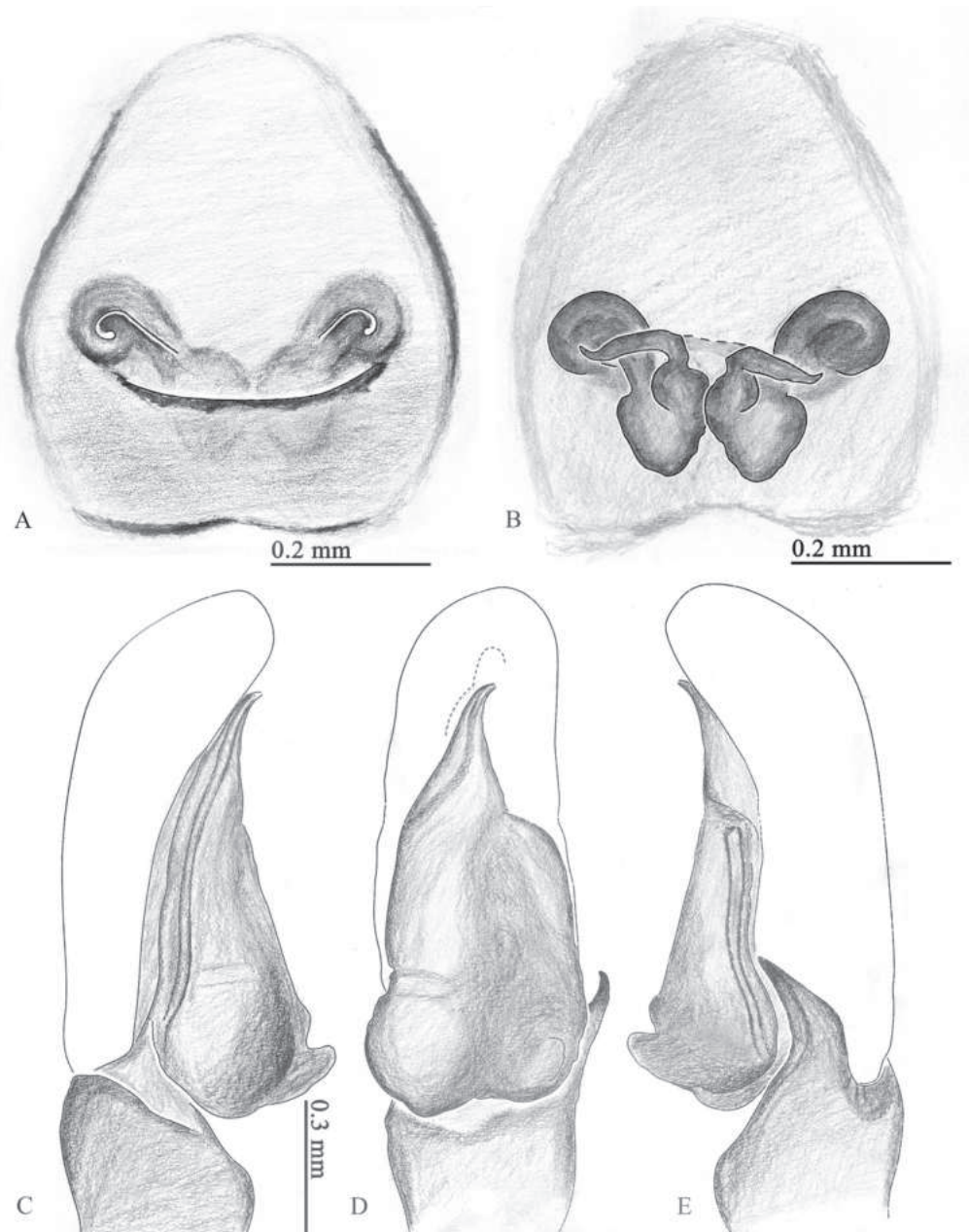


Figure 12. *Ogdenia mutila* (Peckham & Peckham, 1907) from China **A** epigyne, ventral view **B** vulva, dorsal view **C–E** male left palp, prolateral (**C**), ventral (**D**) and retrolateral (**E**) views.

Acknowledgements

We thank Dr Gonazalo Giribet, Laura Leibensperger, Shahan Derkarabetian and Adam Baldinger for assistance with the loan of the type specimen of *O. mutila*; Bo Liu, Kun Yu, Yannan Mu, Lu Zhang, Chi Jin, Nathan I. Morehouse, Chen Zhang, Luyu Wang, and Qianle Lu for collecting the specimens for this study. Also, we would like to extend our gratitude to Qianle Lu for providing some of the living spider photographs of the species, and to Kiran Marathe for assistance with photographs of specimens from Singapore and Malaysia. Thank the two reviewers, Dr John T.D. Caleb and Cheng Wang, the subject editor, Dr Shuqiang Li, and the copy editors, Dr Robert Forsyth and Polina Petrakieva for their valuable comments that helped to improve the manuscript.

Additional information

Conflict of interest

The authors have declared that no competing interests exist.

Ethical statement

No ethical statement was reported.

Funding

This work was funded by the National Natural Science Foundation of China to Junxia Zhang (no. 32070422), a grant (code B2024-TTN-05) from the Ministry of Education and Training, Vietnam to Quang Duy Hoang, and the Natural Sciences and Engineering Research Council Canada to Wayne P. Maddison (Discovery Grant RGPIN 2018-05055).

Author contributions

All authors have contributed equally.

Author ORCIDs

Zhiyong Yang  <https://orcid.org/0000-0002-7610-6843>

Quang Duy Hoang  <https://orcid.org/0000-0003-1672-7960>

Weihang Wang  <https://orcid.org/0000-0003-2460-4514>

Wayne P. Maddison  <https://orcid.org/0000-0003-4953-4575>

Junxia Zhang  <https://orcid.org/0000-0003-2179-3954>

Data availability

All of the data that support the findings of this study are available in the main text.

References

- Joseph KHK, David JC, Chris SPA, Paul YCN (2022) A photographic guide to Singapore spiders. Singapore Botanic Gardens, Singapore, 774 pp.
- Linnaeus C (1758) *Systema naturae per regna tria naturae, secundum classes, ordines, genera, species, cum characteribus, differentiis, synonymis, locis*. Tomus I. Editio Decima Reformata. Laurentii Salvii, Holmiae, Stockholm, 823 pp. <https://doi.org/10.5962/bhl.title.542>
- Peckham GW (1908) The generic name *Rooseveltia*. *Bulletin of the Wisconsin Natural History Society* 6: 171.
- Peckham GW, Peckham EG (1907) The Attidae of Borneo. *Transactions of the Wisconsin Academy of Sciences, Arts, and Letters* 15(2): 603–653.
- Prószyński J (1984) Atlas rysunków diagnostycznych mniej znanych Salticidae (Araneae). *Zeszyty Naukowe Wyższej Szkoły Rolniczo-Pedagogicznej w Siedlcach* 2: 1–177.
- Prószyński J (2017) Pragmatic classification of the world's Salticidae (Araneae). *Ecologica Montenegrina* 12: 1–133. <https://doi.org/10.37828/em.2017.12.1>
- Zeng H, Zhao D, Zhang Z, Gao H, Zhang W (2023) Imperfect ant mimicry contributes to local adaptation in a jumping spider. *iScience* 26(6): 106747. <https://doi.org/10.1016/j.isci.2023.106747>

The *Leptogenys* Roger, 1861 (Formicidae, Ponerinae) of Hong Kong SAR with additional records from Guangdong, China

Matthew T. Hamer¹, Jonathan Hon Chung Lee¹, Cheung Yau Leo Tse¹, Thiago S. R. Silva¹, Benoit Guénard^{1,2}

¹ School of Biological Sciences, The University of Hong Kong, Kadoorie Biological Sciences Building, Pok Fu Lam Road, Hong Kong SAR, China

² The Hong Kong Biodiversity Museum, The University of Hong Kong, Hong Kong SAR, China

Corresponding author: Matthew T. Hamer (matt.hamer@hotmail.co.uk)

Abstract

Leptogenys is the most diverse genus of the ant subfamily Ponerinae and is widely distributed across the world's tropical and subtropical regions. More than 40 species are known from the Oriental realm displaying a wide range of ecologies, although their life history traits remain poorly understood, and new species are frequently discovered. Here, a faunal review of the genus from Hong Kong SAR, southern China is provided. A total of nine species are recorded, with one new species, *Leptogenys grohli* Hamer, Lee & Guénard, **sp. nov.** described. Ecological and biogeographic information, including new information on reproductive modes for two species are provided with the ergatoids of *L. binghamii* Forel, 1900 and *L. rufida* Zhou et al., 2012 described. Additional records for five of these species within the neighbouring province of Guangdong are also provided. Finally, an illustrated key to species known from Hong Kong is presented, as well as notes on each species' distribution, ecology, and behaviour. An updated provincial distributional checklist of the *Leptogenys* species of Mainland China and Taiwan is also supplied.

Key words: Ants, Foo Fighters, Hymenoptera, taxonomy

Introduction

The ant genus *Leptogenys* is currently recognised as the most diverse genus within Ponerinae, comprising 318 species and 14 subspecies (Bolton 2023). The genus is pantropically distributed, with its greatest diversity encountered within tropical regions, and a limited number of species extending to higher latitudes into warm temperature regions (Janicki et al. 2016; Guénard et al. 2017). Based on a molecular phylogenetic study (Schmidt 2013), the genus is hypothesised to have an Old World origin and to confirm this, a broader understanding of its taxonomic and ecological diversity is paramount. *Leptogenys* species are highly predatory, with epigeaic and leaf-litter foragers that predominantly hunt upon isopods, diplopods, earthworms, termites, earwigs, and other leaf litter invertebrates (Maschwitz et al. 1979; Steghaus-Kovac and Maschwitz 1993, Dejean and Evraerts 1997; Schmidt and Shattuck 2014; Peeters and De Greef 2015; Mizuno et al. 2022). Predatory behaviours range from solitarily foraging, to mass raiding reminiscent of doryline army ants, with a continuum of foraging and recruitment modes between both



Academic editor: Brendon Boudinot

Received: 4 February 2024

Accepted: 10 April 2024

Published: 17 May 2024

ZooBank: <https://zoobank.org/CBF2BDAA-5111-4F23-B0DC-FD172CDD17D7>

Citation: Hamer MT, Lee JHC, Tse CYL, Silva TSR, Guénard B (2024) The *Leptogenys* Roger, 1861 (Formicidae, Ponerinae) of Hong Kong SAR with additional records from Guangdong, China. ZooKeys 1202: 169–211. <https://doi.org/10.3897/zookeys.1202.120214>

Copyright: © Matthew T. Hamer et al.
This is an open access article distributed under terms of the Creative Commons Attribution License (Attribution 4.0 International – CC BY 4.0).

extremes (Maschwitz et al. 1989; Duncan and Crewe 1994; Janssen et al. 1997; Schmidt and Shattuck 2014; Mizuno et al. 2022). Nests are often ephemeral and typically found within soil, dead wood, or leaf litter, with the whole colony moving to new nest sites frequently (Maschwitz and Mühlenberg 1975; Schmidt and Shattuck 2014), with species of the *procellanalis* group even forming temporary bivouacs (Maschwitz et al. 1989). Colonies are often queenless, with reproductive functions performed by ergatoid individuals, and with some species reproducing via a gamergate system (Peeters 1991; Ito 1997; Schmidt and Shattuck 2014). The high species diversity, wide variety of life histories, including varying forms of predation, foraging and reproduction, make *Leptogenys* an ideal taxon for the study of evolution, and behavioural ecology (Dejean and Evraerts 1997).

Leptogenys has seen several regional taxonomic treatments in the last few decades, particularly from Asia where Xu and He (2015) provided a revision of the Oriental species and a preliminary regional key. Subsequent work has been produced by Zryanin (2016), Arimoto (2017), Wachkoo et al. (2018), Arimoto and Yamane (2018) for select Oriental species and for species such as the *L. chalybaea* and *L. modiglianii* species groups. Numerous species across the Oriental realm, however, remain undescribed (Arimoto 2017; AntWeb 2024), and many regions remain woefully under-sampled and/or lacking contemporary taxonomic revisions. In China specifically, most of the taxonomic studies for the genus are geographically restricted to a few provinces (e.g., Zhou 2001 and Zhou et al. 2012 for Guangxi, Xu 2000 for Yunnan, and Chen et al. 2024 for Hainan) with the vast majority of regions and provinces of China still lacking local taxonomic revisions for this genus.

Here we review the *Leptogenys* of Hong Kong SAR, one of the most densely populated regions of 6,700 people per square kilometre. Hong Kong, though highly urbanised, comprises surprisingly high biodiversity, including many newly recorded and newly described ant species following intensive sampling from early 90s to the present day (Fellowes 1996; Luo and Guénard 2016; Pierce et al. 2019; Tang et al. 2019; Brassard et al. 2020; Wong and Guénard 2021; Hamer et al. 2023a, Hamer et al. 2023b; Silva et al. 2023; Tang and Guénard 2023). Here, a total of nine *Leptogenys* species are recorded from Hong Kong including four newly recorded species, and one new species to science, *Leptogenys grohli* sp. nov. Along with the taxonomic accounts, we provide high resolution images, an illustrated dichotomous identification key, and discussions on the morphology as well as the ecology for all species known from Hong Kong. Ergatoid queens of *L. binghamii* and *L. rufida* are also described. Records for five of the overall nine species occurring in Hong Kong are provided for the neighbouring Chinese province Guangdong.

Materials and methods

Sampling

Most sample collections were performed using leaf litter sampling through Winkler extractors by Dr. John Fellowes between 1993–2002 and members of the Insect Biodiversity and Biogeography Laboratory (IBBL, HKU) between 2014–2023 in Hong Kong. Other sampling methods were conducted during the same periods, including pitfall trapping, baiting and hand collection comprising of nesting locations and general forager collections.

Measurements and images

Here we use the core set of linear measurements and indexes broadly used in ant taxonomic studies, as well as specialised measurements suggested by Arimoto and Yamane (2018) (Fig. 1). The lengths of the pedicel (**AII**) and the first two flagellar segments (**AFI–AFII**) are also included here. Measurements for all specimens as well as specimen images were gathered using a DMC5400 Camera attached to a Leica M205C Stereomicroscope and processed in Leica Application Suite (LASX). Based on scaled micrometre calibration, measurements are accurate to 0.01 mm. Image artefacts were removed in Adobe Photoshop with plates produced in Adobe InDesign. Illustrations were made using high-resolution images as base for tracing in Adobe Illustrator.

Linear measurements and indices abbreviations

HL	Head length: the length of head from the anteriormost point of the clypeal lobe to the posteriormost point of the head capsule, measured in full face view.
HLL	Lateral head margin length: length of head from mandibular base to posteriormost margin of head capsule, measured in full face view.
HLA	Anterior head length: length of head from mandibular base to anteriormost point of eye, measured in full face view.
CML	Clypeal median lobe length: length of the clypeal lobe from anteriormost margin to the anterior margin of the torulus, measured in full face view.
HW	Head width: maximum width of head, excluding eyes, measured in full face view.
SL	Scape length: diagonal length of scape excluding the neck and basal condyle.
AII	Antennal segment II length: maximum length of pedicel (antennal segment II), measured in dorsal view.
AFI	Antennal flagellomere I length: maximum length first flagellar segment, measured in dorsal view.
AFII	Antennal flagellomere II length: maximum length of second flagellar segment, measured in dorsal view.
EL	Eye length: the maximum diameter of the compound eye in lateral view.
ML	Mandibular length: length of mandible from base to apex, measured in full face view.
PrL	Pronotal length: diagonal length of pronotum measured from anteriormost point of pronotum (excluding neck), to posteriormost margin, measured in lateral view.
PrH	Pronotal height: height of pronotum from the posterior base of the pronotum to the highest point of pronotum dorsum, measured in lateral view.
PrW	Pronotal width: maximum width of pronotum, measured in dorsal view.
WL	Weber's length: diagonal length of mesosoma from anteriormost point of pronotum (excluding neck) to posteriormost point of propodeal lobe, measured in lateral view.

- PeL** Petiole length: length of petiole from the anteriormost point of the petiole (including petiole peduncle) to the posteriormost point, measured in lateral view.
- PeH** Petiole height: height of petiole from the most ventral margin of the subpetiolar process to the highest point of petiolar dorsal margin, measured in lateral view.
- PeW** Petiole width: maximum width of petiole in dorsal view.
- DpeL** Dorsal petiole length: length of petiole in dorsal view, from anteriormost point of the petiole (including peduncle) to the posteriormost point, measured in dorsal view.
- CI** Cephalic index: $HW / HL \times 100$
- CLI** Clypeus index: $CML / HL \times 100$
- SI** Scape index: $SL / HW \times 100$
- OI** Ocular index: $EL / HLL \times 100$
- LPI** Lateral petiole index: $PeH / PeL \times 100$
- DPI** Dorsal petiole index: $PeW / DpeL \times 100$

Depository institution abbreviations

- HKBM** Hong Kong Biodiversity Museum, University of Hong Kong.
- IBBL** Insect Biodiversity and Biogeography Laboratory, The University of Hong Kong.
- SKYC** Seiki Yamane Collection, Kitakyushu Museum of Natural History and Human History, Kitakyushu, Fukuoka, Japan
- ZRC** Zoological Reference Collection, Lee Kong Chian Natural History Museum, Singapore.

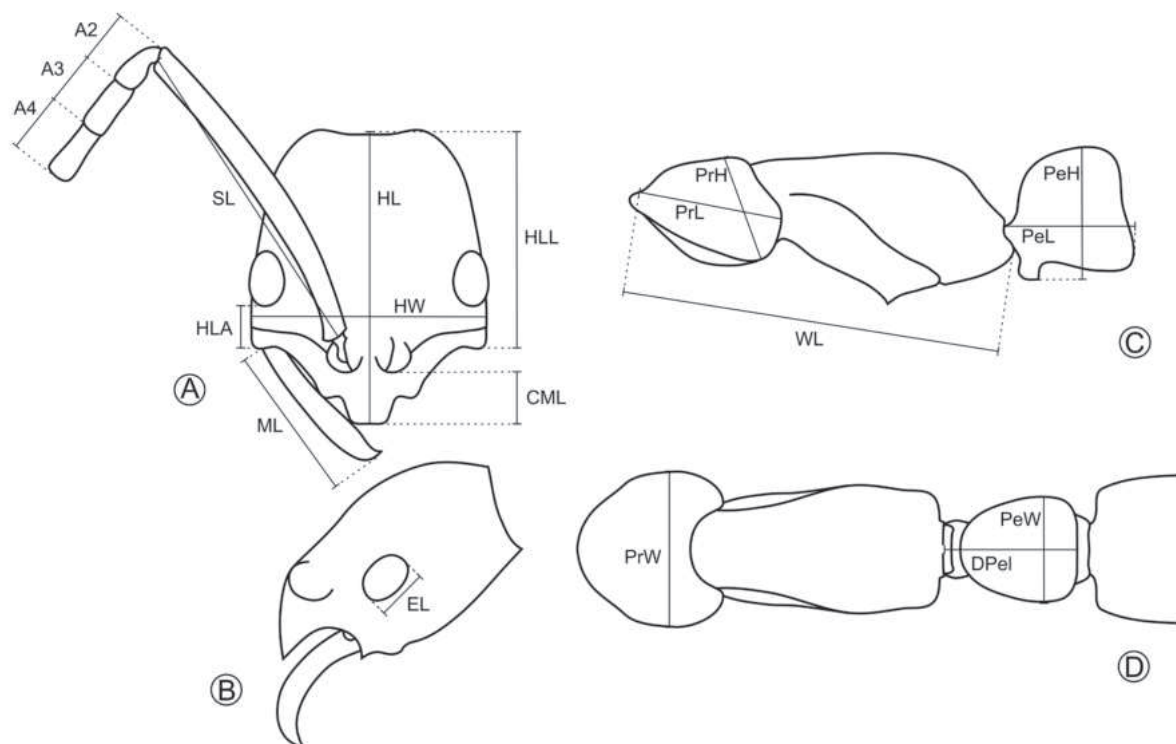


Figure 1. Schematic diagram of the linear measurements used within this study **A** head measurements **B** eye diameter **C** lateral mesosomal and petiole measurements **D** dorsal mesosomal and petiole measurements.

Results

Key to *Leptogenys* workers of Hong Kong SAR

- 1 Anterior clypeal margin terminating in a narrowly convex point (Fig. 2A)...**2**
- Anterior clypeal margin terminating in a distinct truncation (Fig. 2B).....**4**

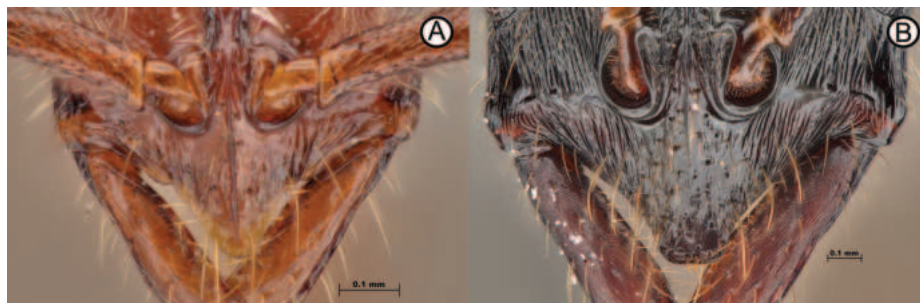


Figure 2. Differing anterior clypeal shapes **A** *Leptogenys rufida* (RHL1259) **B** *L. kraepelini* (ANTWEB1010120).

- 2 Pedicel as long as flagellomere I (All 0.17–0.19; AFI 0.13–0.15) (Fig. 3A); in lateral view, petiole subquadrate, as long as high (LPI 82.61–114.29) (Fig. 3C).....**Leptogenys rufida**
- Flagellomere I considerably longer than pedicel (All 0.17–0.24; AFI 0.31–0.39) (Fig. 3B); in lateral view, petiolar node triangular, either longer than high or as long as high (LPI 74.93–97.24) (Fig. 3D)**3**

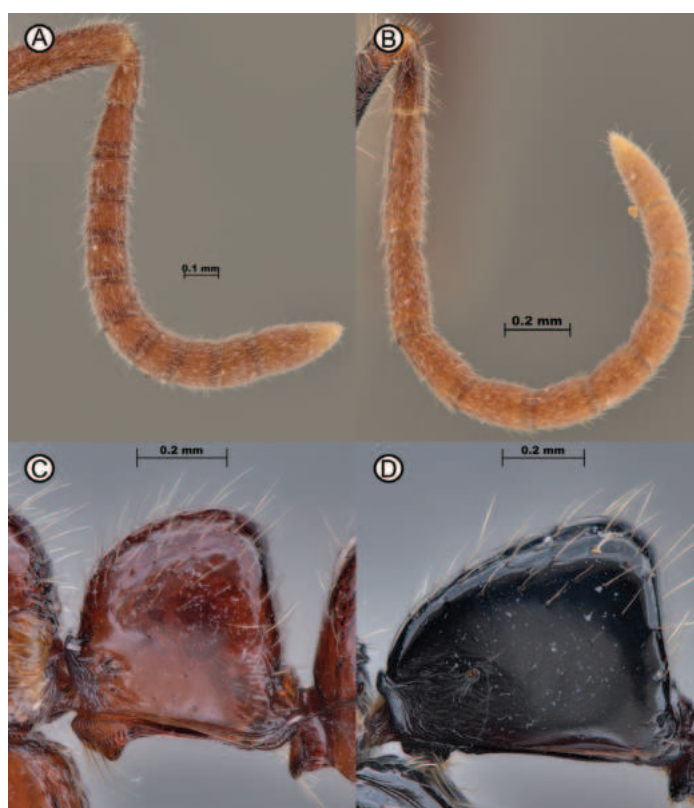


Figure 3. Differences between antennal segment lengths and petiolar shapes **A** *Leptogenys rufida* (MBS006585) **B** *L. peuqueti* (ANTWEB10096169) **C** *Leptogenys rufida* (MBS015251) **D** *L. peuqueti* (RHL003347).

- 3 In full-face view, head lateral margin convex; head dorsum predominantly smooth, with very sparse punctation; eye larger (EL 0.29–0.37).....
..... ***Leptogenys peuqueti***
- In full-face view, head lateral margin straight to weakly tapering posteriorly; head dorsum densely punctate; eye smaller (EL 0.22–0.27).....
..... ***Leptogenys grohli* sp. nov.**
- 4 Masticatory margin of mandible with 3–5 teeth (Fig. 4A); head dorsum smooth, with sparse hair bearing punctures only ***Leptogenys strena***
- Masticatory margin of mandible edentate, or with a single tooth (Fig. 4B); head dorsum sculpture varying, not as above..... **5**



Figure 4. Mandibular masticatory margin differences **A** *Leptogenys strena* (ANTWEB1010114) **B** *L. diminuta* (GYOT070).

- 5 Lateral clypeal margin with conspicuous angulate lobes (Fig. 5A); first and second gastral tergites densely sculptured throughout (Fig. 5C).....
..... ***Leptogenys binghamii***
- Lateral clypeal margin lacking conspicuous angulate lobes (Fig. 5B); first and second gastral tergites smooth and shiny (Fig. 5D)..... **6**



Figure 5. Clypeus lobes of *Leptogenys binghamii* and *L. diminuta*, as well as tergite sculpture differences between the same species **A** *L. binghamii* (RHL01659) **B** *L. diminuta* (GYOT070) **C** *L. binghamii* (ANTWEB1010113) **D** *L. diminuta* (ANTWEB1010183).

- 6 Petiole almost as long as high in lateral view (LPI 89.2–99.35); dorsal margin with a distinct anterior to posterior curvature (Fig. 6A)..... ***Leptogenys kraepelini***
 – Petiole as high as long or higher than long in lateral view (LPI 107.12–158.96); dorsal margin flat, lacking conspicuous anterior to posterior curvature (Fig. 6B) **7**

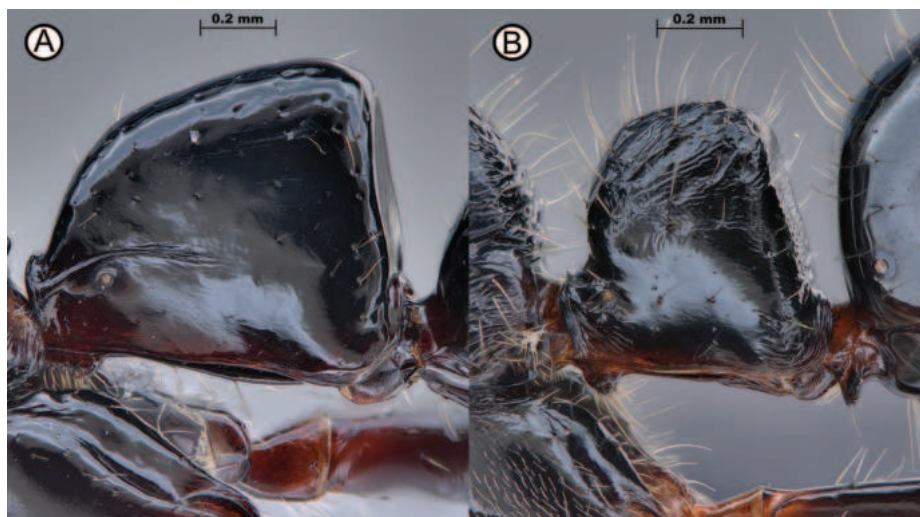


Figure 6. Contrasting petiole shapes between *L. kraepelini* and *L. diminuta* **A** *L. kraepelini* (ANTWEB1010121) **B** *L. diminuta* (ANTWEB1010183).

- 7 Head dorsum smooth, other than hair bearing punctation; clypeus with a conspicuous median longitudinal carina (Fig. 7A); pronotum entirely smooth..... ***Leptogenys laeviterga***
 – Head dorsum with longitudinal costulae; clypeus either entirely lacking median carina or with a weakly produced, inconspicuous carina (Fig. 7B); pronotum variably sculptured..... **8**

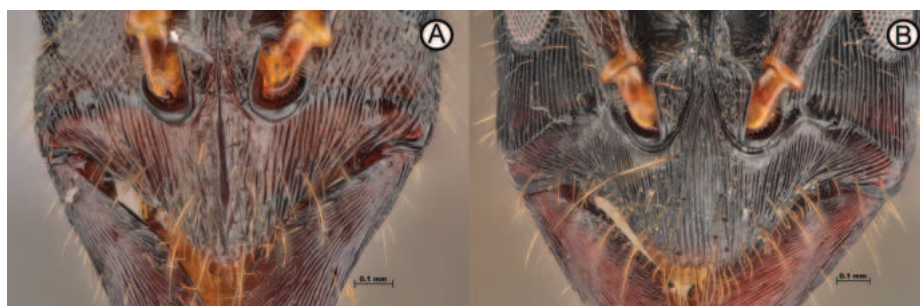


Figure 7. Clypeus differences between *Leptogenys laeviterga* and *L. kitteli* **A** *L. laeviterga* (ANTWEB1010142) **B** *L. kitteli* (RHL02795).

- 8 Sides of pronotum smooth, finely rugulose or finely reticulate (Fig. 8A); masticatory margin with a single tooth; generally a smaller species (WL 2.33–2.53) ***Leptogenys diminuta***
 – Sides of pronotum longitudinally striate (Fig. 8B); masticatory margin without teeth; generally a larger species (WL 2.64–2.87) ***Leptogenys kitteli***



Figure 8. Diverging mesosomal sculpture between *L. diminuta* and *L. kitteli* **A** *L. diminuta* (ANTWEB1010183) **B** *L. kitteli* (PFL1T2W5-1).

Taxonomic accounts

Leptogenys binghamii Forel, 1900

Figs 5A, C, 9, 20A

Leptogenys (*Lobopelta*) *binghamii* Forel, 1900f: 310 (w.) Myanmar.

Lobopelta binghamii: Bingham 1903: 58.

Leptogenys (*Lobopelta*) *binghamii*: Emery 1911e: 102.

Ergatoid description. With characters of worker but head as wide anteriorly as posteriorly; pronotum wider than remaining mesosoma in dorsal view; mesosoma stout and robust, less elongated as worker; petiole nodiform, distinctly higher than long in lateral view; about as wide as long in dorsal view. Metasomal segments III–VII enlarged, segment III distinctly wider than petiole. Same colour as the worker.

Measurements. Worker ($n = 14$): HL 1.66–1.84; HLL 1.31–1.47; HLA 0.24–0.3; HW 1.18–1.33; CML 0.31–0.39; SL 1.94–2.13; All 0.21–0.33; AFI 0.43–0.51; AFII 0.37–0.41; EL 0.31–0.36; ML 0.84–1.03; PrL 1.04–1.25; PrH 0.77–1.13; PrW 1.04–1.2; WL 2.76–3.1; PeL 0.8–1.04; PeH 0.95–1.18; PeW 0.77–0.92; DPL 0.87–0.95; CI 69.36–74.97; CLI 17.58–22.49; SI 156.26–166.48; OI 21.98–26.37; LPI 104.64–124.38; DPI 84.67–98.51.

Ergatoid paratype ($n = 1$): HL 1.67; HLL 1.29; HLA 0.31; HW 1.25; CML 0.39; SL 1.77; All 0.23; AFI 0.39; AFII 0.31; EL 0.34; ML 0.96; PrL 1.03; PrH 0.76; PrW 1.04; WL 2.56; PeL 0.75; PeH 1.06; PeW 0.62; DPL 0.83; CI 74.7; CLI 23.33; SI 141.31; OI 26.49; LPI 142.49; DPI 73.98.

Morphological variation. Little to no variation, other than morphometric values, were detected in the specimens examined from Hong Kong.

Comparative notes. *Leptogenys binghamii* is a relatively large, highly sculptured species, with distinctly linear mandibles, small anteriorly positioned eyes and highly angulated lateral clypeal lobes which makes it recognisable within the *Leptogenys* found in Hong Kong. Within the wider *Leptogenys* fauna of the Indomalayan region, *L. binghamii* might be mistaken for *L. punctiventris* (Mayr, 1879) and *L. yandii* (Xu & He, 2015). *Leptogenys binghamii* is distinguishable from *L. yandii* by antennal flagellomere I longer than antennal flagellomere II, the longer scape, and larger overall size (5.2–5.7 vs 9–10 mm total length for *L. yandii* and *L. binghamii*, respectively; Xu and He 2015). *Leptogenys binghamii* can be differentiated from *L. punctiventris* by the smaller eyes, the first gastral



Figure 9. *Leptogenys binghamii* (ANTWEB1010110) and ergatoid (ANTWEB1010225) **A** worker in lateral view **B** worker in dorsal view **C** worker in head in full face view **D** ergatoid in lateral view **E** ergatoid in lateral view and **F** ergatoid in dorsal view.

tergite being highly punctate, lacking any smooth and shiny regions as well as total size (5–6 vs 9–10 mm total size for *L. punctiventris* and *L. binghamii*, respectively; Xu and He 2015). Both *L. punctiventris* and *L. yandii* are not recorded from Hong Kong. With these species presenting more meridional and occidental distributions within Asia, respectively.

Distribution. This species is known from Myanmar (type locality), India (Assam and Meghalaya), China (Guangxi, Yunnan, and Hong Kong), and Vietnam (Janicki et al. 2016; Guénard et al. 2017). There are no records from Guangdong, Hainan, or Macao, but its presence is expected in the first two Chinese provinces with more sampling efforts. Its presence in Macao is less likely due to the level of urbanisation and isolation of natural areas for this species to oc-

cur. The first record of *L. binghamii* in Hong Kong was Fellowes (1996), here we provide additional new records across the eastern limits of its range.

Ecology. In Hong Kong, colonies have been found within decaying wood and underneath stones, predominantly within Feng Shui Woods, secondary forests and shrubland. Colonies appear relatively small, with one partial colony collection including 23 workers, 1 male, 5 cocoons, 4 larvae, and 2 eggs (MTH collection code MTH163). One ergatoid queen was extracted from a partial colony collection (MTH268). Specimens are known from pitfall traps, leaf litter, and hand collection events. This species is suspected to be a solitary foraging species, with no group hunting yet observed. However, unless nesting sites are located, *L. binghamii* is rarely observed diurnally and is therefore suspected to be predominately a nocturnal foraging species. A second colony, kept in captive colony consisted of 24 workers and one ergatoid queen. Workers fed upon isopod prey and showed no interest in cockroaches, millipedes, and termites. In Hong Kong, the species reaches the northern limit of its distribution range with all records found under 500 m a.s.l.. Further sampling is nonetheless required to confirm if the species can colonize higher and cooler elevations.

Material examined. Worker ($n = 52$): CHINA • 1 worker; Hong Kong SAR, Ng Fai Tong, East Central New Territories; 23 Aug. 1996; J.R.Fellowes leg.; HKBM MBS015249. • 3 workers; Hong Kong SAR, Pak Ngau Shek; 24 Oct. 1996; J.R.Fellowes leg.; HKBM MBS006888, MBS015265, MBS06604. • 1 worker; Hong Kong SAR, Yau Ping San UK, East Central NT; 3 Oct. 1996; J.R.Fellowes leg.; HKBM MBS015263. • 2 workers; Hong Kong SAR, Kadoorie Farm Botanical Garden; 22.4302, 114.1192; 280 m a.s.l.; 14 Sep. 2015; R.H.Lee leg.; Secondary forest, Pitfall trap; IBBL RHL02700 RHL02717. • 1 worker; Hong Kong SAR, Lion Rock; 22.35805, 114.17699; 150 m a.s.l.; 13 Jul. 2015; R.H.Lee leg.; Secondary forest, Pitfall trap; IBBL RHL01659. • 1 worker; Hong Kong SAR, Pak Tam Chung; 22.401, 114.33; 130 m a.s.l.; 5 Jun. 2015; R.H.Lee leg.; Shrubland, Pitfall trap; IBBL RHL02373. • 1 worker; Hong Kong SAR, Shing Mun; 22.39678, 114.1531; 240 m a.s.l.; 14 May. 2015; R.H.Lee leg.; Feng Shui Forest, Pitfall trap; IBBL RHL000350. • 1 worker; Hong Kong SAR, Pok Fu Lam; 22.267, 114.1438; 248 m a.s.l.; 7 Jul. 2016; M.Pierce leg.; Secondary forest, Bait trap; IBBL ANTWEB1009150. • 1 worker; Hong Kong SAR, Lion Rock; 22.357, 114.17504; 140 m a.s.l.; 15 Aug. 2017; R.H.Lee leg.; Secondary forest, Pitfall trap; IBBL RHL03531A. • 1 worker; Hong Kong SAR, Tai Po Kau; 22.42285, 114.18082; 200 m a.s.l.; 6 Jun. 2017; R.H.Lee leg.; Secondary forest, Pitfall trap; IBBL RHL03550. • 4 workers; Hong Kong SAR, Ngong Ping SSSI; 22.25364, 113.90129; 438 m a.s.l.; 24 May. 2022; M.T.Hamer leg.; Secondary forest, Nest ex. Decay wood; IBBL ANTWEB1010110, ANTWEB1010111, ANTWEB1010112, ANTWEB1010113. • 1 worker; Hong Kong SAR, Tai Mo Shan; 22.40549, 114.16352; 468 m a.s.l.; 19 May. 2023; L.Xuan leg.; Secondary forest, Hand collection; IBBL ANTWEB1010125. • 5 workers; Hong Kong SAR, Tai Mo Shan; 22.40403, 114.1069; 471 m a.s.l.; 26 Aug. 2023; M.T.Hamer leg.; Secondary forest, un. Rock; IBBL MTH163. • 5 workers; Hong Kong SAR, Lantau; 22.31701, 114.0173; 179 m a.s.l.; 29 Aug. 2023; M.T.Hamer leg.; Young secondary, ex. Decaying log; IBBL MTH221. • 1 worker; Hong Kong SAR, Lantau; 22.31701, 114.01733; 179 m a.s.l.; 29 Aug. 2023; M.T.Hamer leg.; Young secondary forest, Nest ex. Decay log; IBBL ANTWEB1010173. • 12 workers; Hong Kong SAR, Tai Mo Shan; 22.40452, 114.10645; 490 m a.s.l.; 27 Sep. 2023; M.T.Hamer leg.; Secondary forest, ex. Soil; IBBL MTH563. • 1 worker;

Hong Kong SAR, Tai Mo Shan; 22.40549, 114.16352; 468 m a.s.l.; 19 May. 2023; L.Xuan leg.; Secondary forest, Hand collection; IBBL ANTWEB1010125.

Paratype ergatoid ($n = 1$): CHINA • 1 ergatoid; Hong Kong SAR, Tai Mo Shan; 22.40403, 114.10691; 470 m a.s.l.; 3 Sep. 2023; M.T.Hamer leg.; secondary forest, ex. Decaying log; IBBL ANTWEB1010225.

***Leptogenys diminuta* (F. Smith, 1857)**

Figs 4B, 5B, D, 6B, 8A, 10, 20B

Ponera diminuta Smith, 1857a: 69 (w.) BORNEO (East Malaysia: Sarawak).

Lobopelta diminuta: Mayr 1862: 734.

Leptogenys diminuta: Emery 1895: 461.

Leptogenys diminuta bismarckensis [senior synonym] Forel, 1901c: 7 (w.) NEW GUINEA: Wilson 1958c: 118; Bolton 1995b: 231; Zhou 2001a: 43. Of *Leptogenys diminuta deceptrix* Forel, 1901m: 46 (w.): Xu and He 2015: 138. Of *Leptogenys ferox* Smith, 1865a: 70 (w.) INDONESIA: Wilson 1958c: 118; Bolton 1995b: 231; Zhou 2001a: 43. Of *Leptogenys hodgsoni* Forel, 1900f: 308 (w.) MYANMAR: Xu and He 2015: 144. Of *Leptogenys diminuta palliseri* Forel, 1900f: 307 (w.m.) INDIA: Xu and He 2015: 138. Of *Leptogenys diminuta santschii* Mann, 1919: 299 (w.eq.m.) SOLOMON IS: Wilson 1958c: 118; Bolton 1995b: 231; Zhou 2001a: 43. Of *Leptogenys diminuta sarasinorum* Forel, 1900f: 307 (w.) SRI LANKA: Xu and He 2015: 138. Of *Leptogenys simillima* Smith, 1860b: 104 (w.) INDONESIA: Roger 1863b: 19; Mayr 1863a: 428; Bolton 1995b: 231; Zhou 2001a: 43. Of *Leptogenys diminuta stitzi* Viehmeyer, 1934c: 310: Wilson 1958c: 118; Bolton 1995b: 231; Zhou 2001a: 43. Of *Leptogenys diminuta striatula* Emery, 1895m: 461 (w.) MYANMAR: Xu and He 2015: 138. Of *Leptogenys diminuta woodmasoni* Forel, 1886d: 246 (w.) INDIA: Xu and He 2015: 138. of *Leptogenys diminuta yarrabahna* Forel 1915b: 29 (w.m.) AUSTRALIA: Taylor 1988: 34; Bolton 1995b: 231; Zhou 2001a: 43.

Measurements. Worker ($n = 10$): HL 1.53–1.62; HLL 1.15–1.33; HLA 0.34–0.39; HW 1.09–1.17; CML 0.36–0.41; SL 1.56–1.72; All 0.22–0.225; AFI 0.29–0.34; AFII 0.23–0.32; EL 0.3–0.36; ML 0.67–0.83; PrL 0.85–0.99; PrH 0.57–0.72; PrW 0.81–0.89; WL 2.32–2.53; PeL 0.49–0.66; PeH 0.65–0.73; PeW 0.4–0.48; DPL 0.42–0.5; CI 70.01–74.19; CLI 23.53–26.32; SI 137.99–155.25; OI 24.21–27.27; LPI 107.12–135.85; DPI 84.24–103.9.

Ergatoid ($n = 1$): HL 1.59; HLL 1.29; HLA 0.39; HW 1.18; CML 0.43; SL 1.63; All 0.25; AFI 0.32; AFII 0.24; EL 0.34; ML 0.83; PrL 0.94; PrH 0.66; PrW 0.89; WL 2.61; PeL 0.56; PeH 0.7; PeW 0.47; DPL 0.47; CI 74.15; CLI 26.66; SI 137.82; OI 26.43; LPI 124.73; DPI 99.57.

Morphological variation. Studied specimens showed clear variation in dorsal head sculpturing, with the shape of concentric costulae medially ranging from broadly curved to angulate, and the regularity of costulae varying subtly among specimens. Additionally, we observed the presence of smooth patches in the middle of the head, with varying sizes among certain specimens; when present, these patches were between the concentric costulae. The dorsal margin of the node is completely foveate in most specimens, but fine costulae was observed in the ventral margin of the petiole of one specimen. Fine and

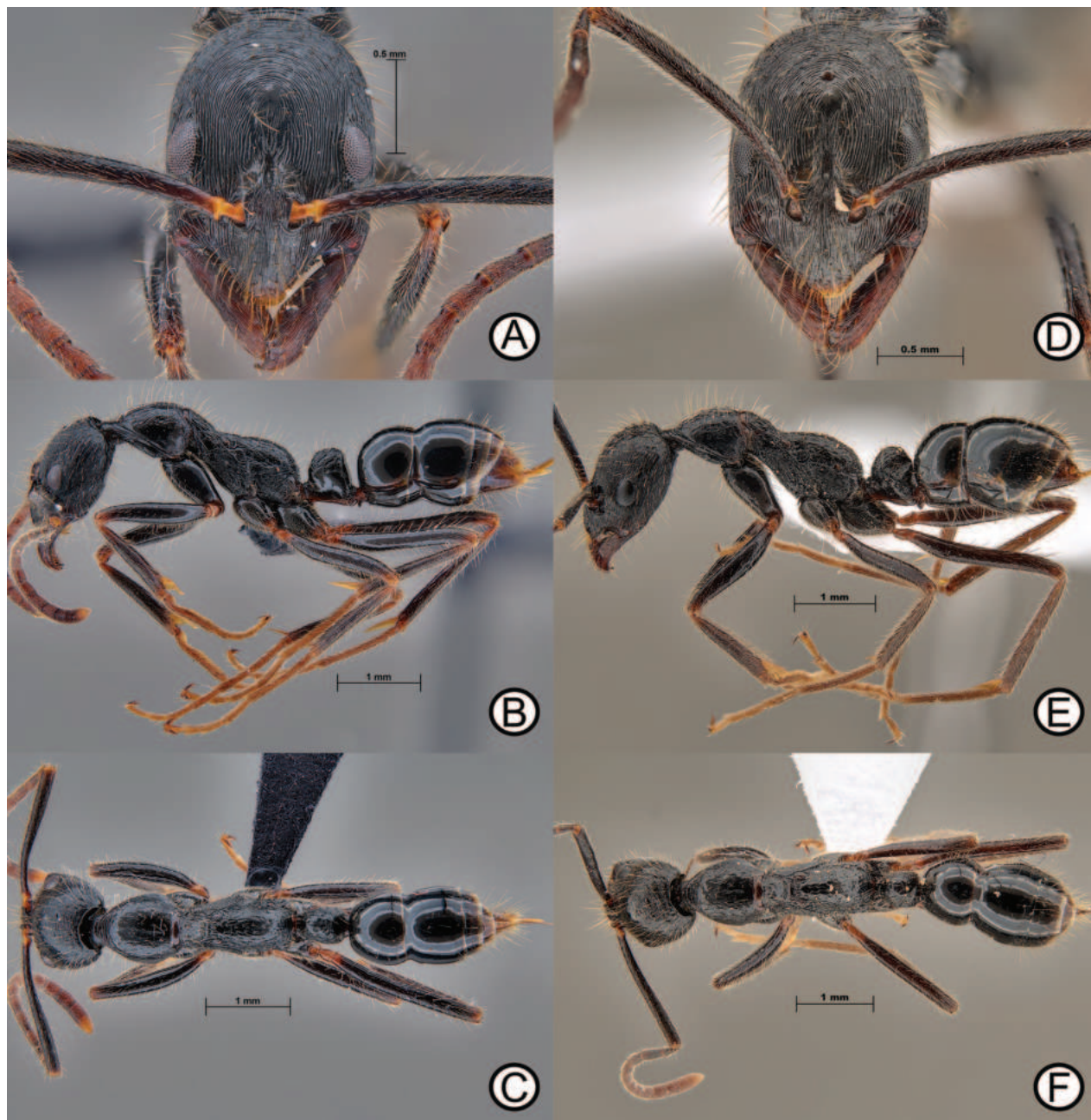


Figure 10. *Leptogenys diminuta* worker (ANTWEB1010183) and *L. diminuta* ergatoid (ANTWEB1010180) **A** worker specimen in lateral view **B** worker specimen in dorsal view **C** worker specimen in full face view **D** ergatoid in lateral view **E** ergatoid in lateral view and **F** ergatoid in dorsal view.

faint costulae was also observed on the metapleuron of one specimen, contrary to the general pattern of rugulose sculpture found in other specimens of *L. diminuta*. *Leptogenys diminuta* is known to be a highly morphologically variable species, both on a wider geographical scope, as well as within Hong Kong. This is also reflected through the complex taxonomic history of this species and the numerous associated subspecies, either considered as valid or synonyms. Given such morphological diversity, *L. diminuta* is likely a species complex with numerous cryptic species found across its distribution (Wilson 1958).

Comparative notes. *Leptogenys diminuta* resembles and is frequently confused with *L. kitteli*. However, *L. diminuta* can be readily separated from *L. kitteli*

in Hong Kong based upon the often smooth to finely reticulate pronotum, the presence of a single tooth on the mandibular masticatory margin, as well as its much smaller size relative to *L. kitteli*.

Distribution. A very wide ranging species, or species complex, known from numerous regions across Asia and Oceania, including the Australasian region (Australia, New Guinea, Solomon Islands), the Indomalayan region (Bangladesh, Borneo, mainland China [Guangdong (additional records provided here), Fujian, Hainan, Guangxi, Hunan, Hong Kong], India, Indonesia, Lanka, Laos, Malaysia, Myanmar, Nepal, Philippines, Singapore, Sri Lanka, Taiwan, Thailand, and Vietnam), as well as the Palaearctic region [part of southwestern China (Sichuan)] (Wilson 1958; Bakhtiar and Chiang 2010; Xu and He 2015; Bharti et al. 2016 Janicki et al. 2016; Guénard et al. 2017). The absence of this species from various countries and provinces (e.g., Cambodia and Guizhou, China) likely reflects lack of sampling efforts.

Ecology. *Leptogenys diminuta* is a group-hunting species, forming long columns of workers that move through their habitat in search of prey. Colonies are moderately populous with 200–400 individuals per nest and move nesting locations throughout the year (Ito 1997). Nest locations in Hong Kong have included rotting logs, underneath rocks and within leaf litter. The species has ergatoids (Fig. 10D–E) and likely disperses through colonial budding (Ito 1997; Ito and Ohkawara 2000). Records are predominantly known from young to old growth secondary forests, and similar to *L. peuqueti*, it is one of the most frequently encountered *Leptogenys* in Hong Kong.

Material examined. Workers ($n = 67$): CHINA • 1 worker; Hong Kong SAR, Sunset Peak; 25 Jul. 1992; J.R.Fellowes leg.; IBBL MBS006900. • 3 worker; Hong Kong SAR, Kadoorie Farm; 10 Aug. 1996; J.R.Fellowes leg.; IBBL MBS006880, MBS006881, MBS006882. • 1 worker; Hong Kong SAR, Lantau, Tei Tong Tsai; 5 Nov. 1996; J.R.Fellowes leg.; HKBM MBS015302. • 3 workers; Guangdong Prov., Gu Tian; 10 Apr. 1997; J.R.Fellowes leg.; HKBM MBS006883, MBS006884, MBS006885. • 2 workers; Hong Kong SAR, The Peak; 27 Jun. 1999; SK.Yamane leg.; SKYC ANTWEB1010191, ANTWEB1010192. • 1 worker; Hong Kong SAR, Victoria Park; 27 Jun. 1999; SK.Yamane leg.; SKYC MBS006607. • 1 worker; Hong Kong SAR, Kadoorie Farm Botanical Garden; 6 Sep. 1999; J.R.Fellowes leg.; HKBM MBS015275. • 1 worker; Hong Kong SAR, Kadoorie Farm Botanical Garden; 448–480 m a.s.l.; 21 Sep. 1999; J.R.Fellowes leg.; HKBM MBS015282. • 1 worker; Hong Kong SAR, The Peak; 10 Sep. 2000; SK.Yamane leg.; SKYC ANTWEB1010193, ANTWEB1010195, ANTWEB1010196, ANTWEB1010197. • 1 worker; Hong Kong SAR, Kadoorie Farm Botanical Garden; 22.42947, 114.12145; 350 m a.s.l.; 3 Jul. 2011; P.S.Ward leg.; Secondary forest, Hand collection; IBBL ANTWEB1010181. • 1 worker; Hong Kong SAR, Lin Fa Shan; 22.39963, 114.09654; 423 m a.s.l.; 18 Jul. 2015; T.Tsang leg.; Winkler leaf litter Ex; IBBL TT01320. • 1 worker; Hong Kong SAR, Tai Lam; 22.3952, 114.09072; 440 m a.s.l.; 26 Oct. 2015; R.H.Lee leg.; Shrubland, Hand collection; IBBL RHL01371. • 1 worker; Hong Kong SAR, Ng Tong Chai; 22.42415, 114.13185; 420 m a.s.l.; 26 Jun. 2016; R.H.Lee leg.; Secondary forest, Hand collection; IBBL RHL02822. • 1 worker; Hong Kong SAR, Lung Fu Shan; 22.2758, 114.13546; 260 m a.s.l.; 30 Jun. 2016; R.H.Lee leg.; Secondary forest, Hand collection; IBBL RHL-SIA-008. • 1 worker; Hong Kong SAR, Clear Water Bay; 22.2918, 114.30208; 114 m a.s.l.; 19 Jul. 2016; M.Pierce leg.; ground forager; IBBL ANTWEB1017020. • 1 worker; Hong Kong SAR, Tai Po; Lam

Tseun; 22.43449, 114.11728; 171 m a.s.l.; 30 Aug. 2016; M.Pierce leg.; forest, Hand collection; IBBL ANTWEB1009148. • 1 worker; Hong Kong SAR, Tai Po; Lam Tseun; 22.43449, 114.11728; 171 m a.s.l.; 30 Aug. 2016; M.Pierce leg.; forest, Hand collection; IBBL ANTWEB1009378. • 1 worker; Hong Kong SAR, Lung Fu Shan; 22.2811, 114.1369; 150 m a.s.l.; 5 Oct. 2016; B.Worthington leg.; Hand collection (night); IBBL BMW02340. • 1 worker; Hong Kong SAR, Tsing Yi; 22.3405, 114.1003; 300 m a.s.l.; 12 Feb. 2017; R.H.Lee leg.; Open rock, general forager; IBBL RHL003394. • 1 worker; Hong Kong SAR, Hatton Road; 22.2792, 114.1365; 237 m a.s.l.; 12 Feb. 2022; M.T.Hamer leg.; Young secondary, Hand collection; IBBL ANTWEB1010183. • 1 worker; Hong Kong SAR, Pok Fu Lam; 22.25988, 114.13944; 213 m a.s.l.; 13 Jun. 2022; M.T.Hamer leg.; Hand collection; IBBL ANTWEB1010184. • 3 workers; Hong Kong SAR, Ngong Ping; 22.25298, 113.90457; 455 m a.s.l.; 4 May. 2023; M.T.Hamer leg.; Secondary forest, Hand collection; IBBL ANTWEB1010128, ANTWEB1010129, ANTWEB1010130. • 1 worker; Hong Kong SAR, Wong Lung Hang; 22.26368, 113.95375; 400 m a.s.l.; 11 May. 2023; M.T.Hamer leg.; Young secondary forest, Hand collection; IBBL ANTWEB1010133, ANTWEB1010134. • 1 worker; Hong Kong SAR, Yi O; 22.22342, 113.84714; 13 m a.s.l.; 20 Jun. 2023; M.T.Hamer leg.; Young secondary forest, Winkler leaf litter Ex; IBBL ANTWEB1010126, ANTWEB1010127. • 1 worker; Hong Kong SAR, Ngong Ping SSSI; 22.25252, 113.90662; 455 m a.s.l.; 29 Jun. 2023; M.T.Hamer leg.; Secondary Forest, Hand collection; IBBL ANTWEB1010124. • 2 workers; Hong Kong SAR, Tai Mo Shan; 22.40403, 114.1069; 471 m a.s.l.; 22 Aug. 2023; C.Y.L.Tse leg.; Secondary forest, ex. Nest; IBBL MTH243. • 1 worker; Hong Kong SAR, Tai Mo Shan; 22.40384, 114.10549; 491 m a.s.l.; 26 Aug. 2023; C.Y.L.Tse leg.; Secondary forest, Gen. forager; IBBL MTH80, MTH242. • 4 workers; Hong Kong SAR, Tai Mo Shan; Kap Lung Forest Trail; 22.41084, 114.10423; 450 m a.s.l.; 3 Sep. 2023; M.T.Hamer leg.; Secondary forest, ex.decaying log; IBBL MTH222. • 5 workers; Hong Kong SAR, Nei Lak Shan; 22.26524, 113.9064; 500 m a.s.l.; 6 Sep. 2023; M.T.Hamer leg.; Young Secondary Forest, Hand coll. in trail; IBBL MTH303. • 5 workers; Hong Kong SAR, Tai Mo Shan; 22.40452, 114.10645; 490 m a.s.l.; 27 Sep. 2023; M.T.Hamer leg.; Secondary forest, un. rock; IBBL MTH574.

Ergatoid: CHINA • 1 ergatoid; Hong Kong SAR, Tai Mo Shan; Kap Lung Forest Trail; 22.40422, 114.10591; 470 m a.s.l.; 22 Aug. 2023; C.Y.L.Tse leg.; Nest ex.; IBBL ANTWEB1010180.

***Leptogenys grohli* Hamer, Lee & Guénard, sp. nov.**

<https://zoobank.org/12FD252A-BAE4-488A-80F7-C5EAA46972D0>

Figs 11, 12, 13, 20C

Diagnosis. Head isosceles trapezoid, longer than wide; mandible linear, basal margin longer than masticatory margin; basal margin edentate, masticatory margin with one proximal and one apical tooth. Scape extending beyond posterior head margin by three tenths of its length; antennal flagellomere I longer than pedicel and antennal flagellomere II. Promesonotal articulation and notopodeal sulcus present. Propodeum with a pair of broadly rounded, posterior facing cuticular lobes. In lateral view, petiole slightly longer than high, trapezoidal in shape with posterior margin higher than anterior margin; dorsum subtly convex, curving gradually downwards anteriorly. Head dorsum between eye,

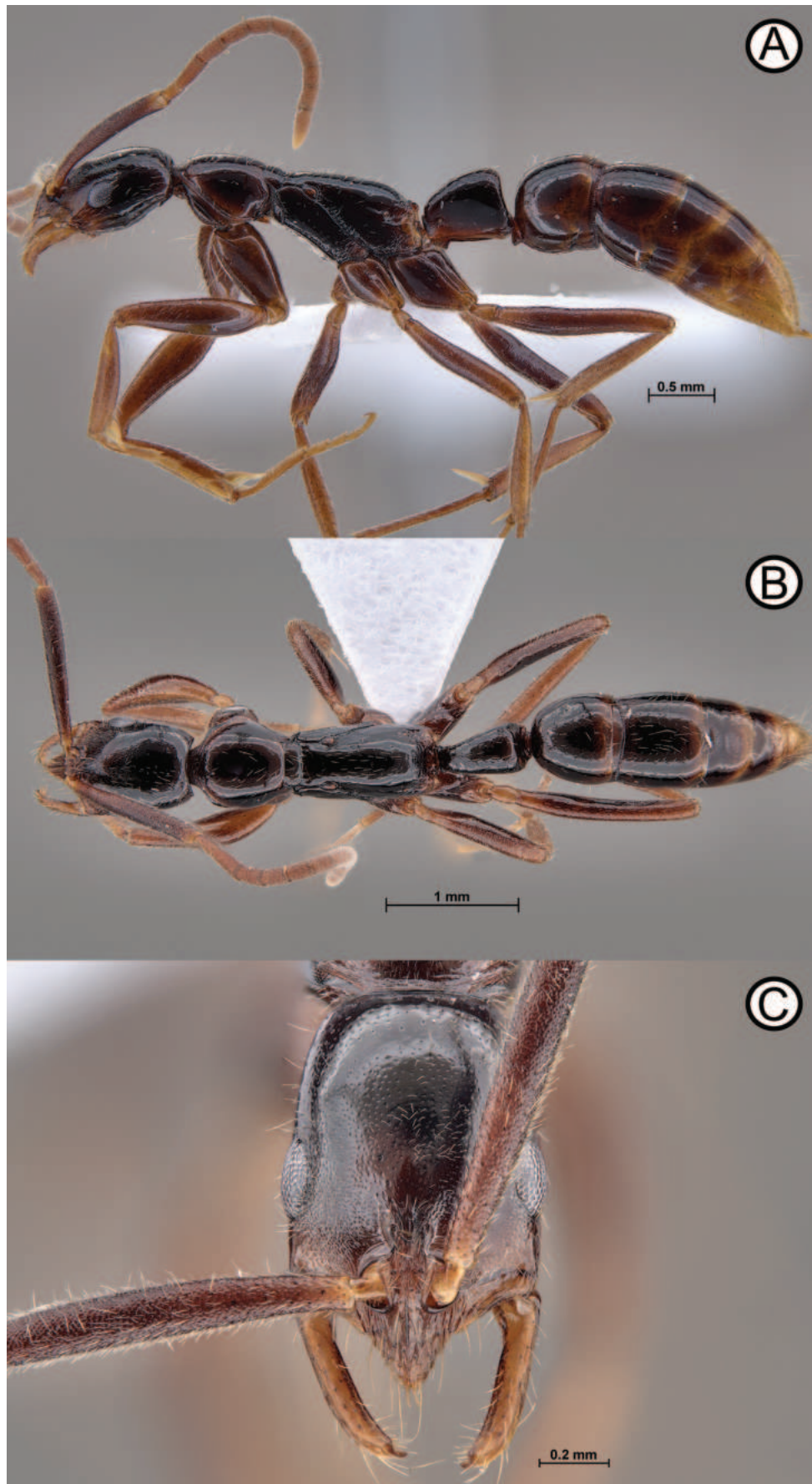


Figure 11. *Leptogenys grohli* holotype (ANTWEB1010093) **A** lateral view **B** dorsal view **C** head in full face view.

clypeus, and frontal lobe with numerous and dense hair-bearing micro-punctulae. Mesosomal dorsum smooth and shining with large, sparse punctures. Anteriormost point clypeal margin with a pair of stout, tubular peg-like setae and two decumbent hairs adjacent to the peg-like setae.

Description. Head. In full face view, head isosceles shaped as trapezoid, longer than wide, widest at mandibular insertion; lateral margin subtly convex and subtly widening beyond eye to posterior margin; posterolateral corner of head blunt; posterior margin of head straight. Mandible linear, basal margin longer than masticatory margin; distinct angle between basal and masticatory margin present; basal margin weakly sinuous and edentate, masticatory margin with one proximal (formed by angle between basal and masticatory margin) and one apical tooth; gap formed between clypeus and mandible when closed. In lateral view, masticatory margin of mandible curves ventrad at apex; mandibular groove present, beginning $\frac{1}{3}$ the width of the mandible from base, terminating at ventrolateral mandible apex. Mandalus ovoid, visible at base of mandible when closed. In full face view, anterior clypeal lobe broadly triangular, extending into intermandibular space; $\frac{1}{5}$ of head length; terminating in an acute convex point; lateral clypeal margin gradually curving to lateral head margins with inconspicuous lobes; longitudinal clypeal carina present and conspicuous. Frontal lobes small, $\frac{2}{3}$ of antennal condyle visible. Frontal groove short, terminating at anterior eye margin. Occipital carina present, extending to ventral surface meeting at an acute angle ventrally. Eye convex, located dorsolaterally in full face view; interrupting lateral head outline; length $\frac{1}{4}$ of lateral head length; maximum number of ommatidia across maximum eye length 14 or 15. Antennae with ten flagellar segments; scape long, extending beyond posterior head margin by $\frac{3}{10}$ of its length; scape reaching maximum width medially; antennal flagellomere I longer than pedicel and antennal flagellomere II; apical most flagellomere tapering to a point. Hypostomal teeth present; in ventral view, located laterally, adjacent to mandibular base. Palp formula 4:4 (one worker dissected).

Mesosoma. In lateral view, promesonotum feebly to distinctly convex; promesonotum higher than propodeum; propodeal dorsal outline straight to feebly convex; dorsal surface longer than declivitous face; angle between dorsal and declivitous face gradually curving. In dorsal view, pronotum wider than long; pronotum wider than maximum propodeal width. Prosternal process present, anteriorly convex, and posteriorly acutely angled. Promesonotal articulation present but feebly impressed. Mesonotum wider than long. Notopropodeal sulcus present, impressed, with longitudinal cross-ribs. Angle between dorsal and lateral surfaces smoothly curved. Posterolateral propodeum at spiracular height with broadly rounded lobe that extend posteriorly; propodeal declivitous surface concave. In lateral view, mesometapleural suture deeply impressed, with cross-ribs; mesopleural margin of suture distinctly marginated. Mesopleuron not visibly divided into anespiternum and katerpisternum. Propodeal spiracle circular, located above midline of lateral propodeum surface within concave cuticular depression anterodorsally. Metapleural gland bulla circular. Distance between metapleural gland and spiracle greater than spiracle diameter. Legs long and slender; tarsomere one with concave cleaning comb basally. Mesotibia with one pectinate and one simple spur; simple spur $\frac{1}{2}$ length of pectinate spur. Metatibia with one long pectinate spur and one simple spur; simple spur $\sim \frac{1}{3}$ the length of the pectinate spur. All tarsal claws pectinate.

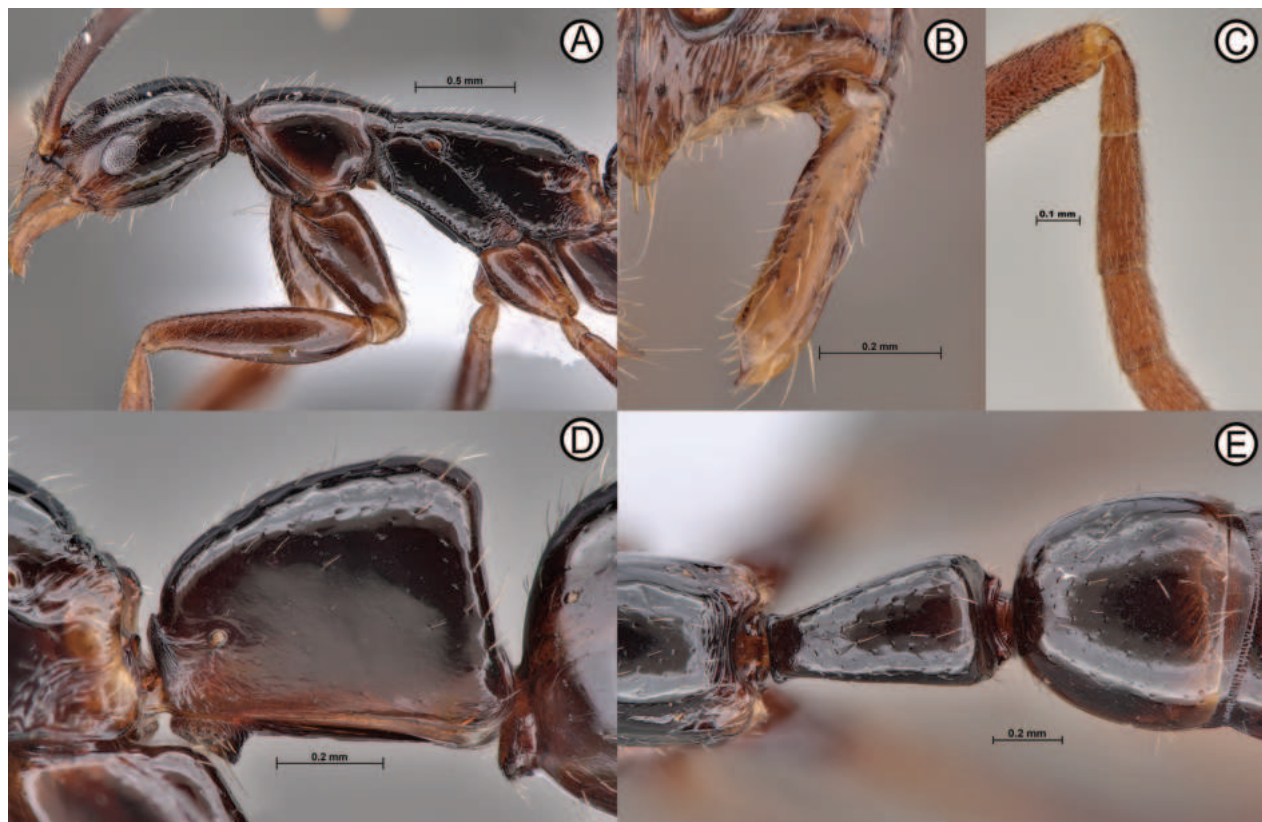


Figure 12. *Leptogenys grohli* sp. nov. holotype (all images are ANTWEB1010093, other than C ANTWEB1010092) close up sections **A** close up of head and mesosoma in lateral view **B** close up of right hand mandible in full face view **C** close up of right antennal scape in full anteroventral view **D** close up of petiole in lateral view **E** close up of propodeum, petiole and first gastral tergite in dorsal view.

Metasoma. In lateral view, petiole slightly longer than high, trapezoidal in shape with posterior margin higher than anterior margin; dorsum subtly convex, curving anteriorly; anterior face straight, ~ 1/2 as high as of posterior face. Peduncle absent. Spiracle small and circular, located laterally on anteromedial surface. In dorsal view, petiole distinctly longer than wide; posterior width twice the anterior width. Subpetiolar process present, located anteroventrally; process triangular with posterior margin longer than anterior margin, posteroventral angle acute. Semi-circular prora lobe present, pointed ventrally. Angle between anterior and dorsal surface of abdominal tergite III broadly rounded in lateral view. Abdominal tergite III widest posteriorly in dorsal view. Cinctus with numerous short, longitudinal cross-ribs. Sting present.

Sculpture. Mandibular dorsum with faint longitudinal striations across whole length. Clypeal dorsum laterally smooth, coarsely striate medially, with scattered hair-bearing punctae. Head dorsum between eye, clypeus, and frontal lobe with numerous, dense hair-bearing punctulae; punctations become larger and sparse posteriorly; ventrolateral head surface mostly smooth and shining with widely spaced hair-bearing punctations. Antennal segments with numerous, dense punctulae, lacking smooth regions. Mesosomal dorsum mostly smooth with large, sparse punctures; distance between punctures much larger than their diameter. Propodeal declivity with conspicuous transverse striations that do not extend to propodeal dorsum; posterior portion of declivity smooth. Lateral surface of pronotum mostly smooth and shining with large, sparse punctures. Mesopleuron

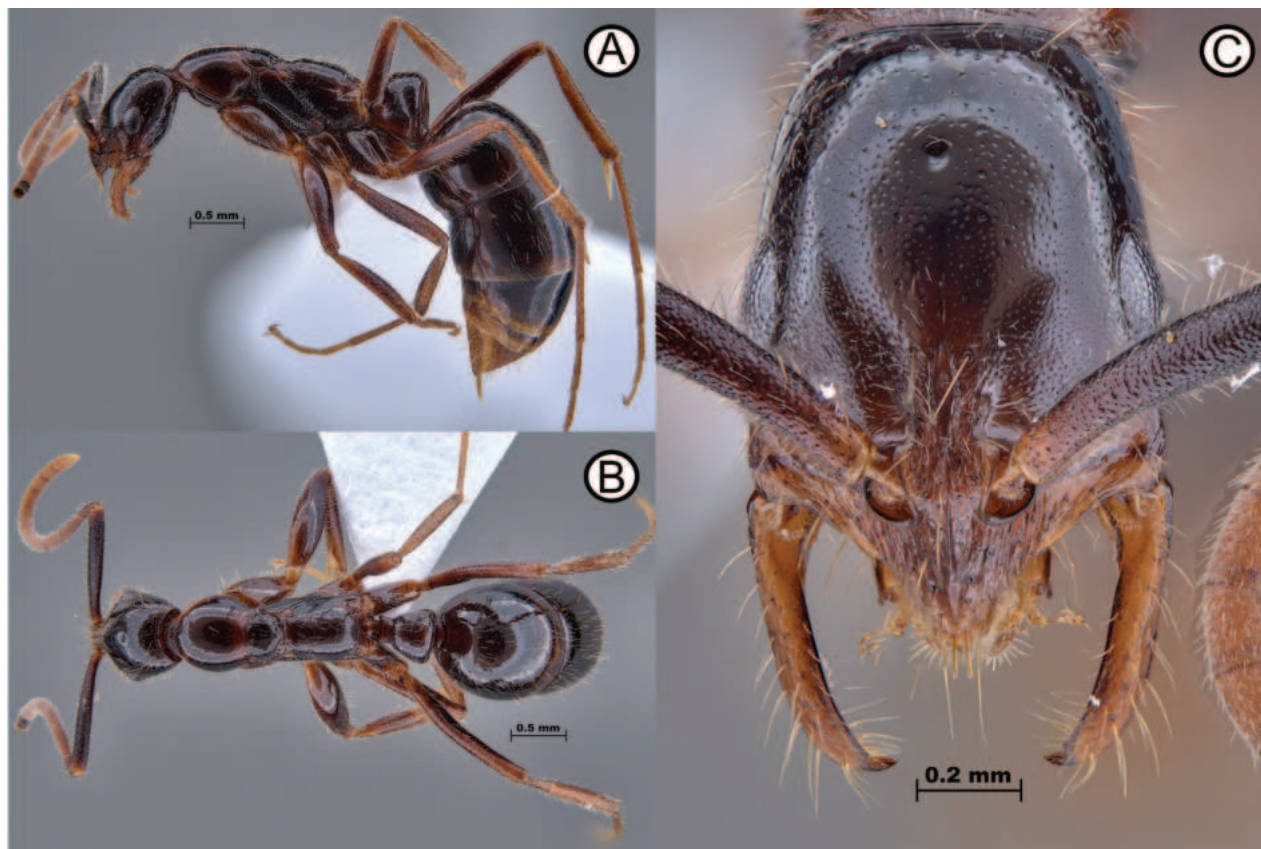


Figure 13. *Leptogenys grohli* ergatoid queen (ANTWEB1010094) **A** lateral view **B** dorsal view **C** head in full face view.

anteroventral and ventral margins with short striations; striations crossing mesopleuron width ventrally; mesopleuron mostly smooth and shining with sparse punctures. Lateral propodeum with striations on ventral margin, around meta-pleural gland bulla, propodeal spiracle and posteroventral corner. All femora with hair-bearing punctures; punctures progressively denser apically on dorsal surface of profemur. All tibiae smooth and shining with dense punctulae and sparse macro hair-bearing punctures throughout. Petiole dorsum mostly smooth and shining with large hair-bearing punctures; lateral petiole surface smooth. Dorsum of first gastral tergite mostly smooth and shining with large, sparse, hair-bearing macro punctures; anterior face smooth and shining. Presternite IV imbricate. Abdominal segment IV with macro-punctures dorsally; sternite with very sparse macro punctures. Pygidium and hypopygium with sparse, hair-bearing macro punctures only.

Pilosity. Mandibular dorsum with stout erect hairs directed inwards along basal margin, and short, decumbent hairs on dorsum. Anteriormost point clypeal margin with pair of long, stout, tubular peg-like setae and two decumbent hairs adjacent to the peg-like setae; clypeal dorsum with numerous, long erect hairs as well as decumbent short hairs sparsely distributed across surface. Head dorsum, between clypeus, antennal foramen, and eye with dense, semi-decumbent, appressed hairs; hairs posteriorly sparse with suberect hairs only; head dorsolaterally with decumbent hairs directed anteriorly. Scape with numerous subdecumbent and suberect hairs; flagella with numerous suberect and decumbent hairs. Mesosomal dorsum with erect and suberect hairs sparsely distributed. Suberect and decumbent hairs present on lateral surfaces of pronotum and propodeum. Coxae with many decumbent hairs reaching highest density on ventral surface.

Femora with suberect hairs dorsally and subdecumbent hairs ventrally; tibiae with dense, decumbent hairs dorsally, and sparse decumbent hairs ventrally. All tarsi I with stout and apically blunt hairs arranged in a series, surrounded by simple decumbent hairs. Petiolar dorsum with decumbent hairs; lateral petiole surface with sparse decumbent hairs, almost glabrous; subpetiolar process with numerous suberect and erect hairs. Prora with numerous, fine, short, erect hairs directed anteriorly. All abdominal tergites and sternites with sparsely distributed suberect and erect hairs. Pygidium and hypopygium with numerous long erect hairs.

Colour. Dark reddish brown across mesosoma, mandibles and legs distinctly paler red to orange in colour.

Ergatoid description. With characters of worker but: lateral head margin not straight, distinctly widening posteriorly noticeably more so than the worker. Mesosoma stout and robust not as elongated as in worker; promesonotum distinctly convex; propodeum shorter, ~ 1/3 longer than propodeal declivity. Petiole nodiform, distinctly higher than long in lateral view; about as wide as long in dorsal view. Metasomal segments III-VII enlarged, segment III wider than petiole. Same colours as the worker.

Measurements. Worker holotype: HL 1.13; HLL 0.87; HLA 0.23; HW 0.72; CML 0.22; SL 1.20; All 0.21; AFI 0.32; AFII 0.24; EL 0.23; ML 0.56; PrL 0.71; PrH 0.49; PrW 0.66; WL 1.92; PeL 0.68; PeH 0.61; PeW 0.38; DPL 0.64; CI 63.57; CLI 19.8; SI 167.31; OI 26.67; LPI 89.66; DPI 59.75.

Worker paratypes ($n = 12$): HL 1.12–1.18; HLL 0.86–0.90; HLA 0.20–0.23; HW 0.69–0.75; CML 0.21–0.23; SL 1.16–1.26; All 0.19–0.24; AFI 0.31–0.36; AFII 0.22–0.26; EL 0.22–0.25; ML 0.54–0.57; PrL 0.66–0.74; PrH 0.49–0.55; PrW 0.64–0.69; WL 1.79–1.99; PeL 0.60–0.69; PeH 0.56–0.61; PeW 0.33–0.39; DPL 0.52–0.67; CI 61.36–64.17; CLI 18.65–20.43; SI 166.25–172.94; OI 26.14–28.93; LPI 85.02–93.55; DPI 55.5–65.71.

Ergatoid paratype ($n = 1$): HL 1.19; HLL 0.90; HLA 0.259; HW 0.80; CML 0.25; SL 1.19; All 0.23; AFI 0.30; AFII 0.22; EL 0.25; ML 0.59; PrL 0.73; PrH 0.56; PrW 0.7; WL 1.88; PeL 0.50; PeH 0.62; PeW 0.49; DPL 0.50; CI 67.31; CLI 21.34; SI 148.06; OI 28.28; LPI 123.01; DPI 97.61.

Non-type workers ($n = 10$): HL 1.12–1.18; HLL 0.82–0.92; HLA 0.16–0.24; HW 0.7–0.75; CML 0.2–0.25; SL 1.17–1.34; All 0.18–0.22; AFI 0.31–0.36; AFII 0.23–0.26; EL 0.22–0.27; ML 0.55–0.61; PrL 0.66–0.74; PrH 0.5–0.55; PrW 0.64–0.71; WL 1.81–1.97; PeL 0.63–0.69; PeH 0.54–0.67; PeW 0.36–0.4; DPL 0.57–0.67; CI 61.82–64.78; CLI 18.01–20.73; SI 163.69–179.7; OI 25.74–31.04; LPI 81.83–97.24; DPI 56.97–68.64.

Morphological variation. A spectrum of mesosomal size was observed, which is reflected in the variation seen within the mesosomal measurements. Moreover, the longitudinal ridges across the notopropodeal sulcus differs across the specimens examined with some showing more ribbing than others. No relationship between the size of a specimen and the longitudinal ridges could be found. Variation in both morphometric and qualitative characters mentioned above differs within the colony type series.

Comparative notes. Within Xu and He (2015), specimens of *L. grohli* will key to the couplet containing both *L. peuqueti* and *L. confucii*. *Leptogenys grohli* is distinguishable from *L. peuqueti* by the more linear lateral margins of the head than the convex lateral margins of *L. peuqueti*; the smaller eye (EL 0.22–0.27); and narrower head (HW 0.70–0.75). Sculptural differences also occur, with

L. grohli having greater density of punctures across the whole head, scapes, mesosomal, petiole and first two gastral tergites than *L. peuqueti*. *Leptogenys peuqueti* is generally larger in all aspects, with *L. grohli* being a smaller, more gracile species. *Leptogenys grohli* is also morphologically similar to *L. confucii*, a species known from Taiwan and Southern Japan, but can be differentiated by the conspicuously defined angle between the basal and masticatory margin of the mandible; a smaller, less conspicuous frontal indentation; more angulated posterior head corner, and the lack of sculpture across the whole mesopleuron and lateral propodeal surfaces.

Distribution. So far *L. grohli* is only known from Hong Kong and Guangdong. This species, however, should be expected from neighbouring Chinese provinces and is likely to have been misidentified previously as *L. peuqueti*.

Ecology. The type series was collected by sifting and extracting leaf litter within an old growth secondary forest. Specimens were noted during leaf litter sample collection, with the nest located within the soil between the tree trunk and its roots. One ergatoid and 16 workers were obtained, likely representing most of the colony. Solitary foraging individuals have been observed and collected during daytime across Hong Kong, with specimens obtained from tree plantations to secondary forests and Feng Shui Woods. Group hunting behaviour was not observed in this species.

Material examined. Holotype worker. CHINA • 1 worker; Hong Kong SAR, Tai Po Kau Nature Reserve; 22.4271, 114.1814; 160 m a.s.l.; 23 Aug. 2022; A.I. Weemaels & M.T.Hamer leg.; Secondary forest, Winkler ex. leaf litter; ZRC ANTWEB1010093.

Paratype workers: 12 workers: Same collection as holotype; ZRC ANTWEB1010085 to ANTWEB1010092. Same collection data as holotype; HKBM ANTWEB1010095 to ANTWEB1010099.

Paratype ergatoid: Same collection data as holotype; ZRC ANTWEB1010094.

Non-type workers ($n = 35$): CHINA • 3 workers; Hong Kong SAR, Tai Po Kau; 19 Jul. 1992; J.R.Fellowes leg.; HKBM MBS006896, MBS006897, MBS006899. • 2 workers; Guangdong Prov., Qi Mu Zhang; 6 Apr. 1997; J.R.Fellowes leg.; HKBM MBS015248. • 1 worker; Hong Kong SAR, Lung Fu Shan; 22.27876, 114.13728; 240 m a.s.l.; 24 Apr. 2015; R.H.Lee leg.; Plantation, Pitfall trap; IBBL RHL00050. • 2 worker; Hong Kong SAR, Lung Fu Shan; 22.2784, 114.1378; 230 m a.s.l.; 30 Apr. 2015; R.H.Lee leg.; Plantation, Pitfall trap; IBBL RHL00129, RHL00152. • 1 worker; Hong Kong SAR, Shing Mun; 22.39693, 114.153; 242 m a.s.l.; 14 May. 2015; R.H.Lee leg.; Feng Shui Forest, Pitfall trap; IBBL RHL00401. • 1 worker; Hong Kong SAR, Sunset Peak; 22.26112, 113.95633; 575 m a.s.l.; 3 Jun. 2015; R.H.Lee leg.; Secondary forest, Pitfall trap; IBBL RHL00892. • 1 worker; Hong Kong SAR, Sunset Peak; 22.26084, 113.95753; 575 m a.s.l.; 3 Jun. 2015; R.H.Lee leg.; Secondary forest, Pitfall trap; IBBL RHL00894. • 2 workers; Hong Kong SAR, Sunset Peak; 22.26392, 113.95376; 470 m a.s.l.; 3 Jun. 2015; R.H.Lee leg.; Secondary forest, Pitfall trap; IBBL RHL00906, RHL00908. • 1 worker; Hong Kong SAR, Sunset Peak; 22.26594, 113.95278; 440 m a.s.l.; 3 Jun. 2015; R.H.Lee leg.; Secondary forest, Pitfall trap; IBBL RHL00931. • 2 workers; Hong Kong SAR, Tai Po Kau; 22.42613, 114.18178; 160 m a.s.l.; 14 Jul. 2015; R.H.Lee leg.; Plantation, Pitfall trap; IBBL RHL00931, RHL02083. • 1 worker; Hong Kong SAR, Tai Po Kau; 22.42285, 114.18082; 200 m a.s.l.; 14 Jul. 2015; R.H.Lee leg.; Secondary forest, Pitfall trap; IBBL RHL02128. • 1 worker; Hong Kong SAR, Tai Po Kau; 22.42706, 114.17999; 180 m a.s.l.; 14 Jul.

2015; R.H.Lee leg.; Plantation, Pitfall trap; IBBL RHL02165. • 2 worker; Hong Kong SAR, Tai To Yan; 22.45479, 114.11821; 420 m a.s.l.; 4 Aug. 2015; R.H.Lee leg.; Secondary forest, Pitfall trap; IBBL RHL02211, RHL02686. • 3 worker; Hong Kong SAR, The Peak; 22.27523, 114.13873; 370 m a.s.l.; 17 Aug. 2015; R.H.Lee leg.; Secondary forest, Pitfall trap; IBBL RHL01090, RHL01099, RHL01106. • 1 worker; Hong Kong SAR, The Peak; 22.2767, 114.1423; 410 m a.s.l.; 17 Aug. 2015; R.H.Lee leg.; Secondary forest, Pitfall trap; IBBL RHL02621. • 2 worker; Hong Kong SAR, The Peak; 22.27603, 114.14199; 410 m a.s.l.; 17 Aug. 2015; R.H.Lee leg.; Secondary forest, Pitfall trap; IBBL RHL02636, RHL02639. • 1 worker; Hong Kong SAR, The Peak; 22.27495, 114.13828; 360 m a.s.l.; 17 Aug. 2015; R.H.Lee leg.; Secondary forest, Pitfall trap; IBBL RHL02655. • 1 worker; Hong Kong SAR, Tai Lam; 22.3956, 114.0928; 420 m a.s.l.; 26–29 Oct. 2015; R.H.Lee leg.; Bamboo forest, Pitfall trap; IBBL RHL02774. • 1 worker; Hong Kong SAR, Lung Fu Shan; 22.2758, 114.13546; 260 m a.s.l.; 30 Jun. 2016; R.H.Lee leg.; Secondary forest, General forager; IBBL RHL-SIA-007. • 1 worker; Hong Kong SAR, Mui Tsz Lam; 22.3892, 114.2345; 220 m a.s.l.; 4 Oct. 2016; R.H.Lee leg.; Secondary forest, Pitfall trap; IBBL RHL003304. • 1 worker; Hong Kong SAR, Tai Po Kau; 22.42613, 114.18178; 160 m a.s.l.; 6 Jun. 2017; R.H.Lee leg.; Secondary forest, Pitfall trap; IBBL RHL03549. • 1 worker; Hong Kong SAR, Tai Po Kau; 22.42706, 114.17999; 180 m a.s.l.; 6 Jun. 2017; R.H.Lee leg.; Secondary forest, Pitfall trap; IBBL RHL03555. • 1 worker; Hong Kong SAR, Lung Fu Shan; 22.2758, 114.13546; 250 m a.s.l.; 11 Oct. 2017; R.H.Lee leg.; Secondary forest, General forager; IBBL RHL-SIA-095. • 1 worker; Hong Kong SAR; Wong Lung Hang; 22.2658, 113.9528; 440 m a.s.l.; 11 May. 2023; M.T.Hamer leg.; Shrubland, General-forager IBBL ANTWEB1010235.

Etymology. Named after the musician Dave Grohl, lead singer, guitarist, and songwriter of the rock band Foo Fighters, drummer of the rock bands Nirvana and Queens of the Stone Age among others, for his positive activism, and ever long musical accompaniment to both first and last author.

***Leptogenys kitteli* (Mayr, 1870)**

Figs 7B, 8B, 14, 20D

Lobopelta kitteli Mayr, 1870b: 966 (w.) INDIA (Sikkim).

Leptogenys kitteli: Emery 1895: 461.

Leptogenys kitteli altisquamis [senior synonym] Forel, 1900f: (w.) MYANMAR: Xu and He 2015: 142. Of *Leptogenys kitteli minor* Forel, 1900f: 307 (w.) INDIA: Xu and He 2015: 142. Of *Leptogenys kitteli siemsseni* Viehmeyer, 1922: 203, fig. 1 (w.) CHINA: Xu and He 2015: 142.

Measurements. Worker ($n = 13$): HL 1.72–1.87; HLL 1.37–1.53; HLA 0.37–0.47; HW 1.3–1.44; CML 0.33–0.45; SL 1.67–1.86; All 0.21–0.32; AFI 0.32–0.37; AFII 0.29–0.33; EL 0.32–0.39; ML 0.73–0.94; PrL 0.97–1.14; PrH 0.7–0.85; PrW 0.97–1.06; WL 2.64–2.87; PeL 0.58–0.82; PeH 0.72–0.93; PeW 0.56–0.74; DPL 0.4–0.52; CI 71.27–81.04; CLI 18.21–25.62; SI 117.83–132; OI 21.94–26.5; LPI 107.98–158.96; DPI 116.12–147.26.

Morphological variation. Specimens of *L. kitteli* show a wide range of variation in sculpture in different parts of the body. In most specimens, the fine costulae on the head run longitudinally across its entire surface; nonetheless, in some other

specimens, some of the costulae converge medially, forming a concentric pattern similar to that found in *L. diminuta*. The mesosomal sculpturing varies even more when compared to the head sculpture; from fine costulae with interspaced foveae to irregular faint costulae throughout the mesosoma. The metanotal groove is deeply incised in the majority of specimens observed, with just a single specimen having a very shallow groove. Similar to *L. diminuta*, *L. kitteli* expresses a large degree of morphological variation across its wider geographical range and is likely a complex of species that would require further taxonomic investigation to resolve.

Comparative notes. *Leptogenys kitteli* is most morphologically similar to *L. diminuta* within Hong Kong. Both species can be differentiated by the distinctly larger absolute size of *L. kitteli*, as well as the longitudinally striate pronotum, and absence of a longitudinal carinae on the clypeal dorsum.

Distribution. *Leptogenys kitteli* is a widely distributed across the Indomalayan region, known from mainland China (Hainan, Guangxi, Yunnan, Sichuan, Guizhou, Hunan, Jiangxi, Fujian Zhejiang, Guangdong, Hubei, and Hong Kong SAR), Taiwan, India, Bangladesh, Myanmar, Thailand, Vietnam, Nepal (; Xu and He 2015; Bharti et al. 2016; Janicki et al. 2016; Guénard et al. 2017; Khachonpisitsak et al. 2020). This species should be expected from Laos and Cambodia.

Ecology. *Leptogenys kitteli* is known to forage in large groups of workers, preying upon termites, as well as earthworms (Fellowes 1996). Similar to *L. diminuta*, colonies are known to move nesting locations and include up to several hundred individuals.

Material examined. Workers ($n = 36$): CHINA • 3 workers; Hong Kong SAR, Tai Mo Shan; 28 Sep. 1992; J.R.Fellowes leg.; HKBM MBS006891, MBS006892. • 1 worker; Hong Kong SAR, Victoria Park; 27 Jun. 1999; K. Eguchi leg.; HKBM MBS006576. • 1 worker; Hong Kong SAR, Victoria Park; 27 Jun. 1999; SK.Yamane leg.; SKYC MBS006586, ANTWEB1010189, ANTWEB1010190. • 3 workers; Guangdong Prov., Hei Shi Ding; 24 Apr. 1997; J.R.Fellowes leg.; HKBM MBS006906, MBS006907, MBS006908. • 1 worker; Guangdong Prov., Nankunshan; 20 Mar. 1997; J.R.Fellowes leg.; HKBM MBS015273. • 1 worker; Guangdong Prov., Qi Mu Zhang; 6 Apr. 1997; J.R.Fellowes leg.; HKBM MBS015271. • 2 workers; Guangdong Prov., Xin Jia Dong; 4 May. 1998; J.R.Fellowes leg.; HKBM MBS006577. • 2 workers; Hong Kong SAR, The Peak; 10 Sep. 2000; SK.Yamane leg.; SKYC ANTWEB1010186, ANTWEB1010187. • 1 worker; Hong Kong SAR, Aberdeen Reservoir; 22.26, 114.163; 160 m a.s.l.; 29 Jun. 2015; Yu-Ying Luo leg.; IBBL YYL00021. • 1 worker; Hong Kong SAR, Tai Tam; 22.2618, 114.2168; 360 m a.s.l.; 27 Jul. 2015; R.H.Lee leg.; Secondary forest, Pitfall trap; IBBL RHL02795. • 1 worker; Hong Kong SAR, The Peak; 22.27603, 114.14199; 400 m a.s.l.; 17 Aug. 2015; R.H.Lee leg.; Secondary Forest, Pitfall trap; IBBL RHL02638. • 1 worker; Hong Kong SAR, Tai Mo Shan; 22.41607, 114.12515; 800 m a.s.l.; 21 Jun. 2016; R.H.Lee leg.; Grassland, Pitfall trap; IBBL RHL03564. • 1 worker; Hong Kong SAR, Lung Fu Shan; 22.27603, 114.14199; 400 m a.s.l.; 11 Jul. 2016; R.H.Lee leg.; Secondary forest, Bait trap; IBBL RHL-SIA-091. • 1 worker; Hong Kong SAR, Southern Shek O; 22.25339, 114.24577; 190 m a.s.l.; 15 Jul. 2016; M.Pierce leg.; Secondary forest, Bait trap; IBBL ANTWEB1009151. • 1 worker; Hong Kong SAR, Deep Water Bay; 22.25483, 114.18338; 107 m a.s.l.; 12 Aug. 2016; M.Pierce leg.; Secondary forest, Hand collection; IBBL ANTWEB1009484. • 1 worker; Hong Kong SAR, Nam Fung Road; 22.2546, 114.1833; 120 m a.s.l.; 20 Aug. 2016; R.H.Lee leg.; Pitfall trap; IBBL RHL003365. • 1 worker; Hong Kong SAR, Deep Water Bay;

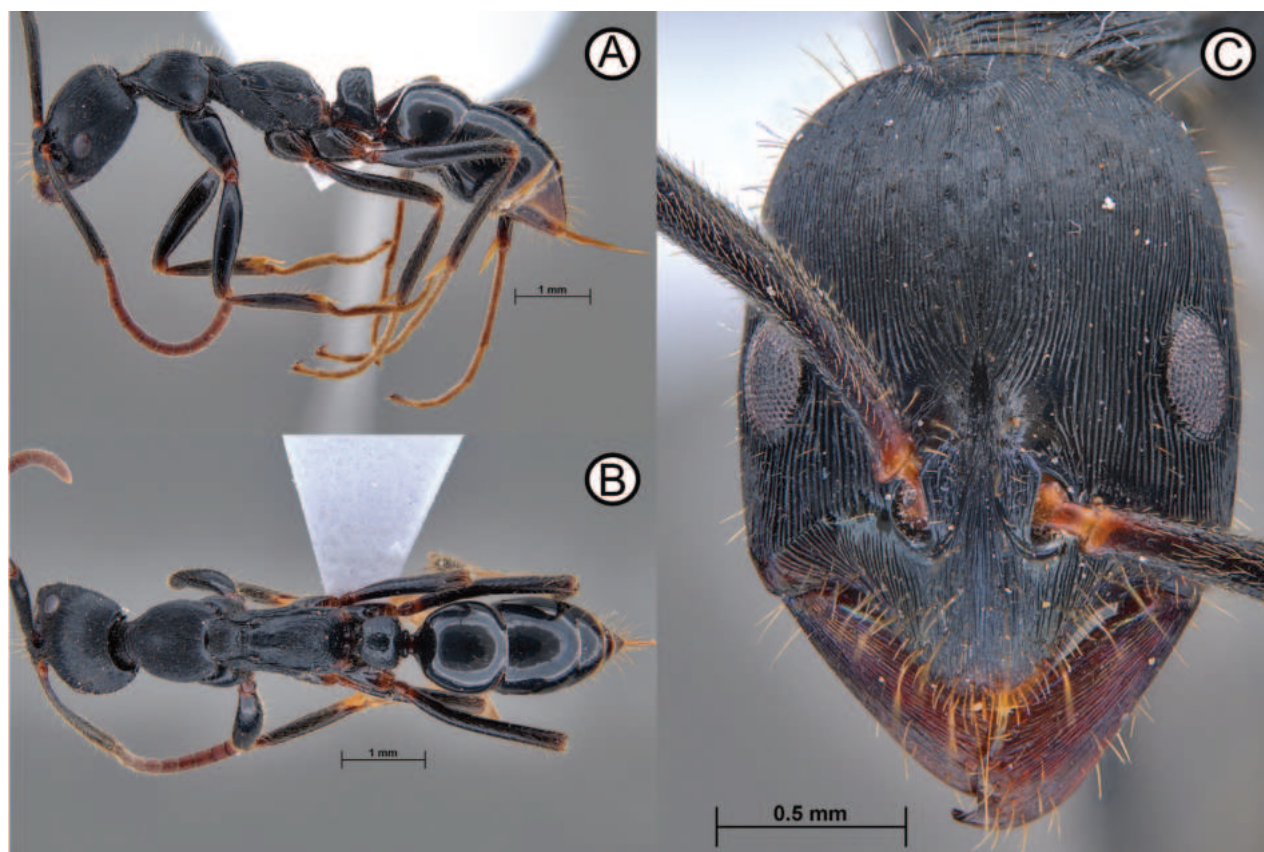


Figure 14. *Leptogenys kitteli* (PFL1T2W3-1) **A** lateral view **B** dorsal view **C** head in full face view.

22.25483, 114.18338; 107 m a.s.l.; 12 Sep. 2016; M. Pierce leg.; Subtropical dry forest, ground forager; IBBL ANTWEB1009664. • 1 worker; Hong Kong SAR, Tai Mo Shan; 22.41099, 114.11917; 737 m a.s.l.; 2 Oct. 2016; C. Leung leg.; Secondary Forest, Bait trap; IBBL ANTWEB1009149. • 2 workers; Hong Kong SAR, Aberdeen; 22.25571, 114.16254; 99 m a.s.l.; 20–23 Oct. 2017; M. Pierce leg.; Secondary forest, Pitfall; IBBL ANTWEB1016994, ANTWEB1009645. • 1 worker; Hong Kong SAR, Tai Mo Shan; 22.4066, 114.12128; 760 m a.s.l.; 3 Oct. 2018; B. Morgan leg.; Hand collection; IBBL ANTWEB1010122. • 3 workers; Hong Kong SAR, Boa Vista; 22.2555, 114.2243; 260 m a.s.l.; 10 Jun. 2020; R. Wang leg.; Pitfall; IBBL RWB1236, RWB1237, RWB1238. • 2 workers; Hong Kong SAR, Pok Fu Lam; 22.26247, 114.1397; 217 m a.s.l.; 7 Apr. 2022; A. I. Weemaels & M.T. Hamer leg.; Secondary Forest, Winkler leaf litter Ex; IBBL PFL1T2W3-1, PFL1T2W5-1. • 6 workers; Hong Kong SAR; Magazine Gap; 22.26819, 114.16578; 255 m a.s.l.; 17 Oct. 2023; C.Y.L. Tse leg.; Young secondary forest, ex. nest; IBBL MTH680.

***Leptogenys kraepelini* Forel, 1905**

Figs 2B, 6A, 15, 21A
new record

Leptogenys (Lobopelta) kraepelini Forel, 1905f: 5 (w.) INDONESIA (Java).

Leptogenys kraepelini baccha [senior synonym] Santschi, 1919: 336 (w.) VIETNAM: Xu and He 2015: 142.

Measurements. Workers ($n = 15$): HL 1.68–1.86; HLL 1.32–1.51; HLA 0.33–0.38; HW 1.09–1.23; CML 0.35–0.43; SL 1.7–2.04; All 0.25–0.31; AFI 0.4–0.5; AFII 0.33–0.39; EL 0.41–0.47; ML 0.78–0.87; PrL 1.03–1.22; PrH 0.63–0.93; PrW 0.97–1.11; WL 2.91–3.26; PeL 0.92–1.07; PeH 0.87–0.99; PeW 0.35–0.65; DPL 0.9–1.02; CI 62.84–67.07; CLI 20.97–24.54; SI 153.66–174.8; OI 29.39–33.12; LPI 89.2–318.31; DPI 39.4–67.12.

Ergatoid queen ($n = 1$): HL 1.63; HLL 1.29; HLA 0.36; HW 1.67; CML 0.4; SL 1.53; All 0.22; AFI 0.35; AFII 0.29; EL 0.42; ML 0.84; PrL 1.05; PrH 0.79; PrW 0.99; WL 2.71; PeL 0.73; PeH 0.84; PeW 0.55; DPL 0.71; CI 102.52; CLI 24.25; SI 91.8; OI 32.87; LPI 114.93; DPI 77.75.

Morphological variation. Specimens collected in Hong Kong match well with the description provided by Forel, 1905 of *L. kraepelini*. However, the sculpture on the propodeum (as ‘sloping surface of the metanotum’ in Forel 1905) is not entirely ‘smooth’ (Forel 1905), but instead with transverse striations of varying degrees of pronounciation from few to many striae. Xu and He (2015) utilised this character (among others) to differentiate *L. kraepelini* from *L. chinensis* (Mayr, 1870), *L. chinensis* having transverse striation and *L. kraepelini* lacking it. Such striations appear absent in the dorsal image of the *L. kraepelini* (CASENT0281936, antweb.org) studied by Xu and He (2015). However, this specimen (from West Java) could represent a morphological extreme for this character. With a large distribution across Southeast Asia, this species likely shows a high degree of morphological variability similar to *L. diminuta* and *L. kitteli*. We suggest that this character should be treated with caution until the holotype specimen and additional material of *L. kraepelini* can be more closely scrutinised. Within Hong Kong, morphological variation appears to be limited. Most variation is associated with colour, with workers varying from reddish brown to jet-black, to black with a blue iridescent shine. The possibility of cryptic species within *L. kraepelini* and *L. chinensis* requires further taxonomic investigation which is not within the scope of this study. As such, despite ergatoids presented here we refrain from describing them.

Comparative notes. This species highly resembles *L. peuqueti* and *L. grohli* within Hong Kong. However, *L. kraepelini* can be separated from both species by its much larger size, the distinctly posteriorly projecting propodeal lobes and the truncated anterior clypeal margin. *Leptogenys kraepelini* has been confused with *L. chinensis* in the past (Xu and He 2015). However, *L. kraepelini* has a rectangular head that does not significantly narrow behind the eyes as in *L. chinensis*; has punctuate sculpture between the clypeus and eyes which *L. chinensis* lacks, and a straight anterolateral clypeal margin which is sinuate in *L. chinensis*. More differing characters will likely be revealed upon closer inspection of type material and the examination of more specimens from across the wider region. Specimens previous determined to be *L. chinensis* from Guangdong were not examined in this study (Wu et al. 2008; Zhao et al. 2009). Such specimens should be re-examined, especially considering *L. kraepelini* is now confirmed from Guangdong and Hong Kong (this study), as well as the previously known misidentifications of *L. chinensis* for *L. kraepelini* (and *L. peuqueti*) in the past.

Distribution. *Leptogenys kraepelini* is widely distributed across Indomalaya, recorded from China (Yunnan and Hong Kong SAR), Vietnam, Laos, Thailand, Malaysia Peninsula, Singapore, Borneo, Sumatra, and Java (Bakhtiar and Chiang 2010; Xu and He 2015; Janicki et al. 2016; Guénard et al. 2017; Khachonpisitsak et al. 2020; Wang et al. 2022). This species is currently absent from

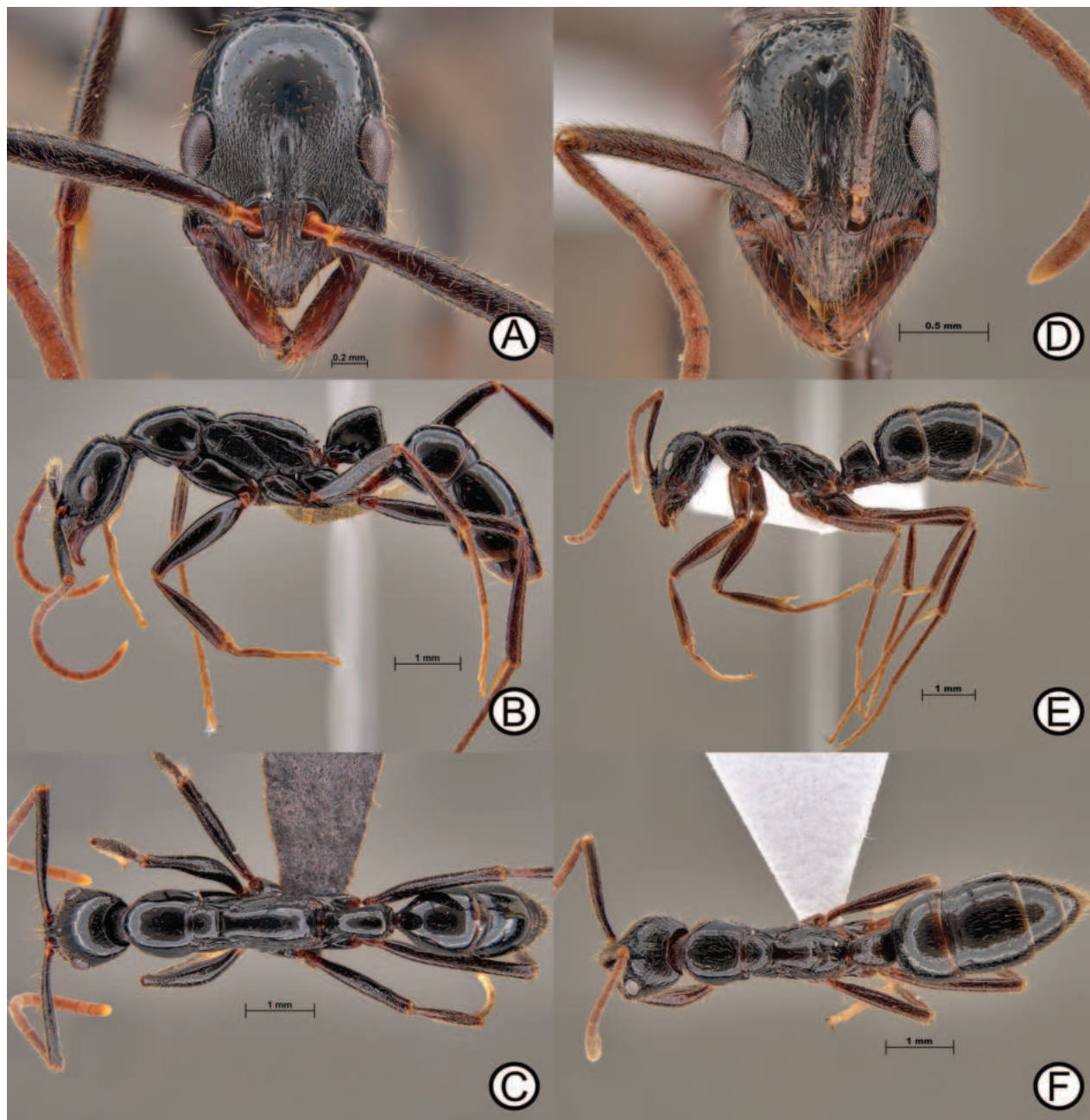


Figure 15. *Leptogenys kraepelini* (RHL00392) and ergatoid (ANTWEB1010172) **A** worker in lateral view **B** worker in dorsal view **C** worker in head in full face view **D** ergatoid in lateral view **E** ergatoid in lateral view and **F** ergatoid in dorsal view.

many southern Chinese provinces which likely reflects sampling effort in these regions, or has been incorrectly identified as *L. chinensis*.

Ecology. This species is known to nest within rotting wood in young to old growth secondary and shrublands but is seemingly absent from highly disturbed environments. Specimens have been collected either individually or in small groups (three individuals) during the day, with colonies reproducing through ergatoid queens (Ito 1997). *Leptogenys kraepelini* appears to have a specialised diet on earwigs (Steghaus-Kovac and Maschwitz 1993) but has been observed preying upon termites in Hong Kong (CYLT pers. obs.).

Material examined. Workers ($n = 38$): CHINA • 1 worker; Hong Kong SAR, The Peak; 13 Jul. 1992; J.R.Fellowes leg.; HKBM MBS006905. • 1 worker; Hong

Kong SAR, Hong Kong Island, The Peak; 24 Sep. 1993; J.R.Fellowes leg.; HKBM MBS015288. • 1 worker; Hong Kong SAR, The Peak; 27 Sep. 1994; J.R.Fellowes leg.; HKBM MBS006660. • 1 worker; Guangdong Prov. Daw U Ling; 28 Apr. 1997; J.R.Fellowes leg.; HKBM MBS015287 • 1 worker; Hong Kong SAR, Victoria Park; 27 Jun. 1999; SK.Yamane leg.; SKYC MBS006658, MBS006659. • 1 worker; Hong Kong SAR, Shing Mun Reservoir; 22.39737, 114.15268; 230 m a.s.l.; 6 Jul. 2011; P.S.Ward leg.; Secondary forest, ex. decay wood; IBBL ANTWEB1010182. • 1 worker; Hong Kong SAR, Shing Mun; 22.39693, 114.153; 240 m a.s.l.; 14 May. 2015; R.H.Lee leg.; Feng Shui Forest, Pitfall trap; IBBL RHL00364, RHL00367, RHL00392, RHL00407. • 1 worker; Hong Kong SAR, Sunset Peak; 22.266, 113.953; 430 m a.s.l.; 3 Jun. 2015; R.H.Lee leg.; Secondary forest, Pitfall trap; IBBL RHL00928. • 1 worker; Hong Kong SAR, Aberdeen Reservoir; 22.259, 114.16; 170 m a.s.l.; 26 Jun. 2015; R.H.Lee leg.; Secondary forest, Pitfall trap; IBBL RHL00861. • 1 worker; Hong Kong SAR, Aberdeen Reservoir; 22.262, 114.16; 180 m a.s.l.; 26 Jun. 2015; R.H.Lee leg.; Secondary forest, Pitfall trap; IBBL RHL01297. • 1 worker; Hong Kong SAR, The Peak; 22.277, 114.143; 450 m a.s.l.; 17 Aug. 2015; R.H.Lee leg.; Secondary forest, Pitfall trap; IBBL RHL02628. • 1 worker; Hong Kong SAR, Kap Lung; 22.41666, 114.10222; 256 m a.s.l.; 19 Sep. 2015; T.Tsang leg.; Winkler leaf litter Ex; IBBL TT01228. • 1 worker; Hong Kong SAR, Tai Tam; 22.396, 114.093; 420 m a.s.l.; 26 Oct. 2015; R.H.Lee leg.; Bamboo, Pitfall trap; IBBL RHL02778. • 1 worker; Hong Kong SAR, Shing Mun; 22.39693, 114.153; 240 m a.s.l.; 17 May. 2016; R.H.Lee leg.; Feng Shui Forest, Winkler leaf litter Ex; IBBL RHL03204. • 1 worker; Hong Kong SAR, Lung Fu Shan; 22.27603, 114.14199; 400 m a.s.l.; 11 Jul. 2016; R.H.Lee leg.; Secondary forest, Winkler leaf litter Ex; IBBL RHL-SIA-89. • 1 worker; Hong Kong SAR, Tai Lam Country Park; 22.37598, 114.04713; 200 m a.s.l.; 3 Nov. 2017; R.Cheung & M.Pierce leg.; Winkler leaf litter Ex; HKBM MBS011437. • 1 worker; Hong Kong SAR, Wong Lung Hang; 22.2668, 113.9524; 400 m a.s.l.; 11 May. 2023; M.T.Hamer leg.; Young secondary forest, Hand collection; IBBL ANTWEB101020. • 1 worker; Hong Kong SAR, Lantau; A Po Long; 22.28186, 113.9835; 200 m a.s.l.; 5 Jun. 2023; M.T.Hamer leg.; Young secondary forest, Hand collection; IBBL ANTWEB1010131, ANTWEB1010132, ANTWEB1010176. • 1 worker; Hong Kong SAR, Sunset Peak, Wong Lung Hang path; 22.2602, 113.95906; 650 m a.s.l.; 7 Jul. 2023; M.T.Hamer leg.; Montane forest, Hand collection; IBBL ANTWEB1010121. • 5 workers; Hong Kong SAR, Tai Mo Shan; 22.40585, 114.1063; 517 m a.s.l.; 26 Aug. 2023; M.T.Hamer leg.; Secondary forest, ex. Decay wood; IBBL MTH70, MTH157. • 1 worker; Hong Kong SAR, Tai Mo Shan; 22.40403, 114.10691; 471 m a.s.l.; 3 Sep. 2023; M.T.Hamer leg.; Secondary forest, Nest ex. decay log; IBBL ANTWEB1010169, ANTWEB1010174. • 1 worker; Hong Kong SAR, Tai Mo Shan; Kap Lung Forest Trail; 22.41088, 114.10451; 450 m a.s.l.; 3 Sep. 2023; M.T.Hamer leg.; Secondary forest, ex.decaying log; IBBL MTH276. • 1 worker; Hong Kong SAR, Severn Road; 22.27044, 114.15621; 380 m a.s.l.; 5 Sep. 2023; C.Y.L.Tse leg.; Nest ex.; IBBL ANTWEB1010168, ANTWEB1010175. • 4 workers; Hong Kong SAR, Wong Lung Hang; 22.26964, 113.95248; 265 m a.s.l.; 5 Sep. 2023; M.T.Hamer leg.; Secondary forest, ex .decaying log; IBBL MTH308, MTH323, MTH335, MTH336.

Ergatoids ($n = 2$): CHINA • 1 ergatoid; Hong Kong SAR, Tai Mo Shan; Kap Lung Forest Trail; 22.41088, 114.10451; 450 m a.s.l.; 3 Sep. 2023; M.T.Hamer leg.; Secondary forest, nest ex. decaying log; IBBL MTH276. • 1 ergatoid; Hong Kong SAR, Severn Road; 22.27044, 114.15621; 380 m a.s.l.; 5 Sep. 2023; C.Y.L.Tse leg.; Nest ex.; IBBL ANTWEB1010172.

***Leptogenys laeviterga* Zhou et al., 2012**

Figs 7A, 16, 21B
new record

Leptogenys laeviterga Zhou et al., 2012: 888, figs 1–3 (w.) CHINA (Guangxi).

Measurements. Worker ($n = 1$): HL 1.58; HLL 1.22; HLA 0.31; HW 1.07; CML 0.4; SL 1.99; All 0.28; AFI 0.43; AFII 0.34; EL 0.28; ML 0.92; PrL 1.03; PrH 0.65; PrW 0.93; WL 2.78; PeL 0.76; PeH 0.84; PeW 0.59; DPL 0.62; CI 67.76; CLI 25.35; SI 185.26; OI 22.89; LPI 110.58; DPI 94.2.

Morphological variation. Owing to the poor quality and quantity of specimens collected, little is known about the morphological variability of this species.

Comparative notes. *Leptogenys laeviterga* is superficially similar to *L. diminuta* owing to similarly shaped triangular mandibles, broad petiole shape, as well as overall body size. However, *L. laeviterga* is readily differentiated by the distinct and conspicuous median clypeal carina; lack of costulate sculpture on the head, lack of teeth on the mandibular masticatory margin, and longer scapes (SL 1.90–1.99). Within the wider Indomalayan *Leptogenys* fauna, *L. laeviterga* is morphologically similar to *L. sunzii* Xu & He, 2015, but can be differentiated by the truncated clypeal apex in *L. laeviterga* (pointed and convex in *L. sunzii*), the smaller eyes (larger in *L. sunzii*), and the higher than long petiole in *L. sunzii* whereas the petiole as long as high in *L. laeviterga* (Xu and He 2015).

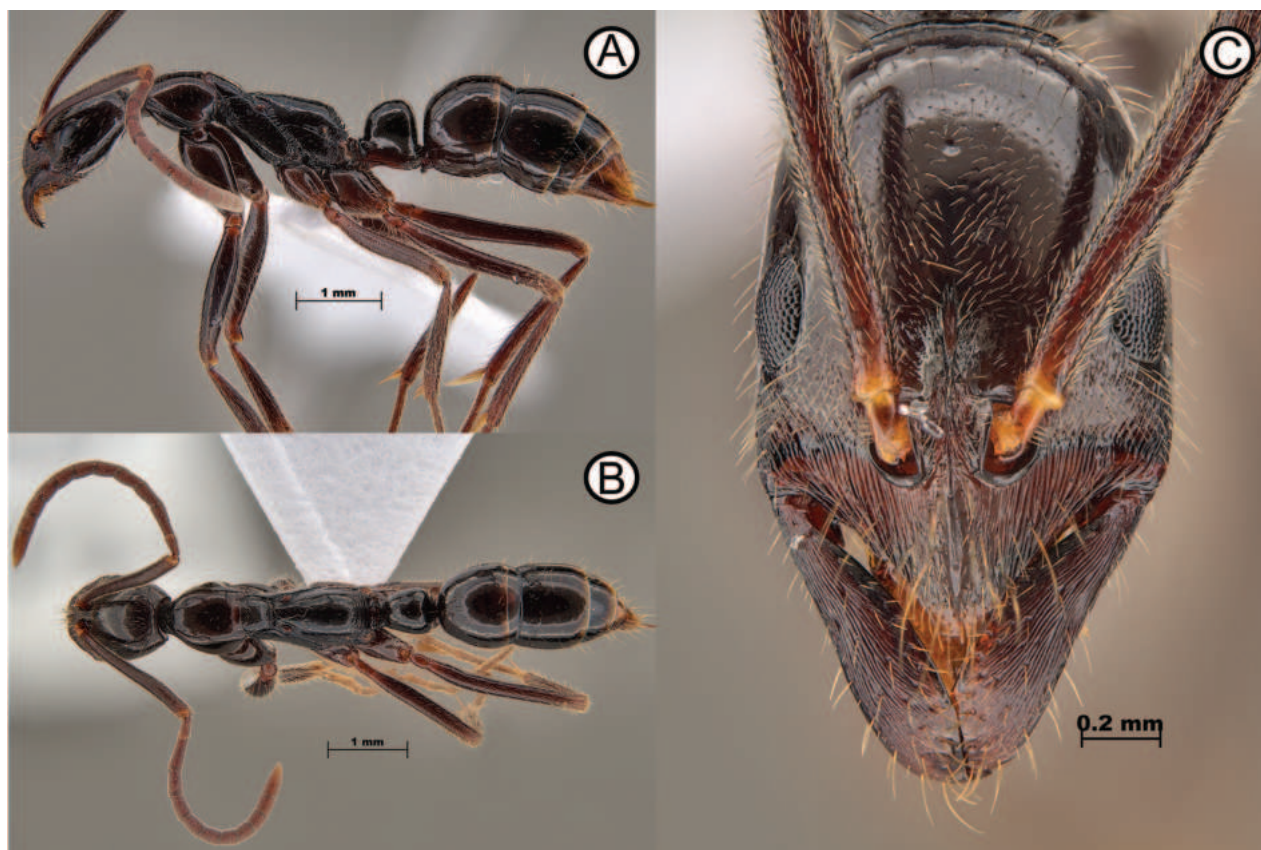


Figure 16. *Leptogenys laeviterga* (ANTWEB1010142) **A** lateral view **B** dorsal view **C** head face view.

Distribution. Previously, *L. laeviterga* was only known from its type locality in Darning Mountain National Nature Reserve, Guangxi (Zhou et al. 2012). Here we provide the first record of the species from Hong Kong, representing the eastern most record for this species thus far. The species should therefore be expected from Guangdong and other neighbouring provinces in China.

Ecology. Very little is known of the ecology of *L. laeviterga*. Specimens (but not the whole colony) from Hong Kong were obtained from within a decaying log from an old growth secondary forest on the southern slopes of Tai Mo Shan (471 m a.s.l.), Hong Kong. Male specimens were obtained on the day of collection. Considering the sampling effort undertaken in Hong Kong, it is surprising that more *L. laeviterga* have not been collected, indicating the potential rarity of this species.

Material examined. Workers ($n = 3$): CHINA • 3 workers; Hong Kong SAR, Tai Mo Shan; 22.40403, 114.10691; 471 m a.s.l.; 26 Aug. 2023; M.T.Hamer leg.; Secondary forest, ex. decay log; IBBL ANTWEB1010142, ANTWEB1010155, ANTWEB1010156.

***Leptogenys peuqueti* (André, 1887)**

Figs 3B, D, 17, 21C

Lobopelta peuqueti André, 1887: 292 (w.) Vietnam.

Leptogenys: Emery, 1895m: 461.

Leptogenys minchinii [senior synonym] Forel, 1900f: 308 (w.) INDIA, MYANMAR: Xu and He 2015: 145. Of *Leptogenys peuqueti watsoni* Forel, 1900f: 309 (w.) MYANMAR: Xu and He 2015: 145.

Measurements. Worker ($n = 15$): HL 1.15–1.31; HLL 0.88–1.02; HLA 0.17–0.28; HW 0.75–0.87; CML 0.23–0.29; SL 1.19–1.39; AII 0.17–0.21; AFI 0.34–0.39; AFII 0.25–0.3; EL 0.29–0.37; ML 0.5–0.65; PrL 0.73–0.85; PrH 0.51–0.74; PrW 0.6–0.76; WL 2.02–2.2; PeL 0.67–0.75; PeH 0.52–0.63; PeW 0.33–0.45; DPL 0.66–0.75; CI 64.63–69.92; CLI 19.91–22.41; SI 156.24–167.09; OI 30.69–37.14; LPI 74.93–90.7; DPI 47.94–65.32.

Morphological variation. Morphological variation with *L. peuqueti* specimens collected from Hong Kong consists of overall size variation, with some specimens being larger and more robust than others collected. Such variation can be seen with the dorsal pronotal width and Webers length (PrW 0.6–0.76; WL 2.02–2.2). Additional variation is associated with colour, with workers varying from jet-black, to black with an iridescent blue shine.

Comparative notes. *Leptogenys peuqueti* is most similar to *L. grohli* and *L. kraepelini* within Hong Kong and Macao, being distinguishable from *L. grohli* by the smooth head dorsum, larger eyes, shorter tubular setae on the anterior clypeal margin, and convex lateral head margins. *Leptogenys peuqueti* highly resembles *L. kraepelini*, but lacks the truncated anterior clypeal margin found in *L. kraepelini*, the posteriorly projecting propodeal lobes and is overall smaller. Within the wider Indomalayan *Leptogenys* species, *L. peuqueti* is most similar to *L. confucii*, as well as other members of the *L. chinensis* group. *Leptogenys peuqueti* can be differentiated by the smooth head dorsum, meso- and metathorax, and propodeum, as well as its black colour.

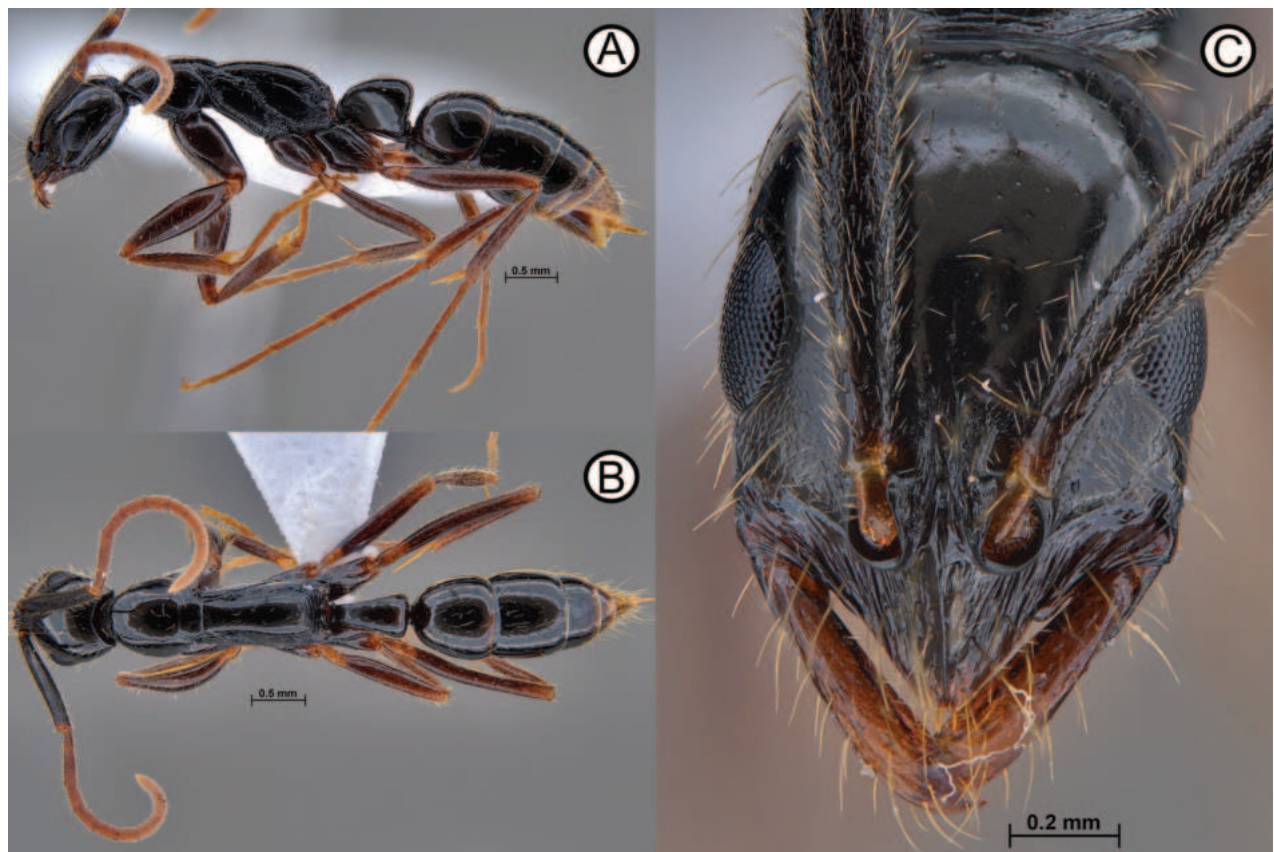


Figure 17. *Leptogenys peuqueti* (FK1T2W5-1) **A** lateral view **B** dorsal view **C** head in full face view.

Distribution. A very wide-ranging species in Indomalaya, *L. peuqueti* is recorded from several Chinese provinces including Fujian, Guangdong, Guangxi, Hainan, Hong Kong Hubei, Hunan, Macao, Yunnan, and Zhejiang (Guénard and Dunn 2012; Xu and He 2015; Janicki et al. 2016; Guénard et al. 2017; Brassard et al. 2021). Other countries include Bangladesh, Bhutan, India (Andaman Islands, Kerala, Meghalaya, Sikkim, and West Bengal), Indonesia (Java), Malaysia (Peninsular and Bornean parts), Myanmar, The Philippines, Singapore, Sri Lanka, and Vietnam (Bakhtiar and Chiang 2010; Janicki et al. 2016; Guénard et al. 2017; Wang et al. 2022). Further sampling effort across the Oriental region will likely produce new country level records of this species (e.g., Cambodia, Laos, Thailand).

Ecology. *Leptogenys peuqueti* is the most common *Leptogenys* recorded from Hong Kong, collected from a wide variety of habitats including forests, shrubland as well as disturbed urban sites. Workers are known to foraging individually but will recruit small numbers of workers to tackle larger prey items (Janssen et al. 1997; MTH pers. obs.). Workers have been noted to feed upon isopods in Hong Kong. Nests have been found within rotting logs, under rocks and within soil (often underneath objects). Colonies are queenless, instead reproducing through gamergates (Ito 1997). One colony collection contained 67 workers, 20 cocoons and four larvae (MTH271), correlating with Ito (1997) who found the number of workers in *L. peuqueti* colonies to range from 5 and 97.

Material examined. Workers ($n = 134$): CHINA • 1 worker; Hong Kong SAR, Sunset Peak; 25 Jul. 1992; J.R.Fellowes leg.; HKBM MBS06893. • 1 worker;

Hong Kong SAR, Lion Rock; 27 Aug. 1992; J.R.Fellowes leg.; HKBM MBS006901. • 1 worker; Hong Kong SAR, Lion Rock; 27 Aug. 1992; J.R.Fellowes leg.; HKBM MBS006902. • 1 worker; Hong Kong SAR, Lion Rock; 27 Aug. 1992; J.R.Fellowes leg.; HKBM MBS006903. • 1 worker; Guangdong Prov., Ding Hu Shan; 25 Sep. 1995; J.R.Fellowes leg.; HKBM MBS015247. • 1 worker; Hong Kong SAR, Luk Tei Tong, Lantau; 7 Oct. 1996; J.R.Fellowes leg.; IBBL MBS006606. • 1 worker; Hong Kong SAR, Lantau, Tong Fuk; 4 Nov. 1996; J.R.Fellowes leg.; HKBM MBS015246. • 1 worker; Hong Kong SAR, Tong Fuk, Lantau Island; 4 Nov. 1996; J.R.Fellowes leg.; IBBL MBS006889. • 1 worker; Hong Kong SAR, Tong Fuk, Lantau Island; 4 Nov. 1996; J.R.Fellowes leg.; HKBM MBS006890. • 1 worker; Hong Kong SAR, Lantau, Tei Tong Tsai; 5 Nov. 1996; J.R.Fellowes leg.; HKBM MBS015261. • 1 worker; Hong Kong SAR, Nam Long, Western New Territories; 7 Nov. 1996; J.R.Fellowes leg.; HKBM MBS015255. • 1 worker; Hong Kong SAR, Kadoorie Farm Botanical Garden; 460 m a.s.l.; 21 Sep. 1999; J.R.Fellowes leg.; HKBM MBS015254. • 1 worker; Hong Kong SAR, The Peak; 10 Sep. 2000; SK. Yamane leg.; SKYC ANTWEB1010194. • 1 worker; Hong Kong SAR, Castle Peak; 22.391, 113.958; 230 m a.s.l.; 30 Jun. 2015; R.H.Lee leg.; Shrubland, Pitfall trap; IBBL RHL01178. • 1 worker; Hong Kong SAR, Castle Peak; 22.391, 113.958; 230 m a.s.l.; 30 Jun. 2015; R.H.Lee leg.; Shrubland, Pitfall trap; IBBL RHL01200. • 1 worker; Hong Kong SAR, Discovery Bay; 22.31, 114.018; 5 m a.s.l.; 2 Jul. 2015; R.H.Lee leg.; Grassland, Pitfall trap; IBBL RHL01907. • 1 worker; Hong Kong SAR, Tai Tam; 22.262, 114.217; 370 m a.s.l.; 27 Jul. 2015; R.H.Lee leg.; Secondary forest, Pitfall trap; IBBL RHL02792. • 2 worker; Hong Kong SAR, Tap Mun; 22.481, 114.361; 100 m a.s.l.; 28 Jul. 2015; R.H.Lee leg.; Shrubland, Pitfall trap; IBBL RHL01540, RHL01547. • 1 worker; Hong Kong SAR, Tap Mun; 22.477, 114.363; 45 m a.s.l.; 28 Jul. 2015; R.H.Lee leg.; Shrubland, Pitfall trap; IBBL RHL01605, RHL01619. • 1 worker; Hong Kong SAR, Chap Lap Kok; 22.29301, 113.93407; 50 m a.s.l.; 17 Sep. 2015; B.Morgan leg.; Winkler leaf litter Ex; IBBL BMW00181. • 1 worker; Hong Kong SAR, Chap Lap Kok; 22.29301, 113.93407; 50 m a.s.l.; 27 Sep. 2015; B.Morgan leg.; Hand collection; IBBL BMW00247, BMW00248. • 1 worker; Hong Kong SAR, Nam Fung Road; 22.25553, 114.18015; 108 m a.s.l.; 1 Oct. 2015; T.Tsang leg.; Winkler leaf litter Ex; IBBL TT01495. • 1 worker; Hong Kong SAR, Chap Lap Kok; 22.29301, 113.93407; 50 m a.s.l.; 12 Oct. 2015; B.Morgan leg.; Winkler leaf litter Ex; IBBL BMW01086. • 1 worker; Hong Kong SAR, Sha Shan; 22.449, 114.145; 50 m a.s.l.; 3 Nov. 2015; R.H.Lee leg.; Feng Shui Forest, Pitfall trap; IBBL RHL02755. • 1 worker; Hong Kong SAR, Chap Lap Kok; 22.2947, 113.9336; 20 m a.s.l.; 19 Mar. 2016; B.Morgan leg.; Winkler leaf litter Ex; IBBL BMW00715. • 1 worker; Hong Kong SAR, Chap Lap Kok; 22.2929, 113.9347; 60 m a.s.l.; 5 Apr. 2016; B.Morgan leg.; Winkler leaf litter Ex; IBBL BMW02365. • 1 worker; Hong Kong SAR, Chap Lap Kok; 22.2918, 113.9333; 30 m a.s.l.; 19 Apr. 2016; B.Morgan leg.; Hand collection; IBBL BMW00581. • 4 worker; Hong Kong SAR, Nam Fung Road; 22.2546, 114.1833; 120 m a.s.l.; 20 Aug. 2016; R.H.Lee leg.; Feng Shui Forest, Pitfall trap; IBBL RHL03518, RHL03360, RHL003381, RHL03391. • 1 worker; Hong Kong SAR, Southern Aberdeen; 22.25109, 114.16259; 99 m a.s.l.; 19 Sep. 2016; M.Pierce leg.; subtropical dry forest, Hand collection; IBBL ANTWEB1009470. • 1 worker; Hong Kong SAR, Tai Po: Kadoorie; 22.43332, 114.1172; 191 m a.s.l.; 21 Sep. 2016; M.Pierce leg.; botanical garden, Hand collection; IBBL ANTWEB1009083. • 2 worker; Hong Kong SAR, Pak Ngan Heung; 22.271, 113.9891; 35 m a.s.l.; 25

Oct. 2016; R.H.Lee leg.; Feng Shui Forest, Pitfall trap; IBBL RHL003347, RHL03508. • 1 worker; Hong Kong SAR, Pak Ngan Heung; 22.27099, 113.98911; 35 m a.s.l.; 25 Oct. 2016; R.H.Lee leg.; Feng Shui Forest, Pitfall trap; IBBL RHL03509. • 1 worker; Hong Kong SAR, Mai Po; 22.487, 114.0392; 1 m a.s.l.; 26–20 Oct. 2016; R.H.Lee leg.; Wetlands, Pitfall trap; IBBL RHL002943. • 1 worker; Hong Kong SAR, Chap Lap Kok; 22.2947, 113.9336; 20 m a.s.l.; 27 Nov. 2016; B.Morgan leg.; Hand collection; IBBL BMW02465. • 1 worker; Hong Kong SAR, Soko Island; 22.18258, 113.91257; 3 m a.s.l.; 2 Dec. 2016; M.Pierce leg.; Forest, Hand collection; IBBL ANTWEB1009836. • 1 worker; Hong Kong SAR, Chap Lap Kok; 22.2947, 113.9336; 30 m a.s.l.; 28 Feb. 2017; B.Morgan leg.; Winkler leaf litter Ex; IBBL BMW02022. • 1 worker; Hong Kong SAR, Lok Ma Chau; 22.51023, 114.06352; 1 m a.s.l.; 9 Apr. 2017; M.Pierce leg.; Pitfall; IBBL ANTWEB1016941, ANTWEB1017005. • 1 worker; Hong Kong SAR, Lok Ma Chau; 22.51044, 114.06348; 21 m a.s.l.; 9–12 May.2017; M.Pierce leg.; Pitfall; IBBL ANTWEB1016958. • 2 worker; Hong Kong SAR, Lok Ma Chau; 22.51117, 114.06576; 6 m a.s.l.; 11–14 Aug. 2017; M.Pierce leg.; Wetland, Pitfall; IBBL ANTWEB1017019, ANTWEB1009760. • 1 worker; Hong Kong SAR, Lion Rock; 22.357, 114.17504; 140 m a.s.l.; 15 Aug. 2017; R.H.Lee leg.; Secondary forest, Pitfall trap; IBBL RHL03526. • 1 worker; Hong Kong SAR, Pak Tam Chung; 22.39474, 114.32314; 70 m a.s.l.; 6 Sep. 2017; R.H.Lee leg.; Shrubland, Pitfall trap; IBBL RHL03492. • 3 worker; Hong Kong SAR, Mai Po; 22.4849, 114.03298; 3 m a.s.l.; 12–15 Sep. 2017; M.Pierce leg.; Pitfall; IBBL ANTWEB1009693, ANTWEB1016943, ANTWEB1009657. • 2 worker; Hong Kong SAR, Mai Po; 22.4849, 114.03298; 3 m a.s.l.; 12–15 Sep. 2017; M.Pierce leg.; Pitfall; IBBL ANTWEB1009657, ANTWEB1009713. • 1 worker; Hong Kong SAR, Mai Po; 22.49413, 114.04014; 3 m a.s.l.; 26–29 Sep.2017; M.Pierce leg.; Pitfall; IBBL ANTWEB1009710. • 4 workers; Hong Kong SAR, Mai Po; 22.49473, 114.03919; 3 m a.s.l.; 26–29 Sep.2017; M.Pierce leg.; Pitfall; IBBL ANTWEB1009614, ANTWEB1009688, ANTWEB1009616, ANTWEB1009783. • 1 worker; Hong Kong SAR, Mai Po; 22.49413, 114.04014; 3 m a.s.l.; 26–29 Sep.2017; M.Pierce leg.; Pitfall; IBBL ANTWEB1009782. • 2 worker; Hong Kong SAR, Tung Ping Chau; 22.5382, 114.4365; 30 m a.s.l.; 2 Oct. 2017; R.Cheung & B.Morgan leg.; Winkler leaf litter Ex; HKBM MBS011433, MBS011434. • 1 worker; Hong Kong SAR, Tung Ping Chau; 22.5443, 114.4317; 1 m a.s.l.; 2 Oct. 2017; R.Cheung & B.Morgan leg.; Winkler leaf litter Ex; HKBM MBS011435. • 2 worker; Hong Kong SAR, Penny's Bay; 22.32588, 114.03384; 22 m a.s.l.; 10–13 Oct.2017; M.Pierce leg.; Pitfall; IBBL ANTWEB1009781, ANTWEB1017072. • 1 worker; Hong Kong SAR, Kam Shan Country Park; 22.3562, 114.15167; 170 m a.s.l.; 18 Oct. 2017; R.Cheung leg.; Winkler leaf litter Ex; HKBM MBS011436. • 2 worker; Hong Kong SAR, Penny's Bay; 22.32719, 114.0336; 21 m a.s.l.; 23–26 Oct.2017; M.Pierce leg.; Pitfall; IBBL ANTWEB1016974, ANTWEB1017001. • 2 worker; Hong Kong SAR, Lung Fu Shan; 22.279, 114.1361; 242 m a.s.l.; 20 Jun. 2019; K.Chan leg.; IBBL ANTWEB1010118, ANTWEB1010119. • 3 worker; Hong Kong SAR, Luk Keng Chan Uk; 22.5183, 114.2187; 10 m a.s.l.; 5 Aug. 2020; R.Wang leg.; IBBL RWB1239, RWB1240, RWB1241. • 1 worker; Hong Kong SAR, Mai Po; 22.47912, 114.03847; 5 m a.s.l.; 18 Aug. 2021; T.Bogar leg.; Grassland, Pitfall; IBBL ANTWEB1010207. • 1 worker; Hong Kong SAR, Mai Po; 22.4801, 114.03814; 5 m a.s.l.; 18 Aug. 2021; T.Bogar leg.; Grassland, Pitfall; IBBL ANTWEB1010208. • 2 worker; Hong Kong SAR, Lok Ma Chau; 22.51093, 114.0652; 5 m a.s.l.; 2 Sep.

2021; T.Bogar leg.; Grassland, Pitfall; IBBL ANTWEB1010210. • 1 worker; Hong Kong SAR, Lok Ma Chau; 22.51106, 114.0656; 5 m a.s.l.; 2 Sep. 2021; T.Bogar leg.; Grassland, Pitfall; IBBL ANTWEB1010211. • 3 worker; Hong Kong SAR, Lok Ma Chau; 22.51093, 114.0652; 5 m a.s.l.; 2 Sep. 2021; T.Bogar leg.; Grassland, Pitfall; IBBL ANTWEB1010212, ANTWEB1010214, ANTWEB1010219. • 1 worker; Hong Kong SAR, Lok Ma Chau; 22.51106, 114.0656; 5 m a.s.l.; 2 Sep. 2021; T.Bogar leg.; Grassland, Pitfall; IBBL ANTWEB1010221. • 1 worker; Hong Kong SAR, Wetlands Park; 22.47236, 114.00401; 1 m a.s.l.; 7 Sep. 2021; A. I. Weemaels & M.T.Hamer leg.; Wetlands, Winkler leaf litter Ex; IBBL WP1T2W2-7. • 1 worker; Hong Kong SAR, Mai Po; 22.47957, 114.03742; 5 m a.s.l.; 14 Sep. 2021; T.Bogar leg.; Grassland, Pitfall; IBBL ANTWEB1010206. • 1 worker; Hong Kong SAR, Lok Ma Chau; 22.51076, 114.06466; 5 m a.s.l.; 16 Sep. 2021; T.Bogar leg.; Grassland, Pitfall; IBBL ANTWEB1010217. • 1 worker; Hong Kong SAR, Lok Ma Chau; 22.51076, 114.06466; 5 m a.s.l.; 16 Sep. 2021; T.Bogar leg.; Grassland, Pitfall; IBBL ANTWEB1010218. • 1 worker; Hong Kong SAR, Lok Ma Chau; 22.51057, 114.06412; 5 m a.s.l.; 16 Sep. 2021; T.Bogar leg.; Grassland, Pitfall; IBBL ANTWEB1010220. • 2 worker; Hong Kong SAR, Lok Ma Chau; 22.51038, 114.06371; 5 m a.s.l.; 28 Sep. 2021; T.Bogar leg.; Grassland, Pitfall; IBBL ANTWEB1010213, ANTWEB1010215. • 1 worker; Hong Kong SAR, Lok Ma Chau; 22.51176, 114.06592; 5 m a.s.l.; 29 Sep. 2021; T.Bogar leg.; Grassland, Pitfall; IBBL ANTWEB1010216. • 1 worker; Hong Kong SAR, Mai Po; 22.48365, 114.03868; 5 m a.s.l.; 2 Oct. 2021; T.Bogar leg.; Grassland, Pitfall; IBBL ANTWEB1010209. • 1 worker; Hong Kong SAR, Cheng Chau Island; 22.19814, 114.0199; 20 m a.s.l.; 25 Nov. 2021; M.T.Hamer leg.; Garden, ex. Decay wood; IBBL MTH635. • 1 worker; Hong Kong SAR, Fung Kong; 22.51322, 114.0937; 30 m a.s.l.; 18 May. 2022; A. I. Weemaels leg.; Young secondary forest, Winkler leaf litter Ex; IBBL FK1T2W5-1. • 2 workers; Hong Kong SAR, Fanling Golf Course; 22.49009, 114.10847; 54 m a.s.l.; 23–25 May. 2022; A. I. Weemaels & M.T.Hamer leg.; Old secondary forest, Pitfall trap; IBBL FGE1SQ2PF4-1. • 1 worker; Hong Kong SAR, Wai Tsai; 22.48284, 114.06153; 29 m a.s.l.; 29 Jun. 2022; M.T.Hamer leg.; Vacuum; IBBL WT2SQ1GVAC3-1. • 1 worker; Hong Kong SAR, Fung Kong; 22.5322, 114.0937; 47 m a.s.l.; 25 Jul. 2022; A. I. Weemaels & M.T.Hamer leg.; Young secondary, Winkler leaf litter Ex; IBBL FK3GC7-17. • 1 worker; Hong Kong SAR, Tai Po Kau Headland; 22.43841, 114.19261; 45 m a.s.l.; 18 Aug. 2022; M.T.Hamer leg.; Old secondary forest, Log Sift; IBBL TPK4GC16-1. • 1 worker; Hong Kong SAR, Tai Po Kau Headland; 22.43471, 114.19264; 52 m a.s.l.; 18 Aug. 2022; M.T.Hamer leg.; Old secondary forest, Log Sift; IBBL TPK4GC17-4. • 2 worker; Hong Kong SAR, Tai Po Kau Headland; 22.43841, 114.19261; 45 m a.s.l.; 18–24 Aug.2022; M.T.Hamer & T.S.R.Silva leg.; Old secondary forest, Pitfall trap; IBBL TPK4SQ1PF4-8, TPK4SQPF1-9. • 4 workers; Hong Kong SAR, Tai Mo Shan; 22.40346, 114.1068; 464 m a.s.l.; 26 Aug. 2023; M.T.Hamer leg.; Secondary forest, ex. Decay wood; IBBL MTH159. • 5 workers; Hong Kong SAR, Lantau; 22.25157, 113.9407; 273 m a.s.l.; 28 Aug. 2023; M.T.Hamer leg.; Young secondary, ex. Decaying log; IBBL MTH214. • 1 worker; Hong Kong SAR, Lantau; 22.2516, 113.94070; 273 m a.s.l.; 28 Aug. 2023; M.T.Hamer leg.; Young secondary forest, ex. Nest; IBBL MTH192. • 5 workers; Hong Kong SAR, Shui Hau; 22.2149, 113.91580 56 m a.s.l.; 31 Aug. 2023; M.T.Hamer leg.; un. Log & ex. Soil, Young secondary forest IBBL MTH271. • 5 worker; Hong Kong SAR, Tai Mo Shan; 22.40403, 114.10691; 471 m a.s.l.; 03 Sep. 2023; M.T.Hamer leg.; sec-

ondary forest, ex. Decaying log; IBBL MTH275. • 1 worker; Hong Kong SAR, Guilford Road; 22.2649, 114.16690; 380 m a.s.l.; 05 Sep. 2023; C.Y.L.Tse leg.; urban green space, ex. Nest; IBBL MTH363. • 5 workers; Hong Kong SAR, Fanling Golf Course; 22.4915, 114.11977; 40 m a.s.l.; 27 Sep. 2023; M.T.Hamer leg.; Old secondary forest, un. Log & ex. Soil; IBBL MTH621.

***Leptogenys rufida* Zhou et al., 2012**

Figs 2A, 3A, C, 18, 21D

new record

Leptogenys rufida Zhou et al., 2012: 891, figs 4–6 (w.) China (Guangxi).

Ergatoid description. With characters of worker but head more square, not as long as in worker. Clypeus terminating in less convex point apically. Propodeum shorter; convex in lateral view. Petiole nodiform, distinctly higher than long in lateral view; wider than long in dorsal view; anterior margin straight in lateral view. Metasomal segments III–VII enlarged, segment III distinctly wider than petiole. Same colour as the worker (Zhou et al. 2012).

Measurements. Workers ($n = 8$): HL 0.93–1.01; HLL 0.76–0.8; HLA 0.18–0.21; HW 0.64–0.67; CML 0.19–0.21; SL 0.84–0.92; All 0.17–0.19; AFI 0.13–0.15; AFII 0.12–0.14; EL 0.16–0.18; ML 0.45–0.46; PrL 0.53–0.6; PrH 0.38–0.44; PrW 0.56–0.59; WL 1.38–1.49; PeL 0.46–0.51; PeH 0.42–0.56; PeW 0.35–0.42; DPL 0.42–0.48; CI 64.29–68.17; CLI 19.36–22.51; SI 129.66–141.82; OI 20.78–23.37; LPI 82.61–114.29; DPI 76.76–90.83.

Ergatoid paratype ($n = 1$): HL 1.04; HLL 0.78; HLA 0.21; HW 0.74; CML 0.25; SL 0.89; All 0.18; AFI 0.14; AFII 0.13; EL 0.19; ML 0.52; PrL 0.66; PrH 0.45; PrW 0.61; WL 1.5; PeL 0.43; PeH 0.61; PeW 0.5; DPL 0.25; CI 71.22; CLI 23.77; SI 120.41; OI 24.55; LPI 141.92; DPI 202.01.

Morphology. Little to no variation is detected with the specimens examined, other than subtle differences in the development of the longitudinal ribbing across the mesonotal notch, however in no specimens was this character absent.

Comparative notes. *Leptogenys rufida* is the smallest *Leptogenys* known from Hong Kong (WL 1.38–1.48) and is further recognisable by the following combined morphological characters; subquadrate petiole with a broadly rounded anterodorsal corner, rugose meso- and metapleural, head dorsum punctate, with relatively small eyes (EL 0.16–0.18). This species could be mistaken for *L. grohli* due to the ribbing across the notopropodeal sulcus, punctate head dorsum and small eyes, but *L. rufida* is smaller, with a more sculptured meso- and metapleural, and flagellomere segment I is as long as flagellomere segment II, shorter clypeal median lobe length (CML 0.19–0.21), and a petiole that is as high as long in lateral view (LPI 82.61–114.29), and as wide as long in dorsal view (DPI 76.76–90.83).

Across the Indochinese *Leptogenys* fauna, *L. rufida* is most similar to members of the *L. zhuangzii* species group (*L. mengzii* Xu, 2000, *L. laozii* Xu, 2000, and *L. zhuangzii* Xu, 2000), and can be differentiated by the following combined characters; petiole in lateral view as long as high, anterodorsal margin distinctly convex, sculptured meso- and metapleural, and red colour. *Leptogenys rufida* and *L. confucii* can be differentiated by the triangular shaped petiole of *L. confucii*,

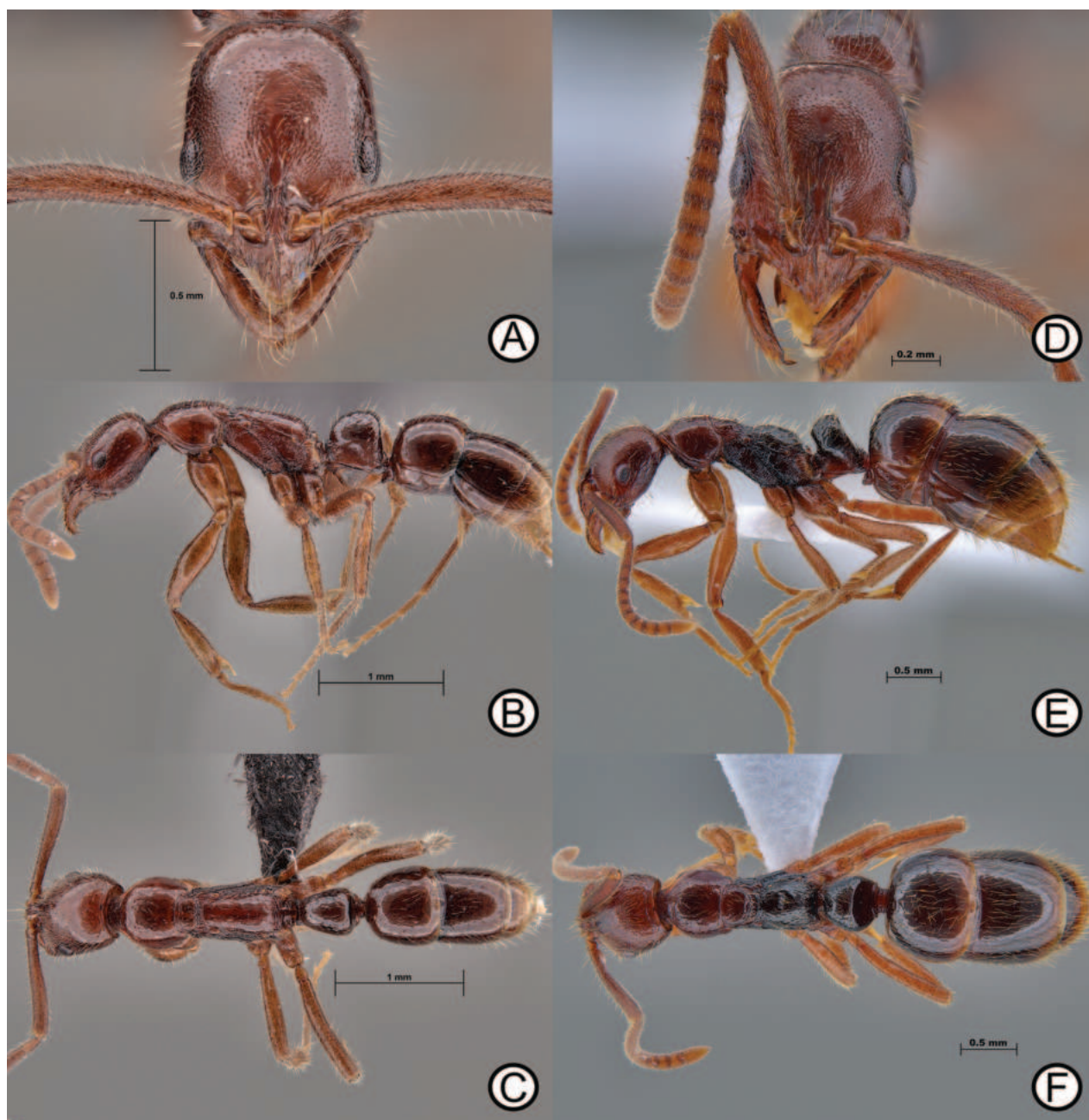


Figure 18. *Leptogenys rufida* (RHL01259) and ergatoid (ANTWEB1010234) **A** worker in lateral view **B** worker in dorsal view **C** worker in head in full face view **D** ergatoid in lateral view **E** ergatoid in lateral view and **F** ergatoid in dorsal view.

the smaller eyes in *L. rufida* and the densely sculptured meso- and metapleural of *L. confucii*.

Distribution. *Leptogenys rufida* is known from China only, including the Chinese provinces of Guangxi, Yunnan, Zhejiang and now Hong Kong SAR (Zhou et al. 2012; Xu and He 2015). To our knowledge, this species is not reported from other southern Chinese provinces but considering the gap in records between Yunnan, Guangxi and Zhejiang, it seems likely to be found in Guangdong and Fujian.

Ecology. Records for *L. rufida* in Hong Kong are sparse, but when collected it has occurred predominantly within pitfall traps, leaf litter samples and hand collection events (predominantly within leaf litter or soil) from secondary forest habitats. Two colony collections are known from Hong Kong. One colony was

located within a half-soil filled metallic pipe buried within leaf litter, consisting of ~ 20 workers and one ergatoid queen, but was not collected. A second nest was located beneath a small rock, with the colony located ~ 4–5 cm below the upper soil layer (MTH403). The colony consisted of one male, one ergatoid, and nine workers. In addition, the latter colony was retained for dietary assessment with workers responding and feeding upon isopods and termites. Foraging workers in the latter colony's collection locality were observed moving within leaf litter, with one worker returning with an isopod held ventrally between the legs.

Material examined. Workers ($n = 13$): CHINA • 1 worker; Hong Kong SAR, Pok Fu Lam; 26 Jun. 1993; J.R.Fellowes leg.; HKBM MBS015252. • 1 worker; Hong Kong SAR, Tai Mo Shan, Central NT; 20 Aug. 1993; J.R.Fellowes leg.; HKBM MBS015253. • 1 worker; Hong Kong SAR, Tai Po Kau; 20 May. 1993; J.R.Fellowes leg.; HKBM MBS015251. • 1 worker; Hong Kong SAR, The Peak; 24 Sep. 1993; J.R.Fellowes leg.; IBBL MBS006585. • 1 worker; Hong Kong SAR, Castle Peak; 22.38993, 113.95493; 426 m a.s.l.; 30 Jun. 2015; R.H.Lee leg.; Secondary forest, Pitfall trap; IBBL RHL01259. • 1 worker; Hong Kong SAR, Lin Fa Shan; 22.3956, 114.0885; 480 m a.s.l.; 15 Jul. 2016; R.H.Lee leg.; Plantation, Pitfall trap; IBBL RHL003291. • 1 worker; Hong Kong SAR, Guildford Road; 22.26715, 114.16248; 280 m a.s.l.; 18 Apr. 2018; C.Y.L.Tse leg.; Hand collection. Leaf litter; IBBL ANTWEB1010123. • 4 workers; Hong Kong SAR, Tai Mo Shan; Kap Lung Forest Trail; 22.41088, 114.10451; 450 m a.s.l.; 3 Sep. 2023; M.T.Hamer leg.; Secondary forest, un. Rock; IBBL MTH403, ANTWEB1010205, ANTWEB1010232, ANTWEB1010233, ANTWEB1010234. • 1 worker; Hong Kong SAR, Tai Mo Shan; Kap Lung Forest Trail; 22.41088, 114.10451; 450 m a.s.l.; 17 Sep. 2023; M.T.Hamer leg.; Secondary forest, Gen. forager; IBBL ANTWEB1010202. • 1 worker; Hong Kong SAR, Tai Mo Shan; Kap Lung Forest Trail; 22.41088, 114.10451; 450 m a.s.l.; 17 Sep. 2023; M.T.Hamer leg.; Secondary forest, Winkler; IBBL ANTWEB1010179.

Paratype ergatoid ($n = 1$): CHINA • 1 ergatoid; Hong Kong SAR, Tai Mo Shan; Kap Lung Forest Trail; 22.41088, 114.10451; 450 m a.s.l.; 3 Sep. 2023; M.T.Hamer leg.; Secondary forest, un. Rock; IBBL ANTWEB1010234.

***Leptogenys strenna* Zhou, 2001**

Figs 4A, 19, 21E

new record

Leptogenys strenna Zhou, 2001a: 40, 229, figs 39, 40 (w.) China (Guangxi).

Measurements. Workers ($n = 8$): HL 1.39–1.47; HLL 1.16–1.23; HLA 0.23–0.31; HW 1.16–1.25; CML 0.21–0.26; SL 1.08–1.18; All 0.2–0.25; AFI 0.18–0.22; AFII 0.15–0.19; EL 0.19–0.23; ML 0.72–0.8; PrL 0.85–0.95; PrH 0.59–0.64; PrW 0.82–0.99; WL 2.18–2.37; PeL 0.34–0.5; PeH 0.72–0.78; PeW 0.46–0.54; DPL 0.2–0.28; CI 82.86–87.03; CLI 15.38–17.74; SI 91.44–97.06; OI 16.6–18.83; LPI 144.33–216.28; DPI 166.19–249.29.

Morphological variation. Upon examination of five specimens from the only collection locality in Hong Kong, it was noted that the number of teeth on the masticatory margin are not consistent but were always between three and five. Teeth were either conspicuous or barely discernible from the mandible margin, suggesting these teeth might be worn down and, or broken. A distinct diastema

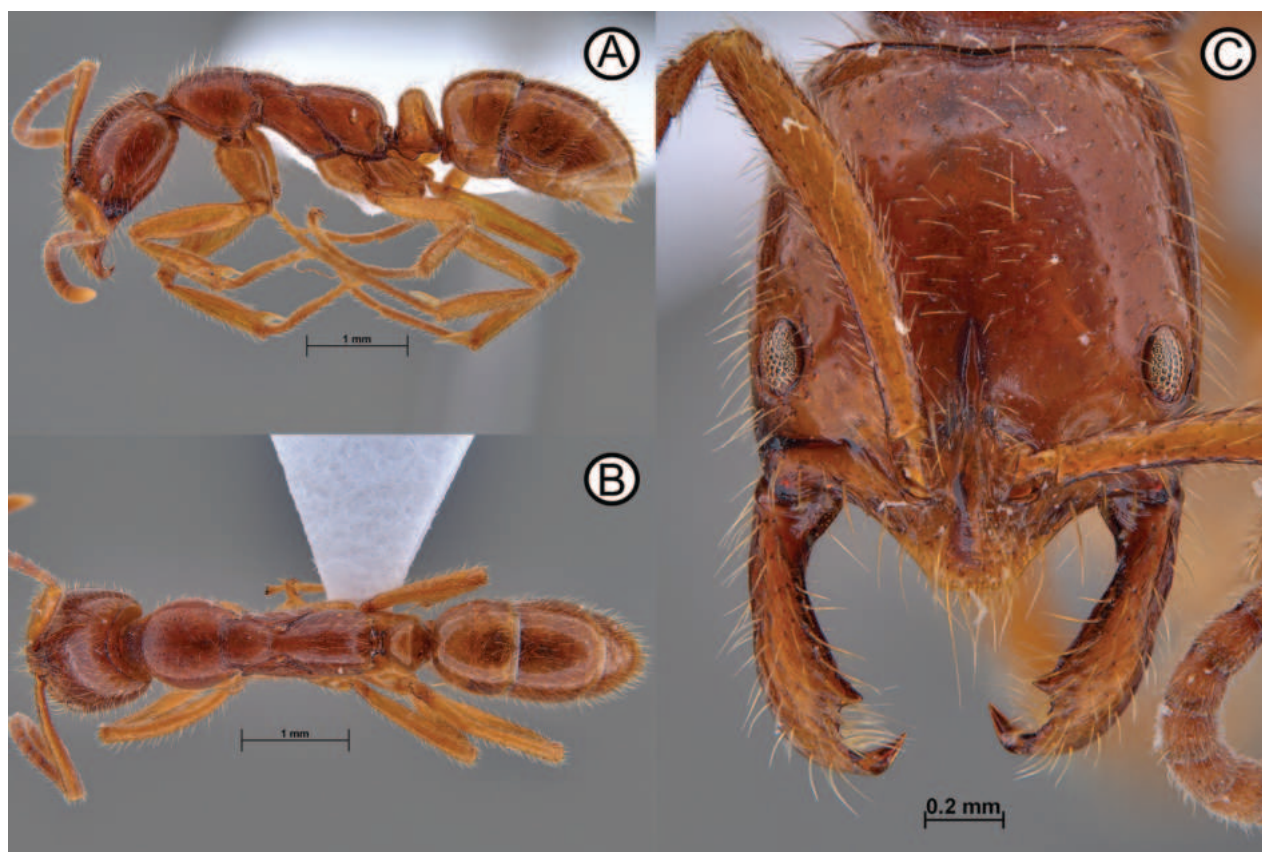


Figure 19. *Leptogenys strenna* (ANTWEB1010114) **A** lateral view **B** dorsal view **C** head in full face view.

between the basal tooth and fourth tooth was, however, always present. The utility of teeth count as a differentiable and diagnosable character should likely be treated with caution unless combined with additional less variable characters.

Comparative notes. *Leptogenys strenna* is immediately recognisable within the *Leptogenys* of Hong Kong by the combined characters of small anteriorly positioned eyes, a subquadrate head, triangular mandibles with 3–5 teeth on the masticatory margin, and a distinctly red body colouration. Within the wider *Leptogenys* fauna of China, *L. strenna* is most similar to *L. lucidula* Emery, 1895 and can be differentiated by the rounded posteroventral corner of the subpetiolar process, fewer teeth on the masticatory margin and the species overall larger size.

Distribution. This species is so far only known from China, including Guangxi (type locality), Hunan, and Guangdong, and Hong Kong SAR (Zhou et al. 2012; Xu and He 2015). Absence from other southern Chinese provinces is likely attributable to sampling effort.

Ecology. Next to nothing is known about the ecology of *L. strenna*. Specimens from Hong Kong are known only from Sunset Peak, Lantau Island. One collection was by J. R. Fellowes in 1992, and another in 2023 by A. Reshchikov using a ground SLAM trap, which was positioned in a tiny fragment of forest near the top of the mountain which yielded one further specimen. Further sampling efforts by members of Insect Biodiversity and Biogeography Laboratory have yet to collect additional specimens from this locality and from Hong Kong at large. The species' small eyes might suggest leaf litter and/or nocturnal foraging.

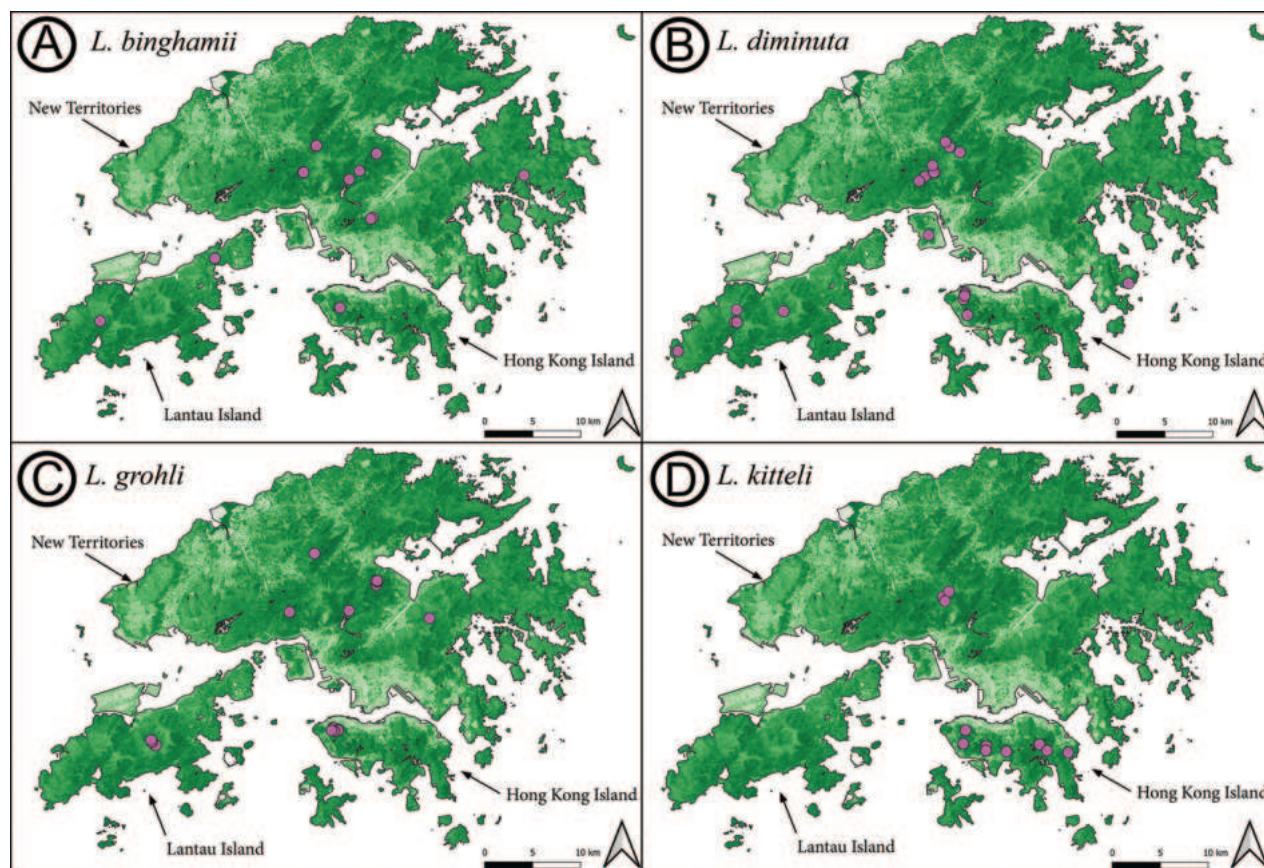


Figure 20. Distribution maps of *Leptogenys* species recorded from Hong Kong **A** *L. binghamii* **B** *L. diminuta* **C** *L. grohli* **D** *L. kitteli*. The base map displayed shows tree canopy cover with the darker green areas indicating greater tree cover.

Material examined. Workers ($n = 13$): CHINA • 8 workers; Hong Kong SAR, Lantau, Sunset Peak; 8 Oct. 1996; J.R.Fellowes leg.; HKBM MBS015294, MBS006591, MBS006592, ANTWEB1010116, ANTWEB1010115, ANTWEB1010114, ANTWEB1010167, ANTWEB1010166. • 4 workers; Guangdong Prov., Bai Yong; 3 May. 1998; J.R.Fellowes leg.; HKBM ANTWEB1010177, ANTWEB1010178, MBS006593. • 1 worker; Hong Kong SAR, Sunset Peak; 22.26104, 113.96683; 625 m a.s.l.; 06–25 May 2023; A. Reshchikov leg.; Secondary forest, SLAM ground; IBBL ANTWEB1010228.

Discussion

Considering the relatively small geographical size (1100 km²), the genus *Leptogenys* is surprisingly rich in Hong Kong. Nine species are now recorded, including one new species, *L. grohli* sp. nov. Hong Kong is now the third most diverse region for this genus across Mainland China and Taiwan even with additional species provided for Guangdong, a considerably larger Mainland Chinese province (Table 1). Such low diversity for Guangdong, as well as Fujian and the more tropical Chinese Province of Hainan (Table 1), is undoubtedly attributable to limited sampling and taxonomic efforts, and is unlikely to reflect true biodiversity patterns. The lack of regional knowledge, especially for a large, mostly epigeic, genus such as *Leptogenys*, indicates our lack of knowledge regarding the biodiversity of this region, a pattern also observed in other recently reviewed ant genera (e.g.,

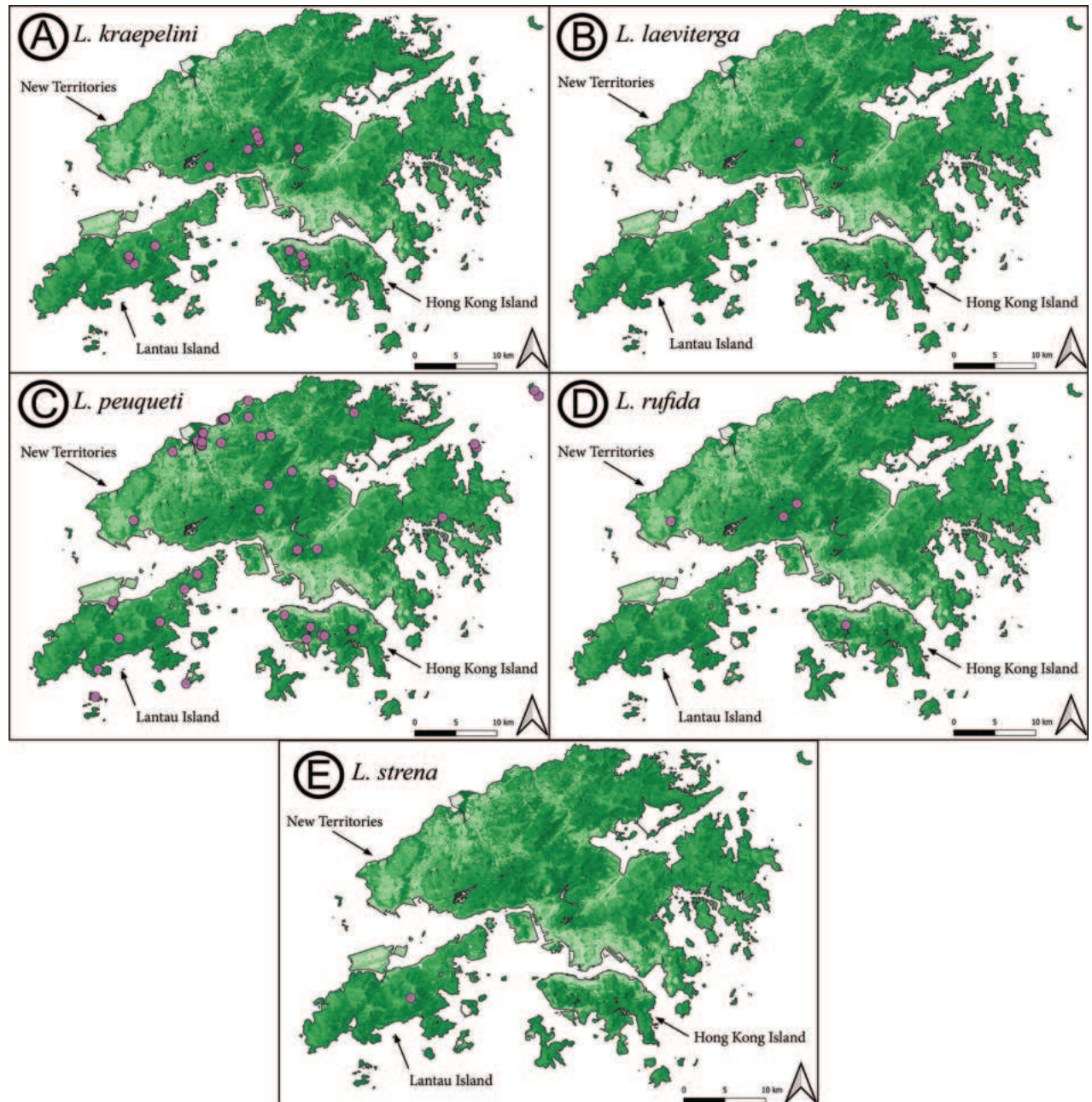


Figure 21. Further distribution maps of *Leptogenys* species recorded from Hong Kong **A** *L. kraepelini* **B** *L. laeviterga* **C** *L. peuqueti* **D** *L. rufida* **E** *L. strenna*. The base map displayed shows tree canopy cover with the darker green areas indicating greater tree cover.

Polyrhachis: Wong and Guénard 2021; *Ponera*: Leung et al. 2023; *Stigmatomma* and *Prionopelta*: Hamer et al. 2023a; *Strumigenys*: Tang and Guénard 2023).

Species of *Leptogenys* are predominately collected via pitfall trapping and hand collection, with fewer known from Winkler samples, at least from Hong Kong. This is likely a result of their more epigeaic, nomadic, and nocturnal nature, at least for a few species. Some species seem to be locally rare, including *L. rufida*, *L. strenna*, and *L. laeviterga*, which are known from just a few localities. *Leptogenys strenna* and *L. laeviterga* are known from a single locality from Sunset Peak, Lantau Island, and Tai Mo Shan, New Territories. Considering the sampling effort carried out across Hong Kong, comprising thousands of pitfall traps, Win-

Table 1. Distributional checklist of the *Leptogenys* species for the provinces of Mainland China and Taiwan. NR indicates new records presented in this study.

Species	Fujian	Guangdong	Guangxi	Guizhou	Hainan	Hong Kong	Hubei	Hunan	Jiangxi	Macao	Sichuan	Taiwan	Xizang	Yunnan	Zhejiang
<i>Leptogenys binghamii</i> Forel, 1900			✓			NR								✓	
<i>Leptogenys birmana</i> Forel, 1900					✓									✓	
<i>Leptogenys chinensis</i> (Mayr, 1870)	✓	✓	✓	✓				✓		✓	✓	✓		✓	
<i>Leptogenys confucii</i> Forel, 1912												✓			
<i>Leptogenys crassicornis</i> Emery, 1895														✓	
<i>Leptogenys davydovi</i> Karavaiev, 1935														✓	
<i>Leptogenys diminuta</i> (F. Smith, 1857)	✓	✓	✓		✓	✓		✓				✓		✓	
<i>Leptogenys grohli</i> Hamer et al., sp. nov.		NR				✓									
<i>Leptogenys hainanensis</i> Chen et al., 2024					✓										
<i>Leptogenys hezhouensis</i> Zhou, 2001			✓												
<i>Leptogenys huapingensis</i> Zhou, 2001			✓												
<i>Leptogenys kitteli</i> (Mayr, 1870)	✓	✓	✓	✓	✓	✓	✓	✓	✓		✓	✓		✓	✓
<i>Leptogenys kraepelini</i> Forel, 1905						✓								✓	
<i>Leptogenys laeviterga</i> Zhou et al., 2012			✓			NR									
<i>Leptogenys laozii</i> Xu 2000														✓	✓
<i>Leptogenys lucidula</i> Emery, 1895														✓	
<i>Leptogenys mengzii</i> Xu 2000													✓	✓	
<i>Leptogenys pangui</i> Xu, 2000														✓	
<i>Leptogenys peuqueti</i> (André, 1887)	✓	✓	✓		✓	✓	✓	✓		✓				✓	✓
<i>Leptogenys processionalis</i> (Jerdon, 1851)														✓	
<i>Leptogenys punctiventris</i> (Mayr, 1879)					✓										
<i>Leptogenys rufida</i> Zhou et al., 2012			✓			NR								✓	✓
<i>Leptogenys strenna</i> Zhou, 2001		NR	✓			NR		✓							
<i>Leptogenys sunzii</i> Xu & He, 2015														✓	
<i>Leptogenys yandii</i> Xu & He, 2015													✓		
<i>Leptogenys zhoui</i> Chen et al., 2024					✓										
<i>Leptogenys zhuangzii</i> Xu, 2000														✓	
Total	4	6	10	2	7	9	2	5	1	2	2	4	2	17	4

kler samples and hand searching events, it is surprising that more material from more localities has not been collected, suggesting that both species are scarce.

Although Xu and He (2015) provided a comprehensive review of the genus in the Oriental region, much is yet to be understood about the taxonomy of the genus in Asia. For example, several species groups have been proposed, based upon limited morphological evidence (but see Arimoto 2017; Arimoto and Yamane 2018). Moreover, several species complexes (e.g., those of *L. diminuta*, *L. kitteli*, and *L. kraepelini*) exist within the region (Wilson 1958; Xu and He 2015). In addition, many regions lack sampling efforts including West and East Malaysia, Vietnam, Laos, and Cambodia. Thus, with known uncertain species groups, new species to science, unsorted species complexes, and lack of regional revisions, the *Leptogenys* is clearly in desperate need of greater taxonomic attention.

Acknowledgements

The authors would like to thank all those who collected specimens including in no particular order: R. H. Lee, S. K. Yamane, K. Eguchi, M. Pierce, T. Tsang, B. Worthington, A. I. Weemaels, T. Bogar, R. Wang, A. Reshchikov, P. Ward, and R. Cheung.

Additional information

Conflict of interest

The authors have declared that no competing interests exist.

Ethical statement

No ethical statement was reported.

Funding

This study was funded by the Environment and Conservation Fund from the Government of the Hong Kong Special Administrative Region, under the 'Environmental Research, Technology Demonstration and Conference Projects' funding scheme – Project number ECF 137/2020.

Author contributions

Conceptualization: MTH, JHCL, BG. Data curation: MTH, JHCL. Formal analysis: MTH. Investigation: JHCL, MTH, CYLT. Methodology: MTH, TSRS. Supervision: BG, TSRS. Visualization: MTH. Writing – original draft: MTH. Writing – review and editing: BG, JHCL, TSRS, MTH, CYLT.

Author ORCIDs

Matthew T. Hamer  <https://orcid.org/0000-0001-6728-9046>

Jonathan Hon Chung Lee  <https://orcid.org/0009-0006-0204-8990>

Cheung Yau Leo Tse  <https://orcid.org/0009-0005-7864-2198>

Thiago S. R. Silva  <https://orcid.org/0000-0002-4239-1500>

Benoit Guénard  <https://orcid.org/0000-0002-7144-1175>

Data availability

All of the data that support the findings of this study are available in the main text or Supplementary Information.

References

- AntWeb (2024) Version 8.106.1. California Academy of Science. <https://www.antweb.org> [accessed 24 October 2023]
- Arimoto K (2017) Taxonomy of the *Leptogenys modiglianii* species group from south-east Asia (Hymenoptera, Formicidae, Ponerinae). *ZooKeys* 651: 79–106. <https://doi.org/10.3897/zookeys.651.10336>
- Arimoto K, Yamane S (2018) Taxonomy of the *Leptogenys chalybaea* species group (Hymenoptera, Formicidae, Ponerinae) from Southeast Asia. *Asian Myrmecology* 10(e010008): 1–31. <https://doi.org/10.20362/am.010008>
- Bakhtiar EY, Chiang SL (2010) *Leptogenys* ants (Hymenoptera: Formicidae: Ponerinae) of Sabah. *Serangga* 15(1–2): 37–55.

- Bharti H, Guénard B, Bharti M, Economo EP (2016) An updated checklist of the ants of India with their specific distributions in Indian states (Hymenoptera, Formicidae). *ZooKeys* 551: 1–83. <https://doi.org/10.3897/zookeys.551.6767>
- Bolton B (2023) An online catalog of the ants of the world. <https://antcat.org> [accessed 20 Dec 2023]
- Brassard F, Leong CM, Chan HH, Guénard B (2020) A new subterranean species and an updated checklist of *Strumigenys* (Hymenoptera, Formicidae) from Macao SAR, China, with a key to species of the Greater Bay Area. *ZooKeys* 970: 63–116. <https://doi.org/10.3897/zookeys.970.54958>
- Brassard F, Leong C-M, Chan H-H, Guénard B (2021) High Diversity in Urban Areas: How Comprehensive Sampling Reveals High Ant Species Richness within One of the Most Urbanized Regions of the World. *Diversity* 13(8): 358. <https://doi.org/10.3390/d13080358>
- Chen C, Chen Z, Xu Z, Fu Q, Fu L (2024) Two new ant species of the genus *Leptogenys* (Hymenoptera, Formicidae) from Hainan, China, with a key to the known Chinese species. *ZooKeys* 1195: 199–217. <https://doi.org/10.3897/zookeys.1195.115889>
- Dejean A, Evraerts C (1997) Predatory behaviour in the genus *Leptogenys*: A comparative study. *Journal of Insect Behavior* 10(2): 177–191. <https://doi.org/10.1007/BF02765551>
- Duncan FD, Crewe RM (1994) Group hunting in a ponerine ant, *Leptogenys nitida* Smith. *Oecologia* 97(1): 118–123. <https://doi.org/10.1007/BF00317915>
- Fellowes JR (1996) Community composition of Hong Kong ants: spatial and seasonal patterns. PhD thesis University of Hong Kong, 367 pages. <http://hub.hku.hk/handle/10722/34436>
- Forel A (1905) Ameisen aus Java. Gesammelt von Prof. Karl Kraepelin 1904. *Mitteilungen aus dem Naturhistorischen Museum in Hamburg* 22: 1–26.
- Guénard B, Dunn RR (2012) A checklist of the ants of China. *Zootaxa* 3558(1): 1–77. <https://doi.org/10.11646/zootaxa.3558.1.1>
- Guénard B, Weiser M, Gomez K, Narula N, Economo EP (2017) The Global Ant Biodiversity Informatics (GABI) database: A synthesis of ant species geographic distributions. *Myrmecological News* 24: 83–89.
- Hamer MT, Pierce MP, Guénard B (2023a) The Amblyoponinae of Hong Kong. *Asian Myrmecology* 16(e016005): 1–37. <https://doi.org/10.1111/jbi.14546>
- Hamer MT, Lee RH, Guénard B (2023b) First record of the genus *Temnothorax* Mayr, 1861 (Formicidae: Myrmicinae) in Hong Kong, with descriptions of two new species. *European Journal of Taxonomy* 879(1): 116–135. <https://doi.org/10.5852/ejt.2023.879.2165>
- Ito F (1997) Colony composition and morphological caste differentiation between ergatoid queens and workers in the ponerine ant genus *Leptogenys* in the Oriental tropics. *Ethology Ecology and Evolution* 9(4): 335–343. <https://doi.org/10.1080/08927014.1997.9522876>
- Ito F, Ohkawara K (2000) Production and behavior of ergatoid queens in two species of the Indonesian Ponerine ant genus *Leptogenys* (*diminuta*-group) (Hymenoptera: Formicidae). *Annals of the Entomological Society of America* 93(4): 869–873. [https://doi.org/10.1603/0013-8746\(2000\)093\[0869:PABOEQ\]2.0.CO;2](https://doi.org/10.1603/0013-8746(2000)093[0869:PABOEQ]2.0.CO;2)
- Janicki J, Narula N, Ziegler M, Guénard B, Economo EP (2016) Visualizing and interacting with large-volume biodiversity data using client-server web-mapping applications: The design and implementation of antmaps.org. *Ecological Informatics* 32: 185–193. <https://doi.org/10.1016/j.ecoinf.2016.02.006>

- Janssen E, Übler E, Bauriegel L, Kern F, Bestmann HJ, Attygalle AB, Steghaus-Kovac̃ S, Maschwitz U (1997) Trail pheromone of the ponerine ant *Leptogenys peuqueti* (Hymenoptera: Formicidae): a multicomponent mixture of related compounds. *Naturwissenschaften* 84(3): 122–125. <https://doi.org/10.1007/s001140050360>
- Khachonpisitsak S, Yamane S, Sriwichai P, Jaitrong W (2020) An updated checklist of the ants of Thailand (Hymenoptera, Formicidae). *ZooKeys* 998: 1–182. <https://doi.org/10.3897/zookeys.998.54902>
- Leung TKC, Leong CM, Hamer MT, Guénard B (2023) Discovery of the formerly Japan-endemic *Ponera kohmoku* Terayama, 1996 (Formicidae, Ponerinae) in Southeast China. *Asian Myrmecology* 16(016008): 1–11.
- Luo YY, Guénard BS (2016) Descriptions of a new species and the gyne in the rarely collected arboreal genera *Paratopula* and *Rotastruma* (Hymenoptera: Formicidae) from Hong Kong, with a discussion on their ecology. *Asian Myrmecology* 8: 1–16.
- Maschwitz U, Mühlenberg M (1975) Strategy of Predation in Some Oriental *Leptogenys* Species (Formicidae: Ponerinae). *Oecologia* 20: 65–83. <https://doi.org/10.1007/BF00364322>
- Maschwitz U, Hahn M, Schönegge P (1979) Paralysis of prey in ponerine ants. *Naturwissenschaften* 66: 213–214. <https://doi.org/10.1007/BF00366035>
- Maschwitz U, Steghaus-Kovac S, Gaube R, Heinz H (1989) A South East Asian ponerine ant of the genus *Leptogenys* (Hym., Form.) with army ant life habits. *Behavioral Ecology and Sociobiology* 24: 305–316. <https://doi.org/10.1007/BF00290907>
- Mizuno R, Likhitrakarn N, Suttiprapan P, Aupanun S, Jaitrong W, Peeters C (2022) Field observations on nestmate recruitment to millipedes in the chain assembling ponerine ant *Leptogenys cyanicatena* (Formicidae: Ponerinae) in northern Thailand. *Asian Myrmecology* 15: e015003.
- Peeters C (1991) Ergatoid queens and intercastes in ants – two distinct adult forms which look morphologically intermediate between workers and winged queens. *Insectes Sociaux* 38(1): 1–15. <https://doi.org/10.1007/BF01242708>
- Peeters C, De Greef S (2015) Predation on large millipedes and self-assembling chains in *Leptogenys* ants from Cambodia. *Insectes Sociaux* 62(4): 471–477. <https://doi.org/10.1007/s00040-015-0426-2>
- Pierce MP, Leong CM, Guénard B (2019) A new species and new record of the cryptobiotic ant genus *Ponera* Latreille, 1804 (Hymenoptera, Formicidae) from Hong Kong. *ZooKeys* 29(867): 9–21. <https://doi.org/10.3897/zookeys.867.36139>
- Schmidt CA (2013) Molecular phylogenetics of ponerine ants (Hymenoptera: Formicidae: Ponerinae). *Zootaxa* 3647(2): 201–250. <https://doi.org/10.11646/zootaxa.3647.2.1>
- Schmidt CA, Shattuck SO (2014) The higher classification of the ant subfamily Ponerinae (Hymenoptera: Formicidae), with a review of ponerine ecology and behavior. *Zootaxa* 3817(1): 1–242. <https://doi.org/10.11646/zootaxa.3817.1.1>
- Silva TSR, Hamer MT, Guénard B (2023) A checklist of *Nylanderia* (Hymenoptera: Formicidae: Formicinae) from Hong Kong and Macao SARs, with an illustrated identification key for species in Southeast China and Taiwan. *Zootaxa* 5301(5): 501–539. <https://doi.org/10.11646/zootaxa.5301.5.1>
- Steghaus-Kovac S, Maschwitz U (1993) Predation on earwigs: A novel diet specialization within the genus *Leptogenys* (Formicidae: Ponerinae). *Insectes Sociaux* 40(3): 337–340. <https://doi.org/10.1007/BF01242370>
- Tang KL, Guénard B (2023) Further additions to the knowledge of *Strumigenys* (Formicidae: Myrmicinae) within South East Asia, with the descriptions of 20 new species. *European Journal of Taxonomy* 907(1): 1–144. <https://doi.org/10.5852/ejt.2023.907.2327>

- Tang KL, Pierce MP, Guénard B (2019) Review of the genus *Strumigenys* (Hymenoptera, Formicidae, Myrmicinae) in Hong Kong with the description of three new species and the addition of five native and four introduced species records. *ZooKeys* 831: 1–48. <https://doi.org/10.3897/zookeys.831.31515>
- Wachkoo A, Maqbool A, Akbar S, Sharaf M (2018) A new species of the ant genus *Leptogenys* Roger, 1861 (Hymenoptera: Formicidae) from India. *Biodiversity Data Journal* 6: e25016. <https://doi.org/10.3897/BDJ.6.e25016>
- Wang WY, Soh EJY, Yong GWJ, Wong MKL, Guenard B, Economo EP, Yamane S (2022) Remarkable diversity in a little red dot: a comprehensive checklist of known ant species in Singapore (Hymenoptera: Formicidae) with notes on ecology and taxonomy. *Asian Myrmecology* 15: e015006. <https://doi.org/10.20362/am.015006>
- Wilson EO (1958) Studies on the ant fauna of Melanesia. I. The tribe Leptogenyini. II. The tribes Amblyoponini and Platythyreini. *Bulletin of the Museum of Comparative Zoology* 118: 101–153.
- Wong TL, Guénard B (2021) Review of ants from the genus *Polyrhachis* Smith (Hymenoptera: Formicidae: Formicinae) in Hong Kong and Macau, with notes on their natural history. *Asian Myrmecology* 13. <https://doi.org/10.20362/am.013001>
- Wu BQ, Lu YY, Zeng L, Liang GW (2008) Influences of *Solenopsis invicta* Buren invasion on the native ant communities in different habitats in Guangdong. *Journal of Applied Ecology* 19(1): 151–156.
- Xu Z-H (2000) Five new species and one new record of the ant genus *Leptogenys* Roger (Hymenoptera: Formicidae) from Yunnan Province, China. *Entomologia Sinica* 7: 117–126. <https://doi.org/10.1111/j.1744-7917.2000.tb00348.x>
- Xu Z-H, He Q-J (2015) Taxonomic review of the ponerine ant genus *Leptogenys* Roger, 1861 (Hymenoptera: Formicidae) with a key to the Oriental species. *Myrmecological News* 21: 137–161.
- Zhao S, Jia FL, Liang GQ, Ke YL, Tian WJ (2009) Ants and their distribution in Guangdong Province, China. *Huanjing Kunchong Xuebao* 31(2): 156–161.
- Zhou S (2001) *Ants of Guangxi*. Guangxi Normal University Press, Guilin, China, 255 pp. [In Chinese]
- Zhou S, Chen Y, Chen Z, Zhou P, Ban D, Huang M (2012) Two new species of the genus *Leptogenys* from Guangxi, China (Hymenoptera: Formicidae). *Sociobiology* 59: 885–892.
- Zryanin VA (2016) A remarkable new species of *Leptogenys* Roger, 1861 (Hymenoptera: Formicidae) from Vietnam. *Evrziatskii Entomologicheskii Zhurnal* 15(1): 50–54.

Supplementary material 1

Leptogenys of Hong Kong measurements

Authors: Matthew T. Hamer, Jonathan Hon Chung Lee, Cheung Yau Leo Tse, Thiago S. R. Silva, Benoit Guénard

Data type: xlsx

Explanation note: Measurements used to construct measurement ranges.

Copyright notice: This dataset is made available under the Open Database License (<http://opendatacommons.org/licenses/odbl/1.0/>). The Open Database License (ODbL) is a license agreement intended to allow users to freely share, modify, and use this Dataset while maintaining this same freedom for others, provided that the original source and author(s) are credited.

Link: <https://doi.org/10.3897/zookeys.1202.120214.suppl1>

Geometric morphometry of the *Rhodnius prolixus* complex (Hemiptera, Triatominae): patterns of intraspecific and interspecific allometry and their taxonomic implications

Ana Carolina P. C. Alvarez¹, Carolina Dale¹, Cleber Galvão²

¹ Laboratório de Entomologia, Instituto Oswaldo Cruz, FIOCRUZ, Av. Brasil 4365, Pavilhão Mourisco, sala 214, Rio de Janeiro, RJ, 21040-360, Brazil

² Laboratório Nacional e Internacional de Referência em Taxonomia de Triatomíneos, Instituto Oswaldo Cruz, FIOCRUZ, Av. Brasil 4365, Pavilhão Rocha Lima, sala 507, Rio de Janeiro, RJ, 21040-360, Brazil

Corresponding author: Cleber Galvão (clebergalvao@gmail.com)

Abstract

In the subfamily Triatominae, the genus *Rhodnius* is one of the most studied, not only because of its epidemiological importance, but also because of the difficulty in differentiating its species. Currently, one of the strategies to control Chagas disease, besides other initiatives such as the analysis of donated blood, is focused on fighting the vector. Correctly identifying triatomines is essential for the entomoepidemiological surveillance of Chagas disease. The objective of the present work was to compare the species of the *R. prolixus* complex using geometric morphometry of hemelytra and heads to evaluate the patterns of intraspecific and interspecific allometry and their taxonomic implications. This method can help in the diagnosis of close species, whose morphological characteristics are insufficient for correct identification. Specimens from five different collections were used, covering the species included in the *R. prolixus* complex (*R. barretti*, *R. dalessandroi*, *R. domesticus*, *R. marabaensis*, *R. milesi*, *R. montenegrensis*, *R. nasutus*, *R. neglectus*, *R. neivai*, *R. prolixus* and *R. robustus*). Morphometric analyses indicated that the hemelytra are not structures with good resolution for separating species and, for this reason, the use of the heads proved to be more adequate for this group (thus allowing differentiation of all species of the *R. prolixus* complex). The results suggest that *R. milesi* is a variant of *R. neglectus* and confirms that *R. prolixus* and *R. robustus* are distinct species. Furthermore, we propose the creation of the *R. neivai* complex comprising *R. domesticus* and *R. neivai*.

Key words: Chagas disease, entomological collections, *Rhodnius nasutus*, *R. neivai* complex, taxonomy, vector

Introduction

Chagas disease is endemic to, and one of the most serious diseases in Latin America, with the number of cases still underreported (Dumonteil and Herrera 2017; Nascimento et al. 2019). Despite having several forms of transmission, including an increase in cases related to oral transmission, the classical form of transmission is through the infected excrements of insect vectors of the



Academic editor: Jader Oliveira
Received: 17 June 2023
Accepted: 7 November 2023
Published: 23 May 2024

ZooBank: <https://zoobank.org/E90D78CB-D96B-40A9-8EEC-1C4691FB0477>

Citation: Alvarez ACPC, Dale C, Galvão C (2024) Geometric morphometry of the *Rhodnius prolixus* complex (Hemiptera, Triatominae): patterns of intraspecific and interspecific allometry and their taxonomic implications. ZooKeys 1202: 213–228. <https://doi.org/10.3897/zookeys.1202.108157>

Copyright: © Ana Carolina P. C. Alvarez et al. This is an open access article distributed under terms of the Creative Commons Attribution License (Attribution 4.0 International – CC BY 4.0).

subfamily Triatominae (Hemiptera: Reduviidae) infected with the parasite *Trypanosoma cruzi* (Chagas, 1909) (Kinetoplastida, Trypanosomatidae) (Dias and Schofield 1999; Schmunis 1999; de Fuentes-Vicente et al. 2023). Triatominae currently includes five tribes, 18 genera and 160 species (Poinar 2019; Alevi et al. 2020; Téllez-Rendón et al. 2023; Zhao et al. 2023), among which the tribes Triatomini and Rhodniini have major epidemiological relevance (Lent and Wygodzinsky 1979; Galvão et al. 2003; Vallejo et al. 2009).

Rhodniini is composed of the genera *Rhodnius* Stål, 1859 and *Psammolestes* Bergroth, 1911. *Rhodnius* is one of the best studied genera, not only for its epidemiological significance, but also for the difficulty in distinguishing its species and/or defining species limits (Lent and Jurberg 1969; Lent and Wygodzinsky 1979; Coutinho 2013). It is well characterized by the insertion of its antennae on the distal portion of the head and by the presence of post-ocular callosities, but its species are difficult to differentiate morphologically although they are genetically distinct (Neiva and Pinto 1923; Lent 1948; Pavan and Monteiro 2007; Coutinho 2013; Zhao et al. 2021). Despite the existence of identification keys, e.g., Lent and Wygodzinsky (1979) and Galvão and Dale (2014), the differentiation of these species is still a major obstacle. At present, there are 21 species considered as valid that are grouped into three complexes following molecular phylogenies based on different sequences (16S mitochondrial rDNA, cytochrome b (Cytb) and 28S nuclear rRNA): *R. pallenscens*, *R. pictipes* and *R. prolixus* (Table 1) (Maia da Silva et al. 2004; Zhao et al. 2021).

Table 1. *Rhodnius* species complexes according to Zhao et al. (2021).

Complex	Species
<i>Rhodnius prolixus</i>	<i>Rhodnius barretti</i> Abad-Franch, Palomeque & Monteiro, 2013
	<i>Rhodnius dalessandroi</i> Carcavallo & Barreto, 1976
	<i>Rhodnius domesticus</i> Neiva & Pinto, 1923
	<i>Rhodnius milesi</i> Carcavallo, Rocha, Galvão & Jurberg, 2001
	<i>Rhodnius marabaensis</i> dos Santos Souza et al., 2016
	<i>Rhodnius montenegrensis</i> da Rosa et al., 2012
	<i>Rhodnius nasutus</i> Stål, 1859
	<i>Rhodnius neglectus</i> Lent, 1954
	<i>Rhodnius neivai</i> Lent, 1953
	<i>Rhodnius prolixus</i> Stål, 1859
<i>Rhodnius robustus</i> Larrousse, 1927	
<i>Rhodnius pictipes</i>	<i>Rhodnius amazonicus</i> Almeida, Santos & Sposina, 1973
	<i>Rhodnius brethesi</i> Matta, 1919
	<i>Rhodnius micki</i> Zhao, Galvão & Cai, 2021
	<i>Rhodnius paraensis</i> Sherlock, Guitton & Miles, 1977
	<i>Rhodnius pictipes</i> Stål, 1872
	<i>Rhodnius stali</i> Lent, Jurberg & Galvão, 1993
<i>Rhodnius zeledoni</i> Jurberg, Rocha & Galvão, 2009	
<i>Rhodnius pallenscens</i>	<i>Rhodnius colombiensis</i> Mejía, Galvão & Jurberg, 1999
	<i>Rhodnius ecuadoriensis</i> Lent & León, 1958
	<i>Rhodnius pallenscens</i> Barber, 1932

The *Rhodnius prolixus* complex was, initially, erected by Carcavallo et al. (2000) with the species *R. domesticus*, *R. nasutus*, *R. neglectus*, *R. prolixus* and *R. robustus*. Zhao et al. (2021) updated the complexes using molecular data, geographical distribution patterns and morphometric analyses. As a result, the number of species belonging to the *R. prolixus* complex was increased from five to eleven, adding to the previous species: *R. barretti*, *R. dalessandroi*, *R. marabaensis*, *R. milesi*, *R. montenegrensis* and *R. neivai*.

Currently, one of the strategies to control the disease, besides other initiatives such as the analysis of donated blood, is focused on fighting the vector, making the correct identification of triatomines essential for the entomoepidemiological surveillance of Chagas disease (The Pan American Health Organization 2023). Studies demonstrate the importance of using other techniques for the identification of species, especially close ones, in triatominae taxa (Gurgel-Gonçalves et al. 2011; Depickère et al. 2020). Over the years, research using new approaches to species differentiation have been published, such as the study of genitalia (e.g., Lent and Jurberg 1969), analysis of the exochorion of eggs (e.g., Barata 1981), description of nymphs (e.g., Rocha et al. 2005), scanning electron microscope (e.g., da Rosa et al. 2014), morphometry (e.g., Gurgel-Gonçalves et al. 2008), isoenzyme analyses (e.g., Dujardin et al. 1999), cytogenetics (e.g., Ravazi et al. 2021), matrix-assisted laser desorption/ionization-time of flight mass spectrometry (MALDI-TOF MS) (Souza 2020), transcriptome (de Carvalho et al. 2017), and more recently DNA analyses (e.g., Montiel et al. 2021). However, even with the advancement of these tools, some species still do not show enough characters for easy diagnosis (Monteiro et al. 2000; Fornel and Cordeiro-Estrela 2012; Coutinho 2013).

The objective of the present work is to compare the species of the *R. prolixus* complex using geometric morphometry of hemelytra and heads to evaluate the patterns of intraspecific and interspecific allometry and their taxonomic implications.

Material and methods

Species samples

The specimens used in the study are from five distinct entomological collections:

Coleção de Triatomíneos do Instituto Oswaldo Cruz (**CTIOC**), of the Laboratório Nacional e Internacional de Referência em Taxonomia de Triatomíneos (**LNIRTT**), FIOCRUZ, Rio de Janeiro, Brazil;

Coleção Entomológica do Instituto Oswaldo Cruz (**CEIOC**), Laboratório de Entomologia (**LABE**), FIOCRUZ, Rio de Janeiro, Brazil;

Entomological collection of the Museum für Naturkunde – Leibniz Institute for Evolution and Biodiversity Science, Berlin, Germany;

Coleção de Triatominae Dr. José Maria Soares Barata, Faculdade de Ciências Farmacêuticas, UNESP, Araraquara, São Paulo, Brazil;

Coleção do Centro de Pesquisa René Rachou (**CPqRR**), FIOCRUZ, Minas Gerais, Brazil. (Suppl. material 1).

For taxonomic identification of adults, the dichotomous keys from Galvão and Dale (2014) were used.

Image acquisition and data analysis

The hemelytra and the heads of specimens belonging to 11 valid species belonging to the *Rhodnius prolixus* complex were photographed using the Leica Automounting Magnifier (DMC 2900): *R. barretti*, *R. dalessandroi*, *R. domesticus*, *R. marabaensis*, *R. milesi*, *R. montenegrensis*, *R. nasutus*, *R. neglectus*, *R. neivai*, *R. prolixus* and *R. robustus* (Fig. 1).

Geometric morphometric analysis

In this study, the geometric morphometry method was employed. The technique involved utilizing previously acquired images and the TPSdig software ver. 2.31 (Rohlf 2005). Following the method of Dujardin (2019), eight type I landmarks were selected on the hemelytra (except for *R. barretti* due to the lack of specimens in the collections) and ten on the heads of each specimen of the *R. prolixus* complex (Fig. 2A, B) (Suppl. material 2). According to Dujardin (2019), type I landmarks “may be considered as anatomical points or patches recognizable from one individual to another”. All landmarks used were identified as regions where structural features converge.

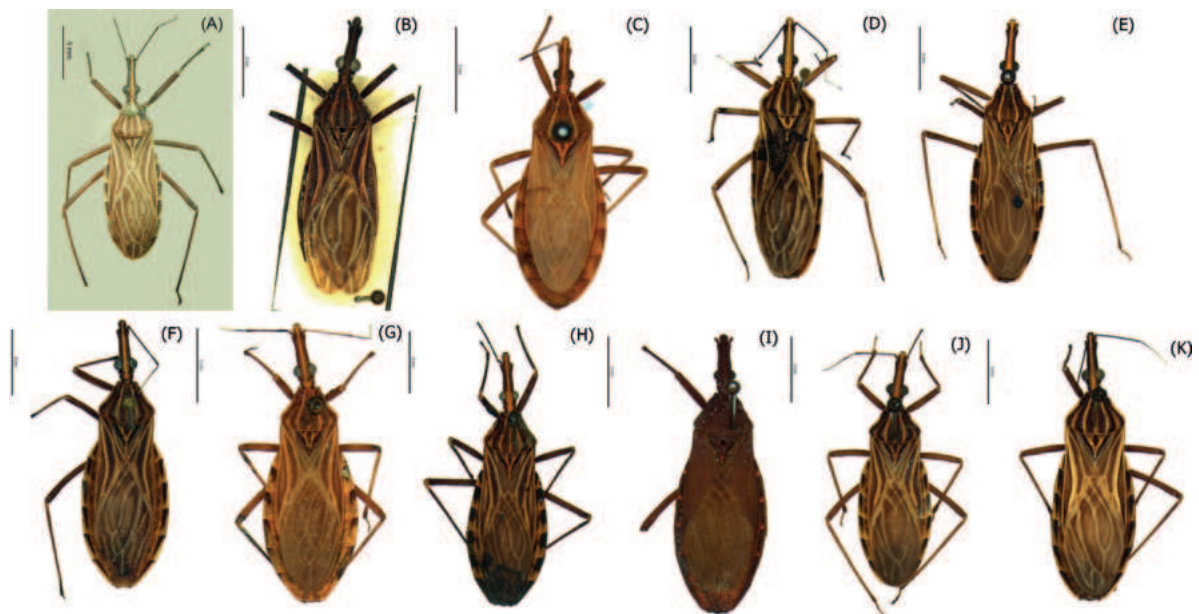


Figure 1. Habitus, dorsal view of **A** *Rhodnius barretti* **B** *Rhodnius dalessandroi* **C** *Rhodnius domesticus* **D** *Rhodnius marabaensis* **E** *Rhodnius milesi* **F** *Rhodnius montenegrensis* **G** *Rhodnius nasutus* **H** *Rhodnius neglectus* **I** *Rhodnius neivai* **J** *Rhodnius prolixus* **K** *Rhodnius robustus*. Scale bars: 5 mm.

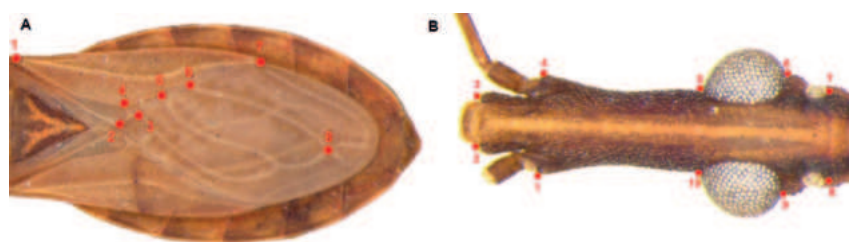


Figure 2. Landmarks in **A** hemelytra of *R. domesticus* and **B** head of *R. prolixus*.

Data transformation and analysis

Using TPSrelw software ver. 1.75 (Rohlf 2005), the data were transformed into numerical coordinates and stored as weighted matrix in an NTS format. Once the matrix was generated, the centroid size, as well as the X and Y uniform components, were calculated for each specimen, following the method outlined by (Coutinho 2017). The X and Y coordinate landmarks underwent Procrustes superimposition (Bookstein 1991), followed by Thin Plate Spline analysis, and subsequently a discriminant analysis. Multivariate analyses and factorial maps were constructed using JMP software ver. 17 (Institute 2000).

Multivariate analysis and software

The data underwent a multivariate principal component analysis (PCA) to show the variability of shapes within the genus, constructing a factor map. Subsequently, the covariance matrix generated by Procrustes coordinate analysis and a multivariate analysis of variance (MANOVA) were conducted to assess shape variation. Species relationships were determined by canonical components (CVA), which can be useful to find shape features and to distinguish the groups of species included in the complex. The statistical tests (including Wilks' Lambda, Pillai's Trace, Hotelling-Lawley and Roy's Max Root) for both hemelytra and head analyses were automatically performed using JMP. Using the same software, factorial maps of principal and canonical components were generated, along with dendrograms employing Mahalanobis distances for cluster analysis of both structures.

Results

Geometric morphometry of hemelytra

Wilks' lambda test for analysis of hemelytra size variation revealed significant differences ($p < 0.0001$) among species (Table 2). PCA resulted in the sum of the values of the first (PC1) and second (PC2) principal components equivalent to 68% of the total shape variability (PC1 = 53.80% and PC2 = 14.20%).

In the plots it is possible to observe the distant distribution of each species. We can see this kind of distribution on the PCA map (Fig. 3) where only *R. robustus* and *R. prolixus* are overlapping. On the CVA map (Fig. 4), there is no species overlap.

The cluster analysis, using the mean distances between species (Mahalanobis distances), produced a dendrogram (Fig. 5) that formed a group including *R. nasutus*, *R. marabaensis* and *R. domesticus*, connected to *R. neglectus* and *R. dalessandroi*; a group formed by *R. prolixus* and *R. robustus* connected to *R. montenegrensis*; *Rhodnius milesi* and *R. neivai* as outgroup species.

Table 2. Statistical tests performed by JMP.

Test	Value	Approx. F	NumDF	DenDF	Prob>F
Wilks' Lambda	0.2901718	5.4757	36	503.9	<.0001
Pillai's Trace	0.9645573	4.8371	36	548	<.0001
Hotelling-Lawley	1.6451934	6.0668	36	352.37	<.0001
Roy's Max Root	0.977472	14.8793	9	137	<.0001

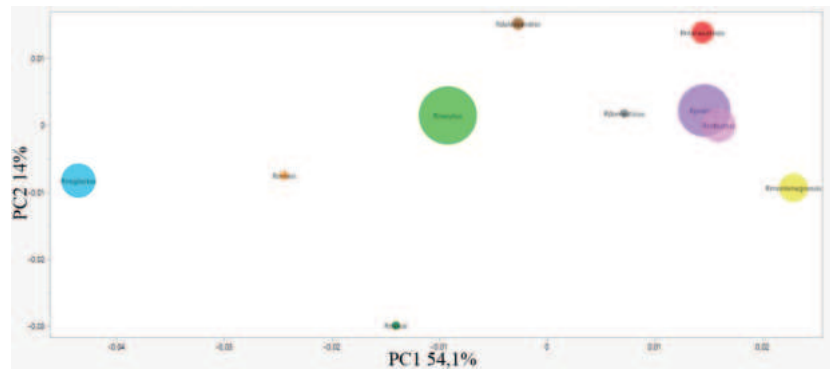


Figure 3. Factorial map containing the principal components of the hemelytra where each species is represented by circles. Brown – *Rhodnius dalessandroi*; Gray – *Rhodnius domesticus*; red – *Rhodnius marabaensis*; orange – *Rhodnius milesi*; yellow – *Rhodnius montenegrensis*; light green – *Rhodnius nasutus*; light blue – *Rhodnius neglectus*; dark green – *Rhodnius neivai*; lilac – *Rhodnius prolixus*; light pink – *Rhodnius robustus* (Suppl. material 2)

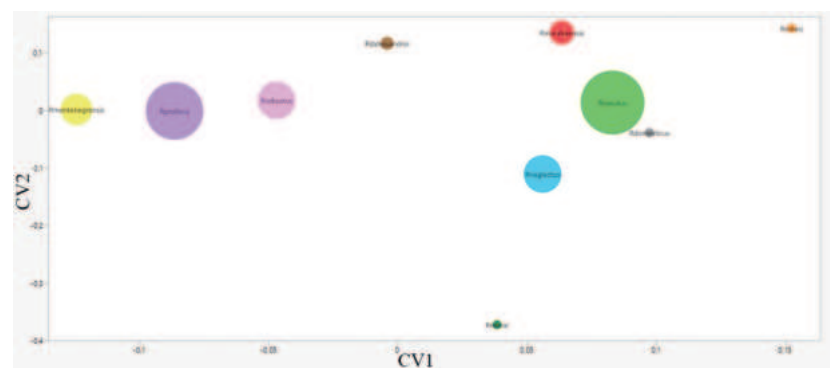


Figure 4. Factorial map containing the canonical variation of the hemelytra where each species is represented by circles. Brown – *Rhodnius dalessandroi*; gray – *Rhodnius domesticus*; red – *Rhodnius marabaensis*; orange – *Rhodnius milesi*; yellow – *Rhodnius montenegrensis*; light green – *Rhodnius nasutus*; light blue – *Rhodnius neglectus*; dark green – *Rhodnius neivai*; lilac – *Rhodnius prolixus*; light pink – *Rhodnius robustus* (Suppl. material 2).

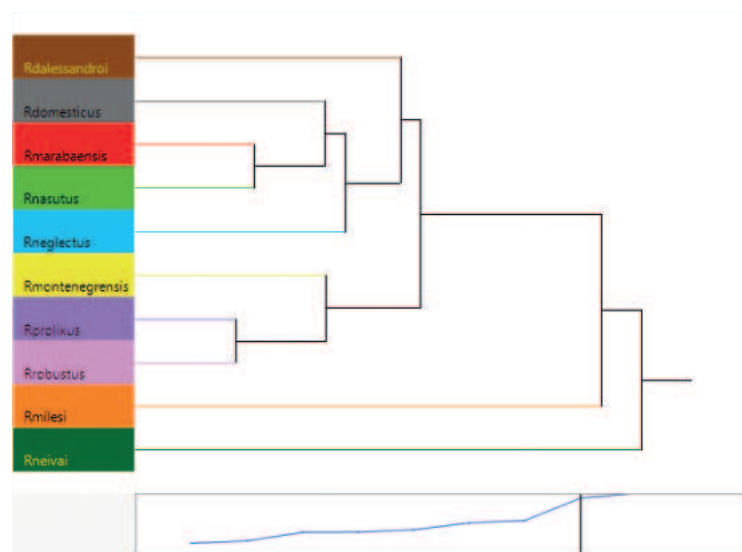


Figure 5. Dendrogram produced by hemelytra cluster analysis of the species of the *Rhodnius prolixus* complex, except *Rhodnius barretti* (Suppl. material 2).

Head geometric morphometry

Wilk's Lambda test for head size variation analysis revealed significant differences ($p < 0.0001$) among species (Table 3). The PCA showed as a result the sum of CP1 and CP2 values equivalent to 77% of the total shape variability (CP1 = 63.50% and CP2 = 13.50%).

Table 3. Statistical tests performed by JMP.

Test	Value	Approx. F	NumDF	DenDF	Prob>F
Wilks' Lambda	0.0180787	35.0464	40	745.06	<.0001
Pillai's Trace	2.0449084	20.8142	40	796	<.0001
Hotelling-Lawley	10.710766	52.1415	40	536.68	<.0001
Roy's Max Root	6.5944871	131.2303	10	199	<.0001

The positioning of each species is observed in the factorial maps of the PCA (Fig. 6) where we see a clear overlap between *R. neglectus* and *R. neivai*; *Rhodnius prolixus* appears distant from *R. robustus* and the group formed by *R. marabaensis*, *R. montenegrensis* and *R. barretti*; *Rhodnius domesticus* appears as an outgroup species. On the CVA map (Fig. 7) we again see *R. prolixus* distant from *R. robustus* and the group formed by *R. barretti*, *R. marabaensis* and *R. montenegrensis*; *Rhodnius domesticus* appears again as an outgroup species.

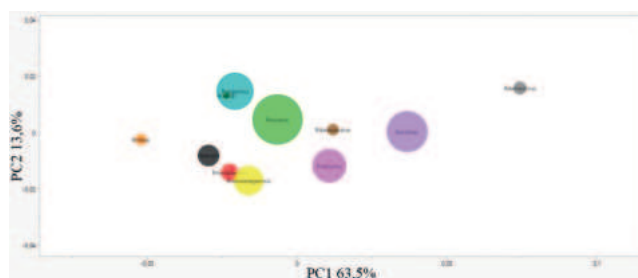


Figure 6. Factorial map containing the principal components of the head where each species is represented by circles. Brown – *Rhodnius dalessandroi*; gray – *Rhodnius domesticus*; red – *Rhodnius marabaensis*; orange – *Rhodnius milesi*; yellow – *Rhodnius montenegrensis*; light green – *Rhodnius nasutus*; light blue – *Rhodnius neglectus*; dark green – *Rhodnius neivai*; lilac – *Rhodnius prolixus*; light pink – *Rhodnius robustus* (Suppl. material 2).

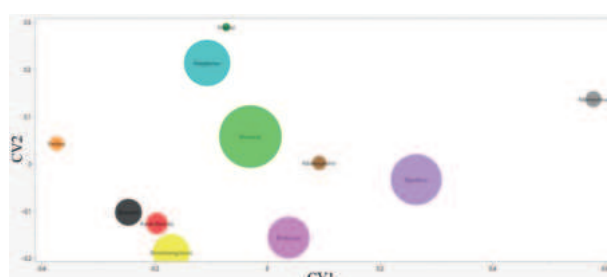


Figure 7. Factorial map containing the canonical components of the head where each species is represented by circles. Brown – *Rhodnius dalessandroi*; gray – *Rhodnius domesticus*; red – *Rhodnius marabaensis*; orange – *Rhodnius milesi*; yellow – *Rhodnius montenegrensis*; light green – *Rhodnius nasutus*; light blue – *Rhodnius neglectus*; dark green – *Rhodnius neivai*; lilac – *Rhodnius prolixus*; light pink – *Rhodnius robustus* (Suppl. material 2).

The cluster analysis using the mean distances among species generated a dendrogram (Fig. 8) that reinforces *R. domesticus* and *R. neivai* as outer groups. In addition, we can visualize a group formed by two inner groups, the first being a group including *R. barretti*, *R. marabaensis*, *R. montenegrensis* and *R. robustus* and the second inserting *R. dalessandroi* close to *R. nasutus* and *R. prolixus*; *Rhodnius milesi* is directly linked to *R. neglectus*.

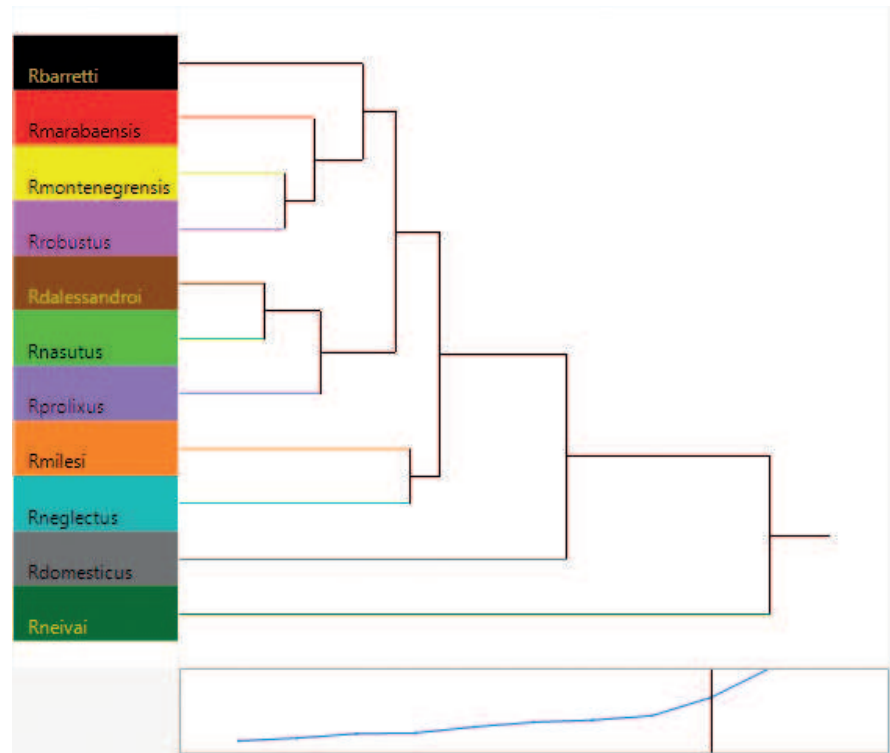


Figure 8. Dendrogram produced by head cluster analysis of the species of the *Rhodnius prolixus* complex (Suppl. material 2).

Discussion

Despite advances in studies related to the taxonomy and systematics of Triatominae, some species still lack sufficient characters for easy diagnosis, such as those belonging to the genus *Rhodnius* (Monteiro et al. 2000; Fornel and Cordeiro-Estrela 2012; Coutinho 2013). Although this genus is easily identified using morphological characters, the differentiation of species is still a major challenge (Neiva and Pinto 1923; Lent 1948; Galvão 2014). Due to their similarities, Zhao et al. (2021) grouped the species of this genus into three complexes according to their distribution: *R. pallescens*, *R. pictipes* and *R. prolixus*. The *R. pallescens* group is considered as trans-Andean, found on the western side of the Andes, while the *R. pictipes* is cis-Andean, distributed on the eastern side of the Andes and also in the Amazon region. In the *R. prolixus* complex, ten species (*R. barretti*, *R. dalessandroi*, *R. domesticus*, *R. marabaensis*, *R. milesi*, *R. montenegrensis*, *R. nasutus*, *R. neglectus*, *R. prolixus* and *R. robustus*) are distributed in the same cis-Andean region of the *R. pictipes* group, and only *R. neivai* has trans-Andean populations (Filée et al. 2022).

Some species in the *R. prolixus* complex are difficult to differentiate using only morphological characters, which can lead to taxonomic conflicts (Filée et al. 2022). Gurgel-Gonçalves et al. (2011) found in *R. neglectus* variations comparing sylvatic and laboratory colonies. Some variations (e.g., size or chromatic) can lead to misidentification, and occasionally to under-reporting of Chagas' disease transmission cases related to different species (Dias 2007; Dias et al. 2014). In cases like those, when chromatic and size variations are significant, geometric morphometry could be a useful method to differentiate species, as seen in Soto Vivas et al. (2007), Gurgel-Gonçalves et al. (2011), Abad-Franch et al. (2021) and Cruz et al. (2023). In addition, geometric morphometry is an important method in studies using specimens from entomological collections, in which molecular analysis can sometimes be inefficient, as presented in Dale et al. (2013).

Lent and Wygodzinsky (1979), cited *R. nasutus* and *R. neglectus* as examples of difficult differentiation, because their phenotypical similarities. The results of head geometric morphometry shows a group formed by *R. nasutus*, *R. dalessandroi* and *R. prolixus*, corroborating the results of Coutinho (2013) who compared the species of *Rhodnius* using the mitochondrial gene cytochrome oxidase I (COI). Meanwhile, *R. neglectus* appears closely related to *R. milesi*, which was described by Valente et al. (2001) as close to *R. dalessandroi*, despite its distant geographical distribution. Coutinho (2013) used COI to verify the great genetic similarity between *R. milesi* and *R. neglectus*, the first being considered as a variant of the second. This result is also found in Monteiro et al. (2018), who used Cytb and ITS-2 sequences. Despite the distribution of the two species in the factorial maps, the relationships between *R. neglectus* and *R. milesi* found in the dendrogram generated by the heads, agree with those found by Coutinho (2013) and Monteiro et al. (2018) in grouping these two species together.

The dendrogram generated by cluster analysis of the head of *R. dalessandroi*, described by Carcavallo and Barreto (1976) as close to *R. brethesi* (a species of the *R. pictipes* complex), appear in the group next to *R. nasutus* and *R. prolixus*, and next to a group formed by *R. neglectus*, *R. nasutus*, *R. marabaensis* and *R. domesticus*. *Rhodnius dalessandroi* have little information in the literature, with Lent and Wygodzinsky (1979) citing that "the published description and illustrations of this *Rhodnius* are not sufficient to recognize it."

The identification key from Lent and Wygodzinsky (1979) and Galvão and Dale (2014), using external morphology, places *R. robustus* and *R. prolixus* as morphologically similar species (which makes their identification difficult). Our analyses of geometric morphometry of the heads showed that these two species are distinct. In fact, *R. robustus* is close to *R. montenegrensis* and *R. prolixus* close to *R. nasutus* and *R. dalessandroi*. Although, in contrast Schofield and Dujardin (1999) considered *R. prolixus* a species domiciliary adapted from a wild *R. robustus* lineage; the results found in the present work agrees with Monteiro et al. (2003), who reiterated that both species were independent taxa (analyzing Cytb), and with Feliciangeli et al. (2007), who comparing the two species using geometric morphometry of hemelytra, showed a possible wild origin of *R. prolixus*.

Monteiro et al. (2003) considered *R. robustus* a paraphyletic group and formed by at least four cryptic species (represented by the author as lineages I, II, III and IV). De Carvalho et al. (2017) used transcriptomic analysis to demonstrate that *R. montenegrensis* and *R. robustus* represented distinct species.

Monteiro et al. (2018) suggested that lineage II of *R. robustus* was described as *R. montenegrensis* and lineage III as *R. marabaensis*. On the other hand, Brito et al. (2019), as well using transcriptomic analysis, observed that *R. montenegrensis* would be genetically indistinguishable from a variant of *R. robustus* II (specimens from Bolivia, Brazil and Ecuador). Brito et al. (2019) also hypothesized that the colonies used as a reference in the description of *R. montenegrensis* were probably a mixture of colonies of *R. prolixus* and *R. robustus*. In the present study, we verified that, in the geometric morphometry of the heads, *R. montenegrensis* was not as close as expected to *R. robustus* and/or *R. prolixus* in the bubble plot (factorial) map, but directly linked to *R. robustus* and closely related to *R. marabaensis* and *R. barretti* in the dendrogram. In the cluster analysis using hemelytra, the species appear external to the group formed by *R. prolixus* and *R. robustus*.

Both hemelytra and head geometric morphometry show *R. neivai* and *R. domesticus* as outgroup species. These results corroborate those obtained by Schofield and Dujardin (1999), Monteiro et al. (2000) and de Paula et al. (2007). These species, considered ancient and isolated, are found geographically far from others present in the *R. prolixus* complex. *Rhodnius domesticus* is commonly found in bromeliads of the Brazilian Atlantic Forest and the *Rhodnius neivai* is found near the Andes Mountains (in Colombia and Venezuela) and in the Maracaibo basin (Abad-Franch et al. 2009; Pita et al. 2013; Monteiro et al. 2018). This fact may justify why these species have such specific characteristics and are located as outliers in the analyses. Carcavallo et al. (2000) cited that *R. domesticus* had sufficient morphological characters to be considered a separate taxon, while Monteiro et al. (2000) stated that *R. neivai* has no support, based on Cytb sequences, to be associated with the *R. prolixus* complex. Schofield and Dujardin (1999) even proposed that *R. neivai* should be grouped with the *R. pictipes* complex. Thus, according to the evidence found in the present work and corroborating the results of Schofield and Dujardin (1999), Monteiro et al. (2000) and de Paula et al. (2007), we suggest the removal of both species from the *R. prolixus* complex and the establishment of a *R. neivai* complex comprising both, *R. domesticus* and *R. neivai*.

Comparing the graphical analysis of the hemelytra and recent published papers as Zhao et al. (2021), we observed that the results using this structure do not always present an adequate resolution for separating the species as expected reflecting molecular phylogeny, indicating that possibly this structure has a lot of homoplasy and very similar morphologies. For this reason, the use of heads to elucidate the differences seems to be more appropriate for this group of species.

Conclusion

The use of different taxonomic methods (integrative taxonomy) is increasingly important in taxonomic studies, especially when dealing with closely related species (Alevi et al. 2020). Through geometric morphometry, it was possible to define the morphometric profiles of the species belonging to the *R. prolixus* complex using both structures, hemelytra, and heads (except for *R. barretti*, for which it was not possible to analyze the hemelytra). Using this method, focusing on the heads, it was possible to differentiate all the species used, which include

R. barretti, *R. dalessandroi*, *R. domesticus*, *R. marabaensis*, *R. milesi*, *R. montenegrensis*, *R. nasutus*, *R. neglectus*, *R. neivai*, *R. prolixus*, and *R. robustus*. These results suggest that *R. milesi* is indeed a variant of *R. neglectus*, emphasizing the need for formal synonymization. They also propose the establishment of the *R. neivai* complex (comprising the species *R. domesticus* and *R. neivai*) (Suppl. material 3) and confirm that *R. prolixus* and *R. robustus* are distinct species.

Acknowledgements

We are very grateful to the curators from CEIOC, Dr Marcio Felix and Cláudia Rodrigues, from CTIOC Dr Hugo Guimarães, and the assistant from the Museum für Naturkunde Birgit Jaenicke for the access in the collections. We are also thankful to Dr Jader Oliveira and the technician Raquel Ferreira for the provided images.

Additional information

Conflict of interest

The authors have declared that no competing interests exist.

Ethical statement

No ethical statement was reported.

Funding

This study was financed in part by the Coordenação de Aperfeiçoamento de Pessoal de Nível Superior - Brasil (CAPES) - Finance Code 001 and also has received financial support from Conselho Nacional de Desenvolvimento Científico e Tecnológico (CNPq, Brazil). CG was supported by CNPq (#305182/2019-6).

Author contributions

Conceptualization: ACPCA, CD, CG. Formal analysis: ACPCA, CD. Funding acquisition: CG. Investigation: ACPCA, CD. Methodology: ACPCA, CD, CG. Project administration: CG. Resources: CD, CG. Supervision: CD, CG. Visualization: ACPCA. Writing – original draft: ACPCA. Writing – review and editing: ACPCA, CD, CG.

Author ORCIDs

Ana Carolina P. C. Alvarez  <https://orcid.org/0000-0002-5853-8298>

Carolina Dale  <https://orcid.org/0000-0002-9526-9242>

Cleber Galvão  <https://orcid.org/0000-0003-4027-9205>

Data availability

All of the data that support the findings of this study are available in the main text or Supplementary Information.

References

Abad-Franch F, Monteiro FA, Jaramillo ON, Gurgel-Gonçalves R, Dias FBS, Diotaiuti L (2009) Ecology, evolution, and the long-term surveillance of vector-borne Chagas disease: A multi-scale appraisal of the tribe Rhodniini (Triatominae). *Acta Tropica* 110(2–3): 159–177. <https://doi.org/10.1016/j.actatropica.2008.06.005>

- Abad-Franch F, Monteiro FA, Pavan MG, Patterson JS, Bargues MD, Zuriaga MÁ, Aguilar M, Beard CB, Mas-Coma S, Miles MA (2021) Under pressure: Phenotypic divergence and convergence associated with microhabitat adaptations in Triatominae. *Parasites & Vectors* 14(1): e195. <https://doi.org/10.1186/s13071-021-04647-z>
- Alevi K, de Oliveira J, Garcia A, Cristal D, Delgado L, de Freitas Bittinelli I, dos Reis Y, Ravazi A, de Oliveira A, Galvão C, de Azeredo-Oliveira M, Madeira F (2020) *Triatoma rosai* sp. nov. (Hemiptera, Triatominae): A new species of Argentinian chagas disease vector described based on integrative taxonomy. *Insects* 11(12): e830. <https://doi.org/10.3390/insects11120830>
- Barata JMS (1981) Aspectos morfológicos de ovos de triatominae: II – Características macroscópicas e exocoriais de dez espécies do gênero *Rhodnius* Stål, 1859 (Hemiptera – Reduviidae). *Revista de Saude Publica* 15(5): 490–542. <https://doi.org/10.1590/S0034-89101981000500006>
- Bookstein F (1991) *Morphometric Tools for Landmark Data*. Cambridge University Press, 435 pp. <https://doi.org/10.1017/CBO9780511573064>
- Brito RN, Geraldo JA, Monteiro FA, Lazoski C, Souza RCM, Abad-Franch F (2019) Transcriptome-based molecular systematics: *Rhodnius montenegrensis* (Triatominae) and its position within the *Rhodnius prolixus*-*Rhodnius robustus* cryptic-species complex. *Parasites & Vectors* 12(1): e305. <https://doi.org/10.1186/s13071-019-3558-9>
- Carcavallo R, Barreto P (1976) A new species of *Rhodnius* in Colombia. *Boletín de la Dirección de Malariología y Saneamiento Ambiental* 16: 176–183.
- Carcavallo RU, Jurberg J, Lent H, Noireau F, Galvao C (2000) Phylogeny of the Triatominae (Hemiptera: Reduviidae): proposals for taxonomic arrangements. *Entomología y Vectores* 7: 1–99. <https://www.documentation.ird.fr/hor/fdi:010024157>
- Coutinho CBD (2013) Caracterização das espécies do gênero *Rhodnius* Stål, 1859 (Hemiptera, Reduviidae, Triatominae) pelo método do Código de Barras de DNA. Fundação Oswaldo Cruz. Instituto Oswaldo Cruz, 1–107.
- Coutinho CBD (2017) Taxonomia integrada de espécies de *Triatoma* Laporte, 1832 (Hemiptera: Reduviidae: Triatominae) do Estado do Rio Grande do Sul, Brasil. Instituto Oswaldo Cruz, Fundação Oswaldo Cruz, 1–101.
- Cruz DD, Ospina-Garcés SM, Arellano E, Ibarra-Cerdeña CN, Nava-García E, Alcalá R (2023) Geometric morphometrics and ecological niche modelling for delimitation of *Triatoma pallidipennis* (Hemiptera: Reduviidae: Triatominae) haplogroups. *Current Research in Parasitology & Vector-borne Diseases* 3: e100119. <https://doi.org/10.1016/j.crpvbd.2023.100119>
- da Rosa J, Mendonça V, Gardim S, de Carvalho D, de Oliveira J, Nascimento J, Pinotti H, Pinto M, Cilense M, Galvão C, Barata JM (2014) Study of the external female genitalia of 14 *Rhodnius* species (Hemiptera, Reduviidae, Triatominae) using scanning electron microscopy. *Parasites & Vectors* 7(1): 1–17. <https://doi.org/10.1186/1756-3305-7-17>
- Dale C, Justi SA, Galvão C (2013) Tropical insect collections and DNA extraction, using *Rhodnius* Stål 1859 (Hemiptera: Heteroptera: Reduviidae: Triatominae). *Zootaxa* 3694(4): e398. <https://doi.org/10.11646/zootaxa.3694.4.8>
- de Carvalho DB, Congrains C, Chahad-Ehlers S, Pinotti H, de Brito RA, da Rosa JA (2017) Differential transcriptome analysis supports *Rhodnius montenegrensis* and *Rhodnius robustus* (Hemiptera, Reduviidae, Triatominae) as distinct species. *PLoS ONE* 12(4): e0174997. <https://doi.org/10.1371/journal.pone.0174997>
- de Fuentes-Vicente JA, Santos-Hernández NG, Ruiz-Castillejos C, Espinoza-Medinilla EE, Flores-Villegas AL, de Alba-Alvarado M, Cabrera-Bravo M, Moreno-Rodríguez A, Vidal-López DG (2023) What Do You Need to Know before Studying Chagas Disease? A

- Beginner's Guide. *Tropical Medicine and Infectious Disease* 8(7): e360. <https://doi.org/10.3390/tropicalmed8070360>
- de Paula AS, Diotaiuti L, Galvão C (2007) Systematics and biogeography of *Rhodnius* (Heteroptera: Reduviidae: Triatominae) based on 16S mitochondrial rDNA sequences. *Journal of Biogeography* 34(4): 699–712. <https://doi.org/10.1111/j.1365-2699.2006.01628.x>
- Depickère S, Ravelo-García AG, Lardeux F (2020) Chagas disease vectors identification using visible and near-infrared spectroscopy. *Chemometrics and Intelligent Laboratory Systems* 197: e103914. <https://doi.org/10.1016/j.chemolab.2019.103914>
- Dias FBS (2007) Ecologia de *Rhodnius nasutus* Stal 1859 (Hemiptera: Reduviidae: Triatominae) em palmeiras da Chapada do Araripe, Ceará, Brasil. *Sciences et Techniques de l'Animal de Laboratoire*. Centro de Pesquisas René Rachou, Fundação Oswaldo Cruz, 1–121.
- Dias J, Schofield C (1999) The evolution of Chagas disease (American Trypanosomiasis) control after 90 years since Carlos Chagas discovery. *Memorias do Instituto Oswaldo Cruz* 94(suppl 1): 103–121. <https://doi.org/10.1590/S0074-02761999000700011>
- Dias FBS, Jaramillo-O N, Diotaiuti L (2014) Description and characterization of the melanic morphotype of *Rhodnius nasutus* Stål, 1859 (Hemiptera: Reduviidae: Triatominae). *Revista da Sociedade Brasileira de Medicina Tropical* 47(5): 637–641. <https://doi.org/10.1590/0037-8682-0007-2014>
- Dujardin J-P (2019) A template-dependent semilandmarks treatment and its use in medical entomology. *Infection, Genetics and Evolution* 70: 197–207. <https://doi.org/10.1016/j.meegid.2019.03.002>
- Dujardin J, Panzera P, Schofield C (1999) Triatominae as a model of morphological plasticity under ecological pressure. *Memorias do Instituto Oswaldo Cruz* 94(suppl 1): 223–228. <https://doi.org/10.1590/S0074-02761999000700036>
- Dumonteil E, Herrera C (2017) Ten years of Chagas disease research: Looking back to achievements, looking ahead to challenges. *PLOS Neglected Tropical Diseases* 11: e0005422. <https://doi.org/10.1371/journal.pntd.0005422>
- Feliciangeli MD, Sanchez-Martin M, Marrero R, Davies C, Dujardin JP (2007) Morphometric evidence for a possible role of *Rhodnius prolixus* from palm trees in house re-infestation in the State of Barinas (Venezuela). *Acta Tropica* 101(2): 169–177. <https://doi.org/10.1016/j.actatropica.2006.12.010>
- Filée J, Merle M, Bastide H, Mougél F, Bérenger J-M, Folly-Ramos E, Almeida CE, Harry M (2022) Phylogenomics for chagas disease vectors of the *Rhodnius* genus (Hemiptera, Triatominae): What we learn from mito-nuclear conflicts and recommendations. *Frontiers in Ecology and Evolution* 9: e750317. <https://doi.org/10.3389/fevo.2021.750317>
- Fornel R, Cordeiro-Estrela P (2012) Morfometria geométrica e a quantificação da forma dos organismos. *Temas em Biologia: Edição comemorativa aos 20*: 101–120.
- Galvão C (2014) Vetores da doença de Chagas no Brasil. *Sociedade Brasileira de Zootologia*, 289 pp. <https://doi.org/10.7476/9788598203096>
- Galvão C, Dale C (2014) Chaves de Identificação Para Adultos. *Vetores da Doença de Chagas no Brasil*. Sociedade Brasileira de Zoologia, Curitiba, 171–208. <https://doi.org/10.7476/9788598203096.0009>
- Galvão C, Carcavallo R, Rocha DDS, Jurberg J (2003) A checklist of the current valid species of the subfamily Triatominae Jeannel, 1919 (Hemiptera, Reduviidae) and their geographical distribution, with nomenclatural and taxonomic notes. *Zootaxa* 202(1): 1–1. <https://doi.org/10.11646/zootaxa.202.1.1>

- Gurgel-Gonçalves R, Abad-Franch F, Ferreira JBC, Santana DB, Cuba CAC (2008) Is *Rhodnius prolixus* (Triatominae) invading houses in central Brazil? *Acta Tropica* 107(2): 90–98. <https://doi.org/10.1016/j.actatropica.2008.04.020>
- Gurgel-Gonçalves R, Ferreira JBC, Rosa AF, Bar ME, Galvão C (2011) Geometric morphometrics and ecological niche modelling for delimitation of near-sibling triatomine species. *Medical and Veterinary Entomology* 25(1): 84–93. <https://doi.org/10.1111/j.1365-2915.2010.00920.x>
- Institute SAS (2000) JMP: Statistics and graphics guide. Sas Inst.
- Lent H (1948) [The genus *Rhodnius* Stal, 1859, Hemiptera, Reduviidae]. *Revista Brasileira de Biologia* 8: 297–339.
- Lent H, Jurberg J (1969) The genus *Rhodnius* Stål, 1859, with a study of the genitalia of the species (Hemiptera, Reduviidae, Triatominae). *Revista Brasileira de Biologia* 29: 487–560.
- Lent H, Wygodzinsky P (1979) Revision of the Triatominae (Hemiptera, Reduviidae), and their significance as vectors of Chagas' disease. *Bulletin of the American Museum of Natural History* 163: 123–520.
- Maia da Silva F, Noyes H, Campaner M, Junqueira AcV (2004) Phylogeny, taxonomy and grouping of *Trypanosoma rangeli* isolates from man, triatomines and sylvatic mammals from widespread geographical origin based on SSU and ITS ribosomal sequences. *Parasitology* 129(5): 549–561. <https://doi.org/10.1017/S0031182004005931>
- Monteiro FA, Wesson DM, Dotson EM, Schofield CJ, Beard CB (2000) Phylogeny and molecular taxonomy of the rhodniini derived from mitochondrial and nuclear DNA sequences. *The American Journal of Tropical Medicine and Hygiene* 62(4): 460–465. <https://doi.org/10.4269/ajtmh.2000.62.460>
- Monteiro FA, Barrett TV, Fitzpatrick S, Cordon-Rosales C, Feliciangeli D, Beard CB (2003) Molecular phylogeography of the Amazonian Chagas disease vectors *Rhodnius prolixus* and *R. robustus*. *Molecular Ecology* 12(4): 997–1006. <https://doi.org/10.1046/j.1365-294X.2003.01802.x>
- Monteiro FA, Weirauch C, Felix M, Lazoski C, Abad-Franch F (2018) Evolution, Systematics, and Biogeography of the Triatominae, Vectors of Chagas Disease. *Advances in Parasitology*. Academic Press, 265–344. <https://doi.org/10.1016/bs.apar.2017.12.002>
- Montiel EE, Panzera F, Palomeque T, Lorite P, Pita S (2021) Satellitome analysis of *Rhodnius prolixus*, one of the main chagas disease vector species. *International Journal of Molecular Sciences* 22(11): e6052. <https://doi.org/10.3390/ijms22116052>
- Nascimento JD, da Rosa JA, Salgado-Roa FC, Hernández C, Pardo-Díaz C, Alevi KCC, Ravazi A, de Oliveira J, de Azeredo Oliveira MTV, Salazar C, Ramírez JD (2019) Taxonomical over splitting in the *Rhodnius prolixus* (Insecta: Hemiptera: Reduviidae) clade: Are *R. taquarussuensis* (da Rosa et al., 2017) and *R. neglectus* (Lent, 1954) the same species? *PLoS ONE* 14(2): e0211285. <https://doi.org/10.1371/journal.pone.0211285>
- Neiva A, Pinto C (1923) Estado actual dos conhecimentos sobre o gênero *Rhodnius* Stal, com a descrição de uma nova espécie. *Brasil-medico* 37: 20–24.
- Pavan MG, Monteiro FA (2007) A multiplex PCR assay that separates *Rhodnius prolixus* from members of the *Rhodnius robustus* cryptic species complex (Hemiptera: Reduviidae). *Tropical Medicine & International Health* 12(6): 751–758. <https://doi.org/10.1111/j.1365-3156.2007.01845.x>
- Pita S, Panzera F, Ferrandis I, Galvão C, Gómez-Palacio A, Panzera Y (2013) Chromosomal divergence and evolutionary inferences in Rhodniini based on the chromosomal location of ribosomal genes. *Memorias do Instituto Oswaldo Cruz* 108(3): 376–382. <https://doi.org/10.1590/S0074-02762013000300017>

- Poinar Jr G (2019) A primitive triatomine bug, *Paleotriatoma metaxytaxa* gen. et sp. nov. (Hemiptera: Reduviidae: Triatominae), in mid-Cretaceous amber from northern Myanmar. *Cretaceous Research* 93: 90–97. <https://doi.org/10.1016/j.cretres.2018.09.004>
- Ravazi A, Olaia N, de Oliveira J, Souza EDS, da Rosa JA, de Azeredo-Oliveira MTV, Alevi KCC (2021) Revisiting the Chromosomal Diversification of the Genus *Rhodnius* (Stål, 1859) (Hemiptera, Triatominae). *The American Journal of Tropical Medicine and Hygiene* 104(2): 656–658. <https://doi.org/10.4269/ajtmh.20-0875>
- Rocha D da S, Patterson JS, Sandoval CM, Jurberg J, Ângulo VM, Esteban AL, Galvão C (2005) Description and ontogenetic morphometrics of nymphs of *Belminus herreri* Lent & Wygodzinsky (Hemiptera: Reduviidae, Triatominae). *Neotropical Entomology* 34(3): 491–497. <https://doi.org/10.1590/S1519-566X2005000300019>
- Rohlf F (2005) Geometric morphometrics simplified. *Trends in Ecology & Evolution* 20(1): 13–14. <https://doi.org/10.1016/j.tree.2004.08.005>
- Schmunis GA (1999) Prevention of transfusional *Trypanosoma cruzi* infection in Latin America. *Memorias do Instituto Oswaldo Cruz* 94(suppl 1): 93–101. <https://doi.org/10.1590/S0074-02761999000700010>
- Schofield CJ, Dujardin J-P (1999) Theories on the evolution of *Rhodnius*. *Actualidades Biológicas* 21(71): 183–197. <https://doi.org/10.17533/udea.acbi.329778>
- Soto Vivas A, Rodríguez C, Bonfante-Cabarcá R, Aldana E (2007) Morfometría geométrica de *Triatoma maculata* (Erichson, 1848) de ambientes doméstico y peridoméstico, estado Lara, Venezuela. *Boletín de Malariología y Salud Ambiental* 47: 231–235.
- Souza ÉDS (2020) Caracterização de espécies do gênero *Rhodnius* Stal, 1859 (Hemiptera, Reduviidae, Triatominae) pelo método MALDI-TOF-MS.
- Téllez-Rendón J, Esteban L, Rengifo-Correa L, Díaz-Albiter H, Huerta H, Dale C (2023) *Triatoma yelapensis* sp. nov. (Hemiptera: Reduviidae) from Mexico, with a Key of *Triatoma* Species Recorded in Mexico. *Insects* 14(4): e331. <https://doi.org/10.3390/insects14040331>
- The Pan American Health Organization (2023) Chagas disease.
- Vallejo GA, Guhl F, Schaub GA (2009) Triatominae–*Trypanosoma cruzi*/*T. rangeli*: Vector–parasite interactions. *Acta Tropica* 110(2–3): 137–147. <https://doi.org/10.1016/j.actatropica.2008.10.001>
- Valente V da C, Valente SA da S, Carcavallo RU, Rocha D da S, Galvão C, Jurberg J (2001) Considerações sobre uma nova espécie do gênero *Rhodnius* Stal, do Estado do Pará, Brasil (Hemiptera, Reduviidae, Triatominae). *Entomologia y Vectores*: 65–80.
- Zhao Y, Galvão C, Cai W (2021) *Rhodnius micki*, a new species of Triatominae (Hemiptera, Reduviidae) from Bolivia. *ZooKeys* 1012: 71–93. <https://doi.org/10.3897/zookeys.1012.54779>
- Zhao Y, Fan M, Li H, Cai W (2023) Review of Kissing Bugs (Hemiptera: Reduviidae: Triatominae) from China with Descriptions of Two New Species. *Insects* 14(5): e450. <https://doi.org/10.3390/insects14050450>

Supplementary material 1

Collection numbers of the specimens studied

Authors: Ana Carolina P. C. Alvarez, Carolina Dale, Cleber Galvão

Data type: xlsx

Explanation note: List of collection numbers of the specimens studied.

Copyright notice: This dataset is made available under the Open Database License (<http://opendatacommons.org/licenses/odbl/1.0/>). The Open Database License (ODbL) is a license agreement intended to allow users to freely share, modify, and use this Dataset while maintaining this same freedom for others, provided that the original source and author(s) are credited.

Link: <https://doi.org/10.3897/zookeys.1202.108157.suppl1>

Supplementary material 2

Colors used to identify the species of *R. prolixus* complex

Authors: Ana Carolina P. C. Alvarez, Carolina Dale, Cleber Galvão

Data type: xlsx

Explanation note: Colors and codes used to identify specimens in hemelytra and head analyzes; Numbers of specimens used on each analyzes.

Copyright notice: This dataset is made available under the Open Database License (<http://opendatacommons.org/licenses/odbl/1.0/>). The Open Database License (ODbL) is a license agreement intended to allow users to freely share, modify, and use this Dataset while maintaining this same freedom for others, provided that the original source and author(s) are credited.

Link: <https://doi.org/10.3897/zookeys.1202.108157.suppl2>

Supplementary material 3

Establishment of the *R. neivai* complex

Authors: Ana Carolina P. C. Alvarez, Carolina Dale, Cleber Galvão

Data type: xlsx

Explanation note: Comprising the species *R. domesticus* and *R. neivai*.

Copyright notice: This dataset is made available under the Open Database License (<http://opendatacommons.org/licenses/odbl/1.0/>). The Open Database License (ODbL) is a license agreement intended to allow users to freely share, modify, and use this Dataset while maintaining this same freedom for others, provided that the original source and author(s) are credited.

Link: <https://doi.org/10.3897/zookeys.1202.108157.suppl3>

Taxonomic study on the genus *Mongoloniscus* Verhoeff, 1930 (Isopoda, Agnaridae) from China: morphological and phylogenetic analyses

Chao Jiang¹, Jing Zhong¹, Zhidong Wang¹, Weichun Li², Luqi Huang¹

¹ State Key Laboratory for Quality Ensurance and Sustainable Use of Dao-di Herbs, National Resource Center for Chinese Materia Medica, China Academy of Chinese Medical Sciences, Beijing 100700, China

² College of Agronomy, Jiangxi Agricultural University, Nanchang 330045, China

Corresponding authors: Weichun Li (weichunlee@126.com); Luqi Huang (Huangluqi01@126.com)

Abstract

A combination of morphological traits and DNA data (COI and 28S rRNA partial sequences) was used to study the genus *Mongoloniscus* Verhoeff, 1930 from China. Four new species are described: *M. crenatus* Jiang, Li & Huang, **sp. nov.**, *M. orientalis* Jiang, Li & Huang, **sp. nov.**, *M. polyacanthum* Jiang, Li & Huang, **sp. nov.**, and *M. parvus* Jiang, Li & Huang, **sp. nov.** Following an in-depth examination of the *Mongoloniscus* species, *Lucasioides vannamei* (Arcangeli, 1927), **comb. nov.** (from *Mongoloniscus*) is proposed, and *M. chevronus* Yang & An, 2021, **syn. nov.** is synonymized with *Koreoniscus racovitzae* (Arcangeli, 1927). A restrictive criterion for recognizing the genus *Mongoloniscus* is also provided in the present study.

Key words: DNA, morphology, new species, Oniscidea, taxonomy



Academic editor: Saskia Brix

Received: 2 October 2023

Accepted: 11 April 2024

Published: 23 May 2024

ZooBank: <https://zoobank.org/B493B7C6-9977-4A6C-B9D4-D4A865468DC8>

Citation: Jiang C, Zhong J, Wang Z, Li W, Huang L (2024) Taxonomic study on the genus *Mongoloniscus* Verhoeff, 1930 (Isopoda, Agnaridae) from China: morphological and phylogenetic analyses. ZooKeys 1202: 229–253. <https://doi.org/10.3897/zookeys.1202.113560>

Copyright: © Chao Jiang et al.
This is an open access article distributed under terms of the Creative Commons Attribution License (Attribution 4.0 International – CC BY 4.0).

Introduction

Agnaridae, one of 38 families within the order Oniscidea worldwide, comprises 14 genera. At present, six genera, namely *Hemilepistus* Budde-Lund, 1879, *Agnara* Budde-Lund, 1908, *Protracheoniscus* Verhoeff, 1917, *Mongoloniscus* Verhoeff, 1930, *Koreoniscus* Verhoeff, 1937, and *Lucasioides* Kwon, 1993 have been recorded (Kwon 1993; Kwon and Taiti 1993; Tang and Gui 2000; Li 2017; Chen 2003; Wang et al. 2022a, 2023). However, taxonomic research on the Chinese woodlice is far from complete. In the present study, we focused on the taxonomy of *Mongoloniscus* from China.

Mongoloniscus was established by Verhoeff (1930) as a subgenus of *Protracheoniscus* Verhoeff, 1917 with *P. (M.) koreanus* Verhoeff, 1930 proposed as its type species. To date, this genus consists of eighteen species. All known species are recorded from East Asia (China, Korea, and Japan) (Schmalfuss 2003; Boyko et al. 2008; Nunomura 2010a, 2010b, 2013; Li 2017) except *M. persicus* Kashani, 2014, which has been reported in Iran (Kashani 2014). Four *Mongoloniscus* spp. have been recorded in China. Among them, *M. sinensis* (Dollfus, 1901) and *M. chevronus* Yang & An, 2021 are endemic to northern China (Chen 2003; Zhao et al.

2016; Yang and An 2021), whereas *M. koreanus* (Verhoeff, 1930) and *M. vannamei* (Arcangeli, 1927) are not only found across several southern Chinese provinces (Kwon 1993; Kwon and Taiti 1993; Chen 2003) but also have been reported in Japan and Korea (Kwon 1993; Saito et al. 2000).

Kwon (1993) proposed a definition for *Mongoloniscus* based on the following morphological traits: (1) triangular median lobe of cephalon, frontal line separated from vertex by a groove; (2) granulated dorsum, numerous gland pores along the whole margin of pereonites; (3) noduli laterales more or less at the same distance from lateral margin; (4) pereonite 1 evenly convex with postero-lateral corners rounded; (5) pleopodal exopods 1–5 with *Protracheoniscus*-type pseudotrachea; (6) male pleopod 1 exopod with bilobed distal part, and male pleopod 2 endopod with a filiform distal part. However, some species have parts of the above characters that have been assigned to *Mongoloniscus*, leading to a heterogeneous grouping (Kashani 2014; Yang and An 2021).

Recently, the integrative methods of morphology combined with DNA data shed light on taxa delimitation in Oniscidea systematics (Dimitriou et al. 2019). Molecular phylogenetics has revealed numerous cryptic Oniscidea species. Dimitriou et al. (2023) revealed cryptic Armadillidiidae diversity within Cyprus island and discovered two new species. Zimmermann et al. (2018) integrated morphology and molecular analyses to delimit Philosciidae species and reveal a new genus from Brazil. This approach has also been applied to other oniscidean isopods and discovered species of *Hemilepistus*, and *Protracheoniscus* (Gongalsky et al 2018; Wang et al. 2022b). In this study, to objectively identifies *Mongoloniscus* species, we studied the genus from China by integrating morphological characters and molecular data.

Materials and methods

The specimens were collected at 48 localities of China (Fig. 1), and preserved in 75% ethanol. All specimens were deposited at the Herbarium, National Resource Center for Chinese Materia Medica, China Academy of Chinese Medical Sciences, China (CMMI).

Morphology

The whole body of the specimens was placed in acid-fuchsin staining buffer for twelve hours. The appendages were dissected and mounted on micro preparations in a neutral balsam mounting medium using a Leica M205 FA microscope. The morphological terminology followed Kwon (1993) and Kwon and Taiti (1993). The taxonomic characters were observed with a Leica M205 FA microscope. Habitus were taken with a Leica M205 MCA camera attached to the microscope. The line drawings were drawn by the GNU Image Manipulation Program (Montesanto 2015).

DNA extraction and fragment amplification

Genomic DNA was extracted from tissue samples of each specimen using the Promega Wizard® SV Genomic DNA Purification Kit (Promega, USA). Polymerase chain reaction (PCR) was used to amplify cytochrome c oxidase subunit I (COI)

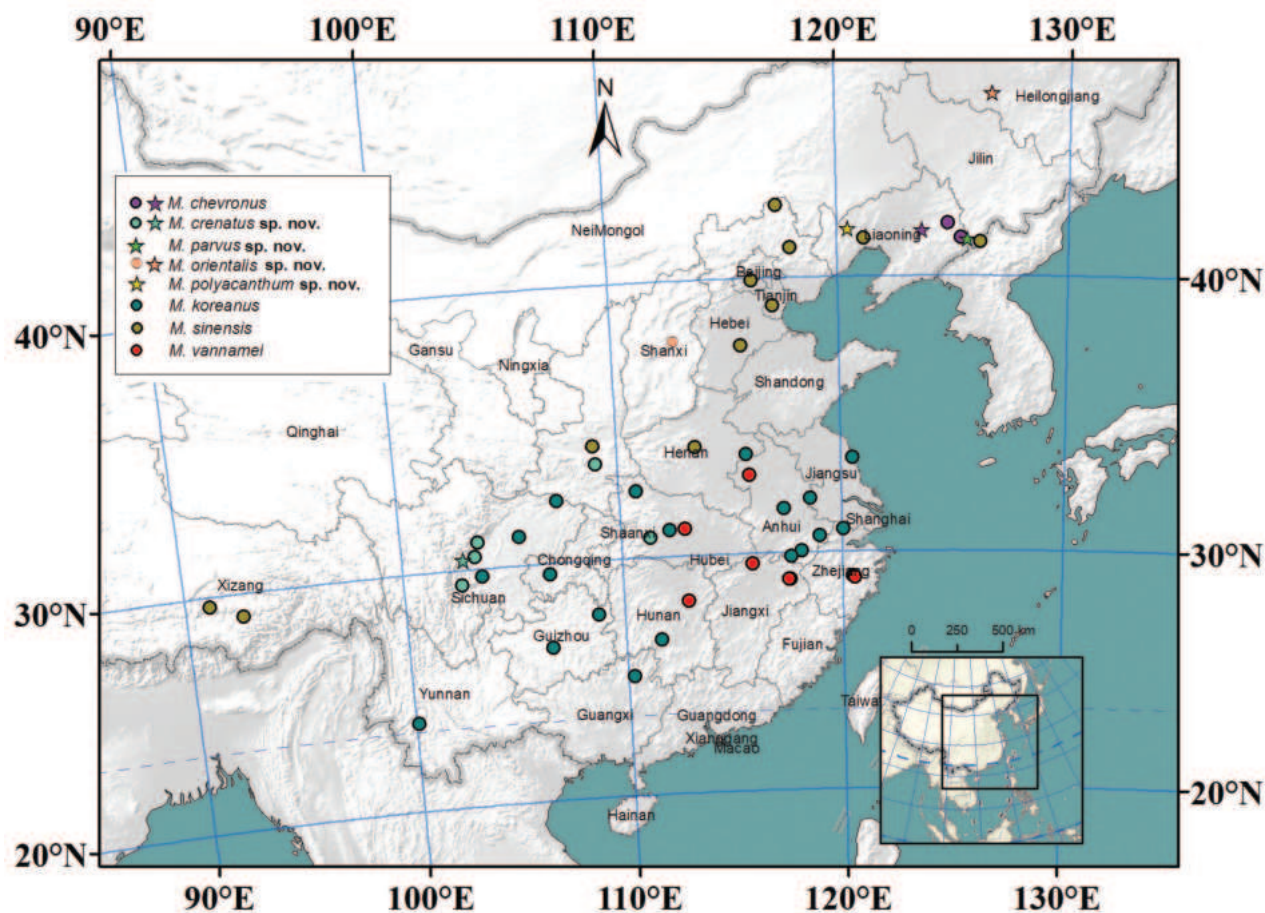


Figure 1. Collected localities of species of *Mongoloniscus* in China. Stars represent type localities.

and nuclear ribosomal DNA 28S fragments. The COI fragments were amplified using primers LCO1490 and HCOoutout (Folmer et al. 1994; Schwendinger and Giribet 2005), 28S fragments were amplified using primers 28Sa and 28Sb (Michael et al. 1997; Joshi and Karanth 2011) followed the procedure described by Chen et al. (2023). All sequences were deposited in GenBank database, with accession numbers listed in Suppl. material 1: table S1.

Molecular analyses

The COI sequences and 28S sequences obtained from this study, as well as data from previous phylogenetic studies obtained from GenBank, were incorporated into the phylogenetic analysis (Poulakakis and Sfenthourakis 2008; Tanaka and Karasawa 2016; Gongalsky et al. 2021; Yang and An 2021; Dimitriou and Sfenthourakis 2022; accession numbers provided as Suppl. material 1: table S1).

Phylogenetic trees were constructed using Bayesian inference (BI) and maximum likelihood (ML) methods, with branch support assessed using standard statistical tests, including bootstrap support (BS) and posterior probability (PP). ML analysis was performed using the IQ-TREE 1.6.8 software tool (Minh et al. 2020) on the PhyloSuite 1.2.3 platform (Zhang et al. 2020) with 250,000 ultrafast bootstraps (Hoang et al. 2018). The evolutionary model for COI was selected under the Akaike information criterion using ModelFinder (Kalyanamoorthy et al. 2017),

GTR+F+I+G4 using Bayesian inference (BI) and TIM+F+I+G4 for maximum likelihood (ML) analyses. BI analyses were conducted using MrBayes 3.2.6 (Ronquist et al. 2012) over 10,000,000 generations, sampled every 1000 generations, with 25% of trees set aside as burn-in. Stationarity was assessed using a split frequency of less than 0.001, and a consensus tree was constructed from the remaining trees. The consensus tree is shown in FigTree 1.4.3 (Rambaut 2016). Several species of *Desertoniscus*, *Hemilepistus*, *Koreoniscus*, *Lucasioides*, *Orthometopon*, and *Protracheoniscus* were included in phylogenetic reconstructions, while *Armadillidium nasatum* Budde-Lund, 1885 was chosen as the outgroup (accession numbers provided as Suppl. material 1: table S1).

Furthermore, pairwise Kimura 2-parameter distances of the COI sequences between *Mongoloniscus* species were calculated by MEGA X (Kumar et al. 2018).

Distribution mapping

The distribution map was made with ArcMap 10.7.1. We illustrated all the collected localities based on the *Mongoloniscus* specimens in the present research.

Results

The specimens collected from China were analyzed using external traits and dissected appendages. As a result, eight members of *Mongoloniscus* were preliminarily recognized, including four known species (*M. koreanus*, *M. sinensis*, *M. vannamei* and *M. chevronus*). Among them, the morphological characters of *M. vannamei* and *M. chevronus* indicate that these two species are more likely to belong to *Lucasioides* and *Koreoniscus*, respectively. It is difficult to verify the taxonomic identities based on traditional morphology.

Molecular analyses

This study involved the sequencing and alignment of mitochondrial COI and nuclear 28S rRNA loci from *Mongoloniscus* species. Sequences from other Agnariidae genera were also included. A final alignment dataset comprising 793 base pairs (bp) of COI and 741 bp of 28S rRNA was obtained. Maximum likelihood and Bayesian methodologies were employed for phylogenetic analysis (Fig. 2). The results indicated that *M. chevronus* and *Koreoniscus racovitzi* formed a clade with high support (PP = 1.00, BS = 100%), and they were sister species to *K. huaguoshanensis* with high support from both likelihood bootstraps (PP = 1.00, BS = 100%). This suggests that *M. chevronus* is a member of *Koreoniscus*, which is supported by morphological characteristics described below. Furthermore, *M. vannamei*, *L. gigliotosi*, and *L. isseli* formed a clade with high support (PP = 1.00, BS = 95%), indicating that *M. vannamei* must be transferred to *Lucasioides* (see below for details in the taxonomic section).

The remaining *Mongoloniscus* species, including *M. koreanus*, *M. crenatus* sp. nov., *M. sinensis*, *M. polyacanthum* sp. nov., *M. parvus* sp. nov., and *M. orientalis* sp. nov. formed a clade with strong support (PP = 0.99, BS = 85%). Notably, *M. crenatus* sp. nov. was found to be a sister to *M. koreanus* with very high support (PP = 1.00, BS = 99%). The two aforementioned species, both found in southern China, formed a clade that is sister to species distributed in northern China (*M. polyacan-*

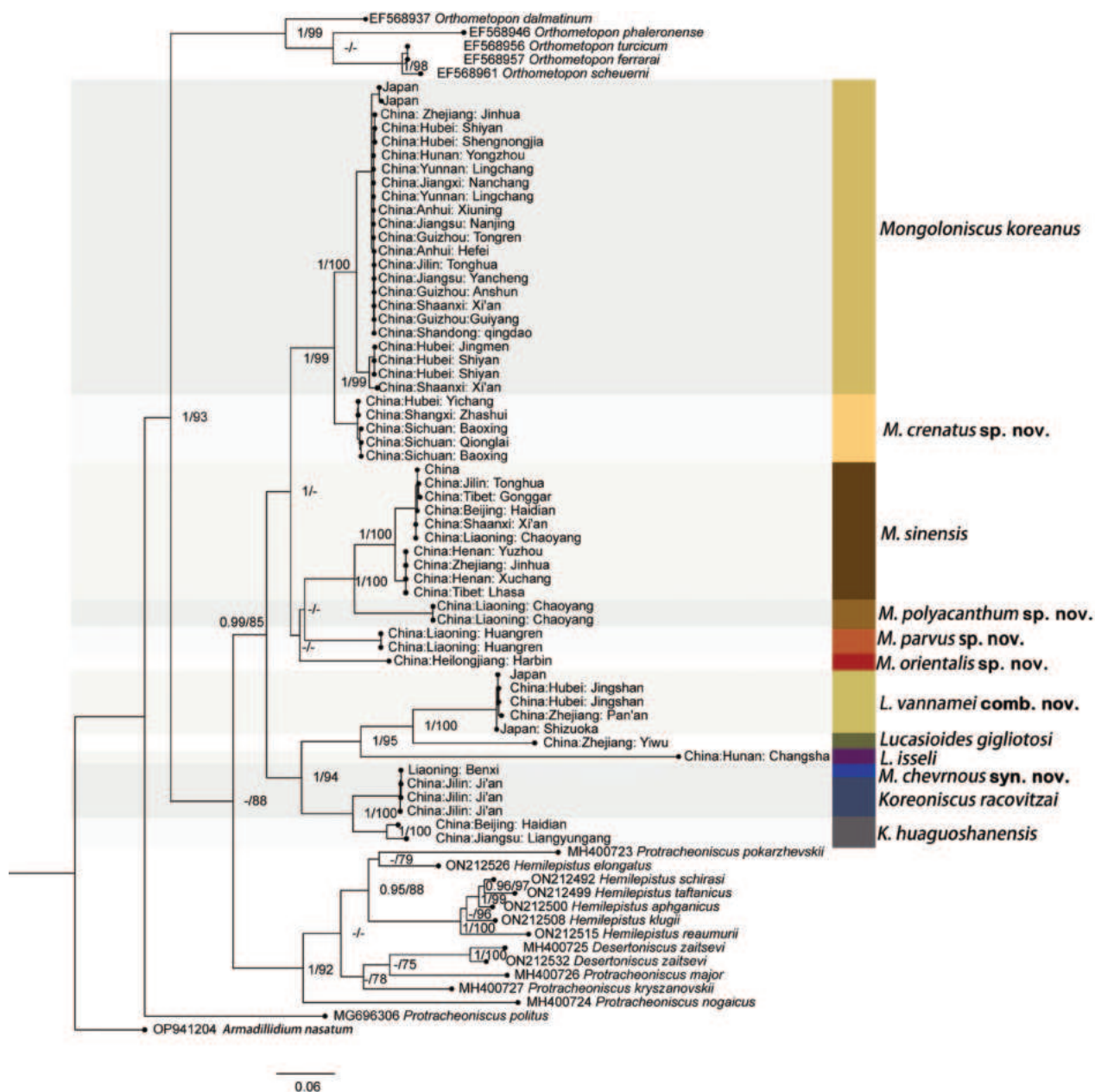


Figure 2. Maximum likelihood phylogenetic tree based on combined COI and 28S data for *Mongoloniscus*. Values above the branches represent the posterior probability (PP) and bootstrap support (BS), BS < 70% or PP < 0.9 are indicated as hyphens.

thum sp. nov., *M. parvus* sp. nov., and *M. orientalis* sp. nov.) or in northern China and Tibet (*M. sinensis*). However, this relationship had moderately low support (PP = 1.00, BS = 50%). *M. koreanus* can be divided into two genotypes with high node support (PP = 1.00, BS = 100%), one widespread in southern China while the other is limited to Hubei Province (these two populations are morphologically indistinguishable and are considered intraspecific variations). Similarly, *M. sinensis* was divided into two well-supported clades with no clear morphological or geographic correlations. Thus, they were considered to belong to the same species. In summary, *Mongoloniscus* in China appears to be a monophyletic taxon which is closely related to *Koreoniscus* and *Lucasioides*.

Genetic distances

Among *Mongoloniscus* species, the average K2P genetic distance of the COI sequences was 14.0%, the intraspecific distances were 0–3%, and the interspecific distances varied from 10% (*M. crenatus* sp. nov. and *M. koreanus*) to 24% (*M. polyacanthum* sp. nov. and *M. crenatus* sp. nov.) (Suppl. material 1: table S2). Although *M. crenatus* sp. nov. and *M. koreanus* had the lowest genetic distances, the intraspecific genetic distances were still lower than the interspecific distances. The genetic distance between *M. chevronus* and *K. racovitzai* was ~ 0%, showing no difference in the result of the phylogenetic analysis. Thus, we proposed a new synonym (see below for details under the taxonomic section of *K. racovitzai*).

Taxonomy

Order Isopoda Latreille, 1817

Suborder Oniscidea Latreille, 1802

Family Agnaridae Schmidt, 2003

Genus *Mongoloniscus* Verhoeff, 1930

Type species. *Mongoloniscus koreanus* Verhoeff, 1930, by subsequent designation.

Notes. Previous studies have ascribed eighteen species to the genus *Mongoloniscus*; however, some do not conform to the criteria proposed by Kwon (1993). In the present study, we provide the typical habitus of the genus (Fig. 3) and adopt a more restrictive interpretation, asserting that a species can be classified as *Mongoloniscus* if exhibiting all the following characters:

1. Dorsum granulated, with numerous gland pores along the entire margin of the pereonites.
2. Noduli laterales more or less at the same distance from lateral margin, with a d/c value less than 0.75.
3. Cephalon with well-developed median lobe and lateral lobes, median one convex or arched on anterior margin.
4. Pereonite 1 posterior margin straight or rounded.
5. Pleopodal exopods 1–5 with monospiracular internal lungs.
6. Pleopod 1 exopod with bilobed apex, and posterior tip of endopod bent outwards.

***Mongoloniscus crenatus* Jiang, Li & Huang, sp. nov.**

<https://zoobank.org/19F87F63-688E-4C59-887E-B78B81A8DF24>

Figs 4A, B, 5, 6

Type material. Holotype. CHINA: ♂ (20210417001), Sichuan Province, Baoxing County, Muping Town, Lengmugou Provincial Geological Park (30.3699°N, 102.8125°E), 1020 m asl., 14.iv.2021, coll. Chao Jiang.

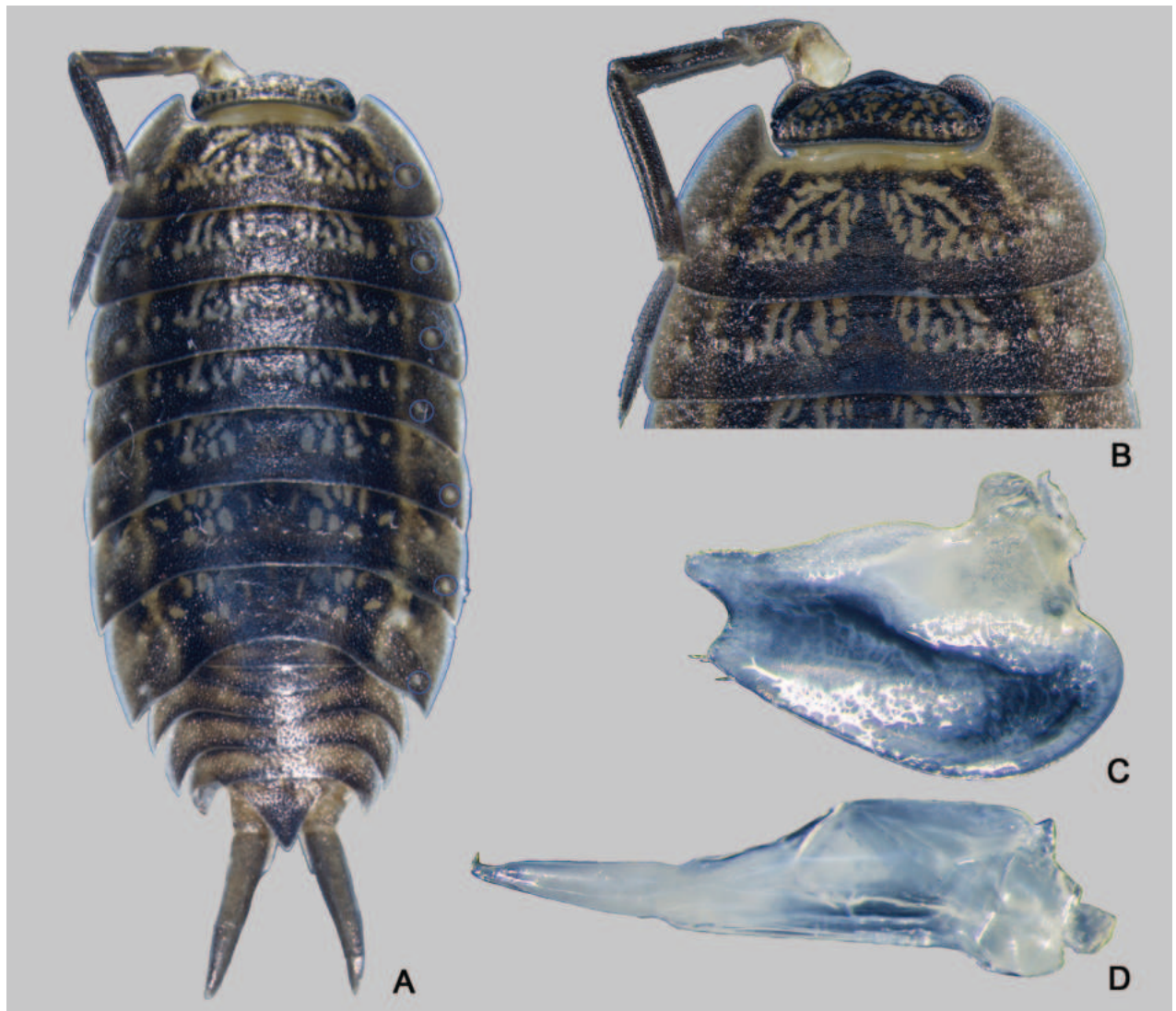


Figure 3. Habitus of *Mongoloniscus sinensis* (Dollfus, 1901), male **A** dorsal view, the blue circles show the noduli laterales arrangement **B** cephalon and pereonites 1 and 2 in dorsal view **C** pleopod 1 exopod **D** pleopod 1 endopod.

Paratypes. CHINA: 3 ♂♂, 8 ♀♀ (20210417002–20210417012), same data as the holotype. 4 ♂♂, 6 ♀♀ (20210412063–20210412066), **Hubei Province**, Yichang, Xiaoxita Forestry Park (30.7853°N, 111.3180°E), 100 m asl., 12.iv.2021, coll. Zhi-dong Wang & Tianyun Chen. 1 ♂ (20210512006), **Shaanxi Province**, Zhashui County, Lengbinggou Village (33.6931°N, 109.0239°E), 1020 m asl., 12.x.2021, coll. Chao Jiang. 3 ♂♂, 1 ♀ (20210417016–20210417019), **Sichuan Province**, Baoxing County, Dengchigou (30.5341°N, 102.9410°E), 1810 m asl., 17.iv.2021, coll. Chao Jiang; 3 ♂♂, 1 ♀ (20210416040–20210416043), Qionglai, Datong Village, Dalong Road (30.5042°N, 103.3063°E), 770 m als., 14.iv.2021, coll. Chao Jiang; 5 ♂♂, 24 ♀♀ (120220827008–20220827025), Hanyuan County, Fuling Town, Hanyuan Service Area (29.4370°N, 102.6343°E), 1080 m asl., 27.viii.2022, coll. Chao Jiang; 6 ♂♂, 9 ♀♀ (20220828036–20220828048), Tianquan County, Binhe Park (30.0584°N, 102.7597°E), 760 m asl., 28.viii.2022, coll. Chao Jiang; 18 ♂♂, 23 ♀♀ (20220829013–20220829028), Wenchuan County, Yingxiu Town (31.0557°N, 103.4887°E), 880 m asl., 29.viii.2022, coll. Chao Jiang.



Figure 4. Habitus of *Mongoloniscus* species **A, C, E, G** male, holotype **B, D, F, H** female, paratype **A, B** *M. crenatus* sp. nov. **C, D** *M. polyacanthum* sp. nov. **E, F** *M. parvus* sp. nov. **G, H** *M. orientalis* sp. nov. The blue circles show the noduli laterales arrangement. Scale bars: 3 mm.

Diagnosis. Cephalon with median lobe convex, medially with a small incision. Antennal flagellum with distal article twice as long as proximal article. Noduli laterales almost at same distance from the lateral margins. Pereopod 6 basis and pereopod 7 ischium fringed with long setae. Pleopod 1 exopod deeply bilobed at apex, inner lobe much longer than outer lobe; apex of male pleopod 1 endopod bent outwards and pointed.

Description. **Body** length of males 7–9 mm and females 8–11 mm. Body elongated and convex, ~ 2–2.5× as long as widest pereonite. Dorsum distinctly granulated, brown-gray color with usual yellowish muscle spots. Numerous gland pores along entire pereonite margin. Pereonite 1 with rounded postero-lateral corner, posterior margin nearly straight. Noduli laterales almost at the same distance from lateral margins (Fig. 4A, B). Telson triangular, approximately twice as wide as long, lateral margins slightly concave at distal one third, posterior apex blunted;

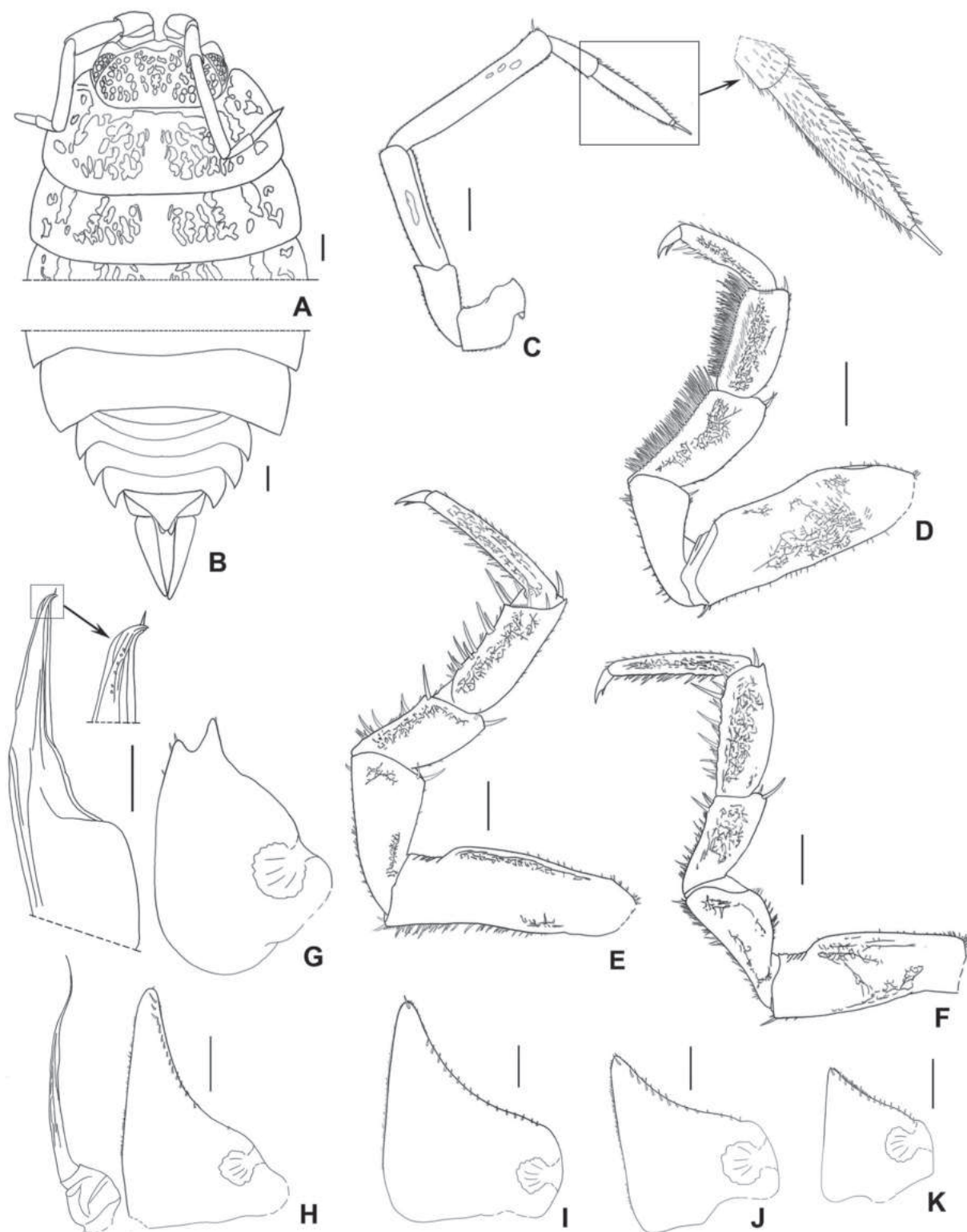


Figure 5. *Mongoloniscus crenatus* sp. nov., holotype **A** cephalon, pereonites 1 and 2 in dorsal view **B** pleonites, telson and uropod in dorsal view **C** second antenna **D** pereopod 1 **E** pereopod 6 **F** pereopod 7 **G** pleopod 1 **H** pleopod 2 **I–K** pleopods 3–5 exopods. Scale bars: 1 mm.

uropodal exopod ~ 2–2.5 and 1.5–2× as long as protopod in males and females, respectively; protopod with an incision on outer margin (Figs 4A, B, 5B).

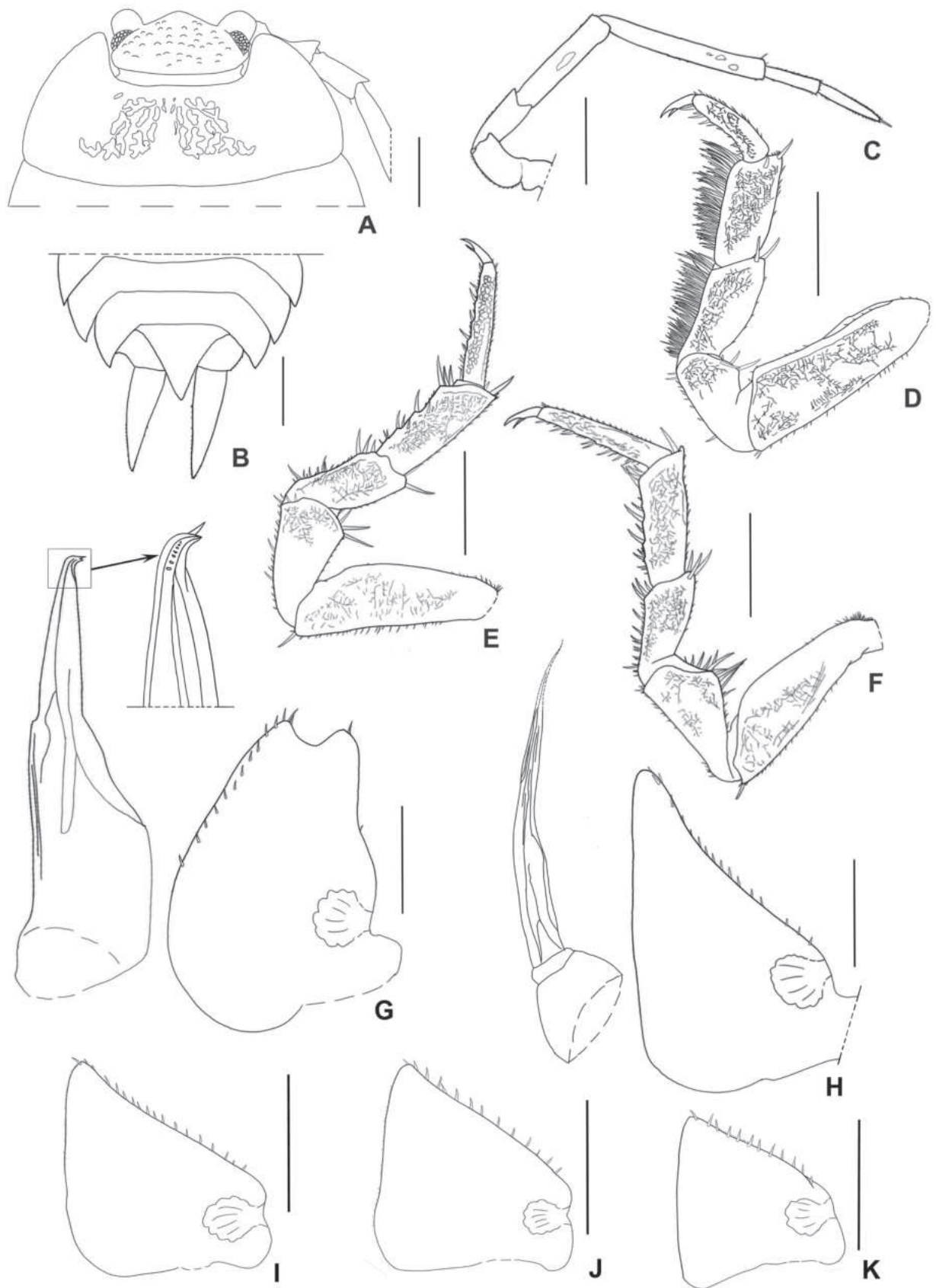


Figure 6. *Mongoloniscus polyacanthum* sp. nov., holotype **A** cephalon and pereonite 1 in dorsal view **B** pleonites, telson, and uropod in dorsal view **C** second antenna **D** pereopod 1 **E** pereopod 6 **F** pereopod 7 **G** pleopod 1 **H** pleopod 2 **I–K** pleopods 3–5 exopods. The abrupt tip of pleopod 2 endopod are indicated as dotted lines. Scale bars: 1 mm (**A–F**); 0.5 mm (**G–K**).

Cephalon with rounded lateral lobe no evidence surpasses eyes, median lobe convex, medially with a small incision (Fig. 5A). Eyes with 15–19 ommatidia. Antenna with fifth article of peduncle longer than flagellum; flagellum with distal article 1.6–2.1× as long as proximal one (Fig. 5C).

Pereopod 1 bearing brush of long setae on its carpus and merus (Fig. 5D). Pereopod 6 basis fringed with long setae and a distal protrusion on sternal margin (Fig. 5E). Pereopod 7 ischium with sternal margin slightly concave and fringed with setae, rostral surface with shallow depression; carpus slightly expanded on the tergal margin (Fig. 5F).

Pleopods 1–5 exopods with monospiracular internal lungs (Fig. 5G–K). Male: pleopod 1 exopod oval, with robust sinuous outer margin; apex deeply bilobed and bearing several setae, inner lobe much longer than outer lobe (Fig. 5G). Pleopod 2 exopod nearly triangular, bearing one line of setae on the outer margin (Fig. 4H). Pleopod 1 endopod with broad basal part, narrowed towards apex, apex bent outwards and pointed (Fig. 5G); pleopod 2 endopod longer than exopod, distal article thin and long (Fig. 5H).

Remarks. The new species resembles *M. koreanus* in morphology. It can be distinguished from the latter by the cephalon median lobe medially with a small incision, pereopod 7 with an unexpanded carpus on the tergal margin, and pleopod 1 endopod with a pointed distal apex. In *M. koreanus*, the cephalon median lobe is medially continuous, pereopod 7 has an expanded carpus on the tergal margin, and the distal apex of the pleopod 1 endopod is blunted. Furthermore, this species and *M. koreanus* formed two clades with high support in the phylogenetic analysis (Fig. 2), and their interspecific distances were much higher than their intraspecific distances (Suppl. material 1: table S2).

Etymology. Latin *crenatus* = notched. The new species name refers to the anterior margin of the cephalon with a small notch in the middle. We suggest the Chinese common name as “刻痕蒙潮虫”.

Distribution. China (Hubei, Shaanxi, Sichuan).

***Mongoloniscus polyacanthum* Jiang, Li & Huang, sp. nov.**

<https://zoobank.org/40D39285-4EF1-4344-B62B-FE91BC37D75E>

Figs 4C, D, 6

Type material. Holotype. CHINA: ♂ (20210908003), Liaoning Province, Chaoyang, Fenghuangshan National Forestry Park (41.54725°N, 120.4743°E), 210 m asl., 8.iv.2021, coll. Chao Jiang.

Paratypes. 1 ♂, 8 ♀♀ (20210908001, 20210908002, 20210908004–20210908010) same data as the holotype.

Diagnosis. Antennal flagellum with distal article ~ 1.2× as long as proximal article. Pereopod 7 ischium sternal margin fringed sparse setae. Pleopod 1 exopod with one line of setae on inner margin, distal apex deeply bilobed, inner lobe as long as outer one, but slightly wider than outer lobe.

Description. **Body** length of males 7–9 mm and females 8–11 mm. Body elongated and convex, ~ 2–2.5× as long as widest pereonite. Dorsum distinctly granulated, brown-gray in color with usual yellowish muscle spots. Numerous gland pores along entire pereonites margin. Pereonite 1 with rounded postero-lateral corner, posterior margin nearly straight. Noduli laterales on pereonites 1–4 much

farther from lateral margins than those on pereonites 5–7. Telson triangular, with slightly concave on lateral margins, posterior apex pointed; uropodal exopod ~ 1.5–2× as long as protopod; protopod with an incision on the outer margin (Figs 4C, D, 6B).

Cephalon with medial lobe triangular, not surpassing the lateral lobes in dorsal view (Fig. 6A). Eyes with 20 ommatidia. Antenna with fifth article of peduncle longer than flagellum; flagellum with distal article 1.2× as long as proximal one (Fig. 6C).

Pereopod 1 bearing a brush of long setae on its carpus and merus (Fig. 6D). Pereopod 7 ischium rostral surface with a shallow depression; carpus not expanded on the tergal margin (Fig. 6F).

Pleopods 1–5 exopods with monospiracular internal lungs (Fig. 6G–K). Male: pleopod 1 exopod oval, apex deeply bilobed, inner lobe as long as outer one, but slightly wider than outer lobe; outer margin sinuous, bearing one seta near middle and apex, respectively; inner margin with one line of setae; (Fig. 6G). Pleopod 2 exopod almost triangular, bearing one line of setae on the outer margin. Pleopod 1 endopod with broad basal part, narrowed towards apex, apex acute and bent outwards, bearing several setae (Fig. 6G); pleopod 2 endopod longer than exopod, distal article thin and long (Fig. 6H).

Remarks. This new species is similar to *M. sinensis* in the large body size, noduli laterales arrangement, and the fringed sparse setae on the pereopod 6 basis and pereopod 7 ischium. However, it can be distinguished from the latter by the distal article of the antennal flagellum longer than the proximal article, carpus of pereopod 7 without a rounded lobe on the tergal margin, and pleopod 1 exopod inner margin bearing a line of well-developed setae. In *M. sinensis*, the antennal flagellum articles are equal in length, the carpus of pereopod 7 has a rounded lobe on the tergal margin, and the pleopod 1 exopod bearing 2–4 setae on the apex of the inner lobe. Furthermore, this species together with *M. sinensis* formed two clades with high support in the phylogenetic analysis (Fig. 2), whose interspecific distances were much higher than their intraspecific distances (Suppl. material 1: table S2).

Etymology. Latin prefix *poly-* = many, plus *acanthum* = spinous. The new species name refers to the setae on the inner margin of pleopod 1 exopod. We suggest the Chinese common name as “多刺蒙潮虫”.

Distribution. China (Liaoning).

***Mongoloniscus parvus* Jiang, Li & Huang, sp. nov.**

<https://zoobank.org/E2A83DFA-2E8F-4BC6-8586-105B10A9A34A>

Figs 4E, F, 7

Type material. Holotype. CHINA: ♂ (20200913004), **Liaoning Province**, Huanren Manchu Autonomous County: Erpengdianzi Town, Yaoqianshu Village (41.1893°N, 125.6383°E), 610 m asl., 13.ix.2020, coll. Chao Jiang.

Paratypes. 3 ♂♂, 2 ♀♀ (20200913003, 2020091300005), same data as the holotype; 3 ♂♂, 2 ♀♀ (20200906002–20200906005), **Liaoning Province**, Huanren Manchu Autonomous County, Erpengdianzi Town (41.236°N, 125.6047°E), 560 m asl., 6.ix.2021, coll. Chao Jiang. 1 ♂, 2 ♀♀ (20200913001, 20200913002), **Jilin Province**, Ji'an, Xihulugou Village (41.3348°N, 125.8893°E), 670 m asl., 13.ix.2020, coll. Chao Jiang.

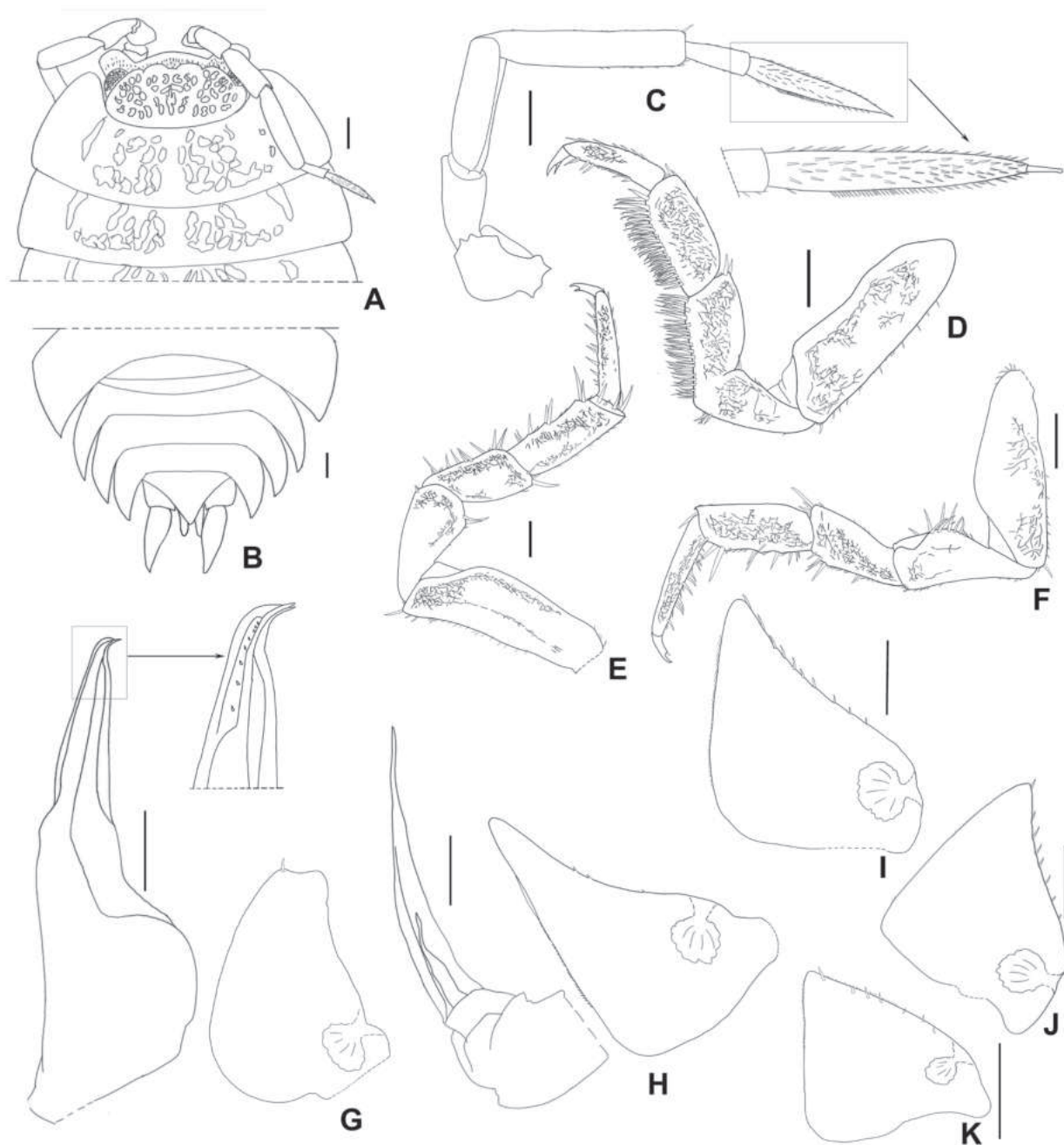


Figure 7. *Mongoloniscus parvus* sp. nov., holotype **A** cephalon, pereonites 1 and 2 in dorsal view **B** pleonites, telson and uropod in dorsal view **C** second antenna **D** pereopod 1 **E** pereopod 6 **F** pereopod 7 **G** pleopod 1 **H** pleopod 2 **I–K** pleopods 3–5 exopods. Scale bars: 1 mm.

Diagnosis. Antennal flagellum distal article approximately twice as long as the proximal article. Pereopod 7 ischium sternal margin fringed with sparse setae; carpus slightly expands on tergal margin. Pleopod 1 exopod oval, distal apex slightly concave, forming two inconspicuous lobes, inner lobe bearing one seta.

Description. **Body** length of males 5–9 mm and females 4–9 mm. Body elongated and convex, ~ 2.3× as long as widest pereonite. Dorsum distinctly granulated, brown-gray color with usual yellowish muscle spots. Numerous gland pores along entire margin pereonites margin (Fig. 4E, F). Pereonite 1 with rounded posterior margin and postero-lateral corners. Noduli laterales on pereonites 1–4

much farther from lateral margins than those on pereonites 5–7. Telson triangular, ~ 1.5× as wide as long, lateral margins slightly concave near middle, posterior apex blunted; uropodal exopod 1.2–1.5× as long as protopod; protopod with an incision on outer margin (Figs 3F, 4E, 7B).

Cephalon with medial lobe arched, not surpassing lateral lobes in dorsal view. Eyes with 14 or 15 ommatidia. Antenna with fifth article of peduncle and flagellum nearly equal in length; flagellum with distal article twice as long as proximal one (Fig. 7C).

Pereopod 1 bearing a brush of long setae on its carpus and merus (Fig. 7D). Pereopod 7 ischium rostral surface with shallow depression; carpus slightly expands on tergal margin (Fig. 7F).

Pleopods 1–5 exopods with monospiracular internal lungs (Fig. 7G–K). Male: pleopod 1 exopod oval, outer margin sinuous, distal apex slightly concave and forming two inconspicuous lobes, inner lobe bearing one seta near apex (Fig. 7G). Pleopod 2 exopod almost triangular, slightly concave on outer margin (Fig. 7H). Pleopod 1 endopod with broad basal part, narrowed towards apical apex, apex bearing several setae, bent outwards and ending with two pointed tips (Fig. 7G); pleopod 2 endopod longer than exopod, distal article thin and long (Fig. 7H).

Etymology. Latin *parvus* = small. The new species name refers to the pleopod 1 with a small exopod. We suggest the Chinese common name as “小蒙潮虫”.

Distribution. China (Liaoning, Jilin).

***Mongoloniscus orientalis* Jiang, Li & Huang, sp. nov.**

<https://zoobank.org/B8C37716-798D-4BEA-8A20-F80F39EEE983>

Figs 4G, H, 8

Type material. Holotype. CHINA: ♂ (20230403006), Heilongjiang Province, Harbin: Xiangfang District, Longrui Residential (126.6821°N, 45.7233°E), 160 m asl., 3.ix.2023, coll. Junjie Zong.

Paratypes. 6 ♂♂, 13 ♀♀ (20230403003–20230403008), same data as the holotype. **CHINA:** 2 ♂♂, 2 ♀♀ (20231030301, -02), Shanxi Province, Taiyuan: Longcheng Forestry Park (37.9228°N, 112.7565°E), 1610 m asl., 30.x.2023, coll. Tianyun Chen, Yuan Xiong & Jiabo Fan.

Diagnosis. Antennal flagellum with distal article as long as proximal article. Pereopod 6 basis fringed with long setae. Pereopod 7 ischium with sternal margin slightly concave and fringed with setae carpus with rounded lamellar lobe on tergal margin. Apex of pleopod 1 exopod bilobed, outer lobe larger than inner one.

Description. Body length of males 8–12 mm and females 7–16 mm. Body elongated and convex, ~ 2.8× as long as widest pereonite. Dorsum distinctly granulated, brown-gray color with usual yellowish muscle spots. Numerous gland pores along entire pereonites margin (Fig. 4G, H). Pereonite 1 with rounded postero-lateral corners, distal margin nearly straight. Noduli laterales on pereonites 1–4 and 7 shifted from lateral margins than those on pereonites 5 and 6. Telson triangular, slightly wider than length, outer margin slightly concave near middle, posterior apex pointed; uropodal exopod ~ 2.8–3.6× as long as protopod in males and ~ 1.2–2× in females; protopod with an incision on outer margin (Figs 4G, H, 8B).

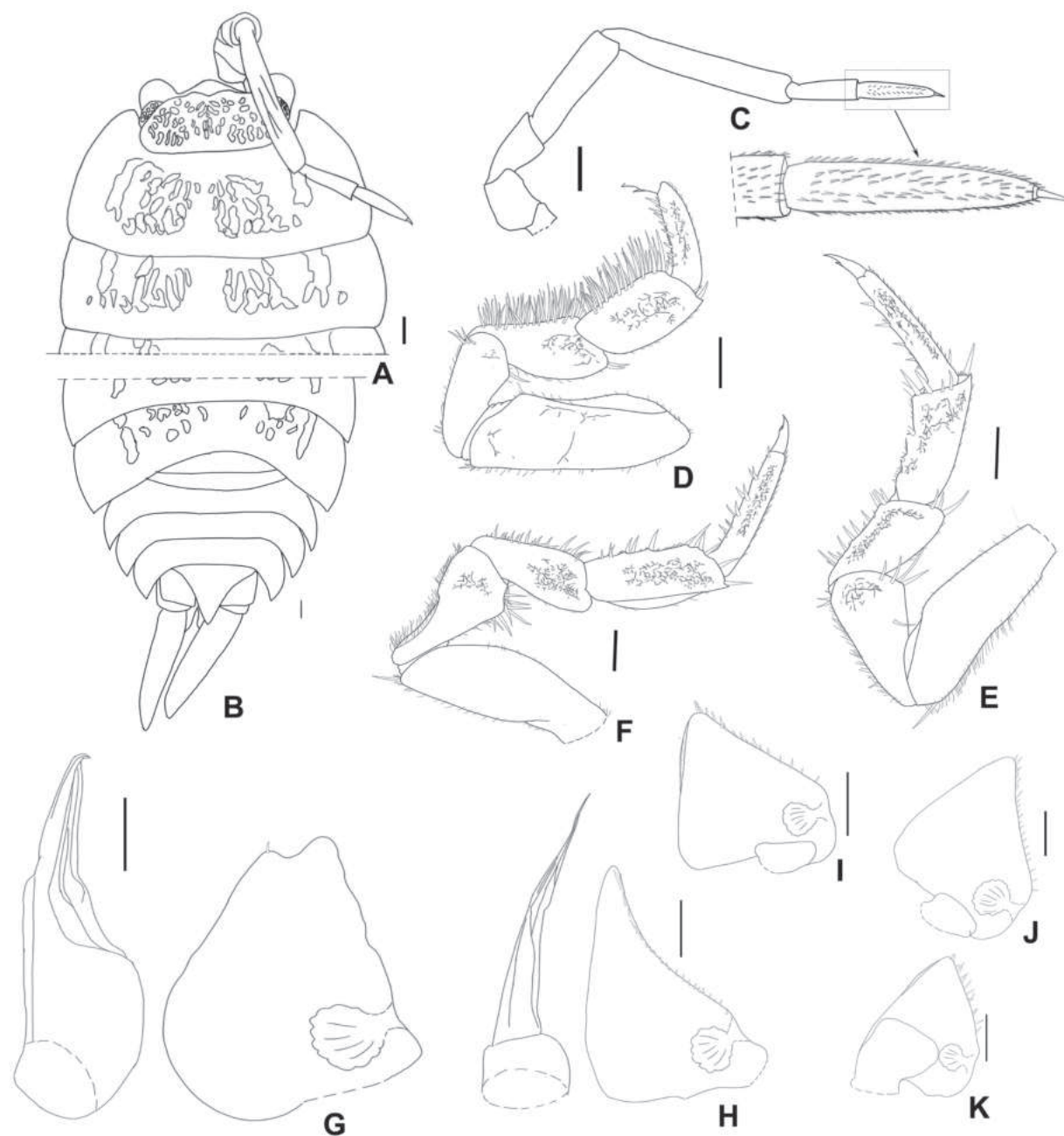


Figure 8. *Mongoloniscus orientalis* sp. nov., holotype **A** cephalon, pereonites 1 and 2 in dorsal view **B** pleonites, telson and uropod in dorsal view **C** second antenna **D** pereopod 1 **E** pereopod 6 **F** pereopod 7 **G** pleopod 1 **H** pleopod 2 **I–K** pleopods 3–5 exopods. Scale bars: 1 mm.

Cephalon with medial lobe triangular, not surpassing lateral lobes in dorsal view. Eyes with 20 ommatidia. Antenna with fifth article of peduncle longer than flagellum; flagellum with distal article as long as proximal one (Fig. 8C).

Pereopod 1 bearing a brush of long setae on its carpus and merus (Fig. 8D). Pereopod 6 basis fringed with long setae (Fig. 8E). Pereopod 7 ischium with sternal margin slightly concave and fringed with setae, rostral surface with shallow depression; carpus with rounded lamellar lobe on tergal margin (Fig. 8F).

Pleopods 1–5 exopods with monospiracular internal lungs (Fig. 8G–K). Male: pleopod 1 exopod drop-like, outer margin sinuous, apex bilobed; outer lobe larger

than inner one, inner lobe bearing one seta at apex (Fig. 8G). Pleopod 2 exopod nearly triangular, bearing one line of setae on outer margin (Fig. 8H). Pleopod 1 endopod with broad basal part, narrowed towards apex, apex bent outwards and pointed (Fig. 8G); pleopod 2 endopod longer than exopod, distal article thin and long (Fig. 8H).

Remarks. This new species resembles *M. koreanus* by basis of pereopod 6 having long setae and a distal protrusion on the sternal margin, ischium of pereopod 7 fringed with setae. However, it can be differentiated from the latter by antenna with two equal flagellum articles, and its noduli laterales on pereonites 1–4 and 7 are much farther from lateral margins than those on pereonites 5 and 6. In *M. koreanus*, the distal article of the flagellum is twice as long as the proximal article, and the noduli laterales are almost at the same distance from the lateral margin. Furthermore, this species together with *M. koreanus* formed two clearly different clades in the phylogenetic analysis (Fig. 2), whose interspecific distances were much higher than their intraspecific distances (Suppl. material 1: table S2).

Etymology. Latin *orientalis* = east. The new species name refers to its distribution in east China. We suggest the Chinese common name as “东方蒙潮虫”.

Distribution. China (Heilongjiang, Shanxi).

***Mongoloniscus koreanus* (Verhoeff, 1930)**

Protracheoniscus (*Mongoloniscus*) *koreanus* Verhoeff, 1930: 117, figs 14, 15.

Mongoloniscus koreanus: Kwon 1993: 149, figs 12, 13; Kwon 1995: 528.

Mongoloniscus nigrogranulatus Kwon & Taiti, 1993: 48, figs 201–208.

Nagurus tsushimaensis Nunomura, 1987: 30, fig. 113.

Nagurus pallidus: Nunomura 1991: 8, fig. 171.

Examined material. CHINA: 2 spms (20200813002, 20200813006), **Anhui Province**, Hefei, Binghu National Forestry Park (31.7230°N, 117.3728°E), 20 m asl., 13.viii.2020, coll. Chao Jiang; 2 spms (20230324029–20230324030), Qimen county: Qishan Town, Qichang Road (29.8666°N, 117.6841°E), 150 m asl., 24.iii.2023, coll. Chao Jiang; 28 spms (20230327116–20230327129), Ningguo County, Yunti She Village, Qianqiushezu (29.8666°N, 117.6841°E), 150 m asl., 27.iii.2023, coll. Chao Jiang; 26 spms (20230326076–20230326088, 20230327102–20230327103), Xi-jin Streets, Cuizhu Park (30.6319°N, 118.9710°E), 60 m asl., 27–28.iii.2023, coll. Chao Jiang; 9 spms (20230324017–20230324021), Xiuning County, Qiyunshan Service Area (29.7540°N, 118.1321°E), 200 m asl., 24.iii.2023, coll. Chao Jiang; 1 spm (20230325071), Huangshan, Tankou Town, Hougu (30.0740°N, 118.1527°E), 510 m asl., 25.iii.2023, coll. Chao Jiang; 12 spms (20230215006–20230215008), Bozhou: Bozhou Cultural Park (33.8286°N, 115.7616°E), 15.ii.2023, coll. Chao Jiang; 2 spms (20230214004, 20230214005), Fuyang, Yingquan district, Wuming Service Area, (33.0458°N, 115.8935°E), 14.ii.2023, coll. Chao Jiang. 2 spms (20201018028, 20201018037), **Chongqing**, Jiangbei District, Tieshanping Forestry Park (29.5957°N, 106.6645°E), 450 m asl., 18.x.2020, coll. Chao Jiang & Zhidong Wang. 13 spms (20201118001, -12, -18, -20, -22, -25, -30, -37, -38, -40, -41, -43), **Guangxi Zhuang Autonomous Region**, Guilin, Guangxi Guilin National Forestry Park (25.2207°N, 110.2543°E), 18.xi.2020, coll. Zhidong Wang. **Guizhou Province**, 20 spms, (20201020001, -4, -7, -9, -10, -14, -16, -17, -20, -21, -24, -25, -27, -29,

-30, -31, -35, -36, -39, -40), Zhengning County, Yelangdong Scenic Area (26.0918°N, 105.6248°E), 1070 m asl., 20.x.2020, coll. Chao Jiang & Zhidong Wang; 8 spms (20210601038–20210601045), Guiyang: Jinhua town, Shangcheng West Road (26.6067°N, 106.57463°E), 1260 m asl., 1.vi.2021, coll. Chao Jiang; 16 spms (20210728020–20210728035), Jiangkou county, Fanjingshan National Nature Reserve (27.8464°N, 108.7733°E), 1510 m asl., 28.vii.2021, coll. Zhidong Wang. 3 spms (20210410069–20210410071), **Hubei Province**, Jingmen, Xiangshan II Road, Youyuan (31.0441°N, 112.1999°E), 80 m asl., 10.iv.2021, coll. Zhidong Wang & Tianyun Chen; 5 spms (20210414063, -64, 20210414066–20210414068), Shennongjia: shennongding (31.4902°N, 110.3583°E), 1840 m asl., 14.iv.2021, coll. Zhidong Wang & Tianyun Chen; 9 spms (20210415051–20210415059), Shiyan, Niutoushan National Forestry Park (32.6118°N, 110.7298°E), 390 m asl., 15.iv.2021, coll. Zhidong Wang & Tianyun Chen; 9 spms (20210415061–20210415069), Yuanyuan Park (32.6113°N, 110.7695°E), 270 m asl., 15.iv.2021, coll. Zhidong Wang & Tianyun Chen; 2 spms (20190321002, 20190321007), **Hunan Province**, Yongzhou, Puliqiao Town (26.6849°N, 111.5997°E), 160 m asl., 21.iii.2019, coll. Chao Jiang; 37 spms (20201107001, -2, -6, -7, -10, -14, -16, -18, -22, -24–30, -32, -33, -35–38, -40, -42, -44, -45, -47, -48, -50, -52–54, -57, -60, -63, -64, -67), **Jiangsu Province**, Yancheng: Jiangsu Yancheng Wetland National Nature Reserve (Rare Birds) (33.6035°N, 120.5042°E), 5 m asl., 7.xi.2020, coll. Zhidong Wang; 9 spms (20201109001, -6, -9, -18, -27, -30, -31, -39, -42), Nanjing, Jiangjunshan Scenic Area (32.1007°N, 118.5861°E), 130 m asl., 9.xi.2020, coll. Zhidong Wang; 2 spms (20210801001, -2), **Jiangxi Province**, Nanchang, Zhaoxian Town, Meiling, (28.7243°N, 115.6848°E), 350 m asl., 1.viii.2021, coll. Zhidong Wang; 32 spms (20230217013–18, -26, -27), Dexing, Yincheng Street, Jishuihu Wetland Park (28.9354°N, 117.5952°E), 70 m asl., 17.ii.2022, coll. Chao Jiang; 23 spms (20230219018–20230219020), Dexing Railway Station (28.9587°N, 117.8544°E), 19.ii.2023, coll. Chao Jiang; 1 spm (20210330053), **Shaanxi Province**, Xi'an, Xi'anbei Railway Station, (34.3741°N, 108.9345°E), 350 m asl., 3.iii.2021, coll. Zhidong Wang; 26 spms (20220909001–20220909026), **Sichuan Province**, Yanting County, Yanting Service Area (31.1481°N, 105.3804°E), 360 m asl., 9.ix.2022, coll. Chao Jiang; 29 spms (20220911007), Tongjiang County: Nuoshuihe Town (32.4320°N, 107.1858°E), 780 m asl., 11.ix.2022, coll. Chao Jiang; 28 spms (20220914002–20220914022), Bazhong, Bazhou District, Jiangbei Road, (31.8718°N, 106.7379°E), 380 m asl., 14.ix.2022, coll. Chao Jiang; 16 spms (20220829070, -71, -73–84), Meishan, Taihe Town, Meishan Service Area, (31.8718°N, 106.7379°E), 380 m asl., 29.viii.2022, coll. Chao Jiang; 17 spms (20220829045, -47–60), Jiajiang County, Jiajiang Bridge (29.7216°N, 103.5754°E), 380 m asl., 29.viii.2022, coll. Chao Jiang; 4 spms (20210528013–20210528015, -18), **Yunnan Province**, Linchang, Manpan Street, (23.9061°N, 100.0985°E), 1430 m asl., 28.v.2021, coll. Chao Jiang; 2 spms (20210531016, -17), Mianning Street (23.8787°N, 100.0983°E), 1430 m asl., 31.v.2021, coll. Chao Jiang; 6 spms (20210506004–20210506009), **Zhejiang Province**, Jinhua, Anwen Street, (29.0169°N, 120.4570°E), 390 m asl., 6.v.2021, coll. Chao Jiang; 27 spms (20230324076–20230324086), Hangzhou, Lin'an Service Area, (30.2076°N, 119.5308°E), 160 m asl., 24.iii.2023, coll. Chao Jiang; 2 spms (20230327058), Tianmushan National Nature Reserve (30.3190°N, 119.4448°E), 350 m asl., 27.iii.2023, coll. Chao Jiang; 11 spms (20230328039–20230328044), Huzhou, Huzhou Railway Station (30.8628°N, 120.0238°E), 160 m asl., 28.iii.2023, coll. Chao Jiang; 8 spms (20230324004–20230324009), Wuxing

District, Zhihe Road (120.0211E, 30.8706N), 20 m asl., 24.iii.2023, coll. Chao Jiang; 12 spms (20230328057–20230328059), Wuxing District, Renhuangshan Mountain, (30.8973°N, 120.0572°E), 80 m asl., 28.iii.2023, coll. Chao Jiang; 4 spms (20230328008–20230328011), Anji County, Fenghuangshan Park (30.6198°N, 119.7013°E), 160 m asl., 28.iii.2023, coll. Chao Jiang.

Remarks. This species closely resembles *M. maculatus* (Iwamoto, 1943) by the noduli laterals at almost the same distance from the lateral margins, and the morphology of pleopod 1 exopod. However, it can be distinguished in having the eyes with 20–24 ommatidia, male pereopod 6 fringed with long setae and bearing a distal protrusion on the sternal margin at the basis, and the ischium of pereopod 7 fringed with setae as well. In *M. maculatus*, its eyes have 15 or 16 ommatidia, the basis of pereopod 6 and the ischium of male pereopod 7 with sparse setae. For detailed descriptions and illustrations of *M. koreanus* see Kwon (1993).

Distribution. China (Anhui, Chongqing, Guangxi, Guizhou, Hubei, Hunan, Jiangsu, Jiangxi, Shaanxi, Sichuan, Yunnan, Zhejiang), Japan, and Korea.

***Mongoloniscus sinensis* (Dollfus, 1901)**

Metoponorthus (*Mongoloniscus*) *sinensis* Dollfus, 1901: 371–374.

Porcellio (*Porcellionides*) *asiaticus*: Arcangeli 1927: 175–178.

Mongoloniscus sinensis: Chen 1993: 260.

Examined material. CHINA: 1 spm (20180901101), **Beijing**, Haidian District, Tiancun, 1.ix.2018, coll. Junduo Zhang; 1 spm (20230408020), **Hebei Province**, Chengde, Weichuang Manchu and Mongolian Autonomous County, Saihanba National Forestry Park (42.408°N, 117.254°E), 1500 m asl., coll. Tianyun Chen, Yangyang Pan & Jiabo Fan; 8 spms (20230330021–2023033004), Hengshui, Taocheng District, near Hengshui Railway Station (37.7467°N, 115.6913°E), 30.iii.2023, coll. Chao Jiang; 12 spms, 20201212013–20201212018, **Henan Province**, Yuzhou, Xiayu Park (34.1387°N, 113.4801°E), 90 m asl., 12.xii.2020, coll. Chao Jiang; 4 spms (20200912009, 20200913002, -3, -5), **Jilin Province**, Ji'an, Koguryo Archaeological Site Park (41.1210°N, 126.1845°E), 210 m asl., 12–13.ix.2020, coll. Chao Jiang; 14 spms (20210908011–20210908024), **Liaoning Province**, Chaoyang, Fenghuangshan National Forestry Park (41.54725°N, 120.4743°E), 210 m asl., 8.iv.2021, coll. Chao Jiang; 15 spms (20210907005–20210907018), Shangzhi Park (41.5891°N, 120.4302°E), 180 m asl., 7.iv.2021, coll. Chao Jiang; 9 spms (20210904019–20210904026), Huanren Manchu Autonomous County, Zhangyue Park (41.2600°N, 125.3480°E), 270 m asl., 04.ix.2021, coll. Chao Jiang; 8 spms (20210904001, -2, -3, -5, -6, -8, -9), Liaoyang, Baita District, Liaoning Research Institute of Cash Crops (41.2605°N, 121.1392°E), 40 m asl., 4.ix.2021, coll. Chao Jiang; 4 spms (20210907030–20210907032), Xinbin Manchu Autonomous County, Yongling Town (124.7979 ° E, 41.7193 ° N), 310 m asl., 4.iv.2021, coll. Chao Jiang, 3 spms (20210907036–20210907038), Nan-zamu Town (41.9422°N, 124.4398°E), 210 m asl., 4.iv.2021, coll. Chao Jiang; 27 spms (20210330042–20210330052, 20210330054–20210330069), **Shaanxi Province**, Xi'an, Xi'anbei Railway Station (34.3741°N, 108.9345°E), 350 m asl., 3.iii.2021, coll. Zhidong Wang. 1 spm (20211007001), **Tianjin**, Nancuiping Park (39.0738°N, 117.1483°E), 7.x.2021, coll. Chao Jiang; 25 spms (20210707014–

20210707038), **Tibet Autonomous Region**, Lhasa, Nanshan Park (29.6315°N, 91.1146°E), 3670 m asl., 7.vii.2021, coll. Chao Jiang; 7 spms (20210710012–20210710018), Gonggar County, Jiazhulin Town (29.2885°N, 90.8958°E), 3560 m asl., 7.x.2021, coll. Chao Jiang; 1 spm (20210709006), Gyatsa County, Anrao Town (29.1029°N, 92.6002°E), 3230 m asl., 7.ix.2021, coll. Chao Jiang.

Remarks. Most male specimens displayed a rounded lobe on the pereopod 7 carpus tergal margin, except for three specimens from Beijing and Henan province. *M. sinensis* is close to *M. satsumaensis* (Nunomura, 1987) in terms of noduli laterales' positions and the morphology of pleopod 1 exopod, but it could differ in the antennal flagellum distal article as long as proximal article rather than 1.5× as long as proximal article.

Distribution. China (Beijing, Hebei, Henan, Jilin, Liaoning, Shaanxi, Tianjin, Tibet).

***Koreoniscus racovitzai* (Arcangeli, 1927)**

Porcellio (*Lucasius*) *Racovitzai* Arcangeli, 1927: 228, fig. 7.

Koreoniscus racovitzai: Verhoeff 1937: 421; Flasarova 1972:102–111, figs 24–47.

Koreoniscus Racovitzai: Arcangeli 1952: 301.

Mongoloniscus chevronus Yang & An, 2021: 265–274, figs 1–3. syn. nov.

Examined material. **CHINA:** 19 spms (20200912002–20200912004, -7, 20200913001, -4, 20200914001–20200914003), **Jilin Province**, Ji'an, Koguryo Archaeological Site Park (41.1210°N, 126.1845°E), 210 m asl., 12–14.ix.2020, coll. Chao Jiang; 8 spms (20200912011–20200912016), Daqiangfenggou (40.9276°N, 125.9505°E), 330 m asl., 12.ix.2020, coll. Chao Jiang. 10 spms (20210904027–20210904034), **Liaoning Province**, Huanren Manchu Autonomous County, Zhangyue Park (41.2600°N, 125.3480°E), 270 m asl., 4.ix.2021, coll. Chao Jiang; 1 spm (20210905002), Gucheng Town (41.4764°N, 125.3832°E), 380 m asl., 5.ix.2021, coll. Chao Jiang; 1 spm (20210907033), Xinbin Manchu Autonomous County (41.7193°N, 124.7979°E), 310 m asl., 7.ix.2021, coll. Chao Jiang.

Remarks. In the present study, we identified the above specimens by integrating morphological characters and COI sequences. The results demonstrate that not only their morphological traits were the same as *M. chevronus*, but also the COI sequences were 100% identical to the sequence from the type material of *M. chevronus* (GenBank: MW792415) (Yang and An 2021). Thus, we used these materials to analyze the relationships between *M. chevronus* and the other species.

Morphologically, this species is distinctly differing from other *Mongoloniscus* species by its pereonite epimera with a “convex-concave-convex” margin. It is noteworthy that this trait is an essential diagnostic character of *Koreoniscus*. Based on further comparison of the descriptions and illustrations of *M. chevronus* (Yang and An 2021: figs 1–3) and *K. racovitzai* (Flasarová 1972: figs 24–31; Kwon 1993: fig. 11), in addition to the above results obtained through phylogenetic analyses (the genetic distance between *M. chevronus* and *Koreoniscus racovitzai* was nearly 0%, Suppl. material 1: table S2; *M. chevronus* and *Koreoniscus racovitzai* formed a clade with high support, Fig. 2), and with the external morphology and the coordinates of noduli laterales on pereonites, we consider *M. chevronus* Yang & An, 2021 as junior synonym of *Koreoniscus racovitzai* (Arcangeli, 1927).

Distribution. China (Liaoning, Jilin), Japan, Korea.

***Lucasioides vannamei* (Arcangeli, 1927), comb. nov.**

Porcellio (*Nagara*) *Van Namei* Arcangeli, 1927: 243.

Porcellio (*Nagara*) *sundaicus*: Arcangeli 1927: 248, fig 15.

Nagara (*Nagara*) *Van Namei*: Arcangeli 1952: 302.

Protracheoniscus (*Mongoloniscus*) *nipponicus* Arcangeli, 1952: 299.

Mongoloniscus nipponicus: Kwon 1993: 150, figs 14, 15.

Mongoloniscus vannamei: Kwon 1995: 527.

Examined material. CHINA: 1 spm (20230214007), **Anhui province**, Fuyang, Yingquan District, Wuming Service Area (33.0458°N, 115.8935°E), 14.ii.2023, coll. Chao Jiang; 50 spms (20230215013–20230215023), Bozhou, Bozhou Cultural Park (33.8286°N, 115.7616°E), 15.ii.2023, coll. Chao Jiang; 10 spms (20230218001–20230218008), **Jiangxi Province**, Dexing, Raoshoukun Park (28.9558°N, 117.5608°E), 18.ii.2023, coll. Chao Jiang; 11 spms (20230219001–20230219008), Dexing Railway Station (28.9587°N, 117.8544°E), 19.ii.2023, coll. Chao Jiang; 15 spms (20230214001–20230214008), Jiujiang, Saiyang Town, near Lushan cable-way Station (29.2926°N, 115.9512°E), 16.ii.2023, coll. Chao Jiang; 32 spms (20230216019–20230216033), Chaisang district, Zhonghuaxianmu Park (29.6144°N, 115.9002°E), 16.ii.2023, coll. Chao Jiang; 9 spms (202302180039, -40), Leping, Hongyan Town, Hongyanxian-jing Scenic Area (29.0442°N, 117.4738°E), 18.ii.2023, coll. Chao Jiang; 19 spms (20230218048–20230218054, -56, -57), Gaojia Town (28.9949°N, 117.4425°E), 18.ii.2023, coll. Chao Jiang; 12 spms (20210409088–20210409090), **Hubei Province**, Jingshan County, Kongshandong Scenic Area (30.9728°N, 113.0415°E), 100 m asl., coll. Zhidong Wang & Tianyun Chen; 3 spms (20210410034), Huzhuashan National Forestry Park (31.0765°N, 112.9009°E), 200 m asl., coll. Zhidong Wang & Tianyun Chen. 2 spms (20210508051, -52), **Zhejiang Province**, Pan'an County, Dapanshan Medicinal Plant Garden (28.9827°N, 120.5536°E), 680 m asl., coll. Chao Jiang.

Remarks. *Mongoloniscus vannamei* distinctly differs from all other *Mongoloniscus* species by the noduli laterales on pereonites 2–4 and 7 which are much farther from the lateral margins than those on pereonites 1, 5, and 6. We recognized this species based on the diagnostic characters among the similar genera *Mongoloniscus*, *Lucasioides*, *Agnara*, *Koreoniscus* and *Protracheoniscus* (Kwon 1993), and found that all the traits of *M. vannamei* match the generic characters of *Lucasioides*, except for its epimeron of pereonite 1 was not bent outwards. Furthermore, *M. vannamei*, *L. gigliotosi* and *L. isseli* formed a clade with high support (PP = 1.00, BS = 95%) according to the results of the phylogenetic analysis (Fig. 2). Thus, *M. vannamei* must be transferred to *Lucasioides*. For species descriptions and illustrations, see Kwon (1993).

Distribution. China (Anhui, Hubei, Hunan, Jiangxi, Zhejiang), Japan, Korea.

Discussion

Currently, all similar genera within the family Agnaridae are separated by the morphological characters, e.g., *Mongoloniscus* Verhoeff, 1930 can be distinguished

from *Lucasioides* Kwon, 1993 by the arrangement of noduli laterals and the shape of the first pereonite (Kwon 1993; Gongalsky et al. 2021). In morphological taxonomy, although eighteen species have been ascribed to the genus *Mongoloniscus* (Boyko et al. 2008), rather than strictly conforming to the criteria proposed by Kwon (1993), several of these species only have some of the diagnostic characters of the genus. These identifications made a dilemma: the species recognition of *Mongoloniscus*, whether based on the only morphological criteria or parts of diagnostic traits, is uncertain.

Considering that the DNA-based approach has revealed an effective way to resolve the taxonomic problems of terrestrial isopods (e.g., Zeng et al. 2021; Khalaji-Pirbalouty et al. 2022; Raupach et al. 2022; Wang et al. 2022a; Yoshino and Kubota 2022), we present mitochondrial COI and nuclear 28S rRNA data based on a broad sample of taxa in the present study (Suppl. material 1: table S1). In the molecular analyses, the results support the use of COI sequences as a useful DNA barcode marker for identifying *Mongoloniscus* species (Suppl. material 1: table S2), and indicate that *Mongoloniscus* is a monophyletic taxon closely related to *Koreoniscus* and *Lucasioides* (Fig. 2). Based on a combination of morphological taxonomy and molecular analyses, we propose *Lucasioides vannamei* (Arcangeli, 1927), comb. nov. out of *Mongoloniscus*, and *M. chevronus* Yang & An, 2021 as junior synonym of *Koreoniscus racovitzai* (Arcangeli, 1927). Furthermore, we provide a more restrictive interpretation of *Mongoloniscus*, making the generic characters more conducive to future species identifications.

If we follow the principle of the restrictive definition, several species previously categorized as *Mongoloniscus* members may be transferred to the other genera, e.g., *M. persicus* Kashani, 2014, *M. katakurai* (Nunomura, 1987), and *M. vannamei* (Arcangeli, 1927) should be transferred to *Lucasioides* because their noduli laterales on pereonites 2–4 are distinctly shifted from the lateral margins than those on the other pereonites, instead of at nearly the same distance from the lateral margin. Other congeners, such as *M. amabilis* Nunomura, 2013, *M. masahitoi* (Nunomura, 1987), *M. arvus* Nunomura, 2010, *M. hokurikuensis* (Nunomura, 1987), *M. persicus* Kashani, 2014, *M. ishikawai* Nunomura, 2013 and *M. circacaudatus* (Nunomura, 1987) etc., have similar taxonomic problems. These findings highlight the need for the genus to be revised in future studies. In this context, integrative taxonomy could be considered an effective method for resolving taxonomic ambiguities.

Acknowledgments

We are grateful to Mr. Junjie Zong for providing specimens. Special thanks are given to two anonymous reviewers for their insightful suggestions.

Additional information

Conflict of interest

The authors have declared that no competing interests exist.

Ethical statement

No ethical statement was reported.

Funding

This research was supported by the National Natural Science Foundation of China (nos. 82073972, 31960100), the Fundamental Research Funds for the Central Public Welfare Research Institutes (no. ZZ13-YQ-089-C1), and the CACMS Innovation Fund (CI2023E002).

Author contributions

Conceptualization: WL, CJ. Data curation: CJ, WL, JZ. Funding acquisition: CJ, WL. Methodology: CJ. Project administration: LH, CJ. Resources: ZW, CJ. Software: JZ. Supervision: CJ, LH. Writing – original draft: CJ. Writing – review and editing: WL.

Author ORCIDs

Chao Jiang  <https://orcid.org/0000-0003-1841-1169>

Weichun Li  <https://orcid.org/0000-0003-0154-861X>

Data availability

All of the data that support the findings of this study are available in the main text or Supplementary Information.

References

- Boyko CB, Bruce NL, Hadfield KA, Merrin KL, Ota Y, Poore GCB, Taiti S, Schotte M, Wilson GDF (2008 [onwards]) World Marine, Freshwater and Terrestrial Isopod Crustaceans database. <https://doi.org/10.14284/365> [accessed 10 July 2023]
- Chen GX (2003) Species construction and distribution of terrestrial Isopoda in typical zones of China. *Journal of Jishou University* 24(1): 14. [Natural Sciences Edition]
- Chen TY, Jiang C, Huang LQ (2023) A new species of *Otostigmus* (Chilopoda, Scolopendromorpha, Scolopendridae) from China, with remarks on the phylogenetic relationships of *Otostigmus politus* Karsch, 1881. *ZooKeys* 1168(5): 161–178. <https://doi.org/10.3897/zookeys.1168.82750>
- Dimitriou AC, Sfenthourakis S (2022) An all-inclusive approach: A universal protocol for the successful amplification of four genetic loci of all Oniscidea. *MethodsX* 9: 101762. <https://doi.org/10.1016/j.mex.2022.101762>
- Dimitriou AC, Taiti S, Sfenthourakis S (2019) Genetic evidence against monophyly of Oniscidea implies a need to revise scenarios for the origin of terrestrial isopods. *Scientific Reports* 9(1): <https://doi.org/10.1038/s41598-019-55071-4>
- Dimitriou AC, Campos-Filho IS, Georgiou A, Taiti S, Sfenthourakis S (2023) Intra-island patterns of cryptic diversity within an oceanic island: Insights from the differentiation of *Schizidium* Verhoeff, 1901 (Oniscidea, Armadillidiidae) within Cyprus, with descriptions of two new species. *Molecular Phylogenetics and Evolution* 187: 107884. <https://doi.org/10.1016/j.ympev.2023.107884>
- Dollfus A (1901) Isopodes. In Horvath's Zoologische Ergebnisse Zichy 2: 371–374.
- Flasarová M (1972) Über einige Isopoden aus Korea (Isopoda, Oniscoidea). *Annales zoologici. Państwowe Wydawnictwo Naukowe* 29(4): 91–113.
- Folmer O, Black M, Hoeh W, Lutz R, Vrijenhoek R (1994) DNA primers for amplification of mitochondrial cytochrome C oxidase subunit I from diverse metazoan invertebrates. *Molecular ultrafast bootstrap approximation. Molecular Biology and Evolution* 35(2): 518–522. <https://doi.org/10.1093/molbev/msx281>

- Gongalsky KB, Turbanov IS, Medvedev DA, Volkova JS (2018) Description of a new species of the genus *Protracheoniscus* Verhoeff, 1917 and redescription of *Protracheoniscus kryszanovskii* Borutzky, 1957 from the southeast of European Russia (Isopoda, Oniscidea, Agnaridae). *ZooKeys* 801: 189–205. <https://doi.org/10.3897/zookeys.801.23167>
- Gongalsky KB, Nefediev PS, Turbanov IS (2021) A new species of the genus *Lucasioides* Kwon, 1993 (Isopoda, Oniscidea, Agnaridae) from Siberia, Russia. *Zootaxa* 4903(1): 140–150. <https://doi.org/10.11646/zootaxa.4903.1.9>
- Hoang DT, Chernomor O, Von Haeseler A, Minh BQ, Vinh LS (2018) UFBBoot2: improving the ultrafast bootstrap approximation. *Molecular Biology and Evolution* 35(2): 518–522. <https://doi.org/10.1093/molbev/msx281>
- Joshi J, Karanth KP (2011) Cretaceous–Tertiary diversification among select scolopendrid centipedes of South India. *Molecular Phylogenetics and Evolution* 60(3): 287–294. <https://doi.org/10.1016/j.ympev.2011.04.024>
- Kalyaanamoorthy S, Minh BQ, Wong TKF, von Haeseler A, Jermiin LS (2017) ModelFinder: Fast model selection for accurate phylogenetic estimates. *Nature Methods* 14(6): 587–589. <https://doi.org/10.1038/nmeth.4285>
- Kashani GM (2014) Description of two new species and redescription of one species of agnarid terrestrial isopods (Oniscidea, Agnaridae) from western Iran. *ZooKeys* 440: 45–56. <https://doi.org/10.3897/zookeys.440.7407>
- Khalaji-Pirbalouty V, Oraie H, Santamaria CA, Wägele JW (2022) Redescription of *Tylos maindroni* Giordani Soika, 1954 (Crustacea, Isopoda, Oniscidea) based on SEM and molecular data. *ZooKeys* 1087: 123–139. <https://doi.org/10.3897/zookeys.1087.76668>
- Kumar S, Stecher G, Li M, Knyaz C, Tamura K (2018) MEGA X: Molecular evolutionary genetics analysis across computing platforms. *Molecular Biology and Evolution* 35(6): 1547–1549. <https://doi.org/10.1093/molbev/msy096>
- Kwon DH (1993) Terrestrial Isopoda (Crustacea) from Korea. *Tongmul Hakhoe Chi* 36: 133–158.
- Kwon DH, Taiti S (1993) Terrestrial isopoda (Crustacea) from Southern China, Macao, and Hong Kong. *Stuttgarter Beitrage zur Naturkunde A (Biologie)* 490: 1–83.
- Li WC (2017) A new species of *Lucasioides* Kwon (Isopoda: Oniscidea: Agnaridae) from China. *Zootaxa* 4216(5): 495–500. <https://doi.org/10.11646/zootaxa.4216.5.6>
- Michael FW, James CC, Quentin DW, Ward CW (1997) The strepsiptera problem: Phylogeny of the holometabolous insect orders inferred from 18S and 28S ribosomal DNA sequences and morphology. *Systematic Biology* 46(1): 1–68. <https://doi.org/10.1093/sysbio/46.1.1>
- Minh BQ, Schmidt HA, Chernomor O, Schrempf D, Woodhams MD, von Haeseler A, Lanfear R (2020) IQ-TREE 2: New models and efficient methods for phylogenetic inference in the genomic era. *Molecular Biology and Evolution* 37(5): 1530–1534. <https://doi.org/10.1093/molbev/msaa015>
- Montesanto G (2015) A fast GNU method to draw accurate scientific illustrations for taxonomy. In: Taiti S, Hornung E, Štrus J, Bouchon D (Eds) *Trends in Terrestrial Isopod Biology*. *ZooKeys* 515: 191–206. <https://doi.org/10.3897/zookeys.515.9459>
- Nunomura N (2010a) A new species of the genus *Mongoloniscus* (Crustacea: Isopoda) from Toyama Plain. *Bulletin of the Toyama Science Museum* 33: 27–31.
- Nunomura N (2010b) Terrestrial crustaceans from Shiga Prefecture, central Japan. *Bulletin of the Toyama Science Museum* 33: 47–63.
- Nunomura N (2013) Isopod crustaceans from Shikoku, western Japan–1, specimens from Ehime Prefecture. *Bulletin of the Toyama Science Museum* 37: 19–78.

- Poulakakis N, Sfenthourakis S (2008) Molecular phylogeny and phylogeography of the Greek populations of the genus *Orthometopon* (Isopoda, Oniscidea) based on mitochondrial DNA sequences. *Zoological Journal of the Linnean Society* 152(4): 707–715. <https://doi.org/10.1111/j.1096-3642.2007.00378.x>
- Rambaut A (2016) FigTree v1.4.3. Molecular evolution, phylogenetics and epidemiology. Edinburgh: University of Edinburgh, Institute of Evolutionary Biology.
- Raupach MJ, Rulik B, Spelda J (2022) Surprisingly high genetic divergence of the mitochondrial DNA barcode fragment (COI) within Central European woodlice species (Crustacea, Isopoda, Oniscidea). *ZooKeys* 1082: 103–125. <https://doi.org/10.3897/zookeys.1082.69851>
- Ronquist F, Teslenko M, van der Mark P, Ayres DL, Darling A, Höhna S, Larget B, Liu L, Suchard MA, Huelsenbeck JP (2012) MRBAYES 3.2: Efficient Bayesian phylogenetic inference and model selection across a large model space. *Systematic Biology* 61(3): 539–542. <https://doi.org/10.1093/sysbio/sys029>
- Saito N, Itani G, Nunomura N (2000) A Preliminary Check List of Isopod Crustaceans in Japan. *Toyama Science Museum* 23: 11–107.
- Schmalfuss H (2003) World catalog of terrestrial isopods (Isopoda: Oniscidea). *Stuttgarter Beiträge zur Naturkunde, Serie A* 654: 1–341.
- Schwendinger PJ, Giribet G (2005) The systematics of the south-east Asian genus *Fangensis* Rambla (Opiliones: Cyphophthalmi: Stylocellidae). *Invertebrate Systematics* 19(4): 297–323. <https://doi.org/10.1071/IS05023>
- Tanaka R, Karasawa S (2016) Growth-related taxonomic character variation in *Mongoloniscus koreanus* Verhoeff, 1930 (Crustacea, Isopoda, Oniscidea), with implications for taxonomic confusion. *Edaphologia* 98: 11–19.
- Tang BP, Gui H (2000) A new species of the genus *Koreoniscus* from China (Crustacea: Isopoda). *Acta Zootaxonomica Sinica* 25(4): 365–368.
- Verhoeff KW (1930) Über Isopoden aus Turkestan. *Zoologischer Anzeiger* 91: 101–125.
- Wang J, Hong X, Li W (2022a) First record of the genus *Hemilepistus* (Isopoda: Agnaridae) from China, with description of two new species. *Zootaxa* 5188(1): 87–94. <https://doi.org/10.11646/zootaxa.5188.1.5>
- Wang J, Yang JB, Zeng XH, Li WC (2022b) Integrative taxonomy on the rare sky-island *Ligidium* species from southwest China (Isopoda, Oniscidea, Ligiidae). *BMC Zoology* 7(1): 26. <https://doi.org/10.1186/s40850-022-00120-1>
- Wang J, Hong X, Jiang C, Li W (2023) First record of the subgenus *Hemilepistus* (Desertellio) (Isopoda, Agnaridae) from China. *Zootaxa* 5389(3): 362–372. <https://doi.org/10.11646/zootaxa.5389.3.4>
- Yang L, An J (2021) A new species of the genus *Mongoloniscus* Verhoeff, 1930 (Crustacea: Isopoda: Agnaridae) from China. *Zootaxa* 5060(2): 265–274. <https://doi.org/10.11646/zootaxa.5060.2.7>
- Yoshino H, Kubota K (2022) Phylogeographic analysis of *Ligidium japonicum* (Isopoda: Ligiidae) and its allied species reveals high biodiversity and genetic differentiation in the Kanto region, Japan. *Entomological Science* 25(2): e12501. <https://doi.org/10.1111/ens.12501>
- Zeng XG, Wang J, Yang JB, Li WC (2021) Integrative taxonomy reveals a new species of the genus *Burmoniscus* (Isopoda, Philosciidae) from the Xuefeng Mountains, China. *ZooKeys* 1055: 123–134. <https://doi.org/10.3897/zookeys.1055.66879>
- Zhang D, Gao F, Jakovlić I, Zou H, Zhang J, Li WX, Wang GT (2020) PhyloSuite: An integrated and scalable desktop platform for streamlined molecular sequence data management

and evolutionary phylogenetics studies. *Molecular Ecology Resources* 20(1): 348–355. <https://doi.org/10.1111/1755-0998.13096>

Zhao Q, Shi E, Li Y, Eberl R, An J (2016) Population genetic structure and demographic history of the Chinese endemic *Mongoloniscus sinensis* (Dollfus, 1901) (Isopoda: Oniscidea). *Zoological Systematics* 41(4): 352–365. <https://doi.org/10.11865/zs.201641>

Zimmermann BL, Campos-Filho IS, Araujo PB (2018) Integrative taxonomy reveals a new genus and new species of Philosciidae (Crustacea: Isopoda: Oniscidea) from the Neotropical region. *Canadian Journal of Zoology* 96(5): 473–485. <https://doi.org/10.1139/cjz-2017-0289>

Supplementary material 1

Supporting Information

Authors: Chao Jiang, Jing Zhong, Zhidong Wang, Weichun Li, Luqi Huang

Data type: docx

Explanation note: **table S1**. Species vouchers and GenBank accession numbers; **table S2**. Pairwise genetic divergence (K2P-distance) among *Mongoloniscus* species of China using COI sequences.

Copyright notice: This dataset is made available under the Open Database License (<http://opendatacommons.org/licenses/odbl/1.0/>). The Open Database License (ODbL) is a license agreement intended to allow users to freely share, modify, and use this Dataset while maintaining this same freedom for others, provided that the original source and author(s) are credited.

Link: <https://doi.org/10.3897/zookeys.1202.113560.suppl1>

Eight new spider species of *Belisana* Thorell, 1898 (Araneae, Pholcidae), with an updated overview of *Belisana* species from Yunnan, China

Ludan Zhang¹, Zheng Wu¹, Shuqiang Li², Zhiyuan Yao¹

¹ College of Life Science, Shenyang Normal University, Shenyang 110034, Liaoning, China

² Institute of Zoology, Chinese Academy of Sciences, Beijing 100101, China

Corresponding authors: Zhiyuan Yao (yaozy@synu.edu.cn); Shuqiang Li (lisq@ioz.ac.cn)

Abstract

In this study, eight new species are described from the subtropical parts of Yunnan Province in southwestern China: *Belisana honghe* Zhang, Li & Yao, **sp. nov.** (♂♀), *B. jiuxiang* Zhang, Li & Yao, **sp. nov.** (♂♀), *B. lincang* Zhang, Li & Yao, **sp. nov.** (♂♀), *B. luxi* Zhang, Li & Yao, **sp. nov.** (♂♀), *B. tengchong* Zhang, Li & Yao, **sp. nov.** (♂♀), *B. tongji* Zhang, Li & Yao, **sp. nov.** (♂♀), *B. yongsheng* Zhang, Li & Yao, **sp. nov.** (♂), and *B. yunnan* Zhang, Li & Yao, **sp. nov.** (♂♀). They add up to a total of 31 *Belisana* species from Yunnan in an updated list provided in this paper.

Key words: Biodiversity, checklist, daddy-long-legs, fogging, invertebrate, morphology, taxonomy



Academic editor: Francesco Ballarin

Received: 26 February 2024

Accepted: 22 April 2024

Published: 27 May 2024

ZooBank: <https://zoobank.org/F2DE6CAC-842E-4275-B3C1-C84D7CEDF5B7>

Citation: Zhang L, Wu Z, Li S, Yao Z (2024) Eight new spider species of *Belisana* Thorell, 1898 (Araneae, Pholcidae), with an updated overview of *Belisana* species from Yunnan, China. ZooKeys 1202: 255–286. <https://doi.org/10.3897/zookeys.1202.121633>

Copyright: © Ludan Zhang et al.
This is an open access article distributed under terms of the Creative Commons Attribution License (Attribution 4.0 International – CC BY 4.0).

Introduction

The family Pholcidae C.L. Koch, 1850 is a highly diverse spider group with 1,969 extant species in 97 genera (WSC 2024). *Belisana* Thorell, 1898 had been a monotypic genus for more than 100 years. Huber (2005) was the first arachnologist to revise this genus: he transferred nine species from *Spermophora* Hentz, 1841 to *Belisana* and described 53 new species from Southeast Asia and northern Australia. Yao and Li (2013) and Yao et al. (2013, 2015) redescribed the type species *B. tauricornis* Thorell, 1898 based on type material from Myanmar, and reported 19 new species from Laos and Vietnam. In China, several researchers have also reported a large number of new species of *Belisana*. For instance, Zhang and Peng (2011) described 11 new species from southern China (in the provinces of Yunnan, Guizhou, Guangxi, Guangdong, and Hainan). Yao and his colleagues identified 17 species from Xishuangbanna in Yunnan, including 15 new species (e.g., Yao et al. 2018; Zhao et al. 2023); they also described 11 new species from Tibet, Sichuan, Guizhou, Guangxi, Guangdong, and Fujian (Zhu et al. 2020a, b; Yang et al. 2023). To date, 62 species have been recorded in southern China (Yang et al. 2023; Zhao et al. 2023; WSC 2024). Altogether, there are currently 148 species of *Belisana* globally, making it the second-largest genus in Pholcidae (WSC 2024). They are distributed mainly in southern China, and

in the Indo-Malayan and Australasian regions (Huber 2005; Zhu et al. 2020a; WSC 2024). They occupy a variety of micro-habitats, e.g., under rocks, in caves, on the underside of leaves, among leaf litter, and amidst foliage in the canopy (Huber 2005; Yao and Li 2013; Yao et al. 2015).

Currently, 23 species of *Belisana* have been recorded from Yunnan in south-western China (WSC 2024). Most of them (19 species) were described from tropical Xishuangbanna in southern Yunnan (Huber 2005; Zhang and Peng 2011; Zhao et al. 2023). Another four species were recorded in the subtropical parts of Yunnan: two in the Hengduan Mountains (western Yunnan) and another two on the Yunnan-Guizhou Plateau (eastern Yunnan) (Huber 2005; Zhang and Peng 2011). This work aims to describe the newly discovered species from these two subtropical sites (Fig. 1) and to provide an updated overview of the diversity of *Belisana* species in Yunnan.

Materials and methods

Specimens were examined and measured with a Leica M205 C stereomicroscope. Left male palps were photographed. Epigynes were photographed before dissection. Vulvae were photographed after being treated in a 10% warm potassium hydroxide (KOH) solution to dissolve soft tissues. Images were captured with a Canon EOS 750D wide zoom digital camera (24.2 megapixels) mounted on the stereomicroscope mentioned above and assembled using Helicon Focus v. 3.10.3 image stacking software (Khmelik et al. 2005). Drawings were done with Procreate 5.0.2 (Savage Interactive Pty. Ltd.). All measurements are given in millimeters (mm). Leg measurements are shown as: total length (femur, patella, tibia, metatarsus, and tarsus). Leg segments were measured on their dorsal sides. The distribution map was generated with ArcGIS v. 10.2 (ESRI Inc.). The specimens studied are preserved in 75% ethanol and deposited in the Institute of Zoology, Chinese Academy of Sciences (IZCAS) in Beijing, China.

Terminology and taxonomic descriptions follow Huber (2005) and Yao et al. (2015). The following abbreviations are used in the descriptions: **ALE** = anterior lateral eye, **AME** = anterior median eye, **PME** = posterior median eye, **L/d** = length/diameter; used in the illustrations: **aa** = anterior arch, **b** = bulb, **ba** = bulbal apophysis, **da** = distal apophysis, **e** = embolus, **ep** = epigynal pocket, **f** = flap, **pa** = proximo-lateral apophysis, **pp** = pore plate, **pr** = procurus.

Taxonomy

Family Pholcidae C.L. Koch, 1850

Subfamily Pholcinae C.L. Koch, 1850

Genus *Belisana* Thorell, 1898

Type species. *Belisana tauricornis* Thorell, 1898.

Notes. A total of eight new species from Yunnan were recognized. Of these, *B. honghe* sp. nov., *B. jiuxiang* sp. nov., *B. tongi* sp. nov., and *B. yongsheng* sp. nov. are from the Yunnan-Guizhou Plateau; *B. lincang* sp. nov., *B. luxi* sp. nov., *B. tengchong* sp. nov., and *B. yunnan* sp. nov. are from the Hengduan Mountains (Fig. 1). A list of all *Belisana* species from Yunnan is provided in Table 1.

Table 1. A list of the *Belisana* species from Yunnan, China.

The Hengduan Mountains	3. <i>B. chenjini</i> Yao & Li, 2018
1. <i>B. lincang</i> sp. nov.	4. <i>B. chuandiani</i> Li, Zheng & Yao, 2023
2. <i>B. luxi</i> sp. nov.	5. <i>B. daxiangi</i> Li, Zheng & Yao, 2023
3. <i>B. nujiang</i> Huber, 2005	6. <i>B. dian</i> Yao & Li, 2018
4. <i>B. pianma</i> Huber, 2005	7. <i>B. fengzheni</i> Li, Zheng & Yao, 2023
5. <i>B. tengchong</i> sp. nov.	8. <i>B. gupian</i> Yao & Li, 2018
6. <i>B. yunnan</i> sp. nov.	9. <i>B. lata</i> Zhang & Peng, 2011
The Yunnan-Guizhou Plateau	10. <i>B. menghai</i> Yao & Li, 2019
1. <i>B. erromena</i> Zhang & Peng, 2011	11. <i>B. mengla</i> Yao & Li, 2020
2. <i>B. honghe</i> sp. nov.	12. <i>B. menglun</i> Yao & Li, 2020
3. <i>B. jiuxiang</i> sp. nov.	13. <i>B. mengyang</i> Yao & Li, 2020
4. <i>B. tongi</i> sp. nov.	14. <i>B. rollofoliolata</i> (Wang, 1983)
5. <i>B. yangi</i> Zhang & Peng, 2011	15. <i>B. schwendingeri</i> Huber, 2005
6. <i>B. yongsheng</i> sp. nov.	16. <i>B. xiaolongha</i> Zhu & Li, 2021
Xishuangbanna	17. <i>B. xishuangbanna</i> Yao & Li, 2019
1. <i>B. bubeng</i> Zhu & Li, 2021	18. <i>B. yangxiaodong</i> Yao & Li, 2018
2. <i>B. cas</i> Yao & Li, 2018	19. <i>B. zhengi</i> Yao, Pham & Li, 2015

***Belisana honghe* Zhang, Li & Yao, sp. nov.**

<https://zoobank.org/4945FF76-8093-4849-AEBC-3F7715FA09B0>

Figs 2, 3, 18A, B, 20A, B

Type material. *Holotype* ♂ (IZCAS-Ar44949) and *paratypes* 2♂ (IZCAS-Ar44950–51) 3♀ (IZCAS-Ar44952–54), Yanzi Cave (23°38.220'N, 103°3.200'E, 1080 m), Mawangzhuang, Miandian Town, Jianshui County, Honghe, Yunnan, China, 29/03/2007, J Liu & Y Lin leg.

Etymology. The specific name refers to the type locality, which is a noun in apposition.

Diagnosis. The new species resembles *B. cheni* Yao, Pham & Li, 2015 (Yao et al. 2015: 5, figs 4A–D, 5A–G, 6A–E) by having similar male chelicerae, bulbal apophyses, and epigyne (Figs 3A, C, D, 20A), but can be distinguished by differences in males: procurus with nearly trapezoidal dorso-distal membranous process (arrow 3 in Figs 2C, 18A vs half-round) and long (as long as dorso-distal membranous process), distally widened ventro-subdistal membranous process (arrow 4 in Figs 2C, 18A vs short and distally pointed); differences in females: pore plates anteriorly pointed and posteriorly wide and blunt (Figs 3B, 20B vs narrow).

Description. Male (holotype): Total length 1.66 (1.74 with clypeus), carapace 0.63 long, 0.67 wide, opisthosoma 1.03 long, 0.84 wide. Leg I: 19.02 (5.05, 0.26, 5.00, 7.05, 1.66), leg II: 14.38 (3.96, 0.25, 3.80, 5.15, 1.22), leg III missing, leg IV: 10.65 (3.16, 0.23, 2.53, 3.96, 0.77); tibia I L/d: 89. Eye inter-distances and diameters: PME–PME 0.13, PME 0.07, PME–ALE 0.02, AME absent. Sternum width/length: 0.50/0.46. Habitus as in Fig. 3E, F. Carapace and sternum yellowish, without marks. Legs whitish, without darker rings. Opisthosoma yellowish, without spots. Thoracic furrow absent. Clypeus unmodified. Chelicerae (Fig. 3D) with a pair of proximo-lateral apophyses and a pair of distal apophyses (distance between tips: 0.19). Palp as in Fig. 2A, B; trochanter with ventral apophysis (arrow 2 in Fig. 2B) and prolateral apophysis (arrow 1 in Fig. 2B); procurus simple proximally but complex distally, with sclerotized prolatero-distal apophysis (arrow 1 in

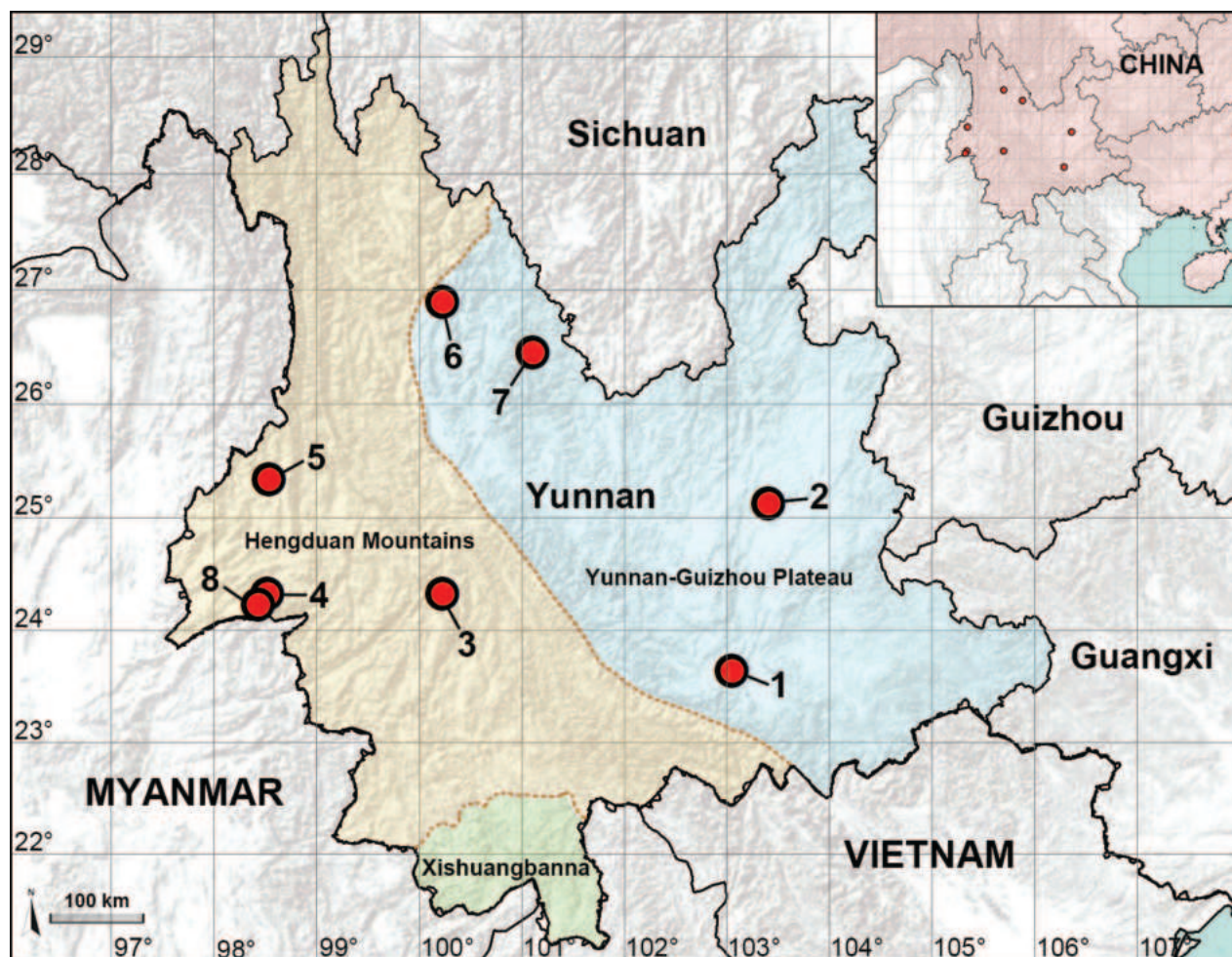


Figure 1. Distribution records of the new *Belisana* species from Yunnan, China 1 *Belisana honghe* sp. nov. 2 *B. jiujiang* sp. nov. 3 *B. lincang* sp. nov. 4 *B. luxi* sp. nov. 5 *B. tengchong* sp. nov. 6 *B. tongi* sp. nov. 7 *B. yongsheng* sp. nov. 8 *B. yunnan* sp. nov.

Figs 2C, 18A), sclerotized distal apophysis (arrow 2 in Figs 2C, 18A), dorso-distal membranous process (arrow 3 in Figs 2C, 18A), ventro-subdistal membranous process (arrow 4 in Figs 2C, 18A), and retrolateral flap (Figs 2D, 18B); bulb (Fig. 3C) with hooked apophysis and simple embolus. Retrolateral trichobothria on tibia I at 9% proximally; legs with short vertical setae on metatarsi; tarsus I with 20 distinct pseudosegments.

Female (paratype, IZCAS-Ar44952): Similar to male, habitus as in Fig. 3G, H. Total length 1.50 (1.62 with clypeus), carapace 0.49 long, 0.55 wide, opisthosoma 1.01 long, 0.80 wide; tibia I: 3.60; tibia I L/d: 61. Eye inter-distances and diameters: PME–PME 0.14, PME 0.06, PME–ALE 0.02, AME absent. Sternum width/length: 0.47/0.44. Epigyne (Figs 3A, 20A) simple and flat, with a pair of postero-lateral pockets 0.32 apart (arrow ep in Figs 3B, 20B, invisible in Figs 3A, 20A). Vulva (Figs 3B, 20B) with ridge-shaped anterior arch and a pair of anteriorly pointed and posteriorly wide and blunt pore plates.

Variation. Tibia I in one male paratype (IZCAS-Ar44950) (leg I missing in IZCAS-Ar44951): 5.64. Tibia I in the other two female paratypes (IZCAS-Ar44953–54): 4.10, 4.25.

Habitat. The species was found in the dark zone inside the cave.

Distribution. China (Yunnan, type locality; Fig. 1).

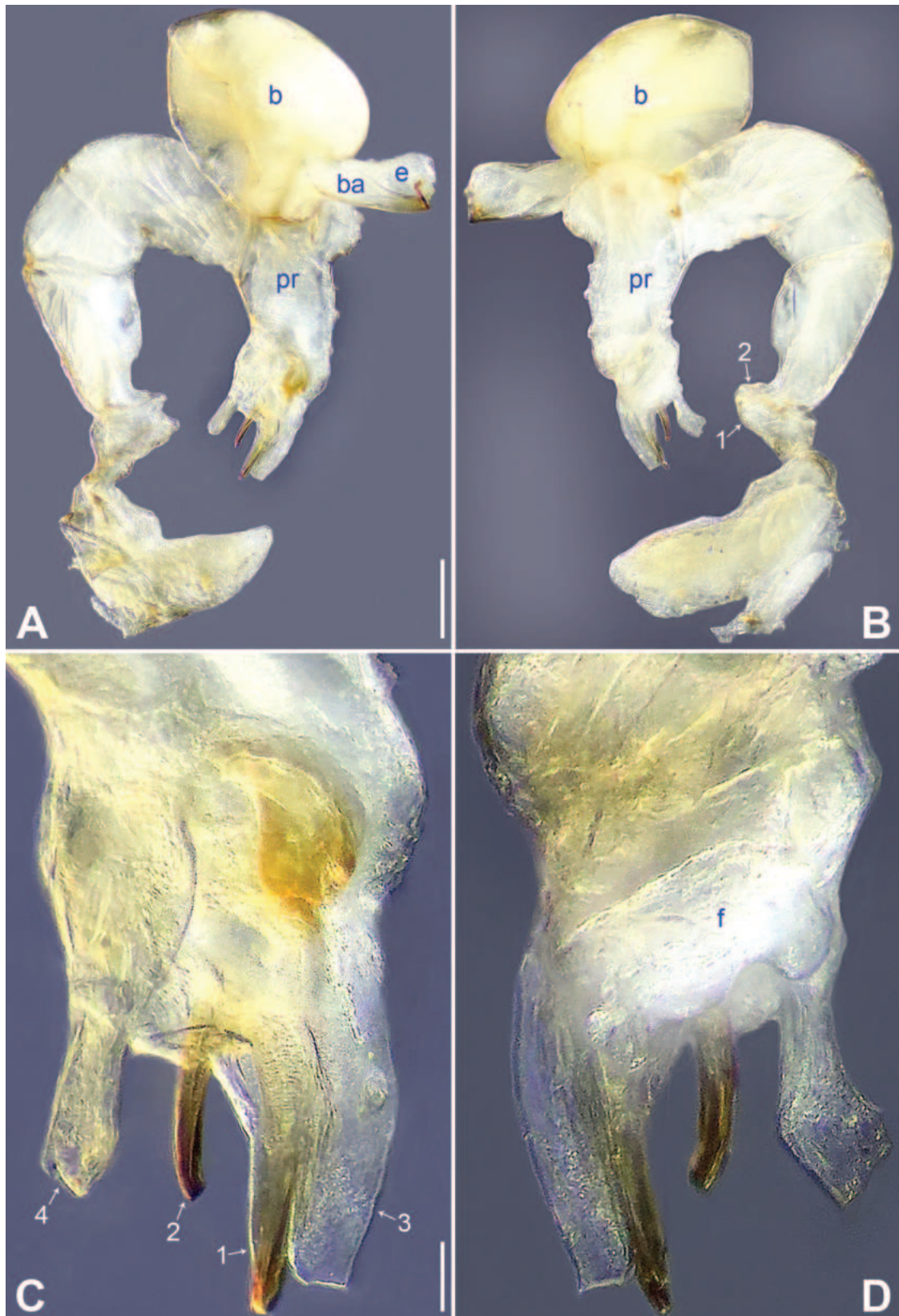


Figure 2. *Belisana honghe* sp. nov., holotype male **A, B** palp (**A** prolateral view **B** retrolateral view, arrow 1 points at retrolateral apophysis, arrow 2 points at ventral apophysis) **C, D** distal part of procurus (**C** prolateral view, arrow 1 points at sclerotized prolatero-distal apophysis, arrow 2 points at sclerotized distal apophysis, arrow 3 points at dorso-distal membranous process, arrow 4 points at ventro-subdistal membranous process **D** retrolateral view). Abbreviations: b = bulb, ba = bulbal apophysis, e = embolus, f = flap, pr = procurus. Scale bars: 0.10 (**A, B**); 0.02 (**C, D**).

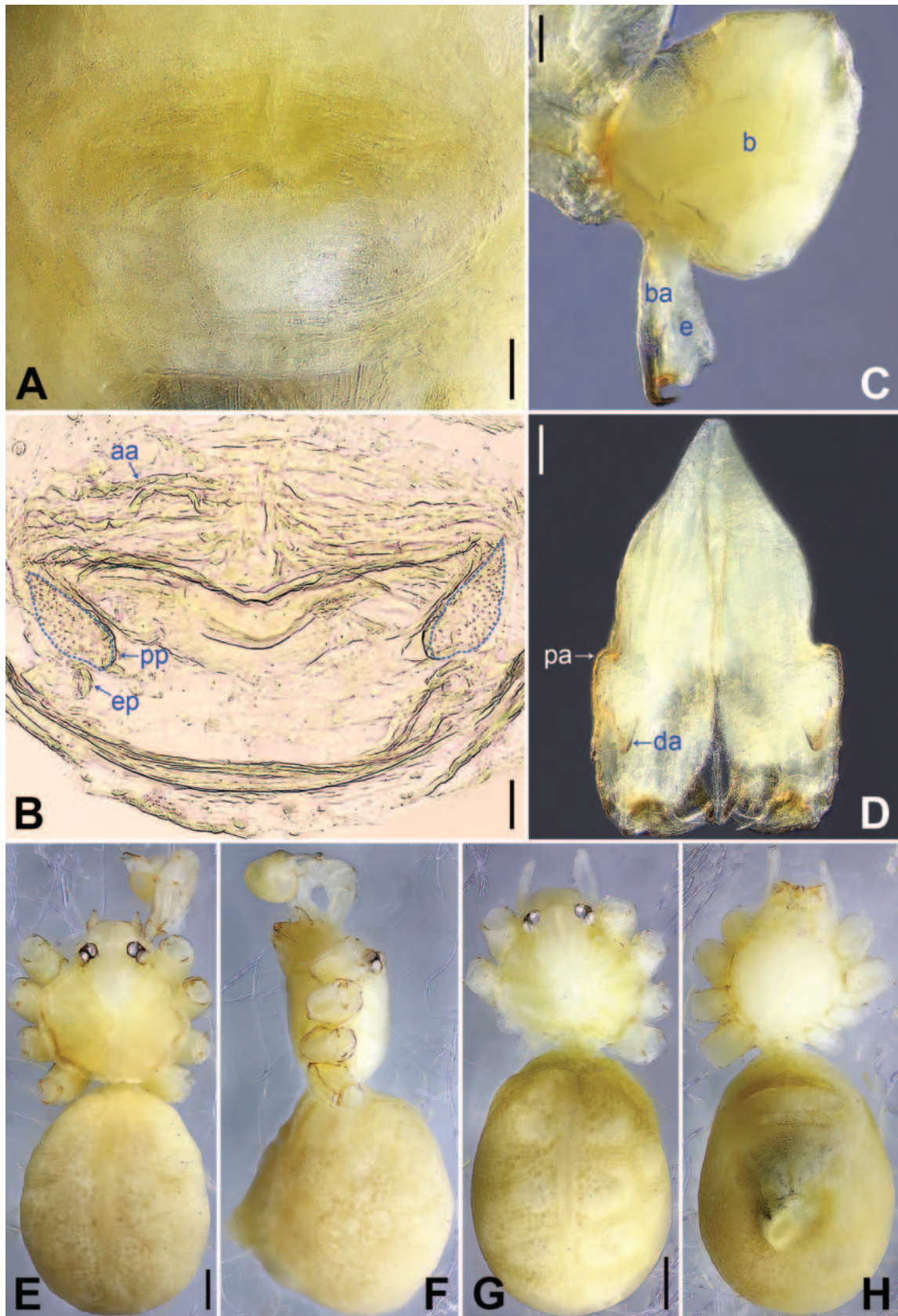


Figure 3. *Belisana honghe* sp. nov., holotype male (C–F) and paratype female (A, B, G, H) **A** epigyne, ventral view **B** vulva, dorsal view **C** bulb, prolateral view **D** chelicerae, frontal view **E–H** habitus (**E, G** dorsal view **F** lateral view **H** ventral view). Abbreviations: aa = anterior arch, b = bulb, ba = bulbal apophysis, da = distal apophysis, e = embolus, ep = epigynal pocket, pa = proximo-lateral apophysis, pp = pore plate. Scale bars: 0.05 (A–D); 0.20 (E–H).

***Belisana jiuxiang* Zhang, Li & Yao, sp. nov.**

<https://zoobank.org/734AE954-74BA-4B1B-81CE-1698150AEF86>

Figs 4, 5, 18C, D, 20C, D

Type material. *Holotype* ♂ (IZCAS-Ar44955) and *paratypes* 2♂ (IZCAS-Ar44956–57) 4♀ (IZCAS-Ar44958–61), Sanjiao Cave (25°8.059'N, 103°23.969'E, 1795 m), Jiuxiang Town, Yiliang County, Kunming, **Yunnan, China**, 08/04/2007, J Liu & Y Lin leg.

Etymology. The specific name refers to the type locality, which is a noun in apposition.

Diagnosis. The new species resembles *B. tianlinensis* Zhang & Peng, 2011 (Zhang and Peng 2011: 65, fig. 10A–G) by having similar male chelicerae and bulbal apophyses (Fig. 5C, D), but can be distinguished by differences in males: clypeus unmodified (Fig. 5E vs with front apophysis), procurus with pointed, sclerotized distal apophysis (arrow 1 in Figs 4C, 18C vs with dorso-distal spine) and dorso-subdistal membranous process (arrow 2 in Figs 4C, 18C vs absent); differences in females: epigyne with median pockets (Figs 5A, B, 20C, D vs lateral), pore plates quadrilateral (Figs 5B, 20D vs nearly triangular).

Description. Male (holotype): Total length 1.64 (1.74 with clypeus), carapace 0.63 long, 0.67 wide, opisthosoma 1.01 long, 0.80 wide. Leg I: 14.84 (3.86, 0.33, 3.80, 5.15, 1.70), leg II: 9.62 (2.64, 0.26, 2.45, 3.17, 1.10), leg III: 6.82 (2.03, 0.19, 1.66, 2.28, 0.66), leg IV: 8.79 (2.56, 0.26, 2.25, 2.94, 0.78); tibia I L/d: 56. Eye inter-distances and diameters: PME–PME 0.13, PME 0.07, PME–ALE 0.02, AME absent. Sternum width/length: 0.53/0.48. Habitus as in Fig. 5E, F. Carapace and sternum yellowish, without marks. Legs whitish, without darker rings. Opisthosoma yellowish, without spots. Thoracic furrow absent. Clypeus unmodified. Chelicerae (Fig. 5D) with a pair of proximo-lateral apophyses and a pair of curved distal apophyses (distance between tips: 0.16). Palp as in Fig. 4A, B; trochanter with ventral apophysis (as long as wide, arrow 1 in Fig. 4B); femur with tiny retrolatero-proximal protrusion (arrow 2 in Fig. 4B); procurus simple proximally but complex distally, with pointed, sclerotized distal apophysis (arrow 1 in Figs 4C, 18C), dorso-subdistal membranous process (arrow 2 in Figs 4C, 18C), and nearly elliptic retrolateral flap (Figs 4D, 18D); bulb (Fig. 5C) with hooked apophysis and simple embolus. Retrolateral trichobothria on tibia I at 8% proximally; legs with short vertical setae on metatarsi; tarsus I with 19 distinct pseudosegments.

Female (paratype, IZCAS-Ar44958): Similar to male, habitus as in Fig. 5G, H. Total length 1.82 (1.92 with clypeus), carapace 0.73 long, 0.80 wide, opisthosoma 1.09 long, 0.83 wide; tibia I: 2.37; tibia I L/d: 36. Eye inter-distances and diameters: PME–PME 0.14, PME 0.06, PME–ALE 0.02, AME absent. Sternum width/length: 0.61/0.60. Epigyne (Figs 5A, 20C) simple and flat, anteriorly slightly sclerotized, with a pair of median pockets 0.15 apart. Vulva (Figs 5B, 20D) with ridge-shaped anterior arch bearing a pair of angular lateral sclerites (arrow in Figs 5B, 20D) and a pair of quadrilateral pore plates.

Variation. Tibia I in two male paratypes (IZCAS-Ar44956–57): 3.91, 4.36. Tibia I in the other three female paratypes (IZCAS-Ar44959–61): 2.84, 3.72, 3.78.

Habitat. The species was found in the dark zone inside the cave.

Distribution. China (Yunnan, type locality; Fig. 1).

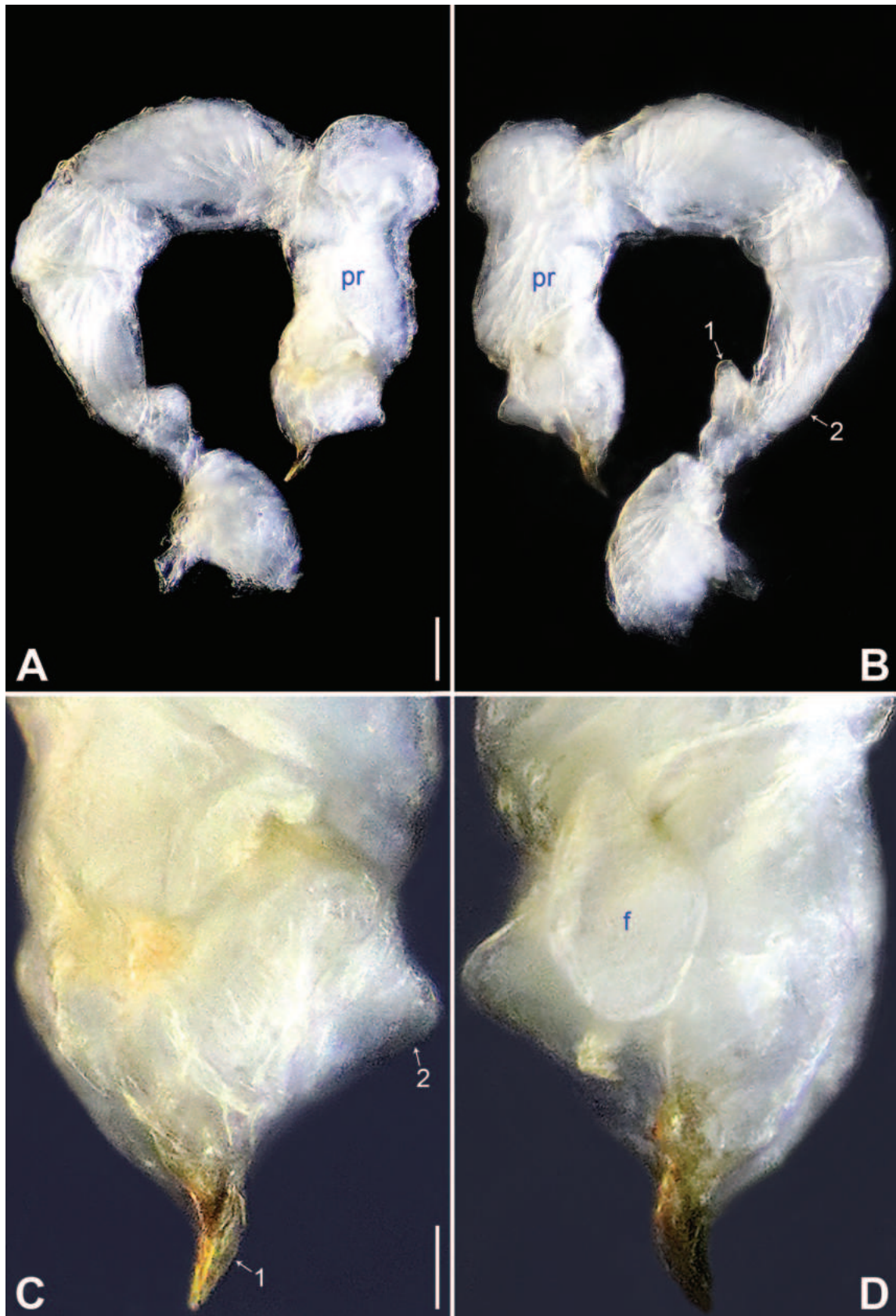


Figure 4. *Belisana juxiang* sp. nov., holotype male **A, B** palp (**A** prolateral view **B** retrolateral view, arrow 1 points at ventral apophysis, arrow 2 points at retrolatero-proximal protrusion) **C, D** distal part of procurcus (**C** prolateral view, arrow 1 points at sclerotized distal apophysis, arrow 2 points at dorso-subdistal membranous process **D** retrolateral view). Abbreviations: f = flap, pr = procurcus. Scale bars: 0.10 (**A, B**); 0.02 (**C, D**).

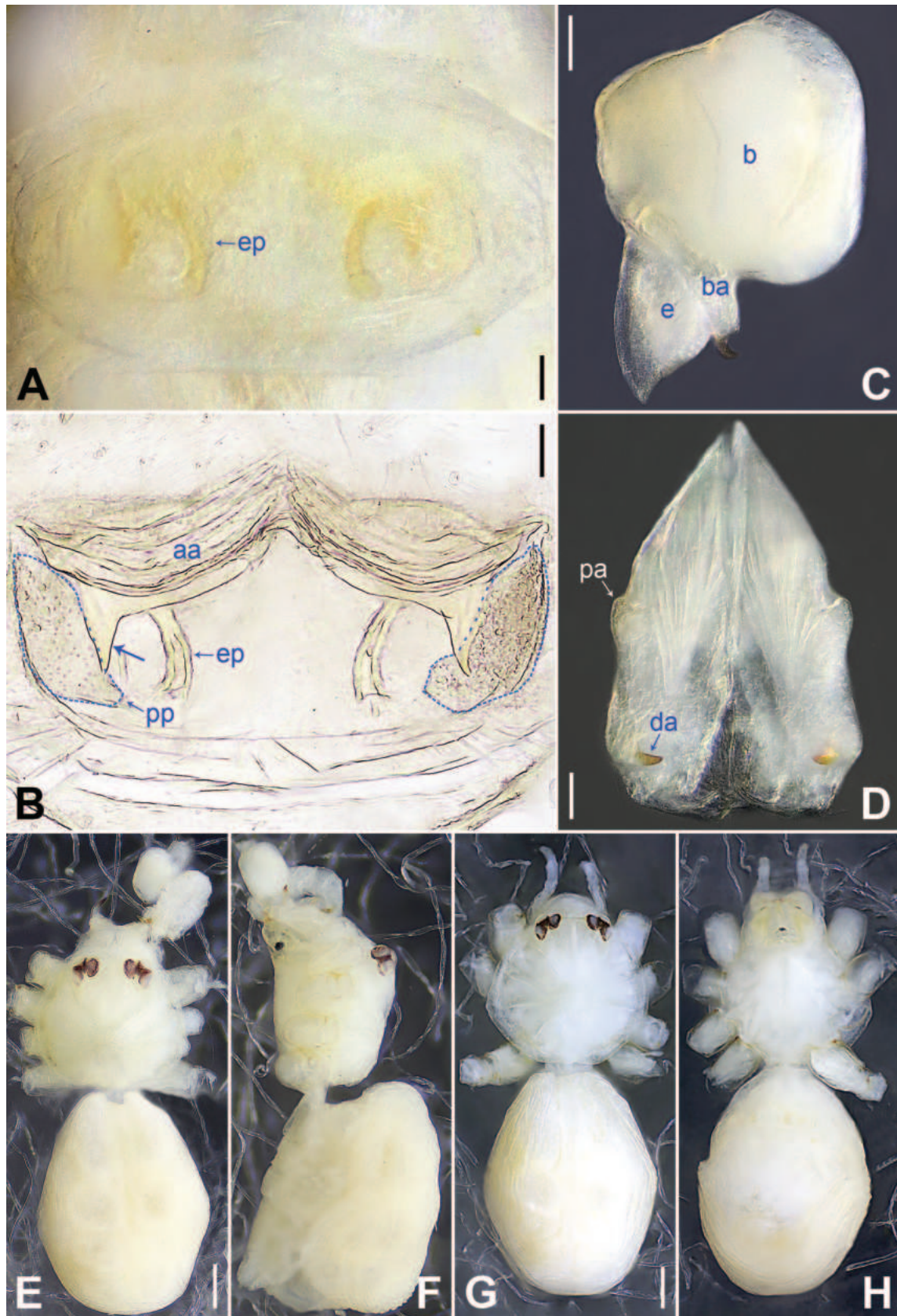


Figure 5. *Belisana juxiang* sp. nov., holotype male (C–F) and paratype female (A, B, G, H) **A** epigyne, ventral view **B** vulva, dorsal view, arrow points at lateral sclerite **C** bulb, prolateral view **D** chelicerae, frontal view **E–H** habitus (**E, G** dorsal view **F** lateral view **H** ventral view). Abbreviations: aa = anterior arch, b = bulb, ba = bulbal apophysis, da = distal apophysis, e = embolus, ep = epigynal pocket, pa = proximo-lateral apophysis, pp = pore plate. Scale bars: 0.05 (A–D); 0.20 (E–H).

***Belisana lincang* Zhang, Li & Yao, sp. nov.**

<https://zoobank.org/7401890D-953B-478C-AFBC-3E8E477689D1>

Figs 6, 7, 18E, F, 20E, F

Type material. *Holotype* ♂ (IZCAS-Ar44962) and *paratype* 1♀ (IZCAS-Ar44963), Bianfu Cave (24°19.862'N, 100°14.001'E, 1619 m), Yankou Village, Laoxu Town, Yun County, Lincang, **Yunnan, China**, 05/08/2010, C Wang, Q Zhao & L Lin leg.

Etymology. The specific name refers to the type locality, which is a noun in apposition.

Diagnosis. The new species resembles *B. phungae* Yao, Pham & Li, 2015 (Yao et al. 2015: 9, figs 19A–D, 20A–G, 21A–E) by having similar male chelicerae, bulbal apophyses, and epigyne (Figs 7A, C, D, 20E), but can be distinguished by differences in males: procurus with dorso-distal membranous lamella (arrow 3 in Figs 6C, 18E vs absent), distally pointed ventro-subdistal membranous lamella (arrow 4 in Figs 6C, 18E vs nearly half-round) and without dorso-subdistal sclerite (Figs 6C, 18E vs present); differences in females: epigynal pockets closer to each other (Figs 7A, B, 20E, F vs widely separated), pore plates curved and narrow (Figs 7B, 20F vs nearly round).

Description. Male (holotype): Total length 1.78 (1.90 with clypeus), carapace 0.85 long, 0.88 wide, opisthosoma 0.93 long, 0.85 wide. Leg I missing, leg II: 6.69 (1.78, 0.31, 1.62, 2.18, 0.80), leg III: 5.18 (1.42, 0.26, 1.19, 1.68, 0.63), leg IV: 6.70 (1.90, 0.28, 1.70, 2.13, 0.69). Eye inter-distances and diameters: PME–PME 0.08, PME 0.09, PME–ALE 0.03, AME absent. Sternum width/length: 0.61/0.56. Habitus as in Fig. 7E, F. Carapace yellowish, with brown median band; sternum yellowish. Legs whitish, without darker rings. Opisthosoma yellowish, without spots. Thoracic furrow absent. Clypeus unmodified. Chelicerae (Fig. 7D) with a pair of proximo-lateral apophyses and a pair of curved distal apophyses (distance between tips: 0.15). Palp as in Fig. 6A, B; trochanter with ventral apophysis (2× longer than wide, arrow 1 in Fig. 6B); femur with tiny retrolatero-proximal protrusion (arrow 2 in Fig. 6B); procurus simple proximally but complex distally, with prolatero-distal membranous process (arrow 1 in Figs 6C, 18E) bearing narrow lateral sclerite, sclerotized prolatero-distal apophysis (arrow 2 in Figs 6C, 18E), dorso-distal membranous lamella (arrow 3 in Figs 6C, 18E), and ventro-subdistal membranous lamella (arrow 4 in Figs 6C, 18E); bulb (Fig. 7C) with distally angular apophysis and simple embolus.

Female (paratype, IZCAS-Ar44963): Similar to male, habitus as in Fig. 7G, H. Total length 2.48 (2.62 with clypeus), carapace 0.86 long, 0.86 wide, opisthosoma 1.62 long, 1.31 wide. Leg I: 9.08 (2.33, 0.33, 2.30, 2.97, 1.15); tibia I L/d: 26. Eye inter-distances and diameters: PME–PME 0.09, PME 0.08, PME–ALE 0.02, AME absent. Sternum approximately as wide as long (0.60). Epigyne (Figs 7A, 20E) simple and flat, with dark internal shade and a pair of postero-median pockets 0.05 apart. Vulva (Figs 7B, 20F) with sac-like structure (arrow in Figs 7B, 20F), sclerotized anterior arch, and a pair of curved, long elliptic pore plates (5× longer than wide). Retrolateral trichobothria on tibia I at 9% proximally; legs with short vertical setae on metatarsi; tarsus I with 20 distinct pseudosegments.

Habitat. The species was found in the dark zone inside the cave.

Distribution. China (Yunnan, type locality; Fig. 1).

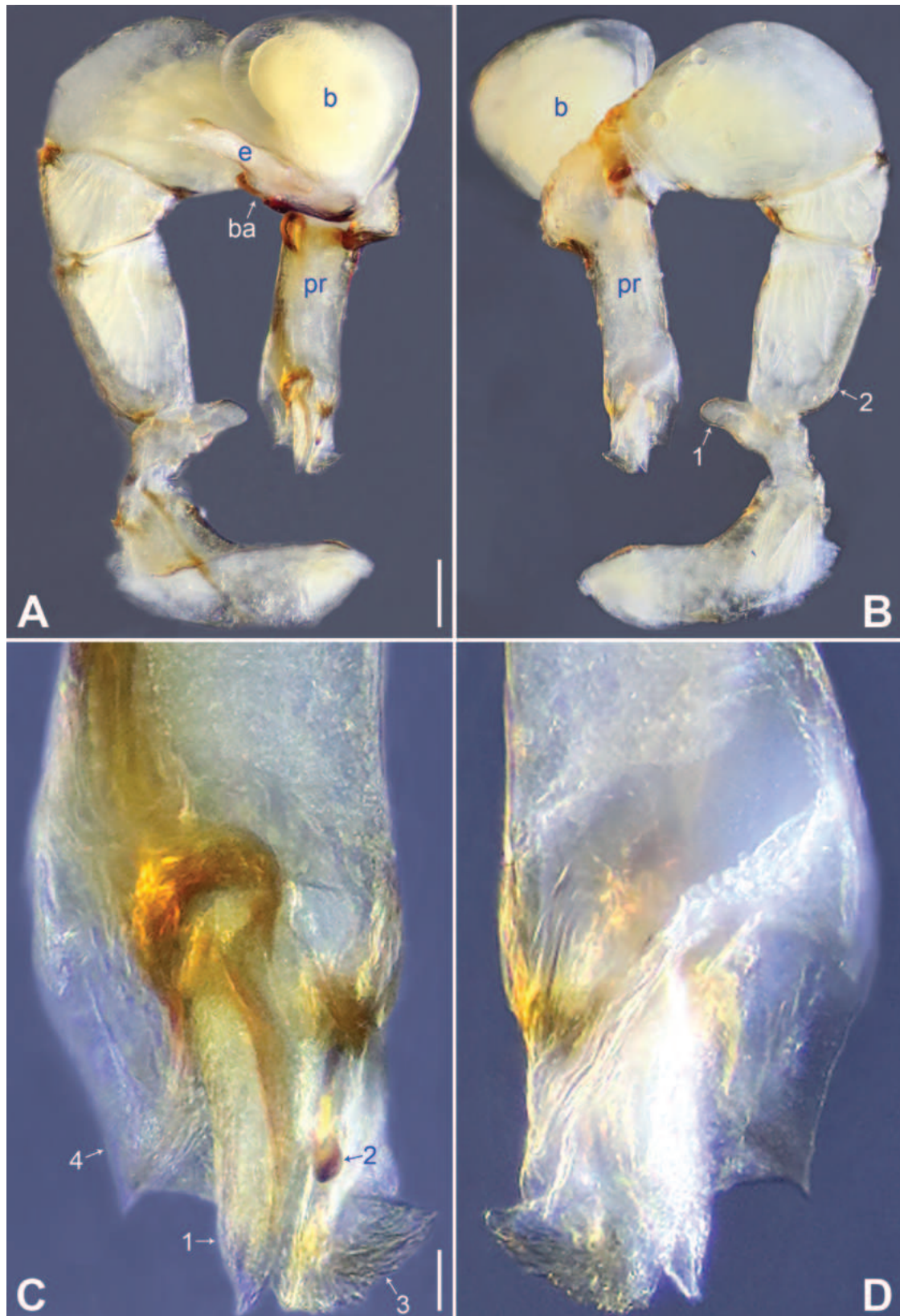


Figure 6. *Belisana lincang* sp. nov., holotype male **A, B** palp (**A** prolateral view **B** retrolateral view, arrow 1 points at ventral apophysis, arrow 2 points at retrolatero-proximal protrusion) **C, D** distal part of procurus (**C** prolateral view, arrow 1 points at prolatero-distal membranous process, arrow 2 points at sclerotized prolatero-distal apophysis, arrow 3 points at dorso-distal membranous lamella, arrow 4 points at ventro-subdistal membranous lamella **D** retrolateral view). Abbreviations: b = bulb, ba = bulbal apophysis, e = embolus, pr = procurus. Scale bars: 0.10 (**A, B**); 0.02 (**C, D**).

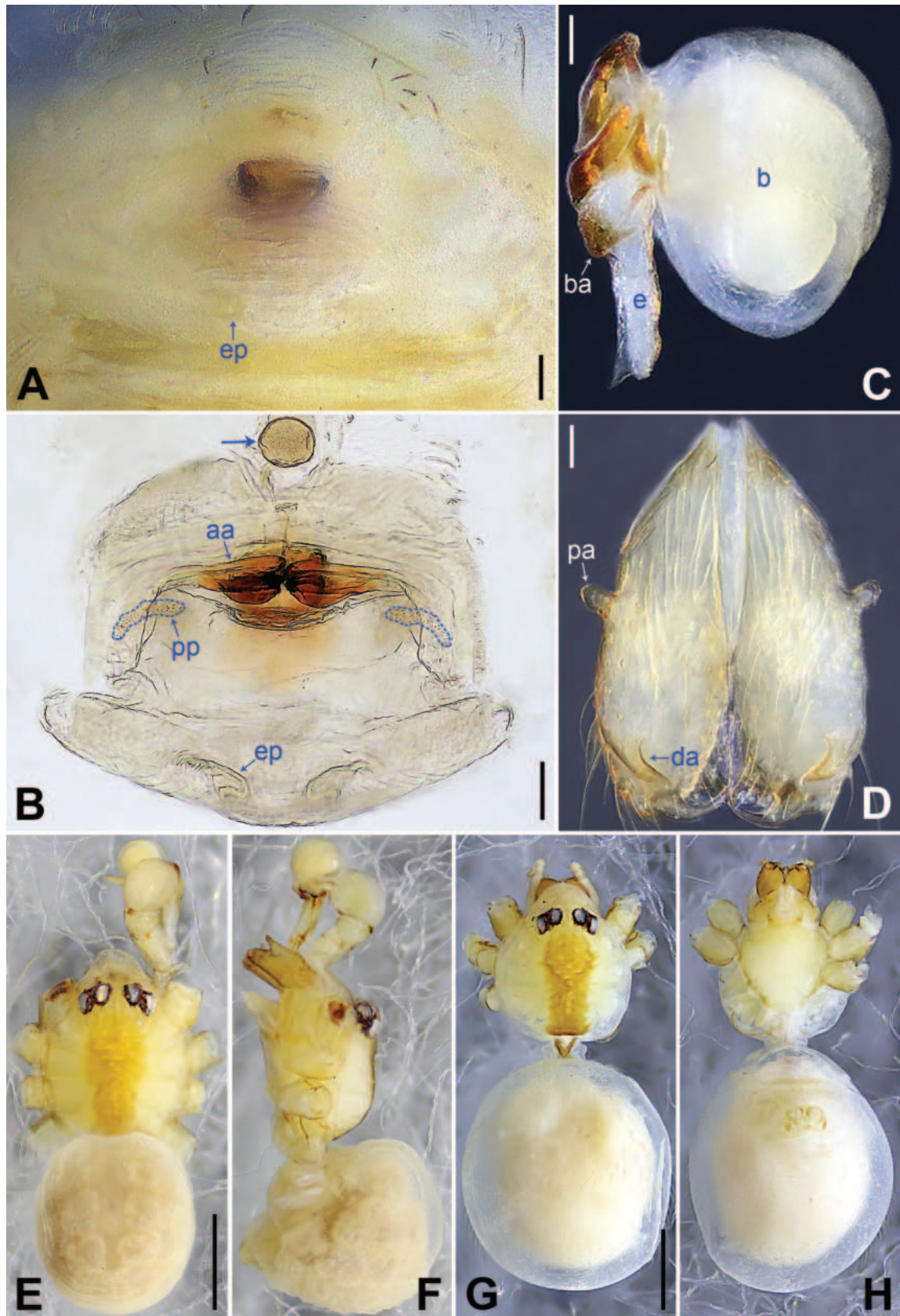


Figure 7. *Belisana lincang* sp. nov., holotype male (C–F) and paratype female (A, B, G, H) A epigyne, ventral view B vulva, dorsal view, arrow points at sac-like structure C right bulb, prolateral view D chelicerae, frontal view E–H habitus (E, G dorsal view F lateral view H ventral view). Abbreviations: aa = anterior arch, b = bulb, ba = bulbal apophysis, da = distal apophysis, e = embolus, ep = epigynal pocket, pa = proximo-lateral apophysis, pp = pore plate. Scale bars: 0.05 (A–D); 0.50 (E–H).

***Belisana luxi* Zhang, Li & Yao, sp. nov.**

<https://zoobank.org/E3307ED5-995B-42A5-9FC8-84D6F6861A61>

Figs 8, 9, 18G, H, 20G, H

Type material. *Holotype* ♂ (IZCAS-Ar44964) and *paratypes* 1♂ (IZCAS-Ar44965) 3♀ (IZCAS-Ar44966–68), Xianfo Cave (24°19.971'N, 98°30.943'E, 1081 m), Mangliu Village, Luxi, Dehong, Yunnan, China, 03/08/2010, C Wang, Q Zhao & L Lin leg.

Etymology. The specific name refers to the type locality, which is a noun in apposition.

Diagnosis. The new species resembles *B. lincang* sp. nov. (Figs 6, 7, 18E, F, 20E, F) by having similar epigyne and pore plates (Figs 9A, B, 20G, H), but can be distinguished by differences in males: cheliceral distal apophyses pointing downwards (Fig. 9D vs inwards), procurus without dorso-distal membranous lamella (Figs 8C, 18G vs present) and with angular ventro-subdistal membranous process (arrow 3 in Figs 8C, 18G vs distally pointed), bulbal apophysis distally blunt (Fig. 9C vs distally angular); differences in females: epigynal pockets widely separated (Figs 9A, B, 20G, H vs closer to each other), vulva without sac-like structure (Figs 9B, 20H vs present), sclerotized part of anterior arch strongly curved (Figs 9B, 20H vs straight).

Description. Male (holotype): Total length 2.25 (2.40 with clypeus), carapace 0.83 long, 0.84 wide, opisthosoma 1.42 long, 1.08 wide. Leg I: 15.92 (4.30, 0.33, 4.20, 5.75, 1.34), leg II: 9.31 (2.48, 0.31, 2.35, 3.40, 0.77), leg III: 6.39 (1.64, 0.29, 1.56, 2.25, 0.65), leg IV: 9.07 (2.56, 0.31, 2.35, 3.09, 0.76); tibia I L/d: 53. Eye inter-distances and diameters: PME–PME 0.11, PME 0.10, PME–ALE 0.04, AME absent. Sternum width/length: 0.65/0.63. Habitus as in Fig. 9E, F. Carapace yellowish, with brown median band; sternum yellowish. Legs whitish, without darker rings. Opisthosoma yellowish, without spots. Thoracic furrow absent. Clypeus unmodified. Chelicerae (Fig. 9D) with a pair of proximo-lateral apophyses and a pair of curved distal apophyses (distance between tips: 0.41). Palp as in Fig. 8A, B; trochanter with ventral apophysis (as long as wide, arrow in Fig. 8B); procurus simple proximally but complex distally, with prolatero-distal membranous process (arrow 1 in Figs 8C, 18G) bearing narrow lateral sclerite, sclerotized dorso-subdistal apophysis (arrow 2 in Figs 8C, 18G), and angular ventro-subdistal membranous process (arrow 3 in Figs 8C, 18G); bulb (Fig. 9C) with distally blunt apophysis and simple embolus. Retrolateral trichobothria on tibia I at 14% proximally; legs with short vertical setae on metatarsi; tarsus I with 20 distinct pseudosegments.

Female (paratype, IZCAS-Ar44966): Similar to male, habitus as in Fig. 9G, H. Total length 2.51 (2.65 with clypeus), carapace 0.89 long, 0.89 wide, opisthosoma 1.62 long, 1.36 wide; tibia I: 2.37; tibia I L/d: 30. Eye inter-distances and diameters: PME–PME 0.09, PME 0.08, PME–ALE 0.03, AME absent. Sternum width/length: 0.61/0.56. Epigyne (Figs 9A, 20G) simple and flat, with a pair of postero-lateral pockets 0.38 apart. Vulva (Figs 9B, 20H) with ridge-shaped, posteriorly sclerotized anterior arch and a pair of curved, long elliptic pore plates (6× longer than wide).

Variation. Tibia I in one male paratype (IZCAS-Ar44965): 3.46. Tibia I in the other two female paratypes (IZCAS-Ar44967–68): 1.78, 2.82.

Habitat. The species was found in the twilight zone (entrance ecotone) of the cave.

Distribution. China (Yunnan, type locality; Fig. 1).



Figure 8. *Belisana luxi* sp. nov., holotype male **A, B** palp (**A** prolateral view **B** retrolateral view, arrow points at ventral apophysis) **C, D** distal part of procurus (**C** prolateral view, arrow 1 points at prolatero-distal membranous process, arrow 2 points at sclerotized dorso-subdistal apophysis, arrow 3 points at ventro-subdistal membranous process **D** retrolateral view). Abbreviations: b = bulb, ba = bulbal apophysis, e = embolus, pr = procurus. Scale bars: 0.10 (**A, B**); 0.02 (**C, D**).

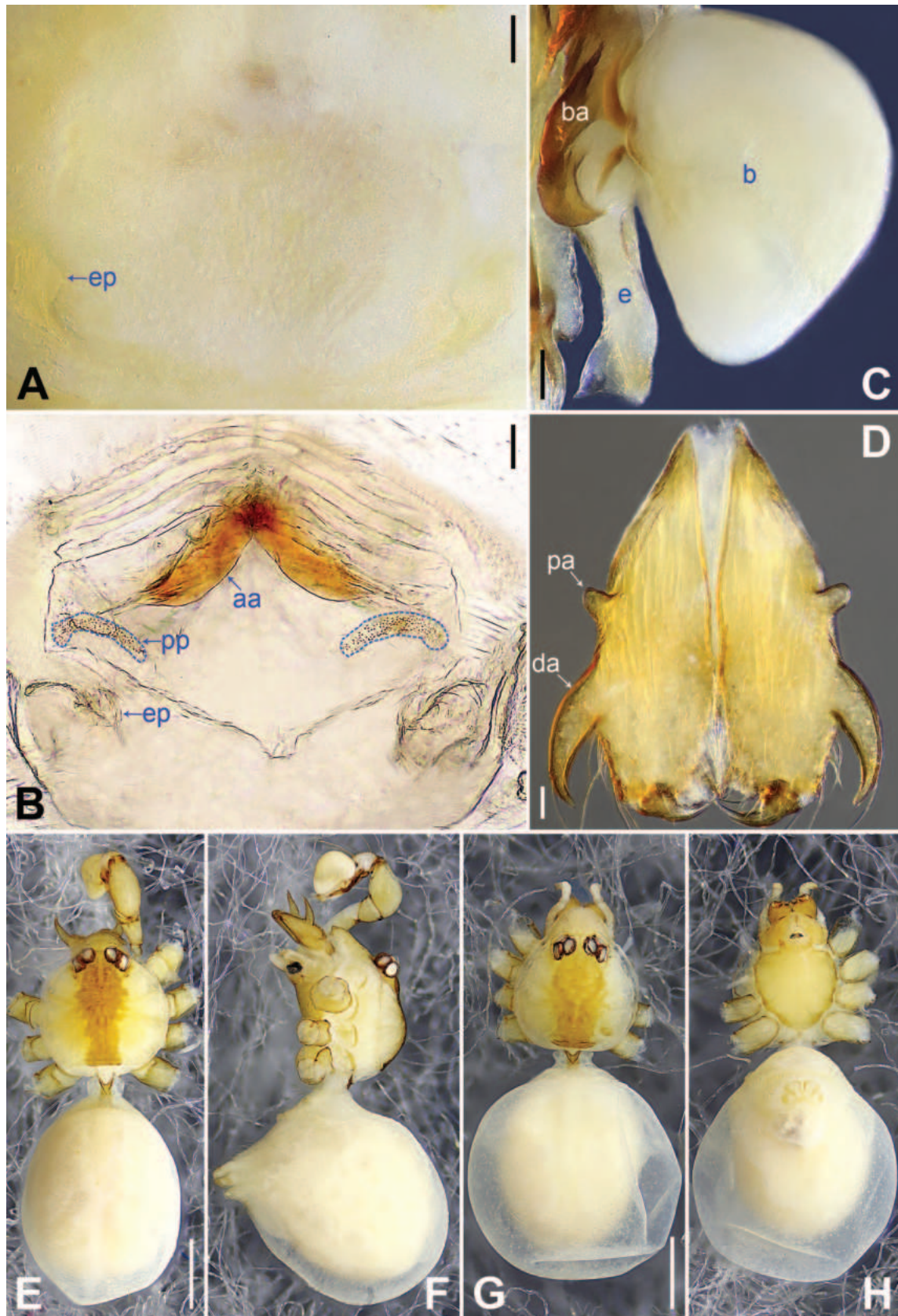


Figure 9. *Belisana luxi* sp. nov., holotype male (C–F) and paratype female (A, B, G, H) **A** epigyne, ventral view **B** vulva, dorsal view **C** bulb, prolateral view **D** chelicerae, frontal view **E–H** habitus (**E, G** dorsal view **F** lateral view **H** ventral view). Abbreviations: aa = anterior arch, b = bulb, ba = bulbal apophysis, da = distal apophysis, e = embolus, ep = epigynal pocket, pa = proximo-lateral apophysis, pp = pore plate. Scale bars: 0.05 (A–D); 0.50 (E–H).

***Belisana tengchong* Zhang, Li & Yao, sp. nov.**

<https://zoobank.org/D21705D9-7D42-4F9A-A4E9-27720466DF1D>

Figs 10, 11, 18I, J, 21A, B

Type material. *Holotype* ♂ (IZCAS-Ar44969) and *paratypes* 2♂ (IZCAS-Ar44970–71) 3♀ (IZCAS-Ar44972–74), Kongming Cave (25°20.447'N, 98°32.297'E, 1802 m), Jiangdong Village, Gudong Town, Tengchong County, Baoshan, Yunnan, China, 18/08/2010, C Wang, Q Zhao & L Lin leg.

Etymology. The specific name refers to the type locality, which is a noun in apposition.

Diagnosis. The new species resembles *B. pianma* Huber, 2005 (Huber 2005: 14, figs 5, 6, 56, 88–92, 112–130) by having similar bulbal apophyses and epigyne (Figs 11A, C, 21A), but can be distinguished by differences in males: clypeus unmodified (Fig. 11E vs with a pair of front apophyses), cheliceral distal apophyses on median part of chelicerae (Fig. 11D vs distal part), procurus without distal spine and dorso-distal sclerite (Figs 10C, 18I vs present), and with angular distal membranous process (arrow 2 in Figs 10C, 18I vs absent); differences in females: pore plates wide and curved (2× longer than wide, Figs 11B, 21B vs narrow, 6× longer than wide).

Description. Male (holotype): Total length 1.95 (2.08 with clypeus), carapace 0.71 long, 0.85 wide, opisthosoma 1.24 long, 0.93 wide. Leg I: 18.34 (4.75, 0.32, 4.90, 6.67, 1.70), leg II: 12.82 (3.56, 0.26, 3.40, 4.55, 1.05), legs III and IV missing; tibia I L/d: 65. Eye inter-distances and diameters: PME–PME 0.14, PME 0.10, PME–ALE 0.03, AME absent. Sternum width/length: 0.56/0.50. Habitus as in Fig. 11E, F. Carapace and sternum yellowish, without marks. Legs whitish, without darker rings. Opisthosoma yellowish, without spots. Thoracic furrow absent. Clypeus unmodified. Chelicerae (Fig. 11D) with a pair of proximo-lateral apophyses and a pair of curved distal apophyses (distance between tips: 0.28). Palp as in Fig. 10A, B; trochanter with ventral apophysis (as long as wide, arrow 1 in Fig. 10B); femur with tiny retrolatero-proximal protrusion (arrow 2 in Fig. 10B); procurus simple proximally but complex distally, with curved, sclerotized prolatero-distal apophysis (arrow 1 in Figs 10C, 18I), angular distal membranous process (arrow 2 in Figs 10C, 18I), and narrow, curved retrolatero-subdistal membranous process (arrow in Figs 10D, 18J); bulb (Fig. 11C) with hooked apophysis and simple embolus. Retrolateral trichobothria on tibia I on 17% proximally; legs with short vertical setae on metatarsi; tarsus I with 17 distinct pseudosegments.

Female (paratype, IZCAS-Ar44972): Similar to male, habitus as in Fig. 11G, H. Total length 2.14 (2.26 with clypeus), carapace 0.66 long, 0.76 wide, opisthosoma 1.48 long, 1.34 wide; tibia I: 3.36; tibia I L/d: 47. Eye inter-distances and diameters: PME–PME 0.10, PME 0.10, PME–ALE 0.02, AME absent. Sternum width/length: 0.54/0.50. Epigyne (Figs 11A, 21A) simple and flat, marginally slightly sclerotized, with a pair of lateral pockets 0.30 apart. Vulva (Figs 11B, 21B) with curved anterior arch and a pair of wide, curved pore plates (2× longer than wide) bearing indistinct teeth.

Variation. Tibia I in two male paratypes (IZCAS-Ar44970–71): 5.45, 5.83. Tibia I in the other two female paratypes (IZCAS-Ar44973–74): 3.45, 4.05.

Habitat. The species was found in the dark zone inside the cave.

Distribution. China (Yunnan, type locality; Fig. 1).

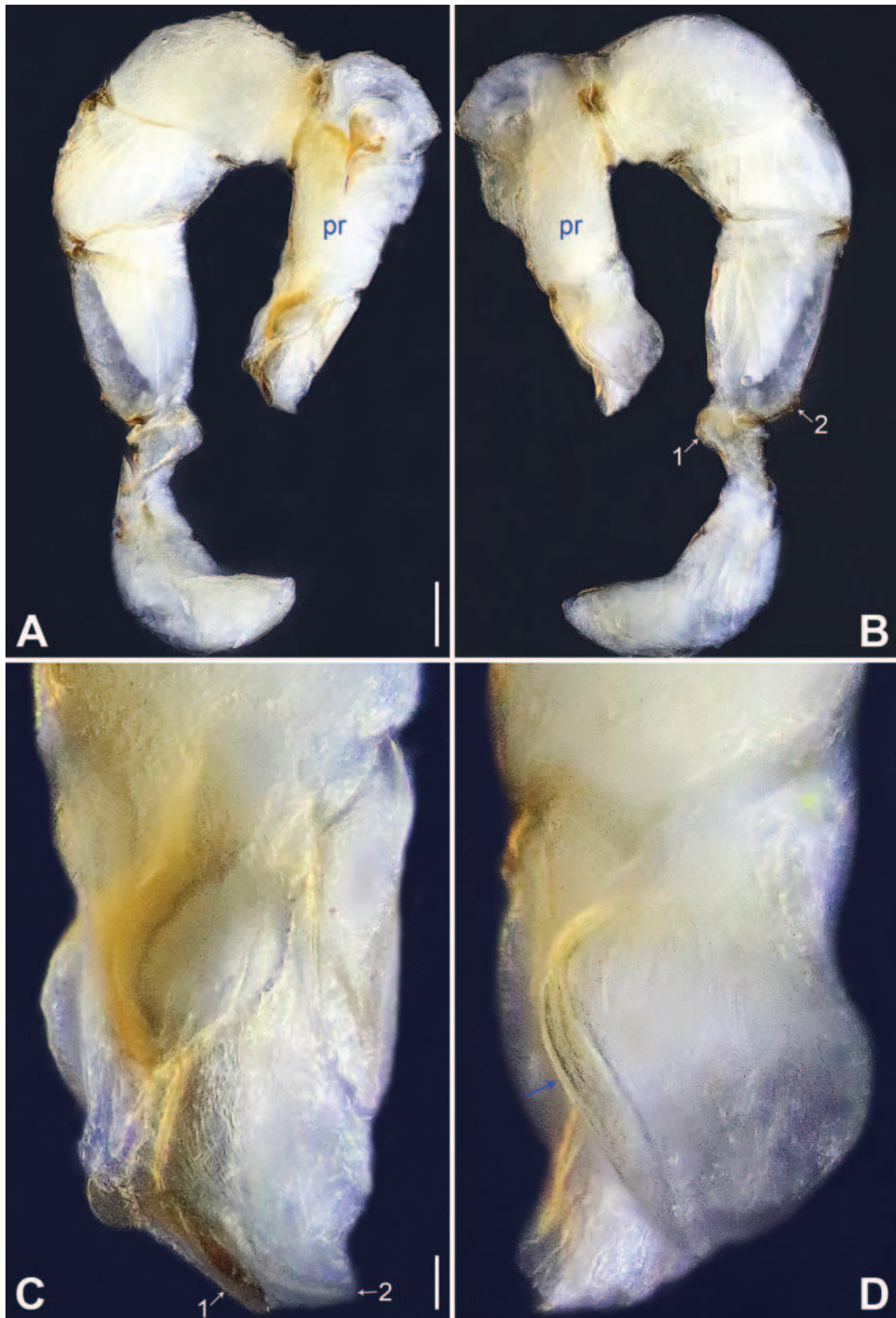


Figure 10. *Belisana tengchong* sp. nov., holotype male **A, B** palp (**A** prolateral view **B** retrolateral view, arrow 1 points at ventral apophysis, arrow 2 points at retrolatero-proximal protrusion) **C, D** distal part of procurcus (**C** prolateral view, arrow 1 points at sclerotized prolatero-distal apophysis, arrow 2 points at distal membranous process **D** retrolateral view, arrow points at retrolatero-subdistal membranous process). Abbreviation: pr = procurcus. Scale bars: 0.10 (**A, B**); 0.02 (**C, D**).

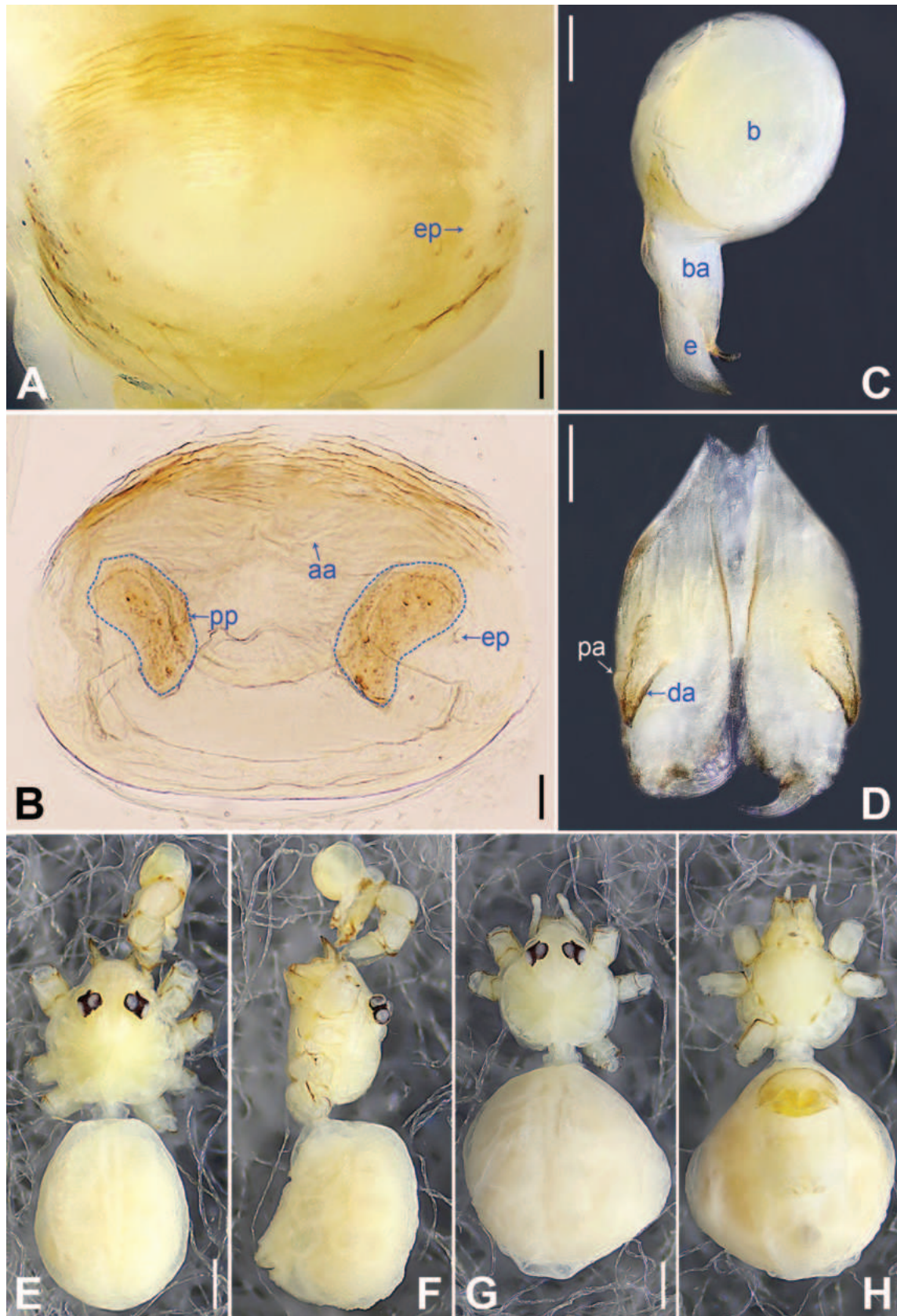


Figure 11. *Belisana tengchong* sp. nov., holotype male (C–F) and paratype female (A, B, G, H) A epigyne, ventral view B vulva, dorsal view C bulb, prolateral view D chelicerae, frontal view E–H habitus (E, G dorsal view F lateral view H ventral view). Abbreviations: aa = anterior arch, b = bulb, ba = bulbal apophysis, da = distal apophysis, e = embolus, ep = epigynal pocket, pa = proximo-lateral apophysis, pp = pore plate. Scale bars: 0.05 (A, B); 0.10 (C, D); 0.30 (E–H).

***Belisana tongi* Zhang, Li & Yao, sp. nov.**

<https://zoobank.org/4C53D853-BD6F-4E49-BBC9-DBBE5987F8A5>

Figs 12, 13, 18K, L, 21C, D

Type material. *Holotype* ♂ (IZCAS-Ar44975) and *paratypes* 4♀ (IZCAS-Ar44976–79), Heilongtan Park (26°53.259'N, 100°14.034'E, 2155 m), Lijiang, Yunnan, China, 15/07/2021, Y Tong & D Bian leg.

Etymology. The specific name is a patronym in honour of the collector Yanfeng Tong, which is a noun (name) in the genitive case.

Diagnosis. The new species resembles *B. yangi* Zhang & Peng, 2011 (Zhang and Peng 2011: 65, fig. 11A–H) by having similar male chelicerae, bulbal apophyses, and epigyne (Figs 13A, C, D, 21C), but can be distinguished by differences in males: procurus with distal membranous process (arrow 2 in Figs 12C, 18K vs absent) and dorso-distal spine (arrow 3 in Figs 12C, 18K vs absent); differences in females: epigyne with posterior pockets (Figs 13A, B, 21C, D vs anterior), vulva with four distinct median teeth (arrows in Figs 13B, 21D vs absent), pore plates nearly triangular (Figs 13B, 21D vs elliptic).

Description. Male (holotype): Total length 1.96 (2.08 with clypeus), carapace 0.71 long, 0.75 wide, opisthosoma 1.25 long, 0.80 wide. Leg I: 12.57 (3.30, 0.32, 3.22, 4.50, 1.23), leg II: 8.49 (2.35, 0.28, 2.03, 2.88, 0.95), leg III missing, leg IV: 7.38 (2.15, 0.26, 1.84, 2.43, 0.70); tibia I L/d: 45. Eye inter-distances and diameters: PME–PME 0.12, PME 0.08, PME–ALE 0.02, AME absent. Sternum width/length: 0.51/0.48. Habitus as in Fig. 13E, F. Carapace yellowish, with a pair of curved median bands; sternum yellowish. Legs yellowish, without darker rings. Opisthosoma yellowish, with dorsal and lateral black spots. Thoracic furrow absent. Clypeus unmodified. Chelicerae (Fig. 13D) with a pair of proximo-lateral apophyses and a pair of long, curved distal apophyses (distance between tips: 0.49). Palp as in Fig. 12A, B; trochanter with ventral apophysis (as long as wide; arrow in Fig. 12A) and small retrolateral apophysis (arrow 1 in Fig. 12B); femur with distinct ventral protrusion (arrow 2 in Fig. 12B); procurus simple proximally but complex distally, with narrow sclerite and teeth on prolatero-subdistal part (arrow 1 in Figs 12C, 18K), distal membranous process (arrow 2 in Figs 12C, 18K), and dorso-distal spine (arrow 3 in Figs 12C, 18K); bulb (Fig. 13C) with hooked apophysis and simple embolus. Retrolateral trichobothria on tibia I at 7% proximally; legs with short vertical setae on metatarsi; tarsus I with 16 distinct pseudosegments.

Female (paratype, IZCAS-Ar44976): Similar to male, habitus as in Fig. 13G, H. Total length 2.13 (2.21 with clypeus), carapace 0.68 long, 0.70 wide, opisthosoma 1.45 long, 1.00 wide; tibia I: 2.91; tibia I L/d: 36. Eye inter-distances and diameters: PME–PME 0.11, PME 0.07, PME–ALE 0.02, AME absent. Sternum width/length: 0.55/0.53. Epigyne (Figs 13A, 21C) simple and flat, anteriorly slightly sclerotized, with dark internal shade and a pair of postero-lateral pockets 0.46 apart. Vulva (Figs 13B, 21D) with ridge-shaped anterior arch, a pair of nearly triangular pore plates bearing distinct teeth, and four distinct median teeth (arrows in Figs 13B, 21D).

Variation. Tibia I in the other three female paratypes (IZCAS-Ar44977–79): 2.25, 2.47, 2.55.

Habitat. The species was found in the leaf litter.

Distribution. China (Yunnan, type locality; Fig. 1).

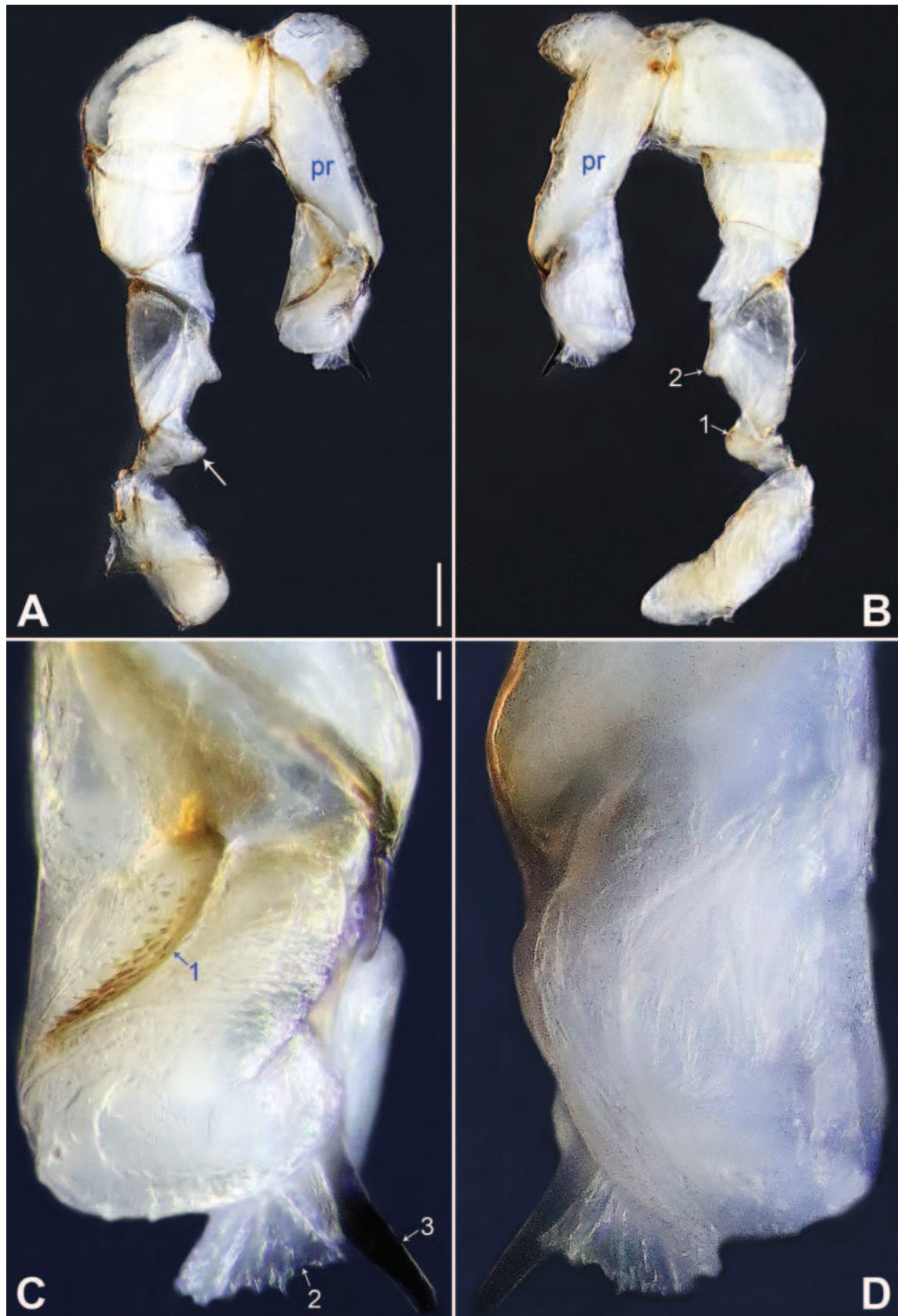


Figure 12. *Belisana tongi* sp. nov., holotype male **A, B** palp (**A** prolateral view, arrow points at ventral apophysis **B** retrolateral view, arrow 1 points at retrolateral apophysis, arrow 2 points at ventral protrusion) **C, D** distal part of procurus (**C** prolateral view, arrow 1 points at prolatero-subdistal part, arrow 2 points at distal membranous process, arrow 3 points at dorso-distal spine **D** retrolateral view). Abbreviation: pr = procurus. Scale bars: 0.10 (**A, B**); 0.02 (**C, D**).

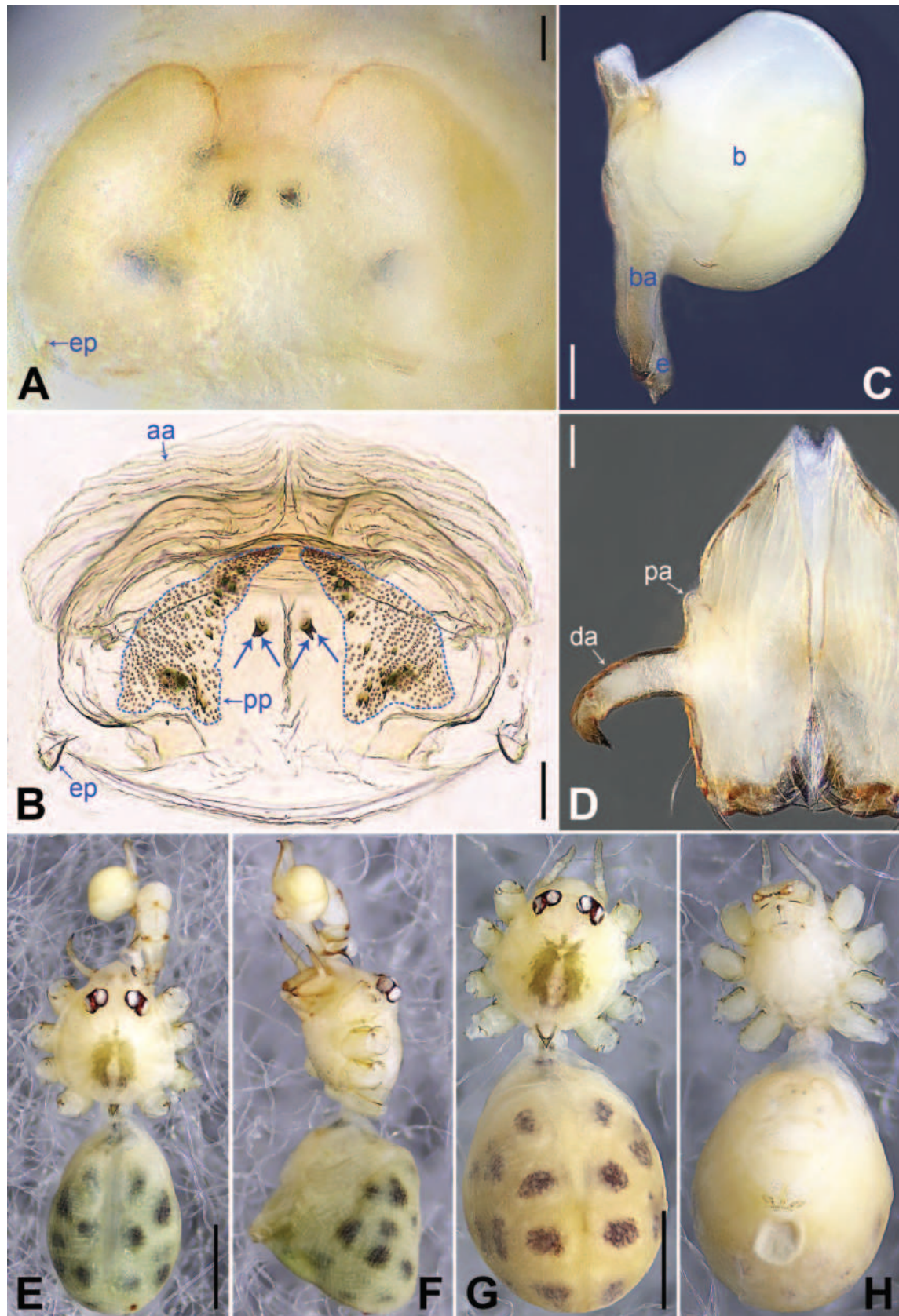


Figure 13. *Belisana tongji* sp. nov., holotype male (C–F) and paratype female (A, B, G, H) A epigyne, ventral view B vulva, dorsal view, arrows point at four distinct median teeth C bulb, prolateral view D chelicerae, frontal view E–H habitus (E, G dorsal view F lateral view H ventral view). Abbreviations: aa = anterior arch, b = bulb, ba = bulbal apophysis, da = distal apophysis, e = embolus, ep = epigynal pocket, pa = proximo-lateral apophysis, pp = pore plate. Scale bars: 0.05 (A–D); 0.50 (E–H).

***Belisana yongsheng* Zhang, Li & Yao, sp. nov.**

<https://zoobank.org/0996FD9D-9FEE-4635-B5D3-D9B14F913191>

Figs 14, 15, 19A, B

Type material. *Holotype* ♂ (IZCAS-Ar44980), Yinhe Cave (26°27.127'N, 101°6.482'E, 2012 m), Renhe Town, Yongsheng County, Lijiang, **Yunnan, China**, 03/08/2010, C Wang, Q Zhao & L Lin leg.

Etymology. The specific name refers to the type locality, which is a noun in apposition.

Diagnosis. The new species resembles *B. halongensis* Yao, Pham & Li, 2015 (Yao et al. 2015: 8, figs 16A–D, 17A–D, 18A–D) by having similar male chelicerae and bulbal apophyses (Fig. 15A, B), but can be distinguished by differences in males: procurus with two sclerotized distal apophyses (arrows in Figs 14C, 19A vs one prolatero-ventral sclerite), retrolateral flap (Figs 14D, 19B vs absent) and without prolatero-distal membranous lamella (Figs 14C, 19A vs present).

Description. Male (holotype): Total length 1.74 (1.79 with clypeus), carapace 0.58 long, 0.65 wide, opisthosoma 1.16 long, 0.80 wide. Leg I: 11.43 (3.10, 0.26, 3.03, 3.76, 1.28), leg II: 7.94 (2.25, 0.24, 1.98, 2.55, 0.92), leg III: 5.65 (1.60, 0.21, 1.38, 1.82, 0.64), leg IV: 7.29 (2.09, 0.23, 1.80, 2.48, 0.69); tibia I L/d: 47. Eye inter-distances and diameters: PME–PME 0.12, PME 0.07, PME–ALE 0.02, AME absent. Sternum width/length: 0.51/0.46. Habitus as in Fig. 15C–E. Carapace yellowish, with brownish radiating marks; sternum yellowish. Legs whitish, without darker rings. Opisthosoma yellowish, without spots. Thoracic furrow absent. Clypeus unmodified. Chelicerae (Fig. 15B) with a pair of proximo-lateral apophyses and a pair of distal apophyses (distance between tips: 0.19). Palp as in Fig. 14A, B; trochanter with ventral apophysis (as long as wide, arrow 1 in Fig. 14B) and retrolatero-ventral apophysis (arrow 2 in Fig. 14B); procurus simple proximally but complex distally, with two sclerotized distal apophyses (arrows in Figs 14C, 19A) and nearly D-shaped retrolateral flap (Figs 14D, 19B); bulb (Fig. 15A) with hooked apophysis and simple embolus. Retrolateral trichobothria on tibia I at 11% proximally; legs with short vertical setae on metatarsi; tarsus I with 20 distinct pseudosegments.

Female: Unknown.

Habitat. The species was found in the dark zone inside the cave.

Distribution. China (Yunnan, type locality; Fig. 1).

***Belisana yunnan* Zhang, Li & Yao, sp. nov.**

<https://zoobank.org/757F74E0-B68C-47E6-9260-5061A26D54A4>

Figs 16, 17, 19C, D, 21E, F

Type material. *Holotype* ♂ (IZCAS-Ar44981) and *paratypes* 2♂ (IZCAS-Ar44982–83) 3♀ (IZCAS-Ar44984–86), Xianren Cave (24°13.929'N, 98°25.563'E, 1636 m), Luxi, Dehong, **Yunnan, China**, 24/08/2010, C Wang, Q Zhao & L Lin leg.

Etymology. The specific name refers to the type locality, which is a noun in apposition.

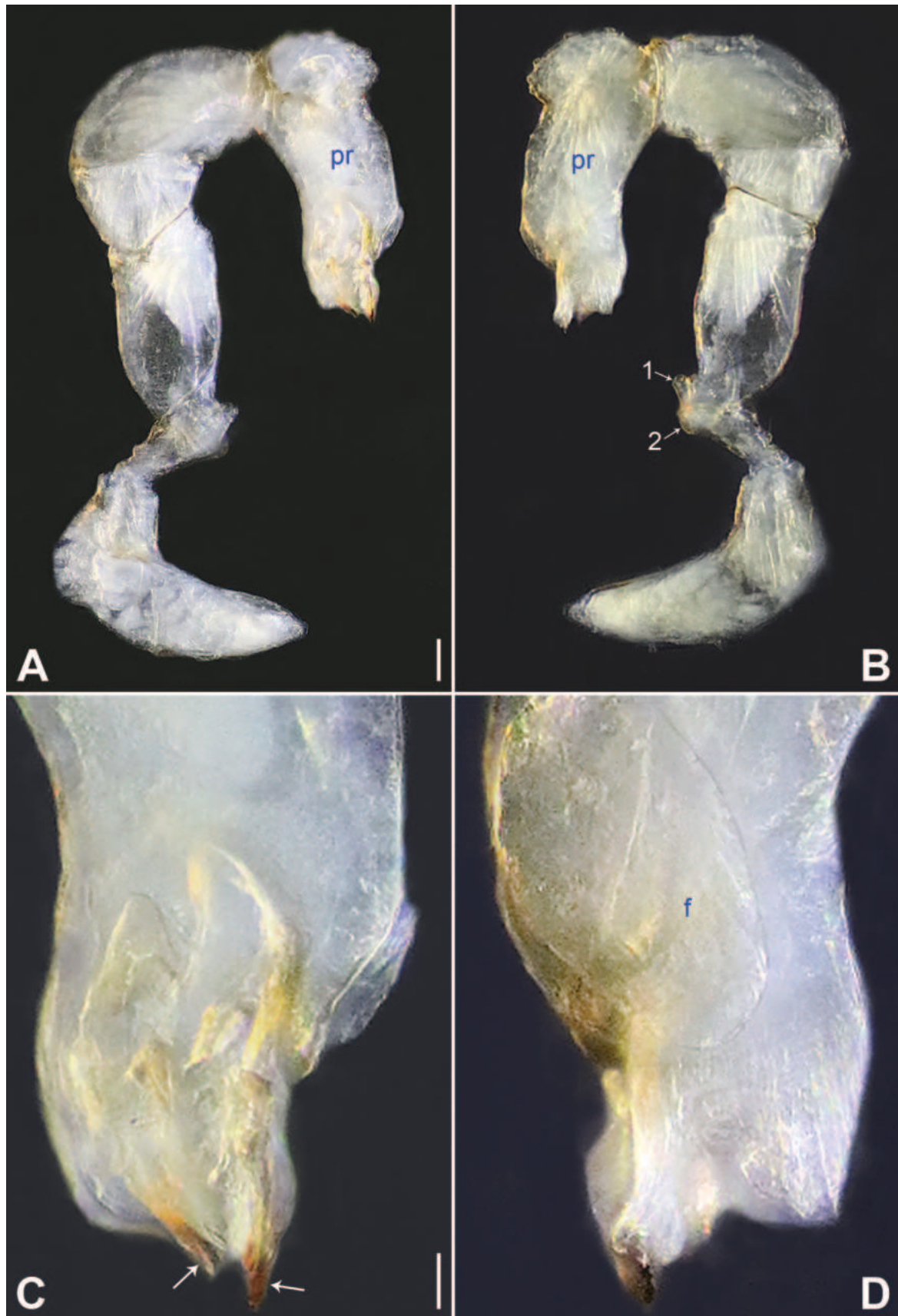


Figure 14. *Belisana yongsheng* sp. nov., holotype male **A, B** palp (**A** prolateral view **B** retrolateral view, arrow 1 points at ventral apophysis, arrow 2 points at retrolatero-ventral apophysis) **C, D** distal part of procurus (**C** prolateral view, arrows point at two sclerotized distal apophyses **D** retrolateral view). Abbreviations: f = flap, pr = procurus. Scale bars: 0.10 (**A, B**); 0.02 (**C, D**).

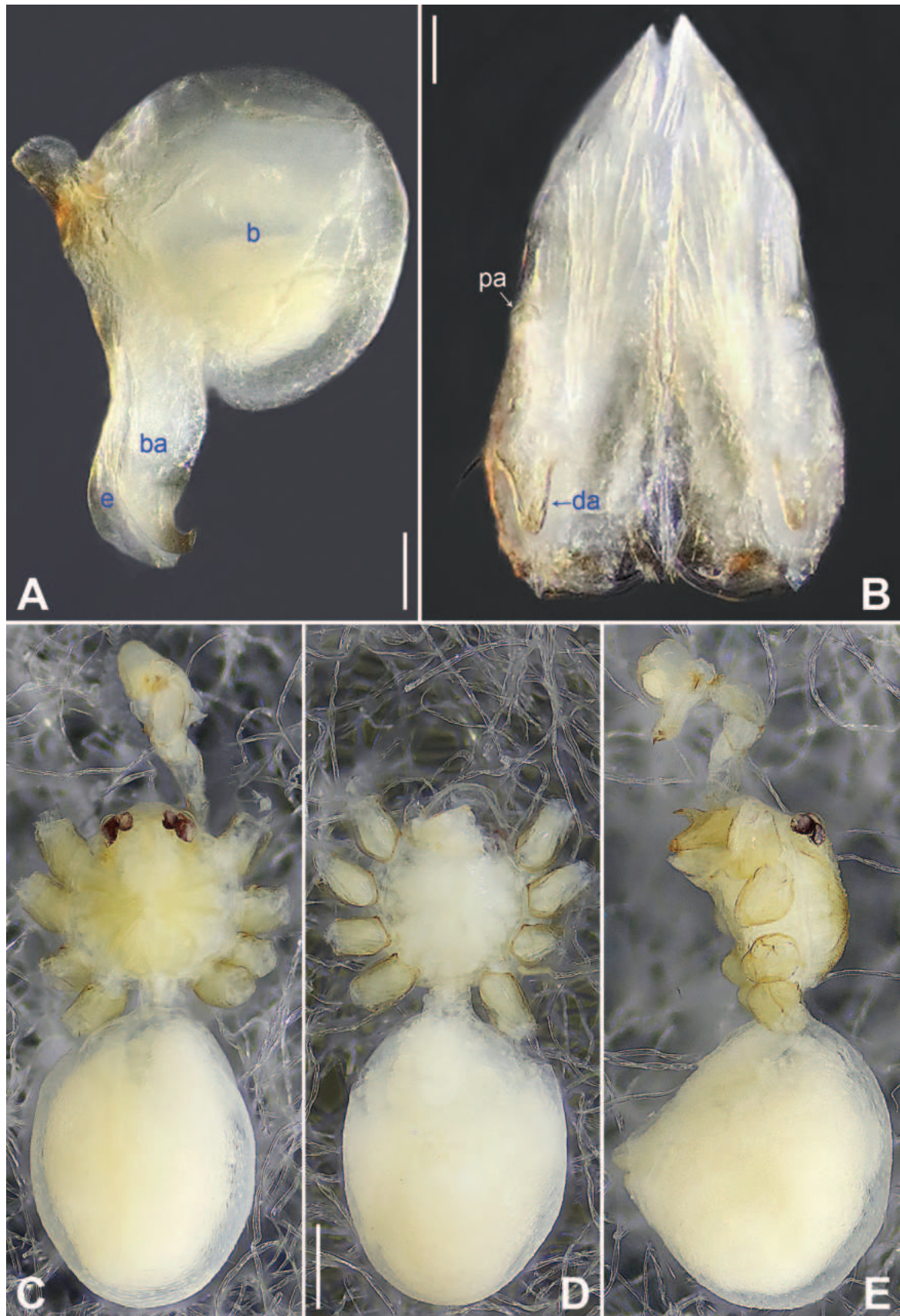


Figure 15. *Belisana yongsheng* sp. nov., holotype male **A** bulb, prolateral view **B** chelicerae, frontal view **C–E** habitus (**C** dorsal view **D** ventral view **E** lateral view). Abbreviations: b = bulb, ba = bulbal apophysis, da = distal apophysis, e = embolus, pa = proximo-lateral apophysis. Scale bars: 0.05 (**A**, **B**), 0.30 (**C–E**).

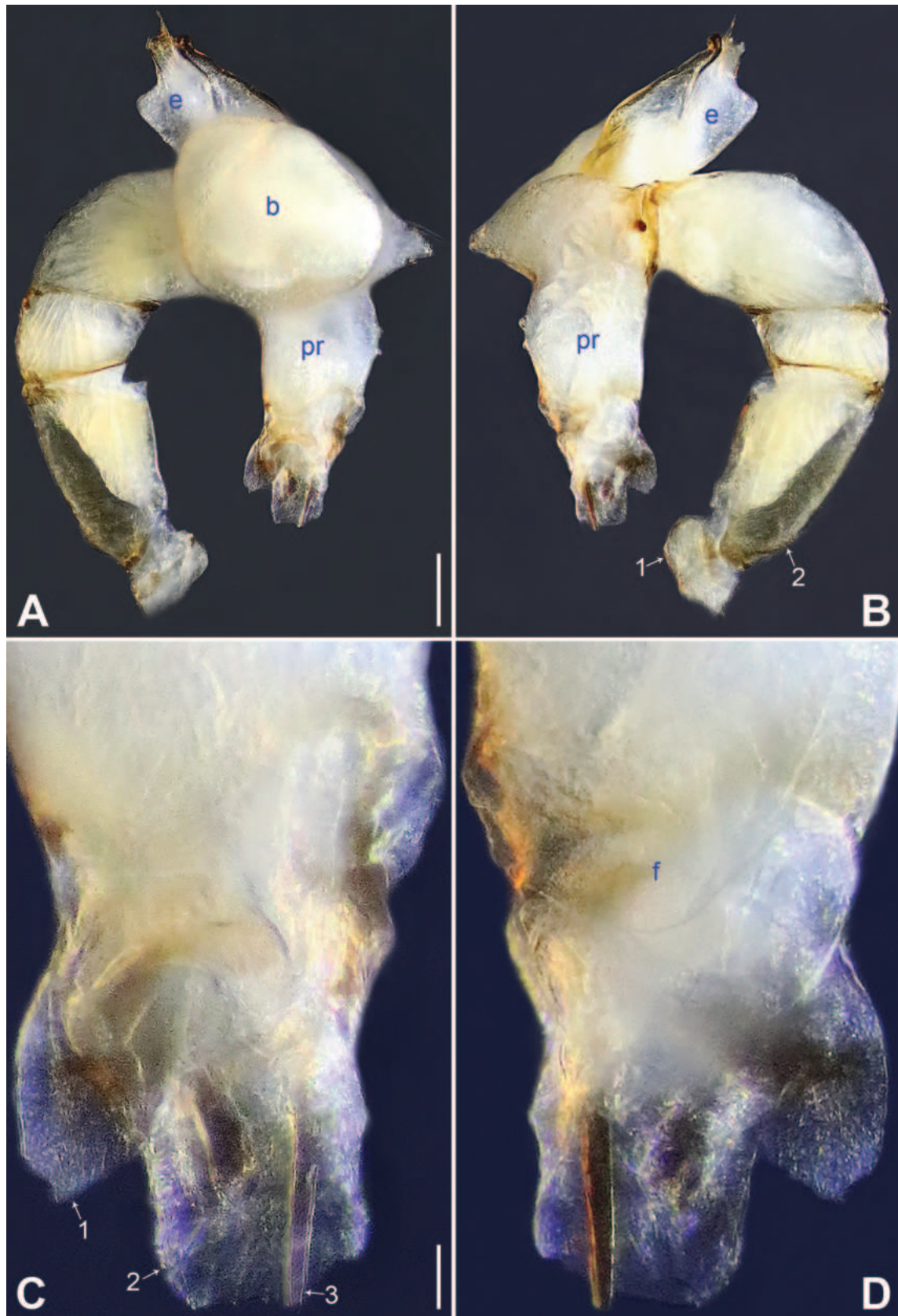


Figure 16. *Belisana yunnan* sp. nov., holotype male **A, B** palp (**A** prolateral view **B** retrolateral view, arrow 1 points at ventral apophysis, arrow 2 points at retrolatero-proximal protrusion) **C, D** distal part of procurus (**C** prolateral view, arrow 1 points at prolatero-ventral membranous lamella, arrow 2 points at distal membranous lamella, arrow 3 points at distal spine **D** retrolateral view). Abbreviations: b = bulb, e = embolus, f = flap, pr = procurus. Scale bars: 0.10 (**A, B**); 0.02 (**C, D**).

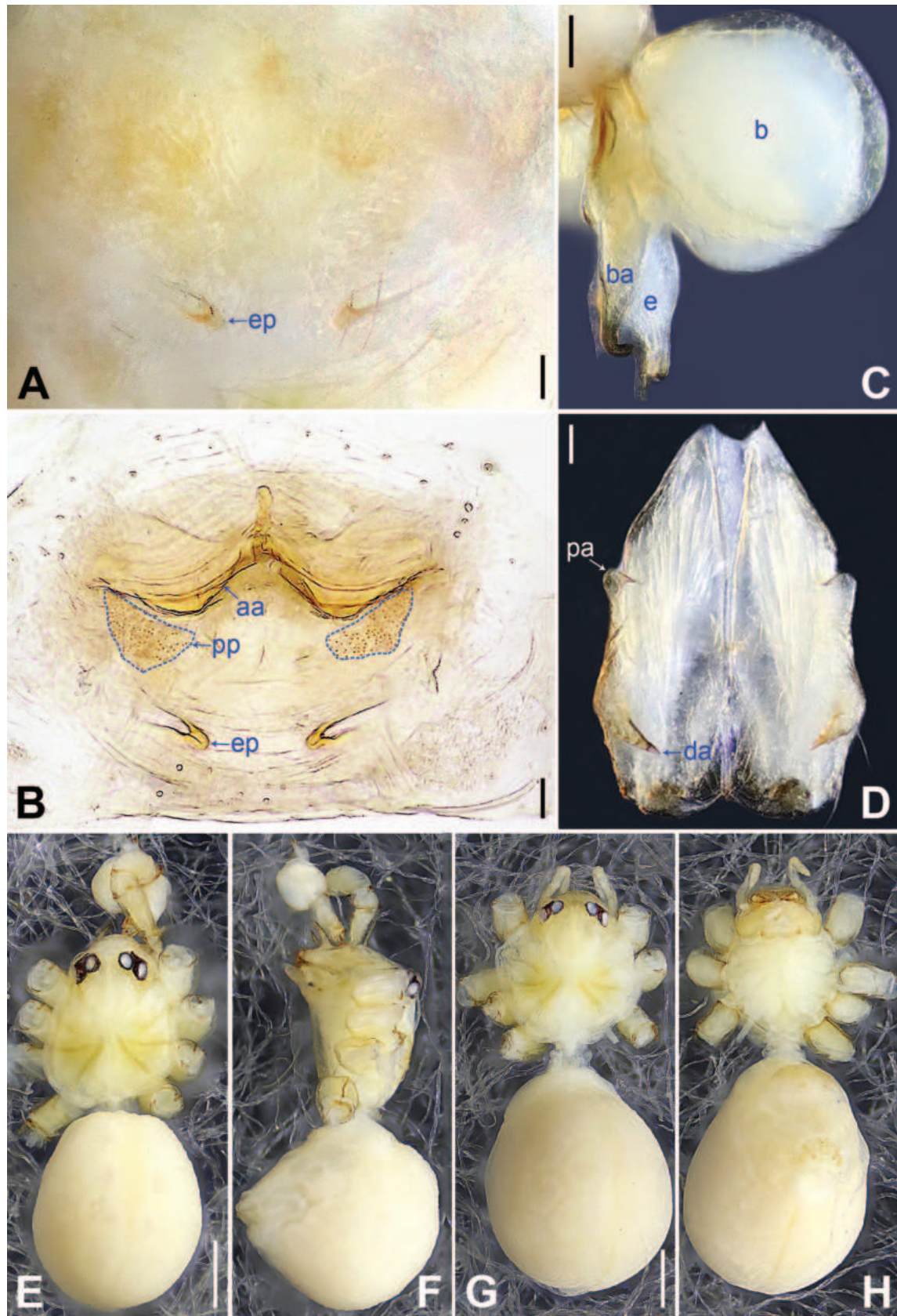


Figure 17. *Belisana yunnan* sp. nov., holotype male (C–F) and paratype female (A, B, G, H) A epigyne, ventral view B vulva, dorsal view C bulb, prolateral view D chelicerae, frontal view E–H habitus (E, G dorsal view F lateral view H ventral view). Abbreviations: aa = anterior arch, b = bulb, ba = bulbal apophysis, da = distal apophysis, e = embolus, ep = epigynal pocket, pa = proximo-lateral apophysis, pp = pore plate. Scale bars: 0.05 (A–D); 0.30 (E–H).

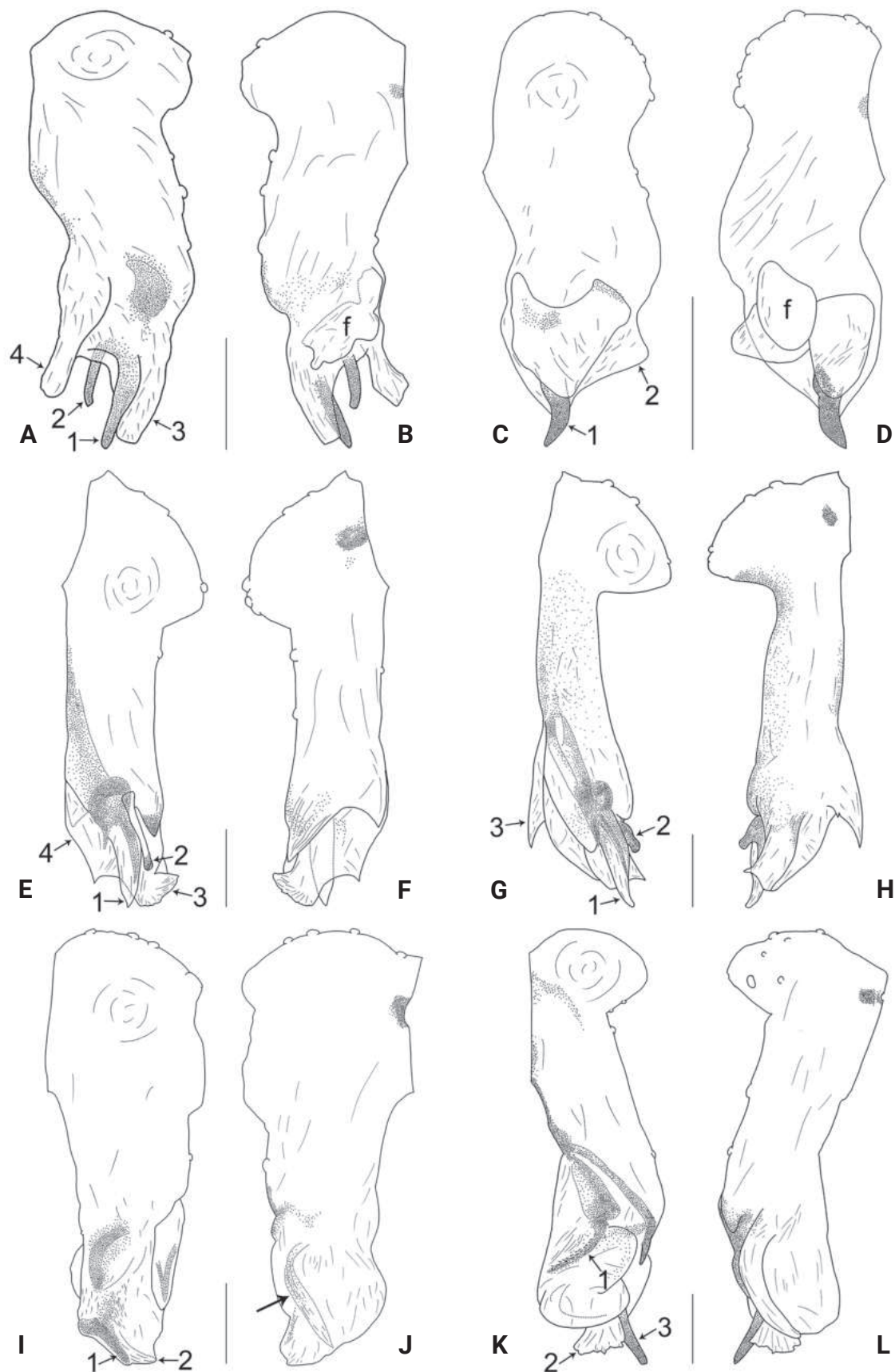


Figure 18. Procurus in prolateral and retrolateral views (arrows point at same structures as photos of each species) **A, B** *Belisana honghe* sp. nov. **C, D** *B. jiuxiang* sp. nov. **E, F** *B. lincang* sp. nov. **G, H** *B. luxi* sp. nov. **I, J** *B. tengchong* sp. nov. **K, L** *B. tongji* sp. nov. Abbreviation: f = flap. Scale bars: 0.10.

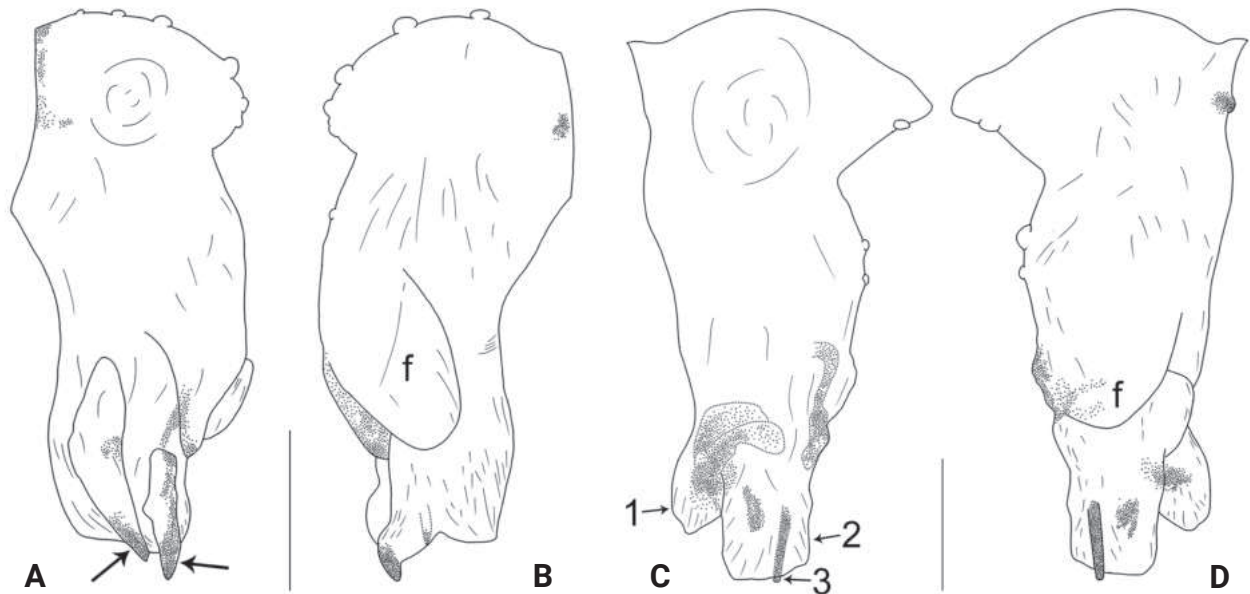


Figure 19. Procurus in prolateral and retrolateral views (arrows point at same structures as photos of each species) **A, B** *Belisana yongsheng* sp. nov. **C, D** *B. yunnan* sp. nov. Abbreviation: f = flap. Scale bars: 0.10.

Diagnosis. The new species resembles *B. yuhaoi* Yang & Yao, 2023 (Yang et al. 2023: 178, figs 2A, B, 3A–D, 4A–H) by having similar bulbal apophyses and epigyne (Figs 17A, C, 21E), but can be distinguished by differences in males: tips of cheliceral distal apophyses closer to each other (Fig. 17D vs widely separated), procurus without sclerotized dorso-subdistal apophysis (Figs 16C, 19C vs present) and with nearly half-round retrolateral flap (Figs 16D, 19D vs angular); differences in females: epigynal pockets closer to each other (Figs 17A, B, 21E, F vs widely separated), pore plates nearly isosceles triangle-shaped (Figs 17B, 21F vs scalene triangle-shaped).

Description. Male (holotype): Total length 1.90 (1.98 with clypeus), carapace 0.79 long, 0.71 wide, opisthosoma 1.11 long, 0.87 wide. Leg I: 18.71 (4.85, 0.56, 4.75, 7.05, 1.50), leg III: 9.35 (2.66, 0.30, 2.25, 3.25, 0.89), legs II and IV missing; tibia I L/d: 59. Eye inter-distances and diameters: PME–PME 0.11, PME 0.08, PME–ALE 0.03, AME absent. Sternum width/length: 0.63/0.60. Habitus as in Fig. 17E, F. Carapace yellowish, with brown radiating marks; sternum yellowish. Legs whitish, without darker rings. Opisthosoma yellowish, without spots. Thoracic furrow absent. Clypeus unmodified. Chelicerae (Fig. 17D) with a pair of proximo-lateral apophyses and a pair of curved distal apophyses (distance between tips: 0.19). Palp as in Fig. 16A, B; trochanter with ventral apophysis (as long as wide, arrow 1 in Fig. 16B); femur with tiny retrolatero-proximal protrusion (arrow 2 in Fig. 16B); procurus simple proximally but complex distally, with prolatero-ventral membranous lamella (arrow 1 in Figs 16C, 19C) bearing median sclerotized part, distal membranous lamella (arrow 2 in Figs 16C, 19C) bearing median sclerotized part, distal spine (arrow 3 in Figs 16C, 19C), and nearly half-round retrolateral flap (Figs 16D, 19D); bulb (Fig. 17C) with hooked apophysis and simple embolus. Retrolateral trichobothria on tibia I at 14% proximally; legs with short vertical setae on metatarsi; tarsus I with 21 distinct pseudosegments.

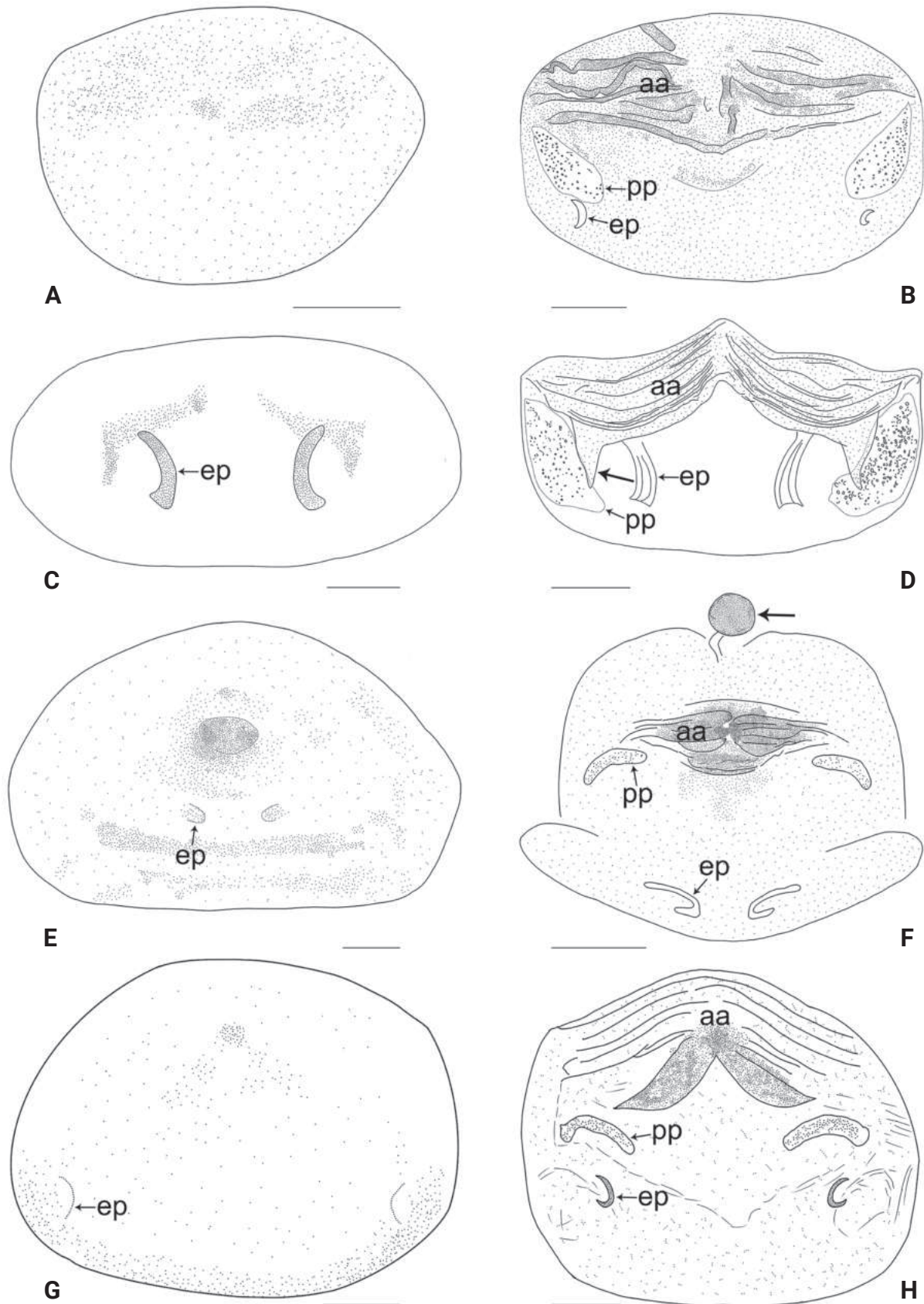


Figure 20. Female genitalia in ventral and dorsal views **A, B** *Belisana honghe* sp. nov. **C, D** *B. jiuxiang* sp. nov., arrow points at lateral sclerite **E, F** *B. lincang* sp. nov., arrow points at sac-like structure **G, H** *B. luxi* sp. nov. Abbreviations: aa = anterior arch, ep = epigynal pocket, pp = pore plate. Scale bars: 0.10.

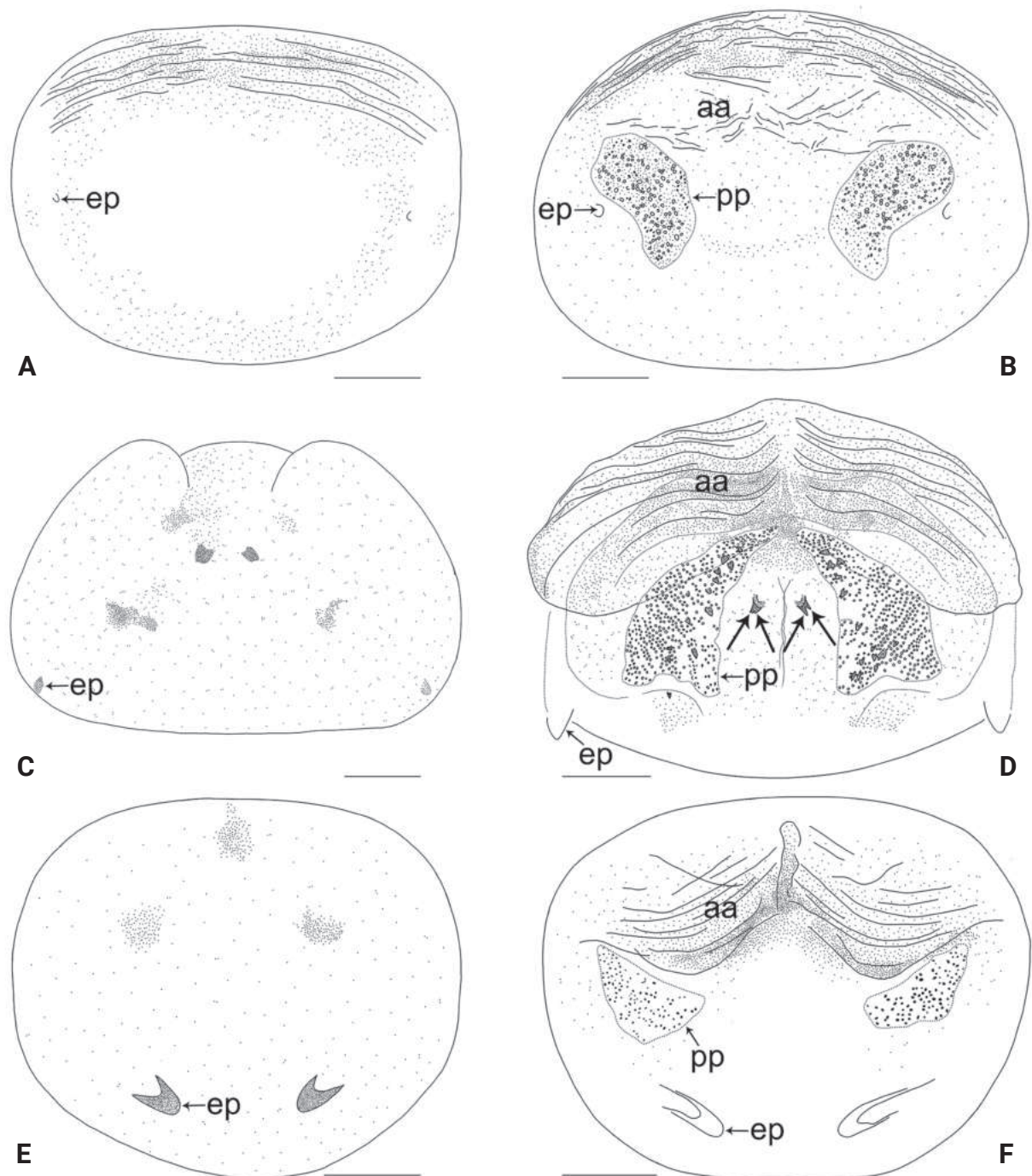


Figure 21. Female genitalia in ventral and dorsal views **A, B** *Belisana tengchong* sp. nov. **C, D** *B. tongi* sp. nov., arrows point at four distinct median teeth **E, F** *B. yunnan* sp. nov. Abbreviations: aa = anterior arch, ep = epigynal pocket, pp = pore plate. Scale bars: 0.10.

Female (paratype, IZCAS-Ar44984): Similar to male, habitus as in Fig. 17G, H. Total length 2.14 (2.20 with clypeus), carapace 0.78 long, 0.77 wide, opisthosoma 1.36 long, 1.00 wide; tibia I: 3.88; tibia I L/d: 52. Eye inter-distances and diameters: PME–PME 0.13, PME 0.07, PME–ALE 0.02. Sternum width/length: 0.62/0.56. Epigyne (Figs 17A, 21E) simple and flat, anteriorly slightly sclerotized, with a pair of postero-median pockets 0.12 apart. Vulva (Figs 17B, 21F) with ridge-shaped anterior arch and a pair of nearly triangular pore plates.

Variation. Tibia I in two male paratypes (IZCAS-Ar44982–83): 5.38, 6.73. Tibia I in the other two female paratypes (IZCAS-Ar44985–86): 3.72, 3.85.

Habitat. The species was found in the dark zone inside the cave.

Distribution. China (Yunnan, type locality; Fig. 1).

Discussion

Altogether, including the eight species described in this paper, there are now 70 species of *Belisana* in China, representing 45% of the global total of the genus. Within China, 31 species (44%) were found in Yunnan. Table 1 shows that within Yunnan, the species count from Xishuangbanna (19 species) far outstrips those of the Hengduan Mountains (six species) and Yunnan-Guizhou Plateau (six species), both of which are geographically larger in area than the Xishuangbanna (Fig. 1). It is easy to speculate on the reasons for the apparent disparity among the three datasets: field collections in Xishuangbanna have been more frequent than in the Hengduan Mountains and the Yunnan-Guizhou Plateau. Although we do not have hard figures in terms of man-hours, it is our general impression that more intensive efforts have been expended in collecting spiders in Xishuangbanna than in the two other localities, partly because fogging was carried out in Xishuangbanna and not elsewhere. In fact, among the 19 species from Xishuangbanna, seven species were collected by fogging. In conclusion, it should not be unreasonable to hypothesize that more new species of *Belisana* may be discovered in the Hengduan Mountains and Yunnan-Guizhou Plateau when a more concerted effort is made to collect from both areas, which differ from Xishuangbanna by their subtropical climate, larger geographic expanse, and by a higher prevalence of karst landforms.

Acknowledgments

The manuscript benefited greatly from comments by Francesco Ballarin, Kadir B Kunt, and Mikhail M Omelko. We thank Joseph KH Koh for his suggestions and language editing.

Additional information

Conflict of interest

The authors have declared that no competing interests exist.

Ethical statement

No ethical statement was reported.

Funding

This study is supported by the Science & Technology Fundamental Resources Investigation Program of China (2023FY100200) and the National Natural Science Foundation of China (NSFC-32170461, 31872193).

Author contributions

ZY and SL designed the study. ZY, SL, and LZ performed morphological species identification. LZ and ZW finished the descriptions and took the photos and drawings. ZY, SL, and LZ drafted and revised the manuscript.

Author ORCIDs

Ludan Zhang  <https://orcid.org/0000-0001-5657-751X>

Shuqiang Li  <https://orcid.org/0000-0002-3290-5416>

Zhiyuan Yao  <https://orcid.org/0000-0002-1631-0949>

Data availability

All of the data that support the findings of this study are available in the main text.

References

- Huber BA (2005) High species diversity, male-female coevolution, and metaphyly in Southeast Asian pholcid spiders: The case of *Belisana* Thorell 1898 (Araneae, Pholcidae). *Zoologica* 155: 1–126.
- Khmelik VV, Kozub D, Glazunov A (2005) Helicon Focus 3.10.3. <https://www.heliconsoft.com/heliconsoft-products/helicon-focus/> [Accessed 27 January 2024]
- WSC (2024) World Spider Catalog, Version 25.0. Natural History Museum Bern. <https://wsc.nmbe.ch> [Accessed 22 April 2024]
- Yang L, Zhao F, He Q, Yao Z (2023) A survey of pholcid spiders (Araneae, Pholcidae) from Guiyang, Guizhou Province, China. *ZooKeys* 1186: 175–184. <https://doi.org/10.3897/zookeys.1186.105736>
- Yao Z, Li S (2013) New and little known pholcid spiders (Araneae: Pholcidae) from Laos. *Zootaxa* 3709(1): 1–51. <https://doi.org/10.11646/zootaxa.3709.1.1>
- Yao Z, Tavano M, Li S (2013) Notes on four pholcid spiders (Araneae: Pholcidae) described by T. Thorell from Southeast Asia. *Zootaxa* 3609(3): 302–310. <https://doi.org/10.11646/zootaxa.3609.3.4>
- Yao Z, Pham DS, Li S (2015) Pholcid spiders (Araneae: Pholcidae) from northern Vietnam, with descriptions of nineteen new species. *Zootaxa* 3909(1): 1–82. <https://doi.org/10.11646/zootaxa.3909.1.1>
- Yao Z, Zhu K, Du Z, Li S (2018) The *Belisana* spiders (Araneae: Pholcidae) from Xishuangbanna Tropical Botanical Garden, Yunnan, China. *Zootaxa* 4425(2): 243–262. <https://doi.org/10.11646/zootaxa.4425.2.3>
- Zhang F, Peng Y (2011) Eleven new species of the genus *Belisana* Thorell (Araneae: Pholcidae) from south China. *Zootaxa* 2989(1): 51–68. <https://doi.org/10.11646/zootaxa.2989.1.2>
- Zhao F, Yang L, Li S, Zheng G, Yao Z (2023) A further study on the *Belisana* spiders (Araneae: Pholcidae) from Xishuangbanna, Yunnan, China. *Zootaxa* 5351(5): 543–558. <https://doi.org/10.11646/zootaxa.5351.5.3>
- Zhu W, Yao Z, Zheng G, Li S (2020a) Six new species of the spider genus *Belisana* Thorell, 1898 (Araneae: Pholcidae) from southern China. *Zootaxa* 4810(1): 175–197. <https://doi.org/10.11646/zootaxa.4810.1.12>
- Zhu W, Yao Z, Zheng G, Li S (2020b) The *Belisana* spiders (Araneae: Pholcidae) from Tibet, China. *Zootaxa* 4802(1): 111–128. <https://doi.org/10.11646/zootaxa.4802.1.7>

Description of three new species of the spider genus *Pseudopoda* Jäger, 2000 (Araneae, Sparassidae) from China, Laos and Thailand, and the female of *P. kavanaughii* Zhang, Jäger & Liu, 2023

Yanrong Wu¹, Rui Zhong², Yang Zhu¹, Peter Jäger³, Jie Liu^{1,4}, He Zhang¹

¹ Hubei Key Laboratory of Regional Development and Environmental Response, Faculty of Resources and Environmental Science, Hubei University, Wuhan 430062, Hubei, China

² The State Key Laboratory of Biocatalysis and Enzyme Engineering of China, College of Life Science, Hubei University, Wuhan 430062, Hubei, China

³ Arachnology, Senckenberg Research Institute, Mertonstraße 17–21, 60325 Frankfurt am Main, Germany

⁴ School of Nuclear Technology and Chemistry & Biology, Hubei University of Science and Technology, Xianning 437100, Hubei, China

Corresponding author: He Zhang (hancyhappy@aliyun.com)

Abstract

With 252 species, *Pseudopoda* Jäger, 2000, is the largest genus in the family Sparassidae and is widely distributed in South (49 species in Bhutan, India, Nepal and Pakistan), East (158 species in China and Japan) and Southeast Asia (51 species in Indonesia, Laos, Myanmar, Thailand and Vietnam). Few species have been found in more than one region. In this paper, three new species of *Pseudopoda* are described from East and Southeast Asia. Among them, one from China: *P. fengtongzhaiensis* Jäger & Liu, **sp. nov.** (♀); one from Laos: *P. baimai* Jäger & Liu, **sp. nov.** (♀); and one from Thailand: *P. inthanonensis* Jäger & Liu, **sp. nov.** (♀). Additionally, the female of *P. kavanaughii* Zhang, Jäger & Liu, 2023 is described for the first time. Photos of the habitus and genitalia, as well as a distribution map of all four species, are provided.

Key words: Heteropodinae, high diversity, Huntsman spiders, taxonomy



Academic editor: Peter Michalik
Received: 20 November 2023
Accepted: 11 April 2024
Published: 27 May 2024

ZooBank: <https://zoobank.org/678BC18A-02A5-4264-BB5C-5A140B4DEABB>

Citation: Wu Y, Zhong R, Zhu Y, Jäger P, Liu J, Zhang H (2024) Description of three new species of the spider genus *Pseudopoda* Jäger, 2000 (Araneae, Sparassidae) from China, Laos and Thailand, and the female of *P. kavanaughii* Zhang, Jäger & Liu, 2023. ZooKeys 1202: 287–301. <https://doi.org/10.3897/zookeys.1202.116007>

Copyright: © Yanrong Wu et al.
This is an open access article distributed under terms of the Creative Commons Attribution License (Attribution 4.0 International – CC BY 4.0).

Introduction

The spider genus *Pseudopoda*, established by Jäger (2000) with *Pseudopoda prompta* (O. Pickard-Cambridge, 1885) as the type species, has a broad distribution across South, East and Southeast Asia. Up to now, 252 species have been reported (World Spider Catalog 2024), with their habitats spanning elevations from 17 m (e.g., *P. spirembolus* Jäger & Ono, 2002) (Jäger and Ono 2002) to 3847 m (e.g., *P. nyingchiensis* Zhao & Li, 2018) (Jiang et al. 2018) above sea level. These spiders inhabit a variety of environments, including foliage, leaf litter, rock crevices, caves, grasslands, under tree bark and stones or synanthropic environments. Most species of this genus typically have a limited distribution range, but at the same time, the genus has a high local diversity (Jiang et al. 2018). Researchers speculate that the actual number of *Pseudopoda* species may far exceed those formally described, hinting at the genus's rich yet partially uncovered biodiversity (Cao et al. 2016; Jiang et al. 2018; Zhang et al. 2023).

To date, nine species groups have been established, primarily based on morphological and molecular characteristics (*daliensis*-group, *interposita*-group, and *signata*-group) or solely on morphological features (*diversipunctata*-group, *latembola*-group, *martensi*-group, *parvipunctata*-group, *prompta*-group, and *schwendingeri*-group) (Jäger 2001; Zhang et al. 2017, 2019; Li et al. 2019). Among these, the *schwendingeri*-group was based only on male characteristics.

One of the notable challenges in studying *Pseudopoda* spiders is the difficulty in collecting mature pairs from the field, leading to many species being described only based on one sex. Currently, more than half of the known species (130) have been documented in this manner. In the course of our research, we have identified three new species from Asia: *P. baimai* Jäger & Liu, sp. nov., *P. fengtongzhaiensis* Jäger & Liu, sp. nov., and *P. inthanonensis* Jäger & Liu, sp. nov. However, only female specimens of these species have been reported. Additionally, during examination of material collected from Kongdang Village, Yunnan Province, China, we found the female of *P. kavanaughi* Zhang, Jäger & Liu, 2023 (Zhang et al. 2023), enabling us to describe the female for the first time in this paper. This study enriches our knowledge of the diversity of the genus *Pseudopoda*.

Material and methods

All specimens were kept in 75% ethanol and examined with an Olympus SZX16 stereomicroscope; details were further investigated with an Olympus BX51 compound microscope. Colouration is described in all species from specimens in ethanol. Copulatory organs were examined and illustrated after dissection from the spider bodies; epigynes were cleared with Proteinase K. Habitus photos were obtained with a Leica DMC4500 digital camera attached to a Leica M205 C digital microscope. Coordinates are given in square brackets when retrieved secondarily from Google Earth. A molecular sample ID and collection acronym is given in brackets.

Leg measurements are shown as total length (femur, patella, tibia, metatarsus, tarsus). The number of spines is listed for each segment in the following order: prolateral, dorsal, retrolateral, ventral (in femora and patellae ventral spines are absent and fourth digit is omitted in the spination formula). The terminology used in text and figure legends follows Jäger (2007). All measurements are given in millimetres.

All specimens treated in the present paper were compared with individuals of described species within a certain distribution range to avoid describing synonyms (e.g., *P. nankunensis* Zhang, Jäger & Liu, 2023 in Zhang et al. 2023).

Abbreviations used in text and figures: **AB**, anterior bands; **ALE**, anterior lateral eyes; **AME**, anterior median eyes; **CH**, clypeus height; **CO**, copulatory opening; **DS**, dorsal shield of prosoma; **EF**, epigynal field; **FD**, fertilization duct; **Fe**, femur; **FW**, first winding; **IDS**, internal duct system; **LL**, lateral lobes; **Mt**, metatarsus; **OS**, Opisthosoma; **Pa**, patella; **PLE**, posterior lateral eyes; **PME**, posterior median eyes; **Pp**, palp; **S**, spermathecae; **Ti**, tibia; **I, II, III, IV**, legs I to IV.

Collections (with curators): **CAS**, California Academy of Science, San Francisco, California, USA (L. Esposito); **CBEE**, Centre for Behavioural Ecology and Evolution, College of Life Sciences, Hubei University, Wuhan, China (J. Liu); **MHNG**, Muséum d'Histoire Naturelle, Geneve, Switzerland (P.J. Schwendinger); **SMF**, Senckenberg Research Institute, Frankfurt, Germany (P. Jäger).

Results

Taxonomy

Family Sparassidae Bertkau, 1872

Subfamily Heteropodinae Thorell, 1873

Genus *Pseudopoda* Jäger, 2000

Type species. *Sarotes promptus* O. Pickard-Cambridge, 1885.

Diagnosis. Small to large Heteropodinae. Species can be diagnosed by: 1) conductor membranous (some species reduced or entirely absent); 2) embolus broadened and flattened (at least in its proximal part); 3) retrolateral tibial apophysis arising proximally or mesially from the tibia; 4) lateral lobes of epigyne distinctly extend beyond the epigastric furrow, covering the median septum in most species; 5) first winding membranous, with bent margins in most species; and 6) first winding or first winding and lateral lobes covering the internal duct system in dorsal view (modified from Jäger 2000, Jiang et al. 2018 and Zhang et al. 2023).

***Pseudopoda baimai* Jäger & Liu, sp. nov.**

<https://zoobank.org/A0DC4815-BE5C-48D8-B349-524C54B51117>

Figs 1, 2, 9

Type material. Holotype female: LAOS, Vientiane Province: Vang Vieng, W of Nam Song, Tham Nam Or Kjem, in cave, 18°55'46.86"N, 102°20'56.82"E, 324 m, 28 July 2016, by hand, by day. P. Jäger leg. (SMF, LAO0008). **Paratype:** 1 female, with same data as for holotype (SMF, LAO0008).

Etymology. The specific name is derived from the Laos word baimai (ໂບໂມ້), meaning foliage and referring to the fact that the holotype female was collected on foliage of a secondary forest; noun in apposition.

Diagnosis. The female of *P. baimai* Jäger & Liu, sp. nov. resembles *P. gongschana* Jäger & Vedel, 2007 (Jäger and Vedel 2007) by: 1) IDS visible through cuticle in ventral view as large circular patches in centre of LL; and 2) posterior margins of LL with median indentation. It can be recognised by: 1) S largely covered by LL in dorsal view; and 2) anterior margins of LL straight, almost "V"-shaped in ventral view, their lateral ends with a bend, laterad (covered by FW, anterior margins distinctly convex, their lateral ends latero-posteriad in *P. gongschana*).

Female (LAO0008): **Measurements:** Medium sized. Body length 11.3, DS length 4.6, width 4.0, OS length 6.7, width 3.8. **Eyes:** AME 0.12, ALE 0.26, PME 0.22, PLE 0.24, AME–AME 0.16, AME–ALE 0.08, PME–PME 0.28, PME–PLE 0.35, AME–PME 0.33, ALE–PLE 0.30, CH AME 0.40, CH ALE 0.34. **Spination:** Pp 131, 101, 2121, 1014; Fe I–III 323, IV 331; Pa I–III 001, IV 000; Ti I–II 2226, III–IV 2026; Mt I–II 2024, III 3024, IV 3036. **Measurements of palps and legs:** Pp 7.1 (2.0, 1.0, 1.6, –, 2.5); I 25.9 (7.7, 2.1, 7.4, 7.0, 1.7); II 28.7 (8.2, 2.5, 8.4, 7.4, 2.2); III 22.2 (6.3, 1.9, 6.8, 5.9, 1.3); IV 24.4 (7.9, 1.2, 7.0, 7.3, 2.0). Leg formula: II-I-IV-III. Promargin of chelicerae with three teeth, retromargin with four teeth, cheliceral furrow with c. 33 denticles.

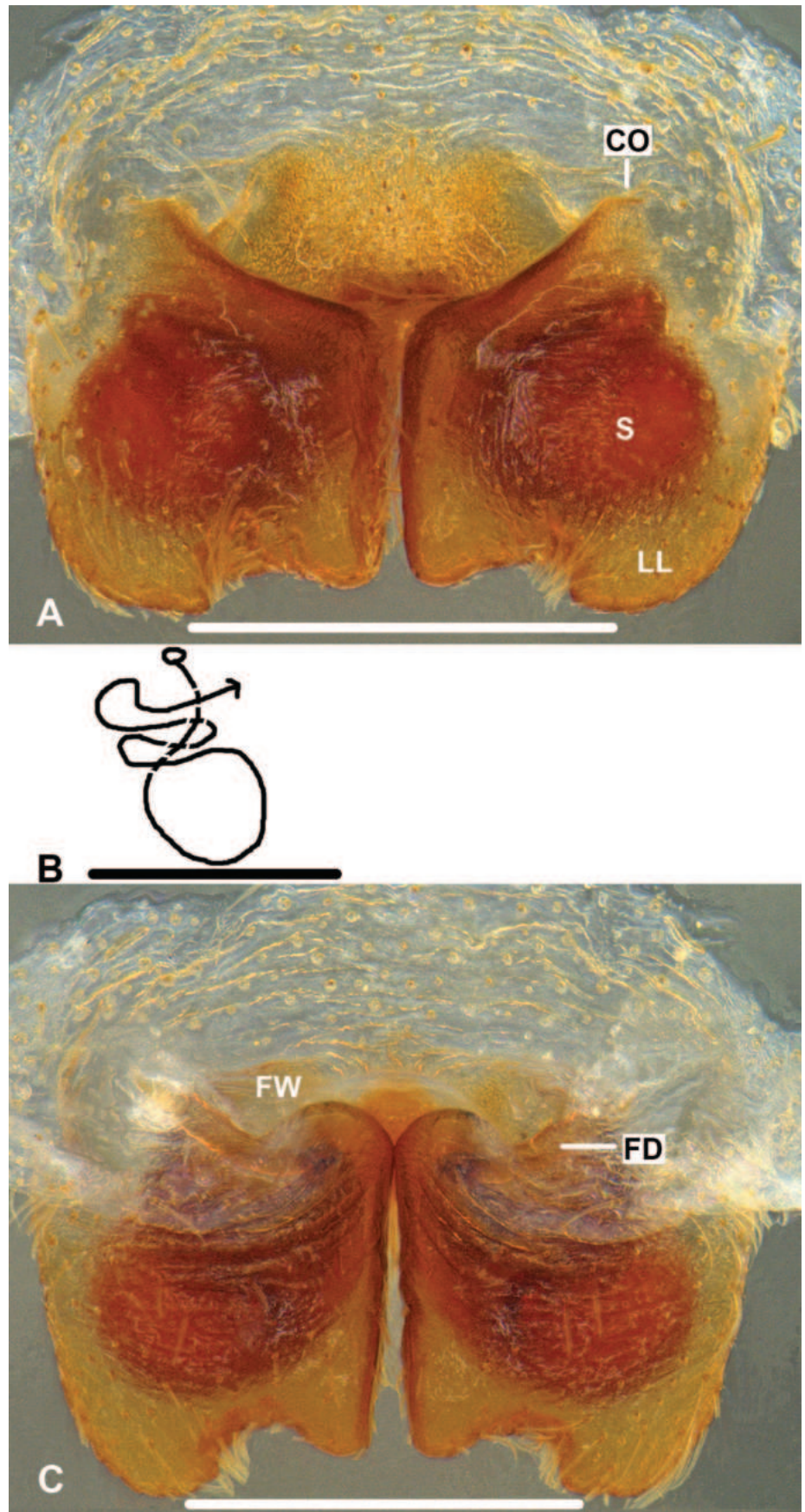


Figure 1. *Pseudopoda baimai* Jäger & Liu, sp. nov., holotype, female **A** epigyne, ventral **B** schematic course of IDS, dorsal **C** vulva, dorsal. Scale bars: 0.5 mm.

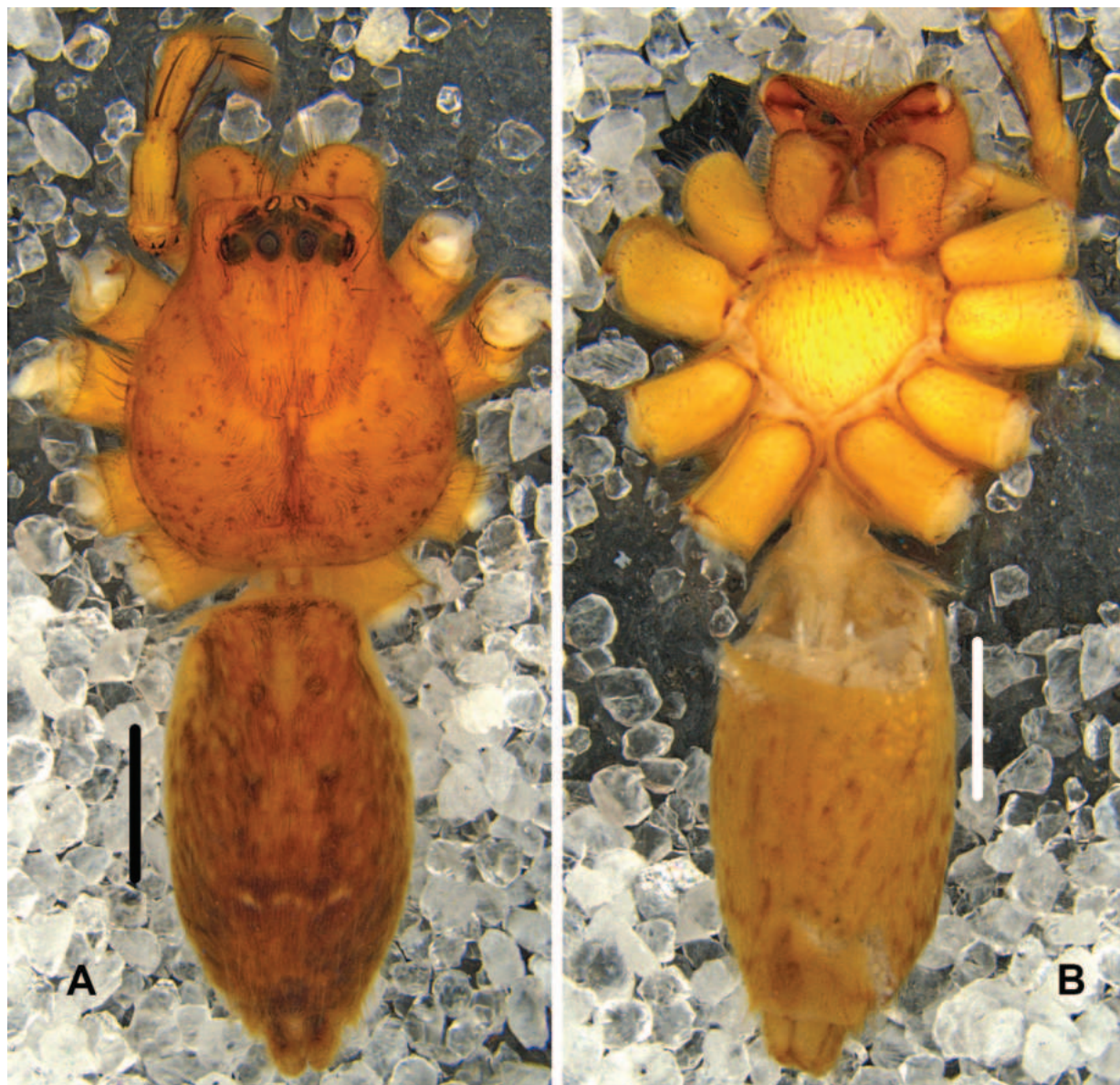


Figure 2. *Pseudopoda baimai* Jäger & Liu, sp. nov., female habitus (A dorsal B ventral). Scale bars: 2 mm.

Epigyne (Fig. 1A–C): As in diagnosis. EF wider than long, without AB. Posterior margins of LL irregularly rounded. S oval-shaped, occupying most part of LL in ventral view. Most parts of FW covered by LL in dorsal view.

Colouration (Fig. 2A, B): DS yellow with dark spots. Fovea distinct. Margin with dark marks. OS dorsally yellowish brown with two light yellow regions at posterior part, ventrally light yellow, with several brown marks, irregularly arranged.

Male: Unknown.

Variation. Female ($N = 1$): body length 12.7, DS length 5.3, OS length 7.4.

Remarks. This species might potentially be conspecific with *P. caudata* Zhang, Jäger & Liu, 2023 (Zhang et al. 2023), given that the two habitats are only about 100 kilometres apart. However, there are subtle differences in coloration and patterns on the dorsal side of the females compared to the males of *P. caudata*, indicating a possible distinction between the two species. Further research and future findings are needed to conclusively resolve this ambiguity.

Distribution. Laos (Vientiane Province) (Fig. 9).

***Pseudopoda fengtongzhaiensis* Jäger & Liu, sp. nov.**

<https://zoobank.org/FE214929-DE51-4FDC-9314-6150FAE50863>

Figs 3, 4, 9

Type material. *Holotype* female: CHINA, Sichuan Province: Ya'an City, Baoxing County, Fengtongzhai National Nature Reserve, 30°34'17"N, 102°52'58"E, 1604 m, 5 May 2016, Y. Zhong leg. (CBEE, LJ2215). **Paratypes:** 3 females, with same data as for holotype (CBEE, LJ2216–LJ2218).

Etymology. The specific name is derived from the type locality, the Fengtongzhai National Nature Reserve; adjective.

Diagnosis. The female of *P. fengtongzhaiensis* Jäger & Liu, sp. nov. is similar to that of *P. emei* Zhang, Zhang & Zhang, 2013 (Zhang et al. 2013) by: 1) LL large, and the length of the lateral margin of LL almost equal to that of median margin in ventral view; and 2) FW well developed. It can be distinguished by: 1) S with a distinct turning in ventral view; and 2) posterior margins of LL rounded and smooth in ventral view (S simple and close to anterior margins of LL, posterior margins of LL with distinct posterior incisions in *P. emei*).

Female (LJ2215): **Measurements:** Medium sized. Body length 15.8, DS length 7.8, width 6.5, OS length 8.0, width 4.9. Eyes: AME 0.22, ALE 0.37, PME 0.24, PLE 0.31, AME–AME 0.13, AME–ALE 0.07, PME–PME 0.18, PME–PLE 0.44, AME–PME 0.27, ALE–PLE 0.23, CH AME 0.38, CH ALE 0.25. **Spination:** Pp 131, 101, 2121, 1014; Fe I–II 323, III–IV 322; Pa I–III 101, IV 100; Ti I 1016, II–IV 2026; Mt I–II 2024, III 3025, IV 3036. **Measurement of palps and legs:** Pp 8.8 (2.5, 1.2, 1.9, –, 3.2); I 25.3 (7.6, 2.3, 7.4, 6.2, 1.8), II 27.9 (8.0, 2.9, 8.3, 6.6, 2.1), III 20.4 (6.8, 1.6, 5.6, 4.9, 1.5), IV 24.7 (7.8, 1.7, 6.8, 6.4, 2.0). Leg formula: II-I-IV-III. Promargin of chelicerae as in *P. baimai* Jäger & Liu, sp. nov., cheliceral furrow with c. 24 denticles.

Epigyne (Fig. 3A–C): As in diagnosis. EF wider than long, with distinct AB. Anterior margins of LL distinctly curved and forming a broad V-shaped, and resembling a heart, in ventral view. FW of IDS well developed, covering entire S, large parts of FW covered by LL in dorsal view. FD long and narrow, suited medially.

Colouration (Fig. 4A, B): DS reddish-brown with dark spots, margin with distinct marks. Fovea and striae distinctly marked and with a few dark dots. OS dorsally dark brown, with lots of yellow and small dots, and several big dots in anterior part, with a transversal yellow line in posterior part. OS ventrally brown, margins with dark hairs, with a yellow region in middle part.

Male: Unknown.

Variation. Females ($N = 3$): body length 15.1–16.3, DS length 7.1–8.0, OS length 8.0–8.3.

Remarks. This species may potentially be conspecific with *P. acutiformis* Zhang, Jäger & Liu, 2023 (Zhang et al. 2023), as they share the same habitat. However, there are notable differences in the coloration and patterns on the dorsal side of the females compared to the males of *P. acutiformis*, suggesting they might be distinct species. Additionally, another species, *P. flexa* Zhang, Jäger & Liu, 2023 (Zhang et al. 2023), is also located in this Reserve. Resolution of these ambiguities will depend on future research and findings.

Distribution. China (Sichuan Province) (Fig. 9).

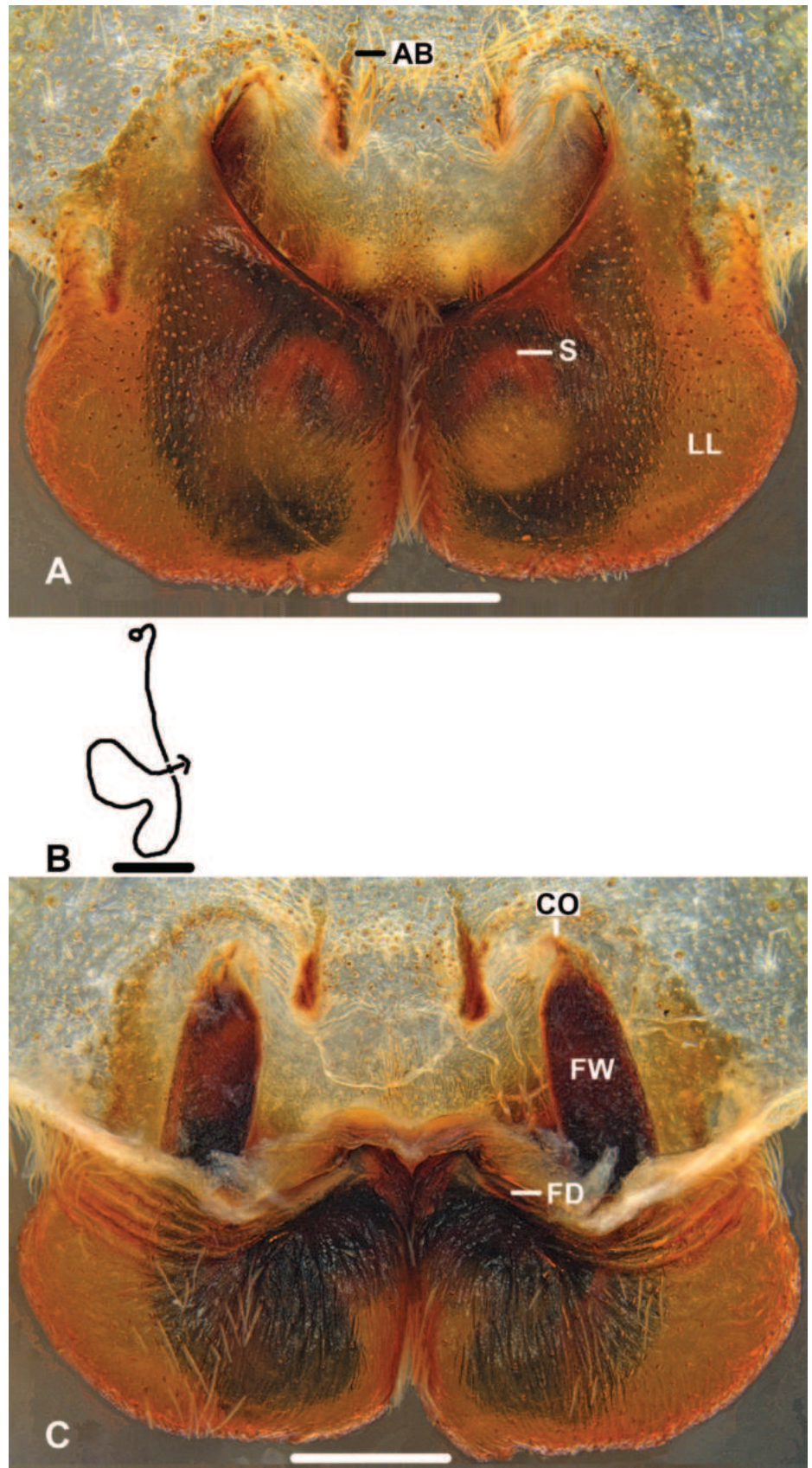


Figure 3. *Pseudopoda fengtongzhaiensis* Jäger & Liu, sp. nov., holotype, female **A** epigyne, ventral **B** schematic course of IDS, dorsal **C** vulva, dorsal. Scale bars: 0.5 mm.



Figure 4. *Pseudopoda fengtongzhaiensis* Jäger & Liu, sp. nov., female habitus (A dorsal B ventral). Scale bars: 2 mm.

***Pseudopoda inthanonensis* Jäger & Liu, sp. nov.**

<https://zoobank.org/E105C872-E060-4202-AA79-6C5DB6EAC7E4>

Figs 5, 6, 9

Type material. *Holotype* female: THAILAND, Chiang Mai Province: Doi Inthanon National Park, [18°35'24"N, 98°28'48"E], 1680 m, 24 October 2002, P. Dankittipakul leg. (MHNG, THI0068).

Etymology. The specific name is derived from the type locality, the Doi Inthanon National Park; adjective.

Diagnosis. The female of *P. inthanonensis* Jäger & Liu, sp. nov. can be distinguished from those of all other *Pseudopoda* species by the posterior margins of LL with a distinct inverted V-shaped indentation at the middle part.

Female (THI0068): Measurements: Medium sized. Body length 12.7, DS length 4.9, width 4.2, OS length 7.8, width 4.5. Eyes: AME 0.24, ALE 0.34, PME 0.27, PLE 0.32, AME–AME 0.19, AME–ALE 0.09, PME–PME 0.21, PME–PLE 0.38, AME–PME 0.30, ALE–PLE 0.26, CH AME 0.36, CH ALE 0.27. **Spination:** Pp 131, 001, 2121, 1004; Fe I–II 323, III 322, IV 331; Pa I–IV 101; Ti I–IV 2026; Mt I–II 2024, III 3024, IV 3036. **Measurement of palps and legs:** Pp 7.8 (2.3, 1.8, 1.0, –, 2.7); I 23.8 (7.0, 2.3, 6.9, 6.1, 1.5), II 28.4 (8.1, 2.5, 8.4, 7.3, 2.1), III 18.4 (6.0, 1.5, 5.1, 4.7, 1.1), IV 24.3 (7.3, 1.8, 6.3, 6.9, 2.0). Leg formula: II-IV-I-III. Promargin of chelicerae as in *P. baimai* Jäger & Liu, sp. nov., cheliceral furrow with c. 27 denticles.

Epigyne (Fig. 5A–C): As in diagnosis. EF wider than long, AB long, but indistinct. LL narrow, with anterior margins slightly curved. S oval-shaped in ventral view, covered by FW and posterior part of LL in dorsal view. FD long, suited medially.

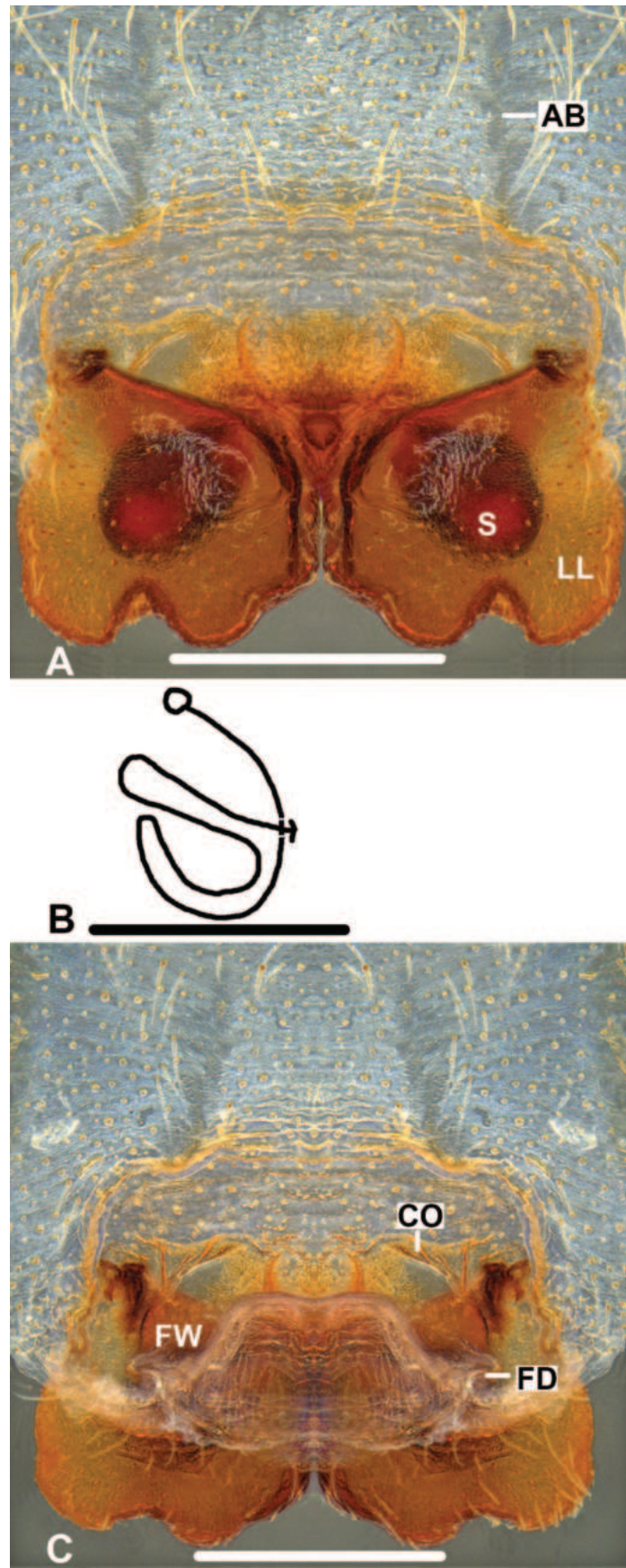


Figure 5. *Pseudopoda inthanonensis* Jäger & Liu, sp. nov., holotype, female **A** epigyne, ventral **B** schematic course of IDS, dorsal **C** vulva, dorsal. Scale bars: 0.5 mm.



Figure 6. *Pseudopoda inthanonensis* Jäger & Liu, sp. nov., female habitus (A dorsal B ventral). Scale bars: 2 mm.

Colouration (Fig. 6A, B): DS reddish-brown with dark spots. Margins with dash dark dots. Fovea and striae distinctly marked. OS dorsally brown, with several dots at anterior part, with two round patches at the posterior half. OS ventrally yellow, with several brown and irregular marks.

Male: Unknown.

Remarks. It is possible that this species is conspecific with *P. columnacea* Zhang, Jäger & Liu, 2023 (Zhang et al. 2023) due to their shared habitat. However, significant variations in the color and patterns on the dorsal side of the females compared to the males of *P. columnacea* suggest they could be different species. Clarifying these uncertainties will require additional research and future discoveries.

Distribution. Thailand (Chiang Mai Province) (Fig. 9).

Pseudopoda kavanaughi Zhang, Jäger & Liu, 2023

Figs 7–9

Pseudopoda kavanaughi Zhang, Jäger & Liu, 2023: 149, figs 135A–C, 136A, B (Holotype male from Yunnan Province, China, deposited in CAS, examined).

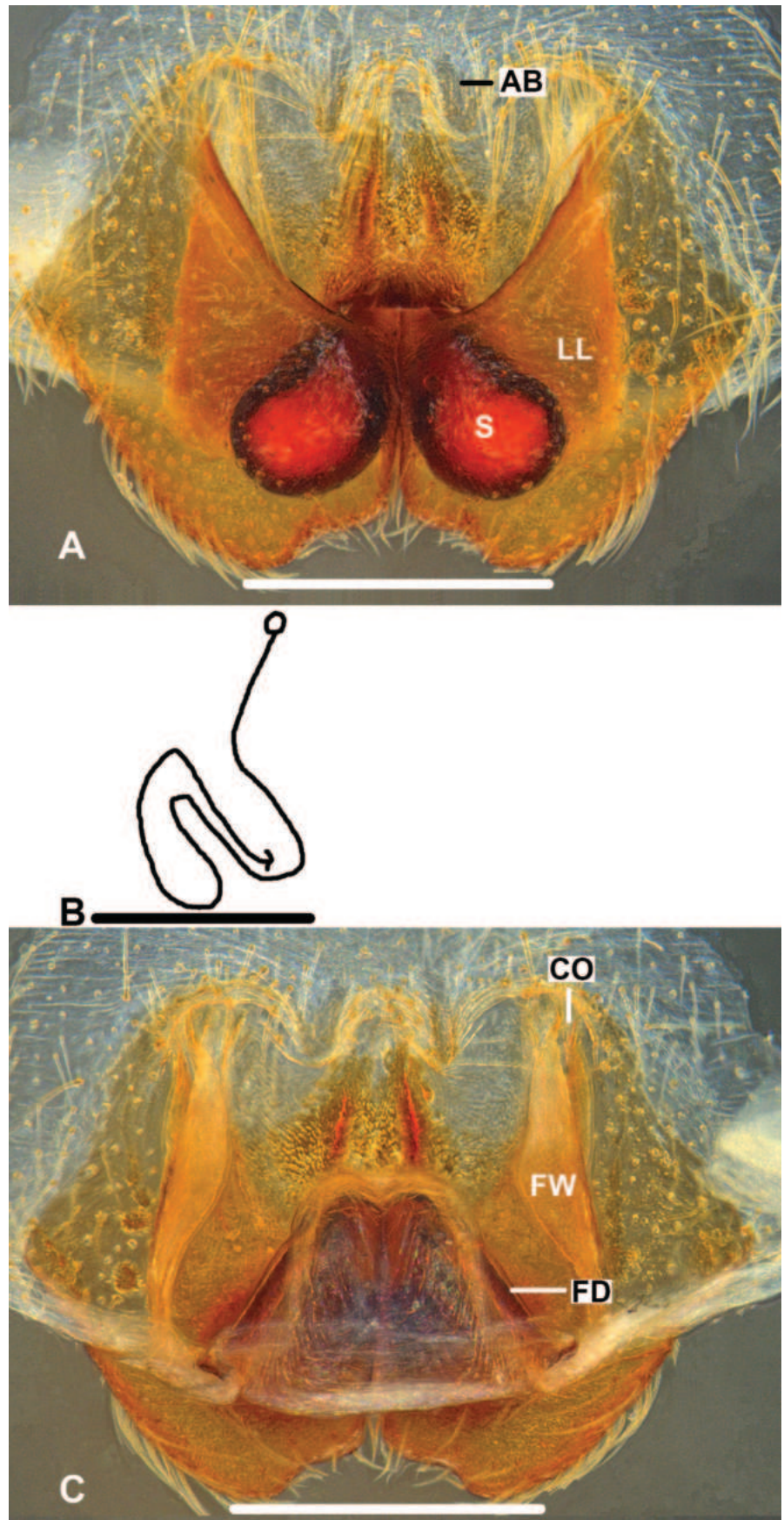


Figure 7. *Pseudopoda kavanaughii* Zhang, Jäger & Liu, 2023, female **A** epigyne, ventral **B** schematic course of IDS, dorsal **C** vulva, dorsal. Scale bars: 0.5 mm.

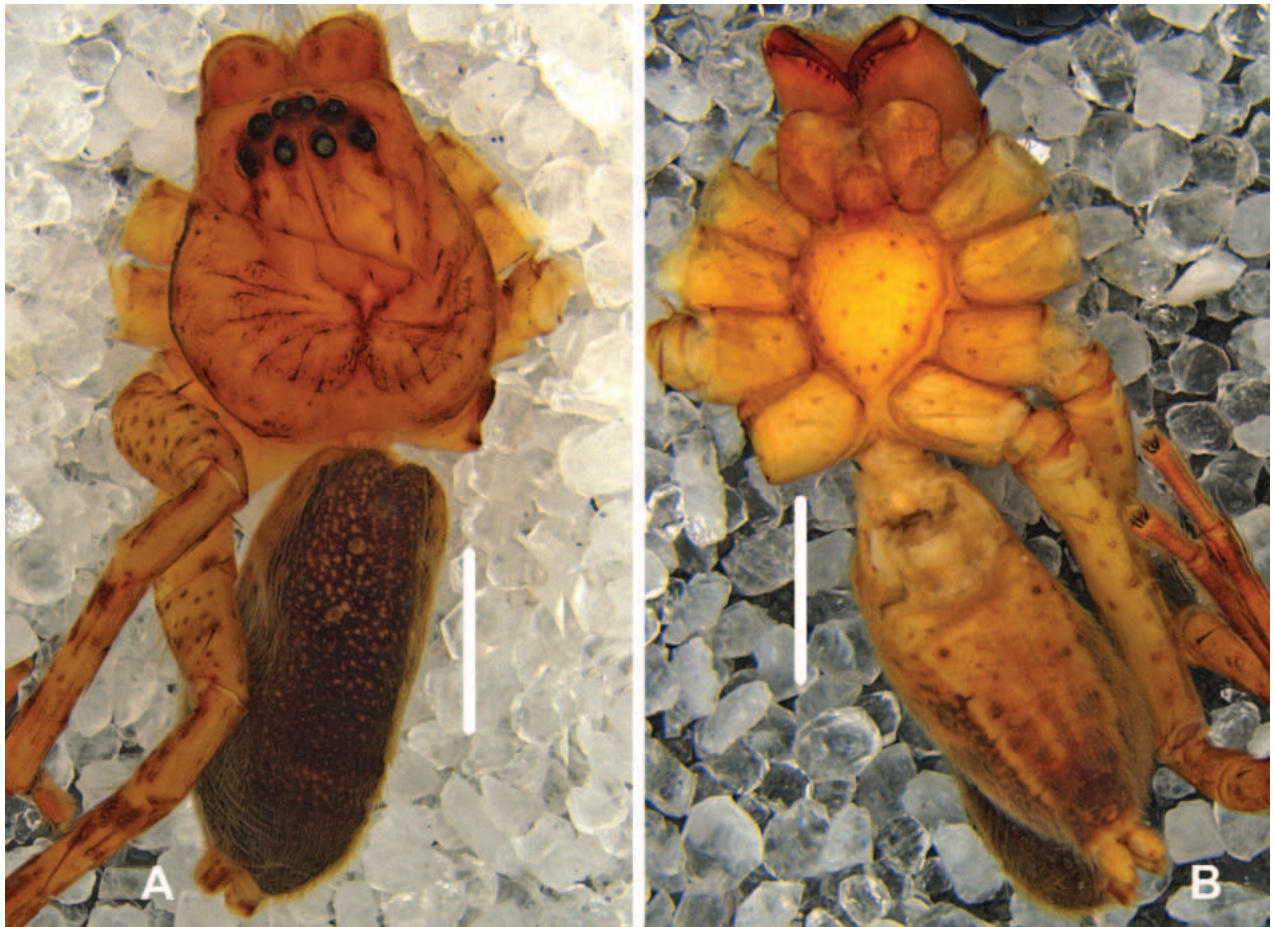


Figure 8. *Pseudopoda kavanaughii* Zhang, Jäger & Liu, 2023, female habitus (A dorsal B ventral). Scale bars: 2 mm.

Material examined. CHINA, Yunnan Province: 1 female, Gongshan County, Dulongjiang Township, 2.3–3.3 km south of Longyuan Village, 28°0'19"N, 98°19'42"E, 1690 m, 2 November 2004, D.H. Kavanaugh leg. (CAS, CAS0035); 1 female, Gongshan County, Dulongjiang Township, Dizheng Wang, across Dulongjiang from Dizhengdang, 28°5'12"N, 98°19'42"E, 1910 m, 20 October 2004, D.H. Kavanaugh leg. (CAS, CAS0034).

Diagnosis. The female of this species is similar to *P. tianpingensis* Zhang, Jäger & Liu, 2023 (Zhang et al. 2023) by: 1) anterior margins of LL U-shaped and almost parallel to posterior margins; and 2) sclerotised part of IDS oval-shaped in ventral view. It can be recognised by the sclerotised part of S forming “八”-shape, extending in oblique downward axis in ventral view (almost parallel to anterior margins and posterior margins, extending in oblique upward axis in ventral view in *P. tianpingensis*).

Female (CAS0034): Measurements: Small sized. Body length 8.2, DS length 3.8, width 3.5, OS length 4.4, width 3.3. Eyes: AME 0.22, ALE 0.35, PME 0.25, PLE 0.33, AME–AME 0.14, AME–ALE 0.08, PME–PME 0.18, PME–PLE 0.38, AME–PME 0.29, ALE–PLE 0.24, CH AME 0.36, CH ALE 0.27. **Spination:** Pp 131, 101, 2121, 1014; Fe I–III 323, IV 321; Pa I–IV 101; Ti I–III 2224, IV 2226; Mt I–II 1014, III 2024, IV 3036. **Measurement of palps and legs:** Pp 5.0 (1.5, 1.0, 0.7, –, 1.8); I 12.6 (3.5, 1.5, 3.7, 2.9, 1.0), II 15.4 (4.3, 1.8, 4.5, 3.3, 1.5), III 10.2 (3.1, 0.9, 2.8, 2.6, 0.8), IV 13.1 (3.9, 1.2, 3.4, 3.1, 1.5). Leg formula: II-IV-I-III.



Figure 9. Distribution map of the four species from the genus *Pseudopoda*. The numbers represent the different species. 1 *P. baimai* Jäger & Liu, sp. nov. 2 *P. fengtongzhaiensis* Jäger & Liu, sp. nov. 3 *P. inthanonensis* Jäger & Liu, sp. nov. 4 *P. kavanaughii* Zhang, Jäger & Liu, 2023.

Promargin of chelicerae as in *P. baimai* Jäger & Liu, sp. nov., cheliceral furrow with c. 16 denticles.

Epigyne (Fig. 7A–C): As in diagnosis. EF wider than long, with short AB. S clearly visible, and slightly bent to anterior margins to LL in ventral view, all covered by FW and posterior part of LL in dorsal view. FD long, suited medially.

Colouration (Fig. 8A, B): DS reddish-brown with dark dots. Fovea and striae distinctly marked. OS dorsally reddish-brown with lots of black dots, ventrally brown with several black marks, with several reddish-brown patches at posterior part.

Male: For details see Zhang et al. (2023).

Variation. Female ($N = 1$): body length 7.7, DS length 3.2, OS length 4.5.

Remarks. This female's location is close to that of the male of *P. kavanaughii*. Although there are slight differences in colouration, we consider it the conspecific female.

Distribution. China (Yunnan Province) (Fig. 9).

Acknowledgments

We thank all institutions and staff as listed in the Material and methods section for loaning material for this study.

Additional information

Conflict of interest

The authors have declared that no competing interests exist.

Ethical statement

No ethical statement was reported.

Funding

This study was supported in part by grants from National Natural Sciences Foundation of China (NSFC-31572236; NSFC-31772420; NSFC-31970406; NSFC-32300378), the China Postdoctoral Science Foundation (2023M731035), Xishuangbanna Tropical Botanical Garden, Chinese Academy of Sciences (19CAS-TFE-3).

Author contributions

Writing – original draft: YW, RZ. Writing – review and editing: YZ, PJ, JL, HZ.

Data availability

All of the data that support the findings of this study are available in the main text.

References

- Cao XW, Liu J, Chen J, Zheng G, Kuntner M, Agnarsson I (2016) Rapid dissemination of taxonomic discoveries based on DNA barcoding and morphology. *Scientific Reports* 6(1): 37066. <https://doi.org/10.1038/srep37066>
- Jäger P (2000) Two new heteropodine genera from southern continental Asia (Araneae: Sparassidae). *Acta Arachnologica* 49(1): 61–71. <https://doi.org/10.2476/asjaa.49.61>
- Jäger P (2001) Diversität der Riesenkrabbenspinnen im Himalaya – die Radiation zweier Gattungen in den Schneetropen (Araneae, Sparassidae, Heteropodinae). *Courier Forschungsinstitut Senckenberg* 232: 1–136.
- Jäger P (2007) Spiders from Laos with descriptions of new species (Arachnida: Araneae). *Acta Arachnologica* 56(1): 29–58. <https://doi.org/10.2476/asjaa.56.29>
- Jäger P, Ono H (2002) Sparassidae from Japan. II. First *Pseudopoda* species and new *Sinopoda* species (Araneae: Sparassidae). *Acta Arachnologica* 51(2): 109–124. <https://doi.org/10.2476/asjaa.51.109>
- Jäger P, Vedel V (2007) Sparassidae of China 4. The genus *Pseudopoda* (Araneae: Sparassidae) in Yunnan Province. *Zootaxa* 1623(1): 1–38. <https://doi.org/10.11646/zootaxa.1623.1.1>
- Jiang TY, Zhao QY, Li SQ (2018) Sixteen new species of the genus *Pseudopoda* Jäger, 2000 from China, Myanmar, and Thailand (Sparassidae, Heteropodinae). *ZooKeys* 791: 107–161. <https://doi.org/10.3897/zookeys.791.28137>
- Li ZC, Zhang H, Jäger P, Liu J (2019) One new *Pseudopoda* group from Yunnan Province, China (Araneae: Sparassidae). *Acta Arachnologica Sinica* 28: 96–105.

- Pickard-Cambridge O (1885) Araneidea. Scientific results of the second Yarkand mission; based upon the collections and notes of the late Ferdinand Stoliczka, Ph. D. Government of India, Calcutta, 115. <https://doi.org/10.5962/bhl.title.119960>
- World Spider Catalog (2024) World Spider Catalog. Version 25.0. Natural History Museum Bern. <http://wsc.nmbe.ch> [accessed on 28 March 2024]
- Zhang F, Zhang BS, Zhang ZS (2013) New species of *Pseudopoda* Jäger, 2000 from southern China (Araneae, Sparassidae). *ZooKeys* 361: 37–60. <https://doi.org/10.3897/zookeys.361.6089>
- Zhang H, Jäger P, Liu J (2017) One new *Pseudopoda* species group (Araneae: Sparassidae) from Yunnan Province, China, with description of three new species. *Zootaxa* 4318(2): 271–294. <https://doi.org/10.11646/zootaxa.4318.2.3>
- Zhang H, Jäger P, Liu J (2019) Establishing a new species group of *Pseudopoda* Jäger, 2000 with the description of two new species (Araneae, Sparassidae). *ZooKeys* 879: 91–115. <https://doi.org/10.3897/zookeys.879.35110>
- Zhang H, Zhu Y, Zhong Y, Jäger P, Liu J (2023) A taxonomic revision of the spider genus *Pseudopoda* Jäger, 2000 (Araneae: Sparassidae) from East, South and Southeast Asia. *Megataxa* 9(1): 1–304. <https://doi.org/10.11646/megataxa.9.1.1>

Argopistes Motschulsky from Madagascar with descriptions of six new species (Coleoptera, Chrysomelidae, Galerucinae, Alticini)

Maurizio Biondi¹, Mattia Iannella¹, Paola D'Alessandro¹

¹ Department of Life, Health and Environmental Sciences, University of L'Aquila, 67100 L'Aquila, Italy
Corresponding author: Paola D'Alessandro (paola.dalessandro@univaq.it)

Abstract

The revision of the flea beetle genus *Argopistes* Motschulsky, 1860 in Madagascar is provided. Six new species are described: *Argopistes janakmoravecorum* **sp. nov.**, *A. laterosinuatus* **sp. nov.**, and *A. vadoni* from the northern area; *A. jenisi* **sp. nov.**, *A. keiseri* **sp. nov.**, and *A. seyrigi* **sp. nov.** from the central area. A new synonym of *Argopistes brunneus* Weise, 1895 is established: *A. sexguttatus* Weise, 1895, **syn. nov.**, since *A. sexguttatus* is shown to be a chromatic form of *A. brunneus*. A diagnostic key of the seven Malagasy *Argopistes* species is provided, with photographs of the habitus, median lobe of the aedeagus, and spermatheca. Finally, based on known occurrences, the current suitable areas for this flea beetle genus in Madagascar are estimated using Ecological Niche Modelling (ENM) techniques.

Key words: Afrotropical region, Ecological Niche Modelling, flea beetles, new species, synonymy



Academic editor: Astrid Eben
Received: 13 March 2024
Accepted: 19 April 2024
Published: 27 May 2024

ZooBank: <https://zoobank.org/1C308A71-A36D-4B60-8CD0-45BD70283919>

Citation: Biondi M, Iannella M, D'Alessandro P (2024) *Argopistes* Motschulsky from Madagascar with descriptions of six new species (Coleoptera, Chrysomelidae, Galerucinae, Alticini). ZooKeys 1202: 303–327. <https://doi.org/10.3897/zookeys.1202.122977>

Copyright: © Maurizio Biondi et al.
This is an open access article distributed under terms of the Creative Commons Attribution License (Attribution 4.0 International – CC BY 4.0).

Introduction

Madagascar is considered one of the world's most important biodiversity hotspots thanks to the many field campaigns conducted since the 17th century that documented its species richness (e.g., Andriamialisoa and Langrand 2022). Nevertheless, its faunistic diversity is still only partially known, especially for some invertebrate groups, including flea beetles (Coleoptera, Chrysomelidae, Galerucinae, Alticini) (Iannella et al. 2019). Biondi and D'Alessandro (2012) reported approximately 260 flea beetle species in 39 genera from Madagascar, of which 13 were endemics. Subsequent published papers and additional material preserved in public and private collections demonstrate that these numbers are significantly underestimated (Biondi and D'Alessandro 2013a, 2013b, 2016; D'Alessandro et al. 2014).

The flea beetle genus *Argopistes* Motschulsky, 1860 was described based on a new species from Siberia, *A. biplagiatus* Motschulsky, 1860, the type species by monotypy. The genus was subsequently reported for the Afrotropical, Australian, Neotropical, Oriental, and Palearctic Regions, with a total of 38 species (Blanco and Konstantinov 2013).

Nadein (2015), through a morphological-based cladistic analysis, attributed *Argopistes* to the subtribe Diboliina with *Dibolia* Latreille, *Megistops* Boheman,

and *Paradibolia* Baly. More recent papers based on the use of molecular data considered *Argopistes* closely related to *Apteropeda* Chevrolat (Hlaka et al. 2022), *Dibolia*, and *Apteropeda* (Letsch and Beran 2023), or *Dibolia* and *Sphaeroderma* Stephens (Douglas et al. 2023). Nevertheless, all authors agreed that additional molecular data and denser taxon sampling are required to provide a robust basis for establishing internal relationships among Alticini and possible subtribal classifications.

Blanco and Konstantinov (2013) recognized nine valid *Argopistes* species in the Afrotropical Region, including Madagascar, but at least 13 new species are currently being described from that area, based on new unpublished material (M. Biondi, unpublished data). In this paper, we provided a revision of the Malagasy *Argopistes* species. We described *Argopistes janakmoravecorum* sp. nov., *A. laterosinuatus* sp. nov., and *A. vadoni* sp. nov. from the northern area, and *A. jeni* sp. nov., *A. keiseri* sp. nov., and *A. seyrigi* sp. nov. from the central area. We proposed a new synonym of *Argopistes brunneus* Weise, 1895, *A. sexguttatus* Weise, 1895, syn. nov. Finally, based on the known occurrences, we reconstructed the current high suitability areas for the *Argopistes* species in Madagascar using Ecological Niche Modelling (ENM) techniques.

Materials and methods

Material examined consisted of dried pinned specimens preserved in the institutions listed in the Abbreviations section. Specimens were examined, measured, and dissected using a Leica M205C stereomicroscope. Photographs were taken using a Leica DMC5400 camera and compiled with the focus stacking technique using Zerene Stacker software v. 1.04. Scanning electron micrographs were taken using a Hitachi TM-1000. Terminology followed Schmitt et al. (2023) for the median lobe of the aedeagus, and Döberl (1986) and Suzuki (1988) for the spermatheca. Geographic coordinates were reported in the Degrees and Decimal Minutes format (DDM) using the WGS84 datum; information included in square brackets was added by the authors, using the Google Earth website for coordinates and geographic information. Chorotypes follow Biondi and D'Alessandro (2006). Vegetation division names refer to Sayre et al. (2013). Abbreviations for the depositories followed the list on the website The Insect and Spider Collections of the World (Evenhuis 2023). Exact label data were cited for all type specimens of the examined or described species; a double slash (//) divided the data on different labels and a single slash (/) divided the data in different rows.

Ecological Niche Models (ENMs) were built based on all the known occurrences, and on 19 temperature- and precipitation-related “bioclimatic” raster variables selected as candidate predictors from the Worldclim.org repository (Fick and Hijmans 2017), namely **BIO1**: annual mean temperature, **BIO2**: mean diurnal range (mean of monthly (max temp–min temp)), **BIO3**: isothermality (BIO2/BIO7) (×100), **BIO4**: temperature seasonality (standard deviation ×100), **BIO5**: max temperature of warmest month, **BIO6**: min temperature of coldest month, **BIO7**: temperature annual range (BIO5–BIO6), **BIO8**: mean temperature of wettest quarter, **BIO9**: mean temperature of driest quarter, **BIO10**: mean temperature of warmest quarter, **BIO11**: mean temperature of coldest

quarter, **BIO12**: annual precipitation, **BIO13**: precipitation of wettest month, **BIO14**: precipitation of driest month, **BIO15**: precipitation seasonality (coefficient of variation), **BIO16**: precipitation of wettest quarter, **BIO17**: precipitation of driest quarter, **BIO18**: precipitation of warmest quarter, and **BIO19**: precipitation of coldest quarter. To avoid potential correlation among variables, which leads to the lowering of the model's performance, we measured both the variance inflation factor (VIF), setting the threshold = 10 (Guisan et al. 2017), and Pearson's r ($|r| < 0.75$, following Dormann (2007) and Elith et al. (2006)); for this purpose, we used the 'vifstep' and 'vifcor' functions of the 'usdm' R package (Naimi 2017). The variables obtained as the analyses' outcomes were then selected as predictors to calibrate the models. The ENMs were performed using the "Presence-only Prediction (Maxent)" tool in the ArcGis Spatial Analyst. This tool permits to infer, based on a set of environmental predictors and occurrence localities (specifically, a presence-only dataset), the suitability of a certain taxon across an area, also giving marginal response curves of the predictors with respect to the predicted suitability. Its main advantage in terms of model discrimination capability is the possibility to calibrate and evaluate performances through a spatial jackknifing procedure (ESRI, 2023). Moreover, the ENM's performance was evaluated by both assessing the Area Under the Curve (AUC) of the ROC (Phillips et al. 2006), automatically resulting from the ArcGIS tool, and the Continuous Boyce Index (CBI), particularly useful for presence-only models (Hirzel et al, 2006; Leroy et al. 2018), calculated through the 'ecospat.boyce' function in the 'ecospat' R package (Di Cola et al. 2017).

Abbreviations

Collections and repositories

BAQ	Italy, University of L'Aquila, Collection of M. Biondi;
NHMB	Switzerland, Basel, Naturhistorisches Museum;
RMCA	Belgium, Tervuren, Musée Royal de l'Afrique Centrale;
ZMHB	Germany, Berlin, Museum für Naturkunde.

Biometrics

LA	numerical sequence from base to apex of each antennomere, proportional to the length of the first antennomere;
LAED	length of median lobe of the aedeagus;
LAN	length of antennae;
LB	total body length (from apical margin of head to apex of elytra);
LE	maximum length of elytra;
LF	maximum length of hind femora;
LP	medial length of pronotum;
LSPC	maximum length of spermathecal capsule;
WE	maximum width of elytra combined;
WF	maximum width of hind femora;
WP	maximum width of pronotum.

Results

Taxonomy

Argopistes brunneus Weise

Figs 1, 8A

Argopistes brunneus Weise, 1895: 336.

Argopistes sexguttatus Weise, 1895: 336. syn. nov.

Type material examined. *Holotype* of *Argopistes brunneus* ♂: “Madagasc. / Pipitz // Madagasc / 195 / Pipitz” [Madagascar, Dr. Pipitz leg.] [handwritten on light blue cards] “*Argopistes / brunneus / m*” [handwritten on white card], “HOLOTYPUS / *Argopistes brunneus* Weise / labelled by MNHUB” [printed on red card], (ZMHB).

Holotype of *Argopistes sexguttatus* ♂: “Madagasc. / Pipitz // Madagasc / 193 / Pipitz” [Madagascar, Dr. Pipitz leg.] [handwritten on light blue cards] “*Argopistes / 6-guttatus / m*” [handwritten on white card], “HOLOTYPUS / *Argopistes sexguttatus* Weise / labelled by MNHUB” [printed on red card], (ZMHB).

Additional material examined. 1 spec., Madagascar Nord, Antsiranana prov., Amber Gebirge [~12°2.20'S, 49°15.02'E] (ZMHB); 1 spec., Madagascar, Toamasina prov., forêt de Fito, ex Coll. Dr. Breuning, [17°59.99'S, 48°50.50'E] (RMCA); 2 specs, Madagascar, Tamatave [= Toamasina, 18°8.97'S, 49°24.14'E] (ZMHB); 2 specs, ibid, Coll. Clavareau (RMCA); 1 spec., Madagascar, Fianarantsoa prov., Ranomafana env. [21°15.76'S, 47°27.12'E], 28.i–6.ii.1995, Ivo Jeniš leg. (BAQ).

Redescription. Body subrounded in dorsal view, with slightly parallel sides (Fig. 1A, C), strongly convex in lateral view; total length of body (LB) = 3.82 ± 0.13 mm ($3.68 \leq LB \leq 3.98$ mm) in male, and 3.79 ± 0.06 mm ($3.72 \leq LB \leq 3.84$ mm) in female; maximum pronotal width at the base: WP = 2.33 ± 0.05 mm ($2.28 \leq WP \leq 2.40$ mm) in male, and 2.27 ± 0.07 mm ($2.20 \leq WP \leq 2.36$ mm) in female; maximum width of elytra in the middle: WE = 3.15 ± 0.07 mm ($3.08 \leq WE \leq 3.24$ mm) in male, and 3.19 ± 0.10 mm ($3.04 \leq WE \leq 3.24$ mm) in female; WE/WP = 1.35 ± 0.03 ($1.32 \leq WE/WP \leq 1.40$) in male, and WE/WP = 1.41 ± 0.04 ($1.36 \leq WE/WP \leq 1.45$) in female.

Color of the dorsal integument variable (Fig. 1A, C): entirely black; entirely brown; with black elytral disc blending in reddish brown towards the pronotum and the elytral margins; with brown head and pronotum, and black elytra with brown patches; antennae (Fig. 1B) yellowish; hind legs brown or paler; fore- and middle legs generally yellowish (Fig. 1B); ventral parts mostly brownish (Fig. 1B).

Head entirely hidden by the pronotum; vertex with very small, irregular punctation and a pair of large setiferous pores; frontal calli barely delimited, not raised; frons moderately elongate, its surface irregular, roughly wrinkled; frontal ridge elongate, thin and sharp; frontogenal sutures distinctly raised; eyes large, elongate, slightly kidney-shaped; interantennal space clearly narrower than antennal sockets. Antennae (Fig. 1B) filiform, as long as ~ 1/2 the body length: LAN = 1.98 ± 0.08 mm ($1.88 \leq LAN \leq 2.08$ mm) in male, and 1.71 ± 0.08 mm ($1.64 \leq LAN \leq 1.80$ mm) in female, and LAN/LB = 0.52 ± 0.01 ($0.51 \leq LAN/LB \leq 0.53$) in male, and 0.45 ± 0.02 ($0.43 \leq LAN/LB \leq 0.47$) in female; segments 1–2 thicker; segments 3–11 slightly and gradually flattened.

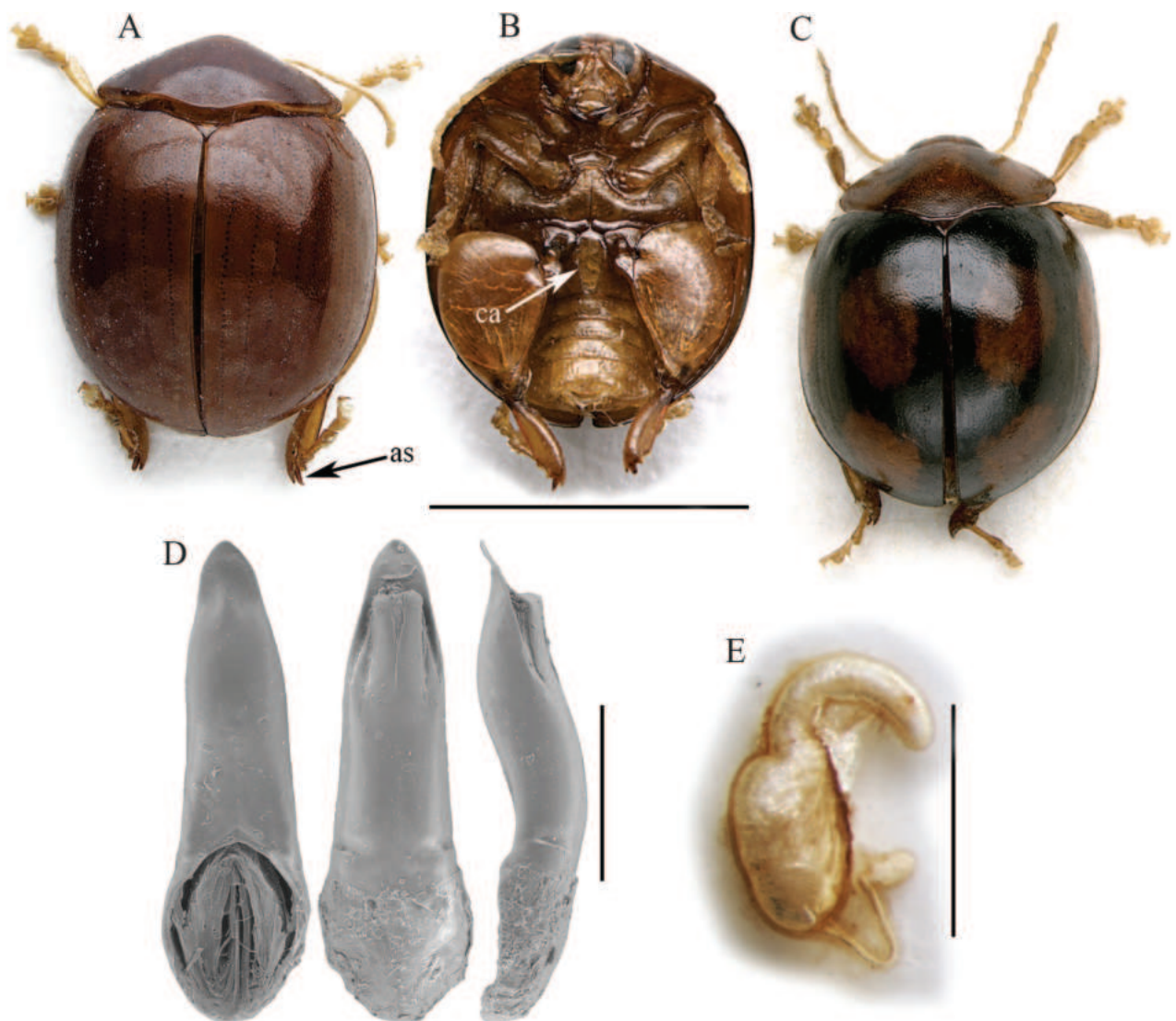


Figure 1. *Argopistes brunneus* Weise. **A** holotype of *A. brunneus*, habitus in dorsal view **B** ibid, ventral view **C** holotype of *A. sexguttatus* Weise, habitus in dorsal view **D** median lobe of the aedeagus, from left to right in dorsal, ventral, and lateral view, from Tamatave **E** spermatheca, from Tamatave. Abbreviations: as: apical spur of hind tibia; ca: central area of the first abdominal sternite bordered by ridges. Scale bars: 3 mm (**A, B, C**); 500 μ m (**D**); 300 μ m (**E**).

Pronotum (Fig. 1A, C) distinctly transverse: LP = 1.06 ± 0.06 mm ($1.00 \leq$ LP ≤ 1.12 mm) in male, and 1.05 ± 0.04 mm ($1.00 \leq$ LP ≤ 1.08 mm) in female, and WP/LP = 2.20 ± 0.07 ($2.14 \leq$ WP/LP ≤ 2.28) in male, and 2.16 ± 0.05 ($2.09 \leq$ WP/LP ≤ 2.20) in female; lateral margins strongly convergent anteriorly, weakly curved to straight, very weakly expanded, not visible in dorsal view; basal margin arcuate and moderately sinuate; surface smooth, sparsely micropunctate, with very dense, small punctation; surface barely raised parallel to the lateral margins, near the posterior angles; a large setiferous pore at the anterior angles. Scutellum small, subtriangular.

Elytra (Fig. 1A, C) distinctly curved but slightly parallel in the middle third, moderately longer than wide, jointly rounded apically; lateral margins finely bordered, visible in dorsal view; surface smooth to sparsely micropunctate; main punctation mostly confused, very dense, small, slightly shallower than on pronotum but more impressed laterally; 9 (+ 1 sutural) regular lines are visible in paler speci-

mens due to the blackened punctures (Fig. 1A); $LE = 3.38 \pm 0.10$ mm ($3.24 \leq LE \leq 3.50$ mm) in male, and 3.43 ± 0.09 mm ($3.32 \leq LE \leq 3.52$ mm) in female; $WE/LE = 0.93 \pm 0.2$ ($0.91 \leq WE/LE \leq 0.95$) in male, and 0.93 ± 0.03 ($0.89 \leq WE/LE \leq 0.98$) in female; $LE/LP = 3.19 \pm 0.09$ ($3.09 \leq LE/LP \leq 3.32$) in male, and 3.27 ± 0.16 ($3.07 \leq LE/LP \leq 3.40$) in female. Humeral calli moderately raised. Macropterous.

Prosternum with posteriorly open procoxal cavities and large intercoxal prosternal process. Mesosternum very short. First abdominal sternite approx. as long as fifth (Fig. 1B); its central area bordered by ridges is quite narrow and subrhomboidal. Anterior and middle legs without modifications. Posterior femora greatly swollen ($WF/LF = 0.68 \pm 0.01$), elongate-subtriangular; posterior tibiae thick, distinctly shorter than femora, apically widened and prolonged into a spur-like process on inner side; outer side of hind tibia apically toothed; apical spur of hind tibiae simple, lanceolate; first metatarsomere moderately enlarged in male.

Median lobe of the aedeagus (Fig. 1D) with smooth surface; in ventral view is tapered towards the apex, slightly sinuate laterally; in lateral view moderately curved, with sinuate ventral outline and straight apex; dorsal ligula formed by a medially incised central lobe, and two thinner lateral lobes; its base at apical $\sim 1/3$; $LAED = 1.41 \pm 0.04$ mm ($1.36 \leq LAED \leq 1.48$ mm); $LE/LAED = 2.40 \pm 0.08$ ($2.30 \leq LE/LAED \leq 2.50$).

Basal part of the spermatheca (Fig. 1E) subcylindrical, dorsally enlarged; distal part curved, elongate, uniform in thickness, with collum generally not distinguishable from the apical part; ductus subapically inserted and oriented, thin, quite short, uncoiled; $LSPC = 0.38 \pm 0.01$ mm ($0.36 \leq LSPC \leq 0.38$ mm); $LE/LSPC = 9.14 \pm 0.39$ ($8.74 \leq LE/LSPC \leq 9.61$).

Remarks. *Argopistes brunneus* is distinguishable from the other Malagasy *Argopistes* species by the slightly parallel sides in dorsal view (Fig. 1A, C), and the first abdominal sternite, whose central surface bordered by ridges is narrow and convergent posteriorly (Fig. 1B). The median lobe of the aedeagus and spermatheca (Fig. 1D, E) are also diagnostic. *Argopistes sexguttatus* Weise is here synonymized with *A. brunneus*, simply representing one of its chromatic forms.

Distribution. Northern, eastern, and central Madagascar (Antsiranana, Toamasina, and Fianarantsoa provinces; Fig. 8A). Malagasy chorotype.

Ecological notes. Host plant unknown. Collection localities fall within areas characterized by the vegetation divisions of 'Malagasy Evergreen & Semi-Evergreen Forest' and 'Malagasy Dry Deciduous & Evergreen Forest & Woodland'.

***Argopistes janakmoravecorum* sp. nov.**

<https://zoobank.org/62088B6A-315D-4294-93DD-237DAC0E4BDE>

Figs 2, 8A

Type material. Holotype ♀: "Madagascar Nord / 800-1000 m / 5 km à est d'Andapa / Lembonibona (1265 m) // forêt dégradée, arbres, arbustes / 2.3.1996 / J. Janák + P. Moravec lgt." [printed on white card] [$14^{\circ}40.63'S$; $49^{\circ}41.63'E$] (BAQ).

Diagnosis. *Argopistes janakmoravecorum* sp. nov. is easily distinguishable from the other Afrotropical *Argopistes* species by the combination of black dorsal integuments and clavate antennae with segments 1–5 yellowish and 6–11 blackened (Fig. 2B). Spermatheca is also strongly diagnostic, due to the elongate and distally coiled ductus (Fig. 2C).

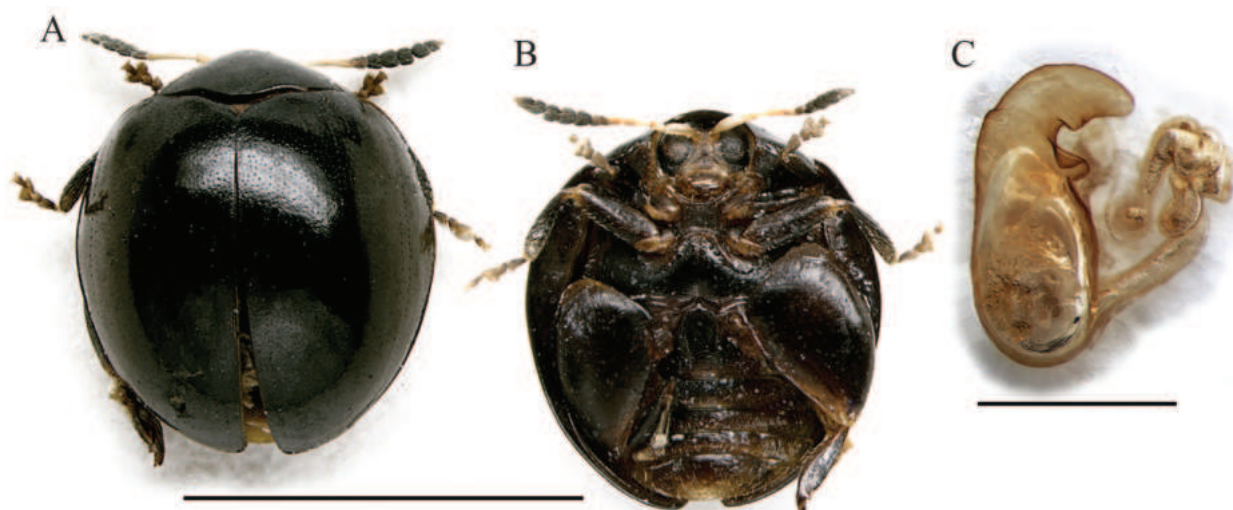


Figure 2. *Argopistes janakmoravecorum* sp. nov. **A** holotype, habitus in dorsal view **B** ibid, ventral view **C** ibid, spermatheca. Scale bars: 3 mm (**A**, **B**); 300 µm (**C**).

Description of the holotype (♀). Body roundish in dorsal view (Fig. 2A), very convex in lateral view; total length of the body (LB) = 3.00 mm; maximum pronotal width at the base (WP = 1.68 mm); maximum width of elytra in the middle (WE = 2.56 mm); WE/WP = 1.52. Dorsal integuments black with weak metallic reflections (Fig. 2A); scutellum brownish; head brownish; frons and mouthparts yellowish; antennae (Fig. 2B) with segments 1–5 yellowish, 6 dark brown, 7–10 black, 11 black but distally paler; ventral parts (Fig. 2B) mostly dark brown; legs with femora and tibiae blackish, tarsi partially dark brown and articulations yellowish (Fig. 2B). Head entirely hidden by the pronotum; vertex irregularly punctate, with a pair of large setiferous pores; frontal calli barely delimited, not raised; frons elongate, with rough, irregular surface; frontal ridge barely detectable; frontogenal sutures weakly raised; eyes large, elongate, slightly kidney-shaped; interantennal space clearly narrower than antennal sockets. Antennae (Fig. 2B) clavate, as long as $\sim 1/2$ the body length (LAN = 1.36 mm; LAN/LB = 0.45); LA = 100:46:32:53:58:42:47:54:49:42:69. Pronotum (Fig. 2A) clearly transverse (LP = 0.78 mm; WP/LP = 2.15); lateral margins strongly convergent anteriorly and slightly folded ventrally, moderately curved, barely expanded, not visible in dorsal view; basal margin arcuate and distinctly sinuate; surface finely microreticulate, with very small and dense punctation; surface moderately raised parallel to the lateral margins; a large setiferous pore at the anterior angles. Scutellum small, subtriangular. Elytra (Fig. 2A) (LE: 2.72 mm, LE/LP = 3.49) strongly curved laterally, slightly longer than wide (WE/LE = 0.94), jointly rounded apically; lateral margins finely bordered, visible in dorsal view; surface sub-smooth, with very small and dense punctation, similar to pronotum, mostly confused but arranged in a couple of lines of slightly larger punctures laterally. Humeral calli moderately raised. Macropterous. Prosternum with posteriorly open procoxal cavities and large intercoxal prosternal process. Mesosternum very short. First abdominal sternite slightly longer than fifth (Fig. 2B); its central area bordered by ridges is quite wide, arcuate anteriorly and slightly narrowing posteriorly. Anterior and middle legs without modifications. Posterior femora greatly swollen (WF/LF = 0.61), elongate-subtriangular; posterior tibiae thick,

distinctly shorter than femora, apically widened and prolonged into a spur-like process on inner side; outer side of hind tibia apically toothed; apical spur of hind tibiae simple, lanceolate. Basal part of the spermatheca (Fig. 2C) sub-pyriform, with a distinct ventral protrusion close to the distal part; collum very short; apical part short, narrowing towards the apex; ductus ventrally inserted, thickset, elongate, distally coiled; LSPC = 0.48 mm; LE/LSPC = 5.67.

Etymology. The specific epithet refers to the two collectors of the new species: Jiří Janák and Pavel Moravec from the Czech Republic, both esteemed experts on Coleoptera Carabidae. The name was composed by the union of the two surnames, applying Latin plural genitive.

Distribution. Northern Madagascar (Antsiranana province; Fig. 8A). Malagasy chorotype.

Ecological notes. Host plant unknown. The only known occurrence locality falls within an area characterized by the vegetation division 'Malagasy Evergreen & Semi-Evergreen Forest'.

***Argopistes jeni* sp. nov.**

<https://zoobank.org/9E7062ED-CDBE-4325-AB7F-E912391A250C>

Figs 3, 8A

Type material. Holotype ♀: "Madagascar / Tamatave prov. / Ambodinifody / 26.12.1996 / Ivo Jeniš leg." [printed on white card] [18°53.20'S; 48°3.04'E] (BAQ).

Diagnosis. *Argopistes jeni* sp. nov. is recognizable by the combination of the following characters: intense black color that contrasts with the yellow antennae, tarsi, and maxillary palpi (Fig. 3A, B); filiform antennae (Fig. 3A, B); wide last abdominal sternite, distinctly longer than first (Fig. 3B). Spermatheca is also diagnostic due to the subglobose basal part ventrally enlarged, and the short ductus, subventrally inserted (Fig. 3C).

Description of the holotype (♀). Body broadly elliptic in dorsal view (Fig. 3A), strongly convex in lateral view; total length of body (LB) = 4.44 mm; maximum pronotal width at the base (WP = 2.60 mm); maximum width of elytra in the middle (WE = 3.76 mm); WE/WP = 1.45. Dorsal integuments (Fig. 3A) entirely black with evident blueish metallic reflections; ventral parts (Fig. 3B) intensively black; head black; frons and mouthparts black, with yellowish maxillary palpi; antennae entirely yellowish (Fig. 3B); legs, including articulations, black, with yellowish tarsi (Fig. 3B). Head entirely hidden by the pronotum; vertex surface rough and distinctly punctate, with a pair of large setiferous pores; area of frontal calli weakly raised; frons elongate, with rough, irregular surface; frontal ridge thin and short; frontogenal sutures strongly raised; eyes large, elongate, slightly kidney-shaped; interantennal space clearly narrower than antennal sockets. Antennae filiform (Fig. 3B), as long as ~ 1/2 the body length (LAN = 2.12 mm; LAN/LB = 0.48); segments 1–2 thicker; segments 3–11 slightly and gradually flattened; LA = 100:42:33:47:47:40:41:44:43:39:64. Pronotum (Fig. 3A) clearly transverse (LP = 1.20 mm; WP/LP = 2.17); lateral margins strongly convergent anteriorly, weakly curved, weakly expanded, not visible in dorsal view; basal margin arcuate and distinctly sinuate; surface smooth, with very small and very dense punctation; surface moderately raised parallel to the lateral margins;

a large setiferous pore at the anterior angles. Scutellum small, subtriangular. Elytra (LE = 4.04 mm; LE/LP = 3.37) distinctly curved laterally (Fig. 3A), distinctly longer than wide (WE/LE = 0.93), jointly rounded apically; lateral margins finely bordered, visible in dorsal view; surface smooth; punctation very small, dense, and confused; points slightly larger towards lateral and apical parts, and partially arranged in some longitudinal lines. Humeral calli moderately raised. Macropterous. Prosternum with posteriorly open procoxal cavities and large intercoxal prosternal process. Mesosternum very short. First abdominal sternite distinctly shorter than fifth (Fig. 3B); its central area bordered by ridges is moderately wide, rounded anteriorly, laterally subparallel. Anterior and middle legs without modifications. Posterior femora greatly swollen (WF/LF = 0.68), elongate-subtriangular; posterior tibiae thick, distinctly shorter than femora, apically widened and prolonged into a spur-like process on inner side; outer side of hind tibia apically toothed; apical spur simple, lanceolate. Spermatheca (LSPC = 0.38 mm; LE/LSPC = 10.63) with apparently wrinkled surface (Fig. 3C); basal part subglobose, with a small protrusion just below the distal part; apical part moderately elongate, narrowing towards the apex; ductus subventrally inserted, quite narrow and short, uncoiled.

Etymology. The specific epithet refers to the collector of the new species: Ivo Jeniš from the Czech Republic, renowned expert on Coleoptera Cerambycidae.

Distribution. Central-eastern Madagascar (Toamasina province; Fig. 8A). Malagasy chorotype.

Ecological notes. Host plant unknown. The only known occurrence locality falls within an area characterized by the vegetation division 'Malagasy Evergreen & Semi-Evergreen Forest'.

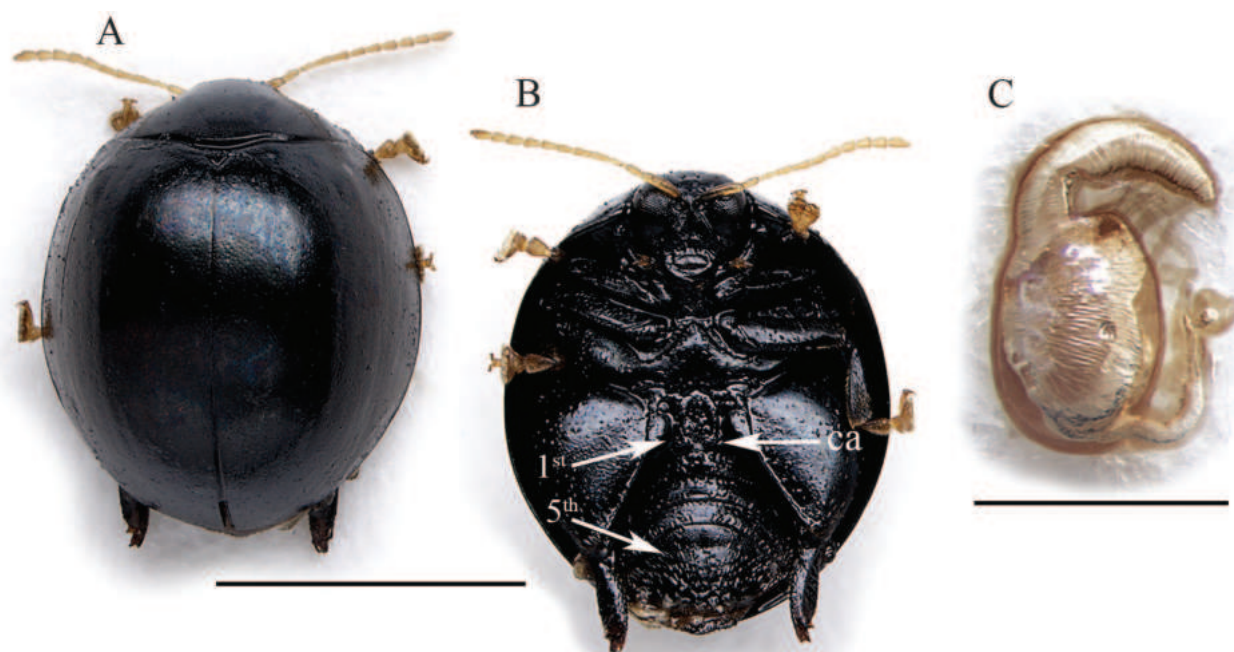


Figure 3. *Argopistes jenisi* sp. nov. **A** holotype, habitus in dorsal view **B** ibid, ventral view **C** ibid, spermatheca. Abbreviations: 1st: first abdominal sternite; 5th: fifth abdominal sternite; ca: central area of the first abdominal sternite bordered by ridges. Scale bars: 3 mm (**A**, **B**); 300 µm (**C**).

***Argopistes keiseri* sp. nov.**

<https://zoobank.org/D3E13A53-73C9-4BFC-9031-CA836A3E7775>

Figs 4, 8A

Type material. *Holotype* ♂: “Madagascar / Tamatave prov. / Manankazo env. / 11-12.11.1995 / Ivo Jeniš leg.” [printed on white card] [17°59.26'S; 46°54.20'E] (BAQ). Paratypes. 1 ♂ and 1 ♀ “Madagascar Tam. / Moramanga / 20.xii.1957 F. Keiser” [printed on pink card] // “Non Cocc. Det. H. Fürsch” [printed on white card] [18°56.93'S; 48°13.47'E] (NHMB); 2 ♀♀, “Madagascar / Tamatave prov. / Moramanga env. / 24.2-1.3.1995 / Ivo Jeniš leg.” [printed on white card] [18°56.93'S; 48°13.47'E] (BAQ); 2 ♀♀, “Madagascar / Tamatave prov. / Moramanga env. / 25-27.11.1995 / Ivo Jeniš leg.” [printed on white card] [18°56.93'S; 48°13.47'E] (BAQ); 2 ♀♀, “Madagascar / Tamatave prov. / Moramanga env. / 21-24.12.1996 / Ivo Jeniš leg.” [printed on white card] [18°56.93'S; 48°13.47'E] (BAQ); 1 ♂ and 1 ♀, “Madagascar / Tamatave prov. / Maromizaha / 21.II.1995 Ivo Jeniš” [printed on white card] [18°58.57'S; 48°27.90'E] (BAQ); 2 ♂ and 3 ♀, “Madagascar / Fianarantsoa prov. / Ranomafana env. / 28.I-6.II.1995 Ivo Jeniš” [printed on white card] [21°15.76'S; 47°27.12'E] (BAQ).

Diagnosis. *Argopistes keiseri* sp. nov. shows major similarities with *A. seyrigi* sp. nov. Both have the spur of hind tibiae distinctly elongate, extending significantly beyond the tibial apex (Figs 4B, 6B), black dorsal integuments (Figs 4A, 6A), and mostly confused elytral punctation. *Argopistes keiseri* sp. nov. can be distinguished by the blackish abdomen and tibiae (mostly reddish brown in *A. seyrigi* sp. nov.) (Figs 4B, 6B). Both the median lobe of aedeagus and spermatheca are diagnostic for *Argopistes keiseri* sp. nov.: median lobe (Fig. 4D) is thickset, with irregular outline in ventral view, and clearly sinuate in lateral view; spermatheca (Fig. 4C) has sinuate basal part and elongate, U-shaped, and uncoiled ductus.

Description of the holotype (♂). Body roundish in dorsal view (Fig. 4A), strongly convex in lateral view; total length of body (LB) = 3.48 mm; maximum pronotal width at the base (WP = 2.08 mm); maximum width of elytra in the middle (WE = 3.16 mm); WE/WP = 1.52. Dorsal integuments (Fig. 4A) entirely black with weak metallic reflections; ventral parts (Fig. 4B) entirely blackish; head black; frons and mouthparts black, with yellowish maxillary palpi; antennae yellowish (Fig. 4B); legs, including articulations, black, with yellowish tarsi (Fig. 4B). Head entirely hidden by the pronotum; vertex punctate, with a pair of large setiferous pores; area of frontal calli weakly raised; frons moderately elongate, roughly wrinkled; frontal ridge thin, weakly raised; frontogenal sutures thin, strongly raised; eyes large, elongate, slightly kidney-shaped; interantennal space clearly narrower than antennal sockets. Antennae (Fig. 4B) filiform, distinctly shorter than 1/2 the body length (LAN = 1.44 mm; LAN/LB = 0.41); segments 1–2 thicker; segments 3–11 slightly and gradually flattened; LA = 100:51:47:53:37:48:44:64:51:50:88. Pronotum (Fig. 4A) distinctly transverse (LP = 1.00 mm; WP/LP = 2.08); lateral margins strongly convergent anteriorly, straight, weakly expanded, not visible in dorsal view; basal margin arcuate and distinctly sinuate; surface sparsely micropunctate, with dense, small punctation; surface moderately raised parallel to the lateral margins; a large setiferous pore at the anterior angles. Scutellum small, subtriangular. Elytra (LE = 3.20 mm; LE/LP = 3.20) strongly curved laterally (Fig. 4A), approx. as

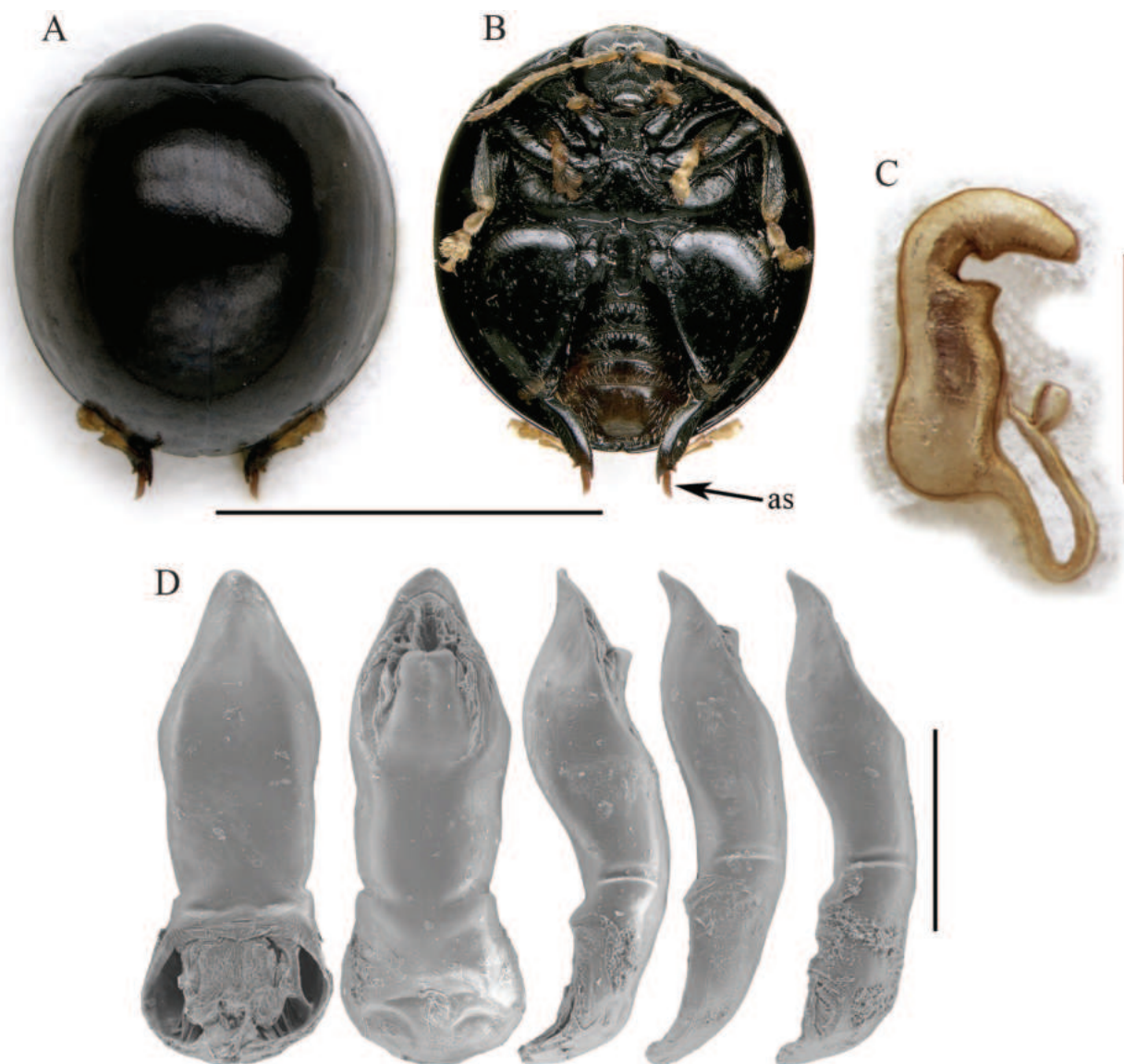


Figure 4. *Argopistes keiseri* sp. nov. **A** habitus in dorsal view, male from Moramanga **B** ibid, ventral view **C** spermatheca, from Ranomafana **D** median lobe of the aedeagus, from left to right in dorsal, ventral, and lateral view, from Ranomafana, and two additional lateral view from Manankazo, and Maromizama. Abbreviations: as: apical spur of hind tibia. Scale bars: 3 mm (**A**, **B**); 300 µm (**C**); 500 µm (**D**).

long as wide ($WE/LE = 1.02$), jointly rounded apically; lateral margins finely bordered, visible in dorsal view; surface smooth; punctation small, dense, mostly confused, but arranged in some regular lines laterally, of which one is made of slightly larger punctures. Humeral calli moderately raised. Macropterous. Prosternum with posteriorly open procoxal cavities and large intercoxal prosternal process. Mesosternum very short. First abdominal sternite slightly longer than fifth (Fig. 4B); its central area bordered by ridges is quite wide, slightly narrowing posteriorly. Anterior and middle legs without modifications. Posterior femora greatly swollen ($WF/LF = 0.68$), elongate-subtriangular; posterior tibiae thick, distinctly shorter than femora, apically widened and prolonged into a spur-like process on inner side; outer side of hind tibia apically toothed; apical spur of hind tibiae simple, lanceolate, very elongate; first metatarsomere moderately enlarged. Median lobe of the aedeagus ($LAED = 1.26$ mm; $LE/LAED = 2.54$) (Fig.

4D) with smooth surface; in ventral view thickset, lanceolate but with slightly irregular outline; in lateral view median lobe moderately curved, thicker at the subapical part, with sinuate ventral outline; apex ventrally oriented; dorsal ligula formed by a central lobe medially incised in the apical part, and two thinner lateral lobes; its base at apical $\sim 1/3$.

Variability. Male ($n = 5$; mean and standard deviation; range): LE = 3.08 ± 0.13 mm ($2.88 \leq LE \leq 3.20$ mm); WE = 2.98 ± 0.13 mm ($2.82 \leq WE \leq 3.16$ mm); LP = 0.92 ± 0.06 mm ($0.86 \leq LP \leq 1.00$ mm); WP = 1.98 ± 0.09 mm ($1.88 \leq WP \leq 2.08$ mm); LAN = 1.39 ± 0.15 mm ($1.16 \leq LAN \leq 1.52$ mm); LAED = 1.38 ± 0.09 mm ($1.26 \leq LAED \leq 1.48$ mm); LB = 3.37 ± 0.12 mm ($3.20 \leq LB \leq 3.48$ mm); LE/LP = 3.35 ± 0.11 ($3.20 \leq LE/LP \leq 3.50$); WE/WP = 1.50 ± 0.03 ($1.44 \leq WE/WP \leq 1.53$); WP/LP = 2.16 ± 0.04 ($2.08 \leq WP/LP \leq 2.19$); WE/LE = 0.97 ± 0.03 ($0.94 \leq WE/LE \leq 0.99$); LAN/LB = 0.41 ± 0.04 ($0.35 \leq LAN/LB \leq 0.45$); LE/LAED = 2.24 ± 0.18 ($2.04 \leq LE/LAED \leq 2.54$). Female ($n = 11$; mean and standard deviation; range): LE = 3.35 ± 0.04 mm ($3.32 \leq LE \leq 3.40$ mm); WE = 3.20 ± 0.06 mm ($3.12 \leq WE \leq 3.24$ mm); LP = 1.02 ± 0.03 mm ($0.98 \leq LP \leq 1.04$ mm); WP = 2.10 ± 0.05 mm ($2.02 \leq WP \leq 2.12$ mm); LAN = 1.34 ± 0.08 mm ($1.28 \leq LAN \leq 1.44$ mm); LSPC = 0.40 ± 0.01 mm ($0.38 \leq LSPC \leq 0.40$ mm); LB = 3.66 ± 0.07 mm ($3.58 \leq LB \leq 3.72$ mm); LE/LP = 3.30 ± 0.07 ($3.23 \leq LE/LP \leq 3.39$); WE/WP = 1.53 ± 0.01 ($1.51 \leq WE/WP \leq 1.54$); WP/LP = 2.06 ± 0.04 ($2.04 \leq WP/LP \leq 2.12$); WE/LE = 0.96 ± 0.02 ($0.94 \leq WE/LE \leq 0.98$); LAN/LB = 0.37 ± 0.01 ($0.35 \leq LAN/LB \leq 0.39$); LE/LSPC = 8.49 ± 0.19 ($8.30 \leq LE/LSPC \leq 8.74$).

Male and female paratypes very similar in shape, size, and color to the holotype. The arrangement of elytral punctation in 9 (+ 1 sutural) regular rows is better visible in some specimens. Spermatheca (Fig. 4C) with subcylindrical, sinuate basal part; collum short; apical part moderately elongate, gradually narrowing, slightly wrinkled; ductus subventrally inserted, quite thickset, elongate, U-shaped, uncoiled.

Etymology. The specific epithet refers to the first collector of the new species: Alfred "Fred" Kaiser (1895–1969) from Switzerland, renowned expert on Diptera Syrphidae from Madagascar.

Distribution. Central-Eastern Madagascar (Toamasina province; Fig. 8A). Malagasy chorotype.

Ecological notes. Host plant unknown. Collection localities fall within areas characterized by the vegetation division 'Malagasy Evergreen & Semi-Evergreen Forest'.

***Argopistes laterosinuatus* sp. nov.**

<https://zoobank.org/193ADA5E-1C06-4FB2-9337-AFC426E6D6A3>

Figs 5, 8A

Type material. *Holotype* ♀: "Coll. Mus. Congo / Madagascar: Antakotako / 15.i.1939, J. Vadon" [printed and handwritten on white card] [$15^{\circ}12.53'S$; $49^{\circ}47.61'E$] (RMCA).

Diagnosis. *Argopistes laterosinuatus* sp. nov. is easily recognizable among the Afrotropical *Argopistes* species due to its subovate outline in dorsal view (Fig. 5A) and sinuate sides in lateral view (Fig. 5C). Spermatheca is also diagnostic, due to the combination of pyriform basal part, with a distinct protrusion

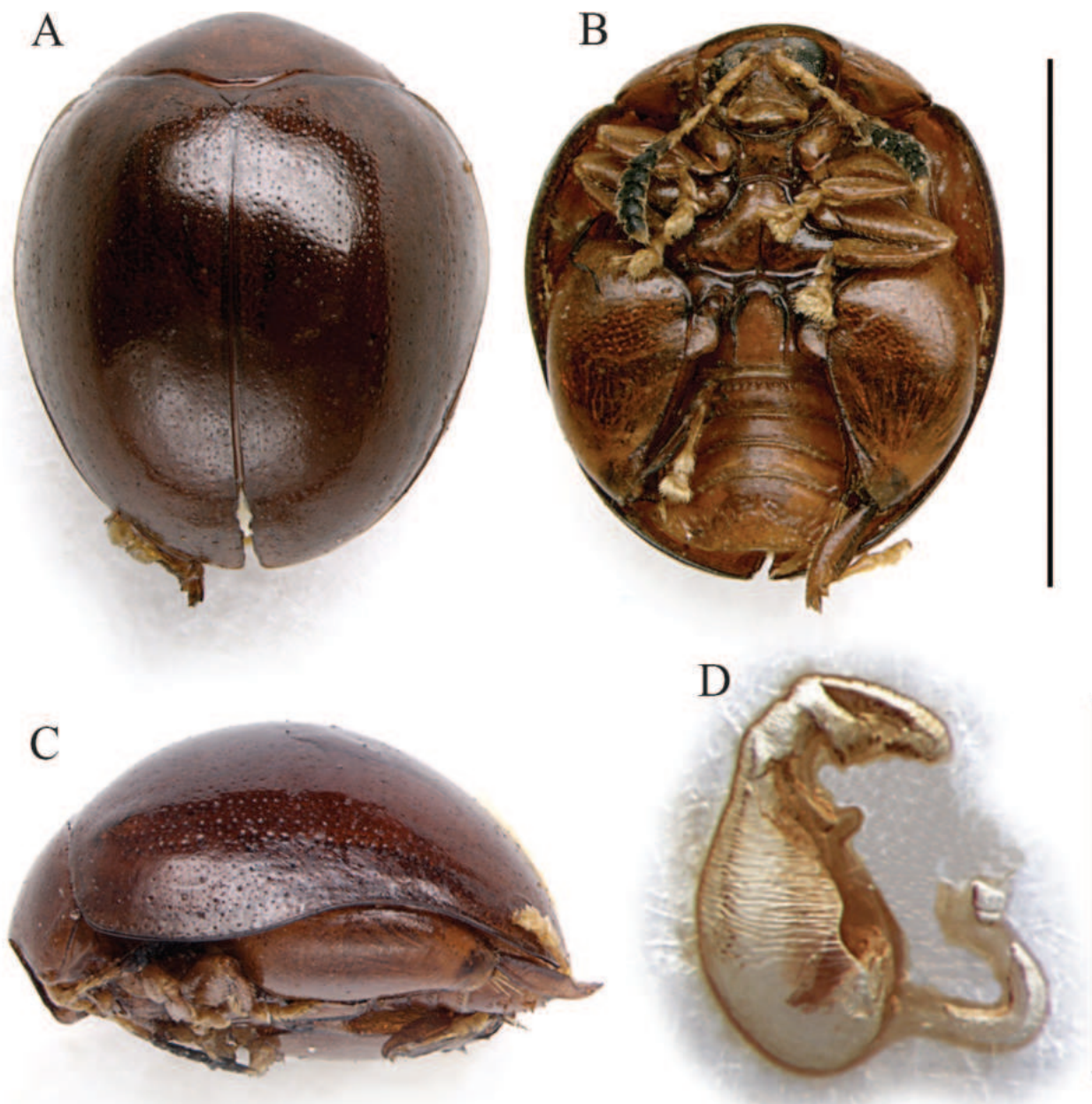


Figure 5. *Argopistes laterosinuatus* sp. nov. **A** holotype, habitus in dorsal view **B** ibid, ventral view **C** ibid, lateral view **D** ibid, spermatheca. Scale bars: 3 mm (**A**, **B**, **C**); 300 μ m (**D**).

close to the collum, apical part clearly narrowing towards the apex, and ductus ventrally inserted, thickset, uncoiled (Fig. 5D).

Description of the holotype (♀). Body largely subovate in dorsal view (Fig. 5A), very convex in lateral view (Fig. 5C); total length of body (LB) = 3.18 mm; maximum pronotal width at the base (WP = 1.80 mm); maximum width of elytra at the basal third (WE = 2.72 mm); WE/WP = 1.51. Dorsal integuments (Fig. 5A) reddish brown with weak metallic reflections; ventral parts (Fig. 5B) light brown; head light brown; frons and mouthparts light brown; antennae (Fig. 5B) with segments 1–5 yellowish, 6 dark brown, 7–10 black, 11 black but distally lighter; legs entirely light brown (Fig. 5B). Head entirely hidden by the pronotum; vertex with small, irregular punctation, and a pair of large setiferous pores; frontal calli

joined, moderately raised, with V-shaped posterior delimitation; frons moderately elongate, flat, roughly microreticulate; frontal ridge short; frontogenal sutures distinctly raised; eyes large, elongate, slightly kidney-shaped; interantennal space clearly narrower than antennal sockets. Antennae (Fig. 5B) clavate, slightly shorter than 1/2 the body length (LAN = 1.36 mm; LAN/LB = 0.43); LA = 100:36:53:47:48:52:44:46:49:52:79. Pronotum (Fig. 5A) strongly transverse (LP = 0.80 mm; WP/LP = 2.25); lateral margins strongly convergent anteriorly and slightly folded ventrally, weakly curved, weakly expanded, not visible in dorsal view; basal margin arcuate and distinctly sinuate; surface finely microreticulate, with very small and dense punctation; surface weakly raised near the lateral margins; a large setiferous pore at the anterior angles. Scutellum small, subtriangular. Elytra (LE = 2.92 mm; LE/LP = 3.65) slightly longer than wide (WE/LE = 0.93), strongly curved laterally in dorsal view (Fig. 5A) and distinctly sinuate in lateral view (Fig. 5C), jointly rounded apically; lateral margins finely bordered, visible in dorsal view; surface subsmooth, with very small and moderately dense, mostly confused punctation; slightly larger punctures are arranged in 9 (+ 1 sutural) regular rows. Humeral calli moderately raised. Macropterous. Prosternum with posteriorly open procoxal cavities and large intercoxal prosternal process. Mesosternum very short. First abdominal sternite approx. as long as fifth (Fig. 5B); its central area bordered by ridges is wide, rounded anteriorly, laterally subparallel. Anterior and middle legs without modifications. Posterior femora greatly swollen (WF/LF = 0.61), elongate-subtriangular; posterior tibiae thick, distinctly shorter than femora, apically widened and prolonged into a spur-like process on inner side; outer side of hind tibia apically toothed; apical spur of hind tibiae simple, lanceolate. Basal part of the spermatheca pyriform, with a distinct ventral protrusion close to the distal part (Fig. 5D); collum short, apical part short, narrowing towards the apex; ductus ventrally inserted, thick-set, moderately elongate, uncoiled; LSPC = 0.32 mm; LE/LSPC = 9.13.

Variability. Only the female holotype of the new species is known so far.

Etymology. The specific epithet refers to the sinuate lateral margin of each elytra, a character absent in all other *Argopistes* species known to date for Madagascar.

Distribution. North-eastern Madagascar (Toamasina province) (Fig. 8A). Malagasy chorotype.

Ecological notes. Host plant unknown. The only known occurrence locality falls within an area characterized by the vegetation division 'Malagasy Evergreen & Semi-Evergreen Forest'.

***Argopistes seyrigi* sp. nov.**

<https://zoobank.org/62E50B82-6B80-4939-9127-07D64E0E9381>

Figs 6, 8A

Type material. *Holotype* ♂: "Coll. Mus Congo. / Madagascar: Mandraka / II.1944 / A. Seyrig" [printed on white card] [18°54.89'S; 47°55.61'E] (RMCA).

Diagnosis. Among the Malagasy *Argopistes* species, *A. seyrigi* sp. nov. shows strong similarities with *Argopistes keiseri* sp. nov. Both have the spur of hind tibiae distinctly elongated, extending significantly beyond the tibial apex (Figs 4B,



Figure 6. *Argopistes seyrigi* sp. nov. **A** holotype, habitus in dorsal view **B** ibid, ventral view **C** ibid, median lobe of the aedeagus. Abbreviations: as: apical spur of hind tibia. Scale bars: 3 mm (**A**, **B**); 500 μ m (**C**).

6B), black dorsal integuments (Figs 4A, 6A), and mostly confused elytral punctation. *Argopistes seyrigi* sp. nov. can be distinguished by the mostly reddish brown abdomen and tibiae (blackish in *A. keiseri* sp. nov.) (Figs 4B, 6B). Median lobe of aedeagus of *A. seyrigi* sp. nov. has a clearly diagnostic value, due to the parallel sides in ventral view and the thinner apical part in lateral view (Fig. 6C).

Description of the holotype (♂). Body roundish in dorsal view (Fig. 6A), strongly convex in lateral view; total length of body (LB) = 3.52 mm; maximum pronotal width at the base (WP = 2.08 mm); maximum width of elytra at the middle (WE = 3.00 mm); WE/WP = 1.44. Dorsal integuments (Fig. 6A) entirely black with evident blueish metallic reflections; ventral parts (Fig. 6B) black, with mostly brownish abdomen; head black; frons and mouthparts black, with yellowish maxillary palpi; antennae yellowish (Fig. 6B); legs with black femora, hind tibiae dark brown, anterior and middle tibiae mostly light brown, and tarsi yellowish (Fig. 6B). Head entirely hidden by the pronotum; vertex punctate, with a pair of large setiferous pores; frontal calli joined, weakly delimited and weakly raised; frons short, roughly wrinkled; frontal ridge thin; frontogenal sutures quite thick and clearly raised; eyes large, elongate, slightly kidney-shaped; interantennal space clearly narrower than antennal sockets. Antennae (Fig. 6B) slightly shorter than 1/2 the body length (LAN = 1.44 mm; LAN/LB = 0.41), filiform; segments 1–2 thicker, segments 3–11 slightly and gradually flattened; LA = 100:46:37:44:40:39:41:43:43:38:75. Pronotum (Fig. 6A) clearly transverse (LP = 0.96 mm; WP/LP = 2.17); lateral margins strongly convergent anteriorly, straight, weakly expanded, not visible in dorsal view; basal margin arcuate and distinctly sinuate; surface microreticulate and micropunctate, with dense, small punctation; surface weakly raised parallel to the lateral margins; a large setiferous pore at the anterior angles. Scutellum small, subtriangular. Elytra (LE = 3.16 mm; LE/LP = 3.29) strongly curved laterally (Fig. 6A), approx. as long as wide (WE/LE = 0.95), jointly rounded apically; lateral margins finely bordered, visible in dorsal view; surface smooth; punctation very small, dense, less impressed than on pronotum, mostly confused, but arranged in some more impressed, barely visible regular lines, laterally. Humeral calli moderately raised. Macropterous. Prosternum with posteriorly open procoxal cavities and large intercoxal prosternal process. Mesosternum very short. First abdominal sternite approx. as long as fifth (Fig. 6B); its central area bordered by ridges is quite narrow, and slightly narrower posteriorly. Anterior and middle legs without modifications. Posterior femora greatly swollen (WF/LF = 0.69), elongate-subtriangular; posterior tibiae thick, distinctly shorter than femora, apically widened and prolonged into a spur-like process on inner side; outer side of hind tibia apically toothed; apical spur of hind tibiae simple, lanceolate, very elongate (Fig. 6B). Median lobe of the aedeagus (LAED = 1.36 mm; LE/LAED = 2.32) (Fig. 6C) with smooth surface; in ventral view lanceolate; in lateral view median lobe thicker in the middle part, moderately curved in the basal part, with sinuate ventral outline and straight apex; dorsal ligula formed by a central lobe, medially incised apically, and two thinner lateral lobes; its base at approx. the middle.

Variability. Only the male holotype of the new species is known so far.

Etymology. The specific epithet refers to the collector of the new species: André Seyrig (1897–1945) from France, an expert on Hymenoptera: Ichneumonidae, and a tireless collector of insects and plants in Madagascar.

Distribution. Central-eastern Madagascar (Antananarivo province; Fig. 8A). Malagasy chorotype.

Ecological notes. Host plant unknown. The only known occurrence locality falls within an area characterized by the vegetation division 'Afromontane Moist Forest'.

***Argopistes vadoni* sp. nov.**

<https://zoobank.org/F6866CF3-7109-43B3-8073-594223862553>

Figs 7, 8A

Type material. *Holotype* ♂: “Coll. Mus. Tervuren / N.E. Madagascar: / Ambo-
divoangy VII.1961/ J. Vadon” [printed on white card] [15°17.30'S; 49°36.88'E]
(RMCA). *Paratype* ♀: “Coll. Mus. Congo / Madagascar: Antakotako / 15.i.1939
/ J. Vadon” [printed on white card] [15°12.53'S; 49°47.61'E] (RMCA).

Diagnosis. *Argopistes vadoni* sp. nov. is one of the species with black or
blackish dorsal integuments, and yellow and filiform antennae, but is distin-
guishable by the regular elytral punctation (Fig. 7A). Median lobe of the ae-
deagus and spermatheca are both diagnostic. Median lobe of the aedeagus
is easily recognizable by the apical part, distinctly slender in ventral view (Fig.
7C). Spermatheca is unique for the combination of pyriform basal part, distal
part homogenously thickened, and ductus subapically inserted, quite thickset,
moderately elongated, and uncoiled (Fig. 7D).

Description of the holotype (♂). Body roundish in dorsal view (Fig. 7A),
strongly convex in lateral view; total length of body (LB) = 3.32 mm; maximum
pronotal width at the base (WP = 2.00 mm); maximum width of elytra in the
middle (WE = 2.84 mm); WE/WP = 1.42. Dorsal integuments (Fig. 7A) entirely
black with weak blueish metallic reflections; ventral parts (Fig. 7B) dark reddish
brown; head dark brown; frons and mouthparts brown, with yellowish maxil-
lary palpi; antennae (Fig. 7B) yellowish; legs, including articulations, reddish
brown, with yellowish tarsi (Fig. 7B). Head entirely hidden by the pronotum;
vertex punctate, with a pair of large setiferous pores; frontal calli joined, clearly
delimited and straight posteriorly; frons elongate, flat, roughly wrinkled; fron-
tal ridge elongate, thin and sharp; frontogenal sutures distinctly raised; eyes
large, elongate, slightly kidney-shaped; interantennal space clearly narrower
than antennal sockets. Antennae (Fig. 7B) filiform, as long as ~ 1/2 the body
length (LAN = 1.76 mm; LAN/LB = 0.53); segments 1 and 2 thicker; segments
3–11 slightly and gradually flattened; LA = 100:42:33:47:47:40:41:44:43:39:64.
Pronotum (Fig. 7A) distinctly transverse (LP = 0.96 mm; WP/LP = 2.08); lateral
margins strongly convergent anteriorly, weakly curved, weakly expanded, not
visible in dorsal view; basal margin arcuate and distinctly sinuate; surface finely
wrinkled, with very dense, small punctation; surface weakly raised parallel to
the lateral margins; a large setiferous pore at the anterior angles. Scutellum
small, subtriangular. Elytra (LE = 2.98 mm; LE/LP = 3.10) strongly curved later-
ally (Fig. 7A), approx. as long as wide (WE/LE = 0.95), jointly rounded apically;
lateral margins finely bordered, visible in dorsal view; surface micropunctate;
main punctation small, arranged in 9 (+ 1 sutural) regular rows, more confused
along lateral parts. Humeral calli moderately raised. Macropterous. Prosternum
with posteriorly open procoxal cavities and large intercoxal prosternal process.
Mesosternum very short. First abdominal sternite (Fig. 7B) slightly longer than
fifth; its central area bordered by ridges is wide, subovate. Anterior and middle
legs without modifications. Posterior femora greatly swollen (WF/LF = 0.67),
elongate-subtriangular; posterior tibiae thick, distinctly shorter than femora,
apically widened and prolonged into a spur-like process on inner side; outer
side of hind tibia apically toothed; apical spur of hind tibiae simple, lanceolate;
first metatarsomere moderately enlarged. Median lobe of the aedeagus (LAED

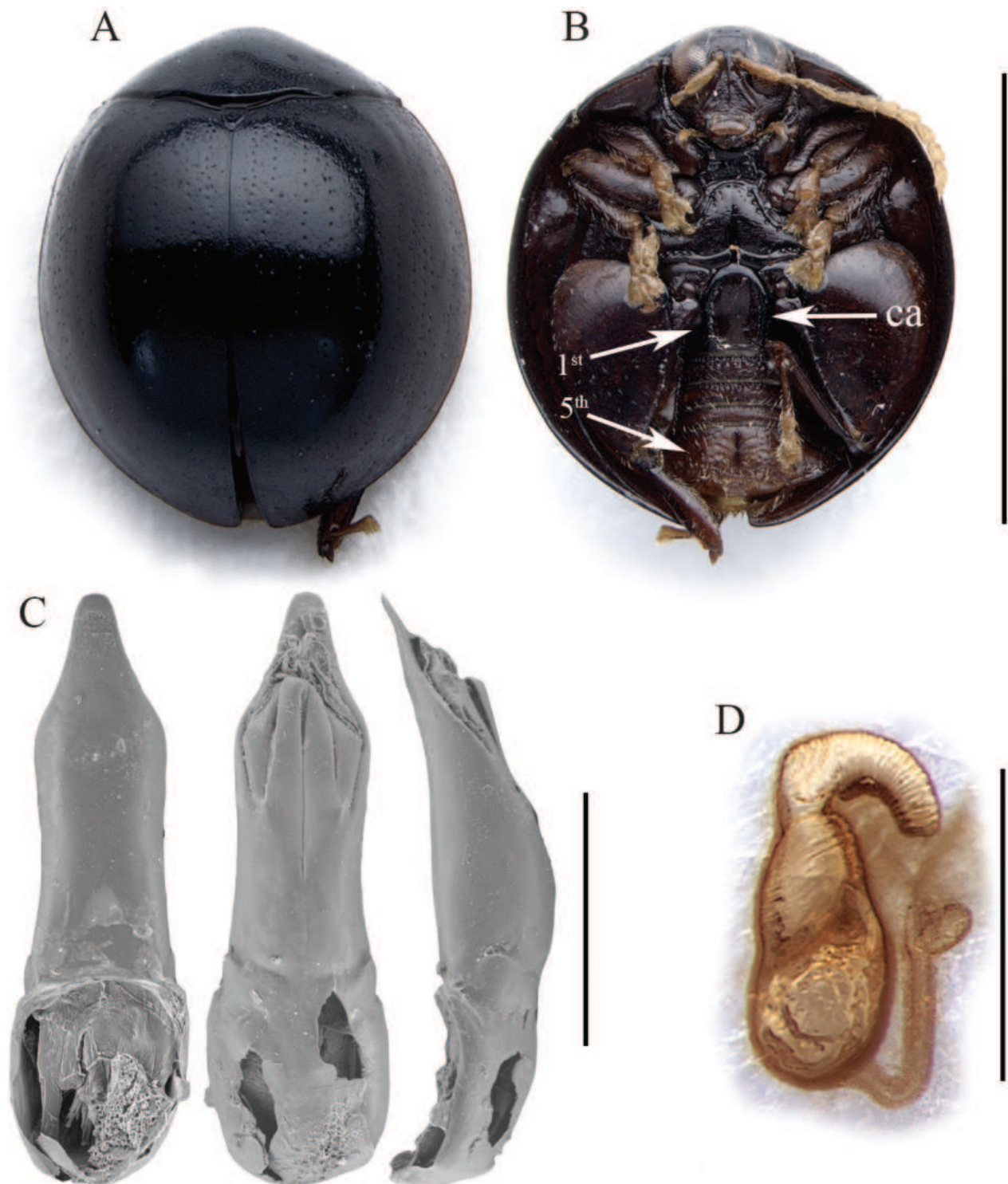


Figure 7. *Argopistes vadoni* sp. nov. **A** holotype, habitus in dorsal view **B** ibid, ventral view **C** ibid, median lobe of the aedeagus **D** spermatheca, from Antakotako. Abbreviations: 1st: first abdominal sternite; 5th: fifth abdominal sternite; ca: central area of the first abdominal sternite bordered by ridges. Scale bars: 3 mm (**A**, **B**); 500 μ m (**C**); 300 μ m (**D**).

= 1.24 mm; LE/LAED = 2.40) (Fig. 7C) with smooth surface; widest at the basal opening in ventral view, slightly curved inwardly; distal part distinctly thinner, sides convergent towards the rounded apex; in lateral view median lobe weakly curved, thicker in the central third; dorsal ligula formed by a central lobe, medially incised, and two lateral lobes; its base at apical $\sim 1/3$.

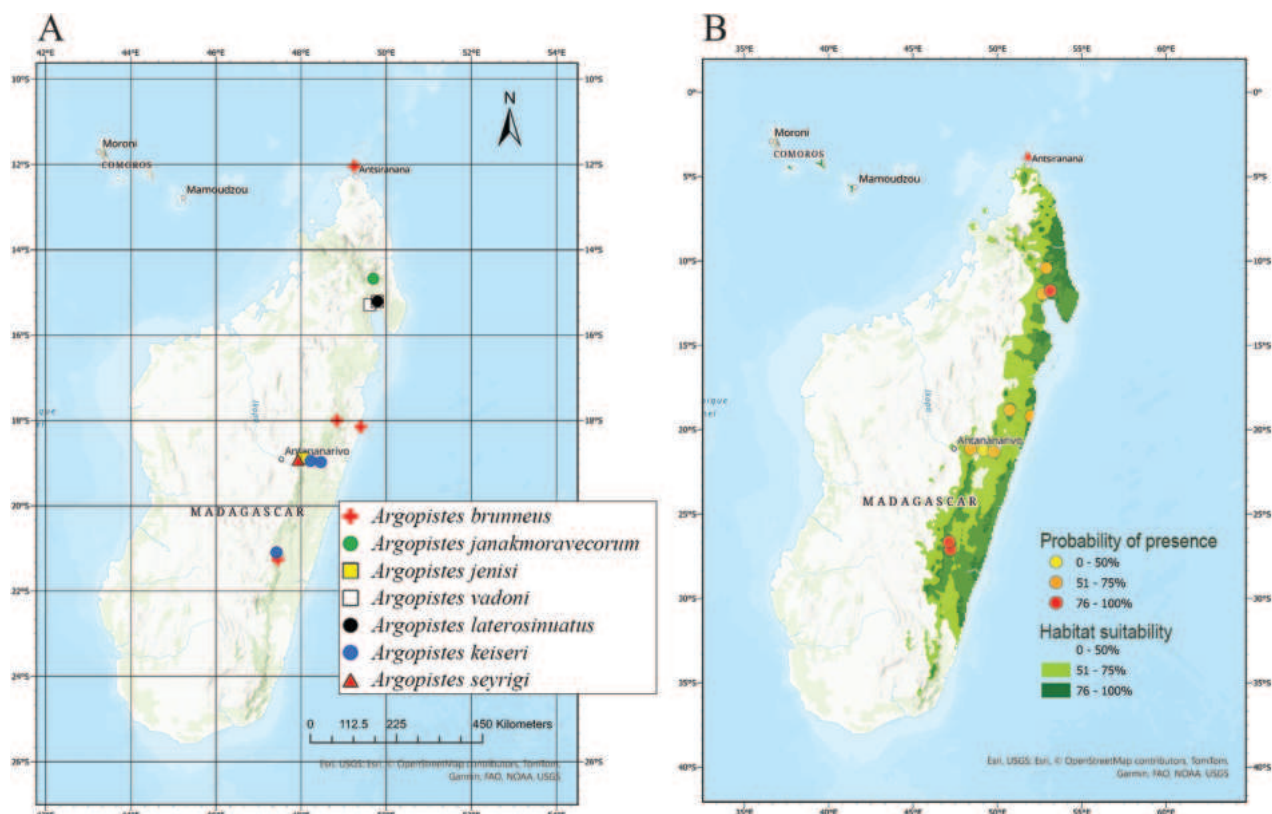


Figure 8. Distribution and habitat suitability of the *Argopistes* species in Madagascar. **A** occurrence locality for each species **B** probability of presence of the occurrence localities, and potential suitability areas for the genus in Madagascar from ENMs.

Variability. Female paratype very similar in shape and color to the holotype. LE = 3.40 mm; WE = 3.16 mm; LP = 1.00 mm; WP = 2.12 mm; LAN = 1.72 mm; LSPC = 0.34 mm; LB = 3.60 mm; LE/LP = 3.40; WE/WP = 1.49; WP/LP = 2.12; WE/LE = 0.93; LAN/LB = 0.48; LE/LSPC = 10.00. First metatarsomere in female not enlarged. Spermatheca (Fig. 7D) apparently wrinkled on most surface; basal part pyriform; collum short; distal part moderately elongate, apically truncate; ductus subapically inserted, quite thickset, moderately elongate, uncoiled.

Etymology. The specific epithet refers to the collector of the new species: Jean Vadon (1904–1970) from France, one of the fathers of the entomological research in Madagascar.

Distribution. Northern-eastern Madagascar (Toamasina province; Fig. 8A). Malagasy chorotype.

Ecological notes. Host plant unknown. The two known occurrence localities fall within areas characterized by the vegetation division ‘Malagasy Evergreen & Semi-Evergreen Forest’.

Key to species

- 1 Antennae clavate, with segments 6–11 clearly dilated and strongly blackened (Figs 2B, 5B) **2**
- Antennae filiform, at most with gradually enlarged distal segments, entirely yellowish (Figs 1B, 3B, 4B, 6B, 7B)..... **3**

- 2 Body shape roundish. Dorsal integuments black. Elytral sides not sinuate in lateral view. Elytral punctation with dense and small punctures on the disc, without evident regular rows (Fig. 2A). Spermatheca with subpyriform basal part; ductus elongate, distally clearly coiled (Fig. 2C). Male unknown.....***Argopistes janakmoravecorum* sp. nov.** (Figs 2, 8A)
- Body shape subovate, more elongate. Dorsal integuments reddish brown. Elytral sides distinctly sinuate in lateral view (Fig. 5C). Elytral punctation with sparser but larger punctures on the disc, with hints of 9 (+ 1 sutural) regular rows (Fig. 5A, C). Spermatheca with pyriform basal part; ductus shorter, uncoiled (Fig. 5D). Male unknown***Argopistes laterosinuatus* sp. nov.** (Figs 5, 8A)
- 3 Apical spur of hind tibiae distinctly elongate, extending significantly beyond the tibial apex (as in Figs 4, 6).....**4**
- Apical spur of hind tibiae shortly extending beyond the tibial apex (as in Fig. 1)**5**
- 4 Dorsal integuments intense black with weak metallic reflections; abdomen and tibiae blackish (Fig. 4B). Median lobe of the aedeagus thickset, clearly sinuate in lateral view (Fig. 4D). Spermatheca with subcylindrical, sinuate basal part; ductus elongate, subapically oriented, uncoiled (Fig. 4C)***Argopistes keiseri* sp. nov.** (Figs 4, 8A)
- Dorsal integuments black but with clear blueish metallic reflections; abdomen and tibiae mostly reddish brown (Fig. 6B). Median lobe of aedeagus slender, in lateral view with narrow and straight apical part (Fig. 6C). Female unknown***Argopistes seyrigi* sp. nov.** (Figs 6, 8A)
- 5 Elytra in dorsal view with slightly parallel lateral margins (Fig. 1A, B). Central area of the first abdominal sternite bordered by ridges is narrow, subrhomboidal (ca: Fig. 1B). Dorsal integuments variable, black to at least partially reddish brown, especially on pronotum; sometimes elytra black with brown elytral patches (Fig. 1A, C). Median lobe of the aedeagus tapered towards the apex in ventral view (Fig. 1D). Spermatheca with subcylindrical, dorsally enlarged basal part; ductus thin, short, subapically oriented (Fig. 1E)***Argopistes brunneus* Weise** (Figs 1, 8A)
- Elytra in dorsal view, with clearly rounded lateral margins (Figs 3A, B, 7A, B). Central area of the first abdominal sternite bordered by ridges is wide, laterally subparallel (ca: Figs 3A, 7A). Dorsal integuments entirely black (Figs 3B, 7B). Median lobe of the aedeagus and/or spermatheca differently shaped**6**
- 6 Elytral punctation small, dense, almost completely unordered (Fig. 3A). Dorsal integuments, ventral integuments, and legs intense black with evident blueish metallic reflections, except the yellowish tarsi (Fig. 3A, B). First abdominal sternite distinctly shorter than fifth (Fig. 3B). Basal part of the spermatheca subglobose, ventrally enlarged; distal part gradually narrowed apically (Fig. 3C). Male unknown.....***Argopistes jeni* sp. nov.** (Figs 3, 8A)
- Elytral punctation with larger punctures ordered in regular rows (Fig. 7A). Dorsal integuments black; ventral integuments and legs brownish, except the yellowish tarsi (Fig. 7B). First abdominal sternite distinctly longer than fifth (Fig. 7B). Spermatheca (Fig. 7D) with pyriform basal part; distal part not narrowed apically. Apical part of the median lobe of aedeagus distinctly slender in ventral view (Fig. 7C) ...***Argopistes vadoni* sp. nov.** (Figs 7, 8A)

Habitat suitability

VIF and Pearson's correlation analyses returned a set of nine uncorrelated bioclimatic variables which were then used to calibrate the models: BIO2, BIO3, BIO8, BIO9, BIO13, BIO14, BIO15, BIO18, and BIO19. The ensemble models for the genus *Argopistes* (Fig. 8) resulted in high performance scores (AUC = 0.899 and CBI = 0.754), indicating a continuous area of habitat suitability in the Eastern part of Madagascar, a region characterized in particular by vegetation formations (cf. Sayre et al. 2013) such as the 'Tropical Lowland Humid Forest' in the central area, mainly with the 'Malagasy Evergreen & Semi-Evergreen Forest' division, and to a lesser extent the 'Tropical Seasonally Dry Forest' to the north, with the 'Malagasy Dry Deciduous and Evergreen Forest and Woodland' division. Based on our model, in Madagascar the areas with high habitat suitability for the genus *Argopistes* are characterized by: a) mean diurnal range temperature (BIO2) with values between 5 and 10 °C; b) mean temperature of wettest quarter (BIO8) between 12 and 24 °C; c) precipitation of wettest month (BIO13) not exceeding 500 mm; d) coefficient of variation (BIO15), as a measure of precipitation inter-annual variability, lower than 30%. Therefore, the western part of Madagascar does not offer optimal conditions for the occurrence of *Argopistes* species (Fig. 8B).

Discussion

Based on our revision, *Argopistes* is present in Madagascar with seven endemic species.

The six new *Argopistes* species here described unequivocally display the typical characters of the genus (Biondi and D'Alessandro 2012; Nadein 2015): body ovate to rounded in dorsal view, strongly convex in lateral view; head generally entirely hidden by the pronotum; antennae short, their length not exceeding 1/2 of the body length; head opisthognathous; eyes very large, kidney-shaped; antennal sockets very close to each other, their distance generally shorter than their diameter; frontogenal sutures (edges of antennal grooves) distinctly raised, often more evident than frontal ridge; frontal calli medially jointed, usually distinctly delimited from vertex; vertex with a pair of large setiferous pores; pronotum always covered with punctures, without evident grooves and impressions; posterior edge clearly bisinuate; scutellum visible, subtriangular; elytra glabrous, with small punctation, confused or arranged in regular striae; epipleura orientation subvertical; prosternum with posteriorly open procoxal cavities and large intercoxal prosternal process; mesosternum very short; central area of the first abdominal sternite bordered by ridges; anterior and middle legs without special modifications; posterior femora considerably swollen, elongate-subtriangular; posterior tibiae thick, short, apically widened and prolonged into a spur-like process on inner side; outer side of hind tibia apically toothed; apical spur of hind tibiae simple, evident. Based on the general body shape, *Argopistes* species are apparently very similar to Coccinellidae, especially of the genus *Exochomus* Redtenbacher, as Motschulsky (1860) highlighted.

Argopistes janakmoravecorum sp. nov. and *A. laterosinuatus* sp. nov. show clear similarities based on the antennal and spermathecal morphology (Figs 2B, C, 5B, D). Some of the spermathecal characters, such as the general shape of

the distal part and a more or less evident, apparently cup-shaped formation on the basal part (Figs 2C, 5D), are present in other *Argopistes* species, also outside the Afrotropical region (Blanco and Konstantinov 2013). However, the clavate and blackened antennae are unique, making the two species taxonomically isolated from the remaining Malagasy and sub-Saharan *Argopistes* species.

Based on the available ecological data, Asian and New World *Argopistes* species and many Afrotropical species are associated with Oleaceae (Blanco and Konstantinov 2013). In sub-Saharan Africa, *Argopistes* species are primarily associated with Olive trees [*Olea europaea* var. *africana* (Mill.)], on which larvae are leaf miners, and adults are defoliators (Biondi and D'Alessandro 2012; Hlaka et al. 2022). No ecological data are available for the Malagasy species. However, based on our habitat suitability model, the western part of Madagascar does not offer optimal conditions for their occurrence (Fig. 8B). Indeed, Malagasy species are distributed in the central and eastern areas of the Island (Fig. 8A). It must be emphasized that Madagascar has been interested in a significant loss of natural habitats over decades so that species described on preserved specimens collected a long time ago might have become rare or even locally extinct (Goodman 2022). That makes it crucial to document Malagasy biodiversity as soon as possible and check its status through field campaigns. Following that principle, in this contribution, we described new species even on single males or females, being confident in the reliability of the diagnostic value of the illustrated characters.

Acknowledgments

We are grateful to the collection managers and curators who enabled us to study their material: Matthias Borer (NHMB), Didier Van den Spiegel and Stéphane Hanot (RMCA), and Joachim Willers (ZMHB). We are also obliged to Jan Bezděk, whose suggestions improved the quality of the manuscript.

Additional information

Conflict of interest

The authors have declared that no competing interests exist.

Ethical statement

No ethical statement was reported.

Funding

No funding was reported.

Author contributions

Conceptualization: MB, PD. Data curation: PD, MB, MI. Formal analysis: MI, MB. Methodology: MB, PD. Resources: MI, MB, PD. Writing - original draft: MB. Writing - review and editing: MI, PD, MB.

Author ORCIDs

Maurizio Biondi  <https://orcid.org/0000-0002-4481-9152>

Mattia Iannella  <https://orcid.org/0000-0003-4695-0194>

Paola D'Alessandro  <https://orcid.org/0000-0002-4481-9152>

Data availability

All of the data that support the findings of this study are available in the main text.

References

- Andriamialisoa F, Langrand O (2022) The History of Zoological Exploration of Madagascar. In: Goodman SM (Ed.) The new natural history of Madagascar, Vol. 1. Princeton University Press, New Jersey, 44 pp. <https://doi.org/10.1515/9780691229409-007>
- Biondi M, D'Alessandro P (2006) Biogeographical analysis of the flea beetle genus *Chaetocnema* in the Afrotropical Region: Distribution patterns and areas of endemism. *Journal of Biogeography* 33(4): 720–730. <https://doi.org/10.1111/j.1365-2699.2006.01446.x>
- Biondi M, D'Alessandro P (2012) Afrotropical flea beetle genera: A key to their identification, updated catalogue and biogeographical analysis (Coleoptera, Chrysomelidae, Galerucinae, Alticini). *ZooKeys* 253: 1–158. <https://doi.org/10.3897/zookeys.253.3414>
- Biondi M, D'Alessandro P (2013a) The genus *Chabria* Jacoby: First records in the Afrotropical region with description of three new species from Madagascar and annotated worldwide species catalogue (Coleoptera, Chrysomelidae, Galerucinae, Alticini). *Zoologischer Anzeiger* 252(1): 88–100. <https://doi.org/10.1016/j.jcz.2012.03.005>
- Biondi M, D'Alessandro P (2013b) *Ntaolaltica* and *Pseudophygasia*, two new flea beetle genera from Madagascar (Coleoptera: Chrysomelidae: Galerucinae: Alticini). *Insect Systematics & Evolution* 44(1): 93–106. <https://doi.org/10.1163/1876312X-04401004>
- Biondi M, D'Alessandro P (2016) Revision of *Diphaulacosoma* Jacoby, an endemic flea beetle genus from Madagascar, with description of three new species (Coleoptera: Chrysomelidae, Galerucinae, Alticini). *Fragmenta Entomologica* 48(2): 14–151. <https://doi.org/10.4081/fe.2016.181>
- Blanco J, Konstantinov A (2013) Review of the New World species of the genus *Argopistes* Motschulsky (Coleoptera: Chrysomelidae: Galerucinae: Alticini). *Zootaxa* 3636(2): 249–267. <https://doi.org/10.11646/zootaxa.3626.2.3>
- D'Alessandro P, Urbani F, Biondi M (2014) Biodiversity and biogeography in Madagascar: Revision of the endemic flea beetle genus *Neoderes* Duvivier, 1891 with description of 19 new species (Coleoptera, Chrysomelidae, Galerucinae, Alticini). *Systematic Entomology* 39(4): 710–748. <https://doi.org/10.1111/syen.12082>
- Di Cola V, Broennimann O, Petitpierre B, Breiner FT, d'Amen M, Randin C, Engler R, Pottier J, Pio D, Dubuis A, Pellissier L, Mateo RG, Hordijk W, Salamin N, Guisan A (2017) ecospat: An R package to support spatial analyses and modeling of species niches and distributions. *Ecography* 40(6): 774–787. <https://doi.org/10.1111/ecog.02671>
- Döberl M (1986) Die Spermathek als Bestimmungshilfe bei den Alticinen. *Entomologische Blätter für Biologie und Systematik der Käfer* 82(1–2): 3–14.
- Dormann CF (2007) Effects of incorporating spatial autocorrelation into the analysis of species distribution data. *Global Ecology and Biogeography* 16(2): 129–138. <https://doi.org/10.1111/j.1466-8238.2006.00279.x>
- Douglas HB, Konstantinov AS, Brunke AJ, Moseyko AG, Chapados JT, Eyres J, Richter R, Savard K, Sears E, Prathapan KD, Ruan Y, Dettman JR (2023) Phylogeny of the flea beetles (Galerucinae: Alticini) and the position of *Aulacothorax* elucidated through anchored phylogenomics (Coleoptera: Chrysomelidae: Alticini). *Systematic Entomology* 48(3): 361–386. <https://doi.org/10.1111/syen.12582>
- Elith J, Graham CH, Anderson RP, Dudik M, Ferrier S, Guisan A, Hijmans RJ, Huettmann F, Leathwick JR, Lehmann A, Li J, Lohmann LG, Loiselle BA, Manion G, Moritz C, Na-

- kamura M, Nakazawa Y, Overton JM, Peterson AT, Phillips SJ, Richardson K, Scachetti-Pereira R, Schapire RE, Soberón J, Williams S, Wisz MS, Zimmermann NE (2006) Novel methods improve prediction of species' distributions from occurrence data. *Ecography* 29(2): 129–151. <https://doi.org/10.1111/j.2006.0906-7590.04596.x>
- ESRI (2023) ArcGIS Pro 3.2. ESRI, Redlands, California.
- Evenhuis NL (2023) The insect and spider collections of the world website. <http://hbs.bishopmuseum.org/codens/> [accessed 06 March 2024]
- Fick SE, Hijmans RJ (2017) WorldClim 2: New 1-km Spatial Resolution Climate Surfaces for Global Land Areas. *International Journal of Climatology* 37(12): 4302–4315. <https://doi.org/10.1002/joc.5086>
- Goodman SM (2022) The new natural history of Madagascar, Vols 1, 2. Goodman SM (Ed.) Princeton University Press, New Jersey, [xxviii +] 2246 pp. <https://doi.org/10.1515/9780691229409>
- Guisan A, Thuiller W, Zimmermann NE (2017) Habitat suitability and distribution models: with applications in R. Cambridge University Press, Cambridge, UK, 478 pp. <https://doi.org/10.1017/9781139028271>
- Hirzel AH, Le Lay G, Helfer V, Randin C, Guisan A (2006) Evaluating the ability of habitat suitability models to predict species presences. *Ecological Modelling* 199(2): 142–152. <https://doi.org/10.1016/j.ecolmodel.2006.05.017>
- Hlaka V, Biondi M, Allsopp E, van Asch B (2022) *Argopistes sexvittatus* and *Argopistes capensis* (Chrysomelidae: Alticini): mitogenomics and phylogeny of two flea beetles affecting Olive trees. *Genes* 13(12): 2195. <https://doi.org/10.3390/genes13122195>
- Iannella M, D'Alessandro P, Biondi M (2019) Entomological knowledge in Madagascar by GBIF datasets: Estimates on the coverage and possible biases (Insecta). *Fragmenta Entomologica* 51(1): 1–10. <https://doi.org/10.4081/fe.2019.329>
- Leroy B, Delsol R, Hugueny B, Meynard CN, Barhoumi C, Barbet-Massin M, Bellard C (2018) Without quality presence–absence data, discrimination metrics such as TSS can be misleading measures of model performance. *Journal of Biogeography* 45(9): 1994–2002. <https://doi.org/10.1111/jbi.13402>
- Letsch H, Beran F (2023) Jumping to new hosts: the diversification of flea beetles (Coleoptera: Chrysomelidae: Alticini) in the context of their host plant associations. *Insect Systematics and Diversity* 7(5)2: 1–12. <https://doi.org/10.1093/isd/ixad019>
- Motschulsky V (1860) Coléoptères de la Sibérie et en particulier des rives de l'Amour. In: Schrenck L von (Ed.) *Reisen ind Forschungen im Amurlande* Vol. 2, St. Petersburg, 79–257.
- Nadein KS (2015) Phylogeny of Diboliina inferred from a morphologically based cladistic analysis (Coleoptera: Chrysomelidae: Galerucinae). *Arthropod Systematics & Phylogeny* 73(1): 65–83. <https://doi.org/10.3897/asp.73.e31816>
- Naimi B (2017) Usdm: Uncertainty Analysis for Species Distribution Models. R Package Version 1.1–15. R Documentation. <http://www.rdocumentation.org/packages/usdm>
- Phillips SJ, Anderson RP, Schapire RE (2006) Maximum entropy modeling of species geographic distributions. *Ecological Modelling* 190(3–4): 231–259. <https://doi.org/10.1016/j.ecolmodel.2005.03.026>
- Sayre RG, Comer P, Hak J, Josse C, Bow J, Warner H, Larwanou M, Kelbessa E, Bekele T, Kehl H, Amena R, Andriamasimanana R, Ba T, Benson L, Boucher T, Brown M, Cress J, Dassering O, Friesen B, Gachathi F, Houcine S, Keita M, Khamala E, Marangu D, Mokua F, Morou B, Mucina L, Mugisha S, Mwavu E, Rutherford M, Sanou P, Syampungani S, Tomor B, Vall A, Van de Weghe J, Wangui E, Waruingi L (2013) A New Map of Stan-

- Standardized Terrestrial Ecosystems of Africa. Association of American Geographers, Washington, DC, USA, 24 pp.
- Schmitt M, Neumann A, Lin S-W (2023) Anatomy of male and female genitalia of *Acanthoscelides obtectus* (Say, 1831) (Coleoptera, Chrysomelidae, Bruchinae) in interaction. In: Chaboo CS, Schmitt M (Eds) Research on Chrysomelidae 9. ZooKeys 1177: 75–85. <https://doi.org/10.3897/zookeys.1177.101621>
- Suzuki K (1988) Comparative morphology of the internal reproductive system of the Chrysomelidae (Coleoptera). In: Jolivet P, Petitpierre E, Hsiao TH (Eds) Biology of Chrysomelidae. Kluwer Academic Publishers, Dordrecht, The Netherlands, 317–355. https://doi.org/10.1007/978-94-009-3105-3_19
- Weise J (1895) Neue Chrysomeliden nebst synonymischen Bemerkungen. Deutsche Entomologische Zeitschrift 1895: 327–352. <https://doi.org/10.1002/mmnd.48018950222>

Contribution to the Chinese *Intybia* Pascoe, 1866 (Coleoptera, Melyridae, Malachiinae), with descriptions of two new species groups and one new species

Yuqi Wang^{1,2}, Zhiqiang Li¹, Ping You², Zhenhua Liu¹

¹ Guangdong Key Laboratory of Animal Conservation and Resource Utilization, Guangdong Public Laboratory of Wild Animal Conservation and Utilization, Institute of Zoology, Guangdong Academy of Sciences, Guangzhou 510260, China

² College of Life Science, Shaanxi Normal University, Xi'an, 710062, China

Corresponding author: Ping You (youping@snnu.edu.cn); Zhenhua Liu (liuzhh_beetle@giz.gd.cn)

Abstract

A contribution to the knowledge of the malachiine genus *Intybia* Pascoe, 1866 from China is given. Two new species groups: *Intybia klapperichi* group and *Intybia eversi* group are defined and described. A new species, *Intybia hainanensis* Wang & Liu, **sp. nov.**, of the *Intybia klapperichi* group is described from Hainan Province. *Intybia erectodentatus* (Wittmer, 1982) and *Intybia concha* Asano, 2015 are redescribed based on new materials collected in mainland China. A key to species groups of the genus *Intybia* Pascoe, 1866 in China is provided.

Key words: Apalochrini, Cleroidea, Hainan, key, redescription, taxonomy



Academic editor: Christopher Majka

Received: 18 November 2023

Accepted: 29 April 2024

Published: 27 May 2024

ZooBank: <https://zoobank.org/59192542-ADBE-4518-855E-E06EE35827A4>

Citation: Wang Y, Li Z, You P, Liu Z (2024) Contribution to the Chinese *Intybia* Pascoe, 1866 (Coleoptera, Melyridae, Malachiinae), with descriptions of two new species groups and one new species. ZooKeys 1202: 329–341. <https://doi.org/10.3897/zookeys.1202.115935>

Copyright: © Yuqi Wang et al.
This is an open access article distributed under terms of the Creative Commons Attribution License (Attribution 4.0 International – CC BY 4.0).

Introduction

The genus *Intybia* Pascoe, 1866 belongs to the tribe Apalochrini of malachiine Melyridae, which is represented by about 170 species from the Asiatic region, making it one of the most diverse genera within the tribe Apalochrini (Wittmer 1997; Plonski 2013; Tshernyshev 2016; Ikeda and Yoshitomi 2017). It is characterized by the following characters: antenna with scape and antennomere 3 dilated and modified in the male; fore leg with tarsus and tibia simple in the male, tarsal formula 5–5–5; and pronotum without bead along lateral or posterior margins. Initially, most species of Apalochrini were included in *Laius* Guérin-Méneville, 1830 (Macleay 1872; Blackburn 1888; Lea 1909). Champion (1921) treated *Intybia* as a subgenus of *Laius*, until Evers (1994) re-diagnosed *Laius* and recognized *Intybia* as an independent genus. This treatment was followed by most researchers, and subsequently, a considerable number of species were transferred from *Laius* to *Intybia* (Wittmer 1995, 1997, 1999; Yoshitomi and Lee 2010; Plonski 2013, 2014a, 2014b; Plonski and Geiser 2014). Plonski and Geiser (2014) and Plonski (2016) divided *Intybia* into 11 species groups mainly based on colouration. A new subgenus, *Intybia (Protolaius)* Tshernyshev, 2020 was described for several species of the *Intybia lombokana* group based on male characters of the fore femora

(Tshernyshev 2020). Tshernyshev (2015) established a new genus, *Troglointybia* Tshernyshev, 2015, for a few species of *Intybia* with a sculptured head; more species from Southeast Asia were transferred to this genus by Tshernyshev (2016). Plonski (2016) suggested eyestalks as the autapomorphy of *Troglointybia* and transferred most species back to *Intybia*, leaving only four species in *Troglointybia*.

Research on the genus *Intybia* is relatively abundant in some Asian regions, including Japan (Ikeda and Yoshitomi 2017; Asano 2021), Philippines (Plonski 2014b; Tshernyshev 2016), the Himalaya region (Tshernyshev 2015) and Indonesia (Wittmer 1995). In China, there are approximately 28 recorded species of the genus *Intybia*, most of which were described by Wittmer (1955, 1956, 1982, 1995, 1996, 1997) and Pic (1907, 1910, 1919, 1921, 1927). According to Plonski (2016), most species of Chinese *Intybia* can be assigned to five species groups: *Intybia guttata* group, *Intybia pelegri* group, *Intybia picta* group, *Intybia rubrithorax* group and *Intybia venusta* group. While *Intybia klapperichi* (Hicker, 1949), *Intybia erectodentatus* (Wittmer, 1982), *Intybia eversi* (Hicker, 1949) and *Intybia concha* Asano, 2015 are not assignable to any species group described by Plonski (2016) based on specimens and original descriptions; thus, two new species groups are described here. One new species collected from Hainan Province, similar to *Intybia klapperichi* and *Intybia erectodentatus*, is also described.

Material and methods

Intybia specimens involved in this study are deposited in the following institutions: **IZGAS**—Institute of Zoology, Guangdong Academy of Sciences, Guangzhou, China; **ZFMK**—Zoologisches Forschungsmuseum Alexander Koenig, Bonn, Germany.

Specimens for dissections were cleared in a 10% solution of KOH for about 10 h at room temperature. The abdomen with the aedeagus was transferred to a cavity slide using fine forceps and the aedeagus was separated from the abdomen using a hooked, fine dissecting needle. Specimens were mounted on cards with white emulsion glue. Genitalia and terminal abdominal segments are preserved in genitalia vials with glycerol.

The habitus images were captured using a Canon 7D DSLR camera, Canon MP-E 65 mm macro lens and Mitutoyo 5× objective lens, mounted on a WeMacro Focus Stacking Rail, with Helicon Remote 3.9.10 and WeMacro software for focus stacking. Male genitalia were photographed using a Zeiss AxioCam HRC digital camera mounted on a Zeiss AX10 compound microscope with the Axio Vision SE64 4.8 software. Layered images of the male genitalia were stacked in Helicon Focus software and edited in Photoshop CC 2022.

The morphological terms used in this paper follow Lawrence and Ślipiński (2013). Measurements were made as follows: body length—from the apical edge of the clypeus to the apex of the elytra; pronotal length—median line from the anterior margin to the posterior margin; pronotal width—maximum width of the pronotum; elytral length—from the base of the scutellum to the elytral apex along the suture; elytral width—maximum width across the elytra.

Taxonomy

Melyridae Leach, 1815

Malachiinae Fleming, 1821

Intybia klapperichi group

Diagnosis. Body size small (less than 2.5 mm). Head black with anterior area yellow, pronotum and elytra entirely black; antenna with basal three segments yellow, antennomeres 4–11 brownish to dark brown; legs yellow with basal 4/5 of femora brown to black (Figs 1A, D, 3A, B). Vestiture of short whitish setae. Dorsal surface without distinct punctuation. Antennomere 3 suboval, with projection along inner edge (Figs 1C, 3D). Pronotum transverse, slightly constricted at base.

Included species. *Intybia erectodentatus* (Wittmer, 1982), *Intybia hainanensis* Wang & Liu, sp. nov., *Intybia klapperichi* (Hicker, 1949).

Distribution. Only known from China: Fujian, Guangdong, Hainan, Taiwan.

Intybia hainanensis Wang & Liu, sp. nov.

<https://zoobank.org/C25966F5-97F1-4B7F-9278-6A67E63296B0>

Figs 1, 2A–C

Type material. Holotype: CHINA • ♂; Hainan, Ledong, Jianfengling; 18.731273°N, 108.873082°E; 17 Mar. 2021; Yuchen Zhao leg; IZGAS. **Paratype:** • 1 ♂; same data as for holotype.

Diagnosis. This species is similar to *Intybia erectodentatus* (Wittmer, 1982) and *Intybia klapperichi* (Hicker, 1949) in body shape and colouration. It can be easily recognized by the shape of antennomere 3 (Fig. 1C), whose inner protrusion is pointed apically (blunt in the other two species).

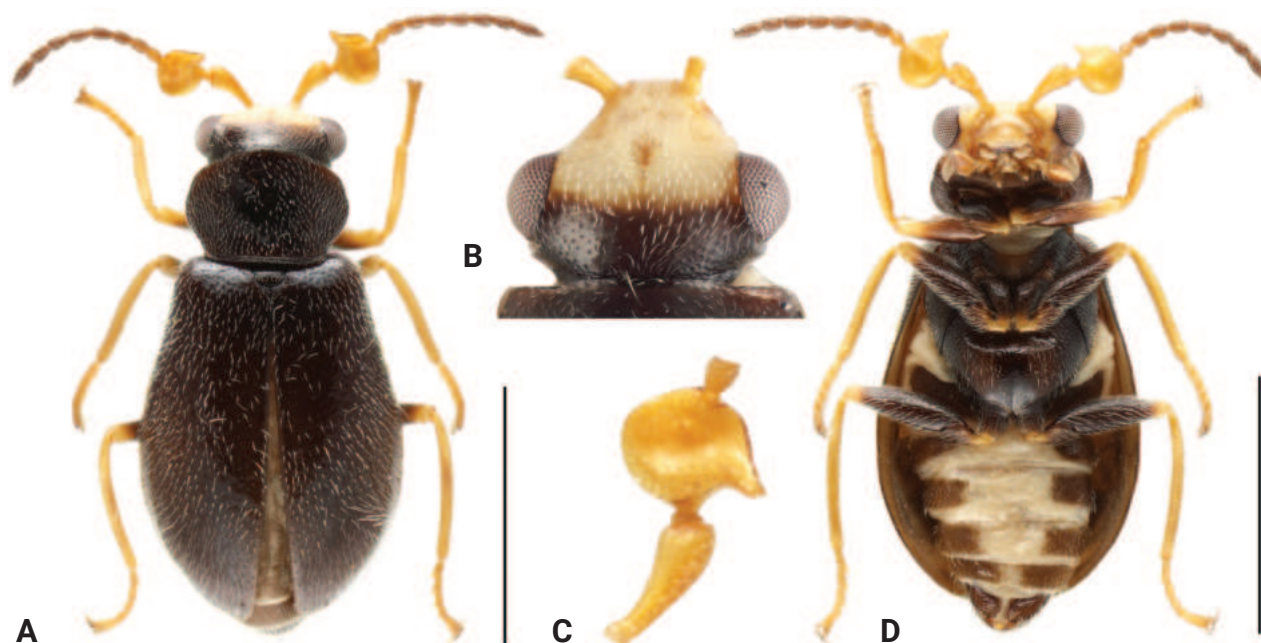


Figure 1. *Intybia hainanensis* sp. nov., holotype **A** habitus, dorsal view **B** head, dorsal view **C** basal antennomeres, dorsal view **D** habitus, ventral view. Scale bars: 1 mm (**A**, **B**).

Description. Male. Length 2.0–2.1 mm. Head yellow, with areas behind middle of eyes black on dorsal surface, frons with darker median spot (Fig. 1B); ventral surface with gular area more or brownish. Mandibles yellow with black apex, maxillary palps and labial palps brownish. Antennae with antennomeres 1–4 yellow, remaining 7 segments brown. Pronotum and elytra black. Legs yellow with basal 4/5 of femora and apex of trochanters dark brown to black. Prosternum dark brown, mesoventrite and metaventrite black; abdominal ventrites dark brown with medial areas of ventrite 2–5 yellow (Fig. 1A, D). Vestiture of short yellowish setae.

Head widest across eyes, nearly as wide as pronotum; dorsal surface flat, covered with dense short setae, clypeus divided into sclerotized postclypeus

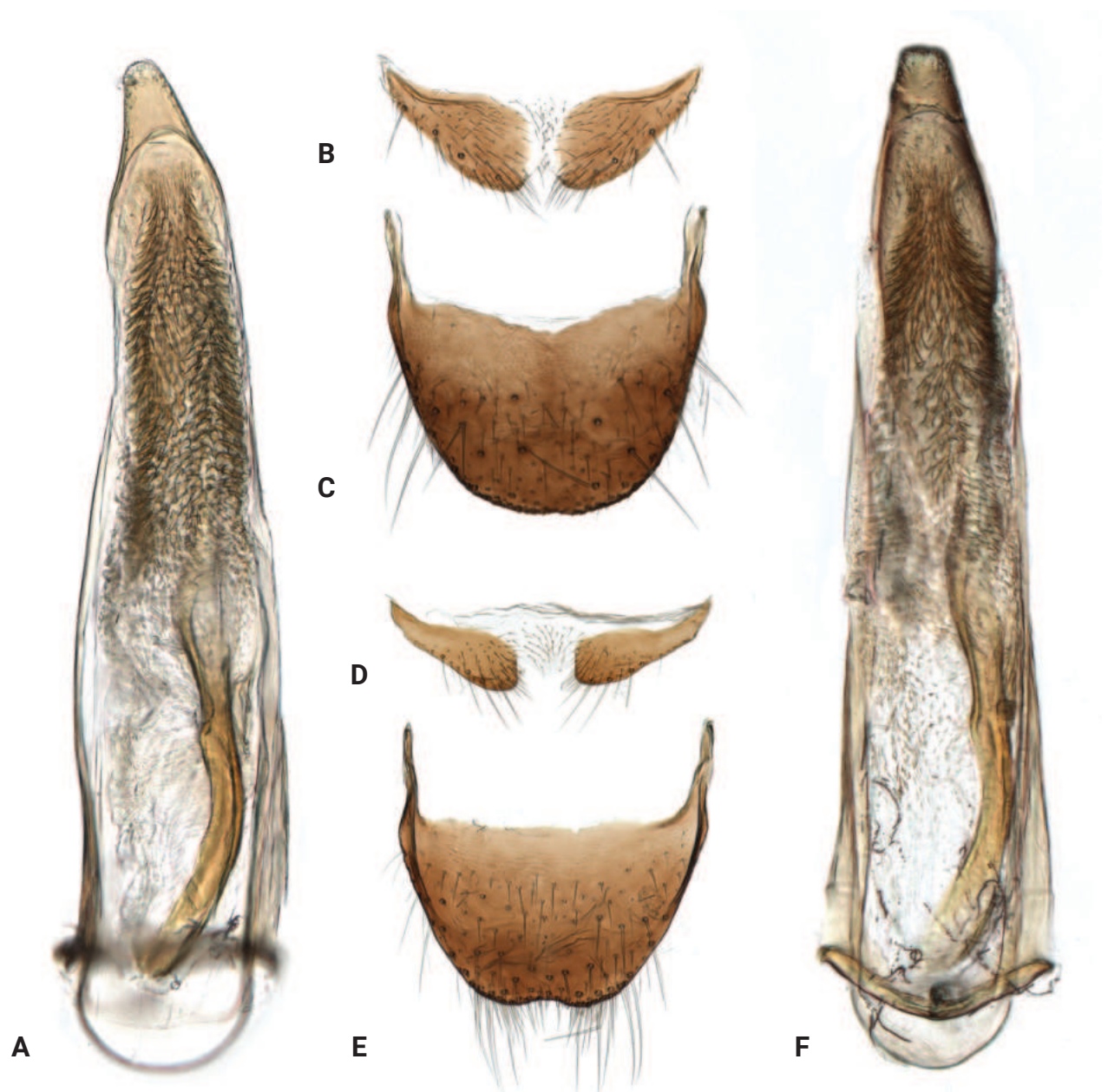


Figure 2. *Intybia hainanensis* sp. nov., paratype (A–C) and *Intybia klapperichi* (Hicker, 1949) (D–F) A, F aedeagus, dorsal view B, D sternite VIII C, E tergite VIII.

and membranous anteclypeus; frons weakly depressed, slightly constricted in front of eyes. Eyes relatively large and laterally protruding. Antenna with 11 segments; scape subtriangular, elongated with slightly enlarged apex; antennomere 3 enlarged and suboval, inner edge with inwardly twisted projections; antennomeres 4–11 covered with short white setae. Labrum transverse, dorsal surface convex. Mandibles bidentate apically, slightly blunt, inner margin straight. Maxillary palps with 4 segments, last segment enlarged and obliquely truncated; labial palps 3 with segments, segment 1 very short, segment 3 conical.

Prothorax transverse; pronotum about 0.7 times as long as wide, widest at about basal third, distinctly constricted at base (Fig. 1A); anterior margin rounded and posterior margin nearly straight. Surface covered with short white setae. Prosternum short, protrochantins exposed. Procoxal cavities transverse and nearly contiguous, posteriorly open; procoxae enlarged and distinct protruding. Scutellum transverse with posterior margin slightly rounded.

Elytra about 1.4 times as long as wide, pear-shaped, widest at about anterior third; humeri rounded and slightly elevated. Surface covered with short white setae. Mesoventrite and metaventrite covered with white setae. Mesoventrite short and subtriangular; mesocoxal cavities large, contiguous at middle, laterally open to mesepimeron; mesocoxae subtriangular, apex slightly swollen, distinctly projecting. Metaventrite enlarged; discrimen distinct, not extending to center, lateral areas with punctures; metanepisternum broad, narrowed posteriorly. Metacoxae transverse, subtriangular, sharply narrowed beside trochanter.

Legs (Fig. 1C) slender, femora slightly enlarged at middle, covered with dense short setae; tibiae slender, with denser setae than femora, which is even denser on inner surface of fore tibiae. Tarsal formula 5–5–5; tarsomeres 3 and 4 slightly shorter than tarsomeres 1 and 2; tarsomere 5 longest, with pair of symmetrical small claws and membranous appendages.

Abdomen with 6 freely movable ventrites; ventrite 1 divided by metacoxae; ventrites 2–4 subequal in length and gradually decreasing in width. Ventrites 2–6 covered with white to light yellow setae on both sides, with longer setae on the last 2 ventrites. Tergite VIII (Fig. 2C) with apical margin broadly rounded, covered with sparse setae; sternite VIII (Fig. 2B) weakly connected at middle. Aedeagus (Fig. 2A) slender, narrowly rounded apically; endophallus with longitudinal sclerite about half as long as penis, curved near base, subapical area with numerous spinules.

Female. Unknown.

Etymology. The species name is derived from the province Hainan, where the type specimens were collected.

Distribution. Hainan.

Intybia klapperichi (Hicker, 1949)

Figs 2D–F, 3

Material examined. Holotype: CHINA • ♂; Fujian, Kwangtseh; 1 Sept. 1937; J. Klapperich leg.; ZFMK-COL-1000188.

Other materials. CHINA • 2 ♂, 4 ♀; Guangdong, Shaoguan City, Ruyuan, Nanling National Forest Park; 24.88487°N, 113.03585°E; 9 May 2023; Zhenhua Liu, Yuqi Wang and Liye Wei leg.; net sweeping; IZGAS.

Diagnosis. It can be distinguished from the other two species within the species group by shape of antennomere 3 (Fig. 3D), with inner protrusion blunt apically and bent toward posterior (inner protrusion pointed apically in *Intybia hainanensis* and bent toward anterior in *Intybia erectodentatus*).

Redescription. Male. Length 2.0–2.4 mm. Head yellow, with areas behind middle of eyes black on dorsal surface (Fig. 1A, G), frons with median area darker (Fig. 3E); ventral surface with gular area dark brown. Mandibles yellow with black apex; maxillary palps and labial palps dark brown. Antennae with scape and antennomere 3 light yellow, antennomeres 4–11 brown to black (Fig. 3D). Pronotum and elytra black. Legs with coxae, trochanters and femora mostly

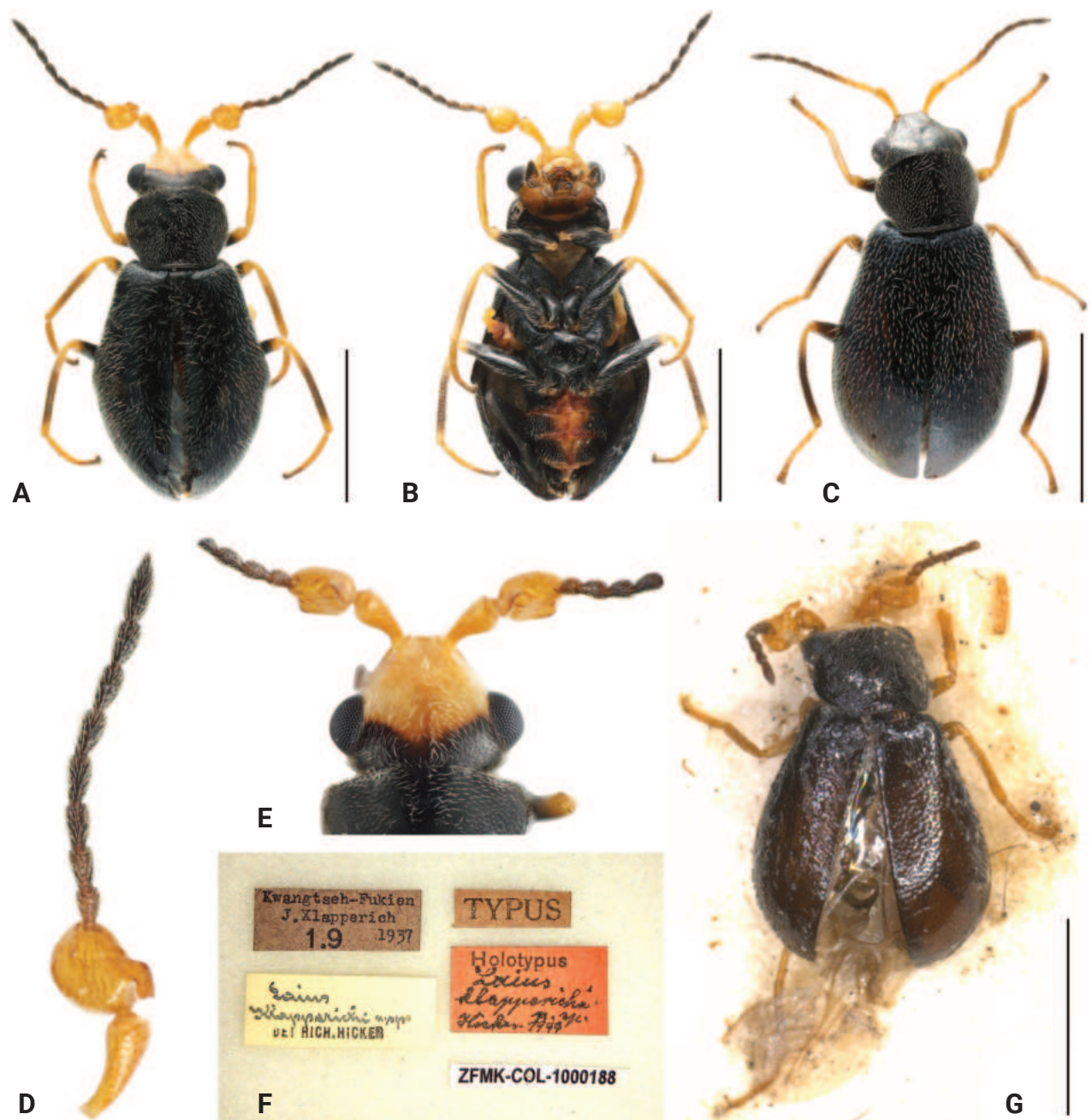


Figure 3. *Intybia klapperichi* (Hicker, 1949) **A** male habitus, dorsal view **B** male habitus, ventral view **C** female habitus, dorsal view **D** male antenna, dorsal view **E** head, dorsal view **F** holotype, labels **G** holotype, dorsal view. Scale bars: 1 mm (**A–C, G**).

black; apex of tarsi, middle areas of middle and hind tibiae brownish to dark brown; remaining part of tibiae and tarsi, joints of coxae and trochanters yellow (Fig. 3B). Prosternum, mesoventrite and metaventrite black; abdominal ventrites black with medial areas yellow to orange. Vestiture of dense white setae.

Head widest across eyes, nearly as wide as pronotum; dorsal surface flat, covered with short setae; clypeus divided into sclerotized postclypeus and membranous anteclypeus; frons slightly constricted in front of eyes. Eyes large and laterally protruding. Antenna with 11 segments; scape elongated and subtriangular; antennomere 3 suboval, inner margin with a hammer-shaped projection twisting towards posterior (Fig. 3D); antennomeres 4–11 densely covered with setae. Labrum transverse, anterior margin strongly arched. Maxillary palps with 4 segments, last segment enlarged and obliquely truncate; labial palps with 3 segments, terminal segment conical.

Prothorax transverse; pronotum about 0.7 times as long as wide, widest at about half; margins smooth, without distinct angles; anterior margin evenly arched, posterior margin nearly straight. Surface densely covered with white short setae. Prosternum short, protrochantin exposed. Procoxal cavities transverse and contiguous at middle; procoxae enlarged, subtriangular. Scutellum subtrapezoid, posterior margin nearly truncated.

Elytra about 1.4 times as long as wide, widest at about anterior third, lateral margins slightly curved; humeri slightly elevated. Surface densely covered with white setae, longer than those on pronotum, punctation indistinct. Mesoventrite transverse and subtriangular; mesocoxal cavities contiguous at middle, laterally open to mesepimeron; mesocoxae enlarged and subtriangular, distinctly projecting, trochantins exposed. Metaventrite transverse, slightly swollen, metanepisternum broad at base, narrowed posteriorly. Metacoxae transverse, subtriangular, sharply narrowed beside trochanter.

Legs (Fig. 3B) slender, femora slightly enlarged at middle, covered with dense short setae; tibiae slender, with denser setae than femora, which is even denser on inner surface of fore tibiae. Tarsal formula 5–5–5, terminal tarsomere with pair of symmetrical small claws and membranous appendages.

Abdomen with 6 freely movable ventrites. Ventrites with long setae on the sides, longer setae on ventrites 4–6. Tergite VIII with posterior margin emarginate (Fig. 2E), covered with sparse setae, denser along apical margin; sternite VIII narrowly weakly connected at middle (Fig. 2D). Aedeagus (Fig. 2F) slender, apex narrowly rounded; endophallus with longitudinal sclerite, about half as long as penis; subapical area with numerous spinules.

Female. Similar to male in body shape and colouration (Fig. 3C), but with head entirely black. Antenna with scape only slightly dilated apically; antennomere 3 simple, rectangular. Fore tarsi distinctly longer than those in male.

Distribution. Fujian, Guangdong.

***Intybia eversi* species group**

Diagnosis. Head, pronotum, scutellum and elytra black, elytra with metallic blue luster (Fig. 4A–C, F). Vestiture of dense short setae. Head with midcranial suture. Pronotum strongly constricted posteriorly, distinctly shorter than elytra at base. Elytra only with dense fine punctures at center, remaining areas nearly

smooth. This species group resembles the *Intybia lombokana* group (Plonski, 2015) in colouration, but can be easily distinguished by the simple vestiture, punctuation on the elytra and shape of the pronotum.

Remarks. Tshernyshev (2020) established the subgenus *Protolaius* for *Intybia lombokana* (Pic, 1910) and *Intybia schillhammeri* (Wittmer, 1966) of the *Intybia lombokana* group, mainly based on the excavate femora in the male, which is absent in *Intybia concha*.

Included species. *Intybia concha* Asano, 2015, *Intybia eversi* (Hicker, 1949).

Distribution. Only known from China (Guangdong, Jiangsu, Shaanxi, Taiwan).

***Intybia eversi* (Hicker, 1949)**

Figs 4, 5

Material examined. Holotype: CHINA • ♂; Fujian, Kwangtseh; 17 July 1937; J. Klapperich leg.; ZFMK-COL-1000176.

Other materials. CHINA • 1 ♂, 1 ♀; Zhejiang, Shaoxing City, Yuecheng District, Fusheng Town; 29.94070°N, 120.73935°E; 14 July 2020; Yuchen Zhao leg.; net sweeping; IZGAS; • 1 ♂; Hubei, Huanggang City, Macheng Aimenguan; 565 m; 31.3856863°N, 115.3231569°E; Fei Ye and Yuqi Wang leg.; IZGAS • 3 ♀; Guangdong, Shaoguan City, Nanling National Forest Park first peak; 24.91971°N, 112.974713°E; 1541 m; 24 Aug.–28 Sept. 2022; Wenfeng Li and Ruonan Zhang leg.; malaise trap; IZGAS.

Diagnosis. This species can be distinguished by its scape with a dark stripe along the inner margin (Fig. 4D), head with a midcranial suture and fine punctations on the elytra. Compared to *Intybia concha*, antennomere 3 of this species has a smoother edge, presenting a more regular spindle shape, with the outer margin slightly blunter than the inner margin.

Redescription. Male. Length 2.7–3.2 mm. Head black, with areas between antennal insertions and anteclypeus yellowish; labrum black at base, apical area yellow, maxillary palps with apex of terminal segment dark yellow. Antenna with basal 3 segments yellow, base of scape black, antennomere with dark stripe along anterior edge on dorsal surface; antennomere 4–11 brownish to dark brown (Fig. 4D). Pronotum black, elytra iridescent dark blue with metallic lustre. Legs deep brown to black with tarsi light brown. Ventral side black, with medial areas and posterior margins of abdominal ventrites 2–5 orange, ventrites 2 to 5 extending yellow regions laterally (Fig. 4B). Vestiture of short white setae.

Head widest across eyes, narrower than pronotum; dorsal surface flat, with distinct midcranial suture; frons slightly constricted in front of eyes; clypeus divided into sclerotized postclypeus and membranous anteclypeus. Eyes large and conspicuously prominent. Antenna with 11 segments; scape subtriangular, with apex distinctly dilated; antennomere 3 strongly transverse, with large transverse concavity, inner edge slightly pointed; antennomeres 4–11 covered with dense white short setae. Labrum transverse and large, nearly semicircular, apical margins strongly arched. Maxillary palps with 4 segments with terminal segment dilated and obliquely truncate; labial palps with 3 segments with terminal segments conical.

Pronotum slightly transverse, about 0.8 times as long as wide, widest at about basal third; lateral margins strongly constricted at base, anterior margin

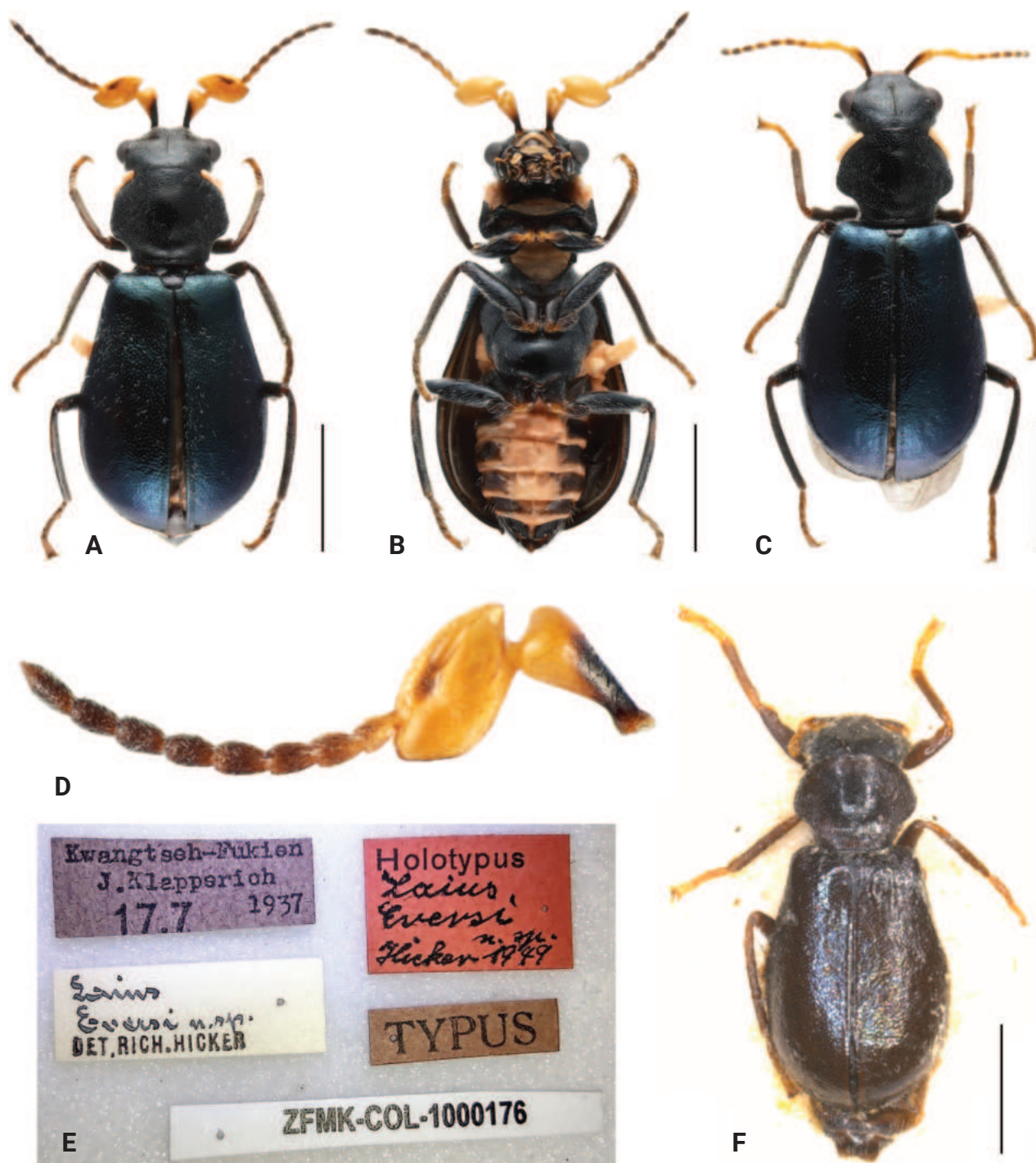


Figure 4. *Intybia eversi* (Hicker, 1949) A male habitus, dorsal view B male habitus, ventral view C female habitus, dorsal view D male antenna, dorsal view E holotype, labels F holotype, dorsal view. Scale bars: 1 mm (A–C, F).

curved, posterior margin almost straight (Fig. 4A, F); disc convex dorsally, slightly depressed posteriorly. Surface nearly smooth, without distinct punctuation; densely covered with short setae. Prosternum short, protrochantins exposed. Procoxal cavities strongly transverse, contiguous at middle; procoxae enlarged and ventrally protruding. Scutellum subtrapezoidal, posterior margin truncate; surface covered with sparse short setae.

Elytra about 1.2 times as long as wide, widest at about apical third, ovoid; humeri slightly elevated; surface covered with dense fine punctures at middle,

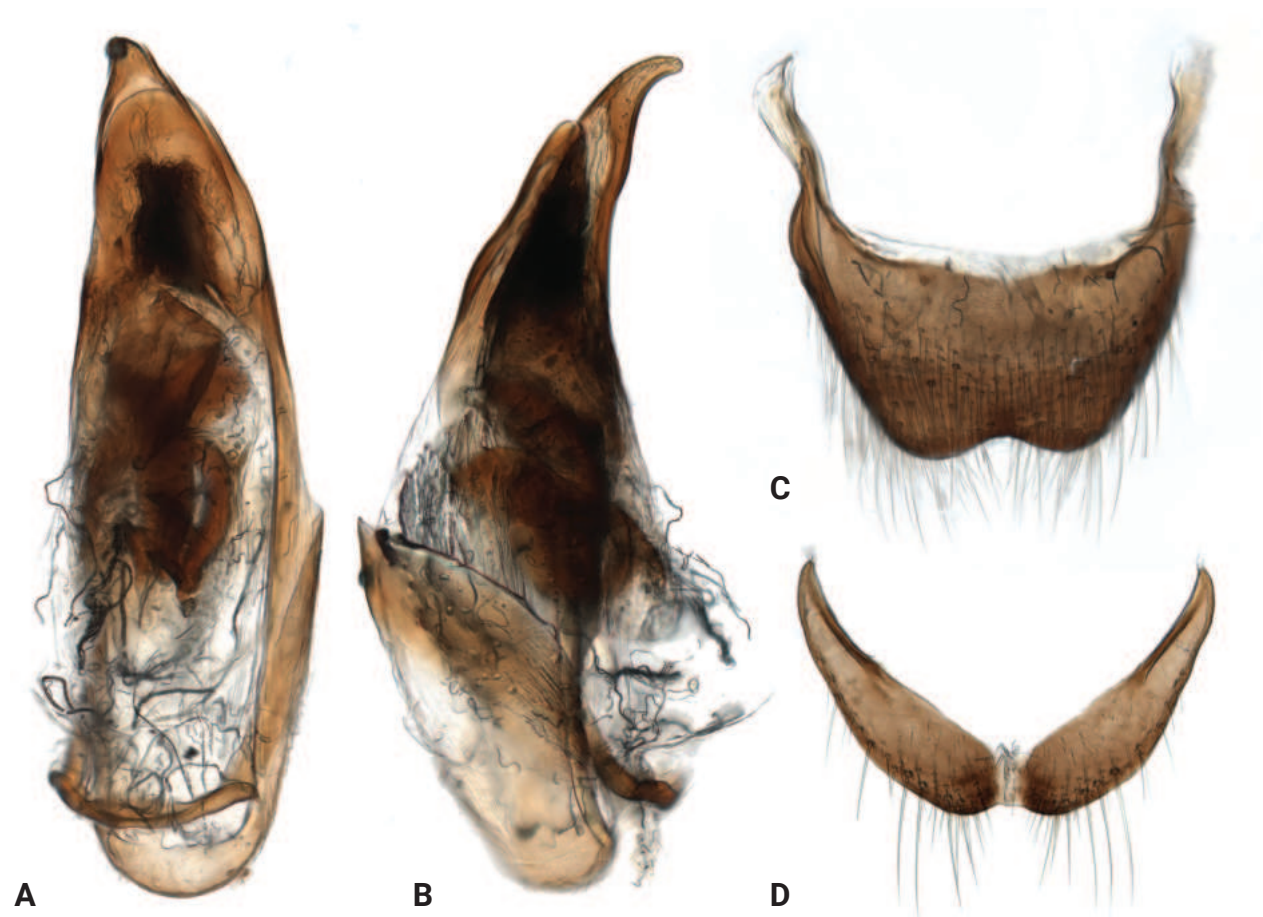


Figure 5. *Intybia eversi* (Hicker, 1949), male genitalia **A** aedeagus, dorsal view **B** aedeagus, lateral view **C** tergite VIII **D** sternite VIII.

remaining areas nearly smooth, covered with dense short setae. Mesoventrite elongated; mesocoxal cavities contiguous at middle, laterally open to mesepimeron; Mesocoxae large and triangular, ventrally protruding. Metaventrite slightly swollen, with short discrimen; metacoxae transverse, subtriangular, sharply narrowed beside trochanters.

Legs slender, femora slightly swollen, covered with white short setae; tibiae slender, with denser setae than femora, which is even denser on inner surface of fore tibiae. Tarsal formula 5–5–5, front tarsi distinctly shorter; terminal tarsomere with pair of symmetrical small claws and membranous appendages underneath.

Abdomen with 6 freely movable ventrites; ventrites 1–4 subequal in length, longer than apical 2 segments, ventrites 4–6 gradually narrowed to apex. Tergite VIII (Fig. 5C) subtrapezoid, with pair of moderately long and curved posterior struts, posterior margin triangularly emarginated; sternite VIII (Fig. 5D) transverse, weakly connected at middle. Aedeagus broad at middle (Fig. 5A), apex acute and curved (Fig. 5B); endophallus with 4 broad and curved sclerites at middle, and 4 small spine-shaped sclerites next to them, 3 at basal and 1 at apical, subapical area with a few thick spinules.

Female. Similar to male in body shape and colouration (Fig. 4C), but antenna with scape only slightly dilated apically, antennomere 3 simple and elongated, front tarsi longer.

Distribution. Fujian, Guangdong.

Key to species groups of the genus *Intybia* Pascoe in China

On the basis of species group designations proposed by Plonski (2016), a key to species groups of *Intybia* in China is provided below:

- 1 Elytra monochrome, without spot or stripe..... **2**
 - Elytra not monochrome, with whitish, yellowish or orange spots or stripes **4**
- 2 Thorax orange-red; elytra dark blue with metallic luster, with dense and coarse punctuation..... ***Intybia rubrithorax* group**
 - Thorax black; elytra black, with or without metallic blue luster, without distinct punctation..... **3**
- 3 Elytra black with metallic blue luster, head with frons black; pronotum strongly constricted at base; body length more than 3.5 mm.....
..... ***Intybia eversi* group**
 - Elytra black without metallic luster, head with frons yellow; pronotum gradually constricted to base; body length less than 2.5 mm
..... ***Intybia klapperichi* group**
- 4 Thorax orange-red; elytra with two transverse orange stripes mixed with white, which are connected along the suture ***Intybia venusta* group**
 - Thorax black; elytra with one transverse stripe or three whitish spots..... **5**
- 5 Elytra black without metallic luster, with three whitish spots, one at about anterior third and two subapical..... ***Intybia guttata* group**
 - Elytra black, sometimes with metallic luster, with one yellow to orange transverse stripe before middle, sometimes continuous across suture
..... ***Intybia pelegri* group**

Acknowledgements

We would like to sincerely thank Dr Dirk Ahrens of ZFMK for photographing the type specimens, and Dr Binglan Zhang of Sun Yat-sen University for help with the photography of male genitalia. We would also appreciate Sergei Tshernyshev and Isidor Plonski for their kind peer reviews. The corresponding author, Zhenhua Liu appreciates Yuchen Zhao for providing specimens of the new species and Dr Makoto Asano for her kind suggestions on this project. And we are also grateful for the support of the Special Project from the Forestry Administration of Guangdong Province.

Additional information

Conflict of interest

The authors have declared that no competing interests exist.

Ethical statement

No ethical statement was reported.

Funding

This project is supported by the National Natural Science Foundation of China (no. 32200374, no. 32070471 and no. 31702039), and GDAS Special Project of Science and Technology Development (2022GDASZH-2022010106, 2020GDASYL-20200102021).

Author contributions

Conceptualization: ZL. Funding acquisition: ZL, ZL. Project administration: ZL. Supervision: ZL, PY. Visualization: YW, ZL. Writing—original draft: YW. Writing—review and editing: ZL, ZL, PY.

Author ORCIDs

Yuqi Wang  <https://orcid.org/0009-0002-0311-8445>

Zhiqiang Li  <https://orcid.org/0000-0003-0064-7165>

Ping You  <https://orcid.org/0000-0002-2913-1544>

Zhenhua Liu  <https://orcid.org/0000-0002-2739-3305>

Data availability

All of the data that support the findings of this study are available in the main text.

References

- Asano M (2015) Taxonomic notes on some malachiid beetles of Taiwan, with description of a new species of the genus *Intybia* Pascoe (Coleoptera: Malachiidae). Japanese Journal of Systematic Entomology 21(1): 77–82.
- Asano M (2021) Larval structures and bionomics of two species of the genus *Intybia* Pascoe (Coleoptera: Melyridae: Malachiinae). Coleopterists Bulletin 75(3): 617–628. <https://doi.org/10.1649/0010-065X-75.3.617>
- Blackburn T (1888) Further notes on Australian Coleoptera with descriptions of new species. Transactions and Proceedings and Reports of the Royal Society of South Australia 10: 177–287.
- Champion GC (1921) Notes on various African and Asiatic species of *Laius*, Guérin, with an account at their accessory ♂-characters. Annals & Magazine of Natural History 9(7): 322–343. <https://doi.org/10.1080/00222932108632526> [Coleoptera]
- Evers AMJ (1994) Zur Phylogenie von *Laius* Guér., *Collops* er. und der verwandten Gattungen. Entomologische Blätter 90(3): 169–181.
- Ikeda H, Yoshitomi H (2017) Revision of the genus *Intybia* (Coleoptera, Malachiidae) from Japan. European Journal of Taxonomy 331(331): 1–31. <https://doi.org/10.5852/ejt.2017.331>
- Lawrence JF, Ślipiński A (2013) Australian Beetles. Vol. 1. Morphology, Classification and Keys. CSIRO Publishing, Collingwood, Victoria, [viii +] 561 pp. <https://doi.org/10.1071/9780643097292>
- Lea AM (1909) Revision of the Australian and Tasmanian Malacodermidae. Transactions of the Royal Entomological Society of London 1(1–2): 45–251. <https://doi.org/10.1111/j.1365-2311.1909.tb02171.x>
- Macleay WJ (1872) Notes on a collection of insects from Gayndah. Second paper. Transactions of the Entomological Society of New South Wales 2(4): 239–318.
- Pic M (1907) Coléoptères exotiques nouveaux ou peu connus (suite). L'Échange. Revue Linnéenne 23: 125–191.
- Pic M (1910) Sur les "*Laius*" Guer. á quatre macules blanches élytrales. L'Échange. Revue Linnéenne 26: 83–84.
- Pic M (1919) Nouveautés diverses. Mélanges Exotico-Entomologiques 30: 1–21.
- Pic M (1921) Diagnoses de Coléoptères exotiques. L'Échange. Revue Linnéenne 37: 6–12. <https://doi.org/10.3406/bsef.1922.26995>

- Pic M (1927) Coléoptères nouveaux de Chine et du Japon. Bulletin de la Société Entomologique de France 32(9): 152–154. <https://doi.org/10.3406/bsef.1927.27826>
- Plonski IS (2013) Studies on the genus *Intybia* Pascoe (Coleoptera: Malachiidae) I. Some nomenclatorial acts and faunistic records. Zeitschrift der Arbeitsgemeinschaft Österreichischer Entomologen 65: 61–68.
- Plonski IS (2014a) Studies on the genus *Intybia* Pascoe, part II. Faunistic and taxonomic notes, with description of a new species of the *I. plagiata*-group. Koleopterologische Rundschau 84: 313–320.
- Plonski IS (2014b) Studies on the genus *Intybia* Pascoe (Coleoptera: Malachiidae) IV. Notes on the fauna of the Philippines. Zeitschrift der Arbeitsgemeinschaft Österreichischer Entomologen 66: 39–45.
- Plonski IS (2015) Studies on the genus *Stenolaius* Wittmer (Coleoptera: Malachiidae) I. Faunistic and ecological notes on known species. Zeitschrift der Arbeitsgemeinschaft Österreichischer Entomologen 67: 39–43.
- Plonski IS (2016) Studies on the genus *Intybia* Pascoe, 1866 (Coleoptera: Malachiidae) V. Contribution to internal classification and taxonomy, with faunistic and nomenclatorial notes. Zeitschrift der Arbeitsgemeinschaft Österreichischer Entomologen 68: 17–38.
- Plonski IS, Geiser M (2014) Studies on the genus *Intybia* Pascoe (Coleoptera: Malachiidae) III. On *Intybia rubrithorax* (Pic) and related taxa. Zeitschrift der Arbeitsgemeinschaft Österreichischer Entomologen 66: 31–38.
- Tshernyshev SE (2015) Soft winged flower beetles (Insecta: Coleoptera: Malachiidae) of the Himalayan region, with notes on Apalochrini. Biodiversität und Naturausstattung im Himalaya 5: 389–405.
- Tshernyshev SE (2016) Taxonomic revision of *Intybia* Pascoe, 1866 species (Coleoptera, Malachiidae) of Thailand and Philippines. Zootaxa 4147(2): 101–123. <https://doi.org/10.11646/zootaxa.4147.2.1>
- Tshernyshev SE (2020) *Intybia (Protolaius)*, a new subgenus of soft winged flower beetles (Coleoptera: Malachiidae) from Indonesia. Russian Entomological Journal 29(2): 173–177. <https://doi.org/10.15298/rusentj.29.2.08>
- Wittmer W (1955) 21. Beitrag zur Kenntnis der Palaearktischen Malacodermata (Coleoptera). Mushi, Fukuoka 29(6): 39–45.
- Wittmer W (1956) Neue Malacodermata aus der Sammlung der California Academy of Sciences (16. Beitrag zur Kenntnis der palaearktischen Malacodermata. Col.). Mitteilungen der Schweizerischen Entomologischen Gesellschaft 29(3): 303–313. 63: 115–161.
- Wittmer W (1982) Zur Kenntnis der Malachiidae von Taiwan (Coleoptera). Entomologica Basiliensia 7: 348–372.
- Wittmer W (1995) Zur Kenntnis der Familie Malachiidae (Coleoptera) 2. Beitrag. Entomologica Basiliensia 18: 287–391.
- Wittmer W (1996) Zur Kenntnis der Familie Malachiidae (Coleoptera). Teil II. Mitteilungen der Schweizerischen Entomologischen Gesellschaft 69: 297–327.
- Wittmer W (1997) Zur Kenntnis der Gattungen *Intybia* Pascoe und *Stenolaius* Wittmer (Coleoptera, Malachiidae). Japanese Journal of Systematic Entomology 3(2): 181–211.
- Wittmer W (1999) Zur Kenntnis der Familie Malachiidae (Coleoptera), 3. Beitrag. Entomologica Basiliensia 21: 171–252.
- Yoshitomi H, Lee CF (2010) Revision of the Taiwanese and Japanese species of the genus *Laius* (Insecta: Coleoptera: Malachiidae). Zoological Studies (Taipei, Taiwan) 49(4): 534–543. <https://doi.org/10.2108/zsj.27.615>

A new species of the genus *Glossobalanus* (Hemichordata, Enteropneusta, Ptychoderidae) from China

Xianan Fu¹, Weijian Guo¹, Zhongwen Ding¹, Wenliang Zhou¹, Fuwen Wei^{1,2,3}

¹ Center for Evolution and Conservation Biology, Southern Marine Science and Engineering Guangdong Laboratory (Guangzhou), Guangzhou, 511458, China

² CAS Key Laboratory of Animal Ecology and Conservation Biology, Institute of Zoology, Chinese Academy of Sciences, Beijing, 100101, China

³ College of Forestry, Jiangxi Agricultural University, Nanchang, 330045, China

Corresponding authors: Wenliang Zhou (zhouwl@gmlab.ac.cn); Fuwen Wei (weifw@ioz.ac.cn)

Abstract

A morphological and molecular analyses of a newly discovered species, *Glossobalanus weii* sp. nov., from Danzhou city, Hainan Island, China is presented. Several morphological characters distinguish this new species, while molecular analyses confirm significant genetic divergence from its recognized congeners (p-distance > 0.25 in mitochondrial genomes). Phylogenetic analyses place the new species in a distinct sister clade to *G. polybranchioporos*, which is afforded first-class state protection in China. An updated retrieval table is provided for the eight species of Hemichordata found in China. Hemichordate diversity remains underestimated and this new species emphasizes the need for their ongoing conservation in southern China.

Key words: Conservation, external morphology, Hainan, molecular analysis, morphometry



Academic editor: Fedor Konstantinov

Received: 29 August 2023

Accepted: 30 April 2024

Published: 27 May 2024

ZooBank: <https://zoobank.org/53C0C4A8-FE2F-4070-B952-403549FC3AA4>

Citation: Fu X, Guo W, Ding Z, Zhou W, Wei F (2024) A new species of the genus *Glossobalanus* (Hemichordata, Enteropneusta, Ptychoderidae) from China. ZooKeys 1202: 343–358. <https://doi.org/10.3897/zookeys.1202.111852>

Copyright: © Xianan Fu et al.
This is an open access article distributed under terms of the Creative Commons Attribution License (Attribution 4.0 International – CC BY 4.0).

Introduction

While Hemichordata now belong to the Ambulacraria clade on a par with Echinodermata, they are nevertheless considered the closest relatives to chordates, because they typically share common features such as bilateral symmetry, gill slits and early axial patterning. Hemichordates occupy an important position in the study of the origin and evolution of deuterostomes. The phylum Hemichordata comprises approximately 130 living species worldwide (Tassia et al. 2016), divided into two classes: Enteropneusta (commonly known as acorn worms) and recently the Graptolithoidea (sea angels) (Swalla and van der Land 2024). The extant and extinct taxa of the Enteropneusta was well reviewed in Maletz (2023). The newly accepted class Graptolithoidea embraces two taxa: Graptolithina and Pterobranchia. The Enteropneusta is further classified into four families: Harrimaniidae Spengel, 1901, Ptychoderidae Spengel, 1893, Spengelidae Willey, 1898, and Torquaratoridae Holland, Clague, Gordon, Gebruk, Pawson & Vecchione, 2005. The family Saxipendiidae is placed within Harrimaniidae according to the Hemichordata World Database (Deland et al. 2010). The Ptychoderidae are characterized by a highly developed branchiogenital region and hepatic sacculations.

Seven species of hemichordates are recorded from China: *Glossobalanus polybranchioporus* Tchang & Liang, 1965; *Saccoglossus hwangtauensis* Tchang & Koo, 1935; *Balanoglossus misakiensis* Kuwano, 1902; *B. carnosus* Müller in Spengel, 1893; *Glossobalanus mortenseni* van der Horst, 1932; *Ptychodera flava* Eschscholtz, 1825, and *Glandiceps qingdaoensis* An & Li, 2005. In China, *G. polybranchioporus* and *S. hwangtauensis* are under first-class state protection and the other five species are under second-class state protection as rare and endangered wildlife. Despite the wide distributional range of the known sixteen species of *Glossobalanus*, from European Seas to the northeast Pacific, many regions of their biogeographic range remain unexplored (Fig. 1).

During recent field surveys along the Chinese coast, we discovered specimens of the genus *Glossobalanus* from Toudong village in Danzhou City, Hainan Province (Fig. 1), which were not previously known. Detailed comparisons with all known *Glossobalanus* species revealed significant morphological differences between this new record and its relatives, particularly in proboscis and collar morphology. Further genetic analyses confirmed its phylogenetic distinctiveness from currently recognized congeners. Here we describe this new species as *Glossobalanus weii* sp. nov. and provide an updated key to identify the different species of hemichordates in China. We also discuss their diversity and conservation issues.

Materials and methods

Taxonomic sampling

Specimens of *Glossobalanus weii* sp. nov. were collected from Toudong village, Danzhou, Hainan Province, China in February and July 2023. Two specimens for histological investigation were fixed in Bouin's solution and dehydrated in a graded series of ethanol. The voucher specimens are stored in 70% ethanol at the Southern Marine Science and Engineering Guangdong Laboratory (Guangzhou) (also named Guangzhou Marine Laboratory, for short GML) Biological Resource Sample Bank. Specimens for comparison of *Glossobalanus polybranchioporus*, *Balanoglossus misakiensis*, and *Glandiceps qingdaoensis* were donated by Professor Xinzheng Li of the Institute of Oceanology, Chinese Academy of Sciences, collected from Jiaozhou Bay, Qingdao, Shandong Province, China. Fresh trunk tissue of these specimens was used for comparative genetic analysis.

Morphological data

Total length (**ToL**), proboscis length (**proL**), collar length (**coll**), hepatic region length (**hepL**), branchial length (**brL**) (from the beginning of branchiogenital region to the end of the gill region), and branchiogenital region length (**brgL**) of the specimens were measured using ImageJ2. Length analysis was performed three times and the average value was taken. For older papers that do have relevant length records, measurements were taken from pictures that included a scale. The specimens for histology investigation were cut into frozen sections (10 µm thickness) after being submerged in optimal cutting temperature compound (OCT). Thin sections from the largest frozen sections were selected for hematoxylin and eosin (HE) staining. Thin sections were viewed and photographed with a Nikon, Eclipse Ti2 photomicroscope. All materials examined are deposited in GML.

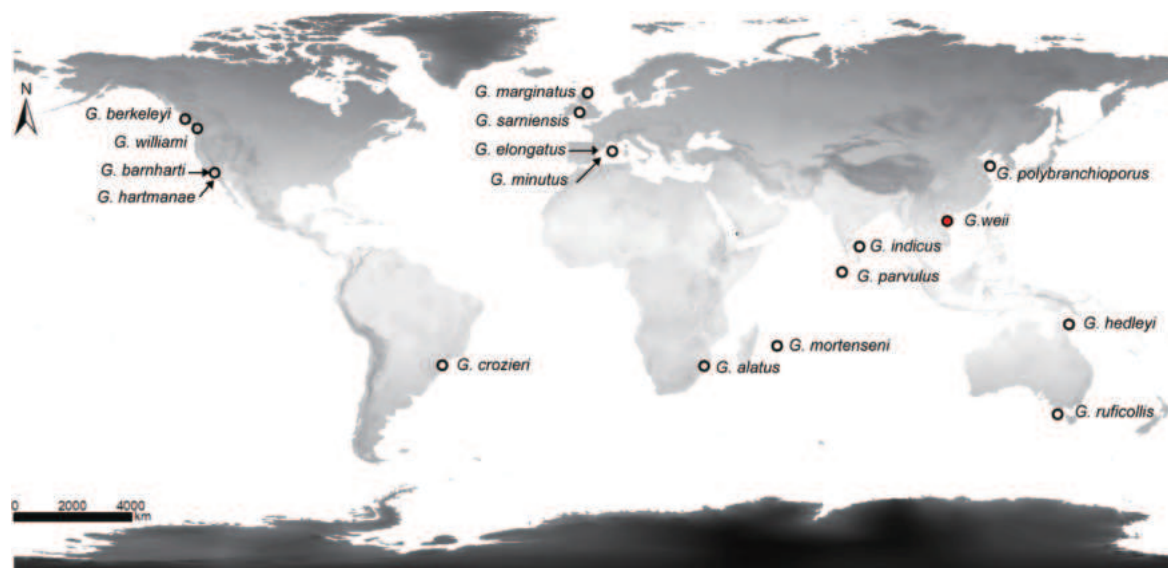


Figure 1. The global distribution of all *Glossobalanus* species. The distributions were compiled from the original description data. The type locality of *Glossobalanus weii* sp. nov. on Hainan Island, China was marked in red.

Genetic data

Molecular genomic DNA was extracted from the trunk of four specimens using the SDS method followed by purification with QIAGEN® Genomic kit (Cat#13343, QIAGEN), according to the standard operating procedure provided by the manufacturer, and was sequenced using the MGI-DNBseqT7 platform. Following the MitoZ tutorial (Meng et al. 2019), a total of 5 G base pairs (bp) of each specimen were obtained respectively, and their complete mitochondrial genome was generated. The assembled mitochondrial genomes were automatically annotated and manually corrected in Geneious Prime 2022.2.2. The mitogenome sequence assembly N_001485032, N_001485033, N_001485034 and N_001485035 were uploaded to China National GeneBank (<https://db.cngb.org/>). In addition, the available mitochondrial genome sequences of congeners were downloaded from GenBank (<https://www.ncbi.nlm.nih.gov/genbank/>). Available accessions are listed in Table 1.

Table 1. Mitochondrial genome sequences used in this study.

Family	Species	Accession No.
Cephalodiscidae	<i>Cephalodiscus hodgsoni</i> Ridewood, 1907	MF374802
Harrimaniidae	<i>Saccoglossus kowalevskii</i> (Agassiz, 1873)	NC_007438
Harrimaniidae	<i>Stereobalanus canadensis</i> (Spengel, 1893)	NC_040107
Ptychoderidae	<i>Balanoglossus carnosus</i> Müller in Spengel, 1893	NC_001887
Ptychoderidae	<i>Balanoglossus clavigerus</i> Delle Chiaje, 1829	NC_013877
Ptychoderidae	<i>Balanoglossus misakiensis</i> Kuwano, 1902	N_001485032
Ptychoderidae	<i>Glossobalanus marginatus</i> Meek, 1922	NC_040109
Ptychoderidae	<i>Glossobalanus polybranchioporus</i> Tchang & Liang, 1965	N_001485033
Ptychoderidae	<i>Glossobalanus weii</i> sp. nov.	N_001485035
Rhabdopleuridae	<i>Rhabdopleura compacta</i> Hincks, 1880	FN908482
Spengelidae	<i>Schizocardium brasiliense</i> Spengel, 1893	NC_040108
Spengelidae	<i>Glandiceps qingdaoensis</i> An & Li, 2005	N_001485034

Species names were checked on WoRMS (www.marinespecies.org). Mitochondrial genome accessions were from GenBank (<https://www.ncbi.nlm.nih.gov/genbank/>) and China National GeneBank (<https://db.cngb.org/>).

Phylogenetic analyses

Sequences were aligned using MAFFT (Kuraku et al. 2013) with the default parameters and further trimmed by trimAl (Capella-Gutiérrez et al. 2009) with parameters -gt 0.6. The aligned DNA sequences of 13 protein-coding genes in the mitochondrion were concatenated in a single dataset (total 11,281 bp) and subjected to Bayesian inference (BI) analyses under the optimal partitioning scheme. The genetic data were partitioned into five unequivocal data blocks and the best-fit nucleotide substitution model for each block was identified using the PartitionFinder v. 2.1.1 (Lanfear, et al. 2017) which nesting in IQ-TREE v. 1.6.12 (Nguyen et al. 2015). The nucleotide models GTR+I+G or GTR +G were used in our analysis, considering the constraints of the available models in MrBayes (Ronquist et al. 2012) and the recommendations provided by PartitionFinder. BI analyses were performed using MrBayes v. 3.2. Two independent Markov chain Monte Carlo (MCMC) runs were performed with three heated and one cold chain for 10^6 generations and sampled every 1,000 generations. To judge convergence and effective sample sizes (ESS) for all parameters, Tracer v. 1.7 (Rambaut et al. 2018) was used to analyze, all the ESS values exceeding 100 after the first 25% generations were discarded. The consensus tree and posterior probabilities were estimated from the remaining generations of two runs and compared for congruence.

Results

Morphological results

The specimens were morphologically consistent with the recognized species from the genus *Glossobalanus*. They differ from the other 16 species of *Glossobalanus* in their combination of morphological characters, including larger size, and proboscis to collar proportions and markings (Table 2). The taxonomic account is as follows.

Taxonomic account

Phylum Hemichordata

Class Enteropneusta

Family Ptychoderidae Spengel, 1893

Genus *Glossobalanus* Spengel, 1901

Glossobalanus weii sp. nov.

<https://zoobank.org/BD53EAB7-7B4C-400C-A441-80CF57B7F22D>

Fig. 2

Material examined. Holotype. GML-23021883041 (Fig. 2A), adult female, collected from Toudong Village, Xinying Town, Lingao County, Danzhou City, Hainan Province, China (19°52.2035'N, 109°32.1094'E), collected by Xianan Fu, Weijian Guo and Wenliang Zhou on 23 Feb 2023 (GML). **Paratypes.** GML-23021883042 (Fig. 2B–D), adult male, same collection information as holotype. GML-23070380011, adult male, same location information as holotype, collected by Xianan Fu and Zhongwen Ding on 4 Jul 2023 (GML).

Table 2. Morphometric measurements and distribution of *G. weii* sp. nov. and all other sixteen species of *Glossobalanus*.

Species	ToL (mm)	proL (mm)	coll (mm)	hepL (mm)	proL/coll	brgL/brL
<i>G. alatus</i> van der Horst, 1940	34.5	2	3	3.7	<1	9–10
<i>G. barnharti</i> * Cameron & Ostiguy, 2013	67	2.1–2.4	1.7–2.1	14.8	1–1.4	3
<i>G. berkeleyi</i> * Willey, 1931	60.7	4.91	3.39	–	1.4	4
<i>G. crozieri</i> * van der Horst, 1924	30–50	2.5–4	3	–	0.8–1.3	2
<i>G. elongatus</i> Spengel, 1904	–	–	–	–	–	–
<i>G. hartmanae</i> Cameron & Ostiguy, 2013	23–45	3.5	3.5	4	1	4.5
<i>G. hedleyi</i> (Hill, 1897)	–	–	–	–	–	–
<i>G. indicus</i> Rao, 1955	–	–	–	–	–	–
<i>G. marginatus</i> Meek, 1922	50	7	5	–	1.4	3–4
<i>G. minutus</i> * (Kowalevsky, 1866)	42	3	2	–	1.5	2–3
<i>G. mortenseni</i> van der Horst, 1932	38.5–67	4.5–4.9	3.2–3.7	4.9–7.6	2–2.4	–
<i>G. parvulus</i> Punnett, 1906	–	–	–	–	–	–
<i>G. polybranchioporus</i> Tchang & Liang, 1965	352–613	10–12	8–10	40–74	1–1.4	4–6
<i>G. ruficollis</i> (Willey, 1899)	–	4–4.5	6.5–7	–	<1	9–10
<i>G. sarniensis</i> (Koehler, 1886)	35–100	–	–	–	~1	6–9
<i>G. williami</i> Cameron & Ostiguy, 2013	130	2.5	1.5	–	1.7	–
<i>G. weii</i> sp. nov.	176–196	11.1–15.9	5.2–6.6	24–26.2	2.1–2.4	5

*Measured according to the picture with standard scale. **G. crozieri* was based on description in Petersen and Ditadi (1971). Abbreviations: branchiogenital region length (brgL); branchial length (brL); collar length (coll); hepatic region (hepL); proboscis length (proL); total length (ToL).

Diagnosis. *Glossobalanus weii* sp. nov. can be differentiated from closely related species by a combination of the following characters: (1) large worms with adult body size of more than 150 mm (Fig. 2A); (2) the proboscis is twice as long as the collar (Fig. 2B); (3) a dark spot on the tip of the proboscis (Fig. 2A, B); (4) a rather broad posterior collar margin and the dorsal margin of the collar is shorter than the ventral margin (Fig. 2B); (5) the collar is covered with longitudinal pleats bound tightly with a ring in the center (Fig. 2B); and (6) a slender brown hepatic region with plump sacculations (Fig. 2E).

Description. Body of the holotype as in Fig. 2. The worm bodies are fragile and easily broken. When placed on a flat surface or photographic canvas they shrink severely and break and it is necessary to examine and measure them in an aqueous or similar solution. The complete living specimen is 176 mm long. There is a dark spot on the tip of the proboscis. The proboscis can stretch freely from 11 to 16 mm. The collar has a number of longitudinal folds with a pale-colored ring in the middle, and on the back, the collar has a raised broad edge forming another ring band (Fig. 2B). The dorsal collar length is 4.7 mm, and ventral collar length is 5.7 mm in the vertical direction; the width is 5–9 mm in the transverse direction. The anterior margin of the collar encircles the base of the proboscis, and there is a conspicuous mouth in the center of the ventral surface of the anterior end at the junction with the proboscis.

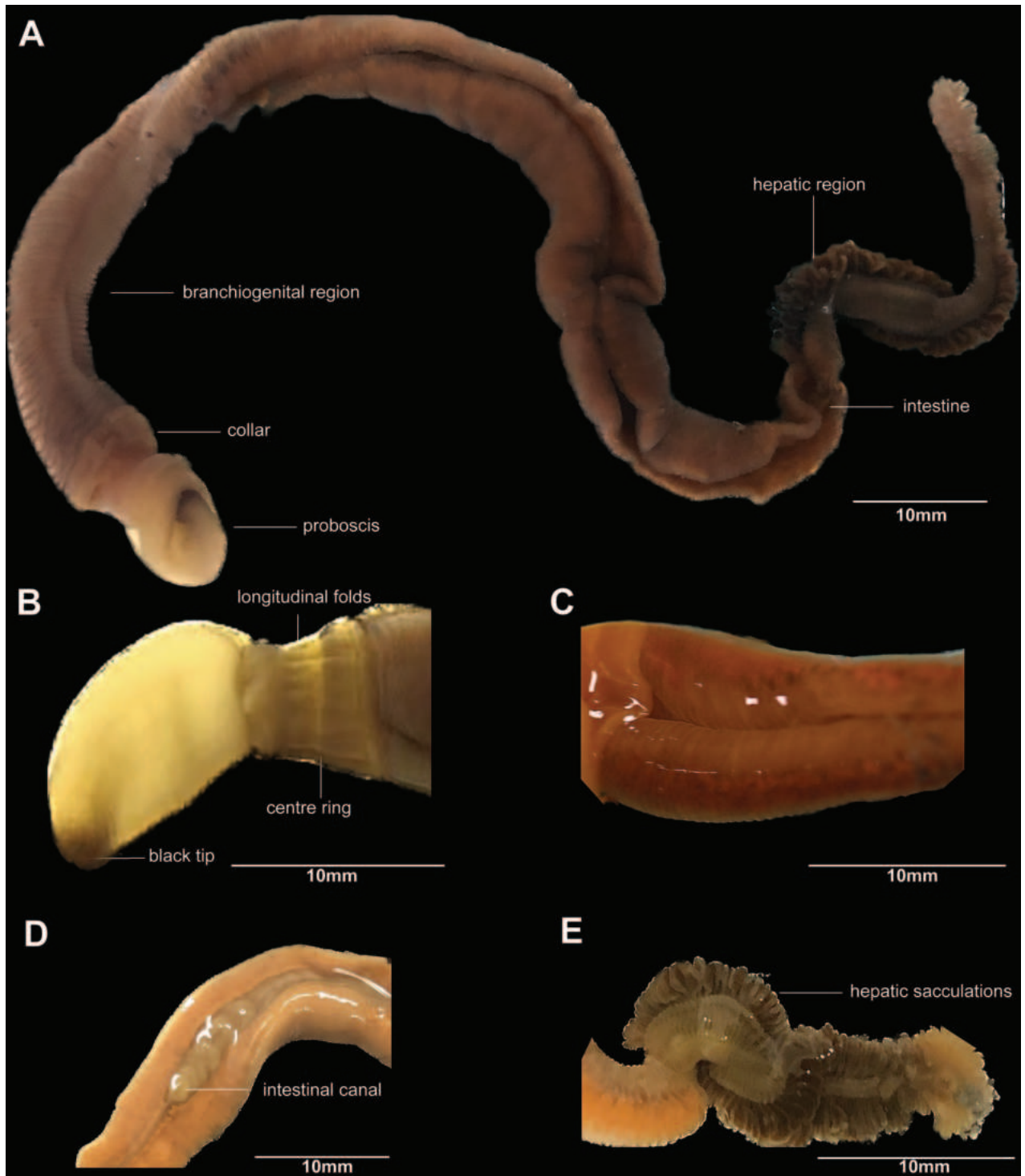


Figure 2. External form of *Glossobalanus weii* sp. nov. **A** whole body of female GML-23021883041 under natural conditions **B** proboscis and collar of paratype male GML-23021883042 **C** branchial region dorsal side photo of paratype male GML-23021883042 **D** intestinal canal containing food **E** hepatic region photo of paratype male GML-23021883042.

Trunk is sub-cylindrical and divided into branchiogenital region, hepatic region, and intestinal region. The branchiogenital region is 105 mm long and 6.2 mm in transverse diameter, sub-cylindrical and slightly furrowed. There are 40 pairs of small gill pores that are invisible without magnification. The beginning of the

branchiogenital region is connected with the posterior margin of the collar and covers the anterior part of the gill region (Fig. 2C). The slender intestinal canal extends from branchiogenital region through the hepatic region. The digestive tract narrows before the hepatic region (Fig. 2D). Hepatic region length is 24–26 mm with about 60 pairs of mature sacculations (Fig. 2E). The arrangement of the hepatic sacculations is plumper and sparser at the anterior, and progressively tighter and neater at the posterior end.

Coloration. In fresh specimens, the body is generally brownish yellow, fading to pale yellow or pale tan in the proboscis and has a black tip. There is a pale, thin ring in the middle of the collar, and a darker colored annular band connects the collar and branchiogenital region of the trunk (Fig. 2B). The branchiogenital region is yellowish brown in females and pale yellow or honey yellow in males. The anterior portion of the hepatic trunk is dark brown and fading to pale brown on the posterior portion (Fig. 2E). The preserved specimens faded to a dull yellow. The hepatic region turned grey after fixation in alcohol.

Anatomical and histological characters. The circular musculature and the epidermis of the proboscis have equal thickness around 0.3 mm (Fig. 3A, B). The proboscis is filled with slender muscles and the circular muscle is outside the longitudinal musculature (Fig. 3A, B). The proboscis cavity is small and may be missed in the transverse section (Fig. 3C). The buccal diverticulum was integrated with the pericardial coelom and surrounded by glomerulus (Fig. 3C). The proboscis bifurcates at the anterior collar into two crura at more than 180° (Fig. 3C). The proboscis has the appearance of a butterfly extending into the median of the collar on the dorsal side (Fig. 3D). The flattened nerve cord is surrounded by the perihemal diverticula (Fig. 3E). The hepatic sacculations are neatly arranged and symmetrical overall (Fig. 3F).

Natural history and distribution. *Glossobalanus weii* sp. nov. is currently only known from the inlet of Toudong village of Danzhou, Hainan Province, China, in the Beibu Gulf (Fig. 1). The new species inhabits humic mudflat intertidal zones with gravelly and shell carcass substrates and is a burrowing filter-feeder (Fig. 4).

Etymology. This species is named after Fuwen Wei to commend his contributions to Zoology and Conservation biology. We propose the common name “魏氏舌形虫” in Chinese.

Genetic results. The validity of *G. weii* sp. nov. was supported by molecular phylogenetic analysis based on the aligned DNA sequences of 13 mitochondrial protein-coding genes (Fig. 5). Bayesian phylogenetic analyses revealed that the specimens form an independent clade with robust support and are closest to *G. polybranchioporus*. The uncorrected pair-wise sequence divergence between the new species and the other recognized relatives was > 25% (Table 3).

The complete mitogenome of *G. weii* sp. nov. is 15,835 bp long with a base composition of 15.8% G, 27.0% A, 25.4% T, and 31.7% C. It encoded 37 genes including 13 protein-coding genes, 22 tRNA genes, 2 rRNA genes, and a control region (Fig. 5B). All these genes were encoded on the heavy strand, except for the ND6 protein-coding gene and seven tRNA genes (tRNA-Ala, tRNA-Cys, tRNA-Asn, tRNA-Pro, tRNA-Gln, tRNA-Ser and tRNA-Tyr) which were located on the light strand.

Combined with the morphological comparison and phylogenetic data, we confirm that the specimens from Danzhou, Hainan Island represent a new species of the genus *Glossobalanus*.

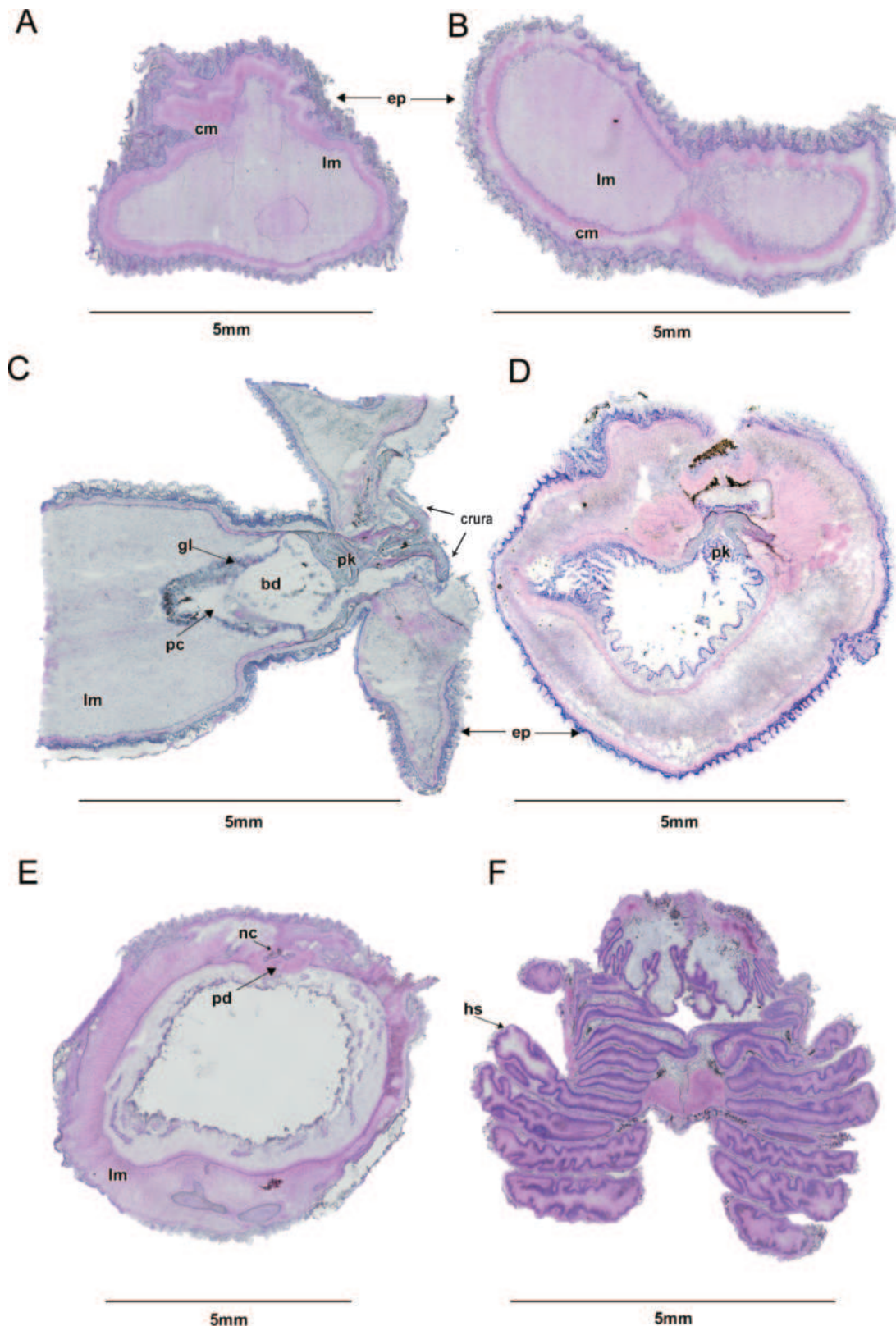


Figure 3. Histological characteristics of *Glossobalanus weii* sp. nov. **A** longitudinal section through the anterior proboscis **B** transverse section through the anterior proboscis **C** frontal section through the posterior proboscis and collar **D** transverse section through the anterior collar **E** transverse section through the posterior collar **F** transverse section through the hepatic region. Abbreviations: buccal diverticulum (bd); circular musculature (cm); epidermis (ep); glomerulus (gl); hepatic sacculations (hs); longitudinal musculature (lm); nerve cord (nc); proboscis cavity (pc); periahaemal diverticula (pd); proboscis skeleton (pk).

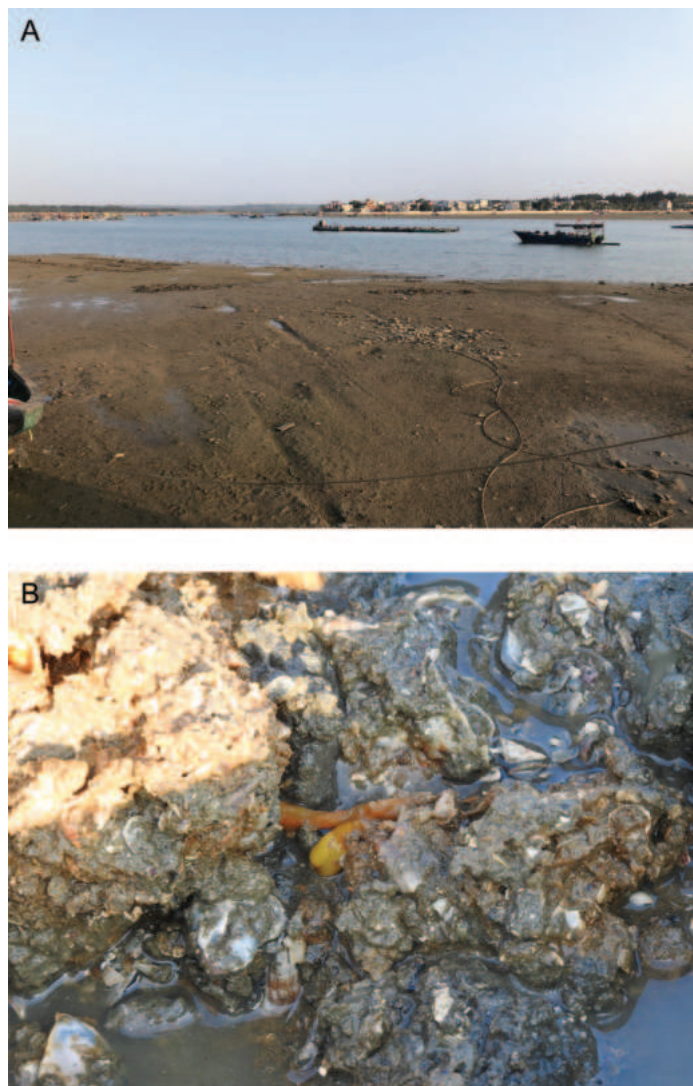


Figure 4. Habitat of *Glossobalanus weii* sp. nov. **A** the intertidal zone habitats at the type locality **B** the humic mudflats intertidal zone with gravelly and shell carcasses substrates feature.

Table 3. Estimates of evolutionary divergence between hemichordates with whole mitochondrial genome.

Species	1	2	3	4	5	6	7	8	9	10	11
<i>Glossobalanus weii</i> sp. nov.											
<i>Glossobalanus polybranchioporus</i>	0.255										
<i>Balanoglossus clavigerus</i>	0.267	0.285									
<i>Balanoglossus misakiensis</i>	0.274	0.281	0.279								
<i>Balanoglossus. carnosus</i>	0.276	0.281	0.258	0.287							
<i>Glossobalanus. marginatus</i>	0.332	0.334	0.352	0.349	0.361						
<i>Schizocardium brasiliense</i>	0.377	0.388	0.401	0.402	0.405	0.407					
<i>Glandiceps qingdaoensis</i>	0.392	0.407	0.402	0.414	0.411	0.419	0.348				
<i>Saccoglossus kowalevskii</i>	0.514	0.516	0.550	0.509	0.547	0.522	0.533	0.546			
<i>Stereobalanus canadensis</i>	0.461	0.464	0.469	0.453	0.471	0.478	0.447	0.476	0.531		
<i>Rhabdopleura compacta</i>	1.091	1.053	1.065	1.039	1.063	1.070	1.013	1.060	1.021	0.953	
<i>Cephalodiscus hodgsoni</i>	1.116	1.080	1.107	1.092	1.096	1.083	1.047	1.093	1.074	1.042	0.815

The number of base substitutions per site from between sequences are shown. Analyses were conducted using the Maximum Composite Likelihood model. This analysis involved 13 nucleotide sequences. All ambiguous positions were removed for each sequence pair (pairwise deletion option). Evolutionary analyses were conducted in MEGA11 (Tamura et al. 2021).

- 4 Proboscis length equal in collar; genital wing initiation separated from posterior margin of the collar by a small segment at the center of the dorsal surface, hepatic sacculations without serrated margins..... *Balanoglossus misakiensis*
- Collar longer than proboscis, genital wing tip joined to posterior margin of collar; hepatic sacculations with serrated margins... *Balanoglossus carnosus*
- 5 Genital ridges beginning at end of gill area, short and not prominent..... *Glossobalanus mortenseni*
- Genital ridges begin at the anterior end of the gill area, long and prominent **6**
- 6 Proboscis length is less than twice of the collar; gill pores 130–160 *Glossobalanus polybranchioporus*
- Proboscis length is more than twice that of the collar; gill pores 30–60.... *Glossobalanus weii* sp. nov.
- 7 Proboscis 3× collar length; proboscis cavity separated completely by the median dorsal-ventral septum..... *Glandiceps qingdaoensis*
- Proboscis 4–9× collar length; proboscis cavity not separated completely by the dorsal-ventral septum *Saccoglossus hwangtauensis*

Discussion

All the specimens of the new species were morphologically consistent with the other recognized species of the genus *Glossobalanus* (Fig. 6). In addition to differences in morphological indicators such as the total length, the branchiogenital region and the collar length, the new species can be distinguished by a black tip to the proboscis, a proboscis that is twice the length of the collar, a broad posterior collar margin and string brown hepatic sacculations. *Glossobalanus polybranchioporus* is the only other *Glossobalanus* species also found in China. The total body length of the new species is 176–196 mm, half the body length of *G. polybranchioporus* (352–613 mm; Tchang and Liang 1965). Meanwhile, the number of branchial pores is around 40, much less than *G. polybranchioporus* (130–160 mm). Our histological analysis also observed that the morphological characteristics of new species is different from other *Glossobalanus* species in a rather small proboscis cavity and > 180° proboscis skeleton bifurcation. The polygenic molecular genetic analysis show that the new species is clustered together with *G. polybranchioporus*. One surprise was that another species, *G. marginatus*, did not cluster in the same clade. This may require a higher level of taxonomic determination, or it may be for other reasons we do not yet know. More attention and research work needs to be devoted to this in the future. Integrating external morphology, histology, and molecular analysis, we present the specimens from Danzhou city, Hainan Island, as a new species of *Glossobalanus* (Enteropneusta).

To better understand the living habits and distribution of *G. weii* sp. nov. in the field, we also conducted field investigation in a wide range. *Glossobalanus weii* sp. nov. usually inhabits benthic gravelly mud, rich in crustacean shells (Fig. 4B), where it occurs over a limited area in discrete patches. This species of acorn worms may require a certain sand quality in their habitat. For example, under experimental conditions, the worms will not burrow in the fine sand from which the shell residue is manually removed, which may greatly limit their

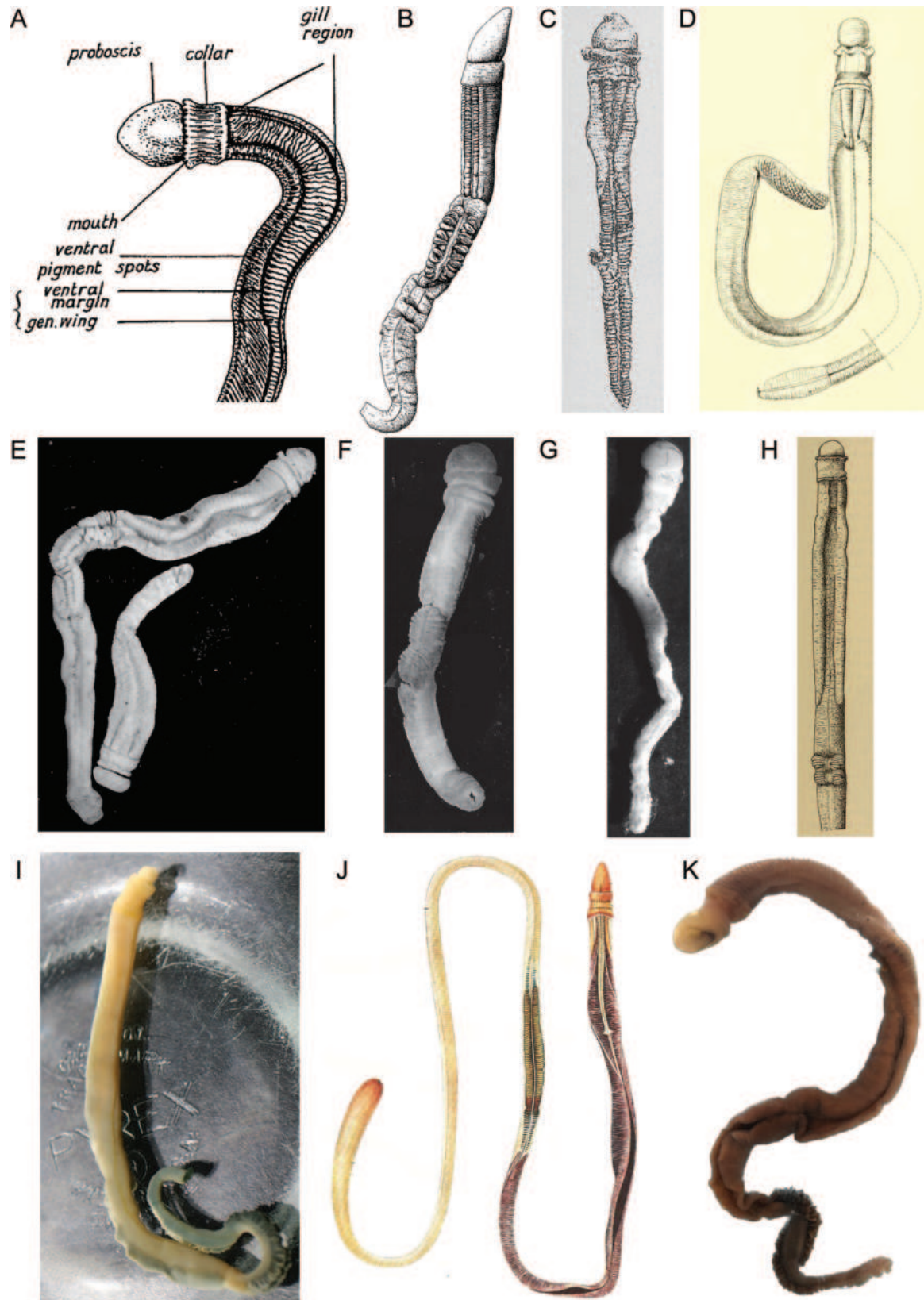


Figure 6. External morphology of genus *Glossobalanus* species **A** *G. marginatus* in Meek (1922) **B** *G. mortenseni* in van der Horst (1932) **C** *G. crozieri* in van der Horst (1924) **D** *G. ruficollis* in Willey (1899) **E** *G. barnharti* in Cameron and Ostiguy (2013) **F** *G. hartmanae* in Cameron and Ostiguy (2013) **G** *G. minutus* in Cameron and Ostiguy (2013) **H** *G. alatus* in van der Horst (1940) **I** *G. berkeleyi*. Photo from Swalla and van der Land (2024). Hemichordata World Database **J** *G. polybranchioporos* in Tchang and Liang (1965) **K** *G. weii* in this article.

movement and ability to avoid enemies. Construction of coastal features with a large amount of fine sand will inevitably adversely affect the survival of this species. On the other hand, according to the current investigation results, the distribution range of *G. weii* sp. nov. is extremely narrow, and the known distribution of *G. polybranchioporus* is 2000 km from its related species (Fig. 1). It is possible that further surveys will extend the range, or that the patchy distribution of these species indicates the demise of an ancient and declining group (Cameron et al. 2010). However, it is unfortunate that the narrow distribution of two acorn worm species overlaps extensively with infrastructure projects development in the coastal zone, which have encroached upon their habitats in recent years. In the future, it is worth thinking about how we and hemichordates will live together.

More than 130 species of hemichordate have been recorded worldwide, and most live in intertidal mudflats or deep-sea environments (Tassia et al. 2016). There is a serious lack of understanding of the distribution and habits of extant hemichordates, mainly due to the lack of public attention, specialized systematic investigation as well as scientific research by researchers on this species group. Most of the known species and even genera have been described only once. In addition, many species may already be endangered or extinct before being formally described. In China, hemichordates have received little attention with only seven species of Enteropneusta being recorded (Liang 1984; An and Li 2005), and their species richness may be greatly underestimated. With this discovery, we aim to shed light on conservation efforts for Chinese hemichordate species. Either way, it is necessary for us to pay more attention to this important group of evolutionary nodes in the future, especially to carry out more detailed studies on the classification and endangered status of them.

Acknowledgements

We are indebted to Prof. X. Li and J. Sui for kindly providing reference material. We thank M. Lawes for his linguistic editing of the paper. Thanks are also due to S. Zhang, M. Huang, and other colleagues for their help in collecting the material.

Additional information

Conflict of interest

The authors have declared that no competing interests exist.

Ethical statement

The collection of all animals used for this study obeyed the Wildlife Protection Act of China. All activities followed the Laboratory Animal Guidelines for the Ethical Review of Animal Welfare (GB/T 35892-2018).

Funding

This study was supported by Ministry of Science and Technology of China (2021YFF0502800), National Natural Science Foundation of China (32301466), Science and Technology Department of Guangdong Province (2021QN02H103), and PI Project of Southern Marine Science and Engineering Guangdong Laboratory (Guangzhou) (GML2020GD0804, GML2022GD0804).

Author contributions

XF: conceptualization, data curation, formal analysis, investigation, visualization, writing-original draft. WG: conceptualization, data curation, investigation, visualization. ZD: investigation. WZ: conceptualization, investigation, funding acquisition, validation, project administration, writing-review, and editing. FW: conceptualization, supervision, funding acquisition. All authors read and approved the final manuscript. #XF and WG contributed equally to this work.

Author ORCIDs

Xianan Fu  <https://orcid.org/0000-0001-9359-6314>

Wenliang Zhou  <https://orcid.org/0000-0002-1240-8842>

Fuwen Wei  <https://orcid.org/0000-0002-5233-1288>

Data availability

All of the data that support the findings of this study are available in the main text.

References

- Agassiz A (1873) The history of *Balanoglossus* and *Tornaria*. *Memoirs of the American Academy of Arts and Sciences* 9(2): 421–436. <https://doi.org/10.2307/25058009>
- An J, Li X (2005) First record of the family Spengeliidae (Hemichordata: Enteropneusta) from Chinese waters, with description of a new species. *Journal of Natural History* 39(22): 1995–2004. <https://doi.org/10.1080/00222930500059902>
- Cameron CB, Ostiguy A (2013) Three new species of *Glossobalanus* (Hemichordata: Enteropneusta: Ptychoderidae) from western North America. *Zootaxa* 3630(1): 143–154. <https://doi.org/10.11646/zootaxa.3630.1.5>
- Cameron CB, Deland C, Bullock TH (2010) A revision of the genus *Saccoglossus* (Hemichordata: Enteropneusta: Harrimaniidae) with taxonomic descriptions of five new species from the Eastern Pacific. *Zootaxa* 2483(1): 1–22. <https://doi.org/10.11646/zootaxa.2483.1.1>
- Capella-Gutiérrez S, Silla-Martínez JM, Gabaldón T (2009) trimAl: A tool for automated alignment trimming in large-scale phylogenetic analyses. *Bioinformatics (Oxford, England)* 25(15): 1972–1973. <https://doi.org/10.1093/bioinformatics/btp348>
- Deland CR, Cameron CB, Rao KP, Ritter WE, Bullock TH (2010) A taxonomic revision of the family Harrimaniidae (Hemichordata: Enteropneusta) with descriptions of seven species from the Eastern Pacific. *Zootaxa* 2408(1): 1–30. <https://doi.org/10.11646/zootaxa.2408.1.1>
- Delle CS (1829) Memorie sulla storia e notomia degli animali senza vertebre del Regno di Neapel. *Napoli* 4: 1–72. <https://doi.org/10.5962/bhl.title.10021>
- Eschscholtz JF (1825) Bericht über die zoologische Ausbeute der Reise von Kronstadt bis St. Peter und Paul. *Isis von Oken* 1825(6): 734–747. <https://www.biodiversitylibrary.org/page/27509188>
- Hill J (1897) XIV The Enteropneusta Part II. *Australian Museum Memoir* 3(5): 336–348. <https://doi.org/10.3853/j.0067-1967.3.1897.500>
- Hincks T (1880) A history of the British marine Polyzoa. John Van Voorst, London, [i-clxii +] 600 pp. <https://doi.org/10.5962/bhl.title.31555>
- Holland ND, Clague DA, Gordon DP, Gebruk A, Pawson DL, Vecchione M (2005) 'Lophenteropneust' hypothesis refuted by collection and photos of new deep-sea hemichordates. *Nature* 434(7031): 374–376. <https://doi.org/10.1038/nature03382>

- Koehler R (1886) Contribution a l'étude des Enteropneustes. Recherch anat. sur le *Balanoglossus sarniensis* nov. sp. Internat Monats Anat Hist 3: 139–190.
- Kowalevsky A (1866) Anatomie des *Balanoglossus*. Mémoires de l'Académie impériale des sciences de St. Pétersbourg 7(10): 16.
- Kuraku S, Zmasek CM, Nishimura O, Katoh K (2013) aLeaves facilitates on-demand exploration of metazoan gene family trees on MAFFT sequence alignment server with enhanced interactivity. Nucleic Acids Research 41(W1): W22–8. <https://doi.org/10.1093/nar/gkt389>
- Kuwano H (1902) On a new Enteropneust from Misaki, *Balanoglossus misakiensis* n. sp. Annotationes Zoologicae Japonenses 4: 77–84. <https://doi.org/10.34434/za000047>
- Lanfear R, Frandsen PB, Wright AM, Senfeld T, Calcott B (2017) PartitionFinder 2: New Methods for Selecting Partitioned Models of Evolution for Molecular and Morphological Phylogenetic Analyses. Molecular Biology and Evolution 34: 772–773. <https://doi.org/10.1093/molbev/msw260>
- Liang X (1984) Studies on the Enteropneusta of the intertidal zones of the China seas. Studia Marina Sinica 22: 127–143. [https://doi.org/10.1016/S0422-9894\(08\)70297-6](https://doi.org/10.1016/S0422-9894(08)70297-6)
- Maletz J (2023) Hemichordata, Including Enteropneusta, Pterobranchia (Graptolithina). Treatise on Invertebrate Paleontology. The University of Kansas Paleontological Institute, V(R2): 5–26.
- Meek A (1922) *Glossobalanus marginatus*, a new species of Enteropneusta from the North Sea. Journal of Cell Science 66: 579–594. <https://doi.org/10.1242/jcs.s2-66.264.579>
- Meng G, Li Y, Yang C, Liu S (2019) MitoZ: A toolkit for animal mitochondrial genome assembly, annotation and visualization. Nucleic Acids Research 47(11): e63. <https://doi.org/10.1093/nar/gkz173>
- Nguyen LT, Schmidt HA, Von Haeseler A, Minh BQ (2015) IQ-TREE: A Fast and Effective Stochastic Algorithm for Estimating Maximum-Likelihood Phylogenies. Molecular Biology and Evolution 32(1): 268–274. <https://doi.org/10.1093/molbev/msu300>
- Petersen JA, Ditadi ASF (1971) Asexual reproduction in *Glossobalanus crozieri* (Ptychoderidae, Enteropneusta, Hemichordata). Marine Biology 9(1): 78–85. <https://doi.org/10.1007/BF00348821>
- Punnett R (1906) The Enteropneusta. In: Gardiner J, (Eds) The Fauna and Geography of the Maldive and Laccadive Archipelagos. Cambridge University Press. London, 641–680.
- Rambaut A, Drummond AJ, Xie D, Baele G, Suchard MA (2018) Posterior summarization in Bayesian phylogenetics using Tracer 1.7. Systematic Biology 67(5): 901–904. <https://doi.org/10.1093/sysbio/syy032>
- Rao KP (1955) *Tornaria* from Madras (Enteropneusta). Hydrobiologia 7(3): 269–278. <https://doi.org/10.1007/BF00046698>
- Ridewood W (1907) Pterobranchia; *Cephalodiscus*. National Antarctic Expedition “Discovery”. Natural History 2: 1–67.
- Ronquist F, Teslenko M, van der Mark P, Ayres DL, Darling A, Höhna S, Larget B, Liu L, Suchard MA, Huelsenbeck JP (2012) MrBayes 3.2: Efficient Bayesian phylogenetic inference and model choice across a large model space. Systematic Biology 61(3): 539–542. <https://doi.org/10.1093/sysbio/sys029>
- Spengel JW (1893) Die Enteropneusten des Golfes von Neapel. in: Fauna und Flora des Golfes von Neapel und der angrenzenden Meeres-Abschnitte. Herausgegeben von der Zoologischen Station zu Neapel, Berlin, 756 pp. <https://doi.org/10.5962/bhl.title.11517>
- Spengel JW (1901) Die Benennung der Enteropneusten-Gattungen. Zoologische Jahrbucher Abteilung fuer Systematik Oekologie und Geographie der Tiere 15(2): 209–218. <https://www.biodiversitylibrary.org/page/9985208>

- Spengel JW (1904) Neue Beiträge zur Kenntnis der Enteropneustenart aus dem Golf von Neapel, nebst Beobachtungen über den postbranchialen Darm der Ptychoderiden. Zoologische Jahrbücher: Abteilung für Anatomie und Ontogenie der Tiere 20: 315–362.
- Swalla BJ, van der Land J (2024) Hemichordata World Database. Graptolithoidea. Accessed through: World Register of Marine Species. <https://www.marinespecies.org> [Retrieved on 27 February 2024].
- Tamura K, Stecher G, Kumar S (2021) MEGA 11: Molecular Evolutionary Genetics Analysis Version 11. Molecular Biology and Evolution 38(7): 3022–3027. <https://doi.org/10.1093/molbev/msab120>
- Tassia MG, Cannon JT, Konikoff CE, Shenkar N, Halanych KM, Swalla BJ (2016) The Global Diversity of Hemichordata. PLoS ONE 11(10): e0162564. <https://doi.org/10.1371/journal.pone.0162564>
- Tchang S, Koo K (1935) Sur deux d'Enteropneustes de la cote de Chine Contr. Institute of Zoology National Academy of Peiping II(4): 1–8.
- Tchang S, Liang X (1965) Description of a new species of Enteropneusta, *Glossobalanus polybranchioporos* from China seas. Dong Wu Fen Lei Xue Bao 2(1): 1–10.
- van der Horst C (1924) West-Indische Enteropneusten. Bijdragen tot de Dierkunde 23(1): 33–60. <https://doi.org/10.1163/26660644-02301004>
- van der Horst C (1932) On some Enteropneusta. Annals of the Transvaal Museum 14(4): 414–430. https://journals.co.za/doi/epdf/10.10520/AJA00411752_627
- van der Horst C (1940) The Enteropneusta from Inyack Island, Delagoa Bay. Annals of the South African Museum 32: 293–380. <https://www.biodiversitylibrary.org/part/76451>
- Willey A (1898) *Spengelia*, a new genus of Enteropneusta. Journal of Cell Science 40(40): 623–630. <https://doi.org/10.1242/jcs.s2-40.160.623>
- Willey A (1899) Enteropneusta from the South Pacific, with notes on the West Indian species. Willey's Zoological Results III: 32–335. <https://www.biodiversitylibrary.org/item/156606#page/1/mode/1up>
- Willey A (1931) *Glossobalanus berkeleyi*, a new enteropneust from the West Coast. Transactions of the Royal Society of Canada 5: 19–28. <https://searchworks.stanford.edu/view/9051289>